Studies in Natural Products Chemistry

Atta-ur-Rahman, FRS
Editor

Volume 36

Elsevier
The Boulevard, Langford Lane, Kidlington, Oxford, OX5 1GB, UK
Radarweg 29, PO Box 211, 1000 AE Amsterdam, The Netherlands

First edition **2012**

British Library Cataloguing in Publication Data
A catalogue record for this book is available from the British Library

Library of Congress Cataloging-in-Publication Data
A catalog record for this book is available from the Library of Congress

ISBN: 978-0-444-53836-9
ISSN: 1572-5995

Contributors

Awdah Al-Hazmi, College of Medicine, University of Hail, P.O. Box 2440, Hail, Saudi Arabia

Mohammed Al-Karrawi, Department of Environmental Technology, Al Iskan, Buraida, Saudi Arabia

Othman A. Al-Sagair, College of Medicine, University of Hail, P.O. Box 2440, Hail, Saudi Arabia

Eric Andrianasolo, Institute of Marine and Coastal Sciences, Rutgers University, New Brunswick, New Jersey, USA

Jamal M. Arif, College of Medicine, University of Hail, P.O. Box 2440, Hail, Saudi Arabia, and Department of Biotechnology, Microbiology and Bioinformatics, Integral University, Lucknow, India,

Marcela M. Baracat, Departamento de Ciencias Farmaceuticas, Centro de Ciencias da Saude, Universidade Estadual de Londrina, Londrina, Parana, Brazil

Renato D.R. Cardoso, Departamento de Ciencias Patologicas, Centro de Ciencias Biologicas, Universidade Estadual de Londrina, Rod. Celso Garcia Cid, Campus Universitario, Londrina, Parana, Brazil

Rubia Casagrande, Departamento de Ciencias Farmaceuticas, Centro de Ciencias da Saude, Universidade Estadual de Londrina, Londrina, Parana, Brazil

Fernando Q. Cunha, Department of Pharmacology, School of Medicine of Ribeirao Preto, University of Sao Paulo, Ribeirao Preto, Sao Paulo, Brazil

Thiago M. Cunha, Department of Pharmacology, School of Medicine of Ribeirao Preto, University of Sao Paulo, Ribeirao Preto, Sao Paulo, Brazil

Salvatore de Rosa, Consiglio Nazionale delle Ricerche Istituto di Chimica Biomolecolare, Pozzuoli, Naples, Italy

Paul Falkowski, Institute of Marine and Coastal Sciences, Rutgers University, New Brunswick, New Jersey, USA

Alvina Farooqui, Department of Biotechnology, Microbiology and Bioinformatics, Integral University, Lucknow, India

Sergio H. Ferreira, Department of Pharmacology, School of Medicine of Ribeirao Preto, University of Sao Paulo, Ribeirao Preto, Sao Paulo, Brazil

Maria J.V. Fonseca, Department of Pharmaceutical Sciences of Ribeirao Preto, University of Sao Paulo, Ribeirao Preto, Sao Paulo, Brazil

Sandra R. Georgetti, Departamento de Ciencias Farmaceuticas, Centro de Ciencias da Saude, Universidade Estadual de Londrina, Londrina, Parana, Brazil

Teppei Kawahara, Graduate School of Environmental Science, Hokkaido University, Kita-ku, Sapporo, Japan

Yanyan Li, Muséum National d'Histoire Naturelle, CNRS-UMR 7245, Unité Molécules de Communication et Adaptation des Micro-organismes, Paris, France

Richard Lutz, Institute of Marine and Coastal Sciences, Rutgers University, New Brunswick, New Jersey, USA

Bastien Nay, Muséum National d'Histoire Naturelle, CNRS-UMR 7245, Unité Molécules de Communication et Adaptation des Micro-organismes, Paris, France

Ifedayo V. Ogungbe, Natural Products Drug Discovery Group, Department of Chemistry, University of Alabama in Huntsville, Huntsville, Alabama, USA

Tatsufumi Okino, Graduate School of Environmental Science, Hokkaido University, Kita-ku, Sapporo, Japan

Mario Sergio Palma, Laboratory of Structural Biology and Zoochemistry, CEIS/Dept. Biology, Institute of Biosciences, São Paulo State University (UNESP), Rio Claro, São Paulo, Brazil

Soizic Prado, Muséum National d'Histoire Naturelle, CNRS-UMR 7245, Unité Molécules de Communication et Adaptation des Micro-organismes, Paris, France

Stephen G. Pyne, School of Chemistry, University of Wollongong, Wollongong, New South Wales, Australia

Thunwadee Ritthiwigrom, Department of Chemistry, Faculty of Science, Chiang Mai University, Chiang Mai, Thailand

William N. Setzer, Natural Products Drug Discovery Group, Department of Chemistry, University of Alabama in Huntsville, Huntsville, Alabama, USA

Mohammad Haris Siddiqui, Department of Biotechnology, Microbiology and Bioinformatics, Integral University, Lucknow, India

Meenakshi Singh, Natural Products Drug Discovery Group, Department of Chemistry, University of Alabama in Huntsville, Huntsville, Alabama, USA

Lik Tong Tan, Natural Sciences and Science Education, National Institute of Education, Nanyang Technological University, Singapore, Singapore

Giuseppina Tommonaro, Consiglio Nazionale delle Ricerche Istituto di Chimica Biomolecolare, Pozzuoli, Naples, Italy

Waldiceu A. Verri Jr., Departamento de Ciencias Patologicas, Centro de Ciencias Biologicas, Universidade Estadual de Londrina, Rod. Celso Garcia Cid, Campus Universitario, Londrina, Parana, Brazil

Fabiana T.M.C. Vicentini, Department of Pharmaceutical Sciences of Ribeirao Preto, University of Sao Paulo, Ribeirao Preto, Sao Paulo, Brazil

Preface

This volume of *Studies in Natural Products Chemistry* is the 36th in the series. The rapid growth in the natural sciences in the current era has created an ever-growing need for books and journals which provide state-of-the-art overviews in specific fields of research. Many aspects of basic research programs are intimately related to natural products.

With chapters written by leading authorities in their respective fields of research, *Studies in Natural Product Chemistry, Volume 36* presents current frontiers and future guidelines for research based on important discoveries made in the field of bioactive natural products. It is a valuable resource for researchers and engineers working in natural product and medicinal chemistry. Elsevier assessed the market needs and launched the *Studies in Natural Product Chemistry* series in 1988 and published Volume 35 in 2005. Taking into consideration the importance of natural product chemistry and the continuing need for a book series on this topic, Elsevier has decided to resume publishing the series after a break of 6 years.

During the past two decades, the series has published more than 700 in-depth comprehensive review articles covering most of the important discoveries and advances made in these disciplines. Volume 36 is devoted to bioactive natural products. The chapters included in these volumes cover the isolation, biological activities, and synthesis of natural products including acylpolyamines from spider venoms, hydrothermal vents as new source of drug discovery, marine cyanobacteria. Also, the readers will find very interesting chapters on chlorosulfolipids, the ecological significance of fungal endophyte, flavonoids as anti-inflammatory and analgesic drugs, and antileishmanial natural products from plant species.

The current volume is another useful addition to this important series of volumes on natural product chemistry which now covers more than 25,000 pages and is generally acknowledged to be the leading book series in Natural Product Chemistry.

I would like to express thanks to Miss Taqdees Malik and Mr. Wasim Ahmad for their assistance in the preparation of the volume. I am also grateful to Mr. Mahmood Alam for his editorial assistance.

Prof. Atta-ur-Rahman, FRS
Patron-in-Chief
International Centre for Chemical & Biological Sciences
University of Karachi
Karachi, Pakistan

Studies in Natural Products Chemistry edited by Atta-ur-Rahman

VOL. 1 Stereoselective Synthesis (Part A)
VOL. 2 Structure Elucidation (Part A)
VOL. 3 Stereoselective Synthesis (Part B)
VOL. 4 Stereoselective Synthesis (Part C)
VOL. 5 Structure Elucidation (Part B)
VOL. 6 Stereoselective Synthesis (Part D)
VOL. 7 Structure and Chemistry (Part A)
VOL. 8 Stereoselective Synthesis (Part E)
VOL. 9 Structure and Chemistry (Part B)
VOL. 10 Stereoselective Synthesis (Part F)
VOL. 11 Stereoselective Synthesis (Part G)
VOL. 12 Stereoselective Synthesis (Part H)
VOL. 13 Bioactive Natural Products (Part A)
VOL. 14 Stereoselective Synthesis (Part I)
VOL. 15 Structure and Chemistry (Part C)
VOL. 16 Stereoselective Synthesis (Part J)
VOL. 17 Structure and Chemistry (Part D)
VOL. 18 Stereoselective Synthesis (Part K)
VOL. 19 Structure and Chemistry (Part E)
VOL. 20 Structure and Chemistry (Part F)
VOL. 21 Bioactive Natural Products (Part B)
VOL. 22 Bioactive Natural Products (Part C)
VOL. 23 Bioactive Natural Products (Part D)

VOL. 24 Bioactive Natural Products (Part E)

VOL. 25 Bioactive Natural Products (Part F)

VOL. 26 Bioactive Natural Products (Part G)

VOL. 27 Bioactive Natural Products (Part H)

VOL. 28 Bioactive Natural Products (Part I)

VOL. 29 Bioactive Natural Products (Part J)

VOL. 30 Bioactive Natural Products (Part K)

VOL. 31 Studies in Natural Products Chemistry: Cumulative Indices Vol. 1–30

VOL. 32 Bioactive Natural Products (Part L)

VOL. 33 Bioactive Natural Products (Part M)

VOL. 34 Bioactive Natural Products (Part N)

VOL. 35 Bioactive Natural Products (Part O)

VOL. 36 Bioactive Natural Products

Chapter 1

Isolation, Biological Activities, and Synthesis of the Natural Casuarines

Thunwadee Ritthiwigrom* **and Stephen G. Pyne†**

*Department of Chemistry, Faculty of Science, Chiang Mai University, Chiang Mai, Thailand

†School of Chemistry, University of Wollongong, Wollongong, New South Wales, Australia

INTRODUCTION

Casuarine **1** [1], casuarine-6-*O*-α-glucoside **2** [2], 6-*epi*-casuarine **3** (uniflorine A) [3–5], and 3-*epi*-casuarine **4** [6] are members of the expanding group of polyhydroxylated 3-hydroxymethylpyrrolizidine natural products (Fig. 1) [7]. This group also includes australine [8], alexine [9] (7a-*epi*-australine), several other *epi*-australines (1-*epi*-australine, 3-*epi*-australine [10], 2,3-di-*epi*-australine, 2,3,7-tri-*epi*-australine) [11], 1-*epi*-australine-2-*O*-α-glucoside, and the more recently isolated hyacinthacine alkaloids of which 19 novel compounds have been identified [12]. This group, along with the polyhydroxylated pyrrolidine, piperidine, indolizidine, and nortropane alkaloids, has glycosidase inhibitory activities and thus has potential utility as antiviral, anticancer, antidiabetic, and antiobesity drugs [7]. Three structurally related synthetic compounds have been marketed as antidiabetic drugs to treat type-II diabetes based on their potent α-glucosidase inhibitory activities, while others have been identified as candidates for therapeutics to treat type-1 Gaucher disease [7]. These potentially useful biological activities, along with the stereochemical richness of these alkaloids (uniflorine A and casuarine have six contiguous stereogenic carbons), have made these compounds attractive and important synthetic targets [13]. This chapter describes the isolation, structure elucidation, glycosidase inhibitory activities, and the synthesis of the four naturally occurring casuarines.

Bioactive Natural Products, Vol. 36. DOI: 10.1016/B978-0-444-53836-9.00018-9

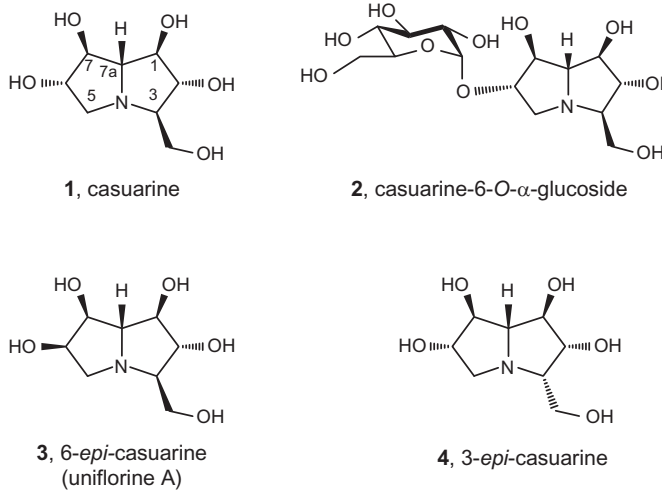

FIGURE 1 Structures of casuarine **1**, casuarine-6-*O*-α-glucoside **2**, 6-*epi*-casuarine **3** (uniflorine A), and 3-*epi*-casuarine **4**.

Isolation of the Natural Casuarines

Casuarina equisetifolia L., or commonly called, Australian pine, Filao or beach she oak, is a plant in the family Casuarinaceae, native to South East Asia, islands of the western Pacific Ocean (including French Polynesia, New Caledonia, Vanuatu), Australia (Northern Territory, north and east Queensland, and northeastern New South Wales), and West Africa. It is an evergreen tree that grows to over 6–35 m in height [14].

The first pentahydroxylated pyrrolizidine alkaloid, with six contiguous stereogenic centers and functional groups on all of the eight carbon atoms, was isolated in 1994 from the bark of *C. equisetifolia* L. [1]. This bark was prescribed as a remedy to treat breast cancer in Western Samoa [2]. Extracts of the wood, bark, and leaves of this plant have also been claimed to be useful for the treatment of diarrhea, dysentery, and colic [1]. This alkaloid was named casuarine **1** ((1*R*,2*R*,3*R*,6*S*,7*R*,7a*R*)-3-(hydroxymethyl)-1,2,6,7-tetrahydroxypyrrolizidine) by Nash *et al*. [1]. This investigation started with a GC–MS analysis of the per-trimethylsilylated bark extract which revealed a pentahydroxylated pyrrolizidine alkaloid and its glycoside as the major alkaloid components. The 75% aqueous ethanol bark extract was purified by ion-exchange column chromatography with Amberlite CG-120 (NH_4^+ form) which was eluted with 0.1 M NH_4OH to afford first the glycoside of casuarine **2** and then casuarine **1** itself (Fig. 1). Both alkaloids were isolated in approximately the same amounts with the latter in 0.013% yield based on the weight of the dried ethanol extract [1]. The absolute configuration of casuarine **1** was established by X-ray crystallographic analysis [1].

Eugenia jambolana is a plant in the family Myrtaceae, native to Bangladesh, India, Nepal, Pakistan, and Indonesia. An evergreen tree, it grows to 30 m in height. The extracts of the fruit pulp from *E. jambolana* have been reported to have antidiabetic properties, although this has been questioned in a more recent study [15]. In 1996, Wormald *et al.* [2] isolated casuarine **1** and its glucoside **2** from the leaves and the seeds of *E. jambolana* using Amberlite CG-120 (NH_4^+ form) ion-exchange chromatography. From 630 g of air-dried leaves they isolated 140 mg of casuarine **1** and 15 mg of the glucoside **2**.

Eugenia uniflora, Surinam cherry, Brazilian cherry, or Cayenne cherry, is a plant in the family Myrtaceae, native to tropical America and widely distributed in Paraguay, Uruguay, Argentina, and Brazil [3]. Decoctions of the leaves of this small tree are used as traditional medicines for a number of ailments, including use as an antidiabetic preparation. A number of studies have been made on the biological activities of the leaf extracts [16–18].

The water-soluble extracts of the leaves of *E. uniflora* L. have been used as an antidiabetic agent in Paraguayan traditional medicine [3]. In 2000, Arisawa *et al.* [3] reported the isolation of uniflorine A and B from the leaves of this tree. The water-soluble extract was purified twice on Amberlite ion-exchange resins and then on silica gel and finally HPLC to give samples of uniflorine A, uniflorine B, and (+)(3α,4α,5β)-1-methylpiperidine-3,4,5-triol in undisclosed amounts. The structures of the alkaloids uniflorine A and uniflorine B were deduced from NMR analysis to be that of the pentahydroxyindolizidine structures **3a** and **1a**, respectively (Fig. 2).

In 2004, Pyne and Davis [19] synthesized the proposed structure of uniflorine A; however, the NMR spectral data for synthetic **3a** did not match with those reported for uniflorine A [3]. The structure of their synthetic **3a** was unequivocally established by a single-crystal X-ray crystallographic study of its pentaacetate derivative. The Wollongong researchers therefore concluded that the structure originally assigned to uniflorine A was not correct [19]. The initial thoughts of several researchers were that uniflorine A was a diastereoisomer of **3a**. In 2006, Dhavale *et al.* [20], in their paper of partial title, "Attempts To Find the Correct Structure of Uniflorine A," reported the second synthesis of compound **3a**. Their sample of **3a** had NMR spectral data identical to those of **3a** that was earlier synthesized by Pyne *et al.* [19]. This paper also reported the synthesis of two diastereomers of **3a**, 8a-*epi*-**3a** and 1,2,8a-tri-*epi*-**3a**. In 2005, Mariano *et al.* [21] reported the synthesis of 1-*epi*-**3a**, while that of 1,2-di-*epi*-**3a** had been reported by Fleet *et al.* in 1996 [22], before uniflorine A was even isolated, and later by Mariano *et al.* [21] and by Pyne *et al.* in 2008 [4]. In 2008, Pyne *et al.* reported the synthesis of 2-*epi*-**3a** (Fig. 3) [4]. Despite these synthetic chemistry efforts, these 1,2,6,7,8-pentahydroxyindolizidine molecules also had NMR spectral data significantly different to those of uniflorine A.

From a reexamination of the original NMR data, Pyne, Davis, and Ritthiwigrom reassigned uniflorine B as the known pyrrolizidine alkaloid

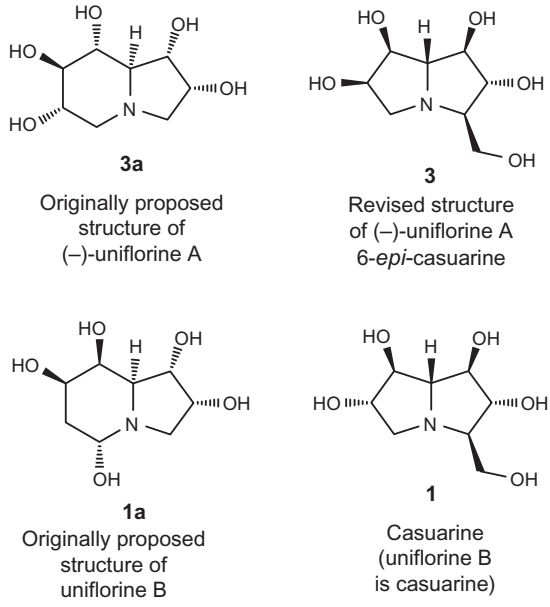

FIGURE 2 Originally proposed and the revised structures of uniflorine A and B.

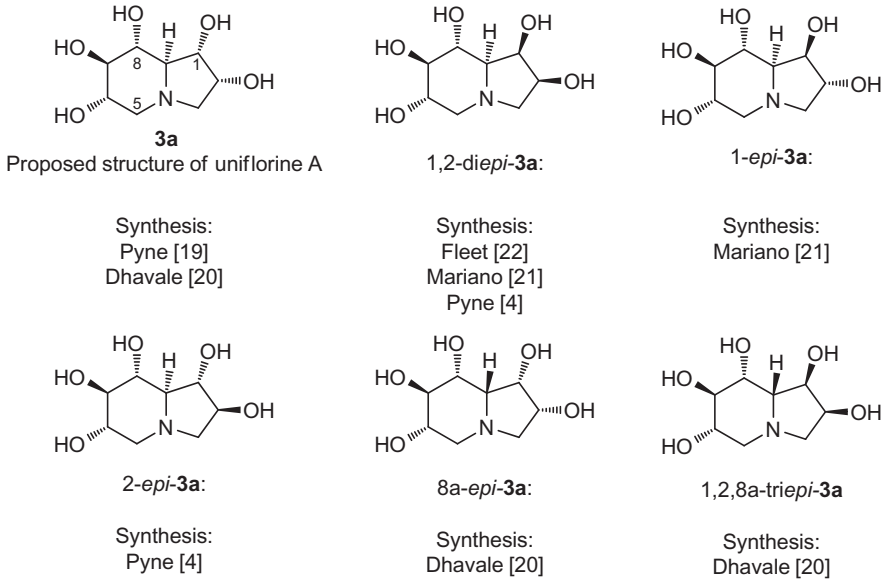

FIGURE 3 Synthesis of diastereomers of structure **3a**.

casuarine **1**, while the structure of (−)-uniflorine A was suggested to be that of 6-*epi*-casusarine **3** (Fig. 2) [4]. The structure of uniflorine A was unequivocally established to be that of 6-*epi*-casuarine **3** by its total synthesis (see synthesis section) [5,23,24].

Myrtus communis L., commonly known as Myrtle or True Myrtle, belongs to the family Myrtaceae. It originates from the Mediterranean, North African, and Western Asia regions. Casuarine **1** and 3-*epi*-casuarine **4** were isolated from *M. communis* L. growing in the grounds of the Institute of Grassland and Environmental Research in Aberystwyth, UK. The isolation was conducted using ion-exchange chromatography. Casuarine **1** was the major alkaloid present, which eluted first with water from the anion-exchange resin Dowex 1 (OH form) followed by 3-*epi*-casuarine **4** ((1*R*,2*R*,3*S*,6*S*,7*R*,7a*R*)-3-(hydroxymethyl)-1,2,6,7-tetrahydroxypyrrolizidine) (Fig. 1). No other epimer of **1** was isolated. Casuarine **1** and 3-*epi*-casuarine **4** were crystallized from warm 95% aqueous ethanol by layering with acetone. The absolute configuration of 3-*epi*-casuarine **4** was established by X-ray crystallographic analysis [6].

GLYCOSIDASE INHIBITORY ACTIVITIES OF THE NATURAL CASUARINES

The inhibitory activities of casuarine **1** and casuarine-6-*O*-α-glucoside **2** against a panel of 14 glycosidases were examined. Casuarine **2** was a much more potent inhibitor of α-D-glucosidases (e.g., rice α-D-glucosidase (IC_{50} 1.2 μM) and rat intestinal maltase (IC_{50} 0.7 μM)) than casuarine-6-*O*-α-glucoside **2** (e.g., rice α-D-glucosidase (IC_{50} 440 μM) and rat intestinal maltase (IC_{50} 260 μM)) [11]. In contrast, casuarine-*O*-α-glucoside **2** was a more active inhibitor of β-D-glucosidase from almond (IC_{50} 7.0 μM). Both compounds **1** and **2** were potent inhibitors of amyloglucosidase from *Aspergillus niger*, with IC_{50} values of 0.7 and 1.1 μM, respectively [11].

Casuarine **1** and casuarine-6-*O*-α-glucoside **2** were found to be inhibitors of the human N-terminal subunit of maltase-glucoamylase (NtMGAM) and *Escherichia coli* trehalose (Tre37A). Casuarine **1** and casuarine-6-*O*-α-glucoside **2** had K_i values of 0.45 and 280 μM, respectively, against human NtMGAM and K_i values of 17 μM and 12 nM, respectively, against Tre37A [25]. The high potency of casuarine-6-*O*-α-glucoside **2** against Tre37A is most significant. These studies confirmed an earlier study that showed casuarine **1** and casuarine-6-*O*-α-glucoside **2** were active inhibitors of trehalase from porcine kidney with IC_{50} values of 12 and 0.34 μM, respectively [11].

There is current interest in inhibitors of these enzymes. Human maltase-glucoamylase is one enzyme involved in the digestion of starch to glucose. Inhibitors of this enzyme can be used to control the rate of glucose production and thus potentially aid in the treatment of type-II diabetes [26]. Trehalase is found mainly in the midgut of insects and converts trehalose, the major sugar in the blood of insects, to glucose which is vital for insect flight. Thus

inhibitors of this enzyme may have potential as insecticides [26,27]. X-ray crystal structures of the complexes of casuarine **1** with human NtMGAM and casuarine-*O*-α-glucoside **2** with Tre37A were determined and revealed similarities in the catalytic sites of these unrelated enzymes [25]. Computer-aided docking studies of casuarine **1** into the active site of NtMGAM were consistent with the X-ray crystal structure and both studies indicated that all five hydroxyl groups of casuarine **1** are involved in H-bonding to amino acid residues in the active site, and the protonated nitrogen atom of casuarine **1** forms a salt bridge with Asp443 [28].

In another study, casuarine-6-*O*-α-glucoside **2** was found to be an nM (nanomolar) inhibitor of trehaloses from midge larvae (*Chironomus riparius*), mammalian pig kidney, and *E. coli*. Significantly, casuarine-6-*O*-α-glucoside **2** and two of its analogues were 10 or more times more potent on the insect trehalase than the other two enzymes indicating their potential as selective insecticides [29]. Other studies showed that casuarine **1** inhibited a membrane-bound trehalase from midge larvae (*C. riparius*) with an IC_{50} of 250 nM [30].

Uniflorine A and B were found to be inhibitors of the α-glucosidases, rat intestinal maltase (IC_{50} values of 12 and 4.0 μM, respectively), and sucrase (IC_{50} values 3.1 and 1.8 μM, respectively) [3]. The biological activity of the leaf extracts may be a result of the glycosidase inhibition activities of the natural product components, including the alkaloids uniflorine A and B [3]. The structures of these two alkaloids were later revised to be that of 6-*epi*-casuarine **3** and casuarine **1**, respectively [5,23,24]. In 2010, the results of the glycosidase inhibitory testing of 6-*epi*-casuarine **3** at 143 μg/mL showed 94–97% inhibition against the α-D-glucosidases of *Saccharomyces cerevisiae* and *Bacillus stearothermophilus* and against the amyloglucosidase of *A. niger*. The IC_{50} values were only determined for the two aforementioned α-D-glucosidases and were found to be modest at 34 and 28 μM, respectively [31]. In the same assays, casuarine **1** had IC_{50} values of 139 and 5.6 μM, respectively [32].

In contrast to casuarine **1**, 3-*epi*-casuarine **4** showed weak activity against three α-D-glucosidases (from yeast, rice, and *Bacillus*) and was more active against β-D-glucosidase from almond (IC_{50} ca. 700 μM). In the same assay, casuarine **1** showed 0% inhibition of this latter enzyme at a concentration of 700 μM, while castanospermine ("the bench mark for β-D-glucosidase inhibition") had an IC_{50} of 20 μM [6].

SYNTHESIS OF THE NATURAL CASUARINES

Synthesis of Casuarine 1

The first synthesis of casuarine **1** was achieved by Denmark and Hurd [33a,b] in four additional steps from a key tandem [4+2]/[3+2] nitroalkene cycloaddition reaction in 20% overall yield. The synthesis commenced with the preparation of the enantiomerically enriched (98% ee) vinyl ether **7** (Scheme 1).

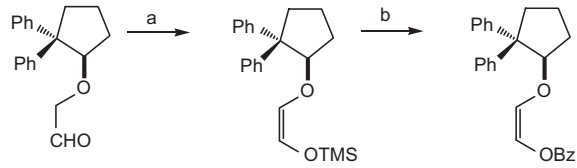

5 **6** **7**

SCHEME 1 Synthesis of the chiral vinyl ether **7**. Reagents and conditions: (a) TMSCl, Et_3N, CH_3CN, 81 °C, 99%; and (b) BzF, TBAF, THF, 0 °C, 2h (81% *Z*:6% *E*).

The chiral, alkoxy aldehyde **5** [33c] was converted to the silyl enol ether **6** in 99% yield as a 10:1 (Z:*E*) mixture. *O*-Benzoylation of **6** with benzoyl fluoride (BzF) and a catalytic amount of tetrabutylammonium fluoride (TBAF) (2mol %) provided **7** as a mixture of *Z* and *E* vinyl ethers, which were separated by silica gel chromatography in yields of 81% and 6%, respectively (Scheme 1).

The chiral nitronate **9**, the 1,3-dipolar component of the [3+2] cycloaddition, was prepared from an *endo*-diastereoselective [4+2]-cycloaddition reaction of the nitroalkene **8** and the chiral vinyl ether **7** in the presence of 2.5 equiv. of $SnCl_4$ in toluene at −78 °C (Scheme 2). The nitronate **9** was not stable and was immediately treated with the 1,1,2-trimethylpropylsilyl (TDS)-protected β-phenyldimethylsilyl enone **10** to give a 45:7:3:2:1:1 mixture of six isomeric cycloadducts in 76% yield. Purification by HPLC afforded the desired nitroso acetal **11** in 55% overall yield. Reduction of the ketone group of **11** with L-selectride at −78 °C led to a 10:1 mixture of epimeric alcohols **12** in 87% yield. Mesylation of the secondary alcohol **12** gave the mesylate **13** in 97% yield. This mesylate was converted to the pyrrolizidine **14** in 64% yield via hydrogenolysis over Raney nickel and then hydrolysis of both benzoate esters under basic conditions. The final step was transformation of the C-1 silyl group to the final hydroxyl substituent (Tamao–Fleming reaction) by dearylation of the phenyldimethylsilyl group with mercuric trifluoroacetate in trifluoroacetic acid (TFA), followed by oxidation with peracetic acid to afford pure casuarine **1** in 84% yield after ion-exchange column chromatography. Since aldehyde **5** can be prepared from diphenylacetonitrile in six overall steps [33c], the total steps in this synthesis of casuarine **1** are 14 (or 13 if you do not count the one-pot reaction going from **8** to **11**).

A synthesis of casuarine **1** and its 6,7-diepimer, in a stereocontrolled manner, was reported by Izquierdo *et al*. [34a]. The synthesis of casuarine **1** began with *N*-Cbz protection of the DMDP derivative **16** [34b] that gave the Cbz compound **17** in 93% yield (Scheme 3). Primary alcohol oxidation and then a Wittig reaction of **18** gave the pyrrolidinic propenoate **19** (in two steps). Dihydroxylation (DH) of **19** using osmium tetraoxide and NMO in the presence of *O*-(4-chlorobenzoyl)hydroquinine (DHQ-CLB) as a chiral ligand gave a mixture of **20** and **21** in yields of 58% and 27%, respectively. The configuration of both diol products could not be determined at this stage. After two

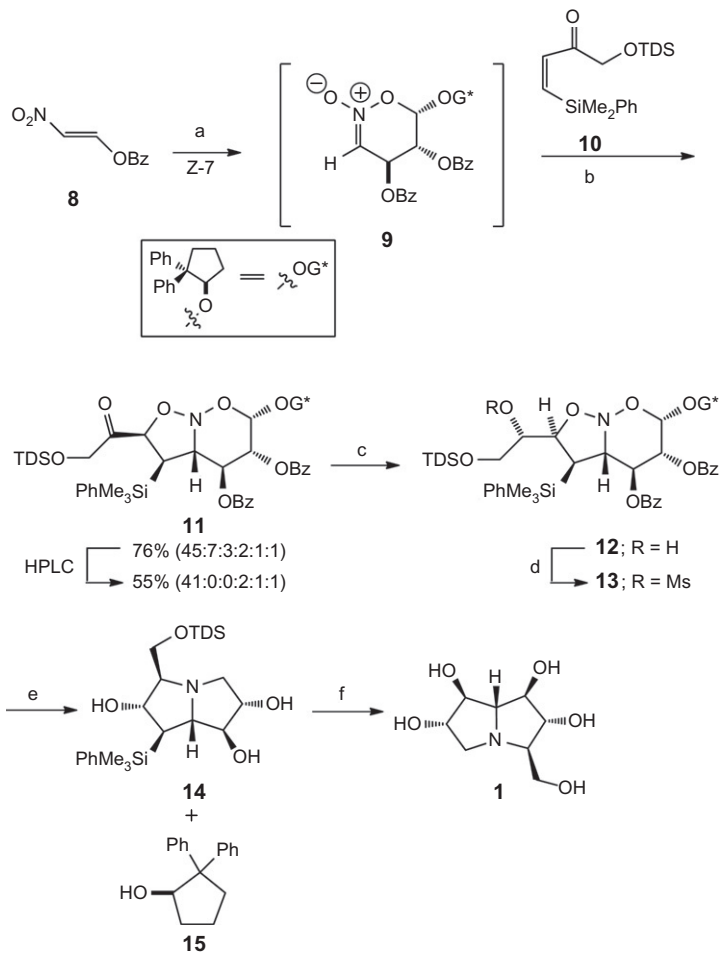

SCHEME 2 Total synthesis of casuarine **1** by Denmark *et al*. [33a,b]. Reagents and conditions: (a) ***Z*-7**, $SnCl_4$, toluene, −78°C; (b) **10**, $CHCl_3$; (c) L-selectride, THF, −78°C, 87% (10:1); (d) Ms_2O, py, 1h, 97%. (e) i: Raney Nickel, MeOH, 260psi H_2; ii: K_2CO_3, MeOH, rt, 64%; and (f) $Hg(OTFA)_2$, TFA, HOAc, AcO_2H, 84%.

more steps, an NOE experiment confirmed that **20** was the desired intermediate to make casuarine **1**. *N*-Deprotection of **20** under hydrogenolysis reaction conditions provided pyrrolidine **22** which was subsequently transformed to **23** by heating a methanol solution at reflux in the presence of a catalytic amount of NaOMe.

Reduction of the lactam carbonyl group of **23** using $BH_3{\cdot}SMe_2$ complex gave **24** in 89% yield. *O*-TBDPS deprotection and then debenzylation of **24** gave **25** in 95% yield. Hydrogenolysis then gave an impure sample of **1**. This sample was further purified by peracetylation which gave **26** in 41% yield.

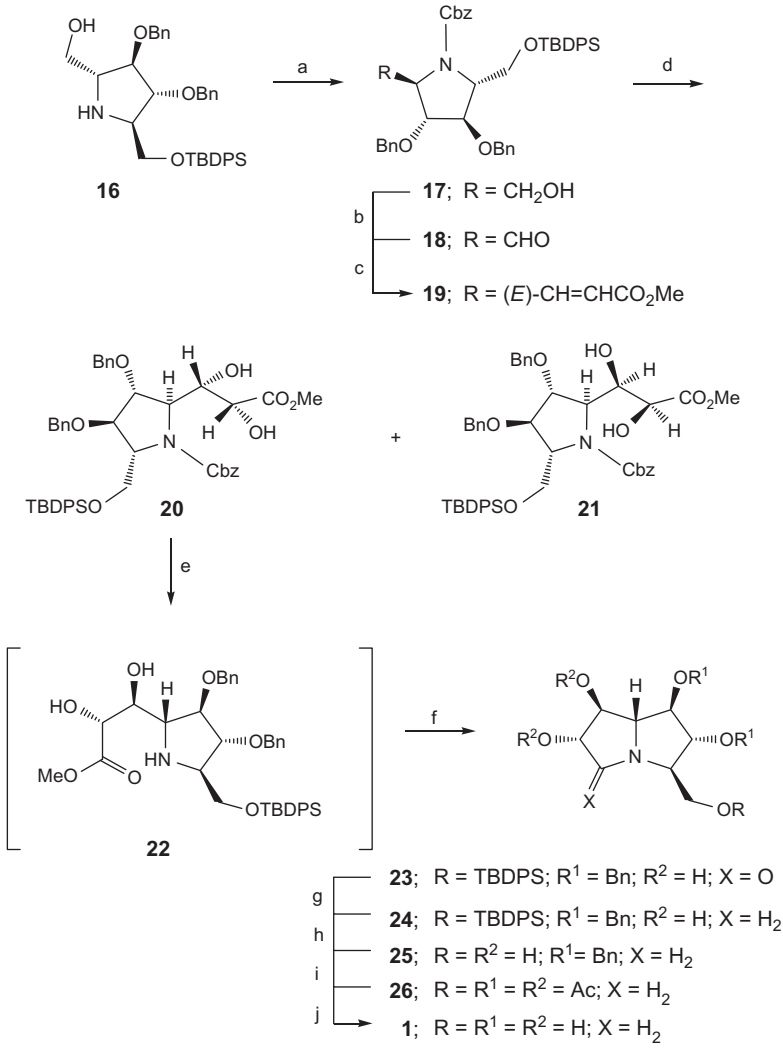

SCHEME 3 Total synthesis of casuarine **1** by Izquierdo *et al*. [34a]. Reagents and conditions: (a) CbzCl, Me_2CO, K_2CO_3, rt, 93%; (b) TPAP, NMO, 4 Å MS, CH_2Cl_2; (c) $Ph_3P{=}CHCO_2Me$, CH_2Cl_2, rt, 85% (from **17**); (d) OsO_4, NMO, DHQ-CLB, acetone/H_2O, rt, 2days (**20**:**21**=58%:27%); (e) H_2, 10% Pd/C, MeOH; (f) cat. MeONa, MeOH, rt, 85%; (g) $BH_3{\cdot}SMe_2$, THF, then MeOH, Δ, 89%; (h) n-$Bu_4N^+F^-{\cdot}3H_2O$, THF, rt, 95%; (i) i: H_2, 10% Pd/C, MeOH, then Amberlite IRA-400 (OH^- form), ii: Ac_2O, py, DMAP, 41%; and (j) cat. NaOMe, MeOH, rt, 93%.

Base-catalyzed deacetylation of **26** afforded casuarine **1** in 93% yield. This synthesis was achieved in eight steps from the DMDP derivative **16** in 13% overall yield. DMDP **16** was prepared in five steps from a compound derived from D-fructose [34b]; thus the total number of synthetic steps using this route is more than 13.

In 2006, Fleet *et al*. [6] published the synthesis of casuarine **1** from D-gluconolactone **27** (Scheme 4). D-Gluconolactone **27** was reacted with 2,2-dimethoxypropane and the open chain diacetonide was subsequently esterified with trifluoromethanesulfonic anhydride to afford the triflate **28** in 72% yield. The triflate group of **28** was displaced with sodium azide in DMF to give the azide **29** in 97% yield. The unsaturated ester **30** was obtained from reduction of the azidoester **29** with DIBAL, followed by treatment of the resulting aldehyde with the Wittig reagent, $Ph_3P{=}CHCO_2Me$, in 75% yield over the two steps. The unsaturated ester **30** had an *E*:*Z* ratio of 10:1. After isolation of the pure *E* isomer of compound **30**, it was converted to a mixture (1:4) of the diols **31** and **32**, using an OsO_4-catalyzed DH reaction, in 72% yield. Hydrogenation of this mixture gave a mixture of amines which cyclized to the pyrrolizidine framework upon heating in toluene. Finally, after treatment of the reaction mixture with TBSCl, the lactam **33** was separated in 70% yield over the three steps. The terminal acetonide of **33** was removed by acid hydrolysis to afford the diol **34** in 69% yield. Selective protection of the primary hydroxyl group of diol **34** with TBSCl gave the secondary alcohol **35** in 81% yield. The remaining secondary hydroxyl group of **35** required inversion of its configuration. This was achieved by treatment with triflic anhydride to afford the unstable triflate **36** which was reacted with caesium trifluoroacetate. Base hydrolysis of the resulting trifluoroacetate gave the inverted alcohol **37** in 20% yield over the three steps. The desired lactam mesylate **38** was obtained in 90% yield by treating **37** with methanesulfonyl chloride. Reduction of the lactam carbonyl group of **38** with $BH_3{\cdot}THF$ gave the amine **39** (57% yield). Finally, pure casuarine **1** was obtained after two more steps, *O*-silyl group hydrolysis with TFA and then cyclization by treatment with sodium acetate (91% yield over the two steps). Overall, the total number of synthetic steps was 13 starting from D-gluconolactone **27**.

In 2009, Goti *et al*. [25a] published the synthesis of casuarine **1** and the first total synthesis of its 6-*O*-α-glucoside **2**. Their key steps were a 1,3-dipolar cycloaddition reaction, a Tamao–Fleming reaction and a Mitsunobu reaction. Their total synthesis (Scheme 5) began with a stereoselective cycloaddition reaction of the nitrone **41** with the alkene **42** in CH_2Cl_2 to give the isoxazolidine **43**. Reductive N—O bond cleavage of **43** with Zn/HOAc and then attack of the resulting amine on to the ester carbonyl group resulted in the lactam **44**. This compound was converted to **45** using the Tamao–Fleming reaction similar to that employed by Denmark (Scheme 2) [33a,b]. Reduction of lactam **45** with $LiAlH_4$ gave **46** in 76% yield, which was debenzylated under standard hydrogenolysis reaction conditions to give pure casuarine **1** in five steps and 44% overall yield from the nitrone **41**. This latter compound is prepared in seven steps from L-xylose or D-arabinose [25b], making the total number of synthetic steps for the synthesis of casuarine **1** as 12 and the total overall yield 19%.

The total synthesis of casuarine by Ritthiwigrom and Pyne was completed in 13 steps and 8% overall yield (Schemes 6 and 7) [23]. The 1,2-*anti*-aminoalcohol

47 was obtained from the boronic acid–Mannich reaction (Petasis reaction) of L-xylose, allylamine, and (*E*)-styrene boronic acid [19,35] in 92% yield as a single diastereomer after purification by ion-exchange chromatography. The amino-tetraol **47** was converted to its *N*-Boc derivative **48** (80% yield) and then the terminal diol functionality of **48** was selectively protected as the acetonide derivative **49** under standard conditions. A ring-closing metathesis reaction of the diene **49** using Grubbs' first-generation ruthenium catalyst **50** provided the 2,5-dihydropyrrole **51** in 97% yield (Scheme 6).

The synthesis of casuarine **1** from the chiral 2,5-dihydropyrrole **51** is shown in Scheme 7. To secure the 6α,7β-configuration of the target molecule, the synthetic plan involved a regioselective ring-opening reaction of the epoxide **58** with an oxygen nucleophile (Scheme 7).

To obtain the key epoxide **58**, the two unprotected secondary hydroxyl groups in **51** were protected as their *O*-benzyl ethers and the resulting

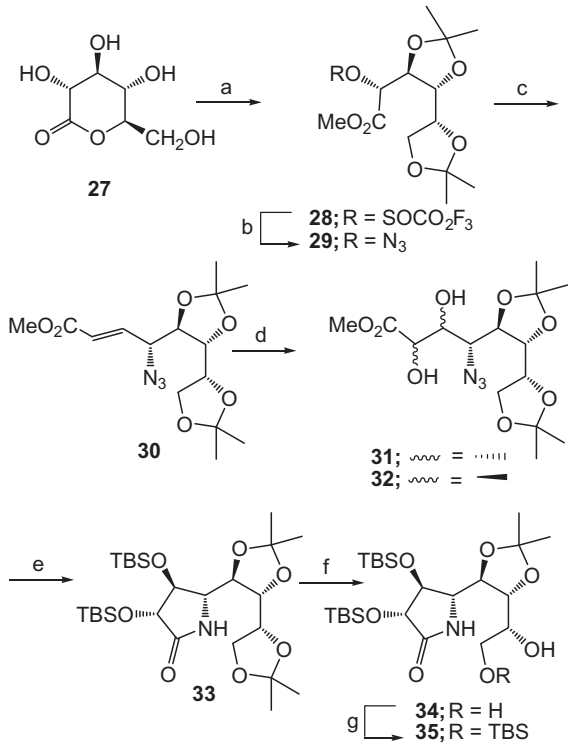

SCHEME 4 Total synthesis of casuarine **1** by Fleet *et al*. [6]. Reagents and conditions: (a) $Me_2C(OMe)_2$, *p*-TsOH, MeOH; then $(CF_3SO_2)_2O$, py, CH_2Cl_2, 72%; (b) NaN_3, DMF, 97%; (c) *t*-Bu_2AlH, −78 °C; then $Ph_3P{=}CHCO_2Me$, toluene (75% over two steps); (d) cat. OsO_4, NMO, *t*-BuOH/H_2O, 72%; (e) H_2, Pd/C, THF; then toluene, Δ; then *t*-$BuMe_2SiCl$, imidazole, THF (70% over three steps); (f) 60% HOAc, H_2O/MeOH, 69%; (g) *t*-$BuMe_2SiCl$, py, 81%;

Continued

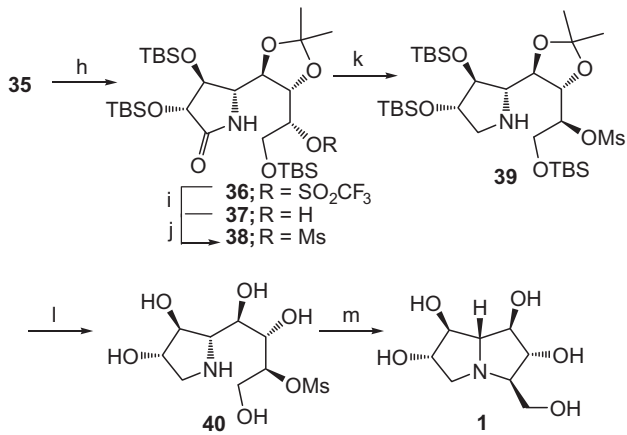

SCHEME 4—cont'd (h) $(CF_3SO_2)_2O$, py, CH_2Cl_2; (i) CF_3CO_2Cs, 2-butanone; then K_2CO_3, MeOH (20% from **35**); (j) CH_3SO_2Cl, Et_3N, CH_2Cl_2, 90%; (k) BH_3·THF, THF, 57%; (l) 90% CF_3CO_2H, H_2O; and (m) NaOAc, H_2O (91% over two steps).

dibenzyl ether **52** (92% yield) was treated under acidic conditions to effect hydrolysis of both the acetonide and *N*-Boc protecting groups and to provide amino diol **53** in 76% yield. Regioselective *O*-silylation of **53** at the primary hydroxyl group gave the TBS ether **54** (81% yield) which was efficiently *N*-protected as its Fmoc derivative **55** in 94% yield. Epoxidation of the alkene moiety of **55** using 1,1,1-trifluoroacetone and oxone [36] provided the epoxide **56** in 81% yield as a single diastereomer. *O*-Mesylation of the free secondary hydroxyl of **56** followed by treatment of the mesylate **57** (94% yield) with piperidine resulted in smooth *N*-Fmoc deprotection and then cyclization of the free cyclic secondary amine to give in 96% yield a 91:9 mixture of the desired pyrrolizidine **58** and the undesired indolizidine **58a**, respectively. It was assumed that **58** arose from *O*-TBS migration under the basic conditions of the *O*-mesylation reaction. Fortunately, pure **58** could be obtained by further separation of the mixture by column chromatography. The structure of the epoxide **58** was confirmed by a single crystal X-ray analysis. Several attempts in our laboratory to ring-open the epoxide group of compounds related to **58** using aqueous acid conditions (e.g., H_2SO_4/water) led to complex mixtures and low yields of diol products. However, when **58** was treated under the conditions reported by Saracoglu [37], using $NaHSO_4$ as both the acid catalyst and the nucleophilic species in dichloromethane at reflux, followed by the addition of water to hydrolyze the intermediate sulfate, then the desired diol **59** was obtained as an 86:14 mixture of regioisomers. Purification of this mixture by column chromatography gave a 92:8 mixture of the diastereomeric diols **59** and 6,7-di-*epi*-**59**, respectively in 51% yield. The regiochemistry of this ring-opening reaction was consistent with that reported on related

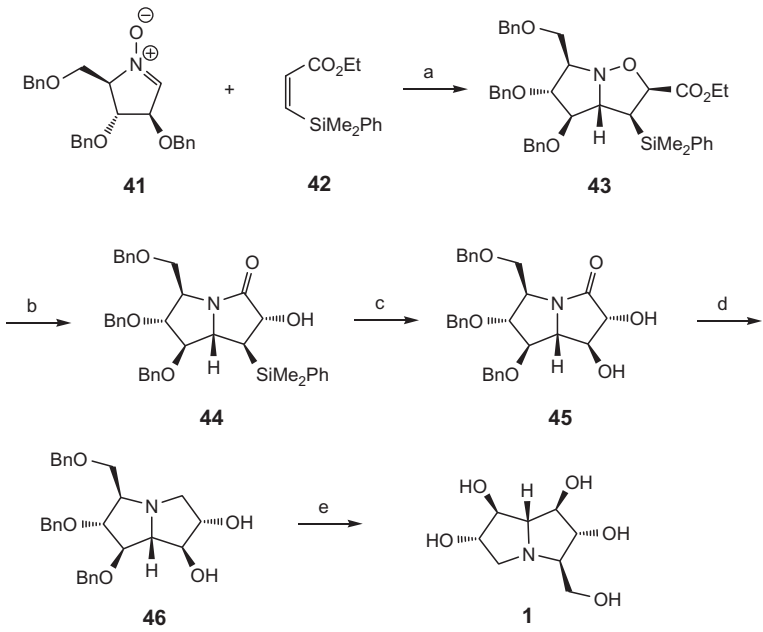

SCHEME 5 Total synthesis of casuarine **1** by Goti *et al*. [25a]. Reagents and conditions: (a) CH_2Cl_2, rt, 36h, 79%; (b) Zn, AcOH/H_2O, 60–65°C, 5h, 93%; (c) $Hg(CF_3CO_2)_2$, TFA, AcOH, AcOOH, $CHCl_3$, 76%; (d) $LiAlH_4$, THF, reflux, 78%; and (e) H_2, Pd/C, MeOH, HCl, 100%.

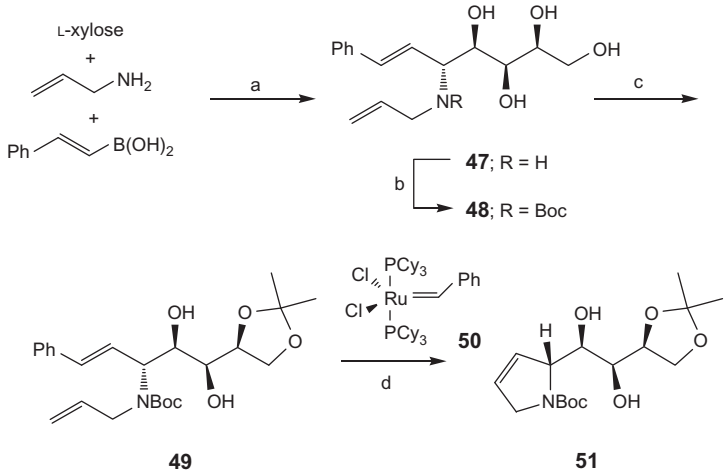

SCHEME 6 Synthesis of **51** [23]. Reagents and conditions: (a) (*E*) PhCH═CHB$(OH)_2$, allyl amine, EtOH, rt, 3days; ion exchange, 92%; (b) $(Boc)_2O$, Et_3N, MeOH, rt, 3days, 80%; (c) DMP, PPTS, acetone, rt, 20h, 64%; and (d) Grubbs' I **50**, CH_2Cl_2, 50°C, 18h, 97%.

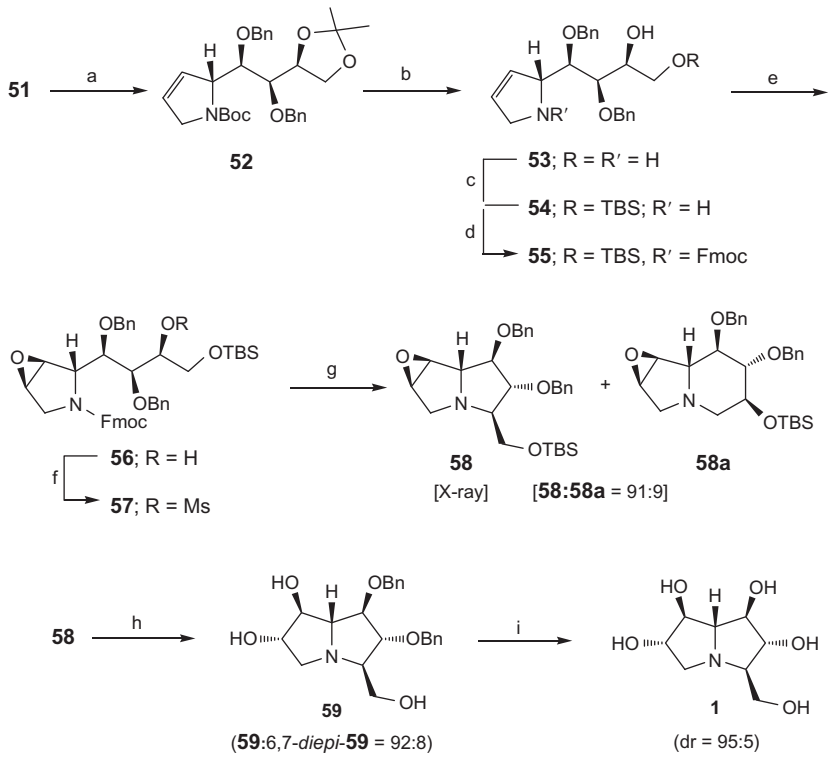

SCHEME 7 Total synthesis of casuarine **1** from the precursor **51** by Ritthiwigrom and Pyne [23]. Reagents and conditions: (a) NaH, BnBr, *n*-Bu_4NI, THF, 18h, 92%; (b) HCl/MeOH, rt, 30 h, 76%; (c) TBSCl, DMAP, imidazole, THF, rt, 1days, 81%; (d) FmocCl, THF, sat. Na_2CO_3, 0° C, 3h, 94%; (e) CF_3COCH_3, oxone, $NaHCO_3$, $MeCN/H_2O$, 0°C, 2h, 81%; (f) MsCl, Et_3N, CH_2Cl_2, N_2, 0°C, 3h, 94%; (g) piperidine, MeCN, rt, 15h, 96%; (h) $NaHSO_4$, CH_2Cl_2, reflux, 2days, water, rt, 1h, 51%; and (i) $PdCl_2$, H_2 (1atm), MeOH, rt, 1.5h; ion exchange, 93%.

epoxy-pyrrolizidines [38] and was expected from stereoelectronic considerations as shown in Scheme 8. For *trans*-1,2-diaxial ring opening of epoxide **58** by HSO_4^-, the two reactive conformations **A** and **B** are possible. Attack on conformation **A** at C-7 is inhibited by 1,3-diaxial interactions between the nucleophile (HSO_4^-) and the pseudoaxial protons H-1α and H-5α and thus addition to conformation **B** at C-6 predominates resulting in **59** as the major regioisomeric product. Hydrogenolysis of **59** over $PdCl_2/H_2$ gave casuarine **1**, in 93% yield after purification by ion-exchange chromatography. The diastereomeric purity of **1** was 95:5 from ^1H NMR spectroscopic analysis.

Thus there have been five total syntheses of casuarine **1**, with that of Goti being the shortest and most efficient with a total of 12 synthetic steps from

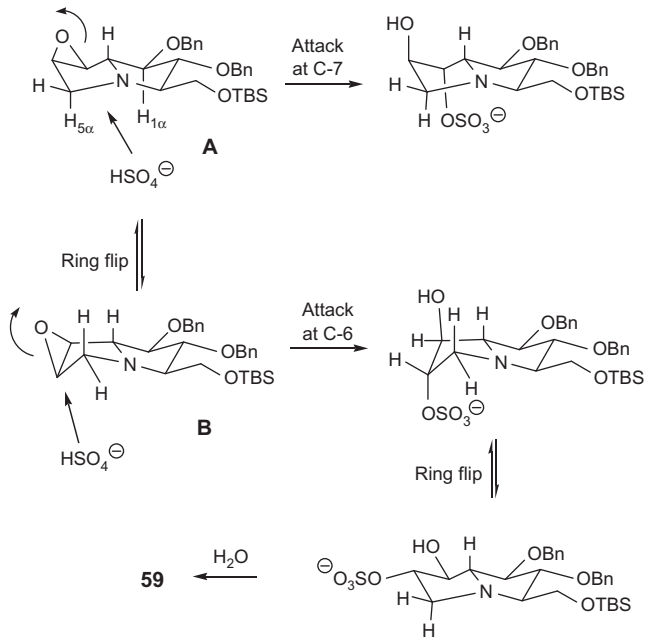

SCHEME 8 Ring-opening reactions of epoxide **58** via conformations A and B [23].

D-arabinose in an overall yield of 19%. The other four syntheses involve 13 or more steps, and unlike that of Goti, include the separation of unwanted regioisomers, diastereomers, or (*E*) and (*Z*) isomers. Further, the Goti synthesis allows for the ready preparation of casuarine-6-*O*-α-D-glucoside **2** (Scheme 9).

Synthesis of Casuarine-*O*-α-Glucoside 2

In 2009, Goti *et al*. [25a] reported the synthesis of casuarine-6-*O*-α-D-glucoside **2** in the same publication in which they reported the synthesis of casuarine **1**. The synthesis of casuarine-6-*O*-α-D-glucoside **2** started with the same precursor **44**, followed by acetylation and the Tamao–Fleming reaction for the oxidation of the C—Si bond to afford the alcohol **60** (Scheme 9).

Then protection of the secondary alcohol of **60** followed by an acetyl group deprotection sequence gave **61** in 75% yield over the two steps. Compound **63** was prepared by a coupling reaction between the alcohol **61** and the trichloroacetimidate **62**. The glucoside alkaloid **2** was obtained by reduction of the lactam carbonyl of **63** and then deprotection of **64** by hydrogenolysis over Pd/C.

Synthesis of 6-*epi*-Casuarine (Uniflorine A) 3

The structural reassignment of uniflorine A to that of 6-*epi*-casuarine **3** was unequivocally confirmed in 2008 by Ritthiwigrom and Pyne on the basis of

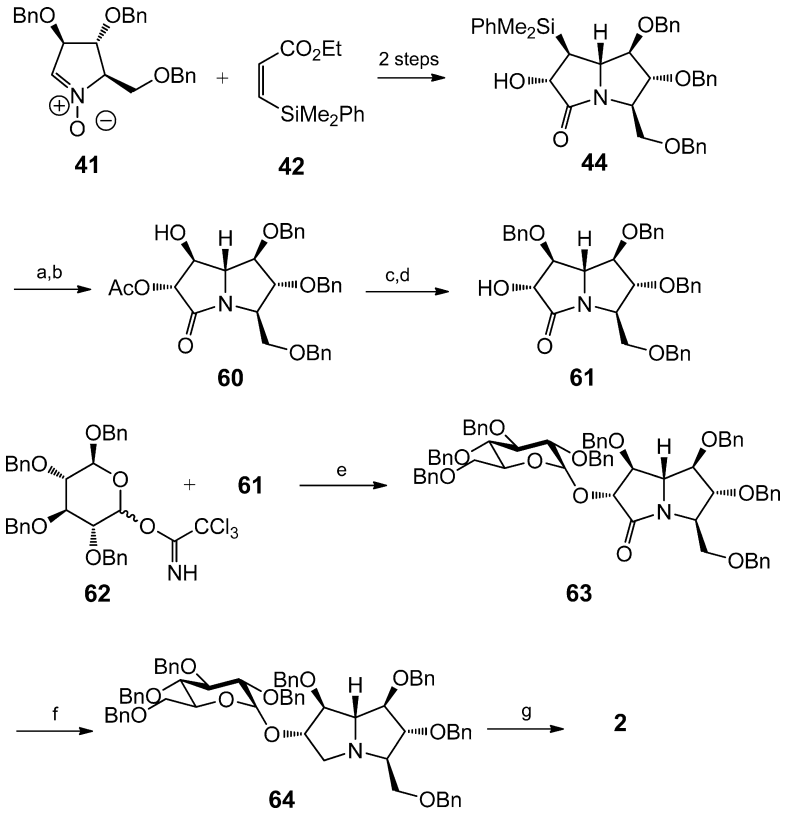

SCHEME 9 Total synthesis of casuarine-6-*O*-α-D-glucoside **2** from the precursor **44** by Goti *et al.* [25]. Reagents and conditions: (a) Ac_2O, pyridine, rt, 15h, 100%; (b) $Hg(CF_3CO_2)_2$, TFA, AcOH, AcOOH, $CHCl_3$, 82%; (c) $BnOC(=NH)CCl_3$, CF_3SO_3H, Et_2O, rt, 3h; (d) Ambersep 900 OH, MeOH, rt, 15h, 75% (two steps); (e) TMSOTf, Et_2O, −20°C, 40min, 72%; (f) $LiBH_4$, BH_3·THF, THF, 23°C, 3days, 68%; and (g) H_2, Pd/C, MeOH, HCl, 77%.

the total synthesis of *ent*-6-*epi*-casuarine **3** [(+)-uniflorine A] from D-xylose in 11 synthetic steps [5]. The NMR spectral data of the synthetic compound matched almost perfectly with that of the natural product. The specific rotation of synthetic (+)-uniflorine A (*ent*-6-*epi*-casuarine **3**) ($[\alpha]_D^{22}=+6.6$ (*c*. 0.35, H_2O)) was essentially equal in magnitude and opposite in sign to that of the natural product (−)-uniflorine A ($[\alpha]_D=-4.4$ (*ca*. 1.2, H_2O)). In 2010, these workers reported the total synthesis of the correct enantiomer of natural uniflorine A in 11 steps and 13% overall yield. This synthesis was the same as the previous one except that the starting material was D-xylose rather than L-xylose [23]. The synthesis of (−)-uniflorine A **3** from the chiral 2,5-dihydropyrrole **51** is shown in Scheme 10. This intermediate was readily prepared on a 4-gram scale from L-xylose in four steps and in 46% overall yield. The 2,5-dihydropyrrole **51** underwent an osmium(VIII)-catalyzed

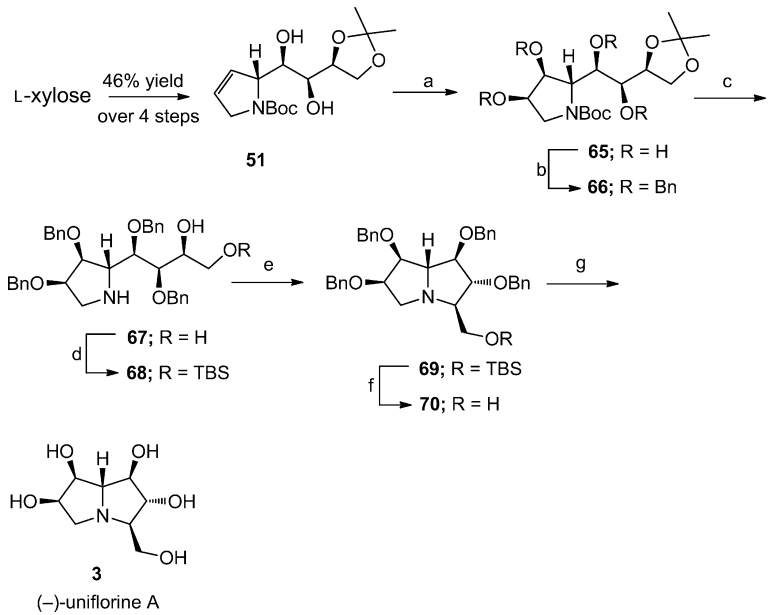

SCHEME 10 Synthetic route for (−)-uniflorine A **3** by Ritthiwigrom and Pyne [23]. Reagents and conditions: (a) $K_2OsO_4{\cdot}H_2O$, NMO, acetone/H_2O, rt, 18h, 72%; (b) NaH, BnBr, *n*-Bu_4NI, THF, 24h, 96%; (c) HCl/MeOH, rt, 18h, 81%; (d) TBSCl, DMAP, imidazole, CH_2Cl_2, rt, 48h, 85%; (e) DIAD, Ph_3P, Et_3NHCl, py, rt, 3days, 76%; (f) HCl/MeOH, rt, 18h, 90%; and (g) $PdCl_2$, H_2 (1atm), MeOH, rt, 24h; ion exchange, 87%.

syn-dihydroxylation reaction to furnish the tetrol **65** as a single diastereomer in 72% yield (Scheme 10). The stereochemical outcome of this DH reaction was expected due to the stereodirecting effect of the C-2 pyrrolidine substituent in **51** [4,19,39,40]. The configuration of this diol was established by ROESY NMR studies on the final product **3**. The tetrol **65** was readily converted to its per-*O*-benzyl protected derivative **66** in 96% yield using standard reaction conditions [19]. Treatment of **66** under acidic conditions (HCl/MeOH) resulted in *N*-Boc and acetonide hydrolysis and gave the amino diol **67** in 81% yield. Regioselective *O*-silylation of **67** with TBSCl/imidazole/DMAP gave the primary silyl ether **68** in 85% yield. In the earlier synthesis of (+)-uniflorine A, compound *ent*-**68** underwent cyclization under Mitsunobu reaction conditions using pyridine [4,41–43] as the solvent to give a mixture (*ca.* 4:1) of the desired pyrrolizidine *ent*-**69** and an indolizidine product (structure not shown) in a combined yield of about 30% after purification of the crude reaction mixture by column chromatography. The undesired indolizidine product arose from first base-catalyzed *O*-TBS migration to the secondary hydroxyl group in *ent*-**68** followed by Mitsunobu cyclization onto the primary carbon of the butyl side chain. It was found that by buffering the reaction mixture with $Et_3N{\cdot}HCl$ [44] the yield of **69** could be dramatically

improved to 76% with little or no formation of the undesired product. Acid hydrolysis of **69** gave the primary alcohol **70** in 90% yield which upon hydrogenolysis using $PdCl_2/H_2$ gave uniflorine A **3** in 87% yield after ion-exchange chromatography in a total of 11 synthetic steps and 13% overall yield from L-xylose.

In 2009, Goti *et al*. [24] reported the total synthesis of (−)-uniflorine A **3** in nine steps and 11% overall yield from **41** or 16 steps from L-xylose or D-arabinose [25b] (Scheme 11). Their syntheses started with the 1,3-dipolar cycloaddition reaction product **43** that they used earlier to prepare casuarine (Scheme 5). The lactam **71** was obtained from cleavage of the N—O bond

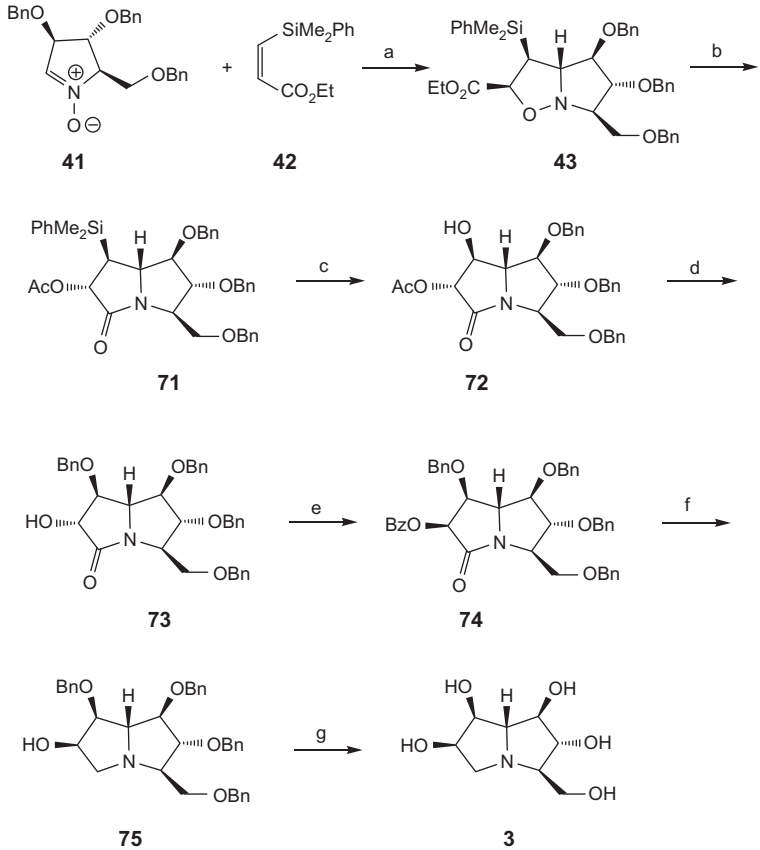

SCHEME 11 Total synthesis of (−)-uniflorine A **3** by Goti *et al*. [24]. Reagents and conditions: (a) CH_2Cl_2, rt, 36h, 79%; (b) i: Zn, AcOH/H_2O, 60–65°C, 5h, 93%; ii: Ac_2O, py, rt, 15h, 100%; (c) $Hg(CF_3CO_2)_2$, TFA, AcOH, AcOOH, $CHCl_3$, 82%; (d) i: $BnOC(=NH)CCl_3$, CF_3SO_3H, Et_2O, rt, 3h; ii: Ambersep 900 OH, MeOH, rt, 15h, 75% (two steps); (e) BzOH, PPh_3, DIAD, THF, rt, 75%; (f) $LiAlH_4$, THF, reflux, 45%; and (g) H_2, 10% Pd/C, MeOH, HCl, rt, then Dowex 50WX8, 6% NH_4OH, 71%.

in **43** with Zn/HOAc followed by attack of the resulting amine onto the ester carbonyl group to form a hydroxy lactam. This intermediate was then acetylated to give the lactam **71** in 93% yield. The Tamao–Fleming reaction ($Hg(CF_3CO_2)_2$, TFA, AcOH, AcOOH) was used to convert the silyl group in **71** to the hydroxyl group in lactam **72** with retention of configuration. Benzylation of this hydroxyl group with $BnOC(=NH)CCl_3$, and CF_3SO_3H in Et_2O, also resulted in deprotection of the acetyl group at C-6 and provided compound **73** in 75% yield. The pyrrolizidine **75** was obtained by inversion of the stereochemistry at the C-6 position of compound **73** by a Mitsunobu reaction with BzOH, PPh_3, DIAD in THF that gave **74** in 75% yield. This was then followed by reduction of the lactam carbonyl group and deprotection of the benzoylated group with $LiAlH_4$. Debenzylation of the pyrrolizidine **75** using standard hydrogenolysis conditions gave (−)-uniflorine A **3** in 71% yield after purification by ion-exchange chromatography with Dowex 50WX8 resin. The ^1H NMR and ^{13}C NMR spectroscopic data was identical with those from our previous synthesis [5]. This synthetic material **3** had an mp 117–180°C and an $[\alpha]_D^{21} = -6.9$ (*c*. 0.42, H_2O).

Synthesis of 3-*epi*-Casuarine 4

In 2006, Izquierdo *et al*. [45] published the synthesis of 3-*epi*-casuarine **4** in the same year that Fleet *et al*. [6] reported its isolation as a natural product and also its synthesis. The synthesis of 3-*epi*-casuarine **4** by Izquierdo *et al*. [45] involved the same methodology that they used for the synthesis of casuarine **1** (Scheme 3) except using the pyrrolidine **76** as the starting material. *N*-Cbz protection of **76** gave the Cbz carbamate **77** in only 25% yield (Scheme 12). The primary alcohol of **77** was oxidized using TPAP and NMO to afford the aldehyde **78** which after a Wittig reaction gave the (*E*)-pyrrolidinic propenoate **79** (93% yield). A *cis*-DH reaction of **79** using osmium tetraoxide and NMO in the presence of DHQ-CLB as a chiral ligand gave the diols **80** (13% yield) and **81** (84% yield). The configuration of these diol products could not be determined at this stage. After two more synthetic steps, an NOE experiment confirmed that **82** was the desired intermediate to prepare 3-*epi*-casuarine **4**. *N*-Deprotection of **81** using catalytic hydrogenolysis provided pyrrolidine **82** which was subsequently transformed to **83** by refluxing in methanol in the presence of a catalytic amount of NaOMe. Acetylation under standard reaction conditions then produced the acetate derivative **84** in an 88% yield. Reduction of the lactam carbonyl group of **84** using $BH_3{\cdot}SMe_2$ complex in THF gave **85** in 96% yield. *O*-TBDPS deprotection and then debenzylation provided **86** in 73% yield. Hydrogenolysis then gave the final compound; however, it was not pure. The product was further purified by per-acetylation that gave **87** in 88% yield. Base-catalyzed deacetylation of **87** afforded 3-*epi*-casuarine **4** in 66% yield. This synthesis was achieved in 12 steps from the pyrrolidine derivative **76** in an overall yield of 2.2%.

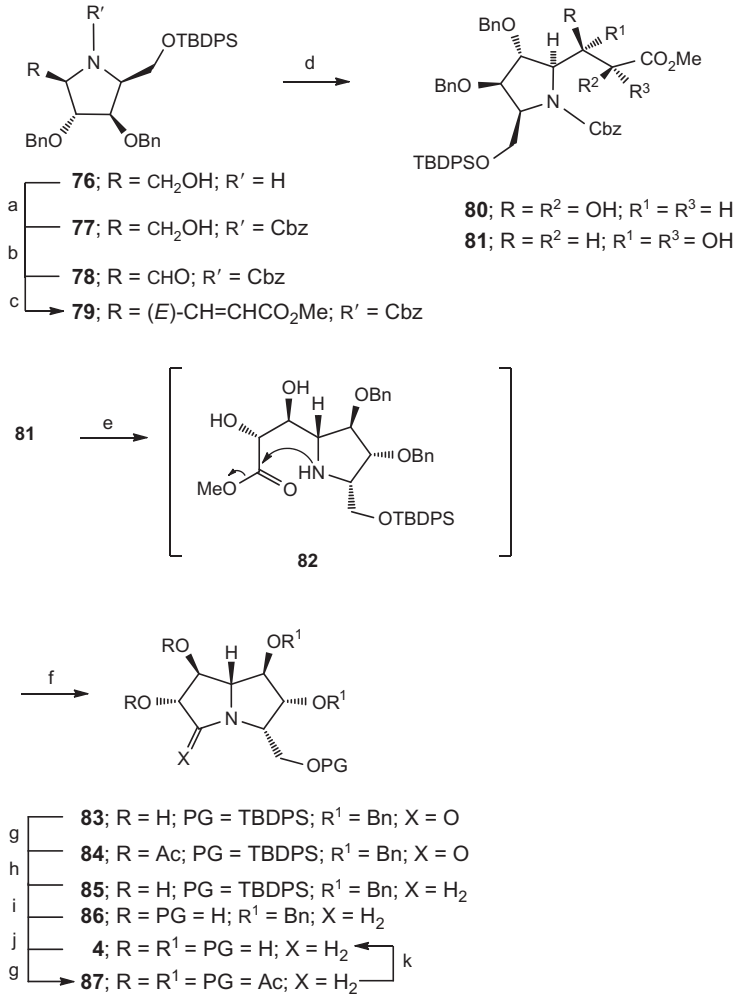

SCHEME 12 Total synthesis of 3-*epi*-casuarine **4** by Izquierdo *et al*. [45]. Reagents and conditions: (a) CbzCl, Me_2CO, K_2CO_3, rt, 25%; (b) TPAP, NMO, 4 Å MS, CH_2Cl_2, 64%; (c) $Ph_3P{=}CHCO_2Me$, CH_2Cl_2, rt, 93%; (d) OsO_4, NMO, DHQ-CLB, acetone/H_2O, rt, 2days (**80**:**81**=13%:84%); (e) H_2, 10% Pd/C, MeOH; (f) cat. NaOMe, MeOH, rt, 63%; (g) Ac_2O, py, DMAP, 88%; (h) $BH_3{\cdot}SMe_2$, THF, then MeOH, Δ, 96%; (i) *n*-$Bu_4N^+F^-{\cdot}3H_2O$, THF, rt, 73%; (j) i: H_2, 10% Pd/C, MeOH, then Amberlite IRA-400 (OH^- form); ii: Ac_2O, py, DMAP, 70%; and (k) cat. NaOMe, MeOH, rt, 66%.

In 2006, Fleet *et al*. [6] reported the synthesis of casuarine **1** (Scheme 4) together with the synthesis of 3-*epi*-casuarine **4** from D-gluconolactone **27** in the same publication (Scheme 13) [6]. He followed the same methodology that he used to synthesize casuarine **1** up to the precursor **34**. Regioselective protection of the primary hydroxyl group of diol **34** with TBSCl and then reaction at the secondary hydroxyl group by treatment with methanesulfonyl

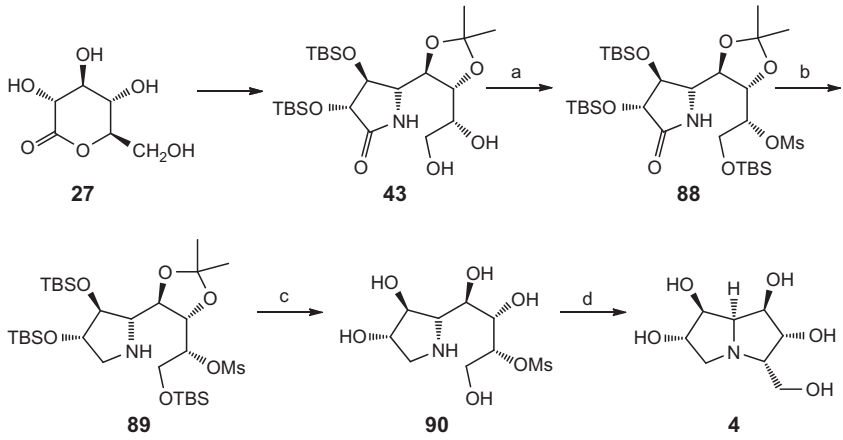

SCHEME 13 Total synthesis of 3-*epi*-casuarine **4** by Fleet *et al.* [6]. Reagents and conditions: (a) *t*-$BuMe_2SiCl$, py; then CH_3SO_2Cl, Et_3N, CH_2Cl_2, 66%; (b) BH_3·THF, THF, 57%; (c) 90% CF_3CO_2H, H_2O; and (d) NaOAc, H_2O (89% over two steps).

chloride generated the mesylate **88** in 66% yield. Reduction of the lactam carbonyl group of **88** with BH_3·THF gave the protected amine **89** (57% yield). Finally, pure 3-*epi*-casuarine **4** was obtained after two more steps: (i) *O*-silyl group hydrolysis with TFA to produce **90** and then (ii) cyclization by treatment with sodium acetate (89% yield over the two steps).

Ritthiwigrom and Pyne's synthesis of 3-*epi*-casuarine **4** [31] started with the precursor **56** which was prepared in nine steps from L-xylose (Scheme 14). Their syntheses required an inversion of the configuration of the butyl side-chain secondary hydroxyl group in **56**. This was achieved by the Mitsunobu reaction of **56** using 4-nitrobenzoic acid [46]. Base treatment (K_2CO_3/MeOH, rt, 1 day) of the resulting secondary 4-nitrobenzoate ester resulted in benzoate hydrolysis. Cyclization under Mitsunobu reaction conditions, using toluene rather than pyridine as the solvent, gave a separable mixture the desired pyrrolizidine **92** in 70% yield and the indolizidine product **93** in 4% yield. The epoxy-pyrrolizidine **92** was treated with $NaHSO_4/CH_2Cl_2$ under the conditions that were described in Scheme 7 except that heating at 50°C was continued for 7 days (Scheme 14). The slower rate of epoxide ring-opening of **92**, when compared to that of 3-*epi*-**92**, was attributed to the increased steric hindrance of the α-face of the epoxide moiety due to the 3-α-CH_2OTBS substituent. Because of the slow reaction rate, hydrolytic cleavage of the OTBS group also occurred resulting in a mixture of products that was difficult to separate. Acetylation of the mixture and then separation by column chromatography gave the desired acetylated product **94** (7% yield), the epoxide **96** in 9% yield, and the undesired tricyclic bridged ether products **95** (8%) and **97** (17%) (Scheme 14). The isolation of epoxide **96** indicated that OTBS cleavage was faster than either the intermolecular or intramolecular (leading to tricyclic bridged ether products) epoxide ring-opening reactions. Unfortunately, several attempts to improve

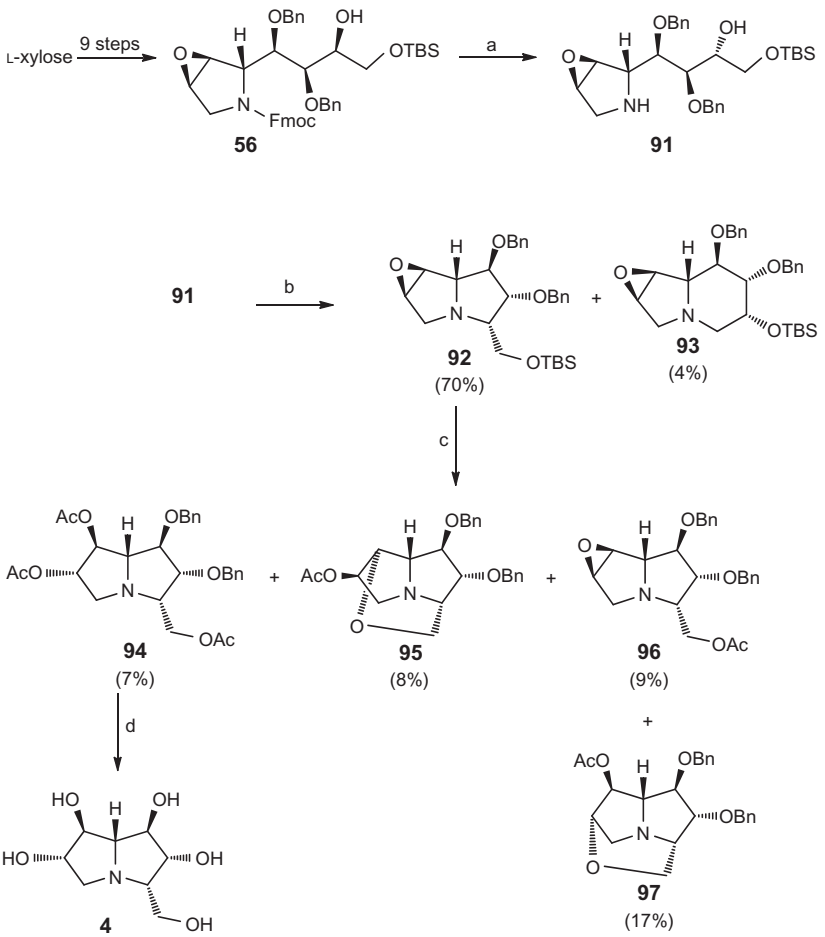

SCHEME 14 Total synthesis of 3-*epi*-casuarine **4** [31]. Reagents and conditions: (a) i: *p*-NO_2Ar-CO_2H, PPh_3, toluene, 80°C, 5h; ii: K_2CO_3, MeOH, rt, 24h, 50%; (b) DIAD, Ph_3P, toluene, 80°C, 3days; (c) i: $NaHSO_4$, CH_2Cl_2, 50°C, 7days; ii: Ac_2O, py, DMAP, 24h; and (d) $PdCl_2$, H_2 (1atm), MeOH, 4days; ion exchange, 77%.

the yield of the desired product **94** were not successful. While the use of a more stable protecting group for the primary alcohol group in **92** may have been more efficient, this variation was not examined. Hydrogenolysis of **94** over $PdCl_2/H_2$ in MeOH for 4days gave diastereomerically pure 3-*epi*-casuarine **4** in 77% yield after purification by ion-exchange chromatography.

CONCLUSIONS

In summary, we have described the isolation, structure elucidation, glycosidase inhibitory activities, and the synthesis of the four naturally occurring

casuarines, namely, casuarine **1**, casuarine-6-*O*-α-D-glucoside **2**, 6-*epi*-casuarine **3** (uniflorine A), and 3-*epi*-casuarine **4**. Casuarine **1** is a potent inhibitor of α-D-glucosidases, whereas casuarine-*O*-α-glucoside **2** was found to be a more active inhibitor of β-D-glucosidase. Both compounds **1** and **2** were potent inhibitors of amyloglucosidase from *A. niger*. Casuarine **1** was found to be a potent inhibitor of the human NtMGAM which could potentially aid in the treatment of type-II diabetes. Casuarine-*O*-α-glucoside **2** was found to be a potent (nM) trehalase inhibitor with potential use as an insecticide. X-ray structural analysis and computer-aided docking studies of these natural products bound to these target enzymes have been carried out. These studies may assist in the design of more potent inhibitors in future studies. The originally assigned structures of uniflorine A and B were found to be incorrect. Based on careful NMR analysis and the total synthesis of uniflorine A, their structures were concluded to be 6-*epi*-casuarine **3** and casuarine **1**, respectively. 6-*Epi*-casuarine **3** was found to be an inhibitor of α-glucosidases and amyloglucosidase from *A. niger*. In contrast to casuarine **1**, 3-*epi*-casuarine **4** showed weak activity against three α-D-glucosidases (from yeast, rice, and *Bacillus*) and was more active against β-D-glucosidase from almond. Future phytochemical studies may unveil other new casuarine epimers or glycoside derivatives as natural products.

ACKNOWLEDGMENTS

We thank the Australian Research Council, the University of Wollongong, and Chiang Mai University for supporting our work in this area.

ABBREVIATIONS

[α]	specific rotation
Ac	acetyl
Bn	benzyl
Boc	*tert*-butoxycarbonyl
Bz	benzoyl
Cbz	benzyloxycarbonyl
DH	dihydroxylation
DHQ-CLB	*O*-(4-chlorobenzoyl)hydroquinine
DIBAL	di-*iso*-butylaluminium hydride
DMAP	4-(*N*,*N*-dimethylamino)pyridine
DMDP	2,5-dihydroxymethyl-3,4-dihydroxypyrrolidine
DMF	dimethylformamide
Fmoc	9-fluorenylmethoxycarbonyl
IC_{50}	50% inhibitory concentration
K_i	the dissociation constant for binding of inhibitor to enzyme
μM	micromolar

nM	nanomolar
NMO	*N*-methylmorpholine *N*-oxide
NOE	nuclear Overhauser effect
NtMGAM	N-terminal subunit of maltase-glucoamylase
ROESY	rotating frame Overhauser effect spectroscopy
TBAF	tetrabutylammonium fluoride
TBDPS	*tert*-butyldiphenylsilyl
TBS	*tert*-butyldimethylsilyl
TDS	1,1,2-trimethylpropylsilyl
THF	tetrahydrofuran
TMS	trimethylsilyl
TPAP	tetrapropylammonium perruthenate
Tre37A	*Escherichia coli* trehalose

REFERENCES

[1] R.J. Nash, P.I. Thomas, R.D. Waigh, G.W.J. Fleet, M.R. Wormald, P.M. de Q. Lilley, D. J. Watkin, Tetrahedron Lett. 35 (1994) 7849–7852.

[2] M.R. Wormald, R.J. Nash, A.A. Watson, B.K. Bhadoria, R. Langford, M. Sims, G.W. J. Fleet, Carbohydr. Lett. 2 (1996) 169–174.

[3] T. Matsumura, M. Kasai, T. Hayashi, M. Arisawa, Y. Momose, I. Arai, S. Amagaya, Y. Komatsu, Pharm. Biol. 38 (2000) 302–307.

[4] A.S. Davis, T. Ritthiwigrom, S.G. Pyne, Tetrahedron 64 (2008) 4868–4879.

[5] For a preliminary communication on the synthesis of (+)-uniflorine A, see:T. Ritthiwigrom, S.G. Pyne, Org. Lett. 10 (2008) 2769–2771.

[6] J. Van Ameijde, G. Horne, M.R. Wormald, R.A. Dwek, R.J. Nash, P.W. Jones, E.L. Evinson, G.W.J. Fleet, Tetrahedron: Asymmetry 17 (2006) 2702–2712.

[7] N. Asano, E. Fattorusso, O. Taglialatela-Scafati (Eds.), Modern Alkaloids: Structure, Isolation, Synthesis and Biology, Wiley-VCH Verlag, Weinheim, 2008, pp. 111–138.

[8] R.J. Molyneux, M. Benson, R.Y. Wong, J.E. Tropea, A.D. Elbein, J. Nat. Prod. 51 (1988) 1198–1206.

[9] R.J. Nash, L.E. Fellows, J.V. Dring, G.W.J. Fleet, A.E. Derome, T.A. Hamor, A.M. Scofield, D.J. Watkin, Tetrahedron Lett. 29 (1988) 2487–2490.

[10] R.J. Nash, L.E. Fellows, A.C. Plant, G.W.J. Fleet, A.E. Derome, P.D. Baird, M.P. Hegarty, A.M. Scofield, Tetrahedron 44 (1988) 5959–5964.

[11] A. Kato, E. Kano, I. Adachi, R.J. Molyneux, A.A. Watson, R.J. Nash, G.W.J. Fleet, M. R. Wormald, H. Kizu, K. Ikeda, N. Asano, Tetrahedron: Asymmetry 14 (2003) 325–331.

[12] (a) A. Kato, I. Adachi, M. Miyauchi, K. Ikeda, T. Komae, H. Kizu, Y. Kameda, A. A. Watson, R.J. Nash, M.R. Wormald, G.W.J. Fleet, N. Asano, Carbohydr. Res. 316 (1999) 95–103; (b) N. Asano, H. Kuroi, K. Ikeda, H. Kizu, Y. Kameda, A. Kato, I. Adachi, A.A. Watson, R.J. Nash, G.W.J. Fleet, Tetrahedron: Asymmetry 11 (2000) 1–8; (c) T. Yamashita, K. Yasuda, H. Kizu, Y. Kameda, A.A. Watson, R.J. Nash, G.W.J. Fleet, N. Asano, J. Nat. Prod. 65 (2002) 1875–1881; (d) A. Kato, N. Kato, I. Adachi, J. Hollinshead, G.W.J. Fleet, C. Kuriyama, K. Ikeda, N. Asano, R.J. Nash, J. Nat. Prod. 70 (2007) 993–997; (e) N. Asano, K. Ikeda, M. Kasahara, Y. Arai, H. Kizu, J. Nat. Prod. 67 (2004) 846–850.

[13] (a) S.G. Pyne, M. Tang, Curr. Org. Syn. 9 (2005) 1395–1418; (b) T. Ritthiwigrom, C.W. G. Au, S.G. Pyne, Curr. Org. Syn. (2012) in press.
[14] Information taken from the Australian National Botanic Gardens, Australian National Herbarium, [http://www.anbg.gov.au/].
[15] M.T. Pepato, D.M. Mori, A.M. Baviera, J.B. Harami, R.C. Vendramini, I.L. Brunetti, J. Ethnopharm. 96 (2005) 43–48.
[16] V.G. Rucker, G.A.A.B. Silva, L. Bause, M. Schikarski, Planta Med. 31 (1977) 322–327.
[17] E. Ferro, A. Schinini, M. Maldonado, J. Rosner, H.G. Schmeda, J. Ethnopharm. 24 (1988) 321–325.
[18] I. Arai, S. Amagaya, Y. Komatsu, M. Okada, T. Hayashi, M. Kasai, M. Arisawa, Y. Momose, J. Ethnopharm. 68 (1999) 307–314.
[19] A.S. Davis, S.G. Pyne, B.W. Skelton, A.H. White, J. Org. Chem. 69 (2004) 3139–3143.
[20] N.S. Karanjule, S.D. Markad, D.D. Dhavale, J. Org. Chem. 71 (2006) 6273–6276.
[21] Z. Zhao, L. Song, P.S. Mariano, Tetrahedron 61 (2005) 8888–8894.
[22] A.W. Bell, L. Pickering, A.A. Watson, R.J. Nash, R.C. Griffiths, M.G. Jones, G.W.J. Fleet, Tetrahedron Lett. 37 (1996) 8561–8564.
[23] T. Ritthiwigrom, A.C. Willis, S.G. Pyne, J. Org. Chem. 75 (2010) 815–824.
[24] C. Parmeggiani, D. Martella, F. Cardona, A.J. Goti, J. Nat. Prod. 72 (2009) 2058–2060.
[25] (a) F. Cardona, C. Parmeggiani, E. Faggi, C. Bonaccini, P. Gratteri, L. Sim, T.M. Gloster, S. Roberts, G.J. Davies, D.R. Rose, A. Goti, Chem. Eur. J. 15 (2009) 1627–1636; (b) F. Cardona, E. Faggi, F. Liguori, M. Cacciarini, A. Goti, Tetrahedron Lett. 44 (2003) 2315–2318.
[26] N. Asano, Glycobiology 13 (2003) 93R–104R.
[27] M.C.P. Silva, A.F. Ribeiro, W.R. Terra, C. Ferreira, Insect Mol. Biol. 18 (2009) 769–784.
[28] S. Nakamura, K. Takahira, G. Tanabe, T. Morikawa, M. Sakano, K. Ninomiya, M. Yoshikawa, O. Muraoka, I. Nakanishi, Bioorg. Med. Chem. Lett. 20 (2010) 4420–4423.
[29] F. Cardona, A. Goti, C. Parmeggiani, P. Parenti, M. Forcella, P. Fusi, L. Cipolla, S. M. Roberts, G.J. Davies, T.M. Gloster, Chem. Commun. 46 (2010) 2629–2631.
[30] M. Forcella, F. Cardone, A. Goti, C. Parmaggiani, L. Cipolla, M. Gregori, R. Schirone, P. Fusi, P. Parenti, Glycobiology 20 (2010) 1186–1195.
[31] T. Ritthiwigrom, R.J. Nash, S.G. Pyne, Tetrahedron 66 (2010) 9340–9347.
[32] T. Ritthiwigrom, R.J. Nash, S.G. Pyne, Unpublished results.
[33] (a) S.E. Denmark, A.R. Hurd, Org. Lett. 1 (1999) 1311–1314; (b) S.E. Denmark, A.R. Hurd, J. Org. Chem. 65 (2000) 2875–2886; (c) S.E. Denmark, M.E. Schnute, J. Org. Chem. 59 (1994) 4578–4595.
[34] (a) I. Izquierdo, M.T. Plaza, J.A. Tamayo, Tetrahedron 61 (2005) 6527–6533; (b) I. Izquierdo, M.T. Plaza, F. Franco, Tetrahedron: Asymmetry 13 (2002) 1503–1508.
[35] N.A. Petasis, I.A. Zavialov, J. Am. Chem. Soc. 120 (1998) 11798–11799.
[36] D. Yang, M.-K. Wong, Y.-C. Yip, J. Org. Chem. 60 (1995) 3887–3889.
[37] H. Cavdar, N. Saracoglu, Tetrahedron 65 (2009) 985–989.
[38] J.-B. Ahn, C.-S. Yun, H. Kim, D.-C. Ha, J. Org. Chem. 65 (2000) 9249–9251.
[39] N. Papaioannou, J.T. Blank, S.J. Miller, J. Org. Chem. 68 (2003) 2728–2734.
[40] K.B. Lindsay, M. Tang, S.G. Pyne, Synlett (2002) 731–734.
[41] K.B. Lindsay, S.G. Pyne, J. Org. Chem. 67 (2002) 7774–7780.
[42] M. Tang, S.G. Pyne, J. Org. Chem. 68 (2003) 7818–7824.

[43] (a) J. Mulzer, H. Dehmlow, J. Org. Chem. 57 (1992) 3194–3202; (b) G. Casiraghi, F. Ulgheri, P. Spanu, G. Rassu, L. Pinna, F.G. Gasparri, F.M.G. Pelosi, J. Chem. Soc., Perkin Trans. I (1993) 2991–2997; (c) M. Naruse, S. Aoyagi, C. Kibayashi, J. Org. Chem. 59 (1994) 1358–1364.
[44] J.C. Anderson, H.A. Chapman, Org. Biomol. Chem. 5 (2007) 2413–2422.
[45] I. Izquierdo, M.T. Plaza, J.A. Tamayo, J. Carbohydr. Chem. 25 (2006) 281–295.
[46] S.F. Martin, J.A. Dodge, Tetrahedron Lett. 32 (1991) 3017–3020.

Chapter 2

The Acylpolyamines from Spider Venoms

Mario Sergio Palma
Laboratory of Structural Biology and Zoochemistry, CEIS/Dept. Biology, Institute of Biosciences, São Paulo State University (UNESP), Rio Claro, São Paulo, Brazil

INTRODUCTION

The use of natural products such as the selective and potent neurotoxins from invertebrate venoms as probes in neurosciences has permitted a dramatic increase in the understanding of the structure and mechanism of action of neurotransmitter receptors [1]. Until the 1980s, it was widely accepted that most neurotoxins from spider and wasp venoms were basically proteins and peptides; however, the discovery of acylpolyamines in the venoms of orb-weaving spiders and parasitic wasps completely changed this viewpoint. The strongest evidence for change was demonstrated when these compounds showed very potent antagonistic action on certain neurotransmitter receptors, in particular, the glutamate receptors (Glu-Rs) [2–4].

Amino acids such as glutamate are potent convulsants in vertebrates, and the Glu-R antagonists are known for their anticonvulsant properties in different experimental models of epilepsy. Because orb-weaving spiders and parasitic wasps are polyphagous animals, which prey on a number of arthropods using acylpolyamines as paralyzing neurotoxins, these discoveries aroused the initial interest of agrichemical industries. Both the venomous solitary hunters and their prey are richly endowed with a series of different subtypes of Glu-Rs. In these animals, these Glu-R subtypes function like the nicotinic acetylcholine receptor (nACh-R) at the neuromuscular junction in vertebrates. The nACh-R is also found in the arthropod central nervous system (CNS). However, the widespread distribution of Glu-Rs in the vertebrate brain and spinal cord later attracted the interest of pharmaceutical companies due to the low molecular mass toxins naturally occurring in the venom of the solitary wasps and orb-weaving spiders [1].

The venoms of orb-weaving spiders are primarily composed of complex mixtures of closely related acylpolyamines. These chemicals share the presence of an aromatic moiety and sometimes one or more amino acid residues

Bioactive Natural Products, Vol. 36. DOI: 10.1016/B978-0-444-53836-9.00019-0

in addition to a polyamine backbone. Meanwhile, the venoms of parasitic solitary wasps generally contain only a few acylpolyamines, typically consisting of spermine and spermidine, and/or analogs of the phyllanthus toxin (PhTX). The elucidation of chemical structures, the study of mechanisms of action, and the investigation of the structure–activity relationships of the PhTX analogs have been the subject of extensive reviews [5,6] and will not be considered in the present review.

SPIDER DIVERSITY AND THE COMPOSITION OF THEIR VENOMS

Spiders are distributed worldwide except for Antarctica. The taxonomy of this group of animals is complex and confusing, with over 20 different classifications proposed to date. Currently, approximately 40,000 spider species are known, which are grouped into 3618 genera and 110 families [7]. Despite this, the structural elucidation of the acylpolyamine toxins contained in the venom of only a limited number of species has been studied. This research gap may be due to a number of reasons, such as the tiny amounts of venom produced by the spiders and the difficulty in obtaining their venom.

Furthermore, spider venoms consist of complex mixtures of peptides, proteins, and low molecular mass organic molecules. Many of these chemicals act on neurons and, in particular, on the ion channels or receptors within the neurons [8]. Among the low molecular mass compounds, the spider venoms contain citric acid, lactic acid, γ-butyric acid, a series of free amino acids, glucose, and biogenic amines such as histamine, diaminopropane, putrescine, cadaverine, spermine, spermidine, dopamine, and epinephrine [9–14]. Spider venoms may also contain at least four types of well characterized, low molecular mass (<1 kDa) toxins: bis-(agmatine)-oxamide isolated from the venom of *Plectreurys tristis*; a gluconucleoside disulfate isolated from the venom of *Hololena curta*; a series of tetrahydro-β-carbolines isolated from the venom of the social spider *Parawixia bistriata*; and the best characterized toxin type in this class, the acylpolyamines isolated from the venoms of several different species of orb-weaving spiders [12,15–18]. These compounds are used by the spider to cause paralysis and/or death in their prey [19].

THE ACYLPOLYAMINE TOXINS: STRUCTURAL ELUCIDATION AND CHEMICAL DIVERSITY

The acylpolyamines are neurotoxic compounds occurring only in the venom glands of spiders at a picomolar level. More than 100 chemical structures of acylpolyamines have been elucidated, which constitute a family of closely related toxins. The most well-characterized chemical structures of acylpolyamine toxins among the Araneidae spiders are those from the orb-web spiders belonging to the Nephilinae subfamily [12,20–26] and from the *Argiope* genus [27].

Until the 1990s, the standard procedure for elucidating the structure of these toxins required an extensive purification from huge amounts of venom. This purification was followed by traditional chemical protocols involving hydrolysis and derivatization, amino acid analysis by Edman degradation chemistry and ^{1}H- and ^{13}C-nuclear magnetic resonance (NMR). Between 1985 and 1990, about 17 different structures were elucidated with this experimental approach from the venom of the spider *Nephila clavata* [21].

The fractionation of the venoms from the orb-weaving spiders using reversed-phase high-performance liquid chromatography (RP-HPLC) with an acetonitrile gradient results in chromatographic profiles in which the toxins are eluted in groups of peaks. These peaks correspond to the type of aromatic moiety that constitutes the chromophore group. For example, the toxins bearing a hydroxyphenyl acetic acid are eluted first, followed by the toxins bearing a hydroxyindole moiety, and then those with an indole group as the chromophore [19]. This observation permitted the establishment of a simple and efficient analytical strategy: the pooling of those fractions presenting a common chromophore. These fractions are later subjected to acidic hydrolysis and repeated chromatography for the collection of the purified chromophore moiety, which is then characterized by NMR analysis [21]. The previous identification of the specific chromophores for each group of toxins made the use of mass spectrometry an important analytical tool for the rapid structural assignment of a large number of different polyamine backbones occurring in each sample. A highly sensitive methodology for the direct detection of these toxins in crude venom was developed using online microcolumn HPLC continuous flow (FRIT) FAB LC/MS and high-energy collision-induced dissociation (CID) methods. CID utilized the attached sodium molecular ions of these toxins to yield information about the structures of this class of compounds in *Nephila clavipes* and *Nephilengys borbonica* [23,26]. The venom of the Brazilian garden spider *Nephilengys cruentata* was investigated using a combination of HPLC/MS, MALDI-TOF, and MALDI-sector mass spectrometry, leading to the structural assignment of some tens of these toxins [24,25]. Even low-resolution mass spectrometry, such as ESI-MS and MS/MS, in a triple quadrupole instrument has been used to elucidate the structures of acylated polyamines from the venom of the spider *Agelenopsis aperta* [28]. A similar approach with LC–MS and MS/MS was used to elucidate many structures in the venom of *A. aperta* [29,30].

Recently, the use of different spectroscopic protocols such as bidimensional NMR, HRMS, and MS/MS has been combined for the structural elucidation of these toxins in complex matrices like the spider venoms. The direct NMR analysis of crude spider venoms (without previous purification) using ^{1}H, dqfCOSY, heteronuclear multiple quantum correlation (HMQC), heteronuclear multiple bond correlation (HMBC), and nuclear Overhauser enhancement spectroscopy (NOESY), complemented by ESI-MS analysis under CID conditions, has permitted the structural characterization of the major

components of many spider venoms including some acylpolyamine toxins from the spider *Coelotes pastoralis* [31].

The analytical efforts made in the past years have resulted in the current knowledge of more than 100 structures of these toxins among the Nephilinae spiders. This vast array has permitted the organization of the acylpolyamine chemical structures from the spider venoms into four parts as follows [19]: part I—a lipophilic, aromatic acyl moiety; part II—a linker amino acid residue; part III—the polyamine backbone chain; and part IV—the backbone tail. These parts are illustrated in Fig. 1. The aromatic acyl group and the polyamine backbone constitute the essential parts of these compounds that are shared by all known toxins of this class. Meanwhile, the linker amino acid(s) and the tail constitute the nonessential parts that are present only in some toxins. The orb-web spiders biosynthesize acylpolyamine toxins containing both the mandatory and optional structural parts, while the toxins from funnel-web, trap door, and tarantula spiders generally present only the mandatory structural parts [19].

Each one of these structural parts is built from simple chemical building blocks. The way that these chemical blocks are connected to each other represents a natural combinatorial chemistry strategy employed by the Nephilinae spiders. This strategy is the result of millions of years of evolution to maximize the efficiency of insect preying. It also reflects the plasticity of this group of spiders to diversify their venom arsenals according to the different prey available in each season and under different ecological niches [19].

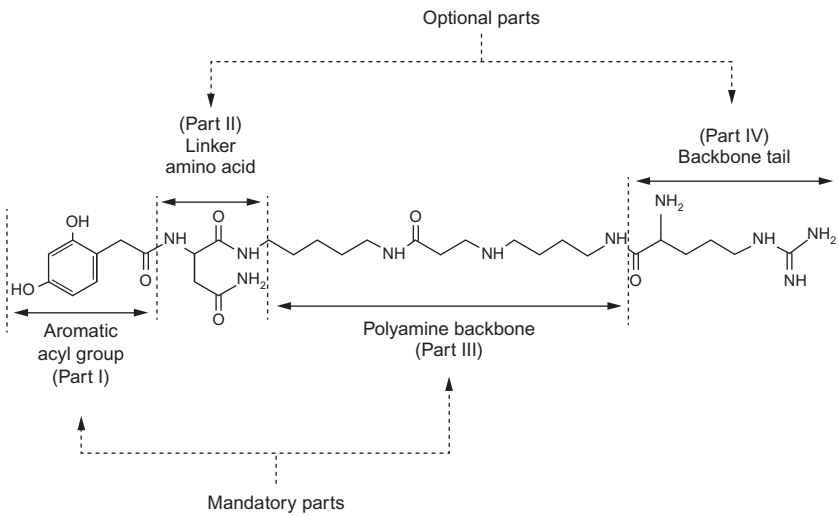

FIGURE 1 Structural parts of the acylpolyamine toxins from spider venoms.

The most studied and well-known toxins are those from the venoms of Nephilinae spiders. Taking into consideration that the structures of these toxins may present the four structural parts mentioned above, their careful examination reveals the following four chemical blocks, as shown in Fig. 2. In part I, the aromatic, lipophilic heads may be a 2,4-dihydroxy phenyl acetyl moiety (**1**), a 4-hydroxyindole acetyl moiety (**2**), or even an indole acetyl moiety (**3**). In part II, the linker amino acid may be an asparagine residue (**4**) or a dipeptide asparaginyl-ornithine (**5**) in the Nephilinae and Argiopidae spiders, while this building block is replaced by a simple amide group in the spiders of the *Agelenopsis* genus. In part III, the polyamine backbones consist of polyamines and amino acid residues. In part IV, the backbone tail is composed of different combinations of amino acid residues such as glycine, alanine, ornithine, and arginine, either between themselves or with putrescine.

Comparing the structures of all known polyamine backbones (a combination of structural parts III and IV), it is possible to identify 70 different polyamine chains. Each one of these backbones is commonly shared among three toxins where the only structural difference is the replacement of the aromatic moiety (part I). Thus, the strategy used by nature to optimize the chemical variability of these toxins was to employ a common polyamine backbone (parts II, III, and IV) in combination with three different aromatic moieties.

Careful examination of part III of the polyamine backbone reveals different subtypes that are produced by the conjugation of five building blocks: three types of polyamines—cadaverine, putrescine, and diaminopropane; and two types of amino acid residues—glycine and alanine. The combination of putrescine and alanine produces a putreanine unit, which frequently appears in tandem as a building block of polyamine backbone chains. Taking into account these structural features, part III polyamine backbones were classified into seven subtypes, from A to G [21,25,27], as follows and illustrated in Fig. 2:

Subtype A has a cadaveryl-putreanyl-diaminopropyl moiety (**6**);
Subtype B has a putrescyl-diaminopropyl-diaminopropyl moiety (**7**);
Subtype C has a cadaveryl-glycyl-putrescyl moiety (**8**);
Subtype D has a cadaveryl-putreanyl moiety (**9**);
Subtype E has a cadaveryl-alanyl-diaminopropyl moiety (**10**);
Subtype F has a cadaveryl-diaminopropyl-diaminopropyl moiety (**11**); and
Subtype G may be considered a pseudo subtype because it contains only a cadaveryl moiety (**12**).

This classification system identifies the toxins by their structural differences as well as their isomeric forms. Thus, it was suggested to include both the molecular mass and the backbone chain subtype in the nomenclature of novel acylpolyamine toxins while maintaining the original nomenclature for the previously known toxins [32]. The occurrence of variable polyamine chain backbones organized into the different subtypes enlarges the structural variability

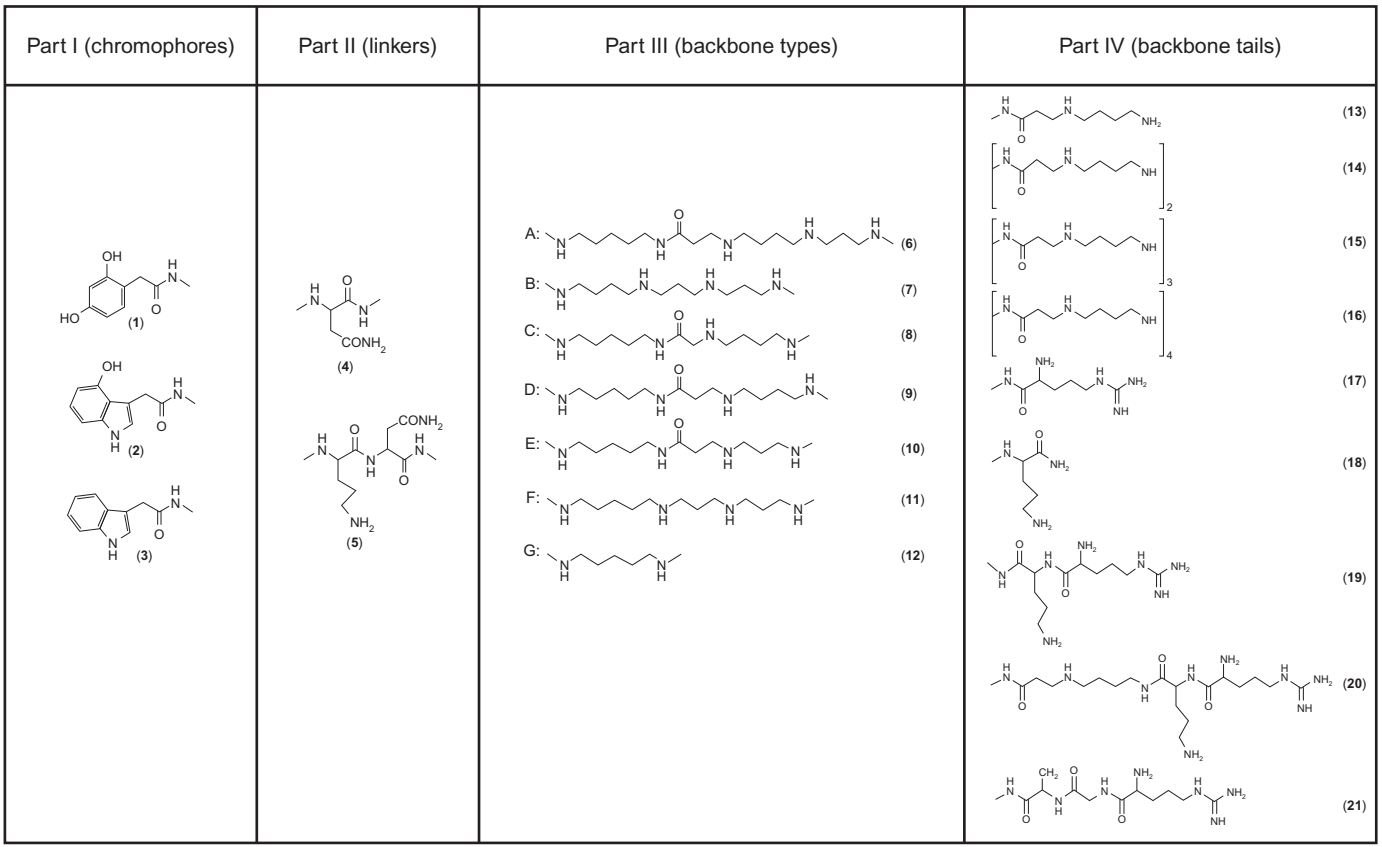

FIGURE 2 Building units of the acylpolyamine toxins from the venoms of Nephilinae orb-weaving spiders.

of toxins, which possibly increases the killing/paralytic arsenal of the Nephilinae spiders.

Observation of part IV of the acylpolyamine backbone chain revealed that nature created nine options for tails among the acylpolyamine toxins from Nephilinae spiders. These tails are summarized as follows and are illustrated in Fig. 2:

- no tail attachment,
- a single putreanyl unit (**13**),
- a diputreanyl in tandem (**14**),
- a triputreanyl in tandem (**15**),
- a tetraputreanyl in tandem (**16**),
- a single arginine residue (**17**),
- a single ornithine residue (**18**),
- a dipeptide ornithyl-arginine (**19**),
- a tripeptide putreanyl-ornithyl-arginine (**20**), and
- a tripeptide alanyl-glycyl-arginine (**21**).

Thus, during evolution, these spiders may have tried different arrays of chemical building blocks to successfully and/or unsuccessfully be used as a paralyzing/killing tool for the types of prey existing in each spider's natural ecosystem. The toxins detected may result from successful trials during evolution, which were incorporated as part of the chemical arsenal of spiders to improve their foraging efficiency. Orb-web spiders are polyphagous animals that prey on a large number of different species of flying arthropods from different orders. For successful prey capture, the venom constitutes an important part of the strategy. As a result, the venom must contain a large number of structurally different acylpolyamine toxins in order to make the spiders adept at catching the most potential prey in each ecological situation.

BIOLOGICAL ACTIVITIES

Acylpolyamines interact strongly with the neuromuscular junctions of insects, which generally are rich in different types of ionotropic Glu-Rs; however, there is relatively high structural similarity between these insect receptors and their homologs in vertebrates [33,34].

The vertebrate Glu-Rs are divided into subclasses based on their responses to exogenous ligands: *N*-methyl-D-aspartate (NMDA)-dependent, α-amino-3-hydroxy-5-methylisoxasole-4-propionic acid (AMPA)-dependent, and kainate (KA)-dependent receptors [35]. Meanwhile, the invertebrate Glu-Rs are classified into four subtypes: (i) quisqualate receptors that gate cation channels (qGlu-R), (ii) ibotenate receptors that gate chloride channels, (iii) a purported KA receptor, and (iv) a purported NMDA receptor [35–37]. The AMPA- and KA-dependent subtypes are involved in synaptic pathways of central signaling, playing different roles in conjunction with each other. Taking into

account the potency, selectivity, low molecular mass, and solubility of the acylpolyamines in water, these toxins constitute lead compounds for targeting Glu-Rs.

Using argiotoxin-636 (**22**) and argiotoxin-659 (**23**) as tools, it was demonstrated that the action of these compounds is use-dependent in relation to the blocking of Glu-Rs. This means that the presence of a receptor agonist is necessary to activate the Glu-Rs, which in turn change their conformations, exposing the inhibitor binding site to the action of the acylpolyamine toxins that then block the receptor [38].

The spider toxin JSTX-3 (**24**) was reported to block the postsynaptic action of Glu-Rs in mammalian central neurons [39–41]. Recombinant expression of AMPA/KA-Glu-Rs in *Xenopus* oocytes permitted the use of sophisticated electrophysiological systems. Using these methods, it was demonstrated that JSTX-3 acts as a specific blocker of the receptor subunit in Glu-R_1, Glu-R_3, Glu-R_4, and Glu-$R_{1/3}$, with a rectifying current–voltage (*I–V*) relationship. JSTX-3 did not affect the Glu-$R_{1/2}$, Glu-$R_{2/3}$, and Glu-R_6 subunits, which present a linear *I–V* relationship [34]. Later, the use of site-directed mutagenesis permitted identification of the transmembrane domain position responsible for the interaction with JSTX-3 (**24**).

Electrophysiological and ligand binding assays suggested that the acylpolyamines are noncompetitive channel blockers of cation-conducting transmitter receptors in nervous systems [3]. A general model of acylpolyamine binding was proposed in which the electrostatic interactions between the protonated amino groups of the toxin and the negatively charged amino acid residues in the interior of the receptor ion channel contribute to binding. Thus, the toxin enters and plugs the open cation channels gated by a Glu-R, sterically inhibiting the ion flow through the channel [36,37]. Due to the complex properties of these toxins and the diversity of cellular responses, the interaction between the acylpolyamines and ion channels is still not completely understood at the molecular level.

It is well known that the acylpolyamine toxins cause paralysis in spiders' prey that may last from several hours to many days, depending on the composition of the toxin cocktail present in the venom [42]. It was reported that the paralytic activity may be strongly potentiated by the presence of Zn^{2+} ions, which naturally occur in high concentrations in spider venoms. The acylpolyamine toxins can form structural complexes with some metal ions due to the nitrogen-crowded conformation assumed by the polyamine backbone that permits the chelation of metal ions. In turn, these metal ions are transported by the toxin until it reaches the binding site region within the ion channel receptor [42]. Next to the acylpolyamine binding site, another binding site exists that is specific for zinc (Zn^{2+}) ions. This neighboring site, once occupied by its ligand, induces conformational changes in the receptor, which promotes the interaction with the binding site of the acylpolyamines and potentiates the paralytic action [43].

Acylpolyamines as Neuroprotective Agents

Ischemia may cause excessive activation of excitatory synapses, followed by sustained influx of calcium (Ca^{2+}) ions (mediated by Glu-Rs). Consequently, the intracellular concentrations of Ca^{2+} ions are elevated, which in turn contributes to neuronal death [44,45]. The use of acylpolyamines as neuroprotective agents is generally associated with the occurrence of long-term ischemia in the brain, as observed in stroke patients or as a result of brain damage. Different neuroprotective agents have been investigated as potential solutions to minimize the problems caused by brain damage; however, most of them cause serious side effects [46–48].

The electrophysiological properties of toxin FTX-3.3 (**25**) isolated from the venom of the spider *A. aperta* inspired the development of a combinatorial chemistry protocol that resulted in the identification of L-arginyl-3,4-spermidine (L-Arg-3,4) (**26**). L-Arg-3,4 is a lead compound for the neuroprotection of neurons from brain slices maintained under culture and subjected to ischemic depolarization [49,50]. The use of electrophysiological recordings of CA1 pyramidal neurons from brain slices demonstrated the neuroprotective effect of JSTX-3 (**24**) and its analog, 1-naphthylacetyl spermine (Naspm) (**27**), against ischemic stress, which generally results in neuronal deaths [47].

JSTX-3 has been used as a tool for studying CNS function and to elucidate the mechanism of some nervous system syndromes. For example, JSTX-3 (**24**) and Naspm (**27**) were used to investigate the selective death of motor neurons potentially responsible for amyotrophic lateral sclerosis (ALS) with the involvement of the AMPA/KA-Glu-Rs using measurements of single channel conductance in neurons under culture [34]. Figure 3 shows the chemical structures of some natural and synthetic acylpolyamines used as tools to dissect the nervous system.

Antiepileptic Effects

Epilepsy is a chronic neurological disorder affecting about 1% of the world's population [51]. The response to therapy is generally good, but up to 30% of patients cannot achieve acceptable seizure control despite adequate trials with potentially effective antiepileptic agents [52,53]. In order to develop new antiepileptic therapeutic strategies, it is important to understand the basic mechanisms involved in epileptic discharges. Many diseases and neuronal disorders are caused by receptor and ion channel dysfunction [54]. Currently, the excitatory amino acid receptors represent promising targets for the development of novel drugs to treat epilepsy.

There is evidence indicating that JSTXs nonselectively block AMPA- and NMDA-Glu-Rs, producing a synergic anticonvulsant effect. The acylpolyamine JSTX-3 (**24**) was reported to present antiepileptogenic action due, at least in part, to the inhibitory action of this toxin on the cationic currents evoked by NMDA receptor activation [53].

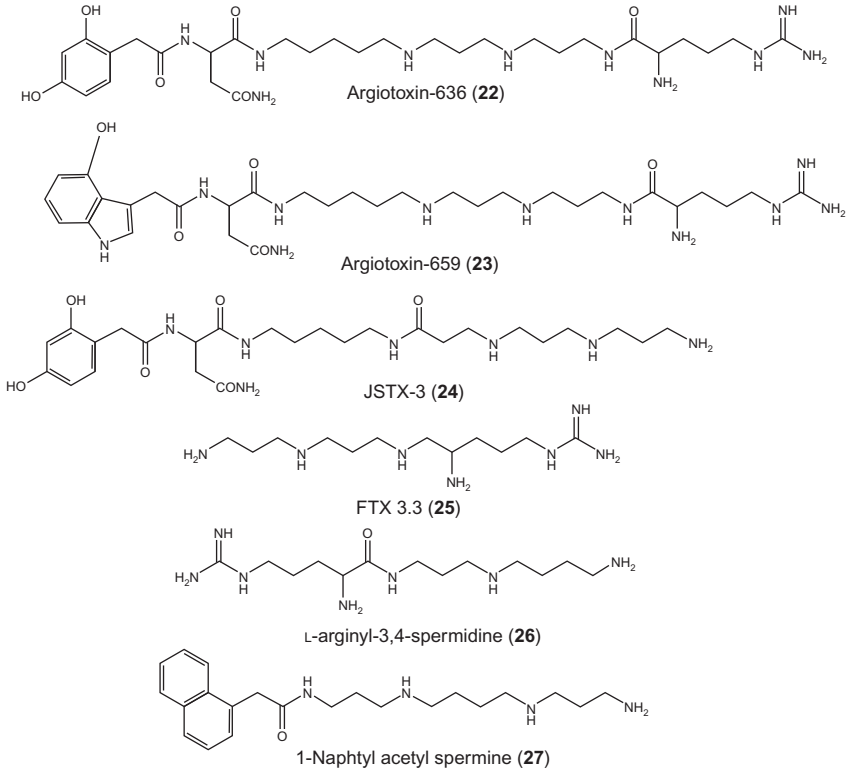

FIGURE 3 Chemical structures of some natural (argiotoxin-636, argiotoxin-659, JSTX-3, and FTX-3.3) and synthetic (L-arginyl-3,4-spermidine and 1-naphthyl acetyl spermine) acylpolyamines.

Glutamate is the major excitatory neurotransmitter in the CNS, and there is an enormous amount of experimental and clinical evidence indicating the importance of this neurotransmitter in the pathogenesis of chronic neuronal degeneration in disorders such as ALS, Huntington's, Alzheimer's, and Parkinson's disease. Therefore, the discovery of novel agonist or antagonist compounds of the vertebrate ionotropic Glu-Rs, like the acylpolyamine toxins, will certainly contribute to the development of a new generation of drugs for neuropharmaceutical use [55,56].

THE CHEMICAL SYNTHESIS OF ACYLPOLYAMINE TOXINS

The structural characterization of the acylpolyamine toxins from spider venoms is rather difficult due to the occurrence of several building blocks used in the synthesis of polyamine backbones that may differ simply by structural isomerism. The different positions of substituents in the aromatic head groups make it relatively difficult to differentiate compounds from each other

in natural samples [30,57]. Generally, a reliable structural characterization of these toxins requires a comparison with reference samples, which are specifically synthesized for this purpose [58]. In addition to this, the large majority of natural spider acylpolyamine toxins lack selectivity toward specific ionotropic receptors, requiring the synthesis of a wide number of different analogs of these compounds to find a suitable drug candidate with the required selectivity and potency [33].

The first synthetic strategies for these compounds utilized solution-phase methods that included frequent use of protecting groups and laborious manipulation of highly polar intermediates, which made these protocols inefficient [27,59]. In order to overcome these difficulties, solid-phase synthesis (SPS) protocols were developed in which the polyamine moiety was immobilized on the surface of a Merrifield resin [57]. This SPS strategy became relatively commonly used for these reduced scale reactions for multiple reasons. First, the ability to manipulate and purify the highly polar intermediates was key and became reduced to simple washing protocols. Also, this strategy allowed the facile use of specific protecting groups. Finally, SPS was a suitable strategy to build combinatorial libraries. However, the first SPS protocols did not allow the synthesis of nonsymmetric polyamine backbones. However, this was later solved by the use of different building blocks in sequential chain elongation [33,60] and was supported by the use of (a) *N*-alkylation reactions [61,62], (b) Mitsunobu reactions [63,64], and (c) reductive methods based on intermediary imines or amides [65–67]. Figure 4 shows an example of the use of the SPS protocol for the synthesis of the acylpolyamine toxin JSTX-4 based on a recently reported protocol [68].

The first methods were further developed to permit linear growth of the polyamine moiety; however, a novel strategy was developed to permit the synthesis of the toxins from the center of the backbone chain [57,69]. Taking into account the proposed organization of the acylpolyamine toxins from Nephilinae spiders as generalized structures classified from A to G (as reported above), another strategy was proposed for the synthesis of these structural types and their analogs. The new strategy involves the construction of the polyamine backbone followed by the successive connection of the lipophilic head and polyamine chain terminus [58]. This strategy applied Fukuyama's protocol that uses reductive alkylation, acetylation, and reduction, or alkylation of sulfonamides, where 2-nitrobenzenesulfonamide is used both as a protecting and an activating group [70], making this protocol very versatile.

CONCLUDING REMARKS

The large number of spider acylpolyamine toxin structures presenting the same chemical nature, mainly among the orb-weaving spiders, offered an interesting opportunity to understand the way that nature has combined a small number of chemical building blocks in a combinatorial array to create

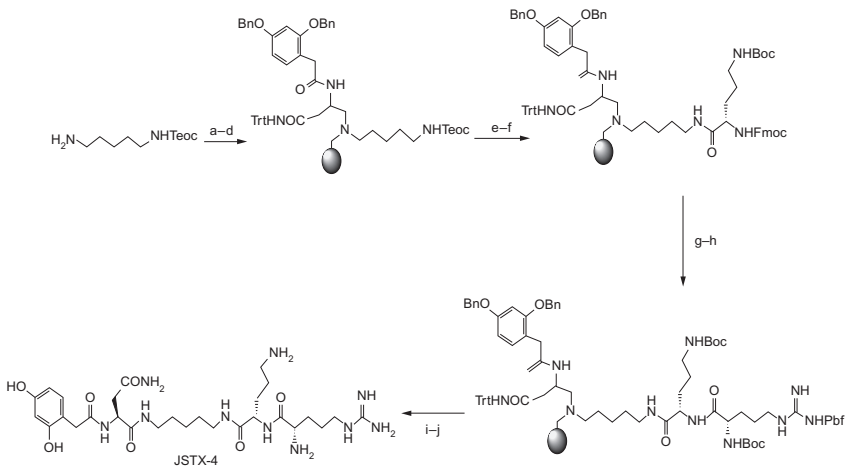

FIGURE 4 The synthetic scheme of the acylpolyamine toxin JSTX-4 using an SPS protocol (modified from [68]): (a) (i) DFPE resin, DMF/acetic acid (9:1), (ii) $NaBH(OAc)_3$; (b) Fmoc-L-Asn(Trt)-OH, HATU, DIPEA, CH_2Cl_2/DMF (9:1); (c) 20% piperidine in DMF; (d) 2-(2,4-bis (benzyloxy)phenyl) acetic acid, HATU, DIPEA, CH_2Cl_2/DMF (9:1); (e) TBAF, THF, 55°C; (f) Fmoc-L-Orn(Boc)-OH, HATU, DIPEA, CH_2Cl_2/DMF (9:1); (g) 20% piperidine in DMF; (h) Boc-L-Arg(Pbf)-OH, HATU, DIPEA, CH_2Cl_2/DMF (9:1); (i) TFA/CH_2Cl_2/TIPS/H_2O (75:20:2.5:2.5); (j) $Pd(OH)_2$/C, H_2, HOAc.

a vast arsenal to kill or paralyze many different types of prey. Despite the well-known predatory nature of spiders, orb-web spiders are almost entirely sedentary animals that use their webs as nests, as prey-traps, and as an interface to interact with the surrounding world.

The use of modern spectroscopic methods permitted the structural elucidation of almost 100 different structures of acylpolyamine toxins among the venoms of orb-weaving spiders. Using the polyamine chain as a structural reference to initiate the biosynthesis of these toxins, seven different subtypes of polyamine moieties (from A to G) were observed in combination with a linker group amino acid residue(s) to produce the polyamine backbone. This backbone, in turn, may be connected to three different aromatic heads, which creates molecules with differing hydrophobicity. Sometimes, a backbone tail may be attached to the polyamine chain in a single building block or even in tandem.

The development of SPS protocols has considerably improved the access to polyamine toxins and has provided ways to confirm many structural assignments. Also, these protocols allow for the synthesis of novel, more potent, and more selective acylpolyamine molecules for the blockage of different subtypes of Glu-Rs. Natural and synthetic acylpolyamines from orb-weaving spiders have become interesting model structures for the development of neuroprotective and/or antiepileptic drugs for therapeutic uses, as well as important tools as probes for receptor structural studies.

ACKNOWLEDGMENTS

This work was supported by a grant from the São Paulo State Research Foundation (FAPESP, BIOprospecTA program 06/57122-7). The research of M.S.P. is for the National Council for Scientific and Technological Development (CNPq).

ABBREVIATIONS

AMPA	α-amino-3-hydroxy-5-methylisoxasole-4-propionic acid
CID	collision-induced dissociation
CNS	central nervous systems
COSY	correlation spectroscopy
DFPE	2-(3,5-dimethoxy-4-formylphenoxy)ethyl polystyrene
DIPEA	*N*,*N*-diisopropylethylamine
DMF	dimethylformamide
ESI-MS	electron spray ionization mass spectrometry
Glu-R	glutamate receptor
HATU	*o*-(7-azabenzotriazol-1-yl)-*N*,*N*,*N*′,*N*′-tetramethyluronium hexaphosphate
HMBC	heteronuclear multiple bond correlation
HMQC	heteronuclear multiple quantum correlation
HRMS	high-resolution mass spectrometry
I–V	current–voltage relationship
JSTX	joro spider toxin
KA	kainic acid
LC–MS	liquid chromatography–mass spectrometry
MS/MS	tandem mass spectrometry
nACh-R	nicotinic acetylcholine receptor
NMDA	*N*-methyl-D-aspartate
NMR	nuclear magnetic resonance
NOESY	nuclear Overhauser enhancement spectroscopy
PhTX	phyllanthus toxin
RP-HPLC	reversed-phase high-performance liquid chromatography
SPS	solid-phase synthesis
TBAF	tetrabutylammoniumfluoride
TFA	trifluoroacetic acid
THF	tetrahydrofuran
TIPS	triisopropylsilane

REFERENCES

[1] P.N.R. Usherwood, I.R. Blagbrougi, Pharmacol. Ther. 52 (1991) 245–268.

[2] P.N.R. Usherwood, G.G. Lunt (Ed.), Neurotox '88: Molecular Basis of Drug and Pesticide Action, Excerpta Medica, Elsevier, Amsterdam, 1988, pp. 383–392.

[3] A.T. Eldefrawi, M.E. Eldefrawi, K. Konno, N.A. Mansour, K. Nakanishi, E. Oltz, P.N. R. Usherwood, Proc. Natl. Acad. Sci. USA 85 (1988) 4910–4913.
[4] T. Piek, B. Hue, 1989, Comp. Biochem. Physiol. 93C (1989) 403–406.
[5] M.R. Jørgensen, C.A. Olsen, I.R. Mellor, P.N.R. Usherwood, M. Witt, H. Franzyk, J. W. Jaroszewski, J. Med. Chem. 48 (2005) 56–70.
[6] S. Frølund, A. Bella, A.S. Kristensen, H.L. Ziegler, M. Witt, C.A. Olsen, K. Strømgaard, H. Franzyk, J.W. Jaroszewski, J. Med. Chem. 53 (2010) 7441–7745.
[7] P.A. Sebastian, K.V. Peter (Eds.), Spiders of India, Universities Press, Hyderabad, India, 2009.
[8] P. Escoubas, S. Diochot, G. Corzo, Biochimie 82 (2000) 893–907.
[9] J.H. Welsh, C.S. Batty, Toxicon 1 (1963) 165–173.
[10] F.L. Schambacher, C.K. Lee, J.E. Hall, I.B. Wilson, D.E. Howell, G.V. Odell, Toxicon 11 (1973) 21–29.
[11] T.K. Chan, C.R. Geren, D.E. Howell, G.V. Odell, Toxicon 13 (1975) 61–66.
[12] Y. Aramaki, T. Yasuhara, T. Higashijima, M. Yoshioka, A. Miwa, N. Kawai, T. Nakajima, Proc. Jpn. Acad. Sci. 62B (1986) 359–362.
[13] S.L. Early, E.K.J. Michaelis, Toxicon 25 (1987) 433–442.
[14] R. Frew, M.G. Hamilton, P.M. Lundy, Toxicon 32 (1994) 511–515.
[15] J. McCormick, J. Meinwald, J. Chem. Ecol. 19 (1993) 2411–2451.
[16] N. Kawai, J. Toxicol. Toxin Rev. 10 (1991) 131–137.
[17] P.N.R. Usherwood, I.R. Duce, P. Boden, J. Physiol. (Paris) 79 (1984) 241–247.
[18] E.V. Grishin, T.M. Volkova, A.S. Arseniev, V.V. Onoprienko, L.G. Magazanik, S. M. Antonov, I.M. Fedorova, Bioorg. Kim. 12 (1986) 11–21.
[19] M.S. Palma, T. Nakajima, Toxin Rev. 24 (2005) 209–234.
[20] Y. Aramaki, T. Yasuhara, T. Higashijima, A. Miwa, N. Kawai, T. Nakajima, Biomed. Res. 8 (1987) 167–172.
[21] T. Toki, T. Yasuhara, Y. Aramaki, K. Osawa, A. Miwa, KawaiN., T. Nakajima, Biomed. Res. 9 (1988) 421–428.
[22] T. Chiba, T. Akizawa, M. Matukawa, H. Pan-Hou, M. Yoshioka, Chem. Pharm. Bull. 42 (1994) 1864–1869.
[23] T. Fujita, Y. Itagaki, M. Hisada, H. Naoki, T. Nakajima, M. Adriantsiferana, Rapid Commun. Mass Spectrom. 11 (1997) 1115–1119.
[24] M.S. Palma, Y. Itagaki, T. Fujita, M. Hisada, H. Naoki, T. Nakajima, Nat. Toxins 5 (1997) 47–57.
[25] M.S. Palma, Y. Itagaki, T. Fujita, H. Naoki, T. Nakajima, Toxicon 36 (1998) 485–493.
[26] Y. Itagaki, Y. Fujita, H. Naoki, T. Yasuhara, M. Andriantsferana, T. Nakajima, Nat. Toxins 5 (1997) 1–13.
[27] A. Schäfer, H. Benz, W. Fiedler, A. Guggisberg, S. Bienz, M. Hesse, G.A. Cordell, A. Brossi (Eds.), The Alkaloids Chemistry and Pharmacology, Academic Press, San Diego, 1994, pp. 1–125 vol. 45.
[28] M. Tzouros, N. Manov, S. Bienz, L. Bigler, J. Am. Soc. Mass Spectrom. 15 (2004) 1636–1643.
[29] S. Chesnov, L. Bigler, M. Hesse, Helv. Chim. Acta 84 (2001) 2178–2197.
[30] N. Manov, M. Tzouros, S. Chesnov, L. Bigler, S. Bienz, Helv. Chim. Acta 85 (2002) 2827–2846.
[31] F.C. Schroeder, A.E. Taggi, M. Gronquist, R.U. Malik, J.B. Grant, T. Eisner, J. Meinwald, Proc. Natl. Acad. Sci. USA 105 (2008) 14283–14287.
[32] Y. Itagaki, T. Nakajima, J. Toxicol. Toxin Rev. 19 (2000) 23–52.

[33] K. Strømgaard, L.S. Jensen, S.B. Vogensen, Toxicon 45 (2005) 249–254.
[34] G. Estrada, E. Villegas, G. Corzo, Nat. Prod. Rep. 24 (2007) 145–161.
[35] G.L. Collingridge, R.A. Lester, Pharmacol. Rev. 41 (1989) 143–210.
[36] S.K. Choi, A.G. Kalivretenosl, P.N.R. Usherwood, K. Nakanishi, Chem. Biol. 2 (1995) 23–32.
[37] I.R. Mellor, P.N.R. Usherwood, Toxicon 43 (2004) 493–508.
[38] M.S. Davies, M.P. Baganoff, E.V. Grishin, T.H. Lanthorn, T.M. Volkova, G.B. Watson, R. C. Wiegand, Eur. J., Pharmacol. Mol. Pharmacol. Sect. 227 (1992) 51–56.
[39] N. Kawai, A. Miwa, M. Saito, H.S. Pan-Hou, M. Yoshioka, J. Physiol. (Paris) 79 (1984) 228–231.
[40] N. Akaike, N. Kawai, N.I. Kiskin, E.M. Kljuchko, O.A. Krishtal, A.Y. Tsyndrenko, Neurosci. Lett. 79 (1987) 326–330.
[41] M. Saito, N. Kawai, A. Miwa, H. Pan-Hou, M. Yoshioka, Brain Res. 346 (1985) 397–399.
[42] M.F. Manzoli-Palma, N. Gobbi, M.S. Palma, Chemoecology 16 (2006) 203–208.
[43] T.W. Stone, Neuropharmacology, W.H. Freeman and Co. Ltd., Oxford, 1995.
[44] N. Kawai, Toxin Rev. 24 (2005) 271–287.
[45] H. Benveniste, M.B. Jorgensen, N. Diemer, A.J. Hansen, Acta Neurol. Scand. 78 (1988) 529–536.
[46] A. Schurr, Curr. Drug Targets 5 (2004) 603–618.
[47] P. Calabresi, D. Centonze, L.M. Cupini, C. Costa, F. Pisani, G. Bernardi, Neurobiol. Dis. 12 (2003) 82–88.
[48] K. Valentino, R. Newcomb, T. Gadbois, SinghT., S. Bowersox, S. Bitner, A. Justice, D. Yamashiro, B.B. Hoffman, R. Ciaranello, Proc. Natl. Acad. Sci. USA 90 (1993) 7894–7897.
[49] B. Morrison, A.K. Pringle, T. McManus, J. Ellard, M. Bradley, F. Signorelli, F. Iannotti, L. E. Sundstrom, Br. J. Pharmacol. 137 (2002) 1255–1268.
[50] A.K. Pringle, B. Morrison, M. Bradley, F. Iannotti, L.E. Sundstrom, Naunyn Schmiedebergs Arch. Pharmacol. 368 (2003) 216–224.
[51] J.W.A.S. Sander, S.D. Shorvon, J. Neurol. Neurosurg. Psychiatry 61 (1996) 433–443.
[52] P. Kwan, M.J. Brodie, N. Engl. J. Med. 42 (2000) 314–331.
[53] S.D. Salamoni, J.C. da Costa, M.S. Palma, K. Konno, K. Nihei, A.A. Tavares, D.S. Abreu, G.T. Venturina, F.B. Cunha, R.M. Oliveira, R.V. Breda, Brain Res. 1048 (2005) 170–176.
[54] B. Hille, Ionic Channels of Excitable Membranes, second ed., Sinauer Associates, Inc., Sunderland, MA, 1984.
[55] P. Quintana, S. Alberi, D. Hakkoum, D. Muller, Eur. J. Neurosci. 23 (2006) 975–983.
[56] D. Giuliani, C. Giaroni, E. Zanetti, L. Canciani, P. Borroni, S. Lecchini, G. Frigo, Neurochem. Int. 48 (2006) 191–200.
[57] N. Manov, M. Tzouros, L. Bigler, S. Bienz, Tetrahedron 60 (2004) 2387–2391.
[58] K. Nihei, M.J. Kato, T. Yamane, M.S. Palma, K. Konno, Bioorg. Med. Chem. Lett. 12 (2002) 299–302.
[59] T. Nishimaru, M. Sano, Y. Yamaguchi, T. Wakamiya, Bioorg. Med. Chem. 17 (2009) 57–63.
[60] K. Strømgaard, K. Andersen, T. Ruhland, P. Krogsgaard-Larsen, J.W. Jaroszewski, Synthesis (2001) 877–884.
[61] T. Kan, H. Kobayashi, T. Fukuyama, Synlett 8 (2002) 1338–1340.
[62] C.A. Olsen, M. Witt, J.W. Jaroszewski, H. Franzyk, Org. Lett. 6 (2004) 1935–1938.
[63] K. Stromgaard, P. Andersen, P. Krogsgaard-Larsen, J.W. Jaroszewski, Mini Rev. Med. Chem. 1 (2001) 317–338.

[64] C.A. Olsen, M. Witt, J.W. Jaroszewski, H. Franzyk, Synlett (2004) 473–476.
[65] S.R. Chhabra, A.N. Khan, B.W. Bycroft, Tetrahedron Lett. 41 (2000) 1095–1098.
[66] D. Jönsson, Tetrahedron Lett. 43 (2002) 4793–4796.
[67] F. Wang, S. Manku, D.G. Hall, Org. Lett. 2 (2000) 1581–1583.
[68] A.F. Barslund, M.H. Poulsen, T.B. Bach, S. Lucas, A.S. Kristensen, K. Strømgaard, J. Nat. Prod. 74 (2011) 483–486.
[69] N. Manov, S. Bienz, Tetrahedron 57 (2001) 7893.
[70] T. Fukuyama, C.K. Jow, M. Cheung, Tetrahedron Lett. 36 (1995) 6373.

Chapter 3

Deep-Sea Hydrothermal Vents as a New Source of Drug Discovery

Eric Andrianasolo, Richard Lutz and Paul Falkowski
Institute of Marine and Coastal Sciences, Rutgers University, New Brunswick, New Jersey, USA

INTRODUCTION

The oceans are the Earth's largest ecosystem and hold great, underexplored potential for drug discovery. Within this vast ecosystem, one area remains particularly enigmatic: deep-sea hydrothermal vents, which are characterized by high concentrations of reduced sulfur compounds [1]. Life is supported by the growth of chemolithoautotrophic bacteria, capable of oxidizing hydrogen sulfide, hydrogen, and other reduced inorganic compounds to provide energy that is used to fuel carbon dioxide fixation into macromolecules. Chemoautotrophic organisms are known to produce chemical defenses against their consumers. Some chemically deterrent species are also known to harbor chemoautotrophic endosymbiotic bacteria, and these microbial symbionts may produce metabolites that defend their host species [2]. The vent mussel *Bathymodiolus thermophilus* is characterized by a considerable flexibility in its sources of nutrition. Symbionts within the gills of this organism were found to be thiosulfate- and sulfide-oxidizing chemoautotrophs [3]. In this review, we investigated the ability of chemolithoautotrophic bacterium, *Thermovibrio ammonificans* and the marine hydrothermal vent mussel, *B. thermophilus*, to produce novel secondary metabolites.

For the treatment of cancer, cytotoxic chemotherapeutics currently in use rely on the ability to selectively target proliferating cells, which are enriched in tumors. Tumor cells progressively evolve genetic mutations that enable not only cell proliferation but also resistance to programmed cell death, or apoptosis, a cell suicide pathway that is the cellular response to oncogene activation or irreparable cellular damage [4–7]. Effective cancer therapeutic strategies often rely on preferential and efficient induction of apoptosis in

Bioactive Natural Products, Vol. 36. DOI: 10.1016/B978-0-444-53836-9.00020-7

tumor cells. Progressive exposure to such molecules commonly leads to selection of resistant cells that are therapeutically associated with both tumor progression and resistance to chemotherapy [4–7]. While many conventional cytotoxic chemotherapeutics trigger apoptosis indirectly by inflicting cellular damage, recent efforts have been directed to developing agents that specifically target or activate the apoptotic pathway irreversibly [8].

To develop a cell-based assay specific for the isolation and identification of apoptosis-inducing compounds that are potential anticancer agents, in this review and especially in our investigation we took advantage of the recently defined mechanism of apoptotic signaling by members of the Bcl-2 family of apoptosis regulators. Two proapoptotic Bcl-2 family member proteins, Bax and Bak, are the functionally redundant, essential downstream regulators of apoptosis in the vast majority of apoptotic signaling pathways [4–6]. Moreover, Bax and Bak are essential for apoptotic function required for suppressing tumor growth and for mediating chemotherapeutic response [9–14]. These discoveries were made, in part, through the step-by-step engineering of immortal isogenic mouse epithelial cell lines derived from wild-type and mutant mice with targeted deletions in apoptosis regulators (*bax*, *bak*, *bim*, and others), separately and in combination [7,11]. Thus, we have genetically matched immortal epithelial cell lines that have apoptosis function intact (wild-type W2) or disabled through specific genetic deletion of both *bax* and *bak* (D3) (U.S. Patent US 6,890,716). D3 cells, by virtue of being deficient in both Bax and Bak, are completely and irreversibly defective for apoptosis, yet all apoptosis regulatory mechanisms upstream (Bcl-2, Bim, etc.) remain intact. Importantly, the vast majority of human cancers with defects in apoptosis have the pathway disabled upstream of Bax and Bak. Thus, screening to identify compounds that have the capacity to kill W2 and not D3 cells should identify those that possess proapoptotic, and potentially anticancer, activity.

In order to situate the scope of research by prospecting unusual sources of bioactive natural products, we primarily display the potential of the deep-sea hydrothermal vents as a source of bioactive marine natural products.

DEEP-SEA HYDROTHERMAL VENTS AS A HOT SPOT FOR BIOACTIVE MARINE NATURAL PRODUCTS DISCOVERY

Over 300 hydrothermal vent sites are known throughout the world [15]. These vent sites generally occur along a nearly continuous underwater mountain chain (mid-ocean ridges) totaling more than 75,000km that remains largely unexplored for hydrothermal activity. Located at the boundaries between the tectonic plates of Earth's crust, these mid-ocean ridges are the sites of incremental seafloor spreading (spreading centers) at which molten rock (magma) rises toward Earth's surface as the tectonic plates move in relation to each other. Hydrothermal vent fields may comprise multiple zones of focused hot

and diffuse (low temperature) fluid flows and range in size from several hundred to several million square meters around ridge axes. Hydrothermal vents are also found behind island arcs along active plate margins in "back-arc spreading centers" and active submarine volcanoes or seamounts located in the center of tectonic plates [16]. As a result of their proximity to the countries primarily involved in deep-sea hydrothermal vent research, the most studied hydrothermal systems are either in the eastern Pacific (East Pacific Rise and the Juan de Fuca, Gorda, and Explorer Ridges) or in the north-central Atlantic (northern Mid-Atlantic Ridge). The distinct geological settings of different hydrothermal vents impact the extent of venting on both spatial and temporal scales and thus influence the biogeography of vent organisms. Therefore, variations in mid-ocean ridge crest dynamics between different ocean basins, as well as regional and local differences in ridge morphology (valley depth, etc.), which affect bottom currents, style of venting, and vent longevity, make it important to keep in mind the geographical context of the general descriptions of vents and their biota [15] (Fig. 1).

The dense invertebrate communities typically associated with deep-sea hydrothermal vents exist in diffuse, warm-water flows that sustain temperatures of 10–40°C and occasionally up to 60°C [18]. Despite the high biomass

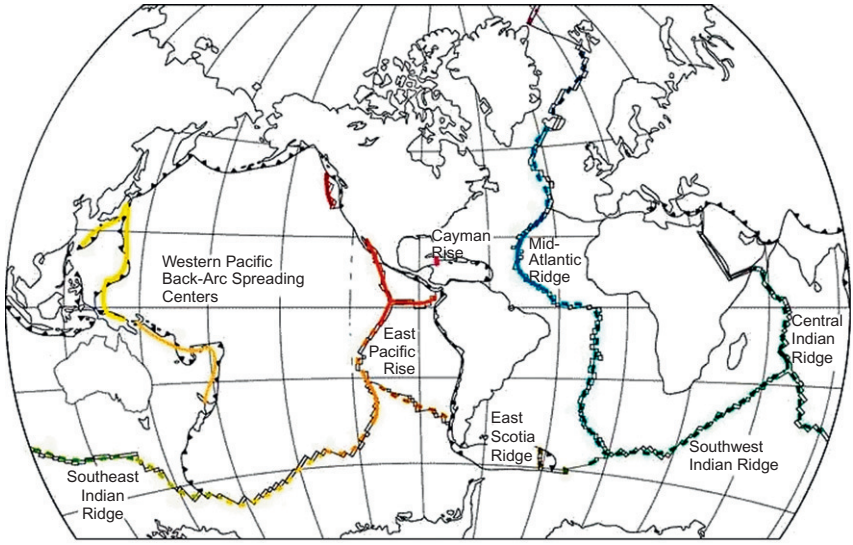

FIGURE 1 Map of selected hydrothermal vents: A model of the global biogeographic differentiation of invertebrate species associated with hydrothermal vents. Colors represent regions that share many of the same species; solid lines reflect areas where vent sites have been relatively well-described; dashed lines and colors interpolate biogeographic similarities between areas that have been explored. Reproduced with permission from Van Dover [17].

associated with hydrothermal vents, there is much lower macrofaunal species diversity relative to other deep-sea communities. This is likely a result of the dynamic and variable fluid conditions both within and between vent habitats that require specialized physiological and biochemical adaptations [18,19] and favor the emergence of dominant species that succeed in a range of fluid conditions [20]. However, the full extent of the species present within hydrothermal vent communities has yet to be discovered considering the vast unexplored ocean ridge systems and the report of new species being described every 2 weeks throughout the 1990s [19]. Over 500 eukaryote species, encompassing 12 animal phyla and more than 150 new genera, have been described in the past three decades from deep vent sites. Arthropods (38.8%), mollusks (28.6%), and annelid worms (17.7%) dominate the megafaunal vent communities throughout the world, while cnidarians (4.6%), chordates (3.7%), and sponges (1.9%) are of notable presence [21]. Although deep ocean currents can disperse larval organisms over vast distances to new hydrothermal fields, many hydrothermal vent fields exhibit a unique range of habitat diversity and a high degree of endemism [18,22]. The Galapagos Rift and East Pacific Rise of the Pacific Ocean have similar communities, whereas different vent communities on the Juan de Fuca Ridge (northeast Pacific) share few species [23]. During a visit to a mature hydrothermal vent site in the eastern Pacific, one might expect to observe scattered aggregations or "bushes" of siboglinid polychaetes (e.g., the vestimentiferan tube worms *Riftia pachyptila* or *Ridgeia piscesae*), which, on closer inspection, host a mix of limpets and snails, alvinellid polychaetes (e.g., the palm worm *Paralvinella palmiformis*), and polynoid polychaetes (e.g., the scale worm *Lepidonotopodium piscesae*), all cloaked in a white microbial mat, with occasional hydrothermal vent shrimp and Yeti crabs. On the Mid-Atlantic Ridge, vent sites are characterized instead by an abundance of hydrothermal vent shrimps (*Rimicaris*) swarming over chimneys near high flows that lack the vestimentiferans and alvinellids of the Pacific vent communities [18]. Nonetheless, at least 40% of the Atlantic genera reported are shared with the Pacific vent fauna. In both oceans, beds of hydrothermal vent clams (*Calyptogena magnifica*) or mussels (*B. thermophilus*) may be observed in lower flow areas. The Kairei and Edmond vent fields of the Indian Ocean contain genera shared with either Atlantic or Pacific vents. However, Indian Ocean communities are different enough to constitute a separate biogeographic province from either Atlantic or Pacific [24].

At deep-sea hydrothermal vents, in the absence of light and the presence of hydrothermal fluids rich in minerals, reduced compounds (including H_2S, CH_4), and CO_2, chemical energy replaces solar energy as the fuel that supports primary production by chemosynthetic bacteria and archaea [18,25]. The archaea comprise a distinct domain of microorganisms that have no cell nucleus or membrane-bound organelles (the same as "prokaryotic" bacteria), but possess unique biochemistry and have several metabolic pathways that are more closely related to those of eukaryotes (especially transcription and

translation) [26]. Bacteria and archaea may be suspended in the ambient water column or hydrothermal plumes or attached to rocks, to sediment, or on/in vent animals, which in turn may feed directly on the microbes or engage in symbiotic associations to acquire fixed carbon and nitrogen [27–29].

Although there has been tremendous scientific interest in the microbial ecology of "hot-spot ecosystems," such as hydrothermal vents, cold seeps, and gas-hydrate systems, the distribution and diversity of functional and taxonomic groups of bacteria and archaea within the deep sea is largely unknown [30]. The diversity of hydrothermal vent microbial communities cannot truly be assessed by methods that rely solely on artificial cultivation, since 99% of marine microbes are considered unculturable [31]. These challenges have been overcome in part by the application of a molecular phylogeny-based approach using nucleotide-sequence analysis of the highly conserved gene for the small subunit (SSU) ribosomal ribonucleic acid (rRNA) molecule (16S rRNA) [32]. This approach has revealed that the global diversity of microorganisms is at least 100 times greater than estimates based on cultivation-dependent surveys; new phylotypes, often representing major new lineages, are consistently shown with each molecular analysis of microbial environments [32–34]. For example, the new archaeal phylum "Nanoarchaeota" [35] has been identified by analysis of polymerase chain reaction-amplified SSU rRNA genes from a defined coculture of hyperthermophilic archaeans, and similar methods have indicated the emergence of a newly defined lineage distributed throughout the global deep-sea vent system referred to as the "Deep-Sea Hydrothermal Vent Euryarchaeoic Group" [36].

In order to understand the strategy of isolation of natural products from deep-sea organisms using the cell-based assay specific for the isolation and identification of apoptosis-inducing compounds, we discuss in detail the main mechanism of apoptosis induction.

MAIN MECHANISM OF APOPTOSIS INDUCTION AND NEW APPROACH IN RESEARCH AND TREATMENT OF CANCER

Tumor cells progressively evolve genetic mutations that enable cell proliferation, metastasis, and chemotherapy resistance, which render successful treatment often problematic. One mechanism of both tumor progression and treatment resistance is achieved through the acquisition of defects in programmed cell death or apoptosis. Apoptosis is a cell suicide pathway whereby cells execute themselves in response to oncogene activation or irreparable cellular damage [4,5,14]. Tumor cells inactivate apoptosis to gain a survival advantage and do so most frequently by overexpressing that antiapoptotic Bcl-2 protein or through inactivating the proapoptotic Bcl-2 antagonist Bim. Understanding the mechanism of apoptosis regulation in normal cells and how it is rendered inactive in tumor cells has been one approach to the development of anticancer therapies.

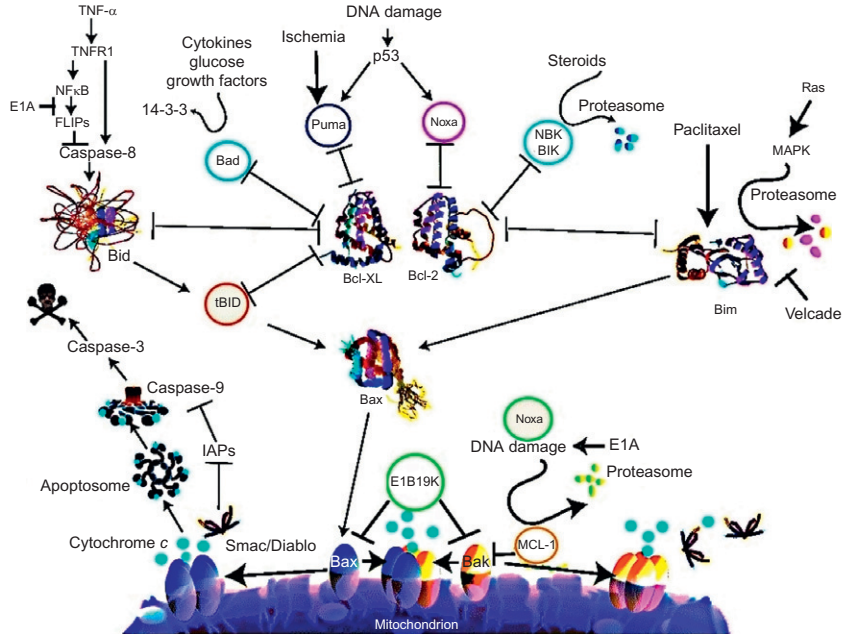

FIGURE 2 Pathway for regulation of apoptosis upstream of Bax and Bak.

Most apoptosis regulation is signaled through members of the Bcl-2 family or proteins (Fig. 2) [4,5]. Multidomain Bcl-2 family members function either to inhibit (e.g., Bcl-2, Bcl-x_L) or to promote (e.g., Bax and Bak) apoptosis. BH3-only Bcl-2 family members (e.g., Bim, Bid, Nbk/Bik, Puma, and Noxa) serve either to antagonize the survival activity of Bcl-2-like proteins or to activate the proapoptotic function of Bax and Bak. Once activated, Bax and Bak form pores and/or oligomerize in the mitochondrial outer membrane rendering it permeable to proapoptotic mitochondrial proteins such as cytochrome *c* and SMAC/Diablo [37]. Once released into the cytoplasm, cytochrome *c* functions to activate the cysteine protease caspase-9 in the apoptosome, whereas SMAC/Diablo functions to antagonize caspase inhibitors (IAPs). Subsequent effector caspase activation (e.g., caspase-3) leads to the orderly dismantling of the cell without activating the innate immune response. This pathway for apoptosis regulation serves as an irreversible molecular switch to terminate cell viability within 30–60 min, once activated, necessitating precise regulation.

This detailed knowledge of apoptosis regulation has led to determination of how common mutations in human tumors disable apoptosis and to the identification and development of therapeutics that restore the apoptotic response. This has enabled the development of small molecule Bcl-2 inhibitors [38], and small molecule SMAC mimetic caspase activators [39,40], that are entering

the clinic. Defining the mechanism of apoptosis induction by chemotherapeutic drugs and how it is disabled in human tumors has led rational approaches to combination chemotherapy to restore apoptosis. One prominent example is our discovery that proapoptotic Bim is the determinant of Taxane responsiveness that is inactivated by its proteasome-mediated degradation in tumors with activated Ras [12]. This led us to demonstrate that combining Taxanes with a proteasome inhibitor (bortezomib/Velcade) was effective in restoring tumor regression in preclinical models [12]. This is currently the basis for a clinical trial for refractory solid malignancies [41]. Further, many of the common signal transduction pathways that are activated in human tumors function to promote tumor cell survival by suppressing apoptosis, and therefore the clinical efficacy of specific inhibitors of these pathways that have been developed is being achieved in part through restoration of apoptotic function [42–46]. Screening small molecule libraries for natural products that induce apoptosis in cancer cells has also attracted interest; however, the best way to perform such a screen has not been entirely clear. Nonetheless, identification of apoptosis modulators for anticancer drug discovery is a fertile area for investigation.

AMMONIFICINS A AND B, HYDROXYETHYLAMINE CHROMAN DERIVATIVES FROM A CULTURED MARINE HYDROTHERMAL VENT BACTERIUM, *T. AMMONIFICANS*

Introduction

Two hydroxyethylamine chroman derivatives, ammonificins A (**1**) and B (**2**), were isolated from the marine hydrothermal vent bacterium, *T. ammonificans*. The molecular structures of these compounds were determined using a combination of NMR (nuclear magnetic resonance), MS (mass spectrometry), and CD (circular dichroism) analyses. Biological activities were determined using an antimicrobial assay and the patented ApopScreen cell-based screen for apoptosis induction and potential anticancer activity. To our knowledge, this is the first report of secondary metabolites from the marine hydrothermal vent bacterium, *T. ammonificans* (Fig. 3).

Experimental Section

T. ammonificans, a thermophilic, anerobic, and chemolithoautotrophic bacterium, was isolated from the walls of an active deep-sea hydrothermal vent chimney on the East Pacific Rise at 9°50′N. Cells of the organism were Gram-negative, motile rods that were about 1.0 μm in length and 0.6 μm in width. Growth occurred between 60 and 80°C (optimum at 75°C), 0.5% and 4.5% (w/v) NaCl (optimum at 2%), and pH 5 and 7 (optimum at 5.5). The generation time under optimal conditions was 1.57 h. Growth occurred under chemolithoautotrophic conditions in the presence of H_2 and CO_2, with

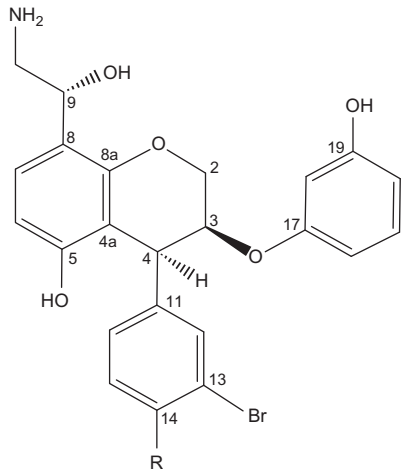

FIGURE 3 Two hydroxyethylamine chroman derivatives, ammonificins A (**1**) and B (**2**).

nitrate or sulfur as the electron acceptor and with concomitant formation of ammonium or hydrogen sulfide, respectively [47].

Forty grams wet weight of the organism were extracted in MeOH (methanol). One part of the MeOH-soluble extract was dissolved in DMSO (dimethyl sulfoxide) and was tested for apoptosis induction as assessed by the ApopScreen protocol [48–50]. Screening should identify compounds that possess proapoptotic, and potentially anticancer, activity.

The extract induced apoptosis and therefore was fractionated, with subsequent purification by analytical RP-HPLC (reverse phase high-pressure liquid chromatography). Using this strategy, two compounds were isolated. The chemical structures of these two compounds (**1** and **2**) were ascertained by standard spectroscopic techniques, as described in the following section.

Structure Elucidation

The LR-ESI-MS (low-resolution electrospray ionization mass spectrometry) of ammonificin A (**1**) displayed ion clusters at *m/z* 488(100)/490(98) indicating the presence of one bromine. The molecular formula of **1** was established as $C_{23}H_{22}BrNO_6$ on the basis of HR-ESI-MS (high-resolution electrospray ionization mass spectrometry) [*m/z* 488.0701 $(M+H)^+$]. The ^1H spectrum of **1** indicated clearly the presence of nine aromatic ring signals: δ_H 6.67 [(d, J=7.9 Hz), H-6], δ_H 7.09 [(d, J=7.9 Hz), H-7], δ_H 7.41 [s, H-12], δ_H 6.77 [(d, J=7.2 Hz), H-15], δ_H 7.26 [(d, J=7.2 Hz), H-16], δ_H 6.65 [s, H-18], δ_H 6.74 [(d, J=7.8 Hz), H-20], δ_H 7.01 [(dd, J=7.8, 7.6 Hz), H-21], and δ_H 6.81

[(d, J=7.6Hz), H-22]. Their corresponding methine carbons were assigned from multiplicity-edited HSQC (heteronuclear single quantum coherence): C-6 (δ 108.0), C-7 (δ 126.8), C-12 (δ 133.1), C-15 (δ 118.4), C-16 (δ 128.8), C-18 (δ 101.4), C-20 (δ 107.3), C-21 (δ 130.5), and C-22 (δ 106.8). Analysis of HMBC (heteronuclear multiple bond correlation) and multiplicity-edited HSQC data suggested the presence of nine quaternary carbons characteristic of signals belonging to aromatic ring systems (δ_C 110.8, 116.1, 119.7, 137.8, 155.7, 156.9, 157.1, 157.9, and 158.9). Given the number of carbon belonging to the aromatic signals, ammonificin A (**1**) was found to possess three aromatic ring systems. Further, three proton signals characteristic of hydroxy groups attached to aromatic ring systems were present in the ^{1}H spectrum: δ_H 8.48 (br, s), δ_H 9.26 (br, s), δ_H 9.47 (br, s). Closer examination of the ^{1}H–^{1}H COSY (correlated spectrometry) along with the ^{1}H NMR spectrum suggested the presence of signals characteristic of a dihydropyran moiety: δ_H 4.35 [(d, J=5.6Hz), H-4], δ_H 4.98 [m, H-3], δ_H 4.45 [m, H-2]. HMBCs between H-6 and C-7 (δ_C 126.8), C-5 (δ_C 155.7), C-4a (δ_C 116.1), H-7 and C-8 (δ_C 119.7), C-8a (δ_C 157.9), H-4 and C-4a (δ_C 116.1), H-2 and C-8a (δ_C 157.9) strongly suggested that **1** has a chroman moiety in its structure. Another interesting group resulting from the ^{1}H–^{1}H COSY analysis is a hydroxyethylamine moiety [51] in **1**: δ_H 4.70 [m, H-9], δ_H 3.45 [m, H-10]. Moreover, this hydroxyethylamine moiety is found to be attached to C-8 according to the HMBC between H-9 and C-8 (δ_C 119.7). The two remaining aromatic rings were established using ^{1}H–^{1}H COSY and HMBCs (Fig. 4). The ^{1}H–^{1}H COSY correlation between H-15 and H-16, HMBCs between H-15 and C-11, C-13, C-14, C-16, and HMBCs between H-12

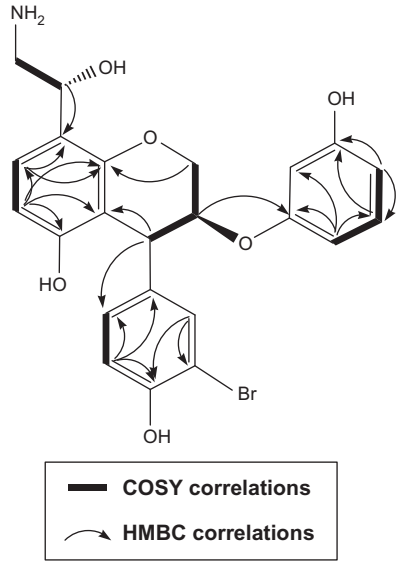

FIGURE 4 Key HMBC and selected COSY correlations for ammonificin A (**1**).

and C-13, C-14, C-16 define a trisubstituted aromatic ring system. The ^{1}H–^{1}H COSY (correlations between H-21 and H-20, H-22, and HMBCs between H-20 and C-19, C-22 and between H-22 and C-17, C-18, C-20) generated a disubstituted aromatic ring system. The connectivity between the chroman moiety and the remaining two ring systems was established by HMBCs: H-4 to C-12, C-16 and H-3 to C-17. The chemical shifts of the quaternary carbons belonging to the aromatic ring systems played an important role in the assignment of the regiochemistry. For example, the chemical shift of the C-5 quaternary carbon (δ_C 155.7) indicated that hydroxy was attached whereas the shift at the C-13 quaternary carbon (δ_C 110.8) indicated bromine was present. Similarly, the chemical shifts at C-14 (δ_C 157.1) and C-19 (δ_C 156.9) indicated that hydroxy groups were attached to these positions.

To determine the absolute configurations at C-3, C-4, and C-9, a CD spectrum of ammonificin A (**1**) was obtained. This experimental CD spectrum was then compared to the predicted CD spectra of all possible stereoisomers. Eight stereoisomers are possible for ammonificin A (**1**). The coupling constant between H-3 and H-4 (J=5.6 Hz) suggested a *cis* relationship between these two protons (H-3 equatorial, H-4 axial) which indicated only four probable stereoisomers: (3*S*,4*S*,9*R*), (3*S*,4*S*,9*S*), (3*R*,4*R*,9*R*), (3*R*,4*R*,9*S*).

These four probable stereoisomers were submitted to geometry optimization by the density functional theory (BLYP/6-31G*) approach [52]. For each minimized geometry, a single CD spectrum was calculated using the TDDFT (time-dependent density functional theory) approach (B3LYP/TZVP) [52]. The overall CD spectra thus obtained were subsequently UV (ultraviolet)-corrected and compared with the experimental one of **1**. An excellent agreement between the CD curve calculated for 3*S*,4*S*,9*R* and the experimental was found (Fig. 5). This indicated that **1** has the following configuration, 3*S*,4*S*,9*R*, and the structure of **1** is established as shown.

The LR-ESI-MS of ammonificin B (**2**) displayed ion clusters at *m*/*z* 550 (51)/552(100)/554(48) indicating the presence of two bromines. The molecular formula of **2** was established as $C_{23}H_{21}Br_2NO_5$ on the basis of HR-ESI-MS [*m*/*z* 549.9857 $(M+H)^+$]. The molecular formula of **2** showed that it has one more bromine atom and one less hydrogen and oxygen atom compared to 1 (Fig. 3).

The strong similarity of its ^{1}H NMR spectrum to that of ammonificin A (**1**) revealed that **1** and **2** share the same general structural features. Further, only two proton signals characteristic of hydroxy groups attached to the aromatic ring system were present in the ^{1}H spectrum of **2** (δ_H 9.27 (br, s), δ_H 9.46 (br, s)), suggesting that one hydroxy group was replaced by one bromine atom. HMBCs between H-16 and C-14 and also between H-12 and C-14 confirmed this suggestion. From the above analyses, it was concluded that the structure of **2** is similar to that of **1** except that the hydroxy group attached to C-14 was replaced by one bromine atom. The absolute configurations

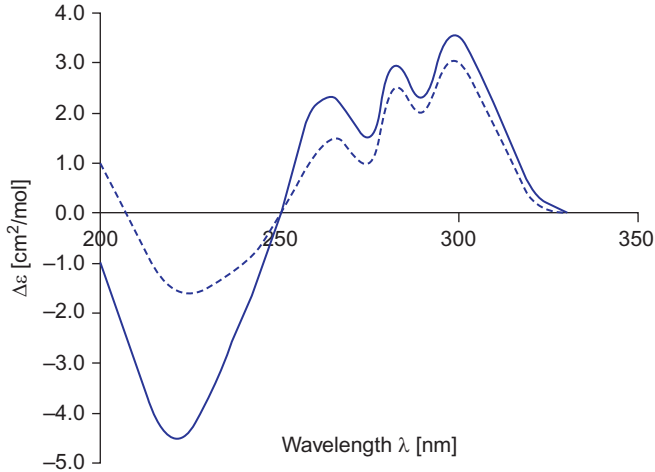

FIGURE 5 Comparison of the experimental CD spectrum (——) of **1** with the spectra calculated (· · ·–· · ·) for 3*S*,4*S*,9*R*.

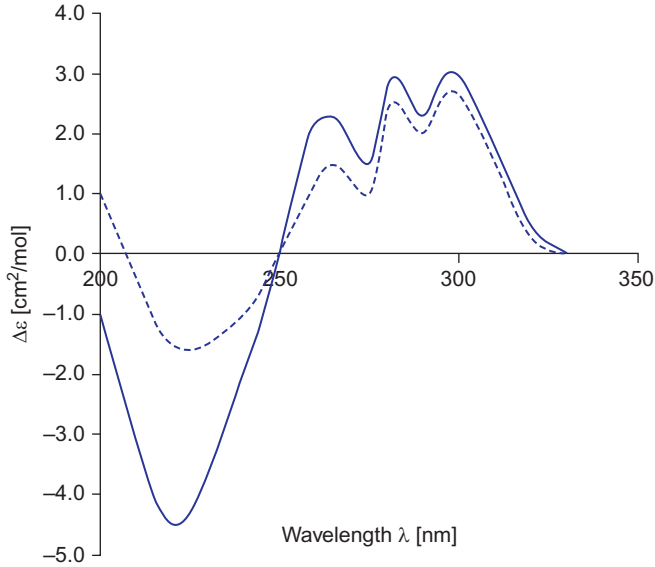

FIGURE 6 Comparison of the experimental CD spectrum (——) of **2** with the spectra calculated (· · ·–· · ·) for 3*S*,4*S*,9*R*.

at C-3, C-4, and C-9 of ammonificin B (**2**) were ascertained by the same methods as described above (Fig. 6). Although chroman derivatives are known structures, the co-occurrence of hydroxyethylamine and phenol in **1** or brominated phenol in **2** with chroman is unique.

Bioassay

The isolated compounds were evaluated in the apoptosis induction assay and with antimicrobial tests, but the results were inconclusive due to the presence of minor inseparable impurities. The original extract showed interesting activity; however, pure compounds that correlated with the activity were not obtained. The minor components that could not be removed during the purification process probably have similar structure and polarity to **1** and **2**. An effort to scale up the culture and reisolate ammonificins A and B as well as the minor components of the extract is still in progress. The compounds described herein represent new chemical structures and may have potential in future drug discovery efforts.

BATHYMODIOLAMIDES A AND B, CERAMIDE DERIVATIVES FROM A DEEP-SEA HYDROTHERMAL VENT INVERTEBRATE MUSSEL, *B. THERMOPHILUS*

Introduction

Two ceramide derivatives, bathymodiolamides A (**1**) and B (**2**), were isolated from the deep-sea hydrothermal vent invertebrate mussel, *B. thermophilus*. The molecular structures of these compounds were determined using a combination of NMR spectroscopy, mass spectrometry, and chemical degradation. Biological activities were assessed in an ApopScreen cell-based screen for apoptosis induction and potential anticancer activity. To our knowledge, this is the first report of secondary metabolites from the marine hydrothermal vent mussel *B. thermophilus* (Fig. 7).

Experimental Section

Thirty specimens of *B. thermophilus* were collected using the deep submergence vehicle *DSV Alvin* from an active hydrothermal vent along the Mid-Atlantic Ridge, northern region, at the Lucky Strike location with a latitude

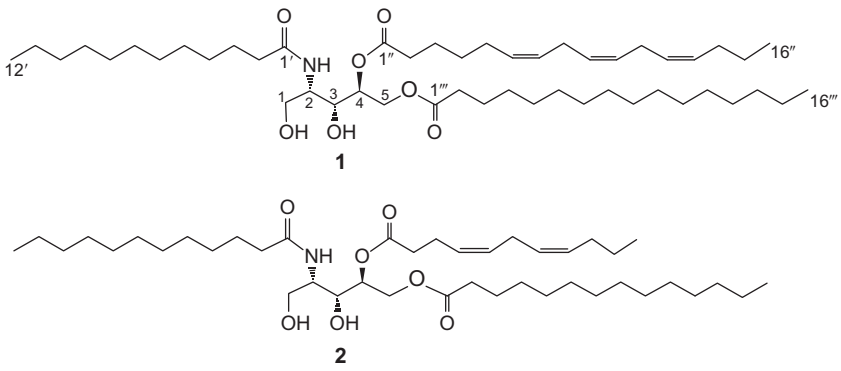

FIGURE 7 Two ceramide derivatives, bathymodiolamides A (**1**) and B (**2**).

of 37°17.63′N, longitude of 32°16.53′W, and depth of 1733 m [53]. Once aboard the research vessel, the mussels were dissected, and samples of adductor muscle, gill, and mantle tissues were frozen at −70 °C for subsequent analyses. One hundred grams wet weight of the tissues from approximately 20 gills were extracted in MeOH. One part of the MeOH-soluble extract was dissolved in DMSO, and was tested for apoptosis induction as assessed by the ApopScreen protocol [48–50]. Screening was expected to identify compounds that possess proapoptotic, and potentially anticancer, activity.

The extract induced apoptosis and therefore was fractionated, with subsequent purification by analytical RP-HPLC. Using this strategy, two compounds were isolated. The chemical structures of these two compounds (**1** and **2**) were ascertained by standard spectroscopic techniques, as described in the following section.

Structure Elucidation

The molecular formula of **1** was established as $C_{49}H_{89}NO_7$ on the basis of HR-MALDI-TOF-MS (high-resolution matrix-assisted laser desorption ionization time-of-flight mass spectrometry) [*m/z* 804.6712 $(M+H)^+$]. The ^{13}C NMR spectrum for **1** clearly indicated resonances for three ester or amide carbonyl carbons (δ_C 173.2, 173.4, 173.8), as well as four oxygen-bearing carbons (δ_C 59.9, 62.5, 63.7, 66.1) and one nitrogen-bearing carbon (δ_C 53.5, δ_H 4.29). Analysis of the multiplicity-edited HSQC spectrum for **1** revealed that these heteroatom-substituted carbons comprise two methylenes (CH_2-1, δ_C 63.7, δ_H 3.65; CH_2-5, δ_C 59.9, δ_{H5a} 4.20, δ_{H5b} 4.45) and three methines (CH-2, δ_C 53.5, δ_H 4.29; CH-3, δ_C 62.5, δ_H 4.01; CH-4, δ_C 66.1, δ_H 5.25). The HMBCs between H-2 and the carbonyl at δ_C 173.2, H-4 and the carbonyl at δ_C 173.4, and H-5a and H-5b and the carbonyl at δ_C 173.8 suggested that **1** has an amide moiety attached to C-2 and two ester moieties attached to C-4 and C-5. Considering the molecular formula and all carbon signals for **1**, the remaining oxygen-bearing carbons C-1 and C-3 are substituted with hydroxy groups, resulting in primary and secondary alcohols at C-1 and C-3, respectively. The connectivity of C-1 through C-5 of **1** was established from COSY data as shown in Fig. 8, confirming the presence of the amino alcohol moiety in **1** (Fig. 8).

The remaining partial structures for **1** could be assigned as three acyl moieties. Given the six degrees of unsaturation of **1** based on its molecular formula, three double bonds must be present in one or more of the three acyl moieties. The HMBCs from δ_H 5.35 to δ_C 26.5 and from δ_H 2.81 to δ_C 127.5, taken together with the 4H integral of the signal at δ_H 2.81 in ^1H NMR spectrum of **1**, indicated the occurrence of four bis-allylic protons and two bis-allylic methylene carbons, suggesting that all three double bonds are located in one branch of the aliphatic side chain. Since bis-allylic carbon signals for *Z* and *E* isomers are observed at ca. δ_C 27 and 32, respectively [54,55], the 26.5 ppm shift suggested that all double bonds have a *cis* geometry (*Z*).

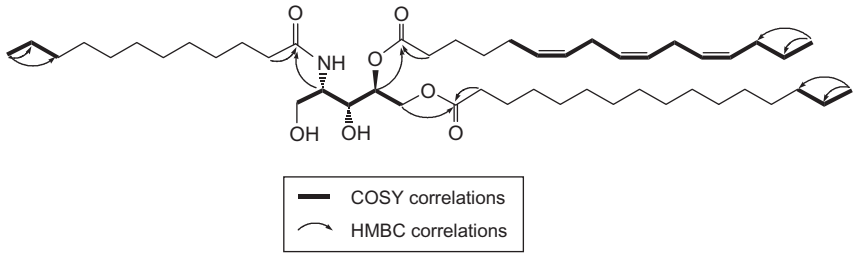

FIGURE 8 Key HMBC and selected COSY correlations for bathymodiolamide A (**1**).

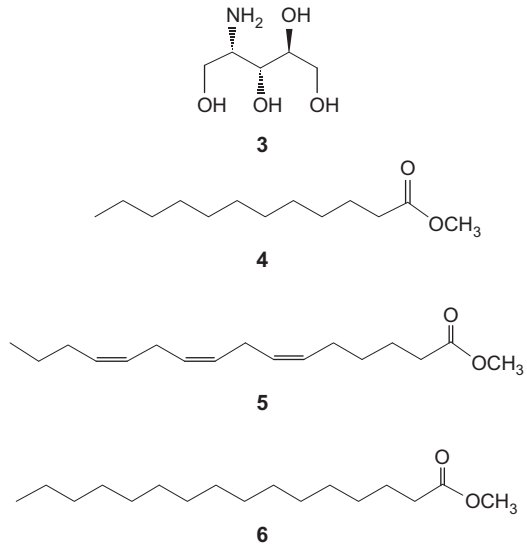

FIGURE 9 Compounds **3**–**6** resulting from chemical degradation of **1**.

To deduce the identity of the fatty acids, **1** was subjected to a transesterification reaction in MeOH/NaOMe (2h). After routine work-up of the reaction, the nonpolar organic extract was analyzed by GC–MS (gas chromatography linked to mass spectrometry) and ESI-MS (electrospray ionization mass spectrometry), and three ion peaks $[M+H]^+$ at *m/z* 215.2010, 265.2166, and 271.2636 were observed, corresponding to dodecanoic acid methyl ester (**4**), hexadecatrienoic acid methyl ester (**5**), and hexadecanoic acid methyl ester (**6**), respectively (Fig. 9).

The regiochemical distribution of these three acyl chains was established using different ionization mass spectrometry analyses. The amide bond was most readily recognized [56] by MALDI-TOF-MS/MS $[M+H]^+$ at *m/z* 184.1, corresponding to the cleavage of the dodecanoyl moiety. ESI-MS [57] was used to differentiate the acyl attached at C-4 and C-5. Fragmentation by positive-mode ESI-MS generated a more stable fragment ion from

cleavage of the acyl chain attached at C-5 than cleavage of the acyl chain attached to C-4. In contrast, the negative-mode ESI-MS fragment ion resulting from cleavage of the acyl chain attached at C-4 is more stable. Successive losses of dodecanoyl and hexadecatrienoyl moieties were observed in the negative-mode ESI-MS (*m/z* 584.2 and 367.1, respectively). From these analyses, it was concluded that the dodecanoyl moiety is attached to C-2, while the hexadecatrienoyl and hexadecanoyl moieties are attached to C-4 and C-5, respectively. To verify this conclusion, a selective enzyme reaction was performed. Upon regioselective enzymic hydrolysis of **1** with lipase enzyme type III in dioxane–H_2O (1:1) at 37°C for 4h [58], only hexadecanoic acid was obtained, as evidenced by ESI-MS and comparison with an authentic sample. Thus, it was concluded that the hexadecanoyl residue is attached to C-5 of **1**.

The aqueous phase from the hydrolysis product of **1** yielded an aminotetraol (**3**), which was identified as (2*S*,3*S*,4*R*)-2-amino-1,3,4,5-pentane tetraol. The relative configuration of **3** was elucidated using the $^3J_{H,H}$ coupling constant analysis from an NMR database for a given stereocluster [59]. Eight stereoisomers are possible for aminotetraol (**3**), depending on the relative position of H-2 and H-3 (S=*Syn* or A=*Anti*) and H-3 and H-4 (S=*Syn* or A=*Anti*), the eight isomers are classified as follows: one pair of SS, one pair AA, one pair of SA, and one pair of AS. According to the value recorded for **3** of $^3J_{H,H}$ coupling constant between H-2 and H-3 (J=2.5Hz) and H-3 and H-4 (J=7Hz), H-2 and H-3 are on the same side (S=*Syn*) and H-3 and H-4 are on the opposite side (A=*Anti*), thus the remaining probable stereoisomers are the pair of SA: (2*S*,3*S*,4*R*)-2-amino-1,3,4,5-pentane tetraol and (2*R*,3*R*,4*S*)-2-amino-1,3,4,5-pentane tetraol. Theoretically, these two isomers should have opposite optical rotation sign. The positive optical rotation of **3** ($[\alpha]^{24}_D$=+8 (ca. 0.05, H_2O)) favors the (2*S*,3*S*,4*R*)-2-amino-1,3,4,5-pentane tetraol configuration as that seen in L-*arabino*-phytosphingosine ($[\alpha]^{25}_D$=+5 (ca. 0.51, pyridine)) [60], which is also the opposite of that observed in D-*arabino*-phytosphingosine ($[\alpha]^{25}_D$=−4.3 (ca. 0.50, pyridine)) [60]. The identical coupling constants between H-2 and H-3 (J=3Hz) and H-3 and H-4 (J=6Hz) along with the optical rotation reported ($[\alpha]^{27}_D$=+9.2 (ca. 0.05, MeOH)) for the sphingosine derivative [61,62,73] and bathymodiolamides A (**1**) further suggested a (2*S*,3*S*,4*R*)-configuration of the sphingosine-like moiety in **1**. From the above data, the structure of **1** was established as shown.

The molecular formula of **2** was established as $C_{42}H_{77}NO_7$ on the basis of HR-MALDI-TOF-MS (*m/z* 730.5594 $[M+Na]^+$). The strong similarity of its ^1H NMR spectrum to that of bathymodiolamide A (**1**) revealed that **1** and **2** share the same general structural features. Upon regioselective enzymic hydrolysis of **2** with lipase enzyme type III in dioxane–H_2O (1:1) at 37°C for 4h [63], only tetradecanoic acid was obtained, as established by ESI-MS analysis and comparison with an authentic sample. Thus, it was concluded that the tetradecanoyl residue is attached to the C-5 position of **2**. The hydrolysis of **2** gave similar results to those observed for **1**, with the exception of

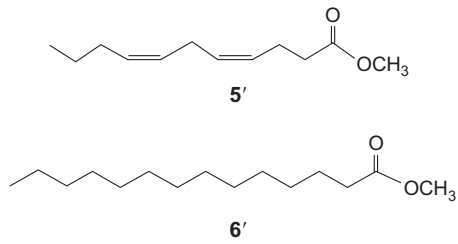

FIGURE 10 Compounds **5′** and **6′** resulting from chemical degradation of **2**.

the presence of undecadienoic acid methyl ester (**5′**) and tetradecanoic acid methyl ester (**6′**) (Fig. 10). The structure of **2** is similar to **1** with undecadienoyl and tetradecanoyl residues at C-4 and C-5, respectively. Thus, the structure of **2** was established as shown.

Bioassay

The isolated compounds were evaluated in the apoptosis induction assay. The results showed that **1** and **2** inhibit the growth of two cancer cell lines [HeLa (cervical cancer) (IC_{50}=0.4 μM for **1** and IC_{50}=0.5 μM for **2**) and MCF7 (breast cancer) (IC_{50}=0.1 μM for **1** and IC_{50}=0.2 μM for **2**)]. The compounds described herein represent new chemical structures and may have potential in future drug discovery efforts. Another interesting observation is that although the deep-sea hydrothermal vents are characterized by high concentrations of reduced sulfur compounds, the presence of sulfur-containing secondary metabolite from the deep-sea hydrothermal vent invertebrate mussel, *B. thermophilus* is not detected.

INDUCTION OF APOPTOSIS BY DITERPENES FROM THE SOFT CORAL *XENIA ELONGATA*

Introduction

Four new diterpenes (**1**–**4**) were isolated from the soft coral *X. elongata* using a novel cell-based screen for apoptosis-inducing, potential anticancer compounds. The molecular structures of the diterpenes were determined using a combination of NMR and MS. The bioactivities were confirmed using a specific apoptosis induction assay based on genetically engineered mammalian lines with differential, defined capacities for apoptosis. The diterpenes induce apoptosis in micromolar concentrations. This is the first report of apoptosis induction by marine diterpenes in xenicane skeletons (Fig. 11).

Bioassay and Efficacy of the Apoptosis Induction Assay for Screening

In order to assess the proapoptotic activities of these compounds as a marker for their potential anticancer efficacy, MeOH-soluble fractions of *Xenia*

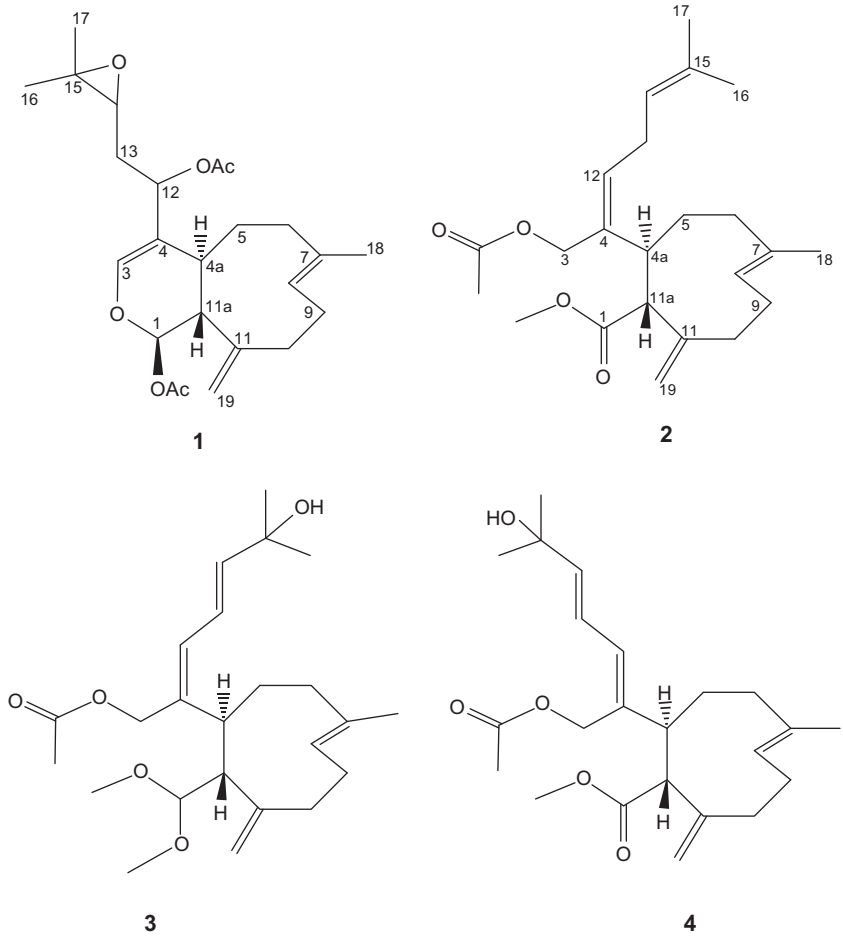

FIGURE 11 Four new diterpenes (**1**–**4**) isolated from the soft coral *Xenia elongata*.

extracts were tested for apoptosis induction in an MTT assay using the apoptosis-competent W2 and apoptosis-resistant D3 cells, as described above. Compounds **1**–**4** induce measurable cell death in W2 but not in D3 cells. To quantify apoptosis induction, viability was determined using an MTT assay. Measurements were taken at time 0 and 48 h after addition of compounds in different concentrations. Viability was calculated as the difference between time 0 (addition of compound) and 48 h. Apoptosis induction was defined as at least 20% death of W2 cells and a 10% or higher growth of D3 cells by MTT assay. The optimal concentration of the compounds for apoptosis induction was determined on the basis of the dose–response of the two cells lines by MTT assay. The results (Fig. 12A) reveal a significant induction of apoptosis by the whole tissue extract and by individual compounds, with the most remarkable induction shown by compound **1** (61% growth of D3 and 50%

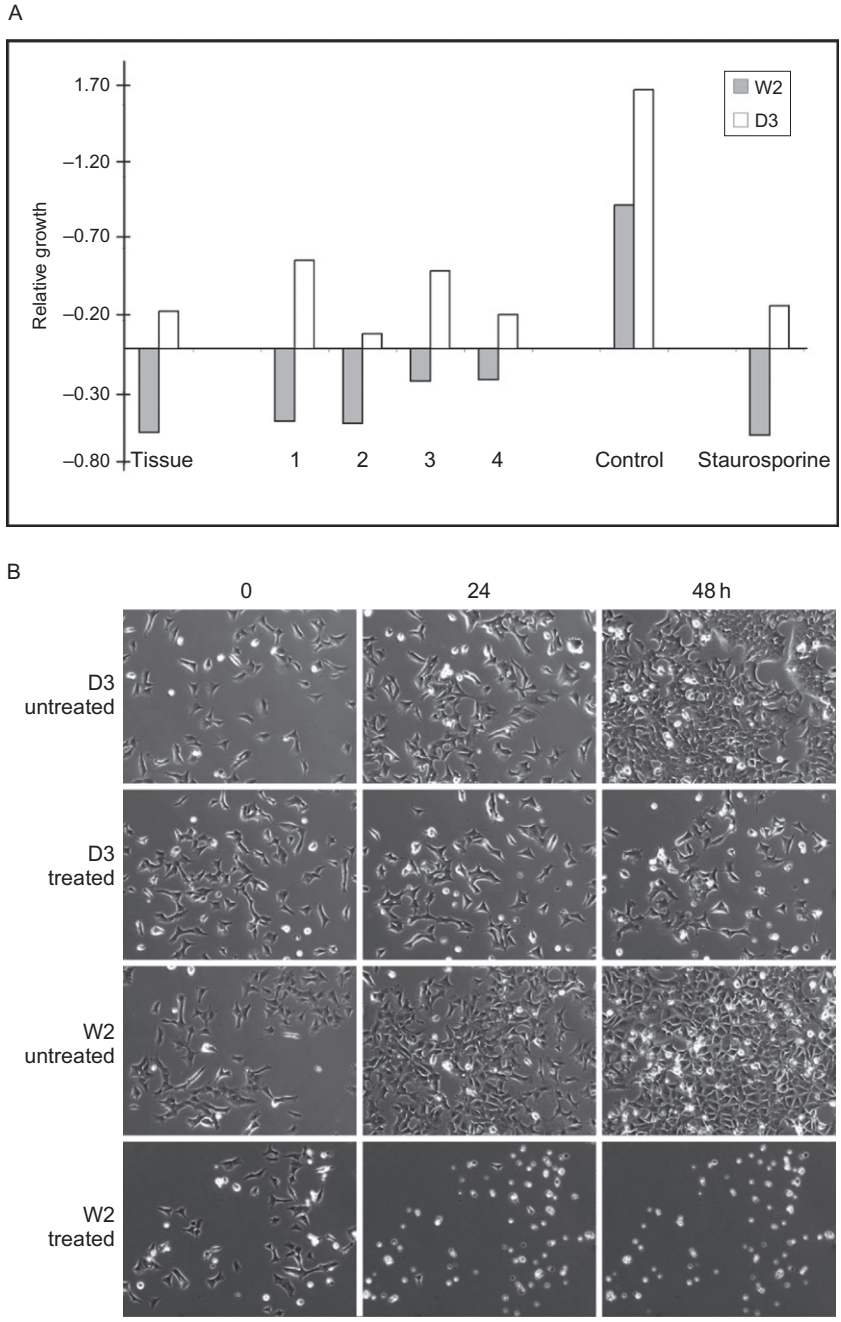

FIGURE 12 (A) Change in relative W2 and D3 cell viability by MTT assay 48 h after addition of whole tissue extract, **1**, **2**, **3**, and **4** (**1**, 12 μM; **2**, 29 μM; **3**, 12 μM; **4**, 11 μM). Staurosporine (0.1 μM), a known apoptosis inducer, and untreated cells were used as positive and negative controls. Values for the compounds are an average of five wells, with a standard deviation of less than

death of W2). Treatment of W2 and D3 cells with 0.1 μM staurosporine, a protein kinase inhibitor and potent inducer of apoptosis, was included as a positive control for apoptosis induction for comparison, which induced apoptosis at comparable levels to compound **1** (Fig. 12A). Thus, the diterpenes we have isolated effectively and specifically activate apoptosis in immortalized mammalian epithelial cells. In order to determine the differential impact of apoptosis induction on cell growth and viability of W2 and D3 cells, we monitored the cell division and viability by time-lapse microscopy. W2 and D3 cells were incubated for 48 h in the presence of compound **1** (12 μM) (Fig. 12B). Both W2 and D3 cell lines showed comparable cell viability in the absence of the drug (Fig. 12B). D3 cells retained their viability in presence of compound **1** even at 48 h, and this viability persisted following 72 h of treatment. There was, however, clear indication of growth arrest in the treated D3 cells. In stark contrast, W2 cells were highly sensitive to apoptosis induced by compound **1**. The apoptosis-competent W2 cells became rounded and detached from the surface between 18 and 24 h of treatment, displaying classic apoptotic morphology by time-lapse microscopy. Survival of the D3 cells for at least 72 h in contrast to the induction of cell death of W2 cells within 18–24 h of treatment with compound **1** suggests that compound **1** induced Bax- and Bak-mediated apoptosis. Taken together, these observations suggest that compound **1** induces apoptosis when the apoptosis pathway is intact and mediates cell growth arrest in the absence of a functional apoptosis pathway.

Soft corals belonging to the genus *Xenia* are a rich source of diterpenoids [64,65], which are characterized by a nine-membered monocarbocyclic ring. The structures of *Xenia* diterpenoids have been divided into three groups: xenicins (containing a dihydropyrancyclononane skeleton), xeniolides (possessing a δ-lactone-cyclononane skeleton), and xeniaphyllanes (with a bicyclo[7.2.0] undecane skeleton) [66,67]. Xenicanes combine unique structural features with interesting biological activities; specifically, they often are cytotoxic against several murine and human cancer cell lines [68,69]. A major limitation regarding the exploration of natural products from marine invertebrates, especially diterpenes, has been the difficulty in obtaining these compounds in sufficient quantities [70,71]. First, attempting to reisolate reasonable amounts of the same compound from the organism is difficult given the changing natural growth environment of these organisms. Second, the framework of nine-membered rings and the particular arrangement of functional groups with multiple embedded stereocenters limit the range of chemical reactions that are applicable to their synthesis. There is little in the existing synthetic literature to define an

15% of the mean. (B) Compound **1** is a specific inducer of apoptosis in mammalian cells. The apoptosis-competent W2 cells and the apoptosis-resistant D3 cells were cultured in the presence or absence of compound **1** (12 μM) under normal physiological conditions (DMEM with 10% FBS, 5% CO_2 at 37°C), and the cell viability was monitored by time-lapse microscopy. D3 cells were viable in the presence of compound **1** beyond 48 h, whereas the apoptosis-competent W2 cells showed massive apoptosis induction and significant loss of viability by 24 h of treatment.

effective strategy for the synthesis of xenicanes [71]. The first total synthesis of an optically active xenicane diterpene has not yet been achieved [71,72]. However, we purified these compounds from *Xenia* grown under optimal conditions in a controlled environment that potentially facilitates reisolation of reasonable amounts of these compounds. In addition, an effort to synthesize these diterpenes is underway.

The compounds described here represent a potential platform for the identification of natural products with specific proapoptotic, and therefore anticancer, activities. This work describes bioactivity of four novel diterpenes from the soft coral *X. elongata* using a high-throughput cell-based screen that we have developed to identify compounds that induce apoptosis in precancerous mammalian epithelial cells. The vast majority of human solid tumors are of epithelial origin, and defects in apoptosis, mostly upstream of Bax and Bak, play important roles in both tumor suppression and mediation of chemotherapeutic response. Consequently, efforts are increasingly focused on developing drugs that can reactivate the apoptotic pathway. The compounds identified here induce apoptosis upstream of Bax and Bak and may have a potential for use as anticancer agents that exploit the apoptosis pathway in tumor cells.

CONCLUSION

Considering the new bioactive natural products discussed here and given the enormous diversity of organism from the hydrothermal vent and following our investigation and finding we demonstrated that it is possible to culture organisms and isolate new bioactive natural products from deep-see hydrothermal vent using rational approach and strategy. The use of ApopScreen, the new cell-based assay specific for the isolation and identification of apoptosis-inducing compounds that are potential anticancer agents, is proven to be very efficient and powerful.

The investigation and exploration of organism from deep-sea hydrothermal vent is just at the early stage of research. The geological setting and geochemical nature of deep-sea vents that impact the biogeography of vent organisms, chemosynthesis, and the known biological and metabolic diversity of eukarya, bacteria, and archaea, including the handful of natural products isolated to date from deep-sea vent organisms, need to be taken into consideration in order to fully demonstrate that the deep-sea hydrothermal vents is probably a new source of drug discovery and may be potential hot spots for natural product investigations.

ACKNOWLEDGMENTS

The authors gratefully acknowledge grants from NSF (OCE 03-27373) and MCB (04-56676) and the fund from Rutgers University through an academic excellence award. Also, we are indebted to Dr. Eileen White and Dr. Kerry McPhail for assistance in the preparation of the manuscript.

ABBREVIATIONS

CD	circular dichroism
COSY	correlated spectrometry
DFT	density functional theory
DHVEG	Deep-Sea Hydrothermal Vent Euryarchaeoic Group
DMSO	dimethyl sulfoxide
DNA	deoxyribonucleic acid
ESI-MS	electrospray ionization mass spectrometry
GC–MS	gas chromatography linked to mass spectrometry
HMBC	heteronuclear multiple bond correlation
HMQC	heteronuclear multiple quantum coherence
HPLC	high-pressure liquid chromatography
HSQC	heteronuclear single quantum coherence
HR-ESI-MS	high-resolution electrospray ionization mass spectrometry
HR-MALDI-TOF-MS	high-resolution matrix-assisted laser desorption ionization time-of-flight mass spectrometry
IC_{50}	the half maximal inhibitory concentration
LR-ESI-MS	low-resolution electrospray ionization mass spectrometry
MeOH	methanol
MS	mass spectrometry
MS/MS	tandem mass spectrometry method
NMR	nuclear magnetic resonance
PCR	polymerase chain reaction
RNA	ribonucleic acid
rRNA	ribosomal RNA
RP-HPLC	reverse phase high-pressure liquid chromatography
SSU	small subunit
TDDFT	time-dependent density functional theory
UV	ultraviolet

REFERENCES

[1] A. Gärtner, J. Wiese, J.F. Imhoff, Int. J. Syst. Evol. Microbiol. 58 (2008) 34–39.
[2] C.E. Kicklighter, C.R. Fisher, M.E. Hay, Mar. Ecol. Prog. Ser. 275 (2004) 11–19.
[3] H.A. Nees, T.S. Moore, K.M. Mullaugh, R.R. Holyoke, C.P. Janzen, S. Ma, E. Metzer, T.J. Waite, M. Yücel, R.A. Lutz, T.M. Shank, C. Vetriani, D.B. Nuzzio, G.W. Luther III, J. Shellfish Res. 27 (2008) 169–175.
[4] J. Adams, Genes Dev. 17 (2003) 2418–2495.
[5] N. Danial, S. Korsmeyer, Cell 116 (2004) 205–219.
[6] C. Gelinas, E. White, Genes Dev. 19 (2005) 1263–1268.
[7] K. Degenhardt, E. White, Clin. Cancer Res. 12 (2006) 5274–5276.
[8] S.W. Fesik, Nat. Rev. Cancer 5 (2005) 876–885.
[9] K. Degenhardt, R. Sundararajan, G. Chen, T. Lindsten, C. Thomson, E. White, J. Biol. Chem. 277 (2002) 14127–14134.

[10] K. Degenhardt, G. Chen, T. Lindsten, E. White, Cancer Cell 2 (2002) 193–203.
[11] K. Degenhardt, R. Mathew, B. Beaudoin, K. Bray, D. Anderson, G. Chen, C. Mukherjee, Y. Shi, C. Gélinas, Y. Fan, Cancer Cell 10 (2006) 51–64.
[12] T.T. Tan, K. Degenhardt, D.A. Nelson, B. Beaudoin, W. Nieves-Neira, P. Bouillet, A. Villunger, J.M. Adams, E. White, Cancer Cell 7 (2005) 227–238.
[13] D.A. Nelson, E. White, Genes Dev. 18 (2004) 1223–1226.
[14] E. White, Cell Death Differ. 13 (2006) 1371–1377.
[15] C.C. Thornburg, T.M. Zabriskie, K.L. McPhail, J. Nat. Prod. 73 (2010) 489–499.
[16] W.E. Seyfried Jr., M.J. Mottl, D.M. Karl (Ed.), The Microbiology of Deep-Sea Hydrothermal Vents, CRC Press, Inc., Boca Raton, FL, 1995, pp. 1–34.
[17] C.L. Van Dover, ICES J. Mar. Sci. 68 (2011) 341–348.
[18] C.L. Van Dover, The Ecology of Deep-Sea Hydrothermal Vents, Princeton University Press, Princeton, NJ, 2000.
[19] J.J. Childress, C.R. Fisher, M. Barnes, A.D. Ansell, R.N. Gibson (Eds.), Oceanography and Marine Biology: An Annual Review, UCL Press Limited, London, 1992, pp. 337–441 vol. 30.
[20] J. Marcus, V. Tunnicliffe, D.A. Butterfield, Deep-Sea Res., Part II 56 (2009) 1586–1598.
[21] D. Desbruyères, M. Segonzac, M. Bright (Eds.), Handbook of Deep-Sea Hydrothermal Vent Fauna, second ed., In: Denisia Series, 18 Biologiezentrum der Oberösterreichischen Landesmuseen, Linz, Austria, 2006.
[22] W.E. Seyfried Jr., M.J. Mottl, D.M. Karl (Ed.), The Microbiology of Deep-Sea Hydrothermal Vents, CRC Press, Inc., Boca Raton, FL, 1995, pp. 1–34.
[23] V. Tunnicliffe, C.M.R. Fowler, Nature 379 (1996) 531–533.
[24] C.L. Van Dover, S.E. Humphris, D. Fornari, C.M. Cavanaugh, R. Collier, S.K. Goffredi, J. Hashimoto, M.D. Lilley, A.L. Reysenbach, T.M. Shank, K.L. Von Damm, A. Banta, R.M. Gallant, D. Gotz, D. Green, J. Hall, T.L. Harmer, L.A. Hurtado, P. Johnson, Z.P. McKiness, C. Meredith, E. Olson, I.L. Pan, M. Turnipseed, Y. Won, C.R. Young III, R.C. Vrijenhoek, Science 294 (2001) 818–823.
[25] D.S. Kelley, J.A. Baross, J.R. Delaney, Annu. Rev. Earth Planet. Sci. 30 (2002) 385.
[26] C.R. Woese, Microbiol. Mol. Biol. Rev. 68 (2004) 173–186.
[27] M.K. Tivey, Oceanus 34 (1991) 68–74.
[28] R.M. Haymon, Nature 301 (1983) 695–698.
[29] V. Robigou, J.R. Delaney, D.S. Stakes, Geophys. Res. Lett. 20 (1993) 1887–1890.
[30] B.B. Jørgensen, A. Boetius, Nat. Rev. Microbiol. 5 (2007) 770–781.
[31] R. Amann, W. Ludwig, K. Schleifer, Microbiol. Rev. 59 (1995) 143–169.
[32] N.R. Pace, Science 276 (1997) 734–740.
[33] M.L. Sogin, H.G. Morrison, J.A. Huber, D.M. Welch, S.M. Huse, P.R. Neal, J.M. Arrieta, G.J. Herndl, Proc. Natl. Acad. Sci. USA 103 (2006) 12115–12120.
[34] J.C. Venter, K. Remington, J.F. Heidelberg, A.L. Halpern, D. Rusch, J.A. Eisen, D. Wu, I. Paulsen, K.E. Nelson, W. Nelson, D.E. Fouts, S. Levy, A.H. Knap, M.W. Lomas, K. Nealson, O. White, J. Peterson, J. Hoffman, R. Parsons, H. Baden-Tillson, C. Pfannkoch, Y.-H. Rogers, H.O. Smith, Science 304 (2004) 66–74.
[35] J.A. Huber, D.A. Butterfield, J.A. Baross, Appl. Environ. Microbiol. 68 (2002) 1585–1594.
[36] K. Takai, K. Horikoshi, Genetics 152 (1999) 1285–1297.
[37] D.R. Green, G. Kroemer, Science 305 (2004) 626–629.
[38] A.M. Petros, J. Dinges, D.J. Augeri, S.A. Baumeister, D.A. Betebenner, M.G. Bures, S.W. Elmore, P.J. Hajduk, M.K. Joseph, S.K. Landis, D.G. Nettesheim, S.H. Rosenberg, W. Shen, S. Thomas, X. Wang, I. Zanze, H. Zhang, S.W. Fesik, J. Med. Chem. 49 (2006) 656–663.

[39] D. Chauhan, P. Neri, M. Velankar, K. Podar, T. Hideshima, M. Fulciniti, P. Tassone, N. Raje, C. Mitsiades, N. Mitsiades, P. Richardson, L. Zawel, M. Tran, N. Munshi, K.C. Anderson, Blood 109 (2007) 1220–1227.
[40] H. Sun, Z. Nikolovska-Coleska, C.-Y. Yang, L. Xu, Y. Tomita, K. Krajewski, P.P. Roller, S. Wang, J. Med. Chem. 47 (2004) 4147–4150.
[41] V. Karantza-Wadsworth, E.H. Rubin, et al., Phase I Study of Paclitaxel (Taxol) and Bortezomib (Velcade) in Patients with Refractory Solid Tumor Malignancies Involving an Activated MAPK Pathway, http://clinicaltrials.gov/show/NCT00667641, 2006.
[42] J.A. Gollob, S. Wilhelm, C. Carter, S.L. Kelley, Semin. Oncol. 33 (2006) 392–406.
[43] J. Marshall, Cancer 107 (2006) 1207–1218.
[44] R. Ohno, Int. J. Clin. Oncol. 11 (2006) 176–183.
[45] R. Schreck, U.R. Rapp, Int. J. Cancer 119 (2006) 2261–2271.
[46] C. Swanton, A. Futreal, T. Eisen, Clin. Cancer Res. 12 (2006) 4377s–4383s.
[47] C. Vetriani, M.D. Speck, S.V. Ellor, R.A. Lutz, V. Starovoytov, Int. J. Syst. Evol. Microbiol. 54 (2004) 175–181.
[48] E.H. Andrianasolo, L. Haramaty, K. Degenhardt, R. Mathew, E. White, R. Lutz, P. Falkowski, J. Nat. Prod. 70 (2007) 1551–1557.
[49] R. Mathew, K. Degenhart, L. Haramaty, C.M. Karp, E. White, Methods Enzymol. 453 (2008) 53–81.
[50] V. Karantza-Wadsworth, E. White, V.T. DeVita, T.S. Lawrence, S.A. Rosenberg (Eds.), Programmed Cell Death. Cancer: Principles and Practice of Oncology, Lippincott, Williams, and Wilkins, Philadelphia, PA, 2008, pp. 93–101.
[51] E. Fahy, B.C.M. Potts, J. Faulkner, J. Nat. Prod. 54 (1991) 564–569.
[52] R. Ahlrichs, F. Furche, C. Hättig, W. Klopper, M. Sierka, F. Weigend, TURBOMOLE 5.10, in: (2008).
[53] H.A. Nees, T.S. Moore, K.M. Mullaugh, R.R. Holyoke, C.P. Janzen, S. Ma, E. Metzer, T.J. Waite, M. Yücel, R.A. Lutz, T.M. Shank, C. Vetriani, D.B. Nuzzio, G.W. Luther III, J. Shellfish Res. 27 (2008) 169–175.
[54] T. Ishii, T. Okino, Y. Mino, J. Nat. Prod. 69 (2006) 1080–1082.
[55] P. Scribe, J. Guezennec, J. Dagaut, C. Pepe, A. Saliot, Anal. Chem. 60 (1988) 928–931.
[56] S. Koster, M.C. Duursma, J.J. Boon, R.M.A. Heeren, S. Ingemaan, R.A.T.M. Van Benthem, C.G. Kostert, J. Am. Soc. Mass Spectrom. 14 (2003) 332–341.
[57] G. Guella, R. Frassanito, I. Mancini, Rapid Commun. Mass Spectrom. 17 (2003) 1982–1994.
[58] I. Kitagawa, K. Hayashi, M. Kobayashi, Chem. Pharm. Bull. 37 (1989) 849–851.
[59] H. Seike, I. Ghosh, Y. Kishi, Org. Lett. 8 (2006) 3861–3864.
[60] J.-J. Park, J.H. Lee, Q. Li, K. Diaz, Y.-T. Chang, S.-K. Chung, Bioorg. Chem. 36 (2008) 220–228.
[61] H.S. Garg, S. Agrawal, J. Nat. Prod. 58 (1995) 442–445.
[62] J. Mulzer, C. Brand, Tetrahedron 42 (1986) 5961–5964.
[63] I. Kitagawa, K. Hayashi, M. Kobayashi, Chem. Pharm. Bull. 37 (1989) 849–851.
[64] A.A.H. El-Gamal, S.-K. Wang, C.-Y. Duh, J. Nat. Prod. 69 (2006) 338–341.
[65] C. Anta, N. Gonzalez, G. Santafe, J.C. Rodriguez, J. Nat. Prod. 65 (2002) 766–768.
[66] Y. Kashman, A. Groweiss, J. Org. Chem. 45 (1980) 3814–3824.
[67] Y.-B. Cheng, J.-Y. Jang, A.T. Khalil, Y.-H. Kuo, Y.-C. Shen, J. Nat. Prod. 69 (2006) 675–678.
[68] C.-Y. Duh, A.A.H. El-Gamal, C.Y. Chiang, C.-J. Chu, S.-K. Wang, C.-F. Dai, J. Nat. Prod. 65 (2002) 1882–1885.
[69] A.A.H. El-Gamal, C.-Y. Chiang, S.-H. Huang, S.-K. Wang, C.-Y. Duh, J. Nat. Prod. 68 (2005) 1336–1340.

[70] E.H. Andrianasolo, D. France, S. Cornell-Kennon, W.H. Gerwick, J. Nat. Prod. 69 (2006) 576–579.
[71] A. Pollex, M. Hiersemann, Org. Lett. 7 (2005) 5705–5708.
[72] C.S. Mushti, J.-H. Kim, E.J. Corey, J. Am. Chem. Soc. 128 (2006) 14050–14052.
[73] T. Natori, M. Morita, K. Akimoto, Y. Koezuka, Tetrahedron 50 (1994) 2771–2774.

Chapter 4

Marine Cyanobacteria: A Treasure Trove of Bioactive Secondary Metabolites for Drug Discovery

Lik Tong Tan

Natural Sciences and Science Education, National Institute of Education, Nanyang Technological University, Singapore, Singapore

INTRODUCTION

Filamentous marine cyanobacteria continue to be a source of unique and biologically active nitrogen-containing secondary metabolites. Currently, there are more than 400 of these natural products isolated from various marine cyanobacterial strains, including the genera *Lyngbya* and *Symploca*. A majority of these compounds are biosynthesized by a hybrid of multimodular enzymatic systems, comprising the polyketide synthases and the nonribosomal polypeptide synthetases [1,2]. Recent biosynthetic and genetic studies on a number of these compounds have revealed tremendous novelty on the enzymology, including tailoring and modifying enzymes, involved in the construction of these molecules [3]. In addition, a high proportion of these molecules have been reported to be highly cytotoxic and neurotoxic with IC_{50}s in the nanomolar to submicromolar range [4]. The antiproliferative nature of some of these marine cyanobacterial compounds is due to their interference with molecular targets, including microtubules, actin, histone deacetylase (HDAC), and serine proteases [4]. Due to the exceptional biological profiles, a number of marine cyanobacterial compounds, including curacin A, dolastatins 10 and 15, and their synthetic analogs, have been selected for further drug development as anticancer agents [4]. For instance, two synthetic dolastatin analogs, soblidotin (= TZT-1027) (**1**, synthetic analog of dolastatin 10) and tasidotin (= Synthadotin/ILX-651) (**2**, synthetic analog of dolastatin 15; Fig. 1), are currently in phase III and II clinical trials as anticancer drugs, respectively [5].

Bioactive Natural Products, Vol. 36. DOI: 10.1016/B978-0-444-53836-9.00021-9

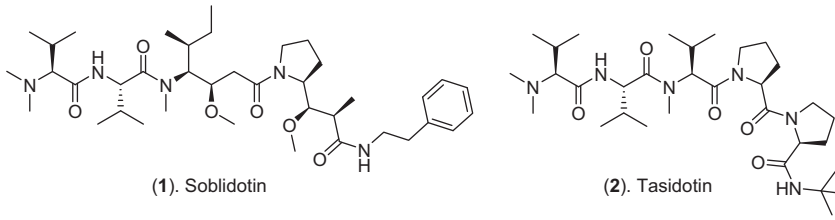

FIGURE 1 Synthetic dolastatin-analogs in clinical trials.

This review covers literature on new reports of marine cyanobacterial nitrogen-containing compounds published between January 2007 and August 2011 (Table 1). A high proportion of these molecules were isolated from cyanobacterial samples collected mainly from Florida, Guam, Papua New Guinea, and Panama. Since 2007, a number of noteworthy novel marine cyanobacterial compounds, such as grassystatins, bisebromoamide, hoiamides, largazole, and coibamide A, with potent biological properties have been reported. In addition, new analogs of previously reported marine cyanobacterial compounds with significant anticancer activities, including apratoxins and aurilides, have been isolated. Reports of these additional new natural analogs provide insight on the structural activity relationship of highly potent marine cyanobacterial compounds. In addition to the myriad of anticancer and neurotoxic molecules, marine cyanobacteria are becoming an important source of antiprotozoal molecules (e.g., lagunamides, venturamides, and viridamides) as well [6]. The chemistry and biology of 112 new natural products are discussed in this chapter and the presentation of these molecules mirrors that of previous reviews by Gerwick *et al.* [1] and Tan [2].

LINEAR LIPOPEPTIDES/PEPTIDES

Tumonoic Acids

Since the initial discovery of tumonoic acids A–C in 1999 by Harrigan *et al.* [7], six additional derivatives, tumonoic acids D (**3**)–I (**8**) (Fig. 2), have been isolated from the marine cyanobacterium, *Blennothrix cantharidomum*, collected from Duke of York Island, Papua New Guinea [8]. *B. cantharidomum* is a ubiquitous mat forming benthic cyanobacterium, and the isolation of these new acyl proline derivatives represents the first report of secondary metabolites from this species. In addition, detailed morphological and phylogenetic studies based on 16S rDNA were also conducted on this marine cyanobacterial strain. The complete chemical structures of these new acyl proline derivatives were accomplished by a combination of NMR, MS spectral data, chiral chromatography, as well as chemical manipulations. Due to their structural similarities to the bacterial signaling molecules, homoserine lactones, they were tested for their effects on bacterial quorum sensing. It was shown that tumonoic acids E (**4**)–H (**7**) exhibited modest inhibition of bioluminescence based on a wild-type strain of *Vibrio harveyi*. Tumonoic acid F (**5**) was the most active with IC_{50} reported at 62 μM. In addition, only tumonoic acid I (**8**) possessed antimalarial activity with IC_{50} of 2 μM [8].

TABLE 1 Nitrogen-Containing Marine Cyanobacterial Natural Products Published from January 2007 to August 2011

Compounds	Species	Location	References
Tumonoic acids (**3**–**8**)	*Blennothrix cantharidomum*	Duke of York Island, Papua New Guinea	[8]
Ethyl tumonoate A (**9**)	*Oscillatoria margaritifera*	Curacao	[9]
Besarhanamides A (**10**) and B (**11**)	*Lyngbya majuscula*	Pulau Hantu, Singapore	[10]
Grenadamides B (**12**) and C (**13**)	*L. majuscula*	Eastern Carribbean	[12]
Palmyrrolinone (**14**)	*Oscillatoria* and *Hormoscilla* sp.	Palmyra Atoll	[13]
8-*epi*-Malyngamide C (**16**) and 8-*O*-acetyl-8-*epi*-malyngamide C (**17**)	*L. majuscula*	True Blue Bay, Grenada	[14]
Isomalyngamide K (**18**)	*L. majuscula*	Alotau Bay, Papua New Guinea	[16]
Malyngamide 2 (**19**)	*L. sordida*	Vicinity of Dutchess Island, Papua New Guinea	[17]
Malyngamide 3 (**20**)	*L. majuscula*	Cocos lagoon, Guam	[18]
Malyngamide X (**22**)	*Bursatella leachii*	Thailand	[19]
Mitsoamide (**23**)	*Geitlerinema* sp.	Nosy Mitso-Ankaraha Island, Madagascar	[24]
Gallinamide A (**24**)	*Schizothrix* sp.	Portobelo National Marine Park, Panama	[25]
Symplostatin 4 (**25**)	*Symploca* sp.	Key Largo, Florida	[26]
Dragomabin (**26**) and dragonamide B (**27**)	*L. majuscula*	Panama	[28]
Dragonamides C (**28**) and D (**29**)	*L. polychroa*	Hollywood Beach, Florida	[29]
Dragonamide E (**30**)	*L. majuscula*	Bastimentos National Park, Panama	[30]

Continued

TABLE 1 Nitrogen-Containing Marine Cyanobacterial Natural Products Published from January 2007 to August 2011—Cont'd

Compounds	Species	Location	References
Almiramides A (**31**)–C (**33**)	*L. majuscula*	Bocas del Toro Marine Park, Panama	[31]
Viridamides A (**35**) and B (**36**)	*O. nigro-viridis*	CARMABI Research Station, Curacao	[32]
Grassystatins A (**37**)–C (**39**)	*L. confervoides*	Grassy Key, Florida	[33]
Lyngbyapeptin D (**40**)	*L. bouillonii*	Finger's Reef, Guam	[34]
Bisebromoamide (**42**) and norbisebromoamide (**43**)	*Lyngbya* sp.	Okinawa	[35,37]
Porpoisamides A (**50**) and B (**51**)	*Lyngbya* sp.	Florida Keys	[46]
Hantupeptins A (**52**)–C (**54**)	*L. majuscula*	Pulau Hantu, Singapore	[47,48]
Palmyramide A (**55**)	*L. majuscula*	Palmyra Atoll	[50]
Cocosamides A (**56**) and B (**57**)	*L. majuscula*	Cocos Lagoon, Guam	[18]
Veraguamides A (**58**)–G (**64**)	*Symploca cf. hydnoides*	Cetti Bay, Guam	[51]
Veraguamides H (**65**)–L (**69**)	*O. margaritifera*	Coiba National Park, Panama	[52]
Carriebowmide (**71**)	*L. majuscula*	Carrie Bow Cay fore-reef, Belize	[53]
Pitiprolamide (**72**)	*L. majuscula*	Piti Bomb Holes, Guam	[54]
Desmethoxymajusculamide C (**73**)	*L. majuscula*	Yanuca Island, Fiji	[55]
Laxaphycins B2 (**75**) and B3 (**76**)	*Anabaena torulosa*	Tahiti	[56]
Lyngbyacyclamides A (**77**) and B (**78**)	*Lyngbya* sp.	Ishigaki Island, Okinawa	[57]
Venturamides A (**79**) and B (**80**)	*Oscillatoria* sp.	Portobelo National Marine Park, Panama	[58]
27-Deoxylyngbyabellin A (**81**) and lyngbyabellin J (**82**)	*L. bouillonii*	Apra Harbor, Guam	[34]

TABLE 1 Nitrogen-Containing Marine Cyanobacterial Natural Products Published from January 2007 to August 2011—Cont'd

Compounds	Species	Location	References
Largazole (**83**)	*Symploca* sp.	Pillars, Key Largo, Florida	[59]
Apratoxin D (**87**)	*L. majuscula* and *L. sordida*	Papua New Guinea	[80]
Apratoxin E (**88**)	*L. bouillonii*	Guam	[81]
Apratoxins F (**89**) and G (**90**)	*L. bouillonii*	Palmyra Atoll	[82]
Grassypeptolides A (**91**)–C (**93**)	*L. confervoides*	Grassy Key, Florida	[85,86]
Grassypeptolides D (**94**) and E (**95**)	*Leptolyngbya* sp.	Red Sea	[87]
Grassypeptolides F (**96**), G (**97**), and Ibu-epidemethoxylyngbyastatin (**98**)	*L. majuscula*	Palau	[88]
Hoiamide A (**99**)	*L. majuscula* and *Phormidium gracile*	Hoia Bay, Papua New Guinea	[89]
Hoiamides B (**100**) and C (**101**)	Various species	Papua New Guinea	[90]
Lyngbyastatin 4 (**102**)	*L. confervoides*	Fort Lauderdale and Pompano Beach, Florida	[91]
Lyngbyastatins 5 (**103**)–7 (**105**)	*L. confervoides*	Fort Lauderdale, Florida	[92]
Lyngbyastatins 8 (**106**)–10 (**108**)	*L. semiplena*	Tumon Bay, Guam	[93]
Bouillomides A (**109**) and B (**110**)	*L. bouillonii*	Guam	[94]
Kempopeptins A (**111**) and B (**112**)	*Lyngbya* sp.	Kemp Channel, Florida	[95]
Molassamide (**113**)	*Dichothrix utahensis*	Molasses Reef, Key Largo, Florida	[96]
Symplocamide A (**114**)	*Symploca* sp.	Sunday Island, Papua New Guinea	[97]
Pompanopeptins A (**115**) and B (**116**)	*L. confervoides*	Fort Lauderdale, Florida	[98]

Continued

TABLE 1 Nitrogen-Containing Marine Cyanobacterial Natural Products Published from January 2007 to August 2011—Cont'd

Compounds	Species	Location	References
Tiglicamides A (**117**)–C (**119**)	*L. confervoides*	Reefs near Port Everglades, Florida	[99]
Coibamide A (**123**)	*Leptolyngbya* sp.	Coiba National Park, Panama	[102]
Itralamides A (**124**) and B (**125**)	*L. majuscula*	True Blue Bay, Grenada	[12]
Laingolide B (**126**)	*L. bouillonii*	Apra Harbor, Guam	[34]
Palmyrolide A (**127**)	*Leptolyngbya cf.* and *Oscillatoria* sp.	Palmyra Atoll	[103]
Alotamide A (**128**)	*L. bouillonii*	Milne Bay, Papua New Guinea	[104]
Lagunamides A (**129**) and B (**130**)	*L. majuscula*	Pulau Hantu, Singapore	[105]
Malevamide E (**131**)	*Symploca laete-viridis*	Oahu, Hawaii	[109]

Based on a novel screening approach using phylogeny, a new compound, ethyl tumonoate A (**9**), was isolated from the marine cyanobacterium, *Oscillatoria margaritifera*, collected from Curacao [9]. The phylogeny-based approach uses genetic information, such as SSU (16S) rRNA genes, to screen filamentous marine cyanobacteria for their capacity to produce related compounds of predicted molecules. Ethyl tumonoate A exhibited *in vitro* anti-inflammatory property, based on the RAW264.7 murine macrophage cell-based nitric oxide assay, having IC_{50} of 9.8 μM. In addition, compound **9** inhibited Ca^{2+} oscillations in neocortical neurons when tested at 10 μM.

Besarhanamides

In our search for novel bioactive compounds from marine cyanobacteria in Singapore, we chanced upon a persistent strain of *Lyngbya majuscula* at the western lagoon of Pulau (= Island) Hantu. Its organic extract showed significant biological activity in the brine shrimp toxicity assay and further purification using RP-HPLC yielded a number of new compounds. The fatty acid amides, besarhanamides A (**10**) and B (**11**) (Fig. 2), were the first series of

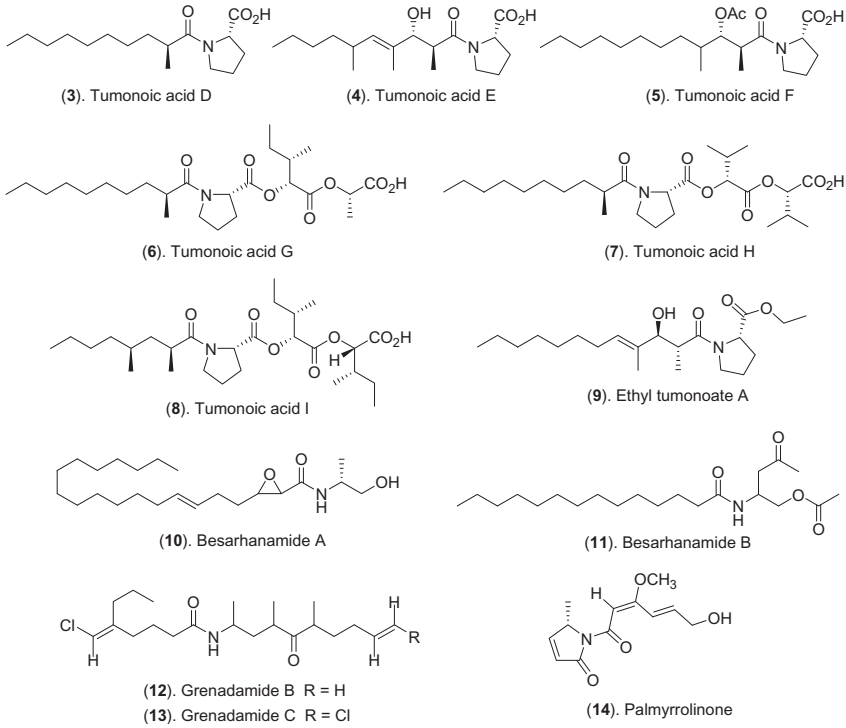

FIGURE 2 Linear lipopeptides (**3**–**14**) from marine cyanobacteria.

new compounds reported from this cyanobacterial strain [10]. The structures of these molecules were deduced mainly from NMR and MS spectral data as well as chemical manipulation involving Marfey's method. Besarhanamides are structurally related to the semiplenamides, previously isolated from a Papua New Guinea strain of *L. majuscula* [11]. When tested in the brine shrimp toxicity assay, only **10** showed moderate activity with LD_{50} observed at 13 μM [10].

Grenadamides

Grenadamides B (**12**) and C (**13**) (Fig. 2) are new chlorinated fatty acid amides, isolated along with the novel cyclic depsipeptides, itralamides A (**124**) and B (**125**), from Eastern Caribbean (True Blue Bay, Grenada) samples of the marine cyanobacterium, *L. majuscula* [12]. The planar structures of these fatty acid amides were determined solely from NMR and MS spectral data. Compounds **12** and **13** contained an unusual terminal substituted vinyl chloride, which is also present in other cyanobacterial lipopeptides, including the malyngamides and jamaicamides. Grenadamides B and C displayed weak insecticidal properties when tested against beet armyworms at 1.0mg/mL, with mortality rates reported at 38% and 50%, respectively [12].

Palmyrrolinone

Palmyrrolinone (**14**) is a new pyrrolidinone-containing molecule isolated recently from a marine cyanobacterial assemblage, consisting of cf. *Oscillatoria* and *Hormoscilla* spp., obtained from Palmyra Atoll [13]. This molecule possesses potent molluscicidal activity when tested against *Biomphalaria glabrata*, with an LC_{50} value of 6.0 μM.

Malyngamide Derivatives

Malyngamide-type molecules are commonly isolated from marine cyanobacterial species belonging to the genus *Lyngbya*. These series of molecules are characterized by a fatty acid chain, usually 7*S*-methoxytetradec-4(*E*)-enoic acid (= lyngbic acid) (**15**), linked via amide bond to a variety of acetate-derived and/or amino acid-derived units. To date, more than 30 malyngamide-type molecules have been reported in the literature. Since 2007, at least three new isomers of known malyngamides have been characterized from *L. majuscula*. Two new stereoisomers of malyngamide C, 8-*epi*-malyngamide C (**16**) and 8-*O*-acetyl-8-*epi*-malyngamide C (**17**) (Fig. 3), were isolated, along with known malyngamides, from *L. majuscula* obtained from True Blue Bay, Grenada [14]. Compound **16** was also reported by Kwan *et al.* from a Floridian (Bush Key, Dry Tortugas) collection of *L. majuscula* [15]. Structural determination of these molecules were based on 1D and 2D NMR and MS spectral data, CD-spectroscopy, as well as a number of chemical manipulation using variable temperature Mosher's method and Mitsunobu reaction [14,15]. 8-*epi*-Malyngamide C (**16**) displayed cytotoxic activity against a panel of cancer cell lines, including NCI-H460, Neuro-2a, and HT29, with IC_{50} values of 9.8, 23.9, and 15.4 μM, respectively [14,15]. Interestingly, malyngamide C was found to exhibit stronger cytotoxic activities with IC_{50} ranging from 3.1 to 5.2 μM [14,15]. When tested against NCI-H460 and Neuro-2a cell lines, compound **17** showed cytotoxic activities at 8.4 and 10.7 μM, respectively. In addition, compound **16** and malyngamide C were found to inhibit bacterial quorum sensing based on a reporter gene assay using pSB1075 [15]. An isomer of malyngamide K, isomalyngamide K (**18**) (Fig. 3), was recently reported from *L. majuscula* collected at Alotau Bay, Papua New Guinea [16]. The structure of this molecule was determined by NMR and mass spectral data, DFT theoretical calculations, and chemical manipulation. No biological activity was reported for this molecule.

Malyngamide 2 (**19**) (Fig. 3), a highly oxidized malyngamide derivative, was isolated from a Papua New Guinea (near Dutchess Island) marine cyanobacterium, *Lyngbya sordida* [17]. Compound **19** contained a trihydroxy cyclohexanone ring moiety and its relative stereochemistry was determined mainly by chemical shift and bond geometry modeling based on homonuclear and heteronuclear coupling constant values coupled with NOE and ROE correlations. Malyngamide 2 displayed anti-inflammatory activity (IC_{50}=8.0 μM)

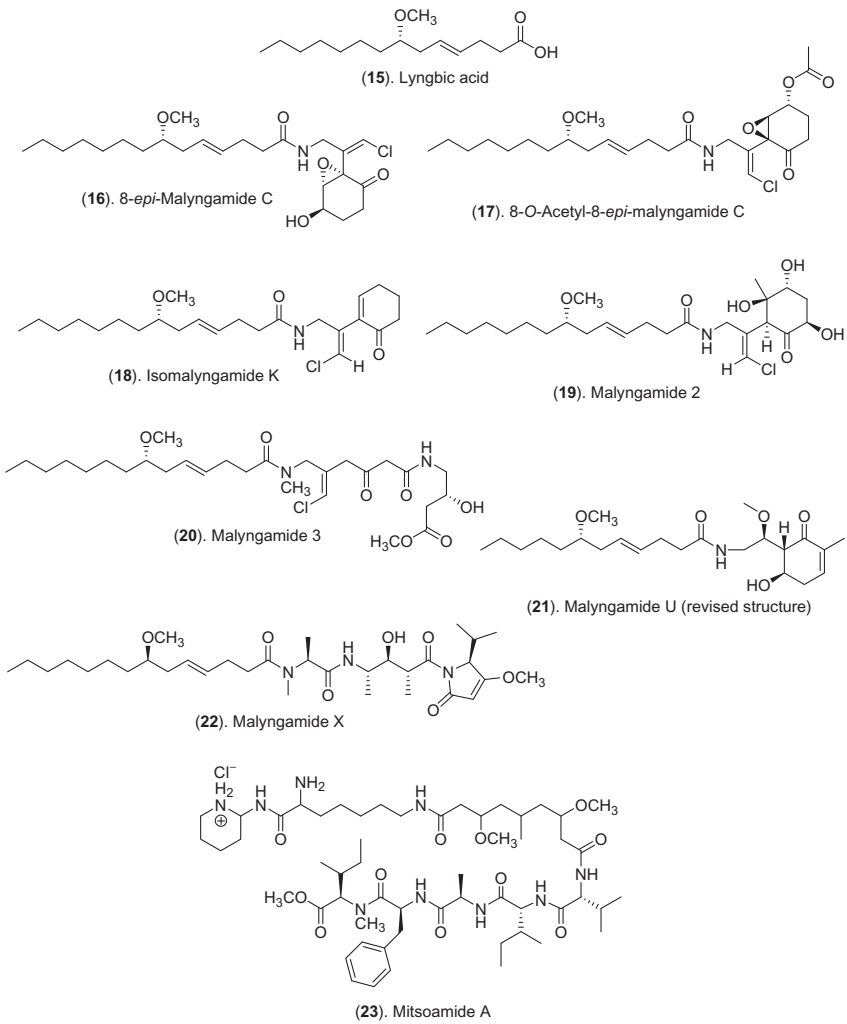

FIGURE 3 Linear lipopeptides (**15**–**23**) from marine cyanobacteria.

when tested on lipopolysaccharide-induced RAW macrophage cells by inhibiting nitric oxide production. When tested against H-460 human lung carcinoma cells, malyngamide 2 showed moderate cytotoxicity with an IC_{50} of 27.3 μM [17]. From a collection of *L. majuscula*, obtained from Cocos lagoon, Guam, malyngamide 3 (**20**) (Fig. 3) was purified along with the new cyclodepsipeptides, cocosamides A (**56**) and B (**57**) [18]. The complete structural elucidation of malyngamide 3 was determined by spectroscopic methods, the modified Mosher's method, and 2D NOE data. Compound **18** showed weak antiproliferative property against MCF7 and HT-29 cancer cells with IC_{50} values of 29 and 48 μM, respectively.

A number of malyngamide derivatives have also been isolated from sea hares and their occurrence could be attributed to the invertebrates' cyanobacterial diet. One such new addition is malyngamide X (**22**) (Fig. 3), which was isolated from the Thai sea hare, *Bursatella leachii* [19]. In addition to NMR and MS spectral data, NMR experiments using chiral solvating agent and chemical synthesis were used to determine the complete structure of **22**. Malyngamide X is the malyngamide-derivative having the (7*R*)-lyngbic acid coupled via amide bond to a tripeptide moiety. Malyngamide X exhibited moderate biological properties, including cytotoxic and antimalarial activities, with ED_{50} values ranging from 4.12 to 8.20 μM. In addition, it showed moderate antitubercular activity against the *Mycobacterium tuberculosis* H37Ra strain with MIC value at 80 μM [19].

At least five known malyngamides, malyngamides O to R, U, and W, have been the subject of total synthesis and as a result their absolute configurations have been revised or confirmed [20–23]. Using a convergent and enantioselective synthetic approach, including Wittig reaction, a DCC/HOBt-promoted amidation, an aldol reaction, and methylation of the enol unit in either base/acid conditions or Mitsunobu reaction, malyngamides O to R and the epimers of malyngamides Q and R were synthesized by Chen *et al.* [22]. In another synthetic report by Li *et al.*, the total synthesis of malyngamide U was achieved in 18 steps starting from (*S*)-(+)-carvone [20]. Based on this synthetic work, the absolute stereochemistry of malyngamide U was revised to compound **21**.

Mitsoamide A

Mitsoamide (**23**) (Fig. 3) is a cytotoxic lipopeptide isolated from the Madagascar (at Nosy Mitso-Ankaraha Island) marine cyanobacterium, *Geitlerinema* sp. [24]. This molecule has a number of unusual structural features, including a 3,7-dimethoxy-5-methyl-nonanedioic acid, a homolysine, and a piperidine aminal unit, along with α-amino acid residues comprising Ala, Ile, *N*Me-Ile, Phe, and Val. Its complete structure was confirmed by NMR, MS spectral data, and chiral HPLC analysis. Mitsoamide was found to possess significant cytotoxic activity when tested against the NCI-H460 human lung tumor cell line with an LC_{50} value at 0.46 μM.

Gallinamide A and Symplostatin 4

Gallinamide A (**24**) (Fig. 4) is a highly functionalized linear lipodepsipeptide, containing a methylmethoxypyrrolinone moiety, isolated from the red-tipped *Schizothrix* sp. obtained from the Portobelo National Marine Park in Panama [25]. This unique molecule exhibited moderate *in vitro* activity against *Plasmodium falciparum* with IC_{50} value of 8.4 μM. It was further observed by Linington *et al.* that linear peptides having either terminal *N*,*N*-dimethylvaline or *N*,*N*-dimethylisoleucine moieties are a potential class of compounds that

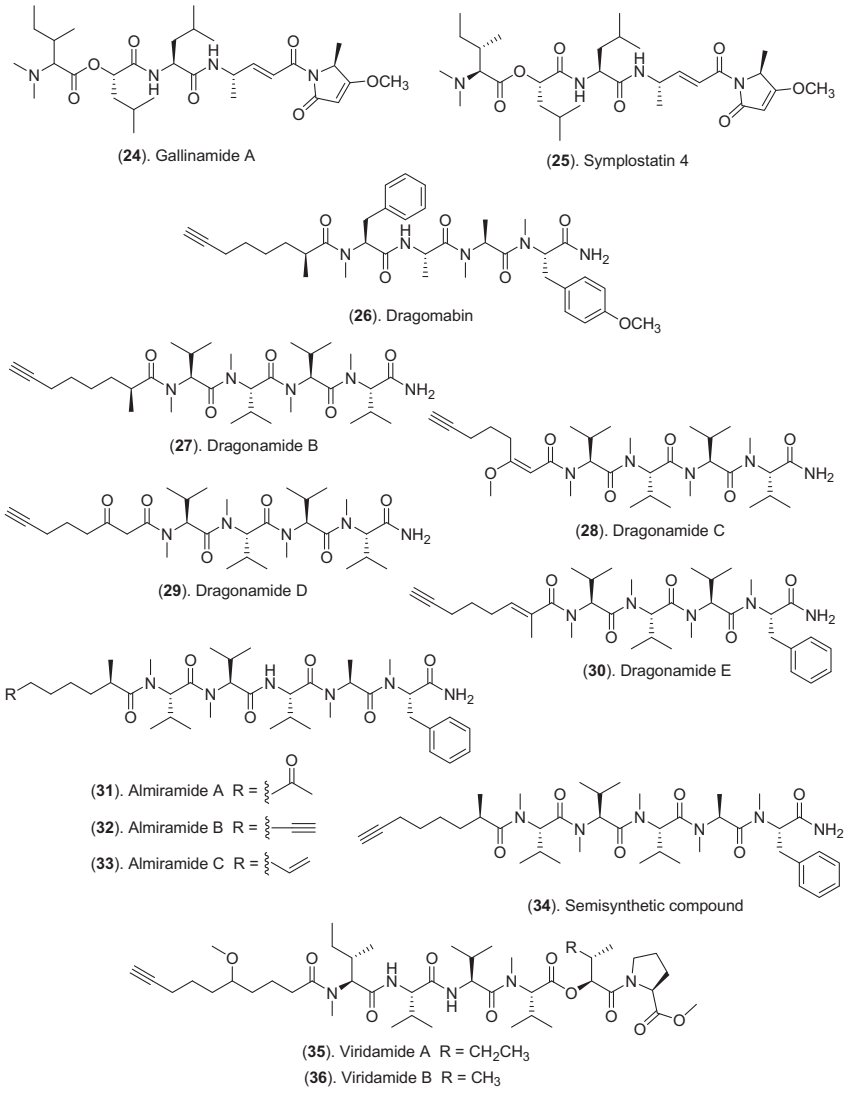

FIGURE 4 Linear lipopeptides (**24**–**36**) from marine cyanobacteria.

possess antiparasitic and anticancer properties [25]. Gallinamide A is structurally related to the highly potent dolastatins 10 and 15. Unlike dolastatins 10 and 15, gallinamide A showed moderate cytotoxicity when tested against Vero cells (TC_{50} of 10.4 μM) and no *in vitro* cytotoxicity when tested against NCI-H460 human lung tumor and neuro-2a mouse neuroblastoma cell lines. In addition, it showed moderate activity against *Leishmania donovani* with IC_{50} reported at 9.3 μM. Symplostatin 4 (**25**) (Fig. 4), with planar structure

identical to **24**, was isolated from a largazole-producing strain of marine cyanobacterium, *Symploca* sp., collected from Key Largo, Florida [26]. The complete structure, including stereochemistry of **25**, was achieved by NMR, MS spectral data, and chemical manipulation. Taori *et al*. showed that the co-occurrence of symplostatin 4 and largazole within the same cyanobacterial strain could exert synergistic effect on target cells [26]. The total synthesis of symplostatin 4 was recently accomplished by Conroy *et al*. [27].

Dragomabin and Dragonamides

Dragomabin (**26**), dragonamides (**27**–**30**), almiramides (**31**–**33**), and viridamides (**35** and **36**) are linear lipopeptides characterized by having a C_8 polyketide-derived moiety linked via amide bond to various amino acid units and are usually terminate with a primary amide functional group (except in viridamides A and B). From a collection of the Panamanian strain of the marine cyanobacterium, *L. majuscula*, two new natural products, dragomabin (**26**) and dragonamide B (**27**) (Fig. 4), along with the known compounds, carmabin A and dragonamide A, were isolated [28]. The planar structures of these new molecules were deduced by NMR and MS spectroscopy, while their stereochemistry determined by chiral HPLC and comparison of optical rotation values and NMR spectral data with known compounds. The antimalarial activities of carmabin A, dragomabin, and dragonamides A and B were evaluated using theW2 chloroquine-resistant malarial strain. It was revealed that carmabin A, dragomabin, and dragonamide A displayed antimalarial activities ranging from 4.3 to 7.7 μM while compound **27** was inactive. The biological data suggested that the aromatic unit is necessary for the observed activity. Further biological evaluation using Vero cells showed that dragomabin was the least active, with IC_{50} value of 182.3 μM, compared to dragonamide A and carmabin [28].

Additional dragonamide derivatives, dragonamides C (**28**)–E (**30**) (Fig. 4), have been reported by Luesch's and Gerwick's research group. Dragonamides C (**28**) and D (**29**) were isolated from the marine cyanobacterium, *Lyngbya polychroa*, collected at Hollywood Beach, Florida, while dragonamide E (**30**) was obtained from *L. majuscula* from Bastimentos National Park, Panama [29,30]. The structures of these compounds were determined by a combination of NMR, MS, chiral HPLC, and Marfey's analysis. Compounds **28** and **29**, when tested against U2OS osteosarcoma cells, showed weak cytotoxic activities with GI_{50} of 56 and 59 μM, respectively [29]. Dragonamide E displayed significant antileishmanial activity when tested against *L. donovani* with IC_{50} value at 5.1 μM [30].

Almiramides

Almiramides A (**31**)–C (**33**) (Fig. 4) are highly *N*-methylated linear lipopeptides isolated from *L. majuscula* from the Bocas del Toro Marine Park in Panama [31]. The chemical structures of almiramides were established by NMR,

MS, as well as chemical manipulations, including Marfey's analysis for determination of their absolute stereochemistry. Almiramides B (**32**) and C (**33**) were reported to exhibit significant *in vitro* antileishmanial activity against *L. donovani*, with IC_{50} values at 2.4 and 1.9 μM, respectively. In addition to the natural compounds, a number of semisynthetic derivatives were synthesized using solid phase peptide synthesis method and provided compound **34** having superior *in vitro* activity with IC_{50} value at 1.6 μM when tested against *L. donovani*. The almiramides are structurally related to other marine cyanobacterial compounds, such as carmabin A, dragomabin, and the dragonamides. In spite of their structural similarities with the almiramides, these related compounds were inactive against *L. donovani* when tested at 10 μg/mL. Antimalarial activity were instead reported for carmabin A (IC_{50} value at 4.3 μM), dragomabin (IC_{50} value at 6.0 μM), and dragonamide A (IC_{50} value at 7.7 μM) when tested against the W2 chloroquine-resistant malaria strain [31]. The discovery of the almiramides could therefore represent new class of leishmaniasis lead compounds.

Viridamides

The linear lipodepsipeptides, viridamides A (**35**) and B (**36**) (Fig. 4), are antiprotozoal compounds isolated from the marine cyanobacterium, *Oscillatoria nigro-viridis*, cultured from an assemblage of *L. majuscula* from the CARMABI Research Station, Curacao [32]. The structures of viridamides A and B consisted of six *N*-methylated amino acids, hydroxy acids, as well as an unusual 5-methoxydec-9-ynoic acid residue. The planar and absolute structural elucidations of these compounds were achieved through NMR and mass spectroscopic methods as well as chemical manipulation involving Marfey's method and chiral HPLC analysis, respectively. Viridamide A (**35**) showed promising activities against three parasitic protozoa, namely, *Trypanosoma cruzi*, *Leishmania mexicana*, and *Plasmodium flaciparum*, with IC_{50} values ranging from 1.1 to 5.8 μM.

Grassystatins

The linear decadepsipeptides, grassystatins A (**37**)–C (**39**) (Fig. 5), are potent cathepsin E inhibitors isolated from the marine cyanobacterium, *Lyngbya confervoides*, collected at Grassy Key, Florida [33]. These statine unit-containing molecules were isolated based on a screening program by profiling the inhibitory activities of natural products against 59 proteases. The structure elucidation of compounds **37**–**39** were deduced by the use of NMR, MS, as well as chiral HPLC analysis. Grassystatins A (**37**) and B (**38**) displayed potent inhibitory activity against cathepsins D and E with IC_{50} values averaging at 16.9 and 0.62 nM, respectively. In addition, grassystatin A was able to reduce antigen presentation by dendritic cells [33].

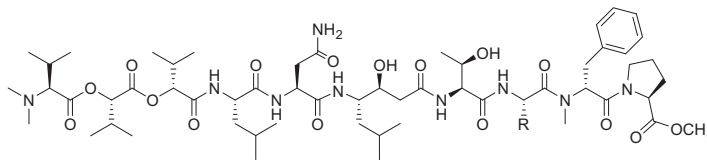

(**37**). Grassystatin A R = Me
(**38**). Grassystatin B R = Et

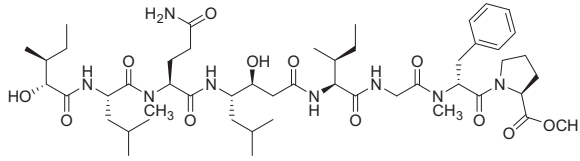

(**39**). Grassystatin C

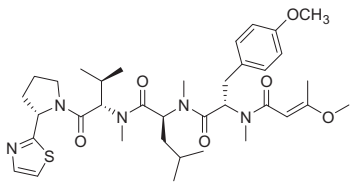

(**40**). Lyngbyapeptin D

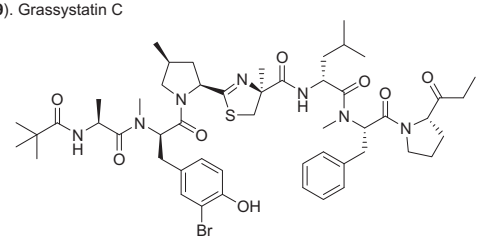

(**41**). Original structure of bisebromoamide

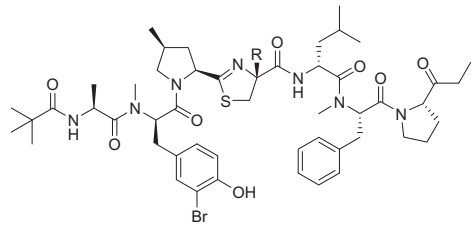

(**42**). Bisebromoamide R = Me (revised structure)
(**43**). Norbisebromoamide R = H

FIGURE 5 Linear lipopeptides (**37**–**43**) from marine cyanobacteria.

Heterocycle-Containing Linear Lipopeptides/Peptides

Lyngbyapeptin D

From the apratoxin-containing organic extract of the marine cyanobacterium, *Lyngbya bouillonii*, collected at Finger's Reef, at least seven new secondary metabolites were isolated. Of these, four are nitrogen-containing analogs of known cyanobacterial compounds, including lyngbyapeptin D (**40**) (Fig. 5), 27-deoxylyngbyabellin A (**81**), lyngbyabellin J (**82**), and laingolide B (**126**) [34]. The structure of the linear thiazole-containing lipopeptide, lyngbyapeptin D (**40**), was determined primarily by NMR and MS spectral data. Lyngbyapeptin D is structurally related to lyngbyapeptin A by having a Val unit

instead of Ile in the former molecule. Unfortunately, **40** decomposed before it could be subjected to further biological testing.

Bisebromoamide and Derivatives

Bisebromoamide (**41**) (Fig. 5) is a cytotoxic linear peptide isolated in 2009 from an Okinawan strain of the filamentous marine cyanobacterium, *Lyngbya* sp. [35]. Its planar structure was determined by 1D and 2D NMR experiments and its complete stereochemistry was established using chemical manipulation and chiral HPLC analysis. This novel compound contained a unique *N*-methyl-3-bromotyrosine, a modified 4-methylproline, a 2-(1-oxo-propyl) pyrrolidine, as well as an *N*-pivalamide unit. Based on the total synthesis of bisebromoamide, recently reported by Gao *et al*., the stereochemistry of the molecule has been revised to compound **42** [36]. The revised structure of bisebromoamide was recently reconfirmed by Sasaki *et al*. based on the reisolation of the molecule from the marine cyanobacterium [37]. In the process of reisolation, a new analog, norbisebromoamide (**43**), was also purified. A highly convergent method of synthesizing bisebromoamide and other simplified analogs was recently developed by Li *et al*. (Scheme 1) [38].

Bisebromoamide possessed cytotoxic property against HeLa S_3 cells with an IC_{50} value 0.04 μg/mL. When tested against a panel of 39 human cancer cell lines, bisebromoamide gave an average GI_{50} value of 40 nM. In addition, a series of biochemical experiments suggested that the ERK (extracellular signal-regulated protein kinase) signaling pathways could potentially be a target for this compound. Structure–activity relationship (SAR) studies on bisebromoamide and synthetic analogs revealed that the stereochemistry of the methylthiazoline moiety and methyl group at the 4-methylproline unit did not influence the cytotoxicity activity significantly [38]. Further, bisebromoamide was identified as an actin filament stabilizer based on cell morphogical profiling analysis [39].

Total Synthesis of Known Linear Lipopeptide/Peptides

Since 2007, a number of synthetic efforts were successfully carried out on the total synthesis of a few marine cyanobacterial compounds, namely, hermitamides A (**44**) and B (**45**), ypaoamide (**46**), belamide A (**47**), tasiamide (**48**), and tasiamide B (**49**) [40–45]. A concise synthesis, based on rhodium-catalyzed conjugate addition reaction, of hermitamides A (**44**) and B (**45**) was reported by Gleave *et al*. [40]. The total synthesis of the hermitamides and its epimers was also reported by Paige *et al*. [41]. In addition, they demonstrated hermitamides to be potent blockers of the human voltage-gated sodium channels (VGSCs). The total synthesis of ypaoamide resulted in the confirmation of the absolute stereochemistry as shown in **46** (Fig. 6), while those of tasiamide and tasiamide B led to reassignment of stereochemistry shown in **48** and **49**, respectively [42–44]. Lan *et al*. reported on the first total synthesis of the antiproliferative compound, belamide A (**47**), in seven steps with an overall yield of about 23% [45].

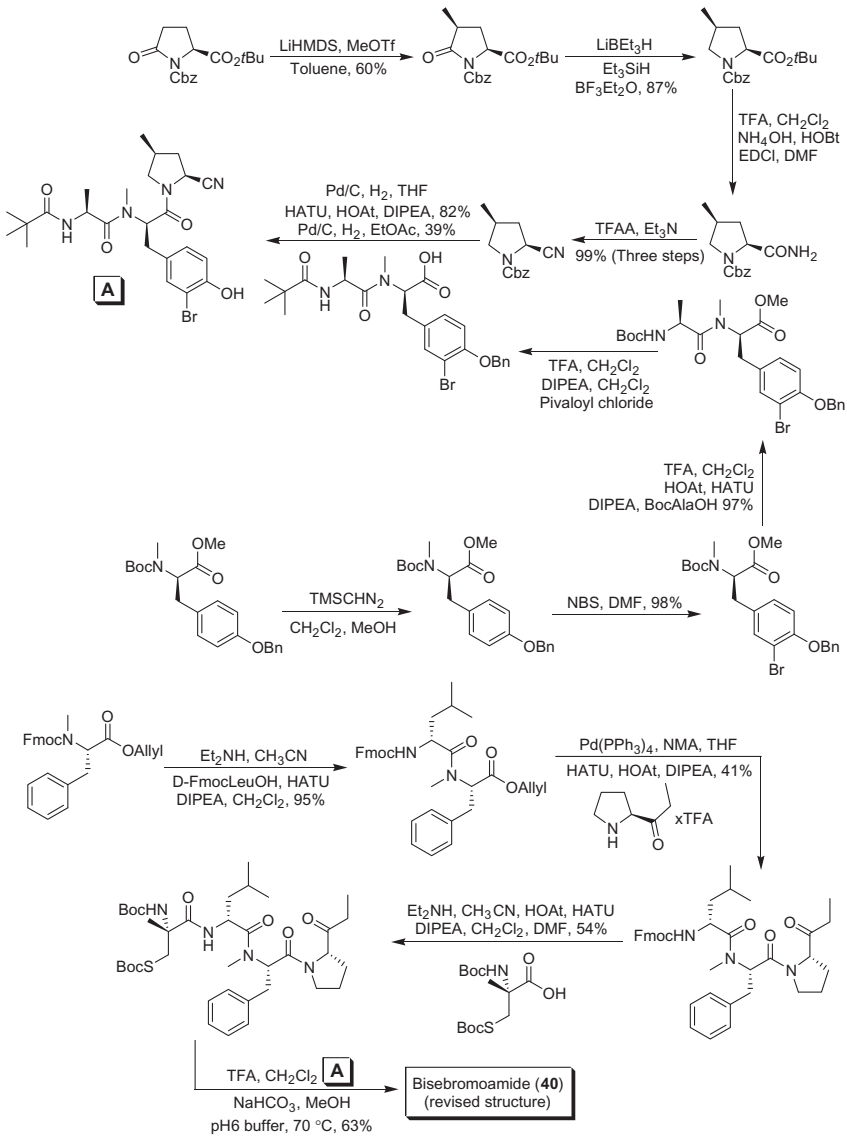

SCHEME 1 Convergent synthetic route of bisebromoamide by Ma and coworkers [38].

CYCLIC DEPSIPEPTIDES/PEPTIDES

Porpoisamides A and B

Porpoisamides A (**50**) and B (**51**) are novel epimeric pair of cyclic depsipeptides purified from a Floridian sample of *Lyngbya* sp. [46]. Each compound consists of five residues, including Ala, *N*Me-Phe, Pro, 2-hydroxy-3-methylpentanoic

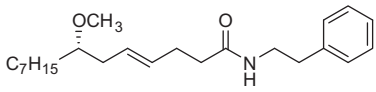

(**44**). Hermitamide A

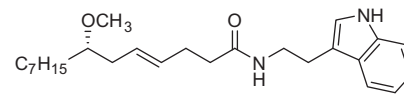

(**45**). Hermitamide B

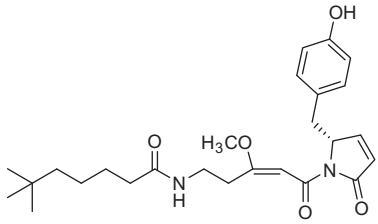

(**46**). (*R*)-Ypaoamide

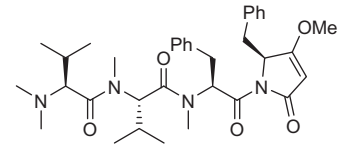

(**47**). Belamide A

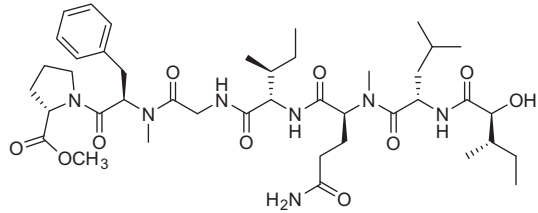

(**48**). Tasiamide

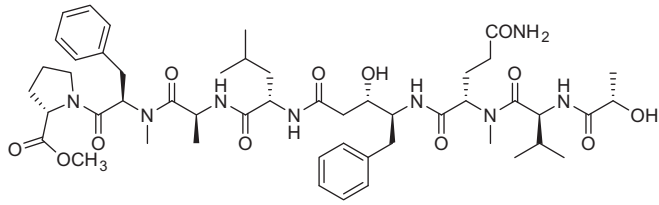

(**49**). Tasiamide B

FIGURE 6 Linear lipopeptides (**44**–**49**) from marine cyanobacteria.

acid, and 3-amino-2-methyloctanoic acid units. They differ only at the stereochemistry at C-2 of the β-amino acid unit. Porpoisamides A and B showed weak cytotoxic activity when tested against HCT-116 colorectal carcinoma and U2OS osteosarcoma cell lines, with IC_{50} values ranging from 21 to 28 μM.

Hantupeptins

Hantupeptin A (**52**) (Fig. 7), a cyclic depsipeptide, is a potent cytotoxic molecule isolated from a persistent strain of *L. majuscula* found at the western lagoon of Pulau Hantu, Singapore [47]. This molecule consisted of four α-amino acids, one α-hydroxy acid, and a PKS-derived β-hydroxy acid residue

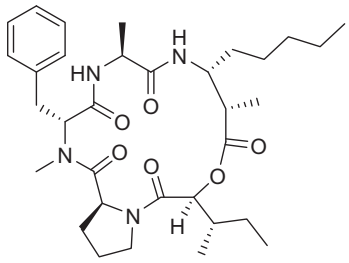

(**50**). Porpoisamide A

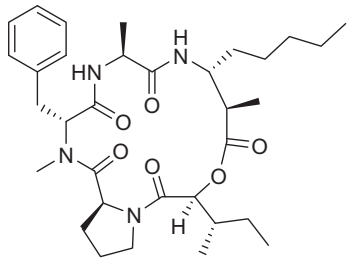

(**51**). Porpoisamide B

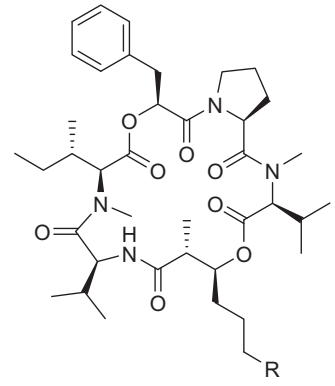

(**52**). Hantupeptin A R =

(**53**). Hantupeptin B R =

(**54**). Hantupeptin C R =

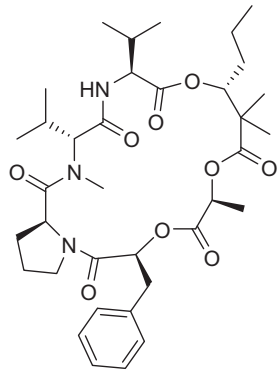

(**55**). Palmyramide A

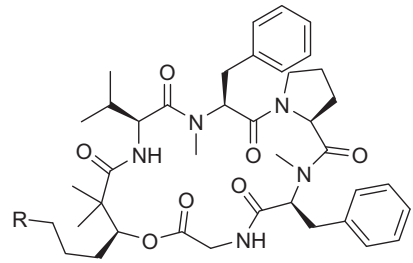

(**56**). Cocosamide A R =

(**57**). Cocosamide B R =

FIGURE 7 Cyclic lipopeptides (**50**–**57**) from marine cyanobacteria.

and its complete structure was determined by extensive NMR experiments and MS data. The presence of the PKS-derived unit of 3-hydroxy-2-methyloctynoic acid residue in **52** appears to be widespread in marine cyanobacterial cyclic depsipeptides. More than 60 cyclic depsipeptides from marine cyanobacteria contain such a PKS-derived unit, usually in the form of β-hydroxy acid or β-amino acid residue [1,2]. In all cases, chain extension occurs at the C-2 position and either single methylation or dimethylation is observed at the C-1 position

of the β-hydroxy acid or β-amino acid unit. Such structural feature is a hallmark of marine cyanobacterial natural products and, together with the different combination of α-amino/hydroxy acids, emphasize the amazing combinatorial biosynthetic capacity of marine cyanobacteria. Hantupeptin A has been reported to display significant cytotoxic activity against the MOLT-4 leukemia cell line with IC_{50} of 32 nM. Further chemical analysis of the organic extract of this cyanobacterial strain led to isolation of hantupeptins B (**53**) and C (**54**) (Fig. 7). These compounds displayed significant *in vitro* cytotoxic property when tested against MOLT-4 and MCF-7 cell lines with IC_{50} values of ranging from 0.2 to 3.0 μM [48]. Other known marine cyanobacterial compounds, including dolastatin 16 and isomalyngamide A, have also been isolated from this cyanobacterial strain. A number of these compounds display various antifouling activities based on an antisettlement assay using barnacle larvae [49].

Palmyramide A

Palmyramide A (**55**) (Fig. 7) is a 19-membered cyclodepsipeptide isolated from an assemblage consisting of the marine cyanobacterium, *L. majuscula*, and the red alga, *Centroceras* sp., collected from a Palmyra Atoll [50]. This molecule consists of six residues, including three α-amino acids of Val, *N*Me-Val, and Pro, and three hydroxy acids of 2,2-dimethyl-3-hydroxyhexanoic acid (Dmhha), lactic acid, and 3-phenyllactic acid. Its complete structure was accomplished by NMR, MS spectral data, and chemical manipulation, including Marfey's analysis. The absolute stereochemistry of the β-hydroxy acid, Dmhha, was determined by the stereoselective synthesis of *S*- and *R*-Dmhha and subjecting them through chiral GC/MS analysis together with the Dmhha unit derived from the acid hydrolysis of palmyramide A. It was only through the use of MALDI-TOF imaging technique that the authors were able to identify the marine cyanobacterium as the true producer of the natural product. When evaluated in the sodium channel blocking assay, compound **55** inhibited the veratridine- and ouabain-induced sodium overload leading to cytotoxicity of neuro-2a cells with an IC_{50} of 17.2 μM. In addition, palmyramide A displayed moderate cytotoxicity against the H-460 human lung carcinoma cells with an IC_{50} value of 39.7 μM [50].

Cocosamides A and B

Along with malyngamide 3 (**20**) (discussed in above section), two new cyclic depsipeptides, cocosamides A (**56**) and B (**57**) (Fig. 7), were isolated from the marine cyanobacterium, *L. majuscula*, from Cocos Lagoon, Guam [18]. The cocosamides consist of six amino/hydroxy units, including *N*Me-Phe (two units), Pro, Gly, Val, and a β-amino acid of 2,2-dimethyl-3-hydroxy-7-octynoic acid (Dhoya) or 2,2-dimethyl-3-hydroxy-7-octenoic acid (Dhoea)

in either **56** or **57**, respectively. The planar structures of these molecules were determined by NMR and MS spectral data, while the absolute stereochemistry was accomplished by Marfey's analysis as well as comparison with the known compound, pitipeptolide A. Compounds **56** and **57** showed moderate cytotoxicity against HT-29 (IC_{50} values of 24 and 11 μM for compounds **56** and **57**, respectively) and MCF7 cancer cells (IC_{50} values of 30 and 39 μM for compounds **56** and **57**, respectively) [18].

Veraguamides

From the dolastatin 16-producing marine cyanobacterium, *Symploca cf. hydnoides*, collected from Cetti Bay, Guam, seven new cyclodepsipeptides, veraguamides A (**58**)–G (**64**) (Fig. 8), were isolated [51]. Their structural elucidations were determined mainly by NMR, MS experiments, HPLC, and Mosher's analysis. In addition to α-amino/hydroxy acid units, these compounds contain a C_8-polyketide-derived β-hydroxy acid residue with tail end occurring as alknyl bromide, alkyne, or vinyl functional group. In addition,

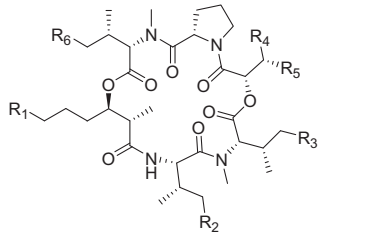

	R_1	R_2	R_3	R_4	R_5	R_6
(**58**). Veraguamide A	≡—Br	H	H	Et	Me	H
(**59**). Veraguamide B	≡—Br	H	H	Me	Me	H
(**60**). Veraguamide C	≡—H	H	H	Et	Me	H
(**61**). Veraguamide D	≡—H	H	H	Et	Me	Me
(**62**). Veraguamide E	≡—H	Me	Me	Et	Me	H
(**63**). Veraguamide F	≡—H	H	H	Ph	H	H
(**64**). Veraguamide G	⌇	H	H	Et	Me	H

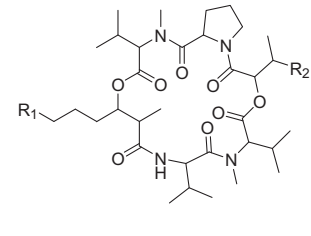

	R_1	R_2
(**65**). Veraguamide H	≡—H	Me
(**66**). Veraguamide I	Et	Et
(**67**). Veraguamide J	Et	Me

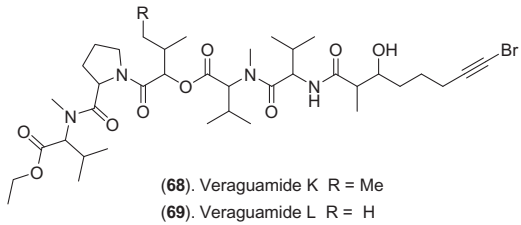

(**68**). Veraguamide K R = Me
(**69**). Veraguamide L R = H

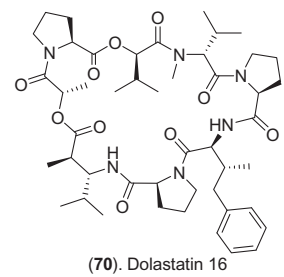

(**70**). Dolastatin 16

FIGURE 8 Cyclic lipopeptides (**58**–**70**) from marine cyanobacteria.

the complete stereochemistry of dolastatin 16 (**70**) was accomplished for the first time since its discovery in 1997. This was achieved by the use of chemical manipulation involving the advanced Marfey's method and the modified Mosher's method based on phenylglycine methyl ester as a chiral anisotropic reagent [51]. Veraguamides D (**61**) and E (**62**) are the most cytotoxic in this series of cyclodepsipeptides, with IC_{50} values ranging from 0.54 to 1.5 μM when tested against the HT29 and HeLa cancer cell lines [51].

Additional natural analogs, veraguamides H (**65**)–L (**69**), were recently isolated from the marine cyanobacterium, cf. *O. margaritifera*, from the Coiba National Park, Panama [52]. These new analogs were isolated along with previously reported veraguamides A–C. In this study, veraguamides A (**58**), B (**59**), C (**60**), K (**68**), and L (**69**) were tested against the H-460 cell lines and only compound **58** showed potent activity with LD_{50} value of 141 nM. Due to the structural similarities of veraguamide A with other known compounds, such as kulomo'opunalide-1 and -2, it was suggested that the alkynyl bromide in **58** is an important structural feature for the potent cytotoxic activity.

Carriebowmide

Carriebowmide (**71**) (Fig. 9) is a new 21-membered cyclic depsipeptide isolated from the marine cyanobacterium, *L. majuscula*, from Carrie Bow Cay fore-reef, Belize [53]. In addition to the six α-hydroxy/α-amino acids, namely, Ala, *N*Me-Leu, Phe, Met, *N*Me-Phe, and 2-hydroxy-3-methylbutyric acid unit, compound **71** contained a β-amino acid unit of 3-amino-2-methylhexanoic acid (Amha). The absolute stereochemistry of the Amha was determined to be 2*R*,3*R* based on the advanced Marfey's method and comparing with the retention time of Amha standards.

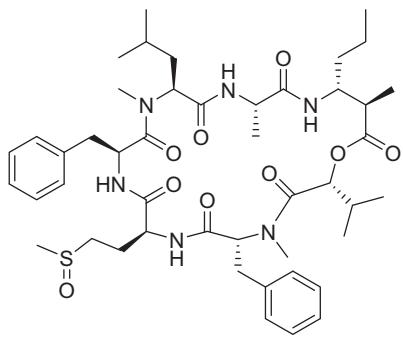

(**71**). Carriebowmide

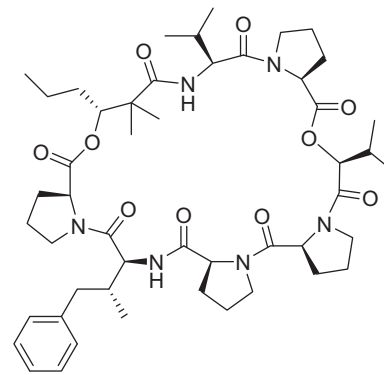

(**72**). Pitiprolamide

FIGURE 9 Cyclic lipopeptides (**71** and **72**) from marine cyanobacteria.

Pitiprolamide

Pitiprolamide (**72**) (Fig. 9), a dolastatin 16 analog, is an unusual cyclic depsipeptide that is enriched with Pro residues. This molecule derived from the organic extract of the marine cyanobacterium, *L. majuscula*, is obtained from Piti Bomb Holes, Guam [54]. In addition to four Pro units, compound **72** contained Val, 2-hydroxy-isovaleric acid, dolaphenvaline, and the β-amino acid, Dmhha residues. The structure of pitiprolamide was deduced by NMR, MS, X-ray crystallography, as well as enantioselective HPLC–MS techniques. Pitiprolamide exhibited weak cytotoxicity property when tested against HCT116 colorectal carcinoma and MCF7 breast adenocarcinoma cell lines with IC_{50} values at 33 μM for both. The natural product also showed weak antibacterial activity against *M. tuberculosis* when tested at 50 μg using the disk diffusion assay [54].

Desmethoxymajusculamide C

Desmethoxymajusculamide C (**73**) (Fig. 10), a new analog of majusculamide C, was isolated from the organic extract of a Fijian (from Kauviti Reef, Yanuca Island) marine cyanobacterium, *L. majuscula* [55]. In addition to NMR, MS/MS and chemical manipulation were used to establish its planar and absolute stereochemistry. Compound **73** is highly potent and showed selective activity when tested against the HCT-116 human colon carcinoma cells with IC_{50} reported at 20 nM. The high potency of this molecule is due to its specific molecular interference with cellular microfilaments [55]. Interestingly, the cytotoxic activity of the linear form of desmethoxymajusculamide C, **74**, generated by base hydrolysis of the natural product, was found to be similar to the cyclic form [55].

Laxaphycin Analogs

Laxaphycin class of molecules are unique cyclopeptides consisting of a number of unusual moieties, including α,β-didehydro-α-aminobutyric acid, 3-hydroxyleucine, 3-hydroxyasparagine, and/or 3-amino-octa/decanoic acids. Laxaphycins B2 (**75**) and B3 (**76**) (Fig. 10) were isolated as minor cyclic peptides from the organic extract of a mixed assemblage of *L. majuscula* obtained from Tahiti [56]. The chemical structures of the major peptides, laxaphycins A and B, and compounds **75** and **76** were determined by spectroscopic methods, including NMR and FAB-MS/MS data, chemical manipulation, and synthesis. From the mixed assemblages, the authors were able to identify the cyanobacterium, *Annabaena torulosa*, as the true producer of the laxaphycins. Biological evaluation on laxaphycins A and B showed the synergistic effect of the former compound by increasing the antiproliferative property of laxaphycin B against sensitive and resistant human cancer cell lines [56].

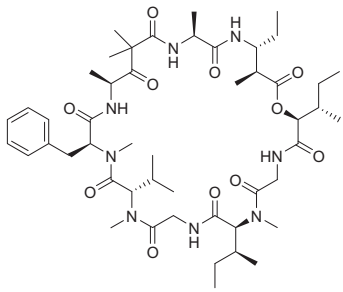

(**73**). Desmethoxymajusculamide C

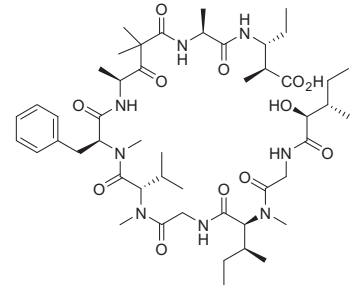

(**74**). Ringed open form of desmethoxymajusculamide C

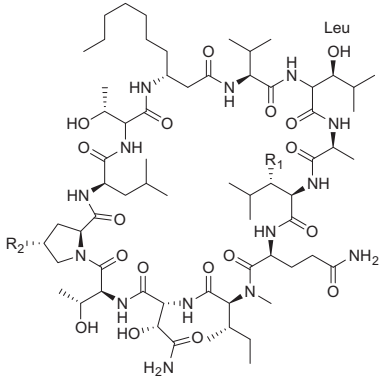

(**75**). Laxaphycin B2 (2R,3S)-3-OH-Leu, R_1 = H, R_2 = H

(**76**). Laxaphycin B3 (2S,3S)-3-OH-Leu, R_1 = OH, R_2 = OH

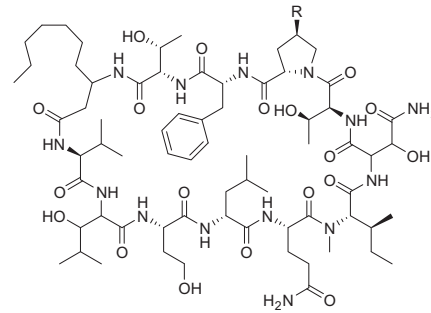

(**77**). Lyngbyacyclamide A R = H

(**78**). Lyngbyacyclamide B R = OH

FIGURE 10 Cyclic lipopeptides (**73** and **75–78**) from marine cyanobacteria and ringed open form of desmethoxymajusculamide C (**74**).

Lyngbyacyclamides

Lyngbyacyclamides A (**77**) and B (**78**) (Fig. 10) are cytotoxic 37-membered cyclic peptides consisting of 11 α-amino acids and one β-amino acid (β-amino-decanoic acid) residue. These molecules were isolated from the marine cyanobacterium, *Lyngbya* sp., collected from Ishigaki Island, Okinawa, Japan [57]. The complete structures of lyngbyacyclamides were deduced by spectroscopic methods and chemical degradation analysis. The lyngbyacyclamides are structurally related to the laxaphycins and they displayed significant cytotoxic property when tested against B16 mouse melanoma cancer cells having IC_{50} values at 0.7 μM for both molecules [57].

Heterocycle-Containing Cyclic Depsipeptides/Peptides

Venturamides

One of the pharmacological trends that has emerged in recent years is the discovery of marine cyanobacterial compounds having significant antiprotozoal

activities, including antimalarial and antileishmanial properties. A number of these compounds have been recovered from natural products research initiated by the Panamanian International Cooperative Biodiversity Group (ICBG) program. One of the aims of this NIH-funded program is to screen terrestrial and marine samples from Panama for compounds against tropical diseases, such as malaria, schistosomiasis, leishmaniasis, and Chagas diseases.

One of the early reports of antimalarial cyanobacterial compounds were venturamides A (**79**) and B (**80**) (Fig. 11), isolated from *Oscillatoria* sp. obtained from Buenaventura Bay, Portobelo National Marine Park, Panama [58]. The chemical structures of these modified cyclic hexapeptides were deduced based on extensive 1D and 2D NMR experiments as well as data comparison with the literature. The venturamides contain interesting structural features, including two thiazole and one methyl-oxazole ring structures. Venturamide A, in particular, showed preferential *in vitro* activity against the W2 chloroquine-resistant strain of the malaria parasite, *P. falciparum*, with IC_{50} at 8.2μM over mammalian Vero cells. Both compounds, **79** and **80**, showed mild activity when tested against other tropical parasites, such as *T. cruzi* and *L. donovani*.

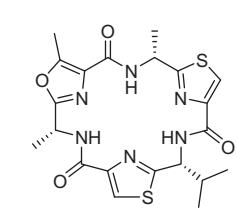

(**79**). Venturamide A

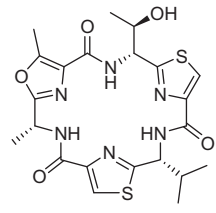

(**80**). Venturamide B

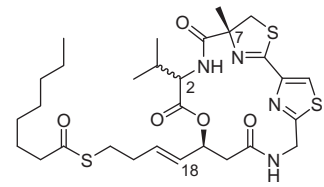

(**83**). Largazole 2*S*
(**84**). 2-*epi*-Largazole 2*R*

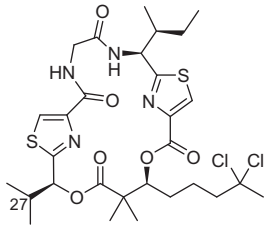

(**81**). 27-Deoxylyngbyabellin A

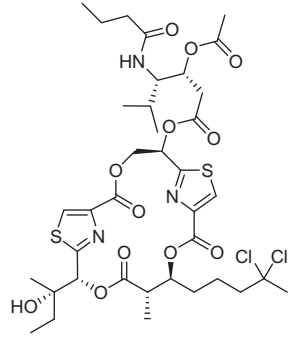

(**82**). Lyngbyabellin J

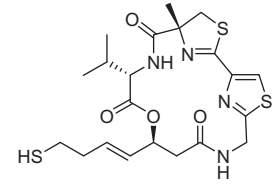

(**85**). Largazole derivative

FIGURE 11 Natural and synthetic heterocycle-containing cyclic depsipeptides/peptides (**79**–**85**).

Lyngbyabellin Derivatives

The lyngbyabellins are a class of thiazole/thiazoline-containing cyclic lipopeptides with dichlorination on the polyketide-derived moiety. A number of these molecules are highly active and are known to interfere with actin cytoskeleton at nanomolar concentrations. Two new lyngbyabellin analogs, 27-deoxylyngbyabellin A (**81**) and lyngbyabellin J (**82**) (Fig. 11), have been isolated from an apratoxin-producing cyanobacterial strain, *L. bouillonii*, obtained from Apra Harbor, Guam [34]. This particular strain appears to be highly prolific in its production of natural products with at least five other molecules, including new lyngbyaloside analogs, laingolide B (**126**) and lyngbyapeptin D (**40**), reported together with **81** and **82** [34]. When compared with lyngbyabellin A, compound **81** displayed higher potency against the HT29 and HeLa cell lines with IC_{50} values reported at 12 and 7.3 nM, respectively. The only difference between lyngbyabellin A and **81** is the presence of hydroxy group at C-27 in the former molecule. Lyngbyabellin J (**82**) has similar cytotoxic activity to lyngbyabellin A when tested against HT29 (IC_{50}=54 nM) and HeLa (IC_{50}=41 nM) cancer cell lines.

Largazole

One of the more exciting cytotoxic marine cyanobacterial compounds discovered in recent years is the report of largazole (**83**) (Fig. 11) in 2008 from the laboratory of Dr. Luesch [59]. This molecule was isolated from the Floridian (Pillars, Key Largo) marine cyanobacterium, *Symploca* sp., and was subsequently found to be a potent class I HDAC inhibitor. Largazole contains a number of unique structural features, including a 4-methylthiazoline linked to a thiazole and an ester of a 3-hydroxy-7-mercaptohept-4-enoic acid unit. Due to its exceptional biological activity, several research groups reported on the total synthesis of this molecule as well as its analogs for further SAR studies. Research groups from Luesch and Hong were the first to report on the concise synthesis (eight steps with overall yield of 19%) of largazole and its derivatives [60,61] (Scheme 2). Since their initial synthetic reports, at least 12 other research groups have successfully attempted the total synthesis of this important molecule. These synthetic reports include Doi [62], Phillips [63], Cramer [64], Ye [65], Bradner and Williams [66–68], Kulkarni [69], Nan [70], Jiang [71], de Lera [72], Forsyth [73,74], Xie [75], and Ganesan [76]. A number of concise syntheses (e.g., Schemes 3 and 4) were outlined for largazole as well as in the generation of analogs for SAR studies.

One of the key findings from the synthetic studies is the revelation of largazole as a pro-drug. Largazole is being converted into the free thiol analog, **85**, within the cell, resulting in cell growth inhibition [60]. A recent review by Tan [4] details the various synthetic studies carried out on largazole. Since the publication of that review, additional synthetic and biological studies on largazole and its derivatives have been published. Zeng *et al*. developed a

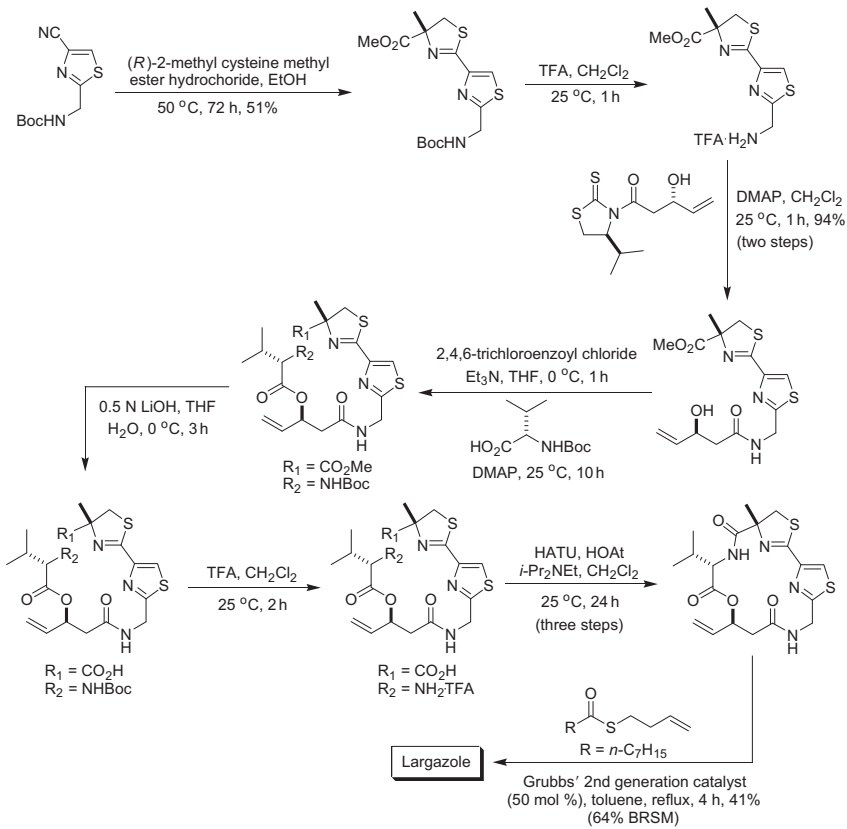

SCHEME 2 Concise synthetic route of largazole by Luesch and Hong [60].

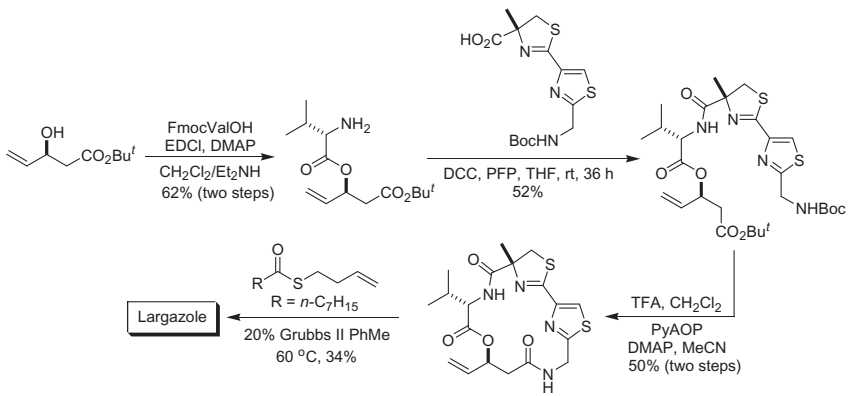

SCHEME 3 Concise synthetic route of largazole by Phillips and coworkers [63].

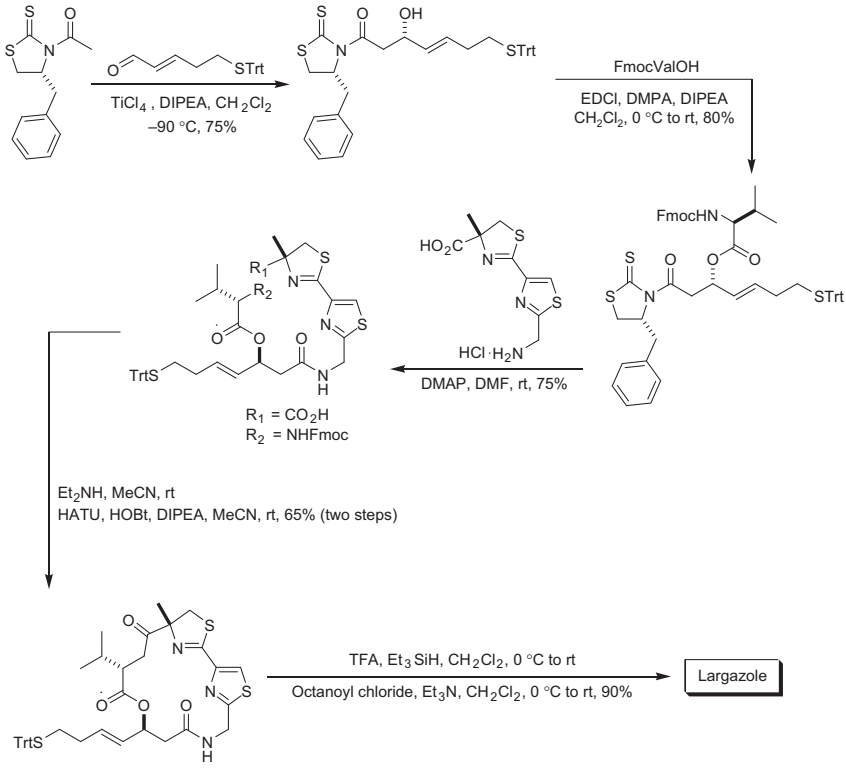

SCHEME 4 Concise synthetic route of largazole by Xie and coworkers [75].

synthetic method for the efficient synthesis (9% overall yield) of largazole as well as other analogs [71]. Their synthetic study revealed that the *trans* geometry of the alkene at C-18 is important for the antiproliferative property of largazole. Further, the replacement of Val with Tyr in largazole enhanced selectivity toward human cancer cells compared with normal cells by more than 100-fold [71]. The synthesis of new largazole analogs with modifications at C-7 and a bithiazole analog based on acyclic cross-metathesis of the respective depsipeptide molecules were recently reported by Souto *et al*. [72]. This study concluded that the HDAC inhibitory activity of the natural product is not affected by changes of the substituent at C-7. In another synthetic and biological study conducted by Wang *et al*., the 2-*epi*-largazole analog, **84**, was found to be more active compared to largazole when tested against the human prostrate cell lines PC-3 and LNCaP [74]. Lastly, a concise total synthesis of largazole, achieved via seven steps with 26.3% overall yield, was reported by Xiao *et al*. [75].

Largazole was screened in the NCI's 60 cancer cell lines and showed that it was preferentially active against colon cancer cell types [77]. Further, it was

found that largazole stimulated histone hyperacetylation in tumor tissue, based on an *in vivo* system using a human HCT116 xenograft mouse model, resulting in the inhibition of tumor growth and induction of apoptosis of tumor cells [77]. A recent report by Lee *et al*. showed largazole to exhibit *in vitro* and *in vivo* osteogenic activity [78].

Apratoxin Analogs

The apratoxin class of molecules is a series of cyclic depsipeptides with potent cytotoxic activities, usually in the nanomolar range, and characterized by a thiazoline unit and an extensive polyketide-derived moiety as part of the macrocyclic structure. The first compound of this series, apratoxin A (**86**) (Fig. 12), was discovered in 2001 from the marine cyanobacterium,

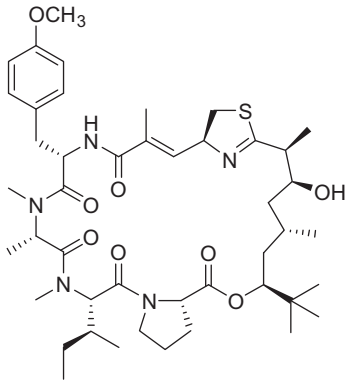

(**86**). Apratoxin A

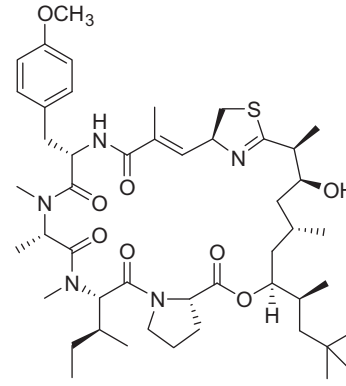

(**87**). Apratoxin D

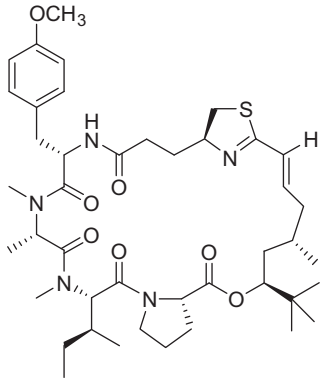

(**88**). Apratoxin E

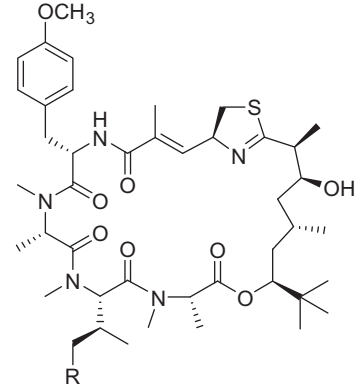

(**89**). Apratoxin F R = CH_3

(**90**). Apratoxin G R = H

FIGURE 12 Apratoxins (**86–90**) from marine cyanobacteria.

L. majuscula, and displayed subnanomolar *in vitro* cytototoxicity against several cancer cell lines [79]. Since 2007, additional analogs, apratoxins D (**87**)–G (**90**), have been discovered from *L. majuscula*, *L. sordida*, and *L. bouillonii*. Apratoxin D (**87**) was isolated from an assemblage of two marine cyanobacteria, *L. majuscula* and *L. sordida*, obtained from Papua New Guinea [80]. Apratoxin D is structurally similar to apratoxin A and differs primarily in the polyketide carbon chain of 3,7-dihydroxy-2,5,8,10,10-pentamethylundecanoic acid unit in the former compound. The structure determination of compound **87** was deduced from extensive NMR and MS data spectral data and by comparison with NMR data of apratoxins A and C. Compound **87** displayed potent *in vitro* cytotoxicity property when tested against H-460 human lung cancer cells having IC_{50} value of 2.6nM.

Apratoxin E (**88**), a dehydrated analog of apratoxin A, was isolated from a Guam collection of the marine cyanobacterium, *L. bouillonii* [81]. Compound **88** showed potent cytotoxicity activity when tested against three cancer cell lines, HT29, HeLa, and U2OS, with IC_{50} values reported at 21, 72, and 59 nM, respectively [81]. Apratoxins F (**89**) and G (**90**) have been reported from a Palmyra collection of *L. bouillonii* [82]. The main difference of these two new molecules is the presence of an *N*-methyl Ala unit in place of a Pro unit in apratoxins A–E. In spite of this difference, apratoxins F and G displayed potent cytotoxicity against H-460 cancer cells with IC_{50} values of 2 and 14 nM, respectively. The synthesis of apratoxin A and its derivatives as well as pharmacological studies were recently reviewed by Tan [4]. Since that review, additional synthetic studies, including Doi *et al*. [83] and Gilles *et al*. [84], were reported for apratoxin A and its analogs. Doi *et al*. developed two synthetic routes based on solid-phase methods for the total synthesis of apratoxin A and its derivatives. They found that the cytotoxicity of the C-34-epimer of **86** was as potent as the natural product and that the replacement of the *O*-methyl-tyrosine with 7-azidoheptyl-tyrosine led to no significant loss of biological activity [83]. The synthetic methods developed by Gilles *et al*. led to a flexible synthesis of the polyketide region of apratoxin A. In addition, their studies allow easy synthesis of oxoapratoxin analogs for future SAR studies [84].

Grassypeptolides

Grassypeptolides A (**91**)–C (**93**) (Fig. 13) are cytotoxic bis-thiazoline-containing cyclic depsipeptides isolated from the marine cyanobacterium, *L. confervoides*, from Grassy Key, Florida [85,86]. Their complete structures, including 3D structures, were determined by a combination of NMR, MS, X-ray crystallography, chemical degradation, and molecular modeling methods.Grassypeptolide A (**91**) displayed significant anticancer activity against four cell lines, including human osteosarcoma (U2OS), cervical carcinoma (HeLa), colorectal adenocarcinoma (HT29), and neuroblastoma (IMR-32), with IC_{50} values reported at 2.2, 1.0, 1.5, and 4.2μM, respectively [85]. Further biological studies showed that

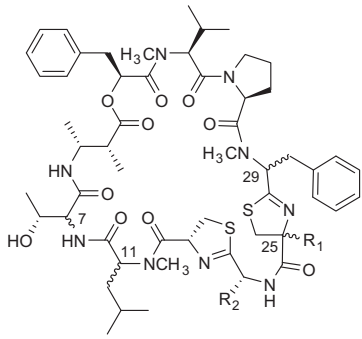

(**91**). Grassypeptolide A 7 *R*, 11*R*, 25*R*, *29*R* H Et
(**92**). Grassypeptolide B 7 *R*, 11*R*, 25*R*, *29*R* H Me
(**93**). Grassypeptolide C 7 *R*, 11*R*, 25*R*, *29*S* H Et
(**94**). Grassypeptolide D 7 *R*, 11*R*, 25*S*, 29*S* Me Et
(**95**). Grassypeptolide E 7 *S*, 11*S*, 25*S*, 29*S* Me Et

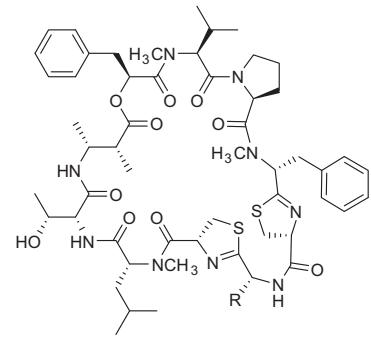

(**96**). Grassypeptolide F R = Et
(**97**). Grassypeptolide G R = Me

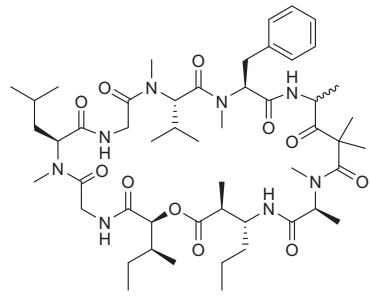

(**98**). Ibu-epidemethoxylyngbyastatin

FIGURE 13 Grassypeptolides (**91**–**97**) and Ibu-epidemethoxylyngbyastatin (**98**) from marine cyanobacteria.

at lower concentrations, compounds **91** and **93** arrest cell cycle at G1 phase while at higher concentrations, they arrest cell cycle at the G2/M phase [86].

Four new analogs, grassypeptolides D (**94**)–G (**97**) were recently isolated from two marine cyanobacterial species, *Leptolyngbya* sp. and *L. majuscula*. Grassypeptolides D (**94**) and E (**95**) were purified, along with a new lyngbyastatin analog (compound **98**) and the known dolastatin 12, from field collections as well as laboratory cultures of the marine cyanobacterium, *Leptolyngbya* sp., obtained from a shipwreck in the Red Sea [87]. Grassypeptolides F (**96**) and G (**97**) were obtained from the marine cyanobacterium, *L. majuscula*, collected from Palau [88]. Grassypeptolides D and E exhibited significant activity against the HeLa and mouse neuro-2a blastoma cell lines with IC_{50} values of 335 and 192 nM and 599 and 407 nM, respectively. Compounds **96** and **97**, on the other hand, showed moderate inhibitory activity when tested against the transcription factor AP-1 with IC_{50} values of 5.2 and 6.0 μM, respectively.

Hoiamides

In recent years, a number of novel polyketide–polypeptide-type neurotoxins have been reported from filamentous strains of marine cyanobacteria. One of these neurotoxins is hoiamide A (**99**) (Fig. 14), isolated from an assemblage of two cyanobacteria *L. majuscula* and *Phormidium gracile* obtained from Hoia Bay, Papua New Guinea [89]. Hoiamide A consists of a number of unique structural features, including an acetate extended isoleucine-derived unit, two methylated thiazoline units, a thiazole unit, and a highly methylated and oxygenated polyketide-derived moiety. Its structure was determined by extensive NMR and chemical manipulation methods. Using neurochemical and pharmacological methods, it was shown that hoiamide A is a potent inhibitor of [3*H*]batrachotoxin binding to VGSCs and it activates sodium influx with IC_{50} and EC_{50} values of 92.8 nM and 2.31 μM, respectively. Since its first discovery in 2009, two more analogs, hoiamides B (**100**), a cyclic depsipeptide, and C (**101**), a linear lipopeptide, have been isolated from various marine cyanobacteria samples from Papua New Guinea [90]. When tested on neocortical neural cells, hoiamide B (**100**) promote sodium influx but reduced spontaneous Ca^{2+} oscillations with EC_{50} values at 3.9 μM and 79.8 nM, respectively.

Lariat-Type Cyclic Depsipeptides

Lynbyastatin Derivatives

At least 14 3-amino-6-hydroxypiperidone (Ahp)-containing cyclic depsipeptides from marine cyanobacteria have been reported and a number of these compounds are known to possess significant serine protease inhibitory properties. Members of this structural class include the lyngbyastatin class of compounds, bouillomides, molassamide, pompanopeptins, symplocamide A, and kempopeptins. Serine proteases, including elastase, chymotrypsin, and trypsin, are a large class of enzymes and play different roles in human health,

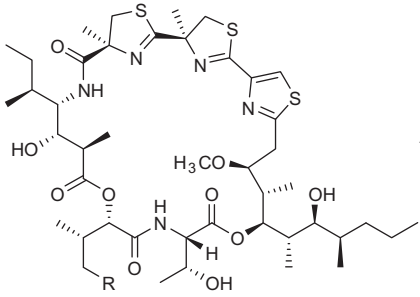

(**99**). Hoiamide A R = H
(**100**). Hoiamide B R = CH_3

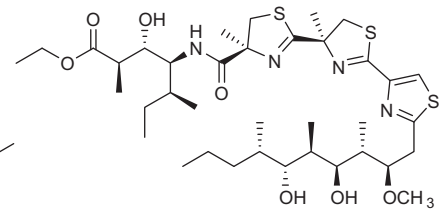

(**101**). Hoiamide C

FIGURE 14 Hoiamides from marine cyanobacteria.

including immune response and blood coagulation. An increase or decrease of protease activity can also induce pathologies, such as cancer, inflammation, heart attack, stroke, and pancreatitis. Lyngbyastatin 4 (**102**) (Fig. 15), isolated from the Floridian (Fort Lauderdale and Pompano Beach) marine cyanobacterium, *L. confervoides*, was found to selectively inhibit elastase and chymotrypsin with IC_{50} values of 30 nM and 0.30 μM, respectively [91]. Three new lyngbyastatin analogs, lyngbyastatins 5 (**103**)–7 (**105**) (Fig. 15), were isolated from *L. confervoides* collected off the coast of Fort Lauderdale, Florida [92]. Compounds **103–105** showed potent elastase inhibitory properties with IC_{50} values at 3.2, 3.3, and 8.3 nM, respectively. A previously known

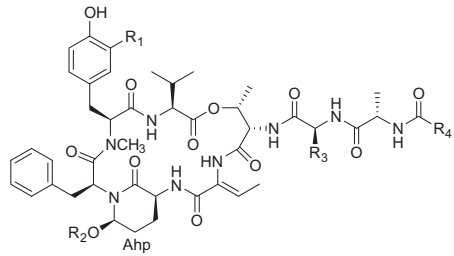

(**102**). Lyngbyastatin 4 R_1 = H, R_2 = H, R_3 = $(CH_2)_2$Ph-OH, R_4 = $CH(OH)CH_2OSO_3H$
(**103**). Lyngbyastatin 5 R_1 = H, R_2 = H, R_3 = $(CH_2)_2$Ph-OH, R_4 = $CH(OH)CH_2$-OH
(**104**). Lyngbyastatin 6 R_1 = H, R_2 = CH_3, R_3 = $(CH_2)_2$Ph-OH, R_4 = $CH(OH)CH_2$-OSO_3Na
(**106**). Lyngbyastatin 8 R_1 = H, R_2 = H, R_3 = *i*-Pr, R_4 = CH_3
(**107**). Lyngbyastatin 9 R_1 = H, R_2 = H, R_3 = *i*-Pr, R_4 = $(CH_2)_2CH_3$
(**108**). Lyngbyastatin 10 R_1 = Br, R_2 = H, R_3 = *i*-Pr, R_4 = $(CH_2)_2CH_3$

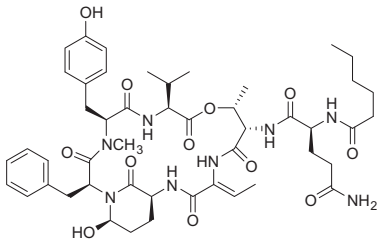

(**105**). Lyngbyastatin 7

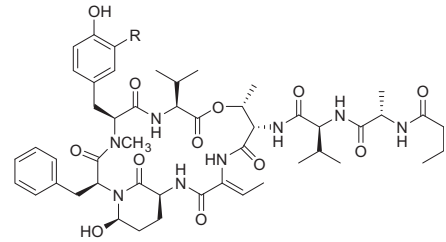

(**109**). Bouillomide A R = H
(**110**). Bouillomide B R = Br

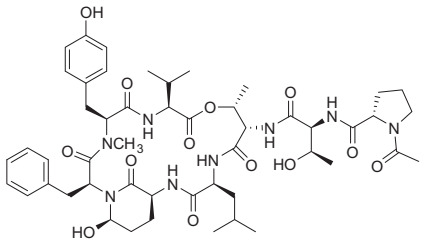

(**111**). Kempopeptin A

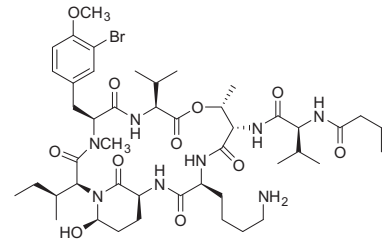

(**112**). Kempopeptin B

FIGURE 15 3-Amino-6-hydroxypiperidone (Ahp)-containing marine cyanobacterial compounds (**102–112**).

compound, somamide B, was also isolated along with these compounds and it was found to inhibit porcine elastase with an IC_{50} of 4.2 nM [92]. Chemical investigation of an organic extract from *L. semiplena* collected from Tumon Bay, Guam, yielded further lyngbyastatin analogs, lyngbyastatins 8 (**106**)–10 (**108**) [93]. The elastase inhibitory activities of these new analogs were found to be less active compared to lyngbyastatins 4 (**102**)–7 (**105**). Their reported IC_{50} values were 123, 210, and 120 nM for compounds **106**, **107**, and **108**, respectively.

Bouillomides

Bouillomides A (**109**) and B (**110**) are new lyngbyastatin/dolastatin 13 analogs isolated from a Guamanian strain of *L. bouillonii* [94]. Their complete structure determination was deduced from NMR, MS, and chemical manipulation involving Marfey's method. Compounds **109** and **110** showed selective serine protease inhibition with IC_{50} values at 1.9 μM for both molecules while the chymotrypsin inhibitory activity were observed at IC_{50} values of 0.17 and 9.3 μM for compounds **109** and **110**, respectively [94].

Kempopeptins

Two Ahp-containing cyclic depsipeptides, kempopeptins A (**111**) and B (**112**) (Fig. 15), were isolated from a collection of a Floridan (mangrove channel at northern part of Kemp Channel, Florida Keys) marine cyanobacterium, *Lyngbya* sp. [95]. The organic extract of this cyanobacterial sample yielded lyngbyastatin 7 as well as somamide B. When evaluated for their inhibitory activity against chymotrypsin and elastase, compound **111** was the more potent molecule with IC_{50} values at 2.6 and 0.32 μM, respectively.

Molassamide

Molassamide (**113**) (Fig. 16) was isolated from the organic extract of the marine cyanobacterial assemblage comprising mostly *Dichothrix utahensis*, collected from Molasses Reef, Key Largo, Florida [96]. This molecule is perhaps the first natural product reported from the cyanobacterial genus *Dichothrix*. The structure of molassamide was determined by NMR methods and chiral HPLC analysis. Compound **113** displayed significant inhibitory activity against elastase and chymotrypsin with IC_{50} values at 32 and 234 nM, respectively [96].

Symplocamide A

Symplocamide A (**114**) (Fig. 16) is both a potent cytotoxin and a chymotrypsin inhibitor isolated from the marine cyanobacterium, *Symploca* sp., from Sunday Island, Papua New Guinea [97]. Compound **114** differs from other Ahp-containing cyclodepsipeptides in having citrulline and *N*,*O*-diMe-Br-Tyr units as part of the cyclic core structure. Symplocamide A inhibits

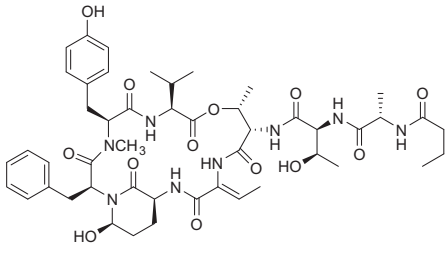

(**113**). Molassamide

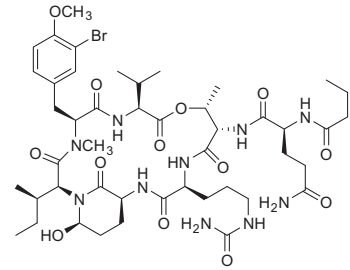

(**114**). Symplocamide A

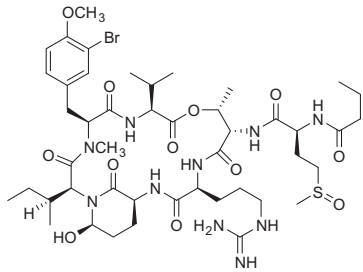

(**115**). Pompanopeptin A

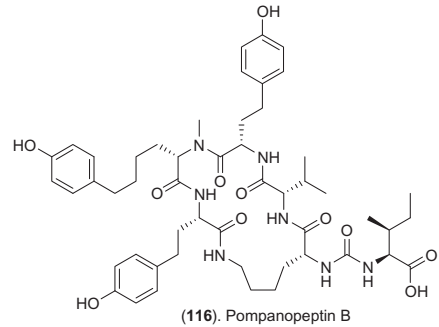

(**116**). Pompanopeptin B

FIGURE 16 3-Amino-6-hydroxypiperidone (Ahp)-containing marine cyanobacterial compounds (**113–115**) and pompanopeptin B (**116**).

chymotrypsin and trypsin with IC_{50} values reported at 0.38 and 80.2 μM, respectively. Further, compound **114** is highly potent when tested against NCI-H460 non-small lung cancer cells and neuro-2a mouse neuroblastoma cells with IC_{50} values at 40 and 29 nM, respectively. When tested against three tropical parasites, compound **114** was found to be more active against W2 *P. falciparum*, with IC_{50} at 0.95 μM [97].

Pompanopeptins

Pompanopeptins A (**115**) and B (**116**) (Fig. 16) are new cyclic peptides isolated from the marine cyanobacterium, *L. confervoides*, procured off the coast of Fort Lauderdale, Florida [98]. Compounds **115** and **116** are not structurally related since the former compound is a Ahp-containing cyclodepsipeptide while the later molecule is a cyclic pentapeptide containing a unique *N*-methyl-2-amino-6-(4′-hydroxy-phenyl)hexanoic acid unit. Compound **115** selectively inhibited trypsin with IC_{50} value reported at 2.4 μM [98].

Tiglicamides

The organic extract from the Floridian (at reefs near Port Everglades Inlet) marine cyanobacterium, *L. confervoides*, yielded new cyclic depsipeptides, tiglicamides A (**117**)–C (**119**), as well as the known compounds largamides A

(**120**)–C (**122**) (Fig. 17) [99]. Since the initial reports of largamides by Plaza and Bewley in 2006 [100], the original structures of largamides A–C have been revised as **120**–**122** based on NMR spectral data and chiral HPLC analysis [101]. These series of compounds differ primarily by only one amino acid unit in the core macrocyclic structure. The inhibitory properties of all six compounds on porcine pancreatic elastase were evaluated and found to display moderate activity with IC_{50} values ranging from 0.53 to 7.28 μM [99,101].

Coibamide A

Coibamide A (**123**) (Fig. 17) is a potent antiproliferative lariat-type cyclic depsipeptide, isolated from the Panamanian marine cyanobacterium, *Leptolyngbya*

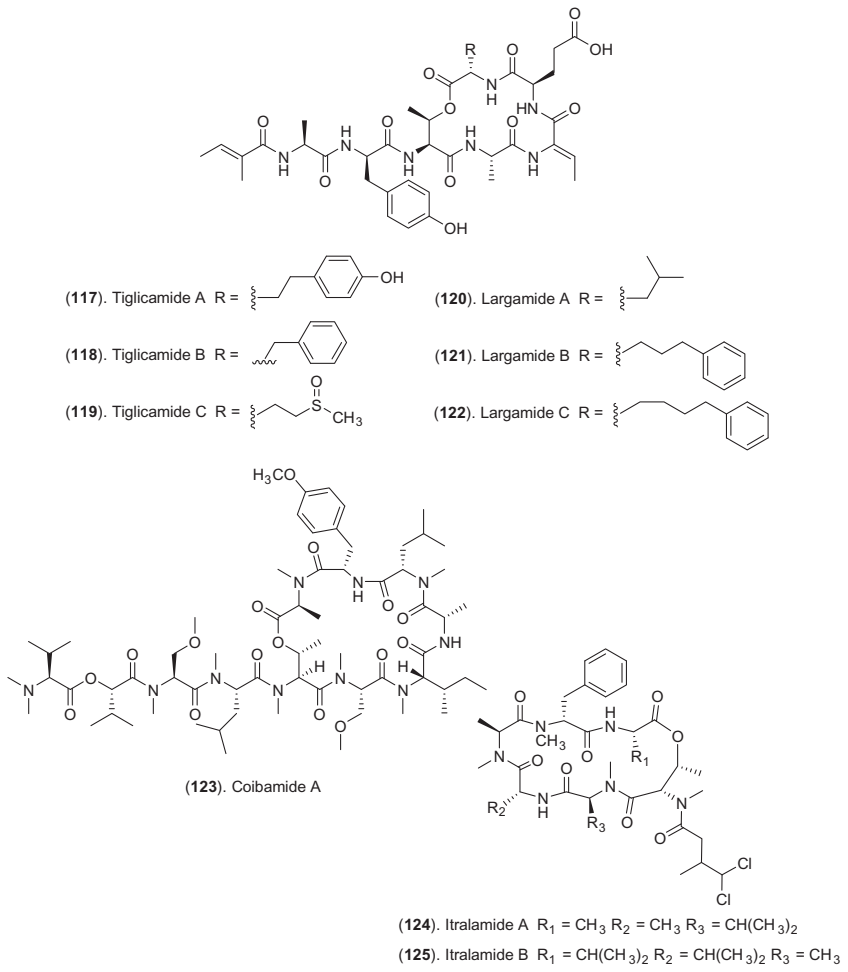

FIGURE 17 Lariat-type marine cyanobacterial compounds (**117**–**125**).

sp. [102]. This compound was isolated as part of an ICBG program, between research groups in the United States and Panama, to screen and identify bioactive compounds from natural sources in the later country. This molecule possesses a high degree of *N*-methylation with 8 out of 11 amino acid residues being *N*-methylated. The chemical structure of compound **123** was established by extensive 2D NMR spectroscopic experiments (e.g., COSY, TOCSY, multiplicity-edited HSQS, HSQC-TOCSY, HMBC, H2BC, $^{1}H–^{15}N$ gHMBC, and ROESY) as well as mass spectroscopic analysis. The absolute stereochemistry of the **123** was determined by Marfey's method as well as chiral HPLC analysis. Coibamide A displayed potent cytotoxicity against NCI-H460 lung cancer cells and mouse neuro-2a cells, with LC_{50} values less than 23 nM. In addition, the compound was evaluated in the NCI's panel of 60 cancer cell lines and it exhibited significant activities against MDA-MB-231, LOX IMVI, HL-60 (TB), and SNB-75 with IC_{50} values at 2.8, 7.4, 7.4, and 7.6 nM, respectively. COMPARE analysis indicated that coibamide A could be inhibiting cancer cell proliferation via a novel mechanism [102].

Itralamides

The cyclic depsipeptides, itralamides A (**124**) and B (**125**) (Fig. 17), were isolated along with grenadamides B (**12**) and C (**13**) (discussed above) from *L. majuscula* collected from True Blue Bay, Grenada [12]. The structures of these molecules were determined mainly by NMR, MS spectral data, and chemical manipulation involving the use of Marfey's method. Itralamides contained an interesting branched chlorinated moiety, 4,4-dichloro-3-methylbutanoic acid, linked via amide bond to *N*Me-Thr. This chlorinated unit could potentially be derived from Val and involves the novel chlorination of unreactive carbon. The presence of chlorinated moieties is found in a number of cyanobacterial compounds, such as barbamide. Itralamide B was found to be an order more toxic (IC_{50}=6 μM) on human embryonic kidney (HEK-293) cells compared to **124**.

Cyclic Depsipeptides with Extensive Polyketide Chain

Laingolide B

Laingolide B (**126**) (Fig. 18) was isolated from the marine cyanobacterial strain, *L. bouillonii*, obtained from Apra Harbor, Guam [34]. It is structurally related to the known laingolide A and the major difference lies in the presence of a branched vinyl chloride functional group at C-7 in **126**. Compound **126** could be biosynthesized from the starter unit of 2,2-dimethyl-propyl CoA and extended by four units of acetyl CoA, linked to a unit of Gly with further extension by a unit of acetyl CoA. Methylation at C-7 and C-4 could derive from *S*-adenosyl-L-methionine (SAM). The exocyclic vinyl chloride moiety in **126** is also present in other marine cyanobacterial compounds, such as the malyngamides. Unfortunately, this molecule degraded before it could be subjected to further biological testing.

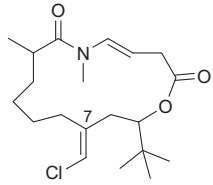

(**126**). Laingolide B

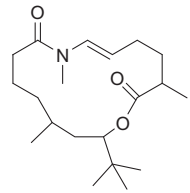

(**127**). Palmyrolide A

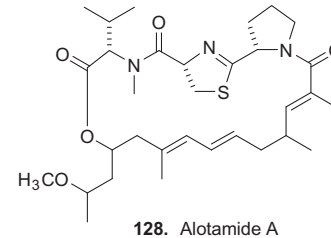

128. Alotamide A

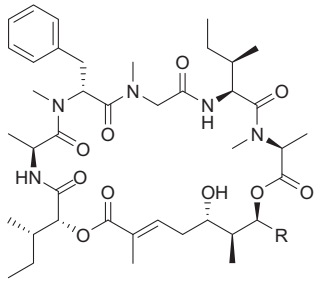

(**129**). Lagunamide A R=

(**130**). Lagunamide B R=

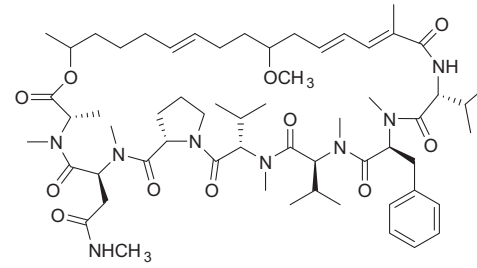

(**131**). Malevamide E

FIGURE 18 Marine cyanobacterial compounds (**126–131**).

Palmyrolide A

Palmyrolide A (**127**) and alotamide A (**128**) (Fig. 18) are two new neurotoxins isolated from marine cyanobacteria from Palmyra Atoll and Milne Bay, Papua New Guinea, respectively [103,104]. These molecules are structurally unique consisting of extensive polyketide portion linking with peptidic residues. Palmyrolide A (**127**) was isolated from a marine cyanobacterial consortium of *Leptolyngbya cf.* and *Oscillatoria* sp. [103]. This molecule is structurally related to the laingolides by featuring a *tert*-butyl group possibly deriving from malonyl-CoA with the methyl groups contributed by SAM. Palmyrolide A was found to suppress calcium influx in cerebrocortical neurons with IC_{50} of 3.7 μM. In addition, it possesses moderate sodium channel blocking activity in neuro-2a cells with IC_{50} of 5.2 μM [103].

Alotamide A

The polyketide portion of alotamide A (**128**) (Fig. 18), obtained from the marine cyanobacterium, *L. bouillonii*, consists of seven acetate units as part of the macrocyclic ring structure [104]. Three other peptidic residues, an *N*Me-Val, a cysteine-derived thiazoline unit and Pro, are linked to the polyketide unit completing the overall macrocyclic structure of the molecule. When

tested on murine cerebrocortical neurons, alotamide A showed unusual Ca^{2+} influx activation profile with EC_{50} of 4.18 μM.

Lagunamides

Recently from our laboratory, we isolated a series of aurilide-related compounds, lagunamides A (**129**) and B (**130**) (Fig. 18), from a collection of *L. majuscula* from Pulau Hantu, Singapore [105]. The chemical structures of these new compounds were established by NMR techniques, HR-MS data, as well as Mosher's and the advanced Marfey's methods. In addition to its nanomolar cytotoxic activities against P388 murine leukemia cell lines (IC_{50} values of 6.4 nM for **129** and 20.5 nM for **130**), the lagunamides A and B displayed significant antimalarial properties when tested against *P. falciparum* with IC_{50} values of 0.19 and 0.91 μM, respectively. Further, these cyanobacterial compounds exhibited moderate antiswarming activities when tested against *Pseudomonas aeruginosa* PA01. The aurilide class of molecules is gaining attention in the scientific community due to its potent cytotoxic properties. Several researchers have reported on the total synthesis of aurilide and its derivative [106,107]. In addition, aurilide was recently showed to activate the OPA1-mediated apoptosis by targeting prohibitin [108].

Malevamide E

A new dolastatin 14 analog, malevamide E (**131**) (Fig. 18), was isolated from the marine cyanobacterium, *Symploca laete-viridis*, procured from coastal waters of Oahu, in the vicinity of Ala Moana Beach Park [109]. The planar structure of malevamide E was achieved through extensive 1D, 2D NMR, and MS/MS analysis, while its absolute stereochemistry was determined mainly by chiral HPLC. Compound **131** displayed dose-dependent inhibition of store-operated Ca^{2+} entry in HEK cells treated with thapsigargin [109].

ACKNOWLEDGMENTS

The author acknowledges NIE AcRF (RI 8/05 TLT and RI 11/10 TLT) for financial support. The author would also like to thank two anonymous reviewers for their useful comments/suggestions.

ABBREVIATIONS

AP-1	Activator protein 1
BF_3Et_2O	Boron triflouride-ethyl ether complex
Bn	Benzyl group
Boc	*tert*-Butyloxycarbonyl group
CD spectroscopy	Circular dichroism spectroscopy
CH_2Cl_2	Dichloromethane
CH_3CN	Acetonitrile

COSY	Correlation spectroscopy
DCC	*N*,*N*′-Dicyclohexylcarbodiimide
DFT	Density functional theory
DIPEA	Diisopropylethylamine
DMAP	4-Dimethylaminopyridine
DMF	Dimethylformamide
ED_{50}	Half maximal effective dosage
EDCI	Ethyl-(*N*′,*N*′-dimethylamino)propylcarbodiimide hydrochloride
Et_3N	Triethylamine
EtOAc	Ethylacetate
EtOH	Ethanol
Et_3SiH	Triethylsilane
FAB-MS	Fast atom bombardment-mass spectrometry
Fmoc	9-Fluorenylmethyloxycarbonyl group
GC	Gas chromatography
H2BC	Heteronuclear 2-bond correlation spectroscopy
H-460	Human lung carcinoma cell line
HATU	(Dimethylamino)-*N*,*N*-dimethyl(3H-[1,2,3]triazolo[4,5-b] pyridin-3-yloxy)methaniminium hexafluorophosphate
HCT-116	Human colorectal carcinoma cell line
HDAC	Histone deacetylase
HEK-293	Human embryonic kidney cell line
HeLa S3	Clonal-derivative of the human epithelial carcinoma cell line
HL-60	Human promyelocytic leukemia cell line
HMBC	Heteronuclear multiple-bond correlation spectroscopy
HOAt	1-Hydroxy-7-azabenzotriazole
HOBt	*N*-Hydroxybenzotriazole
HPLC	High performance liquid chromatography
HSQC	Heteronuclear single-quantum correlation spectroscopy
HT-29	Human colon adenocarcinoma grade II cell line
IC_{50}	Half maximal inhibitory concentration
IMR-32	Human neuroblastoma cell line
***i*-Pr_2NEt**	*N*,*N*-Diisopropylethylamine
LC_{50}	Half maximal lethal concentration
$LiBEt_3H$	Lithium triethylborohydride
LiHMDS	Lithium bis(trimethylsilyl)amide
LiOH	Lithium hydroxide
LOX IMVI	Human melanoma cell line
MALDI-TOF MS	Matrix-assisted laser desorption ionization-time of flight mass spectrometry
MCF-7	Human breast adenocarcinoma cell line

MDA-MB-231	Human breast cancer cell line
MeOTf	Methyl triflate
MOLT-4	Human acute lymphoblastic leukemia cell line
MS	Mass spectrometry
$NaHCO_3$	Sodium bicarbonate
NBS	*N*-Bromosuccinimide
NCI-H460	Non-small cell lung cancer cell line
NH_4OH	Ammonium hydroxide
Neuro-2a	Mouse neuroblastoma cell line
NIH	National Institute of Health
NMA	1-Naphthlenemethylamine
NMR	Nuclear magnetic resonance
NOE	Nuclear Overhauser effect
OPA1	Optic atropy 1 protein
Pd/C	Palladium on carbon
$Pd(PPh_3)_4$	Tetrakis(triphenylphosphine)palladium
PFP	*N*-Pentafluoropropionyl
PKS	Polyketide synthase
PyAOP	Benzotriazol-1-yl-oxytripyrrolidinophosphonium hexafluorophosphate
RAW264.7	Murine macrophage-like cell line
ROE	Rotating frame Overhauser effect
RP-HPLC	Reversed phase-high performance liquid chromatography
SAR	Structure-activity relationship
SNB-75	Human glioma cell line
SSU 16S rRNA	Small subunit 16S ribosomal ribonucleic acid
TC_{50}	Half maximal therapeutic concentration
THF	Tetrahydrofuran
TFA	Trifluoroacetic acid
TFAA	Trifluoroacetic anhydride
$TiCl_4$	Titanium tetrachloride
$TMSCHN_2$	Trimethylsilyldlazomethane
TOCSY	Total correlation spectroscopy
U2OS	Osteosarcoma cell line

REFERENCES

[1] W.H. Gerwick, L.T. Tan, N. Sitachitta, in: G.A. Cordell (Ed.), The Alkaloids: Chemistry and Biology, Academic Press, San Diego, 2001, pp. 75–184 vol. 57.
[2] L.T. Tan, Phytochemistry 68 (2007) 954–979.
[3] A.C. Jones, E.A. Monroe, E.B. Eisman, L. Gerwick, D.H. Sherman, W.H. Gerwick, Nat. Prod. Rep. 27 (2010) 1048–1065.
[4] L.T. Tan, J. Appl. Phycol. 22 (2010) 659–676.

[5] A.M. Mayer, K.B. Glaser, C. Cuevas, R.S. Jacobs, W. Kem, R.D. Little, J.M. McIntosh, D. J. Newman, B.C. Potts, D.E. Shuster, Trends Pharmacol. Sci. 31 (2010) 255–265.
[6] J.K. Nunnery, E. Mevers, W.H. Gerwick, Curr. Opin. Biotechnol. 21 (2010) 787–793.
[7] G.G. Harrigan, H. Luesch, W.Y. Yoshida, R.E. Moore, D.G. Nagle, J. Biggs, P.U. Park, V. J. Paul, J. Nat. Prod. 62 (1999) 464–467.
[8] B.R. Clark, N. Engene, M.E. Teasdale, D.C. Rowley, T. Matainaho, F.A. Valeriote, W. H. Gerwick, J. Nat. Prod. 71 (2008) 1530–1537.
[9] N. Engene, H. Choi, E. Esquenazi, T. Byrum, F.A. Villa, Z. Cao, T.F. Murray, P. C. Dorrestein, L. Gerwick, W.H. Gerwick, J. Nat. Prod. (2011), doi:10.1021/np200236c.
[10] L.T. Tan, Y.Y. Chang, A. Tripathi, Phytochemistry 69 (2008) 2067–2069.
[11] B. Han, K.L. McPhail, A. Ligresti, V. Di Marzo, W.H. Gerwick, J. Nat. Prod. 66 (2003) 1364–1368.
[12] J.I. Jiménez, T. Vansach, W.Y. Yoshida, B. Sakamoto, P. Pörzgen, F.D. Horgen, J. Nat. Prod. 72 (2009) 1573–1578.
[13] A.R. Pereira, L. Etzbach, N. Engene, R. Müller, W.H. Gerwick, J. Nat. Prod. 74 (2011) 1175–1181.
[14] H. Gross, K.L. McPhail, D.E. Goeger, F.A. Valeriote, W.H. Gerwick, Phytochemistry 71 (2010) 1729–1735.
[15] J.C. Kwan, M. Teplitski, S.P. Gunasekera, V.J. Paul, H. Luesch, J. Nat. Prod. 73 (2010) 463–466.
[16] B. Han, U.M. Reinscheid, W.H. Gerwick, H. Gross, J. Mol. Struct. 989 (2011) 109–113.
[17] K.L. Malloy, F.A. Villa, N. Engene, T. Matainaho, L. Gerwick, W.H. Gerwick, J. Nat. Prod. 74 (2011) 95–98.
[18] S.P. Gunasekera, C.S. Owle, R. Montaser, H. Luesch, V.J. Paul, J. Nat. Prod. 74 (2011) 871–876.
[19] S. Suntornchashwej, K. Suwanborirux, K. Koga, M. Isobe, Chem. Asian J. 2 (2007) 114–122.
[20] Y. Li, J.P. Feng, W.H. Wang, J. Chen, X.P. Cao, J. Org. Chem. 72 (2007) 2344–2350.
[21] J.P. Feng, Z.F. Shi, Y. Li, J.T. Zhang, X.L. Qi, J. Chen, X.P. Cao, J. Org. Chem. 73 (2008) 6873–6876.
[22] J. Chen, X.G. Fu, L. Zhou, J.T. Zhang, X.L. Qi, X.P. Cao, J. Org. Chem. 74 (2009) 4149–4157.
[23] X.L. Qi, J.T. Zhang, J.P. Feng, X.P. Cao, Org. Biomol. Chem. 9 (2011) 3817–3824.
[24] E. Andrianasolo, D. Goeger, W.H. Gerwick, Pure Appl. Chem. 79 (2007) 593–602.
[25] R.G. Linington, B.R. Clark, E.E. Trimble, A. Almanza, L.D. Ureña, D.E. Kyle, W. H. Gerwick, J. Nat. Prod. 72 (2009) 14–17.
[26] K. Taori, Y. Liu, V.J. Paul, H. Luesch, ChemBioChem 10 (2009) 1634–1639.
[27] T. Conroy, J.T. Guo, N.H. Hunt, R.J. Payne, Org. Lett. 12 (2010) 5576–5579.
[28] K.L. McPhail, J. Correa, R.G. Linington, J. Gonzalez, E. Ortega-Barrie, T.L. Capson, W. H. Gerwick, J. Nat. Prod. 70 (2007) 984–988.
[29] S.P. Gunasekera, C. Ross, V.J. Paul, S. Matthew, H. Luesch, J. Nat. Prod. 71 (2008) 887–890.
[30] M.J. Balunas, R.G. Linington, K. Tidgewell, A.M. Fenner, L.D. Ureña, G.D. Togna, D. E. Kyle, W.H. Gerwick, J. Nat. Prod. 73 (2010) 60–66.
[31] L.M. Sanchez, D. Lopez, B.A. Vesely, G.D. Togna, W.H. Gerwick, D.E. Kyle, R. G. Linington, J. Med. Chem. 53 (2010) 4187–4197.
[32] T.L. Simmons, N. Engene, L.D. Urena, L.I. Romero, E. Ortega-Barria, L. Gerwick, W. H. Gerwick, J. Nat. Prod. 71 (2008) 1544–1550.

[33] J.C. Kwan, E.A. Eksioglu, C. Liu, V.J. Paul, H. Luesch, J. Med. Chem. 52 (2009) 5732–5747.
[34] S. Matthew, L.A. Salvador, P.J. Schupp, V.J. Paul, H. Luesch, J. Nat. Prod. 73 (2010) 1544–1552.
[35] T. Teruya, H. Sasaki, H. Fukazawa, K. Suenaga, Org. Lett. 11 (2009) 5062–5065.
[36] X. Gao, Y. Liu, S. Kwong, Z. Xu, T. Ye, Org. Lett. 12 (2010) 3018–3021.
[37] H. Sasaki, T. Teruya, H. Fukazawa, K. Suenaga, Tetrahedron 67 (2011) 990–994.
[38] W. Li, S. Yu, M. Jin, H. Xia, D. Ma, Tetrahedron Lett. 52 (2011) 2124–2127.
[39] E. Sumiya, H. Shimogawa, H. Sasaki, M. Tsutsumi, K. Yoshita, M. Ojika, K. Suenaga, M. Uesugi, ACS Chem. Biol. 6 (2011) 425–431.
[40] C. Frost, S.D. Penrose, R. Gleave, Org. Biomol. Chem. 6 (2008) 4340–4347.
[41] E.O. De Oliveira, K.M. Graf, M.K. Patel, A. Baheti, H.S. Kong, L.H. Macarthur, S. Dakshanamurthy, K. Wang, M.L. Brown, M. Paige, Bioorg. Med. Chem. 19 (2011) 4322–4329.
[42] J. Chen, P.Q. Huang, Y. Queneau, J. Org. Chem. 74 (2009) 7457–7463.
[43] T. Sun, W. Zhang, C. Zong, P. Wang, Y. Li, J. Pept. Sci. 16 (2010) 364–374.
[44] Z.H. Ma, N. Song, C.X. Li, W. Zhang, P. Wang, Y.X. Li, J. Pept. Sci. 14 (2008) 1139–1147.
[45] H.Q. Lan, J.L. Ye, A.E. Wang, Y.P. Ruan, P.Q. Huang, Chemistry 17 (2011) 958–968.
[46] T. Meickle, S.P. Gunasekera, Y. Liu, H. Luesch, V.J. Paul, Bioorg. Med. Chem. (2011), doi:10.1016/j.bmc.2011.05.051.
[47] A. Tripathi, J. Puddick, M.R. Prinsep, P.P. Lee, L.T. Tan, J. Nat. Prod. 72 (2009) 29–32.
[48] A. Tripathi, J. Puddick, M.R. Prinsep, P.P. Lee, L.T. Tan, Phytochemistry 71 (2010) 307–311.
[49] L.T. Tan, B.P. Goh, A. Tripathi, M.G. Lim, G.H. Dickinson, S.S. Lee, S.L. Teo, Biofouling 26 (2010) 685–695.
[50] M. Taniguchi, J.K. Nunnery, N. Engene, E. Esquenazi, T. Byrum, P.C. Dorrestein, W. H. Gerwick, J. Nat. Prod. 73 (2010) 393–398.
[51] L. Salvador, J.S. Biggs, V.J. Paul, H. Luesch, J. Nat. Prod. 74 (2011) 917–927.
[52] E. Mevers, W.T. Liu, N. Engene, H. Mohimani, T. Byrum, P.A. Pevzner, P.C. Dorrestein, C. Spadafora, W.H. Gerwick, J. Nat. Prod. 74 (2011) 928–936.
[53] S.P. Gunasekera, R. Ritson-Williams, V.J. Paul, J. Nat. Prod. 71 (2008) 2060–2063.
[54] R. Montaser, K.A. Abboud, V.J. Paul, H. Luesch, J. Nat. Prod. 74 (2011) 109–112.
[55] T.L. Simmons, L.M. Nogle, J. Media, F.A. Valeriote, S.L. Mooberry, W.H. Gerwick, J. Nat. Prod. 72 (2009) 1011–1016.
[56] I. Bonnard, M. Rolland, J.M. Salmon, E. Debiton, C. Barthomeuf, B. Banaigs, J. Med. Chem. 50 (2007) 1266–1279.
[57] N. Maru, O. Ohno, D. Uemura, Tetrahedron Lett. 51 (2010) 6384–6387.
[58] R.G. Linington, J. Gonzalez, L.-D. Urena, L.I. Romero, E. Ortega-Barria, W.H. Gerwick, J. Nat. Prod. 70 (2007) 397–401.
[59] K. Taori, V.J. Paul, H. Luesch, J. Am. Chem. Soc. 130 (2008) 1806–1807.
[60] Y. Ying, K. Taori, H. Kim, J. Hong, H. Luesch, J. Am. Chem. Soc. 130 (2008) 8455–8459.
[61] Y. Ying, Y. Liu, S.R. Byeon, H. Kim, H. Luesch, J. Hong, Org. Lett. 10 (2008) 4021–4024.
[62] Y. Numajiri, T. Takahashi, M. Takagi, K. Shin-ya, T. Doi, Synlett 16 (2008) 2483–2486.
[63] C.G. Nasveschuk, D. Ungermannova, X. Liu, A.J. Phillips, Org. Lett. 10 (2008) 3595–3598.
[64] T. Seiser, F. Kamena, N. Cramer, Angew. Chem. Int. Ed Engl. 47 (2008) 6483–6485.
[65] Q. Ren, L. Dai, H. Zhang, W. Tan, Z. Xu, T. Ye, Synlett 15 (2008) 2379–2383.
[66] A. Bowers, N. West, J. Taunton, S.L. Schreiber, J.E. Bradner, R.M. Williams, J. Am. Chem. Soc. 130 (2008) 11219–11222.

[67] A.A. Bowers, T.J. Greshock, N. West, G. Estiu, S.L. Schreiber, O. Wiest, R.M. Williams, J.E. Bradner, J. Am. Chem. Soc. 131 (2009) 2900–2905.
[68] A.A. Bowers, N. West, T.L. Newkirk, A.E. Troutman-Youngman, S.L. Schreiber, O. Wiest, J.E. Bradner, R.M. Williams, Org. Lett. 11 (2009) 1301–1304.
[69] A.K. Ghosh, S. Kulkarni, Org. Lett. 10 (2008) 3907–3909.
[70] F. Chen, A.H. Gao, J. Li, F.J. Nan, ChemMedChem 4 (2009) 1269–1272.
[71] X. Zeng, B. Yin, Z. Hu, C. Liao, J. Liu, S. Li, Z. Li, M.C. Nicklaus, G. Zhou, S. Jiang, Org. Lett. 12 (2010) 1368–1371.
[72] J.A. Souto, E. Vaz, I. Lepore, A.C. Pöppler, G. Franci, R. Alvarez, L. Altucci, A.R. de Lera, J. Med. Chem. 53 (2010) 4654–4667.
[73] B. Wang, C.J. Forsyth, Synthesis 17 (2009) 2873–2880.
[74] B. Wang, P.H. Huang, C.S. Chen, C.J. Forsyth, J. Org. Chem. 76 (2011) 1140–1150.
[75] Q. Xiao, L.P. Wang, X.Z. Jiao, X.Y. Liu, Q. Wu, P. Xie, J. Asian Nat. Prod. Res. 12 (2010) 940–949.
[76] H. Benelkebir, S. Marie, A.L. Hayden, J. Lyle, P.M. Loadman, S.J. Crabb, G. Packham, A. Ganesan, Bioorg. Med. Chem. 19 (2011) 3650–3658.
[77] Y. Liu, L.A. Salvador, S. Byeon, Y. Ying, J.C. Kwan, B.K. Law, J. Hong, H. Luesch, J. Pharmacol. Exp. Ther. 335 (2010) 351–361.
[78] S.-U. Lee, H.B. Kwak, S.-H. Pi, H.-K. You, S.R. Byeon, Y. Ying, H. Luesch, J. Hong, S. H. Kim, ACS Med. Chem. Lett. 2 (2011) 248–251.
[79] H. Luesch, W.Y. Yoshida, R.E. Moore, V.J. Paul, T.H. Corbett, J. Am. Chem. Soc. 123 (2001) 5418–5423.
[80] M. Gutiérrez, T.L. Suyama, N. Engene, J.S. Wingerd, T. Matainaho, W.H. Gerwick, J. Nat. Prod. 71 (2008) 1099–1103.
[81] S. Matthew, P.J. Schupp, H. Luesch, J. Nat. Prod. 71 (2008) 1113–1116.
[82] K. Tidgewell, N. Engene, T. Byrum, J. Media, T. Doi, F.A. Valeriote, W.H. Gerwick, ChemBioChem 11 (2010) 1458–1466.
[83] T. Doi, Y. Numajiri, T. Takahashi, M. Takagi, K. Shin-ya, Chem. Asian J. 6 (2011) 180–188.
[84] A. Gilles, J. Martinez, F. Cavelier, C. R. Chim. 14 (2011) 437–440.
[85] J.C. Kwan, J.R. Rocca, K.A. Abboud, V.J. Paul, H. Luesch, Org. Lett. 10 (2008) 789–792.
[86] J.C. Kwan, R. Ratnayake, K.A. Abboud, V.J. Paul, H. Luesch, J. Org. Chem. 75 (2010) 8012–8023.
[87] C.C. Thornburg, M. Thimmaiah, L.A. Shaala, A.M. Hau, J.M. Malmo, J.E. Ishmael, D. T. Youssef, K.L. McPhail, J. Nat. Prod. (2011)doi:10.1021/np200270d.
[88] W.L. Popplewell, R. Ratnayake, J.A. Wilson, J.A. Beutler, N.H. Colburn, C.J. Henrich, J.B. McMahon, T.C. McKee, J. Nat. Prod. (2011), doi:10.1021/np2005083.
[89] A. Pereira, Z. Cao, T.F. Murray, W.H. Gerwick, Chem. Biol. 16 (2009) 893–906.
[90] H. Choi, A.R. Pereira, Z. Cao, C.F. Shuman, N. Engene, T. Byrum, T. Matainaho, T. F. Murray, A. Mangoni, W.H. Gerwick, J. Nat. Prod. 73 (2010) 1411–1421.
[91] S. Matthew, C. Ross, J.R. Rocca, V.J. Paul, H. Luesch, J. Nat. Prod. 70 (2007) 124–127.
[92] K. Taori, S. Matthew, J.R. Rocca, V.J. Paul, H. Luesch, J. Nat. Prod. 70 (2007) 1593–1600.
[93] J.C. Kwan, K. Taori, V.J. Paul, H. Luesch, Mar. Drugs 7 (2009) 528–538.
[94] B.K. Rubio, S.M. Parrish, W. Yoshida, P.J. Schupp, T. Schils, P.G. Williams, Tetrahedron Lett. 51 (2010) 6718–6721.
[95] K. Taori, V.J. Paul, H. Luesch, J. Nat. Prod. 71 (2008) 1625–1629.
[96] S.P. Gunasekera, M.W. Miller, J.C. Kwan, H. Luesch, V.J. Paul, J. Nat. Prod. 73 (2010) 459–462.

[97] R.G. Linington, D.J. Edwards, C.F. Shuman, K.L. McPhail, T. Matainaho, W.H. Gerwick, J. Nat. Prod. 71 (2008) 22–27.
[98] S. Matthew, C. Ross, V.J. Paul, H. Luesch, Tetrahedron (2008) 4081–4089.
[99] S. Matthew, V.J. Paul, H. Luesch, Phytochemistry 70 (2009) 2058–2063.
[100] A. Plaza, C.A. Bewley, J. Org. Chem. 71 (2006) 6898–6907.
[101] S. Matthew, V.J. Paul, H. Luesch, Planta Med. 75 (2009) 528–533.
[102] R.A. Medina, D.E. Goeger, P. Hills, S.L. Mooberry, N. Huang, L.I. Romero, E. Ortega-Barria, W.H. Gerwick, K.L. McPhail, J. Am. Chem. Soc. 130 (2008) 6324–6325.
[103] A.R. Pereira, Z. Cao, N. Engene, I.E. Soria-Mercado, T.F. Murray, W.H. Gerwick, Org. Lett. 12 (2010) 4490–4493.
[104] I.E. Soria-Mercado, A. Pereira, Z. Cao, T.F. Murray, W.H. Gerwick, Org. Lett. 11 (2009) 4704–4707.
[105] A. Tripathi, J. Puddick, M.R. Prinsep, M. Rottmann, L.T. Tan, J. Nat. Prod. 73 (2010) 1810–1814.
[106] K. Suenaga, S. Kajiwara, S. Kuribayashi, T. Handa, H. Kigoshi, Bioorg. Med. Chem. Lett. 18 (2008) 3902–3905.
[107] T. Takahashi, H. Nagamiya, T. Doi, P.G. Griffiths, A.M. Bray, J. Comb. Chem. 5 (2003) 414–428.
[108] S. Sato, A. Murata, T. Orihara, T. Shirakawa, K. Suenaga, H. Kigoshi, M. Uesugi, Chem. Biol. 18 (2011) 131–139.
[109] B. Adams, P. Pörzgen, E. Pittman, W.Y. Yoshida, H.E. Westenburg, F.D. Horgen, J. Nat. Prod. 71 (2008) 750–754.

Chapter 5

Novel Bioactive Peptides from Cyanobacteria: Functional, Biochemical, and Biomedical Significance

Jamal M. Arif[*†1], Alvina Farooqui[†], Mohammad Haris Siddiqui[†], Mohammed Al-Karrawi[‡], Awdah Al-Hazmi[*] and Othman A. Al-Sagair[*]

[*]*College of Medicine, University of Hail, P.O. Box 2440, Hail, Saudi Arabia*

[†]*Department of Biotechnology, Microbiology and Bioinformatics, Integral University, Lucknow, India*

[‡]*Department of Environmental Technology, Al Iskan, Buraida, Saudi Arabia*

INTRODUCTION

Nature has equipped living organisms with a wide array of bioactive compounds for their nutritional, functional, defensive, and biochemical needs. The beneficial applications of natural bioactive compounds from marine organisms and plants are not unknown in pharmaceutical, diagnostic, chemical, and agro-food industries. In the recent past, another group of secondary metabolites known as bioactive peptides, emerged with tremendous potential of biochemical and biomedical significance. Bioactive peptides are molecules of peptidic nature or origin formed by a chain consisting of 50 or less amino acids that display a biological behavior like any other bioactive compound.

Despite their presence in plants, algae, and bacteria, the cyanobacteria have been identified as one of the most promising groups of organisms from which more than 600 novel and biochemically active peptides or peptidic metabolites have been isolated [1]. To date, most compounds have been isolated from Oscillatoriales and Nostocales, followed by Chroococcales and Stigonematales; however, very few metabolites are known from Pleurocapsales.

[1] Present address: Department of Biochemistry, College of Medicine, University of Hail, P.O. Box 2440, Hail, Saudi Arabia

Bioactive Natural Products, Vol. 36. DOI: 10.1016/B978-0-444-53836-9.00022-0

The most common genus for production of an array of bioactive peptides has been *Lyngbya*. The important species of this genus include *L. aestuarii*, *L. majuscula*, *L. martensiana*, and *L. wollei* [2]. This species is widely distributed throughout tropical and subtropical regions and are easily cultured in the laboratory for bulk production of compounds. More than 30% of all marine cyanobacterial metabolites yielded from *L. majuscule* indicating its tremendous biosynthetic ability. Furthermore, some of its strains like *L. majuscula* 19L produced several compounds with unique biological potentials.

The majority of these potent nitrogen-rich biomolecules, such as dolastatins, curacin A, hectochlorin, apratoxins, and lyngbyabellins, have been largely synthesized by polyketide synthase (PKS), non-ribosomal polypeptide synthetase (NRPS), as well as the integration of PKS–NRPS pathways [2–4]. These nitrogenous frameworks often contain some unusual chemical modifications like halogenations, methylations, and oxidations. There is also abundance of compounds with amino acids, hydroxy acids, pyrrolidone ring, thiazoline, oxazoline, oxazole, thiazole, and methyl groups [5].

A wide variety of toxins and other bioactive compounds, including lipopeptides (40%), amino acids (5.6%), fatty acids (4.6%), macrolides (4.2%), and amides (9%), are produced by cyanobacteria. Cyanobacterial lipopeptides exhibit cytotoxic (41%), antitumor (13%), antiviral (4%), antibiotics (12%) activities, and the remaining 18% activities include antimalarial, antimycotics, multidrug resistance (MDR) reversers, antifeedant, herbicides, and immunosuppressive agents [6].

This chapter will focus on the recent advancement in the biosynthesis, mechanism(s) of action, and biomedical applications of the selected natural bioactive peptides from cyanobacteria and their synthetic analogues. Accordingly, the chapter has been organized into sections based on the bioactivity of peptides (1, Anticancer Peptides; 2, Antiviral Peptides; 3, Antifungal Peptides; 4, Antibacterial Peptides; 5, Anti-inflammatory Peptides; 6, Molluscicidal Peptides).

ANTICANCER PEPTIDES

The structurally novel bioactive nitrogenous secondary metabolites have been emerged as an important source of anticancer drugs (Tables 1 and 2). The majority of these potent biomolecules target eukaryotic cytoskeleton, such as tubulin and actin microfilaments, making them an attractive source of potential anticancer drugs. Furthermore, a number of these potent peptides have also been reported to modulate cell death and apoptosis in cancer cells as well as target enzymes such as histone deacetylase [36].

Cryptophycins

Cryptophycins are the largest class of peptolides isolated from *Nostoc* sp. [37,38]. Cryptophycin 1, the major representative of >25 naturally occurring analogues, consisting of a phenyl-octenoic acid (unit A) and L-leucic acid

TABLE 1 Selected Anticancer Bioactive Peptides from Cyanobacteria

Peptides	Source	Activity	Class	Reference
Curacin	*Symploca hydnoides*	Strong toxicity toward L1210 leukemic cell lines	Linear peptide	[7]
Scyptolin	*Scytonema hofmanni pcc*	Elastase inhibiting activity	Cyclic peptides	[8]
Obyanamide	*Lyngbya confervoides*	Cytotoxic against KB cells	Cyclic peptide	[9]
Tasipeptins A and B	*Symploca* sp.	Cytotoxic toward KB cells	Depsipeptides lipopeptide	[9]
Tychonamides A and B	*Tychonema* sp.	Cytotoxic activity toward cancer cell lines	Cyclic peptides	[10]
Bisebromoamide	*Lyngbya* sp.	Cytotoxic against HeLa S3cells and a panel of 39 human cancer cell lines	Linear peptide	[11]
Alotamide A	*Lyngbya majuscula* and *Lyngbya sordida*	Cytotoxic against H-460 human lung cancer cells	Cyclic depsipeptides	[12]
Hantupeptins A–C	*L. majuscula*	Cytotoxic against leukemia	Cyclic peptides	[13,14]
Palmyramide A	*L. majuscula*	Blocked the voltage-gated sodium channel in neuro-2a cells and showed mild cytotoxicity against H-460 human lung carcinoma cells	Cyclic peptide	[15]
Dolastatin 16	*L. majuscula*	Extremely cytotoxic against lung, brain, colon, and melanoma cells	Cyclic depsipeptide	[16,17]

Continued

TABLE 1 Selected Anticancer Bioactive Peptides from Cyanobacteria—Cont'd

Peptides	Source	Activity	Class	Reference
Jamaicamides A–C	*L. majuscula*	Cytotoxicity activities against the H-460 human lung and neuro-2a mouse neuroblastoma cell lines	Lipopeptides	[18]
Cryptophycin 52	Synthetic analogue	Cytotoxic to the resistant cancer cells and inhibits microtubule formation	Cyclic depsipeptide	[19]
Lyngbyabellins	*L. majuscula*	Cytotoxicity against various cell lines, including KB and H-460 cancer cells	Cyclic peptides	[20,21]
Apratoxins	*Lyngbya* sp.	Cytotoxicity in various human tumor cell lines	Cyclic peptides	[22]
Aurilide	*L. majuscula*	Cytotoxic against H-460 human lung tumor and neuro-2a mouse neuroblastoma cell lines	Cyclic peptide	[23]
Malyngamides S	*Bursatella leachii*	Cytotoxic and anti-inflammatory	Lipopeptide	[24]
Symplostatin 3	*Symploca* sp.	100-fold less cytotoxic against the KB and LoVo cell lines than dolastatin 10	Linear peptide	[25]
Malevamide D	*S. hydnoides*	Cytotoxic against P-388, A-549, HT-29, and MEL-28 cells	Lipopeptide	[26]
Belamide A	*Symploca* sp.	Cytotoxic against the MCF7 breast-cancer and HCT-116 cells	Lipopeptide	[27]
Wewakpeptins	*Lyngbya semiplena*	Cytotoxic against the H-460 human lung tumor and the neuro-2a mouse neuroblastoma cell lines	Cyclic peptides	[28]

Hectochlorins	*L. majuscula*	Cytotoxic against colon, melanoma, ovarian, and renal cancer cell lines, inhibitory activity against the fungus, *C. albicans*	Cyclic peptides	[29]
Laxaphycins	*L. majuscula*	Antiproliferative activity against multidrug resistance cancer cells	Cyclic peptide	[30]
Homodolastatin 16	*L. majuscula*	Cytotoxic against esophageal and cervical cancer cell lines	Lipopeptide	[31]
Aurilides B and C	*L. majuscula*	Cytotoxic against H-460 human lung tumor	Lipopeptide	[23]
Veraguamide A	*Oscillatoria margaritifera*	Cytotoxic against H-460 human lung cancer cell line	Cyclic depsipeptide	[32]
Desmethoxymajusculamide C	*L. majuscula*	Extremely cytotoxic to HCT-116, H-460, MDA-MB-435, and Neuro-2A	Cyclic depsipeptide	[33]
Minutissamides A–D	*Anabaena minutissima*	Antiproliferative activity against the HT-29 human colon cancer cell line	Cyclic peptide	[34]
Pahayokolides A–B	*Lyngbya* sp.	Growth inhibition in a number of cancer cell lines	Cyclic peptides	[35]

TABLE 2 Structures of Anticancer Peptides

S. no.	Name of peptide	Structure
1 (a)	Cryptophycin 1 R1 = H Cryptophycin 52 R1 = Me	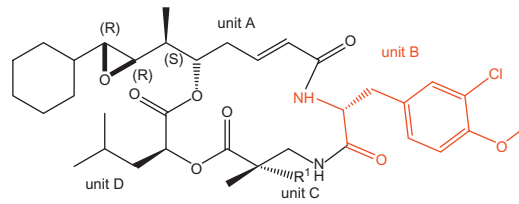
(b)	Clicktophycin 52	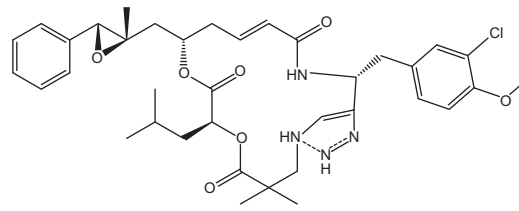
2	Curacin	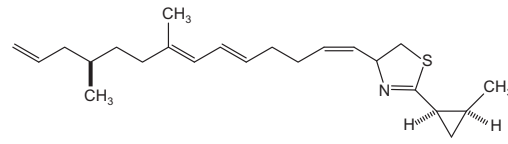
3 (a)	Lyngbyabellin A	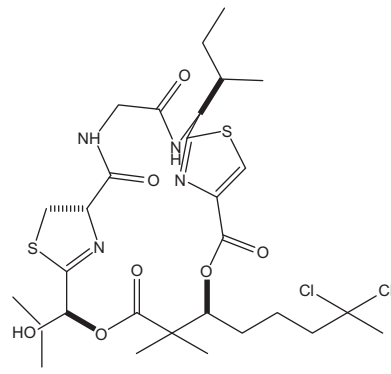

TABLE 2 Structures of Anticancer Peptides—Cont'd

S. no.	Name of peptide	Structure
(b)	Lyngbyabellin B	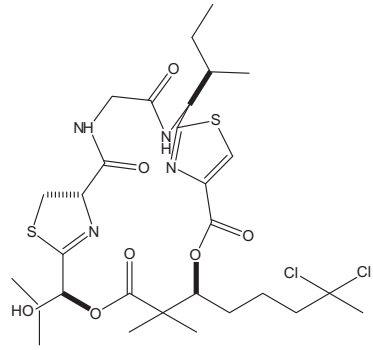
(c)	Lyngbyabellin C	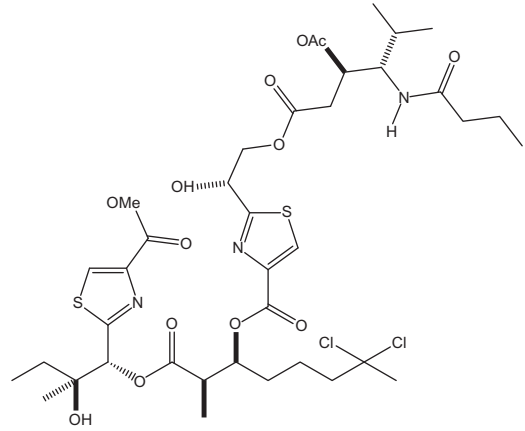
(d)	Lyngbyabellin D	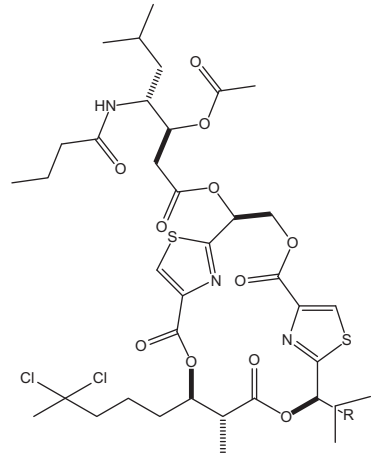

Continued

TABLE 2 Structures of Anticancer Peptides—Cont'd

S. no.	Name of peptide	Structure
(e)	Lyngbyabellin E R = OH Lyngbyabellin H R = H	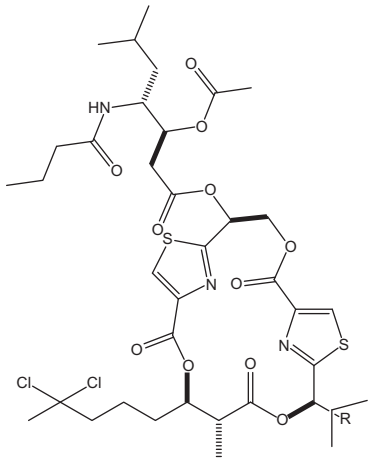
(f)	Lyngbyabellin F R = OH Lyngbyabellin I R = H	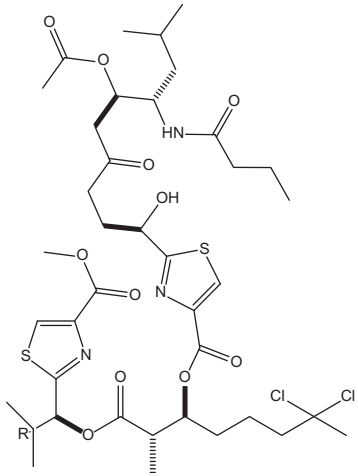
(g)	Lyngbyabellin G	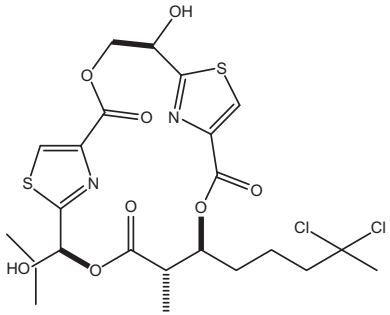

TABLE 2 Structures of Anticancer Peptides—Cont'd

S. no.	Name of peptide	Structure
4 (a)	Jamaicamide A 2R = Br Jamaicamide B 3R = H	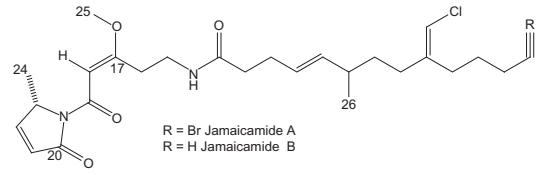
(b)	Jamaicamide C	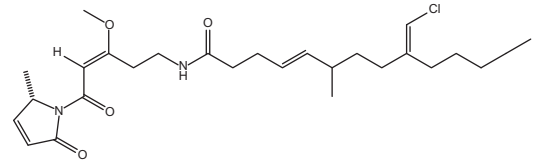
5	Dolastatin 15	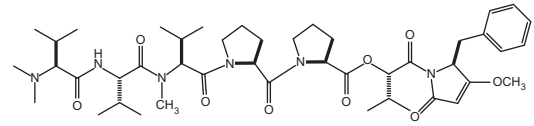
6	Dolastatin 16	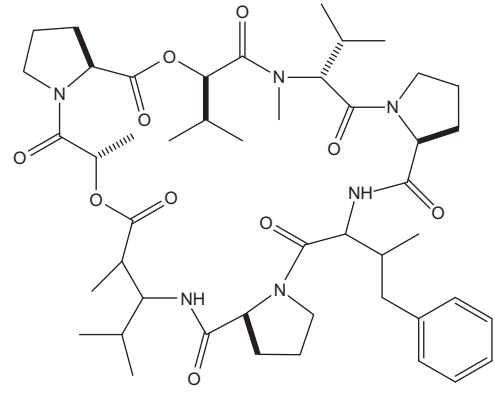

Continued

TABLE 2 Structures of Anticancer Peptides—Cont'd

S. no.	Name of peptide	Structure
7	Homodolastatin 16	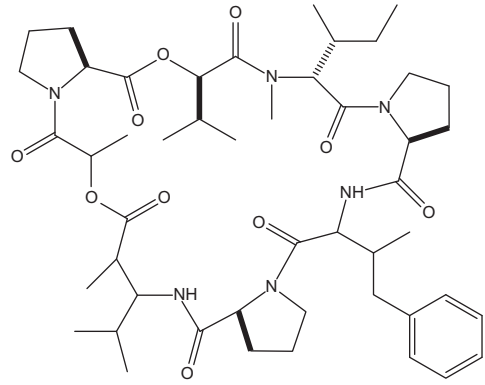
8	Symplostatin 3	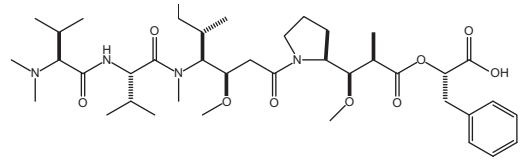
9	Malevamide D	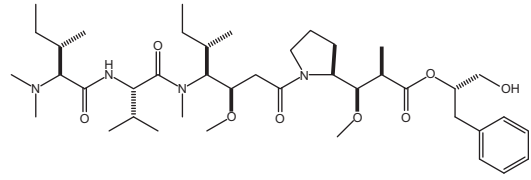
10	Belamide A	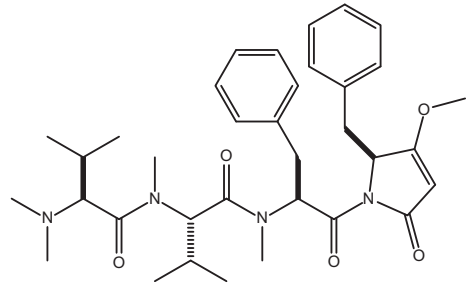

TABLE 2 Structures of Anticancer Peptides—Cont'd

S. no.	Name of peptide	Structure
11	15-Norlyngbyapeptin A	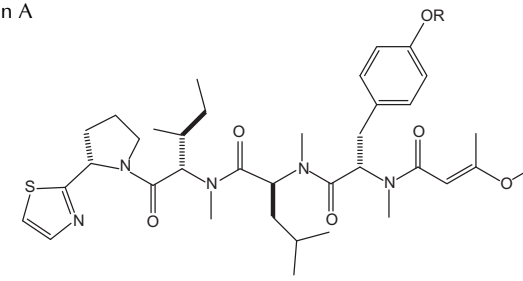
12	Lyngbyapeptin B R = Me Lyngbyapeptin C R = Et	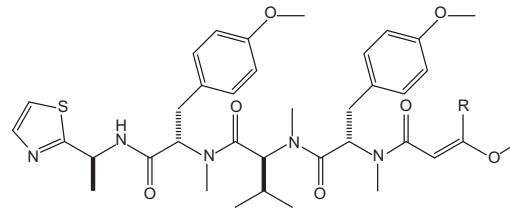
13	Desmethoxymajusculamide	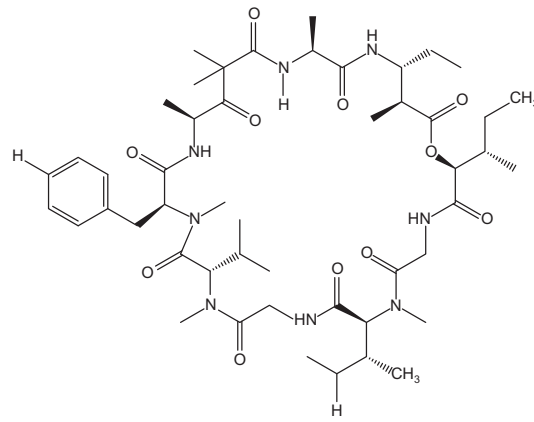

Continued

TABLE 2 Structures of Anticancer Peptides—Cont'd

S. no.	Name of peptide	Structure
14	Veraguamides	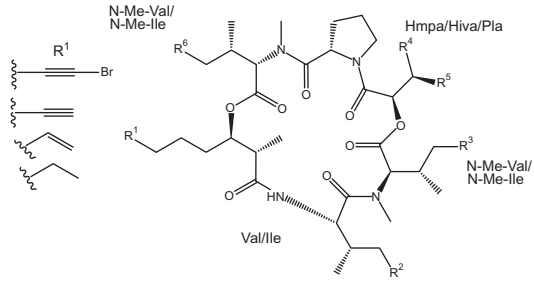
15	Pahayokolides	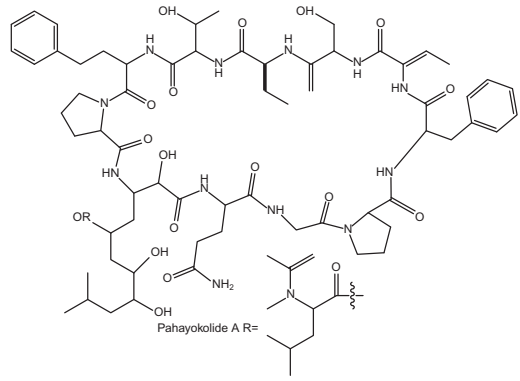
16 (a)	Aurilide B	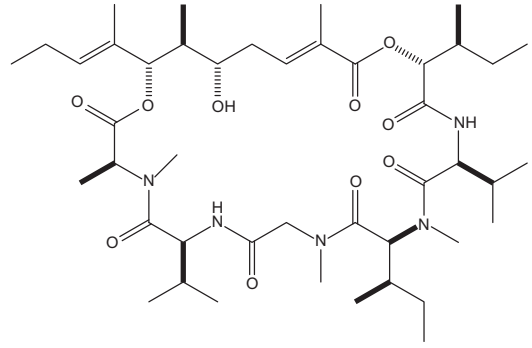

TABLE 2 Structures of Anticancer Peptides—Cont'd

S. no.	Name of peptide	Structure
(b)	Aurilide C	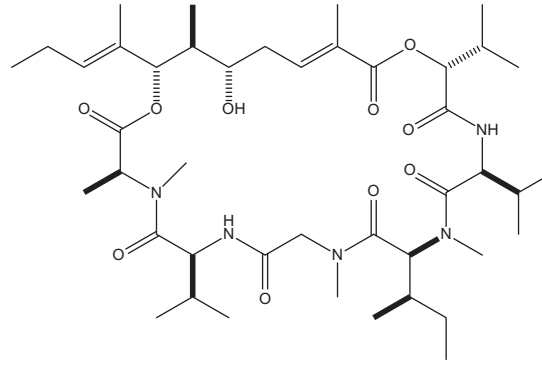
17	Obyanamide	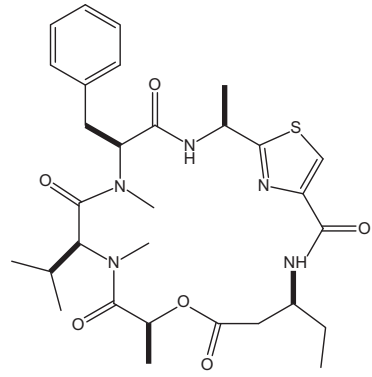
18 (a)	Guineamide A	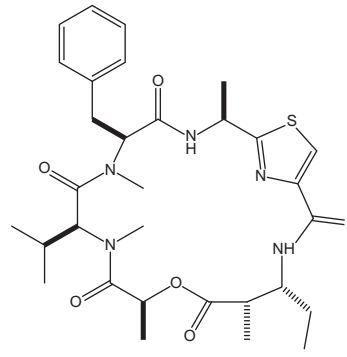

Continued

TABLE 2 Structures of Anticancer Peptides—Cont'd

S. no.	Name of peptide	Structure
(b)	Guineamide B	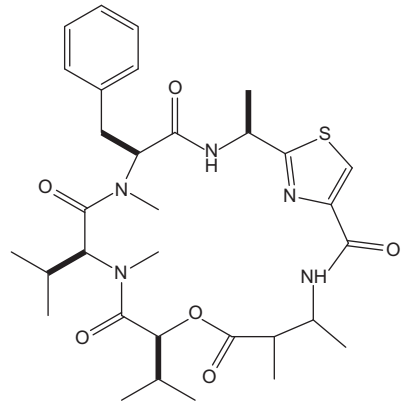
(c)	Guineamide C	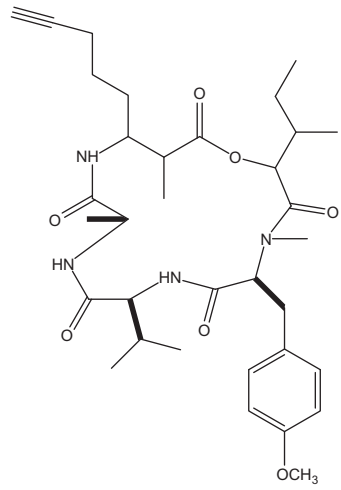
(d)	Guineamide D	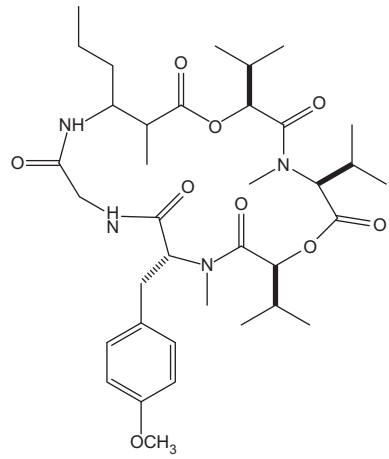

TABLE 2 Structures of Anticancer Peptides—Cont'd

S. no.	Name of peptide	Structure
(e)	Guineamide E	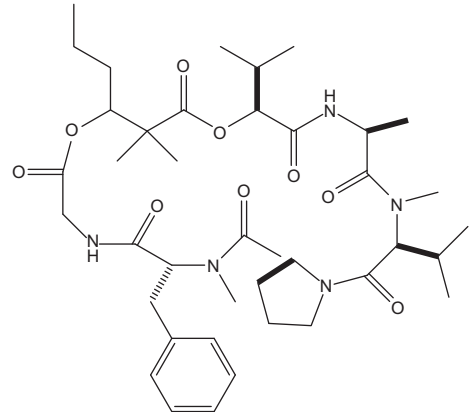
(f)	Guineamide F	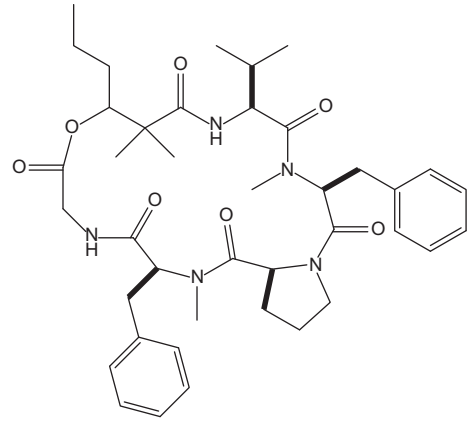
19	Palmyramide	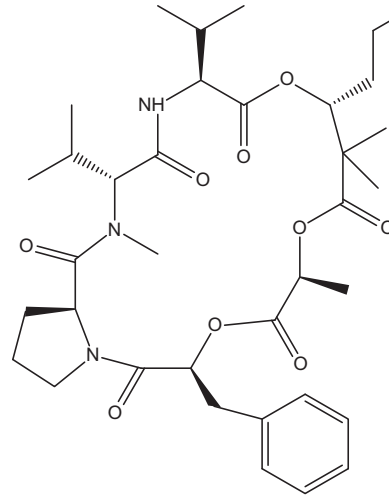

Continued

TABLE 2 Structures of Anticancer Peptides—Cont'd

S. no.	Name of peptide	Structure
20	Trungapeptins	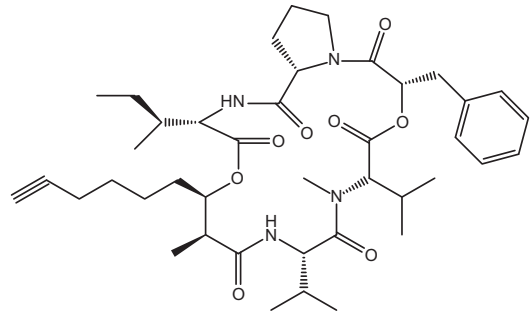
21	Hantupeptin	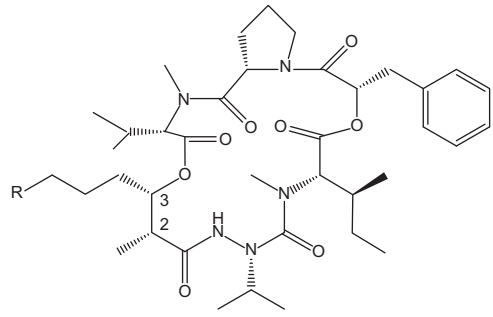
22	Grassypeptolide	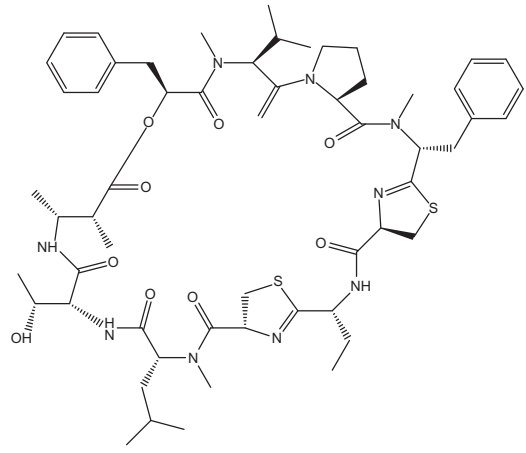

Name	R
Hantupeptin A	$CH{\equiv}C-$
Hantupeptin B	$CH_2{=}CH-$
Hantupeptin C	CH_3CH_2-

TABLE 2 Structures of Anticancer Peptides—Cont'd

S. no.	Name of peptide	Structure
23	Bisebromoamide	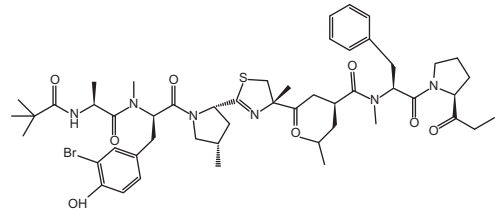
24	Wewakpeptins A and B	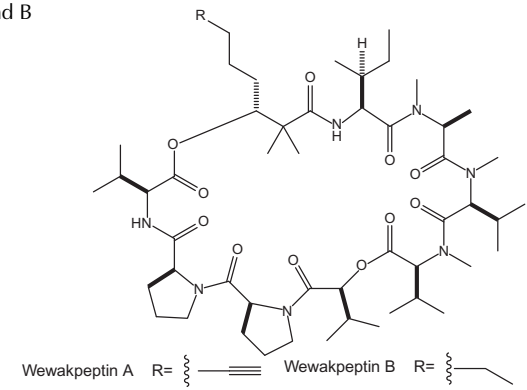
25	Wewakpeptins C and D	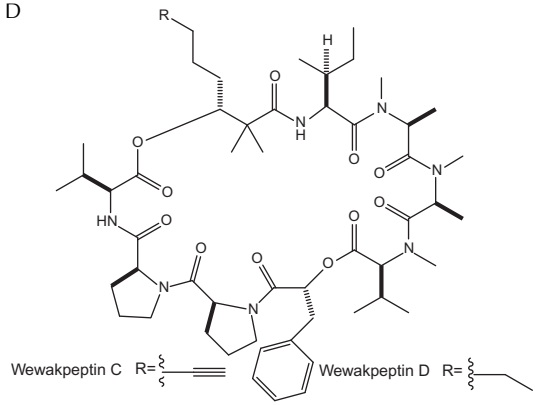

Continued

TABLE 2 Structures of Anticancer Peptides—Cont'd

S. no.	Name of peptide	Structure
26	Laxaphycin	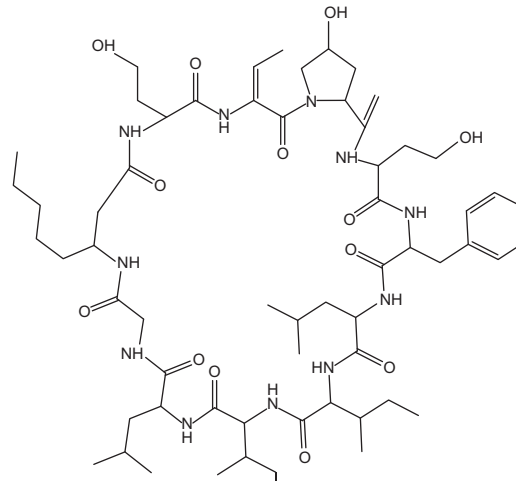
27	Minutissamides	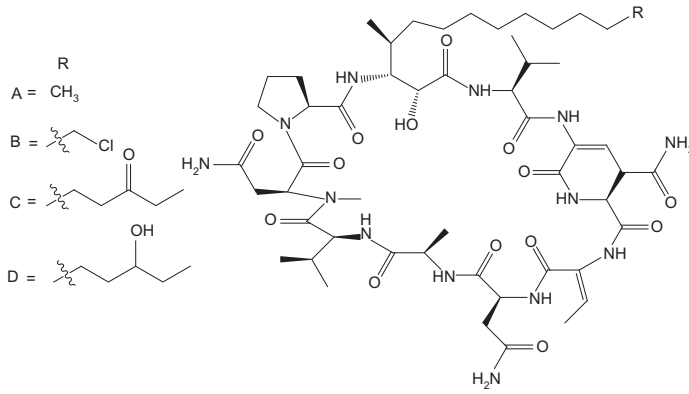

(unit D) and two amino acids, 3-chloro-*O*-methyl-D-tyrosine (unit B) and methyl L-alanine (unit C), linked in a cyclic ABCD sequence [19]. The remaining naturally occurring cryptophycins are analogues that differ structurally from cryptophycin 1 by one or two units in the molecule [19]. Natural cryptophycin variants of a unit A differ in their oxygenation state (e.g., an alkene vs. hydroxyl groups and epoxide vs. styrene) and double bond

configurations (*trans* vs. *cis*) while unit B contains phenylalanine variants. Unit C includes methyl L-alanine or L-alanine, and unit D involves L-hydroxy acid subunit diversity [19]. The Nostoc-derived cryptophycins exhibit extensive variation, indicating versatility of the biosynthetic pathway [19,37–40].

Another notable cryptophycin variation, which does not commonly stem from other PKS and NRPS biosynthetic pathways, is macrocyclic ring size (16- vs. 14-membered peptolide rings) [19,37,39,40].

Cryptophycin Analogues

Cryptophycin 52 (LY355703) is one of the most active synthetic derivatives of the naturally occurring cryptophycin 1, which differs structurally from cryptophycin 1 by an additional methyl group in the C fragment of the molecule.

Cryptophycin-8, another analogue of cryptophycin 1, was prepared by the conversion of the epoxide group on cryptophycin-1 to a chlorohydrin [41]. Clicktophycin-52, the triazole analogue of cryptophycin-52, exhibits an endocyclic *trans*-amide linkage within the macrocyclic antitumor agent cryptophycin-52 which was replaced by a 1,4-disubstituted 1*H*-1,2,3-triazole ring by macrolactamization and Cu(I)-mediated "click"-cyclization [42,43].

Biosynthesis

The cryptophycin gene cluster covers >40kb of the *Nostoc* genome and are assembled with the same reading direction and hence exhibits the biosynthetic assembly-line sequence of events in the same manner. The core of the *crp* gene cluster consisting of PKS genes (*crpA* and *crpB*) and NRPS genes (*crpC* and *crpD*) [44] encode multienzyme complexes for chain elongation. Subsequently, four small genes encoding post-PKS/NRPS tailoring enzymes (*crpE–H*) of which *crpE*, a cytochrome P450 oxygenase is responsible for the epoxide formation in several cryptophycins (e.g., cryptophycins 1, 2, and 52 [19]).

Bioactivity

The cryptophycins are among the most promising anticancer drugs of marine origin, which showed very high cytotoxicity even against MDR cell lines. The main mechanism of action is by interfering with the dynamics of tubulin polymerization and depolymerization thereby inhibiting mitosis of eukaryotic cells through interaction of β-subunit with the α/β-tubulin heterodimers and consequently, apoptotic cell death [45–52]. It arrests tumor cells at the G1-M phase, inducing a block in cellular proliferation, and causes hyperphosphorylation of Bcl-2, triggering the apoptotic cascade [19,53].

Cryptophycin 52 is the most potent suppressor of microtubule dynamics showing significant antiproliferative and cytotoxic activity on cancer cells. It was shown *in vitro* to bind to microtubule ends with high affinity, which

significantly reduced the rate and extent of microtubule shortening and growing without significantly reducing the polymer mass or mean microtubule length [54–57]. Further, picomolar concentration of cryptophycin 52 prevented tumor cells from progressing through the cell cycle by causing them to accumulate in mitotic metaphase and subsequently underwent apoptosis [58]. Relative comparison of antiproliferative activity of cryptophycin 52 with the clinically significant antimicrotubule agents against tumor cells *in vitro* proved cryptophycin 52 to be 40–400-fold more potent. Moreover, cryptophycin 52 seems to be relatively insensitive to the MDR transporters and/or MDR-associated protein [54].

Another analogue, cryptophycin-8, was approximately fourfold less potent than cryptophycin 1 against subcutaneous tumors of both mouse and human origin [41].

Further, clicktophycin-52 exhibited about fivefold (IC_{50} of 3.2 nM) less potent cytotoxic activity than the parent cryptophycin-52 (IC_{50} of 0.7 nM) against the MDR human cervix carcinoma cell line KB-V1 [43].

Curacin A

Curacin A, one of the potent cytotoxin and antiproliferative agent against various human cancer cell lines, is produced by strains of the tropical marine cyanobacterium *L. majuscula* [59]. Its structure is unique in that it contains the sequential positioning of a thiazoline and cyclopropyl ring. Further, it exerts its potent cell toxicity through interaction with the colchicine drug binding site on microtubules. Thus, curacin is an unusual acetogenin entailing a thiazoline ring [60].

Curacin A Analogue

The significance of the C3−C4−(*Z*)-alkene geometry was used to design a novel oxime analogue of curacin A which exhibited almost similar biological properties as the natural curacin A. Accordingly, the oxime moiety is likely to serve as a novel bioisostere of the (*Z*)-alkene group [61].

Biosynthesis

The biosynthetic pathway of curacin A has been identified as a mixed PKS/NRPS [60,62]. Based on the initial analysis, involvement of a number of genes encoding unusual catalytic domains and enzymes such as GCN5-related *N*-acetyltransferase (GNAT)-like domain in the chain initiation module, an HMG enzyme cassette, α-ketoglutarate-dependent non-heme halogenase, and a sulfotransferase domain in the chain termination module has been predicted in this pathway. These intriguing catalytic elements embedded within the curacin A biosynthetic system indicated the combinatory flexibility of modular polyketide assembly lines [63–66].

Bioactivity

Curacin A exhibits potent antiproliferative and cytotoxic activity against colon, renal, and breast-cancer derived cell lines [67]. It also shows strong toxicity toward L1210 leukemic cell lines and inhibits tubulin polymerization by binding at the colchicine site [7]. Further, the oxime analogue was much less lipophilic with only slightly weak human tumor cell growth potential. Further, it was found to be more potent than curacin A at inhibiting the assembly of purified tubulin [67].

Lyngbyabellins

Lyngbyabellins, bithiazole-containing cyclic depsipeptides, possessing the unusual dichlorinated β-hydroxy acid residue, 7,7-dichloro-3-hydroxy-2-methyl-octanoic acid (Dhmoc), are isolated from *Lyngbya* sp., *L. bouillonii*, and *Symploca* sp.

Lyngbyabellin Analogues

Lyngbyabellin B, an analogue of lyngbyabellin A, has been isolated as a minor intermediary metabolite from *L. majuscula* collected at Apra Harbor, Guam [68]. It possesses slightly weaker cytotoxicity than lyngbyabellin A. The known modified tetrapeptide lyngbyapeptin A was also found in the same extract. Further, lyngbyabellin D was also reported from *Lyngbya* sp. collected from Palau and Guam [69,70]. A recent collection of *L. majuscula* from Papua New Guinea yielded five new lyngbyabellins E–I along with a related molecule, dolabellin, originally reported from the sea hare, *Dolabella auricularia* [71].

Biosynthesis

Yokokawa *et al.* [72] described the first total synthesis of lyngbyabellin A, a novel peptolide from the marine cyanobacterium *L. majuscula*. Both functionalized thiazole carboxylic acid units were synthesized using chemical manganese dioxide oxidation from the corresponding thiazolidines. Subsequently, the asymmetric synthesis of the dichlorinated β-hydroxy acid was achieved by the chiral oxazaborolidinone-mediated aldol reaction. Finally, fragment condensation followed by the macrolactamization provided lyngbyabellin A.

Lyngbyabellin C, a dichlorinated thiazole hydroxy acid-containing cytotoxic macrolide, is also related to other lyngbyabellins, dolabellin, and hectochlorin [36].

Bioactivity

Lyngbyabellin A was shown to be a potent disrupter of the cellular microfilament network. Lyngbyabellin B also displayed potent toxicity toward brine shrimp and the fungus *Candida albicans* [3,68]. Lyngbyabellins D, F, and H

displayed significant cytotoxicity against various cancer cell lines, including KB and H-460 cancer cells with IC_{50} or LC_{50} values ranging from 0.1 to 0.4 μM [20,21].

Apratoxin

The apratoxins are a novel class of potent cytotoxic cyclic depsipeptides isolated from strains of *Lyngbya* sp. with morphological similarity to the *L. bouillonii* strain collected from Guam and Palau [22,73,74]. These peptides have five amino acid residues and a polyketide chain as part of the cyclic carbon skeleton. The chemical structure of apratoxin A was determined through extensive 2D NMR techniques as well as chemical manipulations. Further, J-based configuration analysis established the relative stereochemistry of the unique polyketide chain 3,7-dihydroxy-2,5,8,8-tetramethylnonanoic acid [22]. Apratoxin A was found to be acid-sensitive, and it decomposed to its dehydro-derivative. Apratoxin F and G isolated from *L. bouillonii* from Palmyra Atoll in the Central Pacific. 1D and 2D NMR in combination with mass spectrometric methods confirmed their structures [74]. Stereochemistry was explored by using chromatographic analyses of the hydrolytically released fragments in combination with NMR and optical rotation. Apratoxins F and G add fresh insights into the structure–activity relationship (SAR) of this family because they incorporate an *N*-methyl alanine residue at a position where all prior apratoxins have possessed a proline [74].

Apratoxin Analogues

Due to the structural novelty, coupled with the exceptional biological activities of apratoxin A, various research groups initiated total synthesis of this molecule and its analogues for SAR studies [75–80]. An oxazoline analogue of apratoxin A was found to be slightly lower in potency against HeLa cells when compared with the natural compound [80]. Further, SAR studies on synthetic oxazole-containing analogues of apratoxin A revealed the importance of methyl groups at C-37, C-40, as well as the stereochemistry at C-37 for biological activity [80].

Biosynthesis

The biosynthesis of apratoxin A could be rationalized by the involvement of a unique starter unit, 2,2-dimethyl-propionic acid (DPA), followed by polyketide extension with three acetate units catalyzed by PKS. One cysteine and acetyl unit are then added onto this linear intermediate carbon chain via NRPS and PKS enzymes, respectively, followed by the addition of tyrosine, alanine, isoleucine, and proline, to the growing intermediate chain using NRPS. Heterocyclization of cysteine, methylation by *S*-adenosylmethioine, and ring closure between proline and DPA yielded apratoxin A [36,81].

Bioactivity

All extracts derived from these *L. bouillonii* collections were highly cytotoxic due to the presence of apratoxin A or apratoxin C [82]. Apratoxin A exhibited relatively high *in vitro* cytotoxicity in various human cancer cell lines with IC_{50} values ranging from 0.36 nM in LoVo cancer cells to 0.52 nM in KB cancer cells [22]. Furthermore, the presence of the *N*-methylated isoleucine and hydroxyl group at C-35 are important features for biological activities [73]. Moreover, apratoxins F and G possessing an *N*-methyl alanine residue in place of proline, still retain high potency as cytotoxins to H-460 cancer cells with IC_{50} values of 2 and 14 nM, respectively [74].

In terms of the mechanism of action, apratoxin A inhibited cell division by arresting the cell cycle at the G1 phase. In addition, the use of functional genomic methods revealed apratoxin A blocks the FGFR (fibroblast growth factor receptor) pathway by preventing the phosphorylation and activation of STAT3, which is a downstream effector of the FGFR pathway [83].

Jamaicamides

The jamaicamides A–C are a series of potent polyketide–peptide neurotoxins isolated from a chemically rich Jamaican strain of *L. majuscula* [18]. Jamaicamide A is a novel and highly functionalized lipopeptide containing an alkynyl bromide, vinyl chloride, β-methoxy eneone system, and pyrrolinone ring [18].

Jamaicamides Analogues

The carboxylic acid fragment of jamaicamide C contains a methyl stereocenter and a trisubstituted *E* chloroolefin [84]. The non-racemic synthesis of the aliphatic chain of jamaicamide C was performed by installing the methyl stereocenter using Evans' oxazolidinone methodology, and the trisubstituted chloroolefin was set by silylstannylation of a triple bond [84].

Biosynthesis

Edwards *et al*. [18] reported the 58 kbp gene cluster composed of 17 open reading frames that showed an exact colinearity with their expected utilization. A novel cassette of genes appears to form a pendent carbon atom possessing the vinyl chloride functionality containing an HMG-CoA synthase-like motif at its core. The gross structures of these jamaicamides were determined using 1D and 2D NMR spectroscopy. The relative and/or absolute configurations were elucidated by chemical manipulations (Marfey's method, J-based configuration analysis, Mosher analysis, and organic synthesis of the stereoisomers) [85]. The free hex-5-enoic or hex-5-ynoic acid has also been suggested to be the starter unit for the biosynthesis of the jamaicamides [85].

Bioactivity

The jamaicamides A–C exhibited voltage-gated sodium channel blocking properties at approximately 5 μM while moderate cytotoxic activities against the H-460 human lung cancer and neuro-2a mouse neuroblastoma cell lines with LD_{50} of approximately 15 μM [18]. Interestingly, the non-aromatic ring-containing alkynoic lipopeptide jamaicamide B showed weak antimalarial activity (IC_{50}=18.4 μM). However, the terminal bromoacetylene homologue jamaicamide A was inactive in this assay.

Dolastatins

The dolastatins are a series of potent cytotoxic molecules initially isolated from the sea hare, *D. auricularia*, although their discovery in the marine cyanobacteria substantiated their cyanobacterial origin [86,87]. Dolastatin 10 was isolated from the sea hare *D. auricularia* as part of an extensive series of investigations [87–89].

The relative simplicity of the structure and the difficulty of sourcing the natural product made chemical synthesis the preferred approach, and dolastatin 10 have been synthesized [90]. The L-configuration of the lactate residue in dolastatin 16 was originally established from chiral HPLC data. However, several attempts, using both chiral GC analysis and HPLC (with precolumn derivatization), failed to reproducibly establish the stereochemistry of the lactate residue in homodolastatin 16 [31].

Dolastatin Analogues

Additional new dolastatin 10 analogues (symplostatin 3 and malevamide D) and dolastatin 15 analogues (palau'imide and belamide A) have been reported. Examination of the mixed assemblages of *L. majuscule* and *Schizothrix* sp. from the Fijian Islands led to the isolation of somamides A and B which are analogues in structure to symplostatin 2 and dolastatin 13 [91–94]. So far, dolastatin 13 has been found to strongly inhibit growth of the PS cell line derived from pig kidney and exhibit a GI_{50} value of 0.013 μg/mL [94].

Dolastatin 16 and Homodolastatin 16

The known dolastatin 16 was isolated from the *L. majuscula* collection from Antany Mora, Madagascar [16]. In addition, a bioactive cyclic depsipeptide, homodolastatin 16 has been isolated from the cyanobacterium *L. majuscula*, collected from Wasini Island off the southern Kenyan coast [31].

The dolastatin 16 showed strong activity against a wide variety of cancer cell lines, for example, lung (GI_{50}=0.00096 μg/mL), colon (GI_{50}=0.0012 μg/mL), brain (GI_{50}=0.0052 μg/mL), and melanoma (GI_{50}=0.0033 μg/mL) [17]. However, homodolastatin 16, as a higher homologue of dolastatin 16,

exhibited moderate activity against esophageal (IC_{50}=4.3 and 10.1 μg/mL) and cervical cancer cell lines (IC_{50}=8.3 μg/mL) (reviewed in Ref. [3]).

Symplostatin 3

Symplostatin 3 was purified from a tumor selective organic extract of the marine cyanobacterium, *Symploca* sp. VP452, collected from Hawaii [95]. The complete structure elucidation of symplostatin 3 was based on extensive 2D NMR spectrometry, MS/MS data comparison with dolastatin 10, and chemical manipulation. This molecule differs from dolastatin 10 only in the C-terminal unit where the dolaphenine unit in the latter compound is replaced by a 3-phenyllactic acid moiety. Due to this structural difference, the biological activity of symplostatin 3 was found to be about 100-fold less active in comparison with dolastatin 10 against the KB and LoVo cell lines with IC_{50} of 3.9 and 10.3 nM, respectively. In addition, symplostatin 3 was found to cause microtubule depolymerization in A-10 cells.

Malevamide D

Another dolastatin 10 analogue, malevamide D, isolated together with the known molecules, curacin D and symplostatin 1, from a Hawaiian strain of marine cyanobacterium, *Symploca hydnoides* [26]. Malevamide D differs from dolastatin 10 by having an L-Ile and a 3-phenyl-1,2-propanediol unit at the N- and C-terminal ends, respectively. The biological activity was found to be in the subnanomolar range when tested against a panel of different cell lines, including P-388, A-549, HT-29, and MEL-28 cells [26].

Belamide A

The isolation and structure elucidation of belamide A from the marine cyanobacterium *Symploca* sp. has been reported [27]. Belamide A is a highly methylated linear tetrapeptide with the structural analogy to the important linear peptides dolastatins 10 and 15.

The first asymmetric synthesis of belamide A has been achieved in seven steps from (S)-9, with an overall yield of 23.8% [96]. Not only have the structure and absolute configuration of (+)-belamide A been confirmed but also the solvent used for recording the ^{13}C NMR spectrum, the ^{13}C NMR spectrum data correlation, and optical rotation data of natural belamide A have been revised.

Disruption of the microtubule network in A-10 cells was observed at 20 μM and displayed classic tubulin destabilizing antimitotic characteristics. The moderate cytotoxicity of belamide A (IC_{50} 0.74 μM in HCT-116 colon cancer line) provides new insights into the SARs for this drug class [27].

15-Norlyngbyapeptin A, Lyngbyapeptins B and C, and Micromide

These marine cyanobacterial linear lipopeptides purified from filamentous marine cyanobacterial strains showed structural variation of dolaphenine units

in dolastatin 10 [4,25,69,70]. The 15-norlyngbyapeptin A was isolated from a Guamanian *Lyngbya* sp. while lyngbyapeptins B and C were also isolated from another strain of *Lyngbya* sp. procured from Palau. The lyngbyapeptin class of lipopeptides is biosynthetically derived from five amino acid residues and a combination of acetate and possible propionate units giving rise to the terminal polyketide chain. Lyngbyapeptins B and C were found to be not toxic when tested at $<5\mu M$ against KB and LoVo cells.

A collection of *Symploca* sp. from Guam yielded another thiazole-containing linear lipopeptide, micromide, along with guamamide [25]. Micromide consisted of seven amino acid residues as well as a unique β-methoxy acid unit, 3-methoxy-hexanoic acid. Micromide displayed IC_{50} value at $0.26\mu M$ when tested against the KB cell line.

Dolastatins in Human Clinical Trials

Dolastatin 10 binds to tubulin at a distinct site for peptide antimitotic agents near the exchangeable nucleotide and vinca alkaloid sites, thereby inhibiting tubulin polymerization [89]. Dolastatin 10 entered Phase I clinical trials in the 1990s, with the finding that 40% of patients developed moderate peripheral neuropathy [97]. However, it later progressed to National Cancer Institute (NCI), USA, Phase II trials for the treatment of several solid tumors, including liver, bile duct, gallbladder, pancreatic, and advanced kidney cancers, but the results of these trials were not encouraging [98,99].

The novel activity of the dolastatins spurred the development of several analogs, and the simplified analog TZT-1027 was among several analogs selected for further development based on its reduced toxicity as compared with dolastatin 10 [100]. Clinical results to date are mixed, with antitumor activity observed in only some cases [98].

A second derivative in clinical development is the dolastatin 15 analog Tasidotin which is also a tubulin-interactive drug, weakly inhibiting tubulin polymerization to microtubules but strongly suppressing the dynamic instability of microtubules [101]. It has completed Phase I trials [102,103] and is currently in Phase II trials under Genzyme [104].

Desmethoxymajusculamide

Desmethoxymajusculamide C (DMMC), a new cyclic depsipeptide, was discovered from the cytotoxicity-guided fractionation of the organic extract from a Fijian *L. majuscula* [33]. Spectroscopic analysis (1D and 2D NMR, MS/MS), chemical degradation, and derivatization protocol were used to establish the planar structure and stereoconfiguration of DMMC [33].

Desmethoxymajusculamide Analogues

A linear form of DMMC was generated by base hydrolysis, and the amino acid sequence was confirmed by mass spectrometry [33].

Bioactivity

DMMC and its ring-opened form, linear DMMC, demonstrated equivalent efficacy and solid tumor selectivity against four cell lines, including HCT-116, H-460, MDA-MB-435, and Neuro-2A. HCT-116 was the most sensitive cell line, with IC_{50} values of 20 and 16 nM, respectively [33]. This selective anti-solid tumor activity against the HCT-116 human colon carcinoma cell line was via disruption of cellular microfilament networks. Linearized DMMC was also evaluated in the biological assays and found to maintain potent actin depolymerization characteristics while displaying solid tumor selectivity equivalent to DMMC in the disk diffusion assay [33]. Further, therapeutic studies with HCT-116 bearing SCID mice demonstrated efficacy at the highest dose used (%T/C=60% at 0.62 mg/kg daily for 5 days) [33].

Miscellaneous Anticancer Peptides

Veraguamides

Cancer cell cytotoxic cyclodepsipeptides, veraguamides A–C and H–L were isolated from a collection of *Oscillatoria margaritifera* obtained from the Coiba National Park, Panama [32]. The planar structure of veraguamide A was deduced by 2D NMR spectroscopy and mass spectrometry, whereas the remaining structures were mainly determined by a combination of ^{1}H NMR and MS-2/MS-3 techniques.

These new compounds are analogous to the mollusk-derived kulomo'opunalide natural products, with two of the veraguamides (C and H) containing the same terminal alkyne moiety. However, four veraguamides, A, B, K, and L, also feature an alkynyl bromide, a functionality that has been previously observed in only one other marine natural product, jamaicamide A.

Veraguamide A showed potent cytotoxicity to the H-460 human lung cancer cell line (LD_{50}=141 nM).

Pahayokolides

Pahayokolides A and B, cyclic peptides, were produced by a freshwater *Lyngbya* sp. isolated from the Florida Everglades [35]. All the pahayokolides have an unusual β-amino acid, 3-amino-2,5,7,8-tetrahydroxy-10-methylundecanoic acid. Pahayokolides A and B contained the same cyclic undecapeptide core and pahayokolide A contains a pendant *N*-acetyl-*N*-methyl leucine moiety connected via an ester linkage to the 5-hydroxy group of the β-amino acid which is absent in pahayokolide B. Further, it was also confirmed that pahayokolides C–D were conformers of pahayokolide A.

Pahayokolide A inhibits a number of cancer cell lines over a range of concentrations (IC_{50} ranged from 2.13 to 44.57 μM). Pahayokolide A was acutely toxic to zebrafish embryos (LC_{50}=2.15 μM). However, it was only marginally toxic against brine shrimp at the highest concentrations tested (1 mg/mL) [105].

Aurilides

Two aurilide analogues, aurilides B and C, have been recently isolated from the Papua New Guinea *L. majuscula* [23]. Aurilide was previously reported from the sea hare *D. auricularia* and the discovery of these new analogues further supports their cyanobacterial origin.

The biogenesis of the aurilides could be conceived from either a 2-methyl-but-2-enoic acid or 2-methyl-pent-2-enoic acid starter unit extended by three acetate-derived units. Further, methylations on the lipid chain and coupling with six proteinogenic amino acids followed by macrocyclization resulted in the formation of these cyclic molecules [106].

Both aurilides B and C showed *in vitro* cytotoxicity toward H-460 human lung cancer and the neuro-2a mouse neuroblastoma cell lines, with LC_{50} values between 0.01 and 0.13 μM [23]. Aurilide B was evaluated in the NCI 60 cell line panel and exhibited a high level of cytotoxicity and growth inhibitory activities with $GI_{50}<10$ nM against leukemia, renal, and prostate cancer cell lines. Furthermore, aurilide B exhibited tumor cell killing activity in the NCI's *in vivo* model hollow fiber assay [23]. The mechanism of aurilide cytotoxicity further suggests that prohibitin 1 in mitochondria is an apoptosis-regulating protein amenable to modulation by small molecules. Aurilide may serve as a small-molecule tool for studies of mitochondria-induced apoptosis [107].

Obyanamide

Obyanamide, a depsipeptide, was isolated from the marine cyanobacterium *Lyngbya confervoides* collected in Saipan, Commonwealth of the Northern Mariana Islands [9]. This novel depsipeptide contains two *N*-methyl amino acids, an Ala-thiazole unit, and a β-amino acid. Its absolute stereochemistry was deduced by chiral chromatography of the hydrolysis products and comparison of the retention time with authentic and synthetic standards. The stereochemistry of the β-amino acid moiety, 3-amino-2-methylhexanoic acid, was established by advanced Marfey analysis of the acid hydrolyzates (reviewed in Ref. [3]).

Obyanamide was cytotoxic against KB and LoVo cells with an IC_{50} of 0.58 and 3.14 μg/mL, respectively [3,9].

Guineamides

Guineamides A–F are novel cyclic depsipeptides isolated and characterized from a Papua New Guinea collection of the marine cyanobacterium *L. majuscula* [108]. All six possessed *N*-methylated amino acids and β-amino acids, or β-hydroxyl groups. The three β-amino acid residues present in the guineamides are 2-methyl-3-aminobutanoic acid in guineamide A, 2-methyl-3-aminobutanoic acid in guineamide B, and 2-methyl-3-amino-oct-7-ynoic acid in guineamide C. Guineamides E and F contained the 2,2-dimethyl-3-hydroxyhexanoic acid [108].

Guineamides B and C possess moderate cytotoxicity to a mouse neuroblastoma cell line with IC_{50} values of 15 and 16 μM, respectively [108]. The cytotoxicity of guineamide F was not reported [2].

Palmyramide A

Palmyramide A, an unusual cyclic depsipeptide composed of three amino acids and three hydroxy acids, is produced by the marine *L. majuscula* collected from Palmyra Atoll [15].

Pure palmyramide A was assayed for sodium channel blocking and cancer cell cytotoxic activities, presumably due to the presence of one *N*-methyl amide. It occurs as a 95:5 mixture of major and minor conformers by ^{1}H NMR.

In the sodium channel-blocking assay, palmyramide A inhibited the veratridine- and ouabain-induced sodium overload, which resulted cytotoxicity in neuro-2a cells, presumably by blocking the voltage-gated sodium channel with an IC_{50} value of 17.2 μM. However, it only showed mild cytotoxicity against H-460 human lung carcinoma cells (IC_{50}=39.7 μM) [2,15].

Trungapeptins

Trungapeptins A–C were isolated from the marine cyanobacterium *L. majuscula* collected from Trung Province, Thailand [109]. The structures of these peptides contain the unique 3-hydroxy-2-methyl-7-octynoic acid, 3-hydroxy-2-methyl-7-octenoic acid, and 3-hydroxy-2-methyl-7-octanoic acid residues, respectively. The relative stereochemistry of 3-hydroxy-2-methyl-7-octynoic acid of trungapeptin A was elucidated by the application of the J-based configuration analysis [110]. Its absolute stereochemistry was established to be 2*S*, 3*R* by Mosher's method.

Trungapeptin A showed mild brine shrimp toxicity at 10 ppm and mild ichthyotoxicity at 6.25 ppm but did not exhibit cytotoxicity against KB and LoVo cells at 10 μg/mL [109].

Hantupeptins

Hantupeptins A–C, cyclic depsipeptides, isolated from *L. majuscula* from Pulau Hantu Besar, Singapore, showed 100% brine shrimp toxicity at 100 and 10 ppm, which were significantly higher than the activity reported for its close analogue trungapeptin A [13,14].

The *in vitro* cytotoxicity testing of hantupeptins A, B, and C against the breast-cancer cell line MCF-7 resulted in IC_{50} values 4.0, 0.5, and 1.0 μM, respectively, while they showed cytotoxicity against the leukemia cell line MOLT-4 with IC_{50} values of 32 nM, 0.2 μM, and 3.0 μM, respectively [13,14].

Grassypeptolide

Grassypeptolide, a macrocyclic depsipeptide with unusually high D-amino acid content, two thiazolines, and one β-amino acid A, was isolated from

L. confervoides of the Florida Keys, USA [111]. Grassypeptolide inhibited human osteosarcoma (U2OS), cervical carcinoma (HeLa), colorectal adenocarcinoma (HT29), and neuroblastoma (IMR-32) cell lines with IC_{50} values ranging from 1.0 to 4.2 μM.

Bisebromoamide

Bisebromoamide isolated from a *Lyngbya* sp. harvested in Okinawa Prefecture [11]. It possesses a combination of unusual 2-substituted thiazoline-4-methyl-4-carboxylic acid unit fused to a methyl-proline, 2-(1-oxopropyl) pyrrolidine, *N*-methyl-bromine-tyrosine, and *N*-pivalamide. Bisebromoamide exhibited extremely cytotoxic potential against HeLa cells with quite low IC_{50} value (0.04 μg/mL). Further, the average GI_{50} value against a panel of 39 human cancer cell lines (termed JFCR39) was found to be 40 nM.

Wewakpeptins

Wewakpeptins A–D, depsipeptides, were isolated from the marine cyanobacterium *Lyngbya semiplena* collected from Papua New Guinea [28]. Complete structural determination of these cyclic lipopeptides was based on 2D NMR spectral analysis, including HSQC-TOCSY and ROESY, mass spectrometry, and chiral HPLC methods. The wewakpeptins represent an unusual arrangement of amino and hydroxy acid subunits possessing a bis-ester, a 2,2-dimethyl-3-hydroxy-7-octynoic acid or 2,2-dimethyl-3-hydroxyoctanoic acid, and a diprolyl group. Wewakpeptins A and B were the most cytotoxic with an IC_{50} of approximately 0.4 μM to both the H-460 human lung cancer and the neuro-2a mouse neuroblastoma cell lines [6,85,112].

Laxaphycins

Laxaphycins A, B, B1, and B2, cyclic peptides, were isolated from a mixed assemblage of *L. majuscula* [30]. The structures of the two major components, laxaphycins A and B, and of two minor peptides, laxaphycins B2 and B3, were determined by spectroscopic methods and degradative analysis. Absolute configurations of natural and nonproteinogenic amino acids were determined by a combination of hydrolysis, synthesis of noncommercial residues, chemical derivatization, and HPLC analysis.

The antiproliferative activity of laxaphycins was investigated on a panel of solid and lymphoblastic cancer cells. The results demonstrated that in contrast to laxaphycin A, laxaphycin B inhibits the proliferation of sensitive and resistant human cancer cell lines. However, this activity was strongly increased in the presence of laxaphycin A presumably due to an unusual biological synergism [30].

Minutissamides A–D

Minutissamides A–D, cyclic decapeptides, were isolated from the cultured cyanobacterium *Anabaena minutissima* (UTEX 1613) [34]. The planar structures were determined using HRESIMS and 1D and 2D NMR techniques. The absolute configuration of the α-amino acid residues was assigned using Marfey's method after acid hydrolysis. However, the absolute configuration of a β-amino acid residue was assigned by a combination of the advanced Marfey's method, J-based configurational analysis, and ROE spectroscopic analysis [34]. The structures of minutissamides A–D were characterized by the presence of three nonstandard α-amino acid residues (two α,β-dehydro-α-aminobutyric acids and one *N*-methylated Asn) and one β-amino acid residue (2-hydroxy-3-amino-4-methyldodecanoic acid or 2-hydroxy-3-amino-4-methylhexadecanoic acid).

Minutissamides A–D exhibited antiproliferative activity against the HT-29 human colon cancer cell line with IC_{50} values of 2.0, 20.0, 11.8, and 22.7 μM, respectively [34].

ANTIVIRAL PEPTIDES

Cyanovirin-N

Cyanovirin-N (CV-N), discovered as a constituent of a cultured cyanobacterium, *Nostoc ellipsosporum*, is a unique cyclic peptide, 101 amino acids long, 11 kDa protein (Table 3). The primary amino acid structure has <20%

TABLE 3 Selected Antimicrobial Peptides from Cyanobacteria

Peptides	Source	Activity	Class	Reference
Hectochlorins	*Lyngbya majuscula*	Antifungal	Cyclic peptide	[29]
Calophycin	*Calothrix fusca*	Antifungal	Cyclic peptide	[113]
Lobocyclamides A–C	*L. confervoides*	Antifungal	Lipopeptide	[112,114]
Lyngbyabellin B	*L. majuscula*	Antifungal	Cyclic peptide	[68]
Schizotrin A	*Schizotrix* sp.	Antifungal	Cyclic peptide	[115]
Cyanovirin-N	*Nostoc ellipsosporum*	Antiviral	Cyclic peptide	[6]
Lyngbyazothrins A –D	*Lyngbya* sp. *36.91*	Antibacterial	Cyclic peptide	[116]

homology to any known protein and hence providing a unique 3-D structure and sequence.

The crystal structure of CV-N revealed a domain swapped dimmer. It is largely a β-sheet protein with internal twofold pseudo symmetry. The two sequences repeat (residues 1–50 and 51–101) shared 32% of sequence identity but do not form separate domains since the overall fold is dependent on numerous contacts between them. Rather, two symmetrically related domains are formed by strand exchange between the two repeats [117].

CV-N exhibits a high degree of resistance toward all kinds of physicochemical degradation. Treatment with denaturants, detergents, organic solvents, multiple freeze–thaw cycles, and heat has no effect on its antiviral activity.

Biosynthesis

CV-N is produced by recombinant *Escherichia coli*, and purification resulted in monomeric protein [118]. Vector containing pel-B signal peptide sequence is used for production of CV-N in high yield [119]. Production in yeast is also reported for the homologs of CV-N, which are active. The use of CV-N and its analogues could lead to an entirely new class of anti-HIV (human immunodeficiency virus) drugs [120].

Bioactivity

CV-N potently and irreversibly inactivates diverse primary strains of HIV-1, including M-tropic forms involved in sexual transmission of HIV. CV-N also blocks cell-to-cell transmission of HIV infection. CV-N is directly virucidal [121]. It is a fusion medicine supposed to protect the transmission of HIV infection to other people.

Mechanism of Action

Recent data indicated that targeting HIV envelope glycoproteins may provide an effective strategy to prevent HIV-1 infection mediated by either cell-free virus or infected cells [122]. HIV infection commences with the interaction of the viral surface envelope glycoprotein gp120 with the CD4 receptor of the host cell. This binding cause a conformational change in gp120 sufficient to accommodate a subsequent interaction between gp120 and a member of α and β chemokine receptor families, now commonly referred to as co-receptors. CV-N inhibits fusion of virus with CD4 cell membrane by interacting in an unusual manner with the viral envelope, apparently binding with extremely high affinity to poorly immunogenic epitopes on gp120 [123,124]. It has a potent activity against all immunodeficiency viruses (HIV-1, M-, and T-tropic strains of HIV-1, HIV-2, SIV (simian), ebola, and FIV (feline) [6,125,126]).

Thus, potent antiviral activity, lack of toxicity, resistance to physicochemical denaturation, as well as the unusual high genetic barrier to resistance

[123,127,128] suggested that CV-N is a promising anti-HIV molecule for use as a topical microbicidal agent [129,130]. However, it is yet to be approved by FDA for use outside of clinical trial (www.aidsinfo.nih.gov).

CV-N Mutants

The structural studies of CV-N initiated the possibility of rationally designing specific mutants, which could drastically alter some of the characteristics of the protein depicting higher stability and biological activity. In the past, several mutants were discovered with the expectation of higher antiviral potential against HIV compared to the wild-type CV-N, but surprisingly, all the mutants showed substantially less or similar anti-HIV activity [131–137].

ANTIFUNGAL PEPTIDES

Schizotrin A

A cyanobacterium, *Schizotrix* (TAU strain IL-89-2), produces schizotrin A, a cyclic undecapeptide (Tables 3 and 4) [2,115]. Zone-of-inhibition assays demonstrated that it has activity against *C. albicans* and *C. tropicalis*. It also inhibited the radial growth of *Fusarium oxysporum* at 0.05 µg/mL. It shows moderate antibacterial activity (*Bacillus subtilis*: 15 mm zone at 6.7 nM/6 mm disk [138,139]).

Lobocyclamides

Lobocyclamides A–C were isolated from *L. confervoides* (Tables 3 and 4) [3,112,114]. Lobocyclamide A was very similar to the known peptides hormothamnin isolated from *Hormothamnion enteromorphoides* [140] and laxaphycin A, isolated from the terrestrial cyanobacterium *Anabaena laxa* [141–143].

Lobocyclamides A–C exhibited modest antifungal activity when tested against fluconazole-resistant fungi *C. albicans* (150 µg/disk) with zone of inhibitions 7 mm (lobocyclamide A), 8 mm (lobocyclamide B), and 10 mm (lobocyclamide C) in the disk diffusion assay [114]. However, lobocyclamide B showed weak antifungal activity with 6 mm of zone of inhibition and lobocyclamide C had 8 mm zone against *Candida glabrata*. The microbroth dilution assay showed that lobocyclamide A had a MIC of 91 µg/mL against *C. albicans* while lobocyclamide C resulted in 30–100 µg/mL MIC. Interestingly, mixtures of lobocyclamides A and B (1:1 mixture) exhibited significant synergism with higher activity (MIC 10–30 µg/mL) than either of the pure compounds alone [114].

Calophycin

Calophycin, a cyclic decapeptide isolated from the terrestrial cyanobacterium *Calothrix fusca*, exhibits a broad-spectrum activity against fungi (Tables 3

TABLE 4 Structures of Antimicrobial Peptides

S. no.	Name of peptide	Structure
1.	Schizotrin A	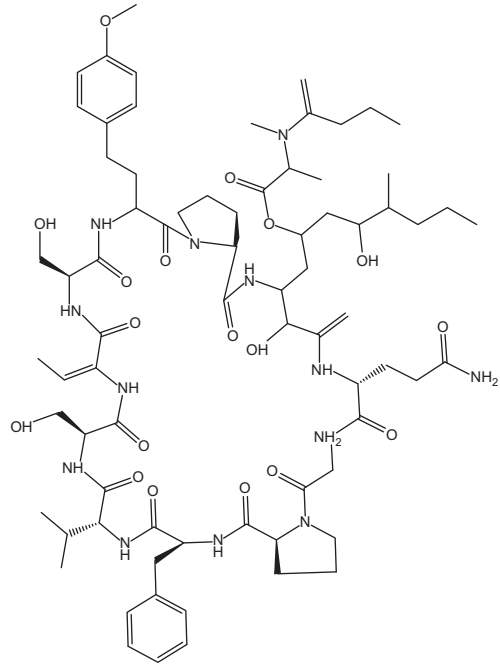
2 (a)	Lobocyclamide A	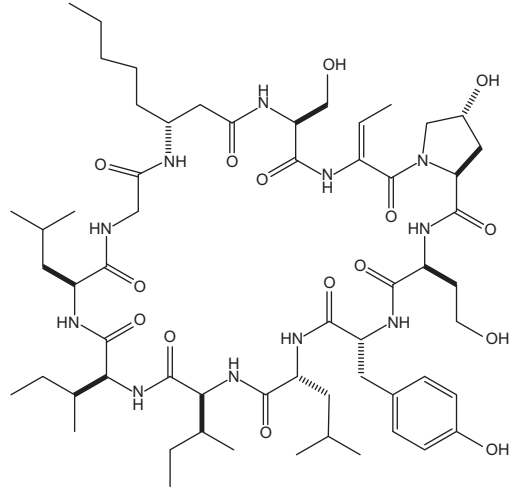

TABLE 4 Structures of Antimicrobial Peptides—Cont'd

S. no.	Name of peptide	Structure
(b)	Lobocyclamide B R = CH_2CH_3 Lobocyclamide C R = H	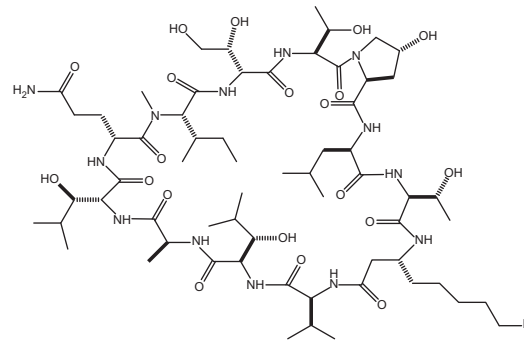
3	Calophycin	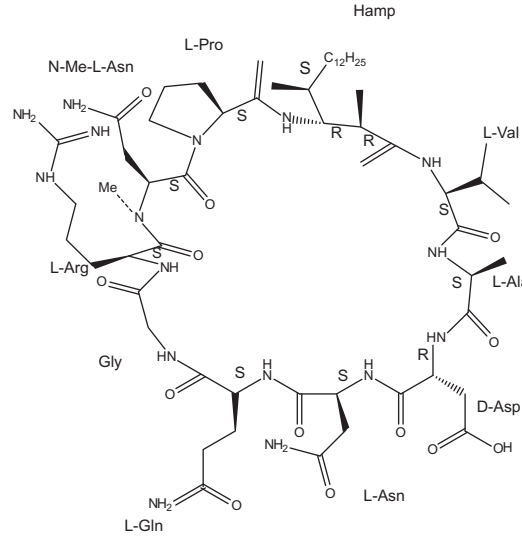
4	Hectochlorin	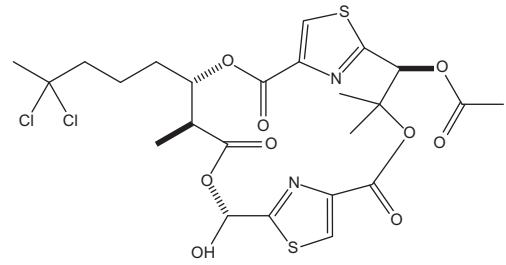

Continued

TABLE 4 Structures of Antimicrobial Peptides—Cont'd

S. no.	Name of peptide	Structure
5	Lyngbyabellin B	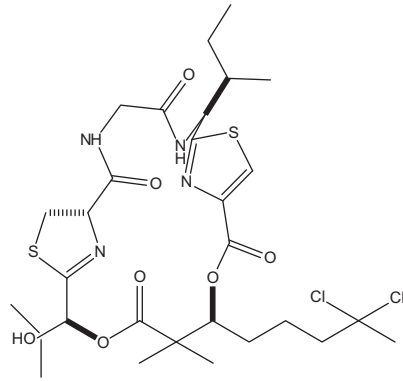
6	Lyngbyazothrins	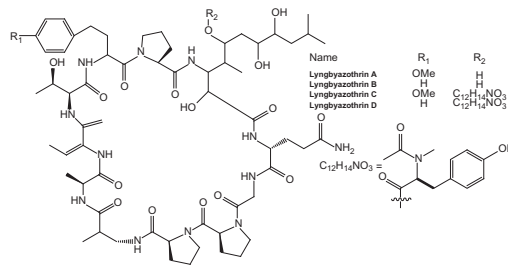

and 4) [113,144]. The structure and absolute configuration of the Hamp moiety have been confirmed by stereoselective synthesis.

Hectochlorin

Hectochlorin possesses the same absolute configuration as dolabellin and lyngyabellins E, G, and H except at the C14 (Tables 3 and 4). Hectochlorin has potent antifungal activity against *C. albicans* [29,145].

Lyngbyabellin B

Lyngbyabellin B was isolated from a marine cyanobacterium, *L. majuscula*, collected near the Dry Tortugas National Park, Florida (Tables 3 and 4) [68]. The planar structure was deduced using 1D and 2D NMR spectroscopic

methods, and the stereochemistry is proposed through a combination of NMR and chiral GC/MS analysis. This new cyclic depsipeptide displayed potent toxicity toward brine shrimp and the fungus *C. albicans*.

ANTIBACTERIAL PEPTIDES

Lyngbyazothrins

Novel cyclic undecapeptides, lyngbyazothrins A–D, were isolated from the cultured *Lyngbya* sp. 36.91 as binary mixtures (Tables 3 and 4) [116]. Their structures were elucidated by analysis of 1D and 2D NMR spectra, ESIMSMS, ESITOFMS, and amino acid analyses. Three unusual amino acids were present and identified as 4-methoxyhomophenylalanine in lyngbyazothrins A and C, homophenylalanine in lyngbyazothrins B and D, and 3-amino-2,5,7,8-tetrahydroxy-10-methylundecanoic acid (Aound) in all compounds. However, lyngbyazothrins C and D have an additional *N*-acetyl-*N*-methyltyrosine unit.

The mixture of lyngbyazothrins A and B showed only low antimicrobial activity against *Micrococcus flavus*, whereas the mixture of lyngbyazothrins C and D was active against *B. subtilis*, *E. coli*, *Pseudomonas aeruginosa*, and *Serratia marcescens*. It seems that the acyl residue at C-5 of the Aound unit plays an important role in antimicrobial activity. This assumption was supported by the activity and structure of pahayokolide A, where the 5-hydroxy group is also substitute by *N*-acetyl-*N*-methylleucine.

ANTI-INFLAMMATORY PEPTIDES

Malyngamides

A predominant class of linear lipopeptides that has become a signature of marine cyanobacterial secondary metabolism is the malyngamides (Tables 5 and 6) [24]. A Puerto Rican and a Papua New Guinea collection of *L. majuscula* provided malyngamides T and U–W, respectively, while a

TABLE 5 Selected Anti-inflammatory and Antioxidant Peptides from Cyanobacteria

Peptides	Source	Activity	Class	Reference
Cyanopeptides β1–β3	C-phycocyanin of *Spirulina fussiformis*	Antioxidant and anti-inflammatory	Peptide	[146]
Malyngamides	*Lyngbya majuscula*	Anti-inflammatory	Linear lipopeptide	[24,147]

TABLE 6 Structures of Anti-inflammatory Peptides

S. no.	Name of peptide	Structure
1 (a)	Malyngamide S	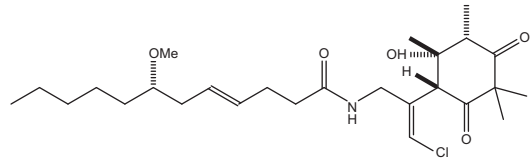
(b)	Malyngamide T	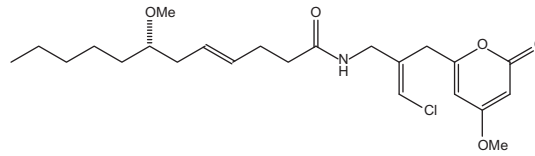
(c)	Malyngamide U	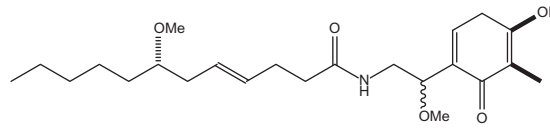
(d)	Malyngamide V	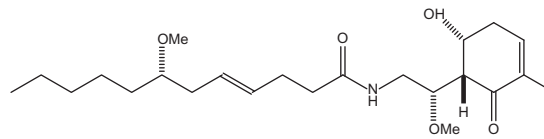
(e)	Malyngamide W	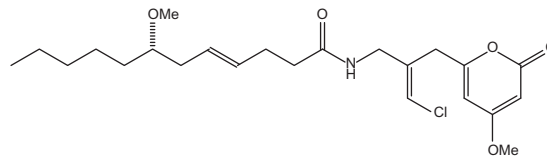

mollusk, *Bursatella leachii*, was the source of malyngamide S [148–152]. These malyngamides consisted of either a 12-carbons or 14-carbons fatty acid moiety termed as lyngbic acid with a methoxy and *trans* double bond at C-7 and C-4, respectively. Chain extension on lyngbic acid by a variety of amino acids (e.g., β-Ala and Gly) and malonyl-CoA-derived acetate units with further modifications, including methylation and chlorination, resulting into

compounds S–W. The presence of a vinyl chloride group could derive from C-2 of the acetate group via tailoring enzymes such as hydratases and halogenases.

A Papua New Guinea collection of *Lyngbya sordida* yielded three known compounds as well as a new PKS–NRPS-derived malyngamide with anti-inflammatory and cytotoxic activity [147]. Malyngamide 2 featured an extensively oxidized cyclohexanone ring and ring core as a 6,8,9-triol. It exhibited anti-inflammatory activity in lipopolysaccharide (LPS)-induced macrophage cells (IC_{50}=8.0μM) with only modest cytotoxicity to the mammalian cell line [147].

Phycocyanin

Phycocyanin, a phycobiliprotein, is the major pigment constituents of blue-green algae (*Spirulina*). Phycobiliproteins are classified into two large groups based on their color, the phycoerythrins (red) and the phycocyanins (blue). The phycocyanins include C-phycocyanin (C-PC), R-phycocyanin, and allophycocyanin. C-PC is the major phycobiliprotein in many blue-green algae [153]. Phycocyanin serves as a protein storage unit and as an antioxidant [154,155]. C-PCs that come from different species, such as *Aphanizomenon* sp. [156], *Spirulina* sp. [157], *Phormidium* sp. [158], *Lyngbya* sp. [154], *Synechocystis* sp. [159], *Synechococcus* sp. [160], have been isolated and studied.

C-PC exhibits a variety of pharmacological properties such as antioxidant, anti-inflammatory, neuroprotective, and hepatoprotective effects [161]. The inhibitory activity of C-PC on LPS-induced NO release and iNOS expression in RAW 264.7 macrophages is probably associated with suppressing TNF-α formation and nuclear NF-κB activation, which may provide an additional explanation for its anti-inflammatory activity and therapeutic effect [162]. It was further reported that the inhibition of NO and prostaglandin E_2 overproduction through suppressing iNOS and COX-2 induction and attenuation of TNF-α formation and neutrophil infiltration into inflammatory sites by C-PC may contribute, at least in part, to its antihyperalgesic activity [163].

The ability of C-PC to induce apoptosis in cancer cells with relatively no toxicity to the normal cells has made it a potential cancer chemopreventive agent [164–166]. Cyanopeptides β1–β3, isolated from C-PC β-chain of *Spirulina fussiformis*, were shown to have antioxidant and anti-inflammatory effects [146].

MOLLUSCICIDAL PEPTIDES

Molluscicides can play an important role in the control of schistosomiasis because snails of the genus *Biomphalaria* act as intermediate hosts for the parasite (Tables 7 and 8). Schistosomiasis is one of 13 neglected tropical diseases with high morbidity and mortality that collectively affect one billion of the world's poorest population, mainly in developing countries [169].

TABLE 7 Selected Molluscicidal and Antiparasitic Peptides from Cyanobacteria

Peptides	Source	Activity	Class	Reference
Barbamide	*L. majuscula*	Molluscicidal	Polyketide	[167,168]
Thiopalmyrone and palmyrrolinone	*Oscillatoria* and *Hormoscilla* spp.	Molluscicidal	Peptides	[169]
Cyanolide A	*L. bouillonii*	Molluscicidal	Peptide	[170]
Almiramides A–C	*L. majuscula*	Antileishmanial or antimalarial	Lipopeptides	[2,171]
Dragonamides A–D	*L. majuscule* *L. polychroa*	Antileishmanial, anticancer	Linear lipopeptides	[2]

TABLE 8 Structures of Molluscicidal and Antiparasitic Peptides

S. no.	Name of peptide	Structure
1	Barbamide	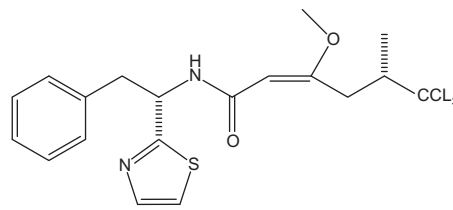
2 (a)	Dragonamide A	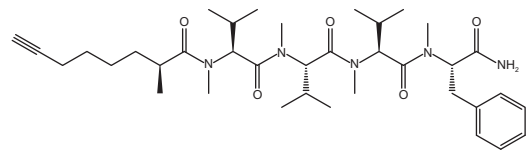
(b)	Dragonamide B	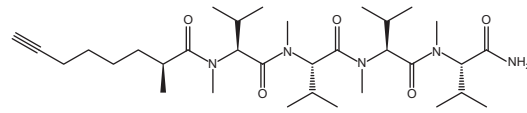

TABLE 8 Structures of Molluscicidal and Antiparasitic Peptides—Cont'd

S. no.	Name of peptide	Structure
(c)	Dragonamide E	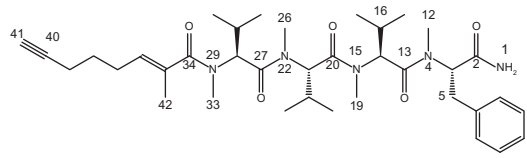
3	Almiramide A R = CH_3CO– Almiramide B R = CH≡C– Almiramide C R = CH_2=CH–	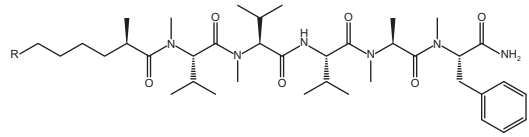
4	Thiopalmyrone	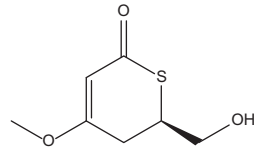
5	Palmyrrolinone	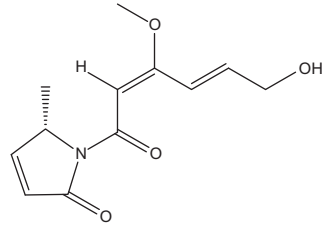
6	Cyanolide A	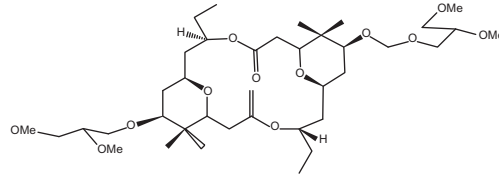

Barbamide

Barbamide was isolated from a Curacao strain of *L. majuscula* and is known to be molluscicidal. Although it is a small molecule, barbamide has complex structural and biosynthetic features, including a thiazole ring and a biosynthetically intriguing trichloromethyl group. The gene cluster of the *L. majuscula* producing barbamide has been reported in literature [167]. The structure of barbamide was determined by spectroscopic methods and was found to contain several unique structural features, including a trichloromethyl group and the methyl enol ether of a β-keto amide [168,172]. Furthermore, high incorporation of labeled exogenous [2-^{13}C]-5,5,5-trichloroleucine implies a direct role for trichloroleucine as an intermediate in the biosynthesis of barbamide [173].

The gene cluster (denoted as *bar*) contains 26kb functional gene sequences, *barA–K* [174]. *BarA* showed high homology to a peptidyl carrier protein of NPRS. *BarR1* and *barB2* and possibly *barC* are likely the candidates for the chlorination of a methyl group of leucine. *BarD* activated trichloroleucine and L-valine in addition to L-leucine. The oxidative decarboxylation of trichloroleucine to trichlorovaleric acid may be carried out by *barJ*. This unusual truncation process was assumed to take place via the α-keto-acid intermediate. *BarE* has features of both NRPS and PKS. Further stages in the biosynthesis include the condensation of the trichlorovaleriate moiety with a malonyl unit (*barF*), *O*-methylation (*barF*), peptide formation with phenylalanine and cysteine (*barG*), and finally thiazolidine ring formation and oxidative decarboxylation (*bar*, *barH*, and *ban*) to complete the structure. Some of the gene functions and exact mechanism of biosynthesis are yet to be clarified [174].

The lipid extract from *L. majuscula* was toxic to the mollusc *Biomphalaria glabrata* with LC_{100}=10μg/mL [168].

Dragonamides

Six structurally related linear lipopeptides, including dragonamide A [175], carmabin A, dragomabin, and dragonamide B [176], dragonamide C and D [177], were isolated from the marine cyanobacteria *L. majuscula* and *L. polychroa* [2]. A unique C8-alkynoate unit has been found in carmabin A, dragomabin, dragonamides A and B. It was reported that carmabin A, dragomabin, and dragonamide A were the only *Lyngbya* metabolites showing good antimalarial activity (IC_{50}=4.3, 6.0, and 7.7μM, respectively), whereas the nonaromatic analogue, dragonamide B, was inactive [2]. The lack of activity for dragonamide B suggests that an aromatic amino acid at the carboxy terminus is necessary for antimalarial activity in this compound series [176]. Dragonamides C–D were not shown to be antiparasitic. Further, dragonamides A and E exhibited antileishmanial activity against *Leishmania donovani* with IC_{50} values of 6.5 and 5.1μM, respectively [178].

Moreover, dragonamides also exhibited cytotoxicity against four neoplastic cell lines P-388, A-549, HT-29, and MEL-28 (IC_{50}>1 μg/mL). Carmabin A was more cytotoxic to Vero cells (IC_{50}=9.8 μM) than dragomabin (IC_{50}=182.3 μM) or dragonamide A (IC_{50}=67.8 μM) [2].

Almiramides

Screening of marine cyanobacteria from the Caribbean coast of Panama led to the identification of two antileishmanial lipopeptides, almiramides B–C and their non-active analog, almiramide A from *L. majuscula* [2,171]. Almiramides B–C showed better antileishmanial potencies (IC_{50}=2.4 and 1.9 μM, respectively), but no antimalarial activity up to 13.5 μM.

Further, lack of antileishmanial activity for almiramide A indicated that an unsaturated terminus on the lipophilic side chain played a critical role for antileishmanial activity in dragonamides and almiramides [2]. Screening of a synthetic library of almiramide analogs with various modifications at the C- or N-terminus afforded several compounds with similar antileishmanial activity but improved selectivity.

Miscellaneous Molluscicidal Peptides

Thiopalmyrone and Palmyrrolinone

These are the metabolites isolated from extracts of a Palmyra Atoll environmental assemblage of two cyanobacteria, cf. *Oscillatoria* and *Hormoscilla* spp., represent new and potent molluscicidal chemotypes against *B. glabrata* (LC_{50}=8.3 and 6.0 μM, respectively) [169]. A slight enhancement in molluscicidal effect (LC_{50}=5.0 μM) was observed when these two natural products were utilized as an equimolar binary mixture.

Cyanolide A

Cyanolide A, isolated from extracts of a Papua New Guinea collection of *L. bouillonii*, is a new and highly potent molluscicidal agent against the snail vector *B. glabrata* (LC_{50}=1.2 μM) [170]. The structure of cyanolide A was elucidated through extensive NMR spectroscopic analyses, yielding a symmetrical dimer that represents the newest addition to the family of glycosidic macrolides from cyanobacteria.

CONCLUSIONS

Thus far, studies have found that the treatment potential of bioactive peptides from cyanobacteria is promising for several cancers, inflammatory diseases, and parasitic tropical diseases (e.g., malaria, leishmaniasis, schistosomiasis). Interestingly, some of the anticancer peptides have even made it into human clinical trials I and II based on assuming their specific biological activities,

such as induction of apoptosis, cancer cell death, and tubulin and actin interactions.

In general, the original natural bioactive peptides produced in cyanobacteria have been found to be relatively more potent compared to their synthetic structural analogues. The diversity in the nature, structure, and bioactivity of these numerous cyanobacterial bioactive peptides are also significantly influenced by the habitats and origins of the cyanobacteria. Moreover, most of these peptidic metabolites have been tested superficially for their biomedical potential in almost only cancer cell lines and in no normal cell lines. Furthermore, all of these so-called potent cyanotoxins that the cyanobacteria produce as internal defense tools may indiscriminately affect both the normal cells and the cancer cells. For example, cyanotoxins were found to be effective at cell killing or apoptosis in almost every cancer cell line tested, with variation found only in their IC_{50} values. This consistency indicates that these bioactive peptides may not be specific for certain types of cancer, which could also mean that they may not discriminate the target from the non-target organs or cells.

Further, one must keep in mind that several marine drugs were withdrawn from advanced human clinical trials due to severe and life-threatening side effects and toxicity, which possibly resulted from the insufficient number of preclinical toxicity studies [179].

Nevertheless, the discovery of new compounds shall continue, but a greater emphasis must be given to the previously discovered (and promising) cyanopeptides during thorough preclinical studies against the targeted diseases.

ACKNOWLEDGMENT

Authors are grateful to Dr. M. Zeeshan for his motivational efforts and critical suggestions.

ABBREVIATIONS

C-PC	C-phycocyanin
CV-N	cyanovirin-N
DMMC	desmethoxymajusculamide C
DPA	2,2-dimethyl-propionic acid
FGFR	fibroblast growth factor receptor
FIV	feline immunodeficiency virus
GI_{50}	concentration that inhibit growth by 50%
HIV	human immunodeficiency virus
IC_{50}	half maximal inhibitory concentration
LC_{50}	lethal concentration 50
LD_{50}	median lethal dose
LPS	lipopolysaccharide

MDR	multidrug resistance
NCI	National Cancer Institute
NRPS	non-ribosomal polypeptide synthetase
PKS	polyketide synthase
SAR	structure–activity relationship
SIV	simian immunodeficiency virus

REFERENCES

[1] J.K. Nunnery, E. Mevers, W.H. Gerwick, Curr. Opin. Biotech. 21 (2010) 787–793.
[2] L. Liu, K.S. Rein, Mar. Drugs 8 (2010) 1817–1837.
[3] L. Liu, Absolute Configuration and Biosynthesis of Pahayokolide A from *Lyngbya* sp. strain 15-2 of the Florida Everglades, (2009) http://digitalcommons.fiu.edu/etd/134 FIU Electronic Theses and Dissertations, Paper 134.
[4] L.T. Tan, B.P.L. Goh, A. Tripathia, M.G. Lim, G.H. Dickinson, S.S.C. Lee, S.L.M. Teo, Biofouling 26 (2010) 685–695.
[5] M. Welker, H. von Dohren, FEMS Microiol. Rev. 30 (2006) 530–563.
[6] A.M. Burja, E.B. Banaigs, MansourA., J.G. Burgess, P.C. Wright, Tetrahedron 57 (2001) 9347–9377.
[7] J.-Y. Lai, J. Yu, B. Mekonnen, J.R. Falck, Tetrahedron Lett. 37 (1996) 7167–7170.
[8] S. Antonopoulou, T. Nomikos, A. Oikonomou, A. Kyriacou, M. Andriotis, E. Fragopoulou, A. Pantazidou, Comp. Biochem. Physiol B 140 (2005) 219–231.
[9] P.G. Williams, W.Y. Yoshida, R.E. Moore, V.J. Paul, J. Nat. Prod. 65 (2002) 29–31.
[10] C. Mehner, D. Müller, A. Krick, S. Kehraus, R. Löser, M. Gütschow, A. Maier, H.H. Fiebig, R. Brun, M. König Gabriele, Eur. J. Org. Chem. 10 (2008) 1723–1739.
[11] T. Teruya, H. Sasaki, H. Fukazawa, K. Suenaga, Org. Lett. 11 (2009) 5062–5065.
[12] I.E. Soria-Mercado, A. Pereira, Z. Cao, T.F. Murray, W.H. Gerwick, A. Alotamide, M. Taniguchi, J.K. Nunnery, N. Engene, E. Esquenazi, T. Byrum, P.C. Dorrestein, W.H. Gerwick, J. Nat. Prod. 73 (2010) 393–398.
[13] A. Tripathi, J. Puddick, M.R. Prinsep, P.P.F. Lee, L.T. Tan, J. Nat. Prod. 72 (2009) 29–32.
[14] A. Tripathi, J. Puddick, M.R. Prinsep, P.P.F. Lee, L.T. Tan, Phytochemistry 72 (2009) 29–32.
[15] M. Taniguchi, J.K. Nunnery, N. Engene, E. Esquenazi, T. Byrum, P.C. Dorrestein, W.H. Gerwick, J. Nat. Prod. 73 (2010) 393–398.
[16] L.M. Nogle, W.H. Gerwick, J. Nat. Prod. 65 (2002) 21–24.
[17] Y. Nakao, W.Y. Yoshida, C.M. Szabo, B.J. Baker, P.J. Scheuer, J. Org. Chem. 63 (1998) 3272–3280.
[18] D.J. Edwards, B.L. Marquez, L.M. Nogle, K. McPhail, D.E. Goeger, M.A. Roberts, W.H. Gerwick, Chem. Biol. 11 (2004) 817–833.
[19] N.A. Magarvey, Z.Q. Beck, T. Golakoti, Y. Ding, U. Huber, T.K. Hemscheidt, D. Abelson, R.E. Moore, D.H. Sherman, ACS Chem. Biol. (2006) 766–779.
[20] F. Yokokawa, H. Sameshima, T. Shioiri, Tetrehedron Lett. 42 (2001) 4171–4174.
[21] J.R. Cetusic, F.R. Green III, P.R. Graupner, M.P. Oliver, Org. Lett. 4 (2002) 1307–1310.
[22] H. Luesch, R. Pangilinan, W.Y. Yoshida, R.E. Moore, V.J. Paul, J. Nat. Prod. 64 (2001) 304–307.
[23] B. Han, H. Gross, D.E. Goeger, S.L. Mooberry, W.H. Gerwick, J. Nat. Prod. 69 (2006) 572–575.

[24] W.H. Gerwick, L.T. Tan, N. Sitachitta, Chem. Biol. 57 (2001) 75–184.
[25] P.G. Williams, W.Y. Yoshida, R.E. Moore, V.J. Paul, J. Nat. Prod. 67 (2004) 49–53.
[26] F.D. Horgen, E.B. Kazmierski, H.E. Westenburg, W.Y. Yoshida, P.J. Scheuer, J. Nat. Prod. 65 (2002) 487–491.
[27] T.L. Simmons, K.L. McPhail, B.E. Ortega, S.L. Mooberry, W.H. Gerwick, Tetrahedron Lett. 47 (2006) 3387–3390.
[28] B. Han, D. Goeger, C.S. Maier, W.H. Gerwick, J. Org. Chem. 70 (2005) 3133–3139.
[29] B.L. Marquez, K.S. Watts, A. Yokochi, M.A. Roberts, P. Verdier-Pinard, J.I. Jimenez, E. Hamel, P.J. Scheuer, W.H. Gerwick, J. Nat. Prod. 65 (2002) 866–871.
[30] I. Bonnard, M. Rolland, J.-M. Salmon, E. Debiton, C. Barthomeuf, B. Banaigs, J. Med. Chem. 50 (2007) 1266–1279.
[31] M.T. Davies-Coleman, T.M. Dzeha, C.A. Gray, S. Hess, L.K. Pannell, D.T. Hendricks, C.E. Arendse, J. Nat. Prod. 66 (2003) 712–715.
[32] E. Mevers, W.-T. Liu, N. Engene, H. Mohimani, T. Byrum, P.A. Pevzner, P.C. Dorrestein, C. Spadafora, W.H. Gerwick, J. Nat. Prod. 74 (2011) 928–936.
[33] T.L. Simmons, L.M. Nogle, J. Media, F.A. Valeriote, S.L. Mooberry, W.H. Gerwick, J. Nat. Prod. 72 (2009) 1011–1016.
[34] H.S. Kang, A. Krunic, Q. Shen, S.M. Swanson, J. Orjala, J. Nat. Prod. (2011), doi:10.1021/np2002226.
[35] T. An, T. Krishnaswamy, S. Kumar, M. Wang, L. Liu, J. Lay Jr., R. Liyanage, J. Berry, M. Gantar, V. Marks, R.E. Gawley, K.S. Rein, J. Nat. Prod. 70 (2007) 730–735.
[36] L.T. Tan, J. Appl. Physiol. 22 (2010) 659–676.
[37] G.V. Subbaraju, T. Golakoti, G.M.L. Patterson, R.E. Moore, J. Nat. Prod. 60 (1997) 302–305.
[38] R.E. Schwartz, C.F. Hirsch, D.F. Sesin, J.E. Flor, M. Chartrain, R.E. Fromtling, G.H. Harris, M.J. Salvatore, J.M. Liesch, K. Yudin, J. Ind. Microbiol. 5 (1990) 113–124.
[39] T. Golakoti, I. Ohtani, D.J. Patterson, R.E. Moore, T.H. Corbett, F.A. Valerlote, L. Demchik, J. Am. Chem. Soc. 116 (1994) 4729–4737.
[40] S. Chaganty, T. Golakoti, C. Heltzel, R.E. Moore, W.Y. Yoshida, J. Nat. Prod. 67 (2004) 1403–1406.
[41] T.H. Corbett, F.A. Valeriote, L. Demchik, L. Polin, C. Panchapor, S. Pugh, K. White, J. Knight, J. Jones, L. Jones, P. LoRusso, B. Foster, R.A. Wiegand, L. Lisow, T. Golakoti, C.E. Heltzel, J. Ogino, G.M. Patterson, R.E. Moore, J. Exp. Ther. Oncol. 1 (1996) 95–108.
[42] J.P. Nandy, M. Prakesch, S. Khadem, P.T. Reddy, U. Sharma, P. Arya, Chem. Rev. 109 (2009) 1999–2060.
[43] M. Nahrwold, T. Bogner, S. Eissler, S. Verma, N. Sewald, Org. Lett. 12 (2010) 1064–1067.
[44] J. Rohr, ACS Chem. Biol. 1 (2006) 747–750.
[45] D.T. Bergstralh, J.P. Ting, Cancer Treat. Rev. 32 (2006) 166–179.
[46] G. Attard, A. Greystoke, S. Kaye, B. De, J. Pathol. Biol. (Paris) 54 (2006) 72–84.
[47] R. Geney, J. Chen, I. Ojima, Med. Chem. 1 (2005) 125–139.
[48] A.T. Fojo, M. Menefee, Semin. Oncol. 32 (2005) S3–S8.
[49] J. Zhou, P. Giannakakou, Curr. Med. Chem. 5 (2005) 65–71.
[50] A. Breier, M. Barancik, Z. Sulova, B. Uhrik, Curr. Cancer Drug Targets 5 (2005) 457–468.
[51] F. Pellegrini, D.R. Budman, Cancer Invest. 23 (2005) 264–273.
[52] N.M. Verrills, M. Kavallaris, Curr. Pharm. Des. 11 (2005) 1719–1733.
[53] K. Lu, J. Dempsey, R.M. Schultz, C. Shih, B.A. Teicher, Cancer Chemother. Pharmacol. 47 (2001) 170–178.

[54] D. Panda, K. DeLuca, D. Williams, M.A. Jordan, L. Wilson, Proc. Natl. Acad. Sci. USA 95 (1998) 9313–9318.
[55] D. Panda, V. Ananthnarayan, G. Larson, C. Shih, M.A. Jordan, L. Wilson, Biochemistry 39 (2000) 14121–14127.
[56] P. Barbier, C. Gregoire, F. Devred, M. Sarrazin, V. Peyrot, Biochemistry 40 (2001) 13510–13519.
[57] K.N. Bhall, Oncogene 22 (2003) 9075–9086.
[58] M.M. Wagner, D.C. Paul, C. Shih, M.A. Jordan, L. Wilson, D. Williams, Cancer Chemother. Pharmacol. 43 (1999) 115–125.
[59] A.V. Blokhin, H.-D. Yoo, R.S. Geralds, D.G. Nagle, W.H. Gerwick, E. Hamel, Mol. Pharmacol. 48 (1995) 523–531.
[60] J.J. Gehret, L. Gu, W.H. Gerwick, P. Wipf, D.H. Sherman, J.L. Smith, J. Biol. Chem. 286 (2011) 14445–14454.
[61] P. Wipf, J.T. Reeves, R. Balachandran, B.W. Day, J. Med. Chem. 45 (2002) 1901–1917.
[62] Z. Chang, N. Sitachitta, J.V. Rossi, M.A. Roberts, P.M. Flatt, J. Jia, D.H. Sherman, W.H. Gerwick, J. Nat. Prod. 67 (2004) 1356–1367.
[63] L. Gu, J. Jia, H. Liu, K. Hakansson, W.H. Gerwick, D.H. Sherman, J. Am. Chem. Soc. 128 (2006) 9014–9015.
[64] L. Gu, B. Wang, A. Kulkarni, T.W. Geders, R.V. Grindberg, L. Gerwick, K. Hakansson, P. Wipf, J.L. Smith, W.H. Gerwick, D.H. Sherman, Nature 459 (2009) 731–735.
[65] A.C. Jones, L. Gerwick, D. Gonzalez, P.C. Dorrestein, W.H. Gerwick, BMC Microbiol. 9 (2009) 247.
[66] D. Khare, B. Wang, L. Gua, J. Razeluna, D.H. Sherman, W.H. Gerwick, K. Håkansson, J.L. Smith, Proc Natl. Acad. Sci. USA 107 (2010) 14099–14104.
[67] P. Verdier-Pinard, J.Y. Lai, H.D. Yoo, J. Yu, B. Marquez, D.G. Nagle, M. Nambu, J.D. White, J.R. Falck, W.H. Gerwick, B.W. Day, E. Hamel, Mol. Pharmacol. 53 (1998) 62–76.
[68] K.E. Milligan, B.L. Marquez, R.T. Williamson, W.H. Gerwick, J. Nat. Prod. 63 (2000) 1440–1443.
[69] H. Luesch, W.Y. Yoshida, R.E. Moore, V.J. Paul, Tetrahedron 58 (2002) 7959–7966.
[70] P.G. Williams, H. Luesch, W.Y. Yoshida, R.E. Moore, V.J. Paul, J. Nat. Prod. 66 (2003) 595–598.
[71] B. Han, K.L. McPhail, H. Gross, D.E. Goeger, S.L. Mooberry, W.H. Gerwick, Tetrahedron 61 (2005) 11723–11729.
[72] F. Yokokawa, H. Sameshima, T. Katagiri, T. Aoyama, T. Shioiri, Tetrahedron 58 (2002) 9445–9458.
[73] H. Luesch, W.Y. Yoshida, R.E. Moore, V.J. Paul, Bioorg. Med. Chem. 10 (2002) 1973–1978.
[74] K. Tidgewell, N. Engene, T. Byrum, J. Media, T. Doi, F.A. Valeriote, W.H. Gerwick, ChemBioChem 11 (2010) 1458–1466.
[75] J.-H. Chen, C.J. Forsyth, Org. Lett. 5 (2003) 1281–1283.
[76] J.-H. Chen, C.J. Forsyth, J. Am. Chem. Soc. 125 (2003) 8734–8735.
[77] J.-H. Chen, C.J. Forsyth, Proc. Natl. Acad. Sci. USA 101 (2004) 12067–12072.
[78] B. Zou, J.-J. Wei, G.-R. Cai, D.-W. Ma, Org. Lett. 5 (2003) 3503–3506.
[79] T. Doi, Y. Numajiri, A. Munakata, T. Takahashi, Org. Lett. 8 (2006) 531–534.
[80] D.W. Ma, B. Zou, G.R. Cai, X.Y. Hu, J.O. Liu, Chemistry 12 (2006) 7615–7626.
[81] R.V. Grindberg, T. Ishoey, D. Brinza, E. Esquenazi, R.C. Coates, W.T. Liu, L. Gerwick, P.C. Dorrestein, P. Pevzner, R. Lasken, W.H. Gerwick, PLoS One 6 (2011) e18565.

[82] S. Matthew, L.A. Salvador, P.J. Schupp, V.J. Paul, H. Luesch, J. Nat. Prod. 73 (2010) 1544–1552.
[83] H. Luesch, S.K. Chanda, R.M. Raya, P.D. DeJesus, A.P. Orth, J.R. Walker, J.C. I. Belmonte, P.G. Schultz, Nat. Chem. Biol. 2 (2006) 158–167.
[84] K.M. Graf, M.G. Tabor, M.L. Brown, M. Paige, Org. Lett. 11 (2009) 5382–5385.
[85] L.T. Tan, Phytochemistry 68 (2007) 954–979.
[86] H. Luesch, G.G. Harrigan, G. Goetz, F.D. Horgen, Curr. Med. Chem. 9 (2002) 1791–1806.
[87] D.G.I. Kingston, J. Nat. Prod. 72 (2009) 507–515.
[88] G.R. Pettit, Y. Kamano, Y. Fujii, C.L. Herald, M. Inoue, P. Brown, D. Gust, K. Kitahara, J. M. Schmidt, D.L. Doubek, C. Michael, J. Nat. Prod. 44 (1981) 482–485.
[89] R. Bai, G.R. Pettit, E. Hamel, Biochem. Pharmacol. 39 (1990) 1941–1949.
[90] C. Mordant, S. Reymond, H. Tone, D. Lavergne, R. Touati, B.B. Hassine, V. Ratovelomanana-Vidal, J.P. Genet, Tetrahedron 63 (2007) 6115–6123.
[91] L.M. Nogle, R.T. Williamson, W.H. Gerwick, J. Nat. Prod. 64 (2001) 716–719.
[92] G.R. Pettit, Y. Kamano, C.L. Herald, C. Dufresne, R.L. Cerny, D.L. Herald, J.M. Schmidt, H. Kizu, J. Am. Chem. Soc. 111 (1989) 5015–5017.
[93] G.G. Harrigan, H. Luesch, W.Y. Yoshida, R.E. Moore, D.G. Nagle, V.J. Paul, J. Nat. Prod. 62 (1999) 655–658.
[94] G.G. Harrigan, H. Luesch, R.E. Moore, V.J. Paul, Spec. Publ. R. Soc. Chem. 257 (2000) 126–139.
[95] H. Luesch, W.Y. Yoshida, R.E. Moore, V.J. Paul, S.L. Mooberry, T.H. Corbett, J. Nat. Prod. 65 (2002) 16–20.
[96] H.Q. Lan, J.L. Ye, A.E. Wang, Y.P. Ruan, P.Q. Huang, Chemistry 17 (2011) 958–968.
[97] E. Flahive, J. Srirangam, G.M. Cragg, D.G.I. Kingston, D.J. Newman (Eds.), Anticancer Agents from Natural Products, CRC Press, Boca Raton, FL, 2005, pp. 191–213.
[98] S. Banerjee, Z. Wang, M. Mohammad, F.H. Sarkar, R.M. Mohammad, J. Nat. Prod. 71 (2008) 492–496.
[99] R. Singh, S. Mukul, P. Joshi, D.S. Rawat, Anti-Cancer Agents Med. Chem. 8 (2008) 603–617.
[100] G.R. Pettit, J.K. Srirangam, J. Barkoczy, M.D. Williams, K.P.M. Durkin, M.R. Boyd, R. Bai, E. Hamel, J.M. Schmidt, J.C. Chapuis, Anti-Cancer Drug Des. 10 (1995) 529–544.
[101] A. Ray, T. Okouneva, T. Manna, H.P. Miller, S. Schmid, L. Arthaud, R. Luduena, M.A. Jordan, L. Wilson, Cancer Res. 67 (2007) 3767–3776.
[102] A.C. Mita, L.A. Hammond, P.L. Bonate, G. Weiss, H. McCreery, S. Syed, M. Garrison, Q.S.C. Chu, J.S. DeBono, C.B. Jones, S. Weitman, E.K. Rowinsky, Clin. Cancer Res. 12 (2006) 5207–5215.
[103] C. Cunningham, L.J. Appleman, M. Kirvan-Visovatti, D.P. Ryan, E. Regan, S. Vukelja, P.L. Bonate, F. Ruvuna, R.J. Fram, A. Jekunen, S. Weitman, L.A. Hammond, J. P. Eder Jr., Clin. Cancer Res. 11 (2005) 7825–7833.
[104] M.S. Butler, Nat. Prod. Rep. 25 (2008) 475–516.
[105] J.P. Berry, M. Gantar, R.E. Gawley, M. Wang, K.S. Rein, Comp. Biochem. Physiol. 139 (2004) 231–238.
[106] K. Suenaga, S. Kajiwara, S. Kuribayashi, T. Handa, H. Kigoshi, Bioorg. Med. Chem. Lett. 18 (2008) 3902–3905.
[107] S. Sato, A. Murata, T. Orihara, T. Shirakawa, K. Suenaga, H. Kigoshi, M. Uesugi, Chem. Biol. 18 (2011) 131–139.
[108] L.T. Tan, N. Sitachitta, W.H. Gerwick, J. Nat. Prod. 66 (2003) 764–771.
[109] S. Bunyajetpong, W.Y. Yoshida, N. Sitachitta, K. Kaya, J. Nat. Prod. 69 (2006) 1539–1542.

[110] N. Matsumori, D. Kaneno, M. Murata, H. Nakamura, K. Tachibana, J. Org. Chem. 64 (1999) 866–876.
[111] J.C. Kwan, E.A. Eksioglu, C. Liu, V.J. Paul, H. Luesch, J. Med. Chem. 52 (2009) 5732–5747.
[112] S. Kosta, R. Jain, A. Tiwari, Ind. J. Microbiol. 50 (Suppl. 1) (2010) 142–143.
[113] S.-S. Moon, J.L. Chen, R.E. Moore, G.M.L. Patterson, J. Org. Chem. 57 (1992) 1097–1103.
[114] J.B. MacMillan, M.A. Ernst-Russell, J.S. de Ropp, T.F. Molinski, J. Org. Chem. 67 (2002) 8210–8215.
[115] I. Pergament, S. Carmeli, Tetrahedron Lett. 35 (1994) 8473–8476.
[116] E.N. Zainuddin, R. Jansen, M. Nimtz, V. Wray, M. Preisitsch, M. Lalk, S. Mundt, J. Nat. Prod. 72 (2009) 1373–1378.
[117] F. Yang, C.A. Bewley, J.M. Louis, K.R. Gustafson, M.R. Boyd, A.M. Gronenborn, J. Mol. Biol. 288 (1999) 403–412.
[118] D.M. Colleluori, D. Tien, F. Kang, T. Pagliei, K.R. Ryan, T. McCormick, K. Watson, K. McRadden, I. Chaiken, R.W. Buckheit Jr., J.W. Romano, Protein Expr. Purif. 39 (2005) 229–236.
[119] T. Mori, K.R. Gustafson, L.K. Pannell, R.H. Shoemaker, L. Wu, J.B. McMahon, Protein Expr. Purif. 12 (1998) 151–158.
[120] T. Mori, L.G. Barrientos, Z. Han, A.M. Gronenborn, J.A. Turpin, M.R. Boyd, Protein Expr. Purif. 26 (2002) 42–49.
[121] T. Mori, R.H. Shoemaker, R.J. Gulakowski, B.L. Krepps, J.B. McMahon, K.R. Gustafson, Biochem. Biophys. Res. Commun. 238 (1997) 218–222.
[122] V. Buffa, D. Stieh, N. Mamhood, Q. Hu, P. Fletcher, R.J. Shattock, J. Gen. Virol. 90 (2009) 234–243.
[123] Q. Hu, N. Mahmood, R.J. Shattock, Virology 368 (2007) 145–154.
[124] S.R. Shenoy, B.R. O'Keefe, A.J. Bolmstedt, L.K. Cartner, M.R. Boyd, J. Pharmacol. Exp. Ther. 297 (2001) 704–710.
[125] F. Helle, C. Wychowski, N. Vu-Dac, K.R. Gustafson, C. Voisset, J. Dubuisson, J. Biol. Chem. 281 (2006) 25177–25183.
[126] L.G. Barrientos, A.M. Gronenborn, Mini Rev. Med. Chem. 5 (2005) 21–31.
[127] J. Balzarini, K. Van Laethem, W.J. Peumans, E.J. Van Damme, A. Bolmstedt, F. Gago, D. Schols, J. Virol. 80 (2006) 8411–8421.
[128] M. Witvrouw, V. Fikkert, A. Hantson, C. Pannecouque, B.R. O'Keefe, J. McMahon, L. Stamatatos, E. de Clercq, A. Bolmstedt, J. Virol. 79 (2005) 7777–7784.
[129] M.R. Boyd, K.R. Gustafson, J.B. McMahon, R.H. Shoemaker, B.R. O'Keefe, T. Mori, R.J. Gulakowski, L. Wu, M.I. Rivera, et al., Antimicrob. Agents Chemother. 41 (1997) 1521–1530.
[130] M.T. Esser, T. Mori, I. Mondor, Q.J. Sattentau, B. Dey, E.A. Berger, M.R. Boyd, J.D. Lifson, J. Virol. 73 (1999) 4360–4371.
[131] L. Matei, A. Zheng, W. Furey, J. Rose, C. Aiken, A.M. Gronenborn, J. Biol. Chem. 285 (2010) 13057–13065.
[132] I.I. Vorontsov, O. Miyashita, Biophys. J. 97 (2009) 2532–2540.
[133] I. Botos, B.R. O'Keefe, S.R. Shenoy, L.K. Cartner, D.M. Ratner, P.H. Seeberger, M.R. Boyd, A. Wlodawer, J. Biol. Chem. 277 (2002) 34336–34342.
[134] B.S. Kelley, L.C. Chang, C.A. Bewley, J. Am. Chem. Soc. 124 (2002) 3210–3211.
[135] L.C. Chang, C.A. Bewley, J. Mol. Biol. 318 (2002) 1–8.
[136] L.G. Barrientos, J.M. Louis, I. Botos, T. Mori, Z. Han, B.R. O'Keefe, M.R. Boyd, A. Wlodawer, A.M. Gronenborn, Structure 10 (2002) 673–686.

[137] C.A. Bewley, Structure 9 (2001) 931–940.
[138] A.J. De Lucca, T.J. Walsh, Antimicrob. Agents Chemother. 43 (1999) 1–11.
[139] A.J. DeLucca, Expert Opin. Investig. Drugs 9 (2000) 273–299.
[140] W.H. Gerwick, Z.D. Jiang, S.K. Agarwal, B.T. Farmer, Tetrahedron 48 (1992) 2313–2324.
[141] W.P. Frankmölle, G. Knübel, R.E. Moore, G.M.L. Patterson, J. Antibiot. 45 (1992) 1458–1466.
[142] W.P. Frankmölle, L.K. Larsen, F.R. Caplan, G.M.L. Patterson, G. Knübel, I.A. Levine, R.E. Moore, J. Antibiot. 45 (1992) 1451–1457.
[143] I. Bonnard, M. Rolland, C. Francisco, B. Banaigs, Lett. Pept. Sci. 4 (1997) 289–292.
[144] M.M. Kulik, Eur. J. Plant Pathol. 101 (1995) 585–599.
[145] L.T. Tan, J. Coastal Dev. 9 (2006) 129–136.
[146] H. Madhyastha, T.M. Vatsala, Ind. J. Exp. Biol. 48 (2010) 486–493.
[147] K.L. Malloy, F.A. Villa, N. Engene, T. Matainaho, L. Gerwick, W.H. Gerwick, J. Nat. Prod. 74 (2011) 95–98.
[148] J.T. Zhang, X.L. Qi, J. Chen, B.S. Li, Y.B. Zhou, X.P. Cao, J. Org. Chem. 76 (2011) 3946–3959.
[149] X.-L. Qi, J.-T. Zhang, J.-P. Feng, X.-P. Cao, Org. Biomol. Chem. 9 (2011) 3817–3824.
[150] K.L. McPhail, W.H. Gerwick, J. Nat. Prod. 66 (2003) 132–135.
[151] L. Nogle, W.H. Gerwick, J. Nat. Prod. 66 (2003) 217–220.
[152] D.R. Appleton, M.A. Sewell, M.V. Berridge, B.R. Copp, J. Nat. Prod. 65 (2002) 630–631.
[153] N.T. Eriksen, Appl. Microbiol. Biotechnol. 80 (2008) 1–14.
[154] A. Patel, S. Mishra, P.K. Ghosh, Ind. J. Biochem. Biophys. 43 (2006) 25–31.
[155] S. Benedetti, F. Benvenuti, S. Pagliarani, S. Francogli, S. Scoglio, F. Canestrari, Life Sci. 75 (2004) 2353–2362.
[156] S. Benedetti, S. Rinalducci, F. Benvenuti, S. Francogli, S. Pagliarani, L. Giorgi, M. Micheloni, G.M. D'Amici, L. Zolla, F. Canestrari, J. Chromatogr. B Analyt. Technol. Biomed. Life Sci. 833 (2006) 12–18.
[157] H.K. Madhyastha, K.S. Radha, M. Sugiki, S. Omura, M. Maruyama, Phytomedicine 13 (2006) 564–5699.
[158] L. Satyanarayana, C.G. Suresh, A. Patel, S. Mishra, P.K. Ghosh, Acta Crystallogr. Sect. F Struct. Biol. Cryst. Commun. 61 (2005) 844–847.
[159] M. Rogner, P.J. Nixon, B.A. Diner, J. Biol. Chem. 265 (1990) 6189–6196.
[160] D.A. Bryant, R. de Lorimier, G. Guglielmi, S.E. Stevens Jr., Arch. Microbiol. 153 (1990) 550–560.
[161] C. Romay, R. González, N. Ledón, D. Remirez, V. Rimbau, Curr. Protein Pept. Sci. 4 (2003) 207–216.
[162] S.-C. Cherng, S.-N. Cheng, A. Tarn, T.-C. Chou, Life Sci. 81 (2007) 1431–1435.
[163] C.M. Shih, S.N. Cheng, C.S. Wong, Y.L. Kuo, T.C. Chou, Anesth. Analg. 108 (2009) 1303–1310.
[164] B. Li, M.H. Gao, X.C. Zhang, X.M. Chu, Biotechnol. Appl. Biochem. 43 (2006) 155–164.
[165] J. Subhashini, S.V. Mahipal, M.C. Reddy, R.M. Mallikarjuna, A. Rachamallu, P. Reddanna, Biochem. Pharmacol. 68 (2004) 453–462.
[166] B.V. Pardhasaradhi, A.M. Ali, A.L. Kumari, P. Reddanna, A. Khar, Mol. Cancer Ther. 2 (2003) 1165–1170.
[167] Z. Chang, P. Flatt, W.H. Gerwick, V.H. Nguyen, C.L. Wills, D.H. Sherman, Gene 296 (2002) 235–247.
[168] J. Orjala, W.H. Gerwick, J. Nat. Prod. 59 (1996) 427–430.

[169] A.R. Pereira, L. Etzbach, N. Engene, R. Mller, W.H. Gerwick, J. Nat. Prod. 74 (2011) 1175–1181.
[170] A.B. Pereira, C.F. McCue, W.H. Gerwick, J. Nat. Prod. 73 (2010) 217–220.
[171] L.M. Sanchez, D. Lopez, B.A. Vesely, G. Della Togna, W.H. Gerwick, D.E. Kyle, R.G. Linington, J. Med. Chem. 53 (2010) 4187–4197.
[172] N. Sitachitta, J. Rossi, M.A. Roberts, W.H. Gerwick, M.D. Fletcher, C.L. Willis, J. Am. Chem. Soc. 120 (1998) 7131–7132.
[173] N. Sitachitta, B.L. Ma´rquez, R.T. Williamson, J. Rossi, M.A. Roberts, W.H. Gerwick, V.-A. Nguyen, C.L. Willis, Tetrahedron 56 (2000) 9103–9113.
[174] Y. Shimizu, Curr. Opin. Microbiol. 6 (2003) 236–243.
[175] J.I. Jiménez, P.J. Scheuer, J. Nat. Prod. 64 (2001) 200–203.
[176] K.L. McPhail, J. Correa, R.G. Linington, J. Gonzalez, E. Ortega-Barría, T.L. Capson, W.H. Gerwick, J. Nat. Prod. 70 (2007) 984–988.
[177] S.P. Gunasekera, C. Ross, V.J. Paul, S. Matthew, H. Luesch, J. Nat. Prod. 71 (2008) 887–890.
[178] M.J. Balunas, R.G. Linington, K. Tidgewell, A.M. Fenner, L.-D. Urea, T.G. Della, D.E. Kyle, W.H. Gerwick, J. Nat. Prod. 73 (2010) 60–66.
[179] J.M. Arif, A.A. Al-Hazzani, M. Kunhi, F.M. Al-Khodairy, J. Biomed. Biotech. 2004 (2) (2004) 93–98.

Chapter 6

Bioactive Marine Prenylated Quinones/Quinols

Salvatore de Rosa and Giuseppina Tommonaro
Consiglio Nazionale delle Ricerche Istituto di Chimica Biomolecolare, Pozzuoli, Naples, Italy

INTRODUCTION

Compounds of mixed biogenesis originating partly from mevalonate and partly from aromatic precursors such as vitamin K, tocopherols, ubiquinones, and plastoquinones are widespread in nature, and they play an important role in cellular metabolism, as catalysts in oxidative metabolism. They serve as respiratory carriers in the electron transport chain, and they are also involved in photosynthesis [1].

Naphthoquinones occur mainly in higher plants, and they have also been found in echinoderms, sea urchins, and starfish. They occur frequently as individuals rather than in mixtures and do not occur as glycosides but may exist *in vivo* in a reduced form [2].

Several linear or cyclic prenyl-hydroquinones and their quinone congeners have been isolated from marine organisms with a terpenoid portion that ranges from one to nine isoprene units and with a linear to cyclic skeleton. Simple benzoquinone and its mono- and diprenyl analogues are known as contact allergens and they also have an important role as chemical defensive agents in anthropoids [3]. Triprenyl- and tetraprenyl-hydroquinones are the most abundant compounds among this class of metabolites. Diprenyl- and triprenyl-hydroquinones are the most extensively studied, and they show a wide variety of biological activities [4].

Structure–activity relationship studies on prenylated hydroquinones/quinones have confirmed that the optimum length of the side chain, for biological activity in the assays used, is in the range of 5–15 carbon atoms [5]. The phenolic moieties are mainly free, but some are cyclized or alkylated hydroquinones, and some of them are polyhydric phenols [4].

Unsubstituted prenylated benzoquinones/hydroquinones are common in marine organisms but they have rarely been discovered in other organisms [4].

Bioactive Natural Products, Vol. 36. DOI: 10.1016/B978-0-444-53836-9.00023-2

The aim of this contribution is to review the more significant prenylated benzoquinones/hydroquinones from marine organisms, and their semisynthetic derivatives which show biological activities, emphasizing those compounds with a potential industrial application. In this review, the structures will be covered on the basis of their number of isoprene units (monoprenyls C_5, monoterpenes C_{10}, sesquiterpenes C_{15}, diterpenes C_{20}, sesterterpenes C_{25}, triterpenes C_{30}, carotenoids C_{40}, and nonaprenylterpenes C_{45}) and then on their carbon skeleton. Previous specific reviews on prenylated benzoquinones/hydroquinones have been published [6,7]. Further, several reviews on quinones [2,3,8] and on marine organisms [9–19] all contain material on prenylated benzoquinones/hydroquinones.

MONOPRENYLS GROUP

The simple monoprenylated hydroquinone (**1**), isolated from the tunicate *Aplidium californicum* together with the quinone (**2**) and the chromene (**3**), showed *in vivo* (mice) activity against P-338 mice lymphoma (treated/control (T/C) ratio=138% at 3.12 mg/kg) [20], and *in vitro* anti-inflammatory activity, inhibiting superoxide production when *N*-formyl-methionyl-leucyl-phenylalanine (fMLP) (IC_{50} 5.1 μM) or phorbol myristate acetate (PMA) (IC_{50} 2.3 μM) were used to activate the respiratory burst [21]. Compounds **1** and **3** significantly inhibited the mutagenic effects of benzo[*a*]pyrene, aflatoxin B_1, and ultraviolet light on *Salmonella typhimurium* and may be cancer protective agents [20].

Cancer is a leading cause of death in industrialized countries. Although mortality rates have been declining in recent years due to earlier detection and more options in treatment, most cancers remain incurable. However, the drug-resistant cancers need the identification of innovative drugs, and marine natural products could answer this need.

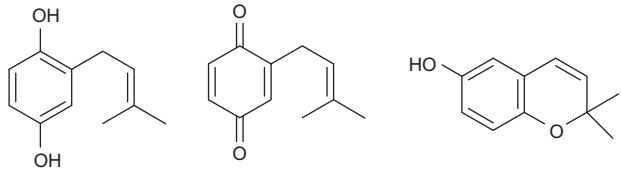

Brown algae of the genus *Perithalia* are sources of rare bis-monoprenylated hydroquinone/quinone, and the quinone **4** and the related chromenyl hydroquinone **5** were isolated from *P. capillaris* growing on the coasts of New Zealand. Compound **4** showed moderate anti-inflammatory activity, inhibiting superoxide production by human neutrophils *in vitro* (IC_{50} 2.1 μM), but was more potent at inhibiting proliferation of HL-60 human leukemia cells (IC_{50} 0.34 μM) [22].

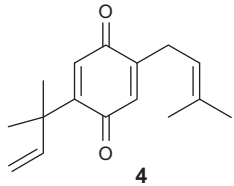

4

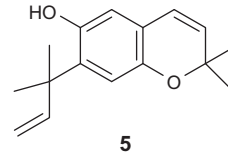

5

Anti-inflammatory activity has been recorded in many marine natural compounds, with a mechanism of action different from those of nonsteroidal anti-inflammatory drugs (NSAID). The inflammatory response has been shown to be involved in a diverse array of pathological conditions such as arthritis, gout, psoriasis, bee stings, and many chemically induced edemas. The inflammatory response is mediated by the biosynthesis of eicosanoids from arachidonic acid (arachidonic acid cascade), as well as other autacoids released locally in response to an irritant. Arachidonic acid is primarily stored in the *sn*-2 position of membrane phospholipids. The hydrolysis of the ester at this position is specifically catalyzed by phospholipase A_2 (PLA_2). Lipoxygenase (LO), cyclooxygenase (COX), and cytochrome P-450 are enzymes from arachidonic acid cascade [23]. The most commonly used nonsteroidal anti-inflammatory agents, indomethacin and the salicylate, inhibit the COX pathway but the use of these inhibitors is associated with an increased risk of gastrointestinal bleeding and renal complications. Thus, the inhibition of release of arachidonic acid by PLA_2 has become an attractive target for investigation. The development of marine inhibitors of PLA_2 offers the prospect for a new generation of anti-inflammatory drugs without side effects, derived from nonselective inhibition of constitutive enzymes.

MONOTERPENOIDS GROUP

Diprenyl quinones and related metabolites are mainly isolated from tunicates and algae, and may have a role as chemical defensive agents against predators.

Linear Monoterpenoids

Tunicates are the main source of linear prenylated 1,4-benzoquinones/hydroquinones. Geranyl hydroquinone (**6**), isolated from several tunicates [24–28] together with the chromenol (**7**), is a cancer protective agent [24], and it showed *in vitro* anti-inflammatory activity, inhibiting superoxide production when fMLP (IC_{50} 1.0 μM) or PMA (IC_{50} 1.1 μM) were used to activate the respiratory burst [21], and significant cytotoxicity against P-388 (IC_{50} 0.2 μg/ml), A-549 human lung carcinoma (IC_{50} 1.0 μg/ml), HT-29 human colon carcinoma (IC_{50} 1.0 μg/ml), and MEL-28 human melanoma (IC_{50} 1.0 μg/ml) cell lines [27]. The chromenol **7** showed antimicrobial activity toward *Micrococcus luteus* (minimum inhibitory concentration (MIC) 0.51 mM) [29]. The Mediterranean

tunicate *Aplidium* sp. contains, together with the geranyl hydroquinone, the hydroxydiprenyl hydroquinone **8** that showed less cytotoxic activity than geranyl hydroquinone against P-388 (IC_{50} 1.2μg/ml), A-549 (IC_{50} 5.0μg/ml), HT-29 (IC_{50} 2.0μg/ml), and MEL-28 (IC_{50} 2.0μg/ml) cell lines [27]. From the tunicate *Amaroucium multiplicatum* were isolated, together with compounds **6** and **7**, four related metabolites **9**–**12** that showed antioxidant activity, inhibiting 15-LO with reduction of lipid peroxides [25]. Compounds **9** and **10** were also isolated from the tunicate *A. savagnyi* [26].

Formation of an excess of lipid peroxide and its accumulation may contribute to cardiovascular diseases, such as arteriosclerosis, hypertension, cardiac insufficiency [25], and to Alzheimer's disease [30].

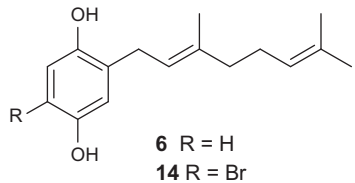

6 R = H
14 R = Br

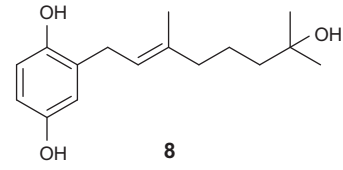

8

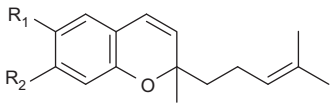

7 R_1 = OH, R_2 = H
11 R_1 = OH, R_2 = OMe
12 R_1 = OMe, R_2 = OH

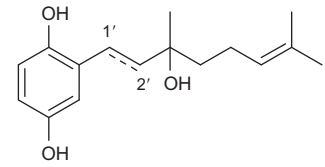

9 C1′-C2′ = single bond
10 C1′-C2′ = *E* double bond

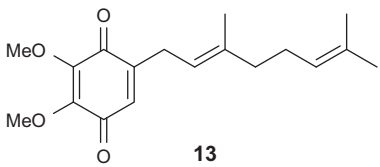

13

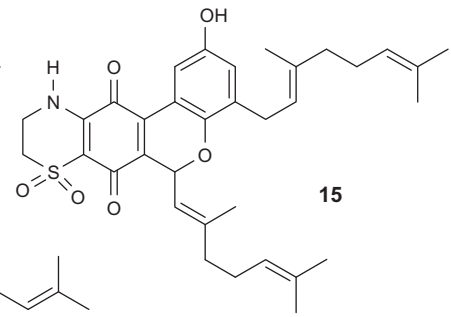

15

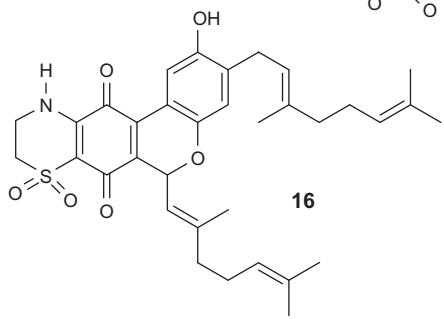

16

From the far-eastern ascidia *Aplidium glabrum* was isolated a desmethylubiquinone Q_2, glabruquinone A (**13**), having cancer preventive activity

in vitro against JB6 $P^{+}Cl$ 41 mouse epidermal cells (IC_{50} 7.3 μM), HCT-116 human colon cancer cells (IC_{50} 12.7 μM), MEL-28 (IC_{50} 17.5 μM), and HT-460 (IC_{50} 50.5 μM) cells [31], and *in vivo* inhibiting the growth of the solid Ehrlich carcinoma in mice (LD_{50} 35 mg/kg) [32].

The cymopols, a group of prenylated bromohydroquinones, were isolated from the green alga *Cymopolia barbata* (Dasycladales). The mayor metabolite, cymopol (**14**), was first isolated from *C. barbata* [33], collected in Bermuda, and it showed antifeedant activity against the herbivorous gastropod mollusc *Littorina irrorata* [34], the sea urchin *Lytechinus variegatus* [35], and herbivorous fishes [36].

From the Mediterranean ascidia *Aplidium conicum* were isolated two prenylated benzoquinones, thiaplidiaquinones A (**15**) and B (**16**), possessing an unprecedented skeleton, where a chromenol unit is fused with a *p*-benzoquinone ring, to which a $NHCH_2CH_2SO_2$ unit is attached to form a 1,4-thiazine ring. Both compounds induced apoptosis in human leukemia T Jukart cells because of a rapid overproduction of intracellular reactive oxygen species, which mediate the collapse of the mitochondrial transmembrane potential [37].

Monocyclic Monoterpenoids

Wall and coworkers reported the isolation of two isomer compounds, cymobarbatol (**17**) and 4-isocymobarbatol (**18**), correlated with cymopol (**14**), from *C. barbata* collected on the north coast of Puerto Rico, which exhibited strong inhibition of the mutagenicity of 2-aminoanthracene and ethyl methanesulfonate toward *S. typhimurium* T-98 and T-100 strains [38]. Subsequently, from a Florida Keys collection of *C. barbata* was isolated debromoisocymobarbatol (**19**) that showed antifeedant activity against the omnivorous pinfish *Lagodon rhomboides* and amphipod *Hyale macrodactyla* [39].

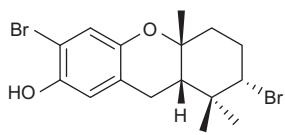

17

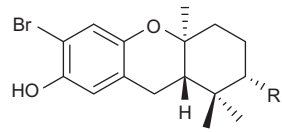

18 R = Br
19 R = H

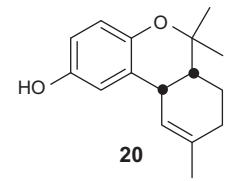

20

From the ascidia *Aplidium aff. densum* collected at Masirah Island (Oman) were isolated a series of monocyclic geranylhydroquinones together with the known chromene **7** [29]. Only epiconicol (**20**) and the chromene **7** showed moderate cytotoxicity against the human leukemic lymphoblastic cells CCRF-CEM with IC_{50} values of 60 and 30 μM, respectively [29]. Further, epiconicol (**20**) also showed cytotoxicity toward a panel of cell lines (P-388, A-549, HT-29, and CV-1 monkey kidney) with an IC_{50} value of 10.0 μg/ml [40] and a weak antimicrobial activity against *M. luteus* (MIC 0.13 mM) [29].

SESQUITERPENOIDS GROUP

The main group of marine prenyl-hydroquinones is those with a sesquiterpenoid side chain, and those with a carbobicyclic skeleton are dominant.

Linear Sesquiterpenoids

Prenylated aromatic compounds with a smaller side chain and without further substituents on the aromatic ring are relatively rare among metabolites of the brown algae but are more common in other marine organisms. Farnesyl hydroquinone (**21**), isolated from the brown seaweed *Dictyopteris undulata*, showed moderate antimicrobial activity against *Saccharomyces cerevisiae* (MIC 25.0 μg/ml), *Sclerotinia libertiana* (MIC 25.0 μg/ml), *Aspergillus oryzae* (MIC 12.5 μg/ml), and *Aspergillus niger* (MIC 12.5 μg/ml) [41].

After the preliminary observation of Tiberio in 1895 [42] and Fleming in 1929 [43] that metabolic products of moulds inhibited the growth of bacteria cultures, and the introduction of penicillin in the treatment of bacterial infections, several antimicrobial drugs were produced. The introduction of antimicrobial drugs for the control of infection is the greatest achievement in the history of medicine. Unfortunately, many bacteria acquire resistance to one or more of the antibiotics to which they were formerly susceptible. Since most antibacterial agents interact with a specific protein or cellular component, modification of the target is a common means by which resistance can be conferred. Pharmaceutical companies are actually developing new antimicrobial agents against resistant bacteria, and marine natural products can be the answer to this requirement.

From a Japanese collection of *D. undulata* was isolated the chromenol of farnesyl hydroquinone, dictyochromenol (**22**), that was ichthyotoxic to killifish (order *Cyprinodontiformes*) at 27 ppm (minimum concentration that kills all fishes within 24 h) [44]. Rossinone A (**23**), an oxygenated derivative of farnesyl hydroquinone, isolated from the Antarctic ascidian *Aplidium* sp., showed *in vitro* anti-inflammatory activity, inhibiting superoxide production when fMLP (IC_{50} 1.0 μM) or PMA (IC_{50} 1.1 μM) were used to activate the respiratory burst [21].

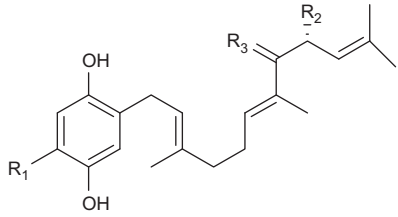

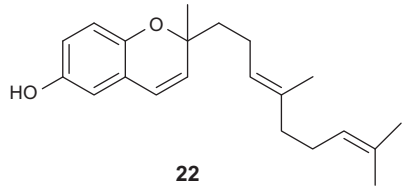

22

21 $R_1 = R_2 = H$, $R_2 = 2H$

23 $R_1 = H$, $R_2 = OH$, $R_3 = O$

24 $R_1 = CH_3$, $R_2 = H$, $R_3 = 2H$

From a marine-derived fungus of the genus *Penicillium* was isolated farnesyl toluquinol (**24**) with potent radical scavenging activity (IC_{50} 12.5 μM) against α,α-diphenyl-β-picrylhydrazyl (DPPH) [45].

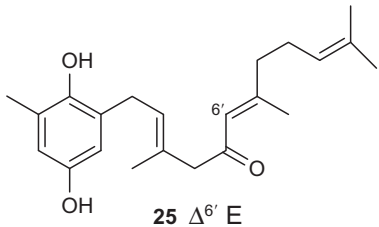

25 $\Delta^{6'}$ E
26 $\Delta^{6'}$ Z

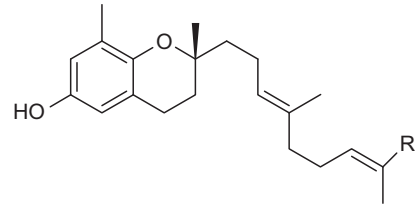

27 R = CHO
28 R = CH_2OH

Two farnesyl toluquinol derivatives (**25** and **26**), isolated from the brown alga *Cystoseira crinite* [46], and two chromanols named sargachromanol A (**27**) and B (**28**), isolated from *Sargassum siliquastrum* [47], showed antioxidant properties. The hydroquinones **25** and **26** showed a potent radical scavenging effect comparable to that of α-tocopherol in DPPH (94.1% and 92.5% scavenging at a concentration of 230 μM, respectively) and thiobarbituric acid (TBARS) (66.8% and 66.5% scavenging at a concentration of 164 μM, respectively) assays [46], while the chromanols **27** and **28** showed less activity in DPPH assay (87.8% and 90.0% scavenging at a concentration of 100 μg/ml, respectively) [47].

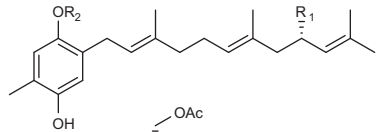

29 R_1 = OH, R_2 =

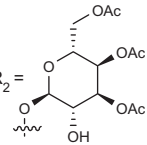

30 R_1 = OH, R_2 =

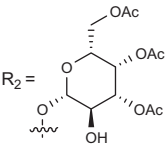

31 R_1 = OAc, R_2 =

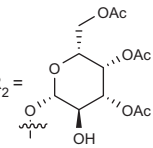

32 R_1 = H, R_2 =

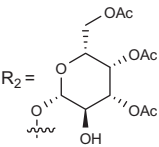

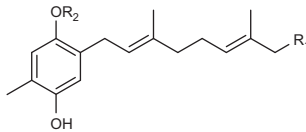

33 R_1 =

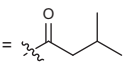

R_2 =

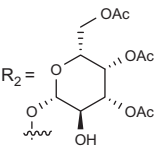

34 R_1 =

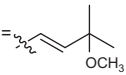

R_2 =

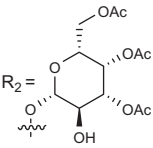

The gorgonian of the genus *Euplexaura* is a source of unusual farnesyl toluquinol glycosides. The 9-hydroxyfarnesyl toluquinol β-D-altrose, named moritoside (**29**), isolated from *Euplexaura* sp., inhibited the first cell division of fertilized starfish (*Asterina pectinifera*) eggs at 1.0 μg/ml [48]. Five farnesyl hydroquinone glycosides, euplexides A–E (**30**–**34**), related to moritoside, were isolated from the Korean *E. anastomasans*. The structures of these compounds differ from each other in that euplexides possessed a β-D-galactose moiety instead of the β-D-altrose of moritoside. Euplexides **30**–**34** exhibited moderate cytotoxicity against the human leukemia cell K-462 with IC_{50} values of 2.6, 3.1, 5.2, 8.1, and 9.4 μg/ml, respectively. Compounds **30** and **31** inhibited PLA_2 (52% and 71%, respectively) at a concentration of 50 μg/ml [49].

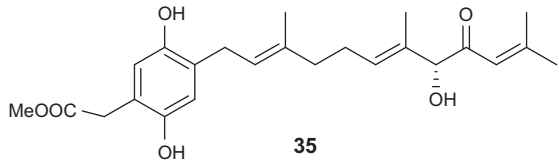

35

From the South African soft coral *Alcyonium fauri* were isolated three related sesquiterpenoid hydroquinones, but only rietone (**35**) exhibited moderate anti-HIV activity against CEM-SS cells with an IC_{50} value of 9.32 μM [50].

Monocyclic Sesquiterpenoids

Farnesyl quinones/quinols with a monocarbocyclic terpenoid skeleton in many instances show structures reminiscent of a rearranged monocyclofarnesyl precursor.

Paniceins are a group of marine metabolites isolated from the Mediterranean sponges *Halicondria panicea* [51], *Reniera fulva* [52], and *R. mucosa* [53], which contain the uncommon feature of an aromatic ring in the sesquiterpenoid moiety that, very likely, originates from a farnesyl precursor by an electrophile-catalyzed cyclization initiated at the isopropylidene group to a monocyclofarnesyl derivative, followed by 1,2-methyl migration and subsequent oxidation, linked to a quinol or a quinol residue [54].

Only paniceins A hydroquinone (**36**), A2 (**37**), B3 (**38**), C (**39**), D (**40**), E (**41**), and F1 (**42**) showed *in vitro* cytotoxicity. Panicein A hydroquinone (**36**) showed activity against CCRF-CEM cells with LC_{50} values of 0.4 mM, while paniceins B3 (**38**) and C (**39**) were active against NCI-H522 non-small lung cancer cells with LC_{50} values of 0.18 and 0.16 mM, respectively [52]. Paniceins A2 (**37**) and D (**40**) showed the same cytotoxicity (ED_{50} 2.5 μg/ml) against P-338, A-549, HT-29, and MEL-28 cell lines. Panicein E (**41**) was more active against P-388 and MEL-20 (ED_{50} 2.5 μg/ml) than to A-549 and HT-29 (ED_{50} 5.0 μg/ml), while panicein F1 (**42**) showed moderate activity (ED_{50} 5.0 μg/ml) against P-388, A-549, and MEL-20 cell lines [53].

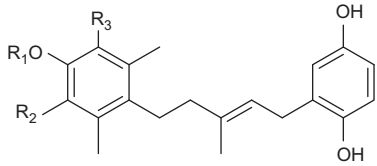

36 $R_1 = R_2 = CH_3$, $R_3 = H$
38 $R_1 = R_3 = H$, $R_2 = CHO$
39 $R_1 = H$, $R_2 = CHO$, $R_3 = OH$
42 $R_1 = CH_3$, $R_2 = CH_2OH$, $R_3 = H$

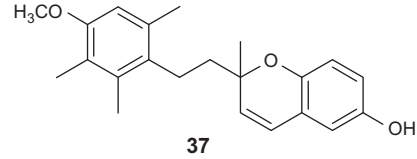

37

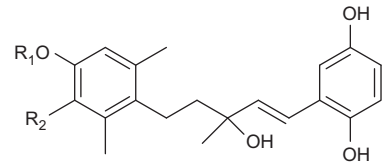

40 $R_1 = H$, $R_2 = CHO$
41 $R_1 = R_2 = CH_3$

Metachromins (**43**–**58**) were isolated from the Okinawan sponges *Hippospongia metachromia* [55–58] and *Spongia* sp. [59–61], and contain the uncommon rearranged monocyclofarnesyl moiety, and showed cytotoxicity against a panel of cells as reported in Table 1.

In addition, metachromins A (**43**) and B (**44**) showed coronary vasodilating activity, markedly inhibiting KCl (40mM)-induced contraction of the rabbit isolated coronary artery with an IC_{50} value of 3.0μM for both compounds [55], and a potent cytotoxicity against COLO-205 human colon cancer cells with IC_{50} values of 0.10 and 0.26μg/ml, respectively [58].

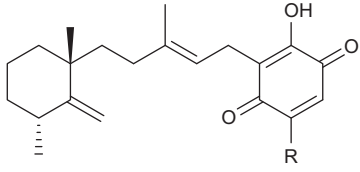

43 R = OCH_3

48 R =

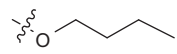

49 R =

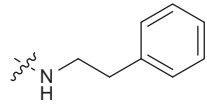

50 R =

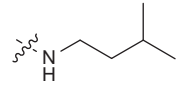

55 R =

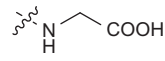

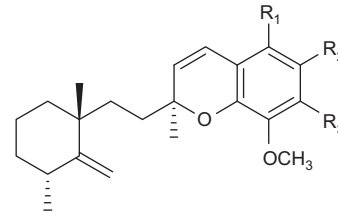

44 $R_1 = OH$, $R_2 = OCH_3$, $R_3 = H$
46 $R_1 = OH$, $R_2 = R_3 = OCH_3$
51 $R_1 = OAc$, $R_2 = OCH_3$, $R_3 = H$
52 $R_1 = R_2 = OAc$, $R_3 = H$

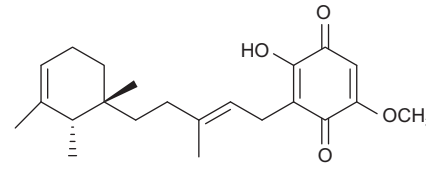

45

TABLE 1 Cytotoxicity (Mean IC_{50} (μg/ml)) of Compounds 43, 44, 46–50, 53–58 Against a Panel of Tumor Cells

Cell Line	Compound												
	43[a]	*44*[a]	*46*[b]	*47*[b]	*48*[b]	*49*[b]	*50*[b]	*53*[c]	*54*[c]	*55*[d]	*56*[d]	*57*[e]	*58*[e]
L-1210	2.4	1.62	3.0	0.2	0.6	1.3	2.0	1.0	>10	4.0	3.5	5.2	3.0
KB	1.8	0.68	10	0.4	1.9	>10	6.4	9.9	>10	4.0	5.4	>10	5.6

[a][55]; [b][57]; [c][59]; [d][60]; [e][61].

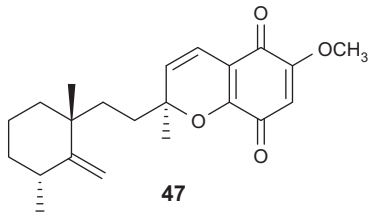

47

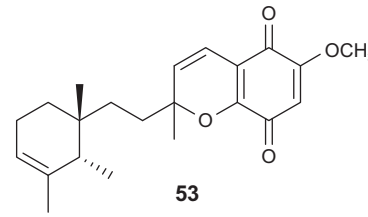

53

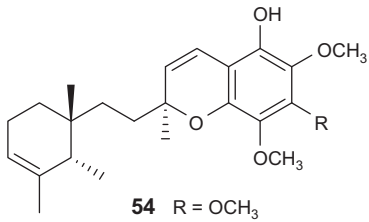

54 R = OCH_3
58 R = H

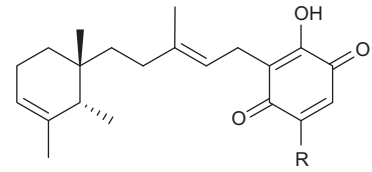

56 R = 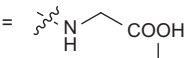

57 R = 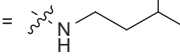

Metachromin B monoacetate (**51**) and hippochromin A diacetate (**52**) exhibited cytotoxicity against COLO-205 (IC_{50} 0.53 and 0.22 μg/ml, respectively) and KB-16 nasopharyngeal carcinoma (IC_{50} 1.32 and 3.06 μg/ml, respectively) cells [58].

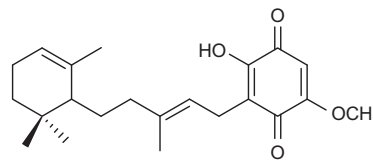

59

From a deep water sponge of the family Spongiidae was isolated isometachromin (**59**) structurally related to metachromin C (**45**), which exhibits *in vitro* cytotoxicity against A-549 cells (IC_{50} 2.6 μg/ml), and it showed moderate antimicrobial activity against *Bacillus subtilis* (MIC 12.5 μg/ml), *Candida albicans* (MIC 6.2 μg/ml), and *Cryptococcus neoformans* (MIC 25.0 μg/ml) [62].

Bicyclic Sesquiterpenoids

Most sesquiterpene quinones/quinols having a bicyclic terpenoid skeleton possess a drimane or rearranged drimane skeleton. Recently, Marcos and coworkers [7] proposed the name aureane and avarane for compounds with 1,2 rearrangements of the drimane skeleton. Within the avaranes, three groups can be characterized. The first includes the avaranes Δ^3, the second the avaranes $\Delta^{4(13)}$ (*trans* fusion in decaline system), and the last the avaranes $\Delta^{4(14)}$ (*cis* fusion in decaline system).

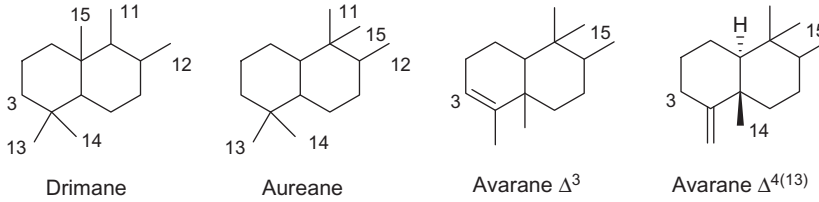

Moreover, we propose the names bolinane and pessyonane for compounds with different 1,2 rearrangements of the drimane skeleton and frondosinane for compounds with a bicyclo[5.4.0]undecane ring system (Fig. 1).

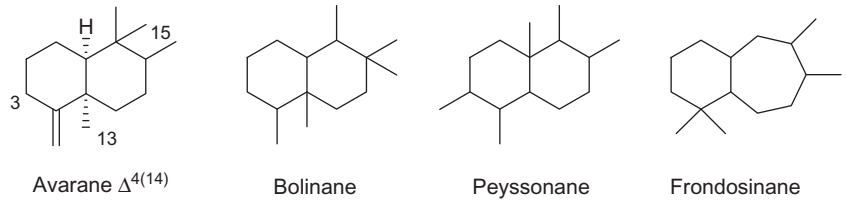

FIGURE 1 Sesquiterpene bicyclic skeletons.

Drimane Skeleton

Sesquiterpene quinones/quinols with a drimane skeleton were mainly isolated from algae and sponges.

Zonarol (**60**) and isozonarol (**61**), isolated from the brown seaweed *Dictyopteris zonarioides*, are the first two farnesyl hydroquinones with a drimane skeleton to be isolated from a marine organism [63]. Both **60** and **61** showed moderate fungitoxicity toward *Phytophthora cinnamomi*, *Rhizoctonia solani*, *Sclerotinia sclerotiorum*, and *Sclerotium rolfsii* [63], and were ichthyotoxic to killifish at 17 ppm (minimum concentration that kills all fishes within 24 h) [44]. From *D. undulata* were isolated zonarone (**62**), isozonarone (**63**), and chromazonarol (**64**), together with zonarol and isozonarol, and all are ichthyotoxic to killifish at 7, 3, 17 ppm, for compounds **62**–**64**, respectively [44].

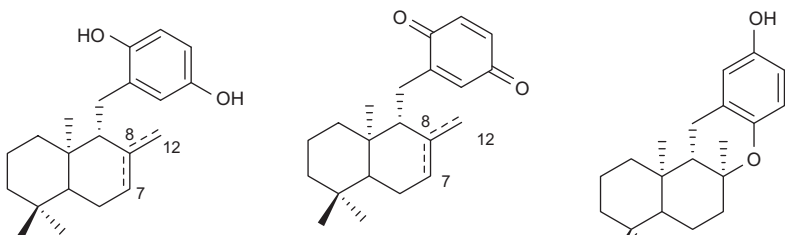

60 $\Delta^{8,12}$
61 Δ^{7}
62 $\Delta^{8,12}$
63 Δ^{7}
64

From *D. undulata* collected in the Bay of Tosa (Japan) was isolated yahazunol (**65**), together with zonarol (**60**) and isozonarol (**61**), which showed a strong antimicrobial activity against yeasts [64]. Further, yahazunol (**65**) exhibited *in vitro* cytotoxicity against HM-02 gastric adenocarcinoma (GI_{50} 4.2 μg/ml), HepG-2 hepatocellular carcinoma (GI_{50} 7.1 μg/ml), and MCF-7 breast carcinoma (GI_{50} 6.0 μg/ml) cells [65]. From the sponge of genus *Dysidea* collected in the Gulf of California were isolated 5′-*O*-acetyl-6′-hydroxy-*ent*-isozanarol (**66**) and *ent*-yahazunol (**67**) that showed cytotoxic activity against MDA-MB-231 mammary gland adenocarcinoma (LC_{50} 11.8 and 27.7 μM, respectively) and A-549 (LC_{50} 11.8 and 17.4 μM, respectively) cells; in addition, compound **66** showed activity against HT-29 cells with an LC_{50} value of 14.0 μM [66].

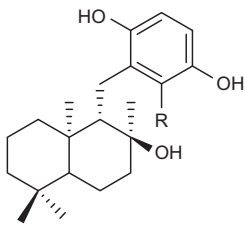

65 R = H
70 R = CHO

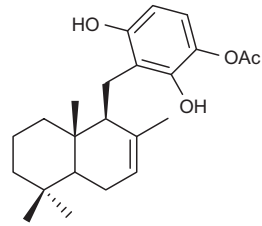

66

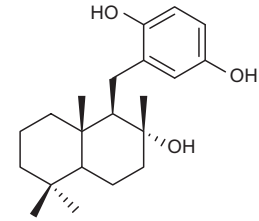

67

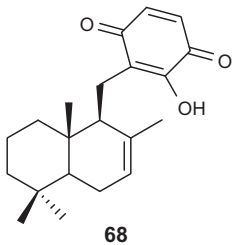

68

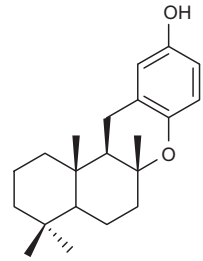

69

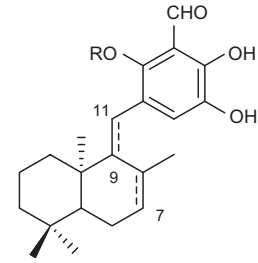

71 R = H, $\Delta^{9,11}$
72 R = SO_3H, Δ^{7}

Compound **66** was also isolated from the New Zealand sponge *Dysidea* cf. *cristagalli* together with the related quinone **68**. Both compounds inhibited *in vitro* superoxide production by human neutrophils with IC_{50} values of 3.0 and 11.0 μM, respectively. In addition, they showed antiproliferative activity against HL-60 cells (IC_{50} 0.37 and 0.34 μM, respectively) [67]. From the sponge *D. pallascens* was isolated *ent*-chromazonarol (**69**) [68] that showed moderate cytotoxicity against P-388, A-549, HT-29, and MEL-28 cells with an IC_{50} value of 15.9 μM [69]. From the sponge *Siphonodictyon coralliphagum* were isolated a series of antimicrobial metabolites named siphonodictyals with drimane or a rearranged drimane skeleton [70,71]. Siphonodictyals A (**70**), B (**71**), and C (**72**) exhibited antimicrobial activity

against *Staphylococcus aureus* and *B. subtilis* in a standard disk assay [70,71]. Siphonodictyal C (**72**) also inhibited the marine bacterium *Vibrio anguillarum* [71] and cyclin-dependent kinase 4 (CDK4)/cyclin D1 complexation with an IC_{50} value of 9.0 μg/ml [72].

CDK4 plays an important role in the G1/S transition phase in the cell cycle. It is inactive in its native form and requires activation by complexation with cyclin D1. The CDK4/cyclin D1 complex phosphorylates the retinoblastoma protein, which then releases the transcription factor that is essential for DNA synthesis. Small molecules that inhibit CDK4/cyclin D1 are potential targets for drug discovery [72].

From a deep water collection of the sponge *S. coralliphagum* was isolated *bis*(sulfato)-cyclosiphonodictyol A (**73**), which inhibited the binding of leukotriene B4 (LT-B4) to human neutrophils with an IC_{50} value of 44.5 μM [73].

Grube and coworkers reported the isolation of metabolites related to siphonodictyal B, from the Caribbean sponge *Aka coralliphagum*, synonymous with *S. coralliphagum*. Siphonodictyals B1 (**74**) and B2 (**75**) showed moderate antibiotic activity against *S. aureus* (12 and 13 mm inhibition zone, respectively) and *Botrytis cinerea* (13 and 15 mm inhibition zone, respectively) in standard disk assays using paper disks of 6 mm spotted with 20 μg of the compound [74]. The compounds **74** and **75** also showed cytotoxic activity against L-929 mouse fibroblast cells with IC_{50} values of 10.0 and 6.0 μg/ml, respectively [74]. Recently, it was reported that siphonodictyal B1 (**74**) increased intracellular calcium levels in PC12 neuroendocrine cells in the presence of either induced release or inhibited uptake of calcium from intracellular calcium stores [75]. From the same sponge were isolated two mixtures of two closely related diastereoisomers of spirosesquiterpene aldehydes, namely corallidictyals, the couple A (**76**), B (**77**) [74,76] and the couple C (**78**), D (**79**) [74]. Both mixtures **76**/**77** and **78**/**79** showed moderate antibiotic activity against *Escherichia coli* (10 and 12 mm inhibition zone, respectively), *S. aureus* (12 and 13 mm, respectively), and *Aspergillus fumigatus* (14 and 19 mm, respectively), while only the mixture **76**/**77** was active against *Mycobacterium phlei* (12 mm), *B. cinerea* (20 mm), and *Pythium debaryanum* (13 mm) in standard disk assays using paper disks of 6 mm spotted with 20 μg of the compound [74].

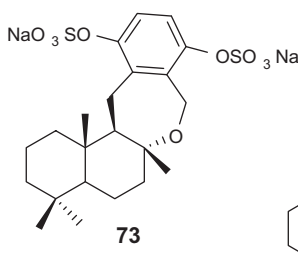

73

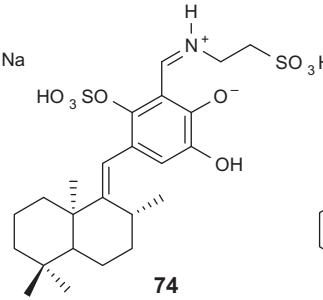

74

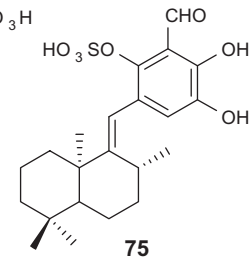

75

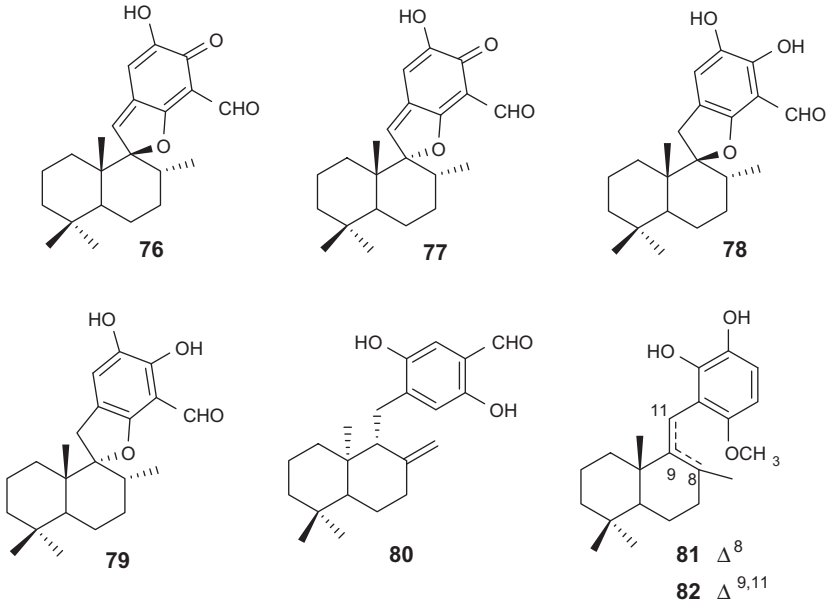

The corallidictyal mixture A and B (**76/77**) inhibited protein kinase C (PKC) (IC_{50} 28 μM) and the growth of cultured Vero (African green monkey kidney) cells (IC_{50} 1 μM) [76].

PKC, an important regulator of cell physiology, is a phospholipid-dependent protein phosphorylating enzyme that is activated by a variety of agonist interactions at the cell surface. In its activated form, it phosphorylates target proteins, which then produce specific physiological responses. Selective inhibitors of PKC are currently developed as potential drugs for cancer, inflammatory, and cardiovascular diseases [76].

From the deep sea-derived fungus, *Phialocephala* sp. was isolated a new sesquiterpene hydroquinone (**80**), which showed strong cytotoxic activity against P-388 (IC_{50} 0.16 μM) and K-562 myelogenous leukemia (IC_{50} 0.05 μM) cells [77].

Wiendendiols A (**81**) and B (**82**) isolated from the sponge *Xestospongia wiedenmayeri* inhibited cholesteryl ester transfer protein (CETP), both with an IC_{50} value of 5 μM [78]. Further, wiendendiol B (**82**) exhibited cytotoxic activity against L-929 (GI_{50} 63.1 μM) and K-562 (GI_{50} 35.8 μM) cells [79].

High levels of low-density lipoprotein (LDL) and low levels of high-density lipoprotein (HDL) in plasma are some of the risk factors which have been identified in cardiovascular diseases. CETP plays an important role in the transfer and exchange of cholesteryl esters and triglycerides between the lipidoprotein classes of human plasma, and it mediates the net transfer of cholesteryl ester from HDL to LDL. Then the inhibition of CETP should increase HDL and decrease LDL levels [80].

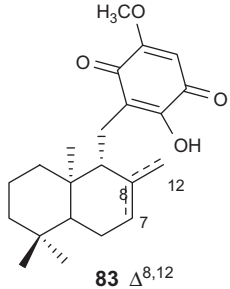

83 $\Delta^{8,12}$

84 Δ^{7}

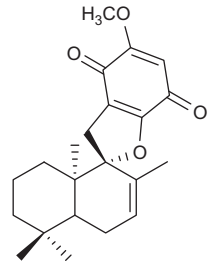

85

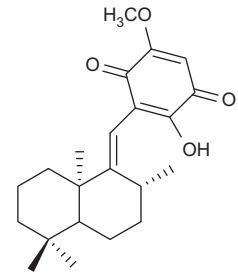

86

Hyatellaquinone (**83**), isolated from the sponge *Hyatella intestinalis* [81] and *Dactylospongia elegans* [82], showed cytotoxic activity against L-929 (GI_{50} 20.9 μM), K-562 (GI_{50} 8.4 μM) [79], HM-02 (GI_{50} 5.3 μg/ml), HepG-2 (GI_{50} 6.0 μg/ml), MCF-7 (GI_{50} 2.4 μg/ml) [65], BC human breast cancer (IC_{50} 4.45 μg/ml), and NCI-H187 (IC_{50} 10.9 μg/ml) cell lines [82]. From *D. elegans*, together with hyatellaquinone (**83**), were also isolated isohyatellaquinone (**84**) and 9-*epi*-7,8-dihydro-cyclospongiaquinone-2 (**85**) that showed cytotoxicity against BC (IC_{50} 6.69 μg/ml) and NCI-H187 (IC_{50} 7.38 μg/ml) cells [82].

Spongiaquinone (**86**), an isomer of hyatellaquinone (**83**), was isolated from *Spongia* sp. [83] and *Stelospongia conulata* [84] and exhibited cytotoxic activity against L-929 (GI_{50} 27.1 μM), K-562 (GI_{50} 13.4 μM) [79], HM-02 (GI_{50} 3.1 μg/ml), HepG-2 (GI_{50} 3.6 μg/ml), MCF-7 (GI_{50} 2.6 μg/ml) [65], and BC (IC_{50} 3.24 μg/ml) cells [85].

From the sponge *S. conulata* [84] was also isolated cyclospongiaquinone (**87**) that showed moderate activity against NCI-H187 cells (IC_{50} 4.96 μg/ml) [85].

A bromo-farnesyl hydroquinone, peyssonol A (**88**), with a *cis* decaline configuration was isolated from the red alga *Peyssonnelia* sp. [81]. Peyssonol A strongly inhibited the reverse transcriptase of human immunodeficiency virus (HIV)-1 RT DNA-dependent (DDDP) (IC_{50} 38.7 μM) and RT RNA-dependent (RDDP) (IC_{50} 6.4 μg/ml), and HIV-2 RT-DDDP (IC_{50} 23.7 μM) and RT-RDDP (IC_{50} 21.3 μg/ml) [86].

Reverse transcriptase (RT), a key enzyme in the cycle of HIV, was the most successful target for the chemotherapeutic treatment of acquired immunodeficiency syndrome (AIDS) [87].

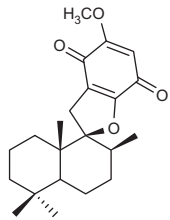

87

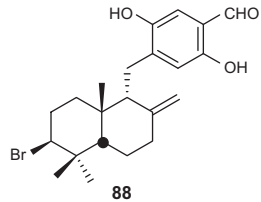

88

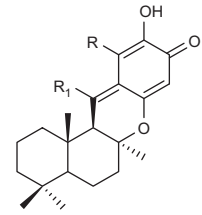

89 R = R_1 = H

90 R = Cl, R_1 = H

91 R = H, R_1 = CN

Puupehenone (**89**) and its derivatives have been isolated from different sponges mainly of order Verongida and Dictyoceratida [88–92]. They are among the most important marine metabolites because they show a wide variety of biological activity. Structurally, puupehenone (**89**) differs from typical natural sesquiterpene quinones by having a quinone–methide system that is certain to cause its unique chemical as well as biological activities. Puupehenone (**89**) showed antimicrobial activity against Gram-positive bacteria, *S. aureus* (MIC 1.2 μg/ml) and *Streptococcus pyogenes* (MIC 1.8 μg/ml), and fungi *C. albicans* (MIC 3.1 μg/ml), *Trichophyton mentagrophytes* (MIC 1.6 μg/ml), and *Trichomonas vaginalis* (MIC 3.1 μg/ml) [88], and *in vitro* antituberculosis activity with 99% inhibition of the growth of *Mycobacterium tuberculosis* (H37Rv) at 12.5 μg/ml [93].

Tuberculosis is a disease that has infected man since the earliest times and currently infects about two billion people (a third of the global population). Resistance to the current antituberculosis therapy is a big problem, and the resurgence of drug-resistant tuberculosis has generated a renewed interest in a strategic search for new drugs.

Further, puupehenone (**89**) showed cytotoxicity against P-388 (IC_{50} 0.25 μg/ml), A-549 (IC_{50} 0.1 μg/ml), HCT-8 (IC_{50} 1.0 μg/ml), MCF-7 (IC_{50} 0.1 μg/ml) [89], HT-29 (IC_{50} 0.5 μg/ml), and CV-1 (IC_{50} 0.5 μg/ml) cell lines [90]; inhibition of CETP (IC_{50} 6 μM) [78]; and antimalarial activity against three strains of *Plasmodium falciparum*: F 32 (IC_{50} 0.6 μg/ml), FcB1 (IC_{50} 2.1 μg/ml), and PFB (IC_{50} 1.5 μg/ml) [92].

The finding of new antimalarial drugs, particularly those against multiresistant *P. falciparum*, is extremely important, because in recent years, the malaria has regained its status as an extremely important threat to the health of the human race. It is estimated that, in the region where the malaria is endemic, about 1.5 million people die from this disease each year.

Several derivatives of puupehenone were isolated and/or synthesized. 21-Chloropuupehenone (**90**), isolated from the Hawaiian sponge of genus *Chondrosia* [88], strongly inhibited the effect of CETP (IC_{50} 0.3 μM) [78] and showed cytotoxicity against P-388 (IC_{50} 0.2 μg/ml), A-549 (IC_{50} 0.5 μg/ml), HT-29 (IC_{50} 0.5 μg/ml), and CV-1 (IC_{50} 0.5 μg/ml) cells [90], and antimicrobial activity against *S. aureus* (MIC 12.5 μg/ml) [94].

15-Cyanopuupehenone (**91**) was isolated from the Hawaiian sponge of order Verongida and showed moderate cytotoxicity against HT-29 (IC_{50} 1.0 μg/ml) cells, antituberculosis activity, *in vitro*, with 96% inhibition of growth of *M. tuberculosis* (H37Rv) at 12.5 μg/ml [93], and a good immunomodulatory (IM) activity with the inhibition of mixed lymphocyte culture (MLC) with an IC_{50} value of 5 μg/ml [90]. From the same sponge was also isolated puupehedione (**92**) with strong IM activity, inhibiting MLC (IC_{50} 2.0 μg/ml), and with moderate cytotoxicity against P-388 (IC_{50} 0.2 μg/ml), A-549 (IC_{50} 0.5 μg/ml), HT-29 (IC_{50} 0.5 μg/ml), and CV-1 (IC_{50} 0.5 μg/ml) cells [90], and 15-cyanopuupehenol (**93**) that showed IM activity with inhibition of MLC (IC_{50} 3.0 μg/ml), and with moderate cytotoxicity against P-388 (IC_{50} 2.0 μg/ml), A-549 (IC_{50} 2.0 μg/ml), HT-29 (IC_{50} 2.0 μg/ml), and CV-1 (IC_{50} 2.0 μg/ml) cells [90].

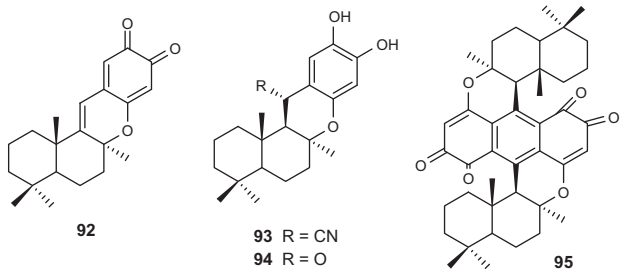

From two Hawaiian sponges of the genus *Hyrtios* was isolated 15-oxopuupehenol (**94**) together with several known compounds related to puupehenone. This new compound showed significant antimalarial activity against two strains of *P. falciparum* D6 (IC_{50} 2.0 μg/ml) and W2 (IC_{50} 1.3 μg/ml); cytotoxicity against P-388 (IC_{50} 1.0 μg/ml), A-549 (IC_{50} 0.5 μg/ml), HT-29 (IC_{50} 2.0 μg/ml), and CV-1 (IC_{50} 1.0 μg/ml) cell lines; and IM activity, inhibiting MLC (IC_{50} 2.8 μg/ml) [91].

From the New Caledonian sponge *Hyrtios* sp. was isolated dipuupehedione (**95**), a dimer of puupehenone, which showed cytotoxic activity on KB cells (EC_{50} 3.0 μg/ml) [95].

Aureane Skeleton

Aureol (**96**) is a sesquiterpene hydroquinone ether, having a secondary methyl group at C-8 and a methyl group at C-9, resulting from rearrangement of the drimane skeleton. It was isolated from the sponge *Smenospongia aurea* and represents the progenitor of this group of compounds [96]. Aureol showed selective cytotoxicity toward A-549 (IC_{50} 4.3 μg/ml), HT-29 (IC_{50} 4.7 μg/ml) [97], and HCT-116 $p53^{+/+}$ parental (IC_{50} 15.9 μM) cell lines [98], and anti-influenza-A virus activity (IC_{50} 11.6 μM) [99]. From the Jamaican sponge *S. aurea*, together with aureol (**96**), was isolated 6′-chloroaureol (**97**) that showed activity against the D6 clone of *P. falciparum* (IC_{50} 3.4 μg/ml) [100].

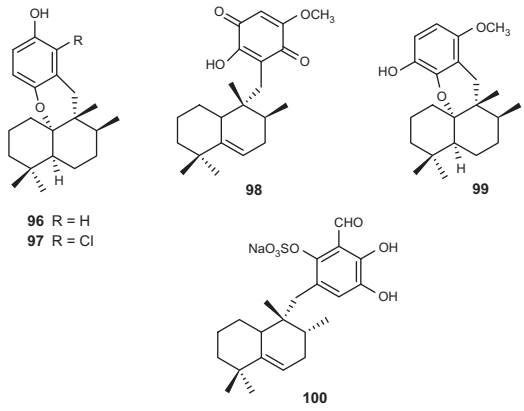

From the Mamanutha Island (Fiji) *Fasciospongia* sp. [101] and from the Australian *D. elegans* [82] was isolated mamanuthaquinone (**98**) that exhibited *in vitro* cytotoxicity toward BC (IC_{50} 2.61 μg/ml), NCI-H187 (IC_{50} 8.78 μg/ml) [82], and HCT-116 (IC_{50} 2 μg/ml) cell lines. Further, it showed *in vivo* activity with a T/C of 118% at 115 mg/kg against P-388 in mice when injected intraperitoneally [101]. Strongylin A (**99**) isolated from the Caribbean sponge *Strongylophora hartmani* inhibited the growth of influenza virus (strain PR-8) with an IC_{50} value of 6.5 μg/ml and exhibited cytotoxic activity against P-388 cells (IC_{50} 13.0 μg/ml) [102]. Siphonodictyal D (**100**) isolated from the sponge *S. coralliphagum* exhibited antimicrobial activity against *S. aureus* and *B. subtilis* in a standard disk assay [71].

Avarane Δ^3 Skeleton

Avarol (**101**) was originally isolated from the Mediterranean sponge *Dysidea avara* along with a minor amount of its oxidized derivative avarone (**102**) [103]. Its structure was determined through degradative and spectroscopic studies [104], and later by chemical synthesis [105]. Avarol represents the first example of a natural sesquiterpene possessing a 9,4-friedodrimane skeleton. Avarol and its derivatives are among the most important marine metabolites because they show a wide spectrum of biological activity and low toxicity.

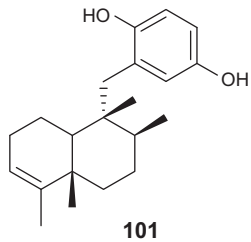

101

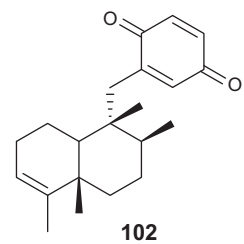

102

Over 100 articles on avarol and/or avarone recorded in *Chemical Abstracts* show the high level of interest in these compounds. In a limited review, it is almost impossible to describe all of the biological activities reported in the literature for both compounds, so only the more significant activities are reported.

Avarone and to a lesser extent avarol are active against a variety of Gram-positive bacteria species. The highest activity was determined for *Streptococcus pneumonia* and *Erysipelothrix rhusiopathiae* (MIC 0.78 μg/ml), while avarol and to a lesser extent avarone displayed antifungal activity against *T. mentagrophytes* (MIC 7.8 μg/ml), *Trichophyton rubrum* (MIC 15.6 μg/ml), and *Microsporum canis* (MIC 15.6 μg/ml) [106]. In cell culture studies, it was established that avarol and avarone exhibited potent cytostatic activities on L-5178Y (ED_{50} 0.93 and 0.62 μM, respectively) [107], L-1210 (ED_{50} 13.9 and 15.6 μM, respectively), and C-8166 (ED_{50} 9.2 and 12.9 μM, respectively) cells [108]. Both compounds also showed potent antileukemic activity *in vivo*, using L-5178Y cells in NMRI mice. At doses of 10 mg/kg for 5 days to mice bearing approximately 10^8 leukemia cells, avarone was curative in about 70% of the

mice (20% for avarol) [107]. Further, they are potent antimutagenic agents, exhibiting an activity as potent as that of the known cytochrome P-450-dependent mono-oxygenase inhibitor benzoflavone [109]. Both avarol and avarone showed a dose-related inhibitory effect on HIV (HTLV-III) replication in human H9 cells as measured by determination of RT activity and the expression of HTLV-III gag proteins p24 and p17 by monoclonal antibodies [110]. Studies with healthy test subjects revealed no side effects of avarol at the dose of 3 mg/kg administered [111]. Subsequently, we have established that both avarol and avarone showed a topical anti-inflammatory activity, with ID_{50} values of 97 and 397 μg/ear, respectively, better than indomethacin, in the tetradecanoyl-phorbol acetate (TPA)-induced ear edema in mice, as well as edema induced by carrageenan (ID_{50} 9.2 and 4.6 mg/kg p.o., respectively) [112]. Avarol was also a moderate inhibitor of the human recombinant synovial PLA_2 (IC_{50} 158 μM) and COX (IC_{50} 1.4 μM), while it was a good inhibitor of LO (IC_{50} 0.6 μM) [112]. Further, avarol showed potent antioxidant activity (IC_{50} 18 μM), evaluated by the free radical scavenging assay using DPPH [113], and it was an inhibitor of *in vitro* induced microsomial lipid peroxidation [114]. Avarone and, to a lesser extent, avarol exerted antiplatelet activity both on platelet-rich plasma and, to a greater extent, on washed platelets. In particular, avarone is a stronger inhibitor of platelet aggregation induced by arachidonic acid or A23187 than by adenosine-5′-diphosphate, platelet-activating factor, or U46619 [115]. Avarol inhibited tumor necrosis factor-α (TNF-α) generation in stimulated human monocytes (IC_{50} 1.0 μM) and TNF-α-induced activation of nuclear factor-κB (NF-κB)–DNA binding in keratinocytes. In the psoriasis-like model of TPA-induced mouse epidermal hyperplasia, topical administration of avarol (0.6–1.2 μmol/site) reduced edema, myeloperoxidase activity, IL-1β, IL-2, and eicosanoid levels in skin. Avarol was also capable of suppressing *in vivo* NF-κB nuclear translocation, determined in mouse skin [116].

Psoriasis is a common skin disease characterized by epidermal hyperplasia, inflammation of the dermis and epidermis, and leukocyte infiltration [117]. It is primarily a keratinocyte proliferation disorder that is due to the pathological development of a hypertrophic physical defence barrier, and classic topical treatments are based principally on antiproliferative or differentiation modifying activity [118]. NF-κB is a crucial factor for the immuno-inflammatory responses which is also implicated in various skin diseases including psoriasis [119]. A crucial link between high levels of TNF-α and NF-κB activation has been found in psoriatic patients and a potential mechanism of action for TNF-targeting agents is the downregulation of NF-κB transcriptional activity [117]. Recently, anti-inflammatory therapies based on blocking TNF-α signaling were shown to be effective in the treatment of psoriasis and could become a highly promising option for the treatment of this skin condition.

The biological activities of these compounds have been correlated with their redox chemistry and their ability to affect radical production, while the terpenoid moiety plays a marginal role in biological processes [120,121].

These properties [122] prompted us to prepare several sulfhydryl derivatives of avarol and to evaluate others.

Avarol-3′-thiosalicylate (**103**) is a potent inhibitor of superoxide generation in human neutrophils and also potently inhibited prostaglandin E_2 (PGE_2) generation in the human keratinocyte HaCaT cell line (IC_{50} 2.5 μM) [123]. Further studies demonstrated that avarol-3′-thiosalicylate reduced, in a concentration-dependent manner, LTB_4 (IC_{50} 1.79 μM), PGE_2 (IC_{50} 17.3 nM), and TNF-α (IC_{50} 4.18 μM) production in activated leukocytes. Oral administration of avarol-3′-thiosalicylate in the mouse air pouch model gave a dose-dependent reduction of all these inflammatory mediators [124]. Avarol-3′-thiosalicylate also inhibited human synovial recombinant PLA_2 activity (IC_{50} 5.9 μM) and the binding of NF-κB to DNA at 5 μM, in HaCaT keratinocytes. These results indicate that avarol-3′-thiosalicylate could be a promising antipsoriatic agent because it inhibits, *in vitro* and *in vivo*, several biomarkers related to the inflammatory response of psoriatic skin [124]. All thio-avarol derivatives obtained by semisynthesis were tested as inhibitors of acetylcholinesterase (AChE). The AChE inhibition tests showed a moderate activity (1 μg) for all thio-avarol derivatives with a carboxylic acid group in the molecule: avarol-3′-thiosalicylate (**103**), avarol-3′-thiolactate (**104**), avarol-4′-thiolactate (**105**), avarol-3′-thioglycolate (**106**), avarol-4′-thioglycolate (**107**), and avarol-3′-thiobenzoate (**108**). In comparison, the alkaloid galanthamine used clinically for the treatment of Alzheimer's disease inhibited the enzyme at 0.01 μg [113].

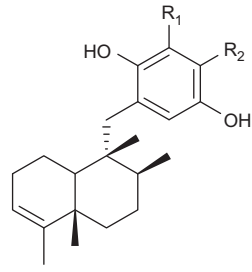

103 R_2 = H, R_1 =

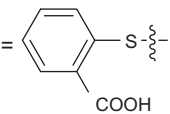

104 R_2 = H, R_1 = $CH_3CH(COOH)S$–

105 R_1 = H, R_2 = $CH_3CH(COOH)S$–

106 R_2 = H, R_1 = $HOOC–CH_2S$–

107 R_1 = H, R_2 = $HOOC–CH_2S$–

108 R_2 = H, R_1 =

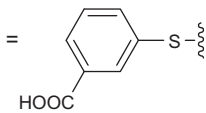

118 R_2 = H, R_1 =

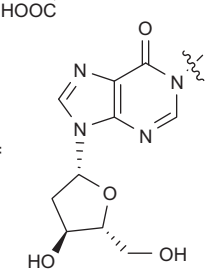

Alzheimer's disease, the most common cause of senile dementia in later life, is accompanied by a deficiency in cholinergic neurotransmission. AChE is the enzyme involved in the metabolic hydrolysis of acetylcholine at cholinergic synapses in the central and peripheral nervous system. AChE inhibitors are nowadays still the best drugs available for the management of this disease [125]. Because most inhibitors of AChE are alkaloids that often possess several side effects, it is important to search for new AChE inhibitors not belonging to this structural class.

Recently, Sladić and coworkers reported the synthesis and biological activity of further thio-avarone derivatives. After preliminary cytotoxic bioassays, only 4′-isobutylthio-avarone (**109**), 3′,4′-ethylenedithio-avarone (**110**), and 4′-phenylthio-avarone (**111**) were selected by NIH-NCI for *in vitro* screening in a panel of human tumor cell lines; the results are reported in Table 2 [126].

The finding of 3′-methylamino-avarone (**112**) and 4′-methylamino-avarone (**113**) that inhibited the cell cleavage of fertilized eggs from the sea urchin

TABLE 2 Cytotoxicity of Compounds 109–111 Against a Panel of Human Tumor Cells [126]

Cell Line	Mean GI_{50} (μM)		
	109	*110*	*111*
CCRF-CEM	1.35	11.0	3.89
K-562	4.47	20.0	19.5
MOLT-4	2.29	21.4	2.57
RIPMI-8226	3.80	14.1	20.4
HOP-92	4.79	31.6	17.0
NCI-H23	5.50	13.2	14.8
LOX-IMVI	4.07	11.2	13.5
SK-MEL-2	20.9	1.70	20.0
IGROV1	10.0	32.4	16.2
RXF 393	6.76	18.6	16.2
MCF7	7.24	20.4	22.4
MDA-MB-435	15.5	8.13	17.0
T-47D	2.63	>100	20.4

Sphaerechinus granularis [127] prompted us to prepare a series of amino derivatives of avarone and evaluate their biological activity [108,128]. 4′-Methylamino-avarone (**113**) and 4′-ethylamino-avarone (**115**) were the most toxic of the compounds, tested in brine shrimp lethality assay as an indicator of cytotoxicity, with an activity (LC_{50} 0.23 and 0.34 ppm, respectively) comparable to that of avarol (LC_{50} 0.18 ppm) [128].

The brine shrimp assay is an in-house assay substituting for KB-9, PS-9, L-5178Y, and L-1210 cytotoxicities [129].

The synthesized amino derivatives were also tested *in vitro* as cytostatic and antitumor agents, and the results of the most active compounds are reported in Table 3 [108]. Generally, the introduction of a methylamino or an ethylamino group in the 3′ position of the quinone ring of avarone results in compounds endowed with higher potency against L-1210, and B- and T-lymphoblast cells. On the other hand, introduction in the 4′ position gives rise to compounds (**113** and **115**) with cytotoxicity comparable to that of avarone (**102**). Modifications in the quinone ring of avarone always result in loss of anti-HIV activity with two exceptions: 4′-leucine-avarone (**116**) and 4′serine-avarone (**117**). Both retain the potency of the parent compound [108].

TABLE 3 Cytostatic and Antiviral Activity of Compounds 101, 102, 112–117 [108]

Cell Line	Compound							
	101	*102*	*112*	*113*	*114*	*115*	*116*	*117*
Cytostatic	Mean ID_{50} (μM)							
Vero	19.5	17.0	14.0	10.2	12.5	12.0	23.5	>100.0
L-1210	13.9	15.6	2.3	15.2	3.4	28.2	11.6	26.3
Raji	11.7	18.1	2.0	18.1	3.9	20.3	9.1	24.0
C-8166	9.2	12.9	1.7	16.2	2.5	18.6	8.8	22.3
H9	13.5	14.2	2.3	22.0	3.7	28.0	9.1	30.1
Antiviral	Mean ED_{50} (μM)							
ASFV	19.0	17.4	14.0	10.5	12.5	12.0	23.5	>100.0
HSV-1	10.5	9.5	4.4	10.2	12.5	12.0	23.5	>100.0
Polio	0.8	0.8	0.6	2.0	0.8	3.3	2.7	3.9

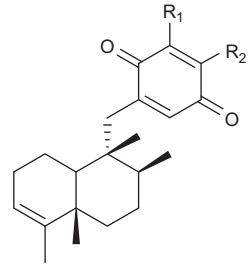

109 R_1 = H, R_2 = 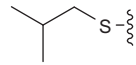

110 R_1 = 
R_2 =

111 R_1 = H, R_2 = 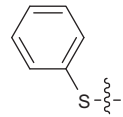

112 R_1 = NHCH$_3$, R_2 = H

113 R_1 = H, R_2 = NHCH$_3$

114 R_1 = NHCH$_2$CH$_3$, R_2 = H

115 R_1 = H, R_2 = NHCH$_2$CH$_3$

116 R_1 = H, R_2 = 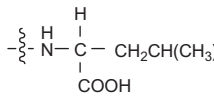

117 R_1 = H, R_2 = 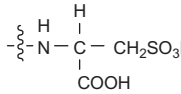

These results indicated that the stability of the quinone form of amino derivatives is at least in part responsible for diminution of some aspects of biological activities, because apparently they can be reduced in biological medium only with difficulty.

Further, several amino-avarone derivatives were also tested as potential antipsoriatic agents. 3′-Methylamino-avarone (**112**) presented the best anti-proliferative profile, by the inhibition of ^{3}H-thymidine incorporation in HaCaT cells (IC_{50} 4.5 μM), with potency similar to the reference compound anthralin but without any cell toxicity. Moreover, compound **112**, by exerting antioxidant properties, could also contribute to reduce the possible undesirable effects derived from respiratory bursts of neutrophils infiltrated in the psoriatic skin [123].

From the sponge *Dysidea* sp. collected in Papua New Guinea was isolated avinosol (**118**), a terpenoid hydroquinone conjugated with a nucleoside, which showed anti-invasion activity against MDA-MB-231 breast cancer cells invaded in a mesenchymal mode, and LS-174T colon carcinoma invaded in an amoeboid manner, with an IC_{50} value of 50.0 μg/ml for both cell lines [130].

From *D. avara* collected from different places in the Gulf of Naples (Italy) were isolated 5′-acetyl avarol (**119**) [131], diacetyl-avarol (**120**), and 6′-hydroxy,5′-acetyl avarol (**121**) [132].

The monoacetyl avarol (**119**) showed a cytotoxicity (LD_{50} 0.09 ppm) twice that of avarol (**101**) [131], while diacetyl-avarol (**120**) (LD_{50} 0.15 ppm) and compound **121** (LD_{50} 1.3 ppm) showed an activity comparable to avarol, in the Brine shrimp assay [132].

Subsequently, Shen and coworkers reported the synthesis and cytotoxicity of several acylated avarol derivatives. Diacetyl avarol (**120**) showed strong cytotoxic activity against KB cells (IC_{50} 1.35 μg/ml), while di-*p*-bromobenzoyl avarol (**122**) was active against HePa (IC_{50} 1.3 μg/ml) cells [133].

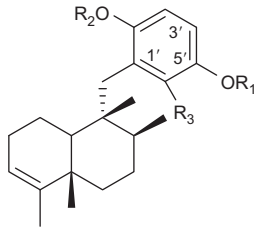

119 R_1 = Ac, R_2 = R_3 = H
120 R_1 = R_2 = Ac, R_3 = H
121 R_1 = Ac, R_2 = H, R_3 = OH

122 R_3 = H, R_1 = R_2 =

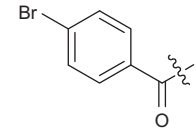

From the Red Sea sponge *Dysidea cinerea* were isolated six avarol and avarone derivatives, 3′-hydroxy avarone (**123**), 3′,6′-dihydroxy avarone (**124**), 6′-acetoxy avarone (**125**), 6′-hydroxy-4′-methoxy avarone (**126**), 6′-hydroxy avarol (**127**), and 6′-acetoxy avarol (**128**) [134].

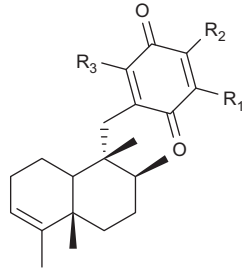

123 R_1 = OH, R_2 = R_3 = H
124 R_1 = R_3 = OH, R_2 = H
125 R_1 = R_2 = H, R_3 = OAc
126 R_1 = H, R_2 = OCH_3, R_3 = OH

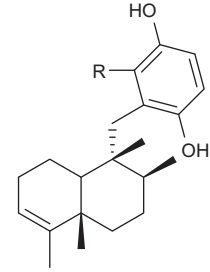

127 R = OH
128 R = OAc

Several of these compounds showed cytotoxic, antimicrobial, and anti-HIV-1 RT activities. Compounds **123**–**126** and **128** were cytotoxic against P-388 cells with IC_{50} values of 0.6, 1.2, 10.0, 20.0, and 0.6 μg/ml, respectively. Modest antifungal activity against *C. albicans* was observed for compounds **123** (MIC 12.5 μg/ml), **124** (MIC 50.0 μg/ml), and **128** (MIC 12.5 μg/ml) [134]. HIV-1 RT-RDDP inhibition was observed for compounds **123** (IC_{50} 6.8 μg/ml), **124** (IC_{50} 5.0 μg/ml), **126** (IC_{50} 1.0 μg/ml), and **127** (IC_{50} 7.0 μg/ml) [135].

Nakijiquinones are sesquiterpene aminoquinone compounds with an avarane Δ^3 skeleton isolated from several collections of Okinawan sponge of family Spongiidae. Nakijiquinones A (**129**), B (**130**) [136], C (**131**), D (**132**) [137], G (**133**), H (**134**), and I (**135**) [138] exhibited cytotoxicity against L-1210 (IC_{50} 3.8, 2.8, 5.8, 8.1, 2.9, 8.5, and 2.4 µg/ml, respectively) and KB (IC_{50} 7.6, 5.0, 6.2, 1.2, 4.8,>10, and 5.6 µg/ml, respectively) cells; in addition, nakijiquinones G (**133**), H (**134**), and I (**135**) were also cytotoxic against P-388 cells with IC_{50} values of 3.2, 2.4, and 2.9 µg/ml, respectively [138].

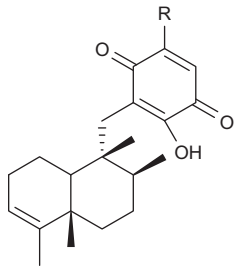

129 R = —$NHCH_2COOH$

130 R = —$NHCH(COOH)CH(CH_3)_2$

131 R = —$NHCH(COOH)CH_2OH$

132 R = —$NHCH(COOH)CH(OH)CH_3$

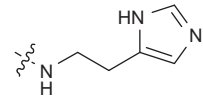

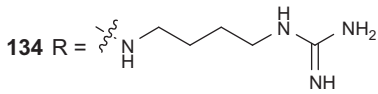

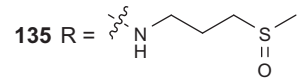

Nakijiquinones A (**129**), B (**130**), and H (**134**) showed antifungal activity against *C. albicans* (MIC values, 2.5, 33.0, and 8.35 µg/ml, respectively) and *A. niger* (MIC values, 5.0, 133.0, and 16.7 µg/ml, respectively) [136,138]; nakijiquinone H (**134**) was also active against the bacteria *M. luteus* (MIC 16.7 µg/ml) and the fungus *C. neoformans* (MIC 8.35 µg/ml) [138]. Nakijiquinones A (**129**), B (**130**), C (**131**), and D (**132**) exhibited inhibition against ErbB-2 tyrosine kinase (IC_{50} 30, 95, 26, and 29 µM, respectively) and PKC (IC_{50} 270, 200, 23, and 220 µM, respectively) [137].

Receptor tyrosine kinases (RTKs) such as Tie-2, insulin-like growth factor 1 receptor (IGF1-R), Her-2/Neu, epidermal growth factor receptor (EGFR), and vascular endothelial growth factor receptors (VEGFR1–3) play crucial roles in the control of cell growth and differentiation. Inhibition of such RTKs has become a major focus of current anticancer drug development, and therefore the discovery of new classes of inhibitors for these signal-transducing proteins is of prime importance [139].

Avarane $\Delta^{4(13)}$ Skeleton

Isoavarol (**136**), a sesquiterpene hydroquinone isomer of avarol (**101**), was isolated from the Pacific sponge *Dysidea* sp. [140]. Simultaneously, the same compound was isolated from the Okinawan *Dysidea* sp. [141] and named neoavarol. Subsequently, it was also isolated from a *Dysidea* sp. collected in the Gulf of California, together with its 5′-acetyl derivative (**137**) that

showed cytotoxic activity against MDA-MB-231 (GI_{50} 21.0 μM) and A-549 (GI_{50} 25.5 μM) cells [66].

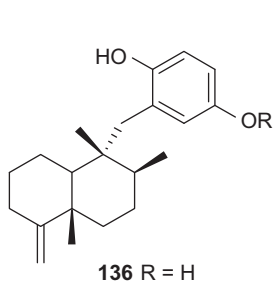

136 R = H
137 R = Ac

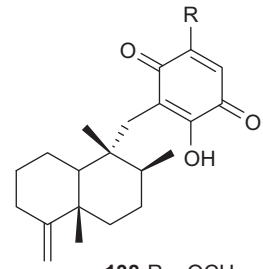

138 R = OCH_3
139 R = NH_2
140 R = $NHCH_2COOH$

Ilimaquinone (**138**) was first isolated from the sponge *H. metachromia* and described as enantiomeric to avarol [142]. Subsequently, the stereochemistry of ilimaquinone was revised establishing that it showed the same absolute stereochemistry as avarol [143]. Ilimaquinone (**138**) showed antimicrobial activity against *S. aureus* (MIC 3.12 μg/ml) [94] and an antiproliferative effect on several types of cancer lines, including Ehrlich ascite tumor cells (ID_{50} 22.4 μg/ml) [94], L-1210 (ID_{50} 4.0 μg/ml) [144], BC (IC_{50} 1.5 μg/ml), NCI-H-187 (IC_{50} 3.37 μg/ml) [82], P-388 (IC_{50} 0.2 μg/ml), KB-16 (IC_{50} 0.7 μg/ml), A-549 (IC_{50} 0.4 μg/ml) [145], and prostate cancer: PC-3 (IC_{50} 2.6 μM), DU-145 (IC_{50} 5.8 μM), and LNCaP (IC_{50} 4.6 μM)], human osteosarcoma MG-63 (IC_{50} 4.9 μM), and Hep-3B (IC_{50} 12.0 μM) [146]. Further, ilimaquinone (**138**) showed inhibitory activity against HIV-1 RT-RDDP (IC_{50}>50 μg/ml), RT-DDDP (IC_{50}>50 μg/ml), and RNase H (IC_{50} 5.4 μg/ml), and retroviral murine leukemia virus (MuLV RT)-RDDP (IC_{50} 19.0 μg/ml), -DDDP (IC_{50} 14.5 μg/ml), and RNase H (IC_{50} 10.3 μg/ml) [147]. Ilimaquinone selectively broke down the Golgi apparatus into small vesicles blocking cellular secretion in a reversible manner [148]. In addition, it inhibited cellular methylation through its interaction with *S*-adenosylhomocysteinase (at 0.05 mM, about 50% of the enzyme activity was inhibited). These studies indicate that the inhibition of secretion by ilimaquinone is the result of its antimethylation activity. It is likely that the ability to fragment the Golgi apparatus is related to the influence of ilimaquinone on methylation chemistry [149]. Ilimaquinone (**138**) showed a dose-related inhibitory effect on the proliferation and induced morphological and ultrastructural changes in promastigotes of *Leishmania mexicana* (LD_{50} 5.6 μM) [150].

Leishmania are parasitic protozoa responsible for a large diversity of clinical manifestations in humans, known as leishmaniasis. The predominant treatment of this disease has been based on the use of pentavalent antimonials. These drugs are very toxic and little is known about their mechanism of

action. Researchers are involved in the discovery of new drugs for the treatment of this disease [150].

Smemospongine (**139**), a sesquiterpene aminoquinone, was isolated from the Red Sea sponge *Smemospongia* sp. [151] that exhibited antibacterial activity against *S. aureus* strain 209 P (MIC 7.0 μg/ml), *Proteus morganii* strain 1510 (MIC 25.0 μg/ml), and *Pseudomonas aeruginosa* strain PYO 9 (MIC 25.0 μg/ml) and strain 8203 S (MIC 25.0 μg/ml) and cytotoxicity against several cell lines including L-1210 (IC_{50} 1.5 μg/ml) [144], A-549 (IC_{50} 5.7 μg/ml), HT-29 (IC_{50} 4.0 μg/ml), B-16/F10 (IC_{50} 4.1 μg/ml), and P-388 (IC_{50} 2.6 μg/ml) cells [152]. From the Philippine, *Fasciospongia* sp. was isolated glycinylilimaquinone (**140**), together with ilimaquinone (**138**) and smenospongine (**139**), which inhibited the growth of HCT-116 (IC_{50} 7.8 μg/ml) cells [153].

Avarane $\Delta^{4(14)}$ Skeleton

From the Pacific sponge *Dysidea arenaria* were isolated arenarol (**141**) and arenarone (**142**), a pair of hydroquinone–quinone compounds, having the same rearranged sesquiterpene skeleton as avarol (**101**) and ilimaquinone (**138**), but with a *cis*- rather than *trans*-decaline stereochemistry. Both showed mild cytotoxicity against P-388 with ED_{50} values of 17.5 and 1.7 μg/ml, respectively [154]. Arenarol (**141**) also exhibited potent antioxidant activity by free radical scavenging DPPH assay (IC_{50} 19 μM) [155]. Isoarenarol (**143**) was isolated from a Papua New Guinea sponge *D. arenaria*, together with arenarol (**141**). Both compounds showed potent and selective *in vitro* inhibition of several protein kinases: the results are reported in Table 4 [156].

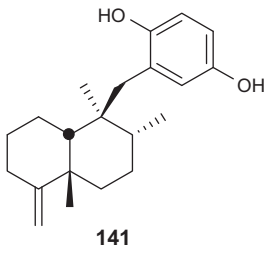

141

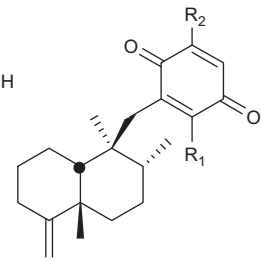

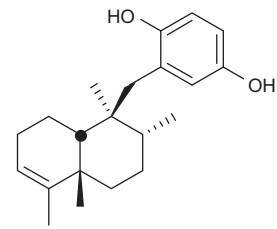

143

142 $R_1 = R_2 = H$
144 $R_1 = OH$, $R_2 = OCH_3$
145 $R_1 = OH$, $R_2 = –NH\text{-}i\text{Bu}$
146 $R_1 = OH$, $R_2 = –NHCH_2CH_2Ph$

5-Epi-ilimaquinone (**144**) was first isolated from the sponge *Fenestraspongia* sp. [157] and subsequently from the Papua New Guinea sponge *D. elegans*, together with epi-smenospongiarine (**145**) and epi-smenospongidine (**146**) [152]. The compounds **144**–**146** showed potent cytotoxicity against a panel of cell lines including A-549 (IC_{50} 0.9, 0.8, and 3.9 μg/ml, respectively), HT-29

TABLE 4 Kinase Inhibition Activities of Arenarol (141) and Isoarenarol (143) on Protein Kinases [156]

Compound	Mean IC_{50} (μM)							
	CDK1	*ERK1*	*GSK3b*	*LCK*	*P70S6K*	*PAK3*	*PIM1*	*PKC*
141	4	13	124	2.0	86	7	16	44
143	4	39	55	6.4	91	6	13	35

(IC_{50} 3.4, 0.9, and 2.4 μg/ml, respectively), B-16/F10 (IC_{50} 1.1, 0.6, and 1.9 μg/ml, respectively), and P-388 (IC_{50} 2.2, 0.7, and 1.9 μg/ml, respectively) [152].

From the Pohnpei (Micronesia) sponge *Dysidea* sp. was isolated popolohuanone E (**147**). Its structure can be derived by enzymatic or possibly nonenzymatic oxidative dimerization of unreported 6′-hydroxyarenarol. Popolohuanone E (**147**) showed topoisomerase-II inhibition (IC_{50} 400 nM) and was selectively cytotoxic against A-549 (IC_{50} 2.5 μg/ml) cells, but it was not appreciably cytotoxic (>20 μg/ml) to CV-1, HT-29, and P-388 cell lines [158].

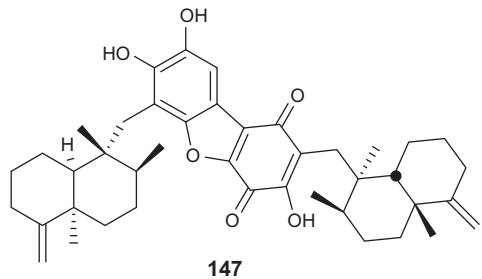

147

Bolinane Skeleton

Bolinaquinone (**148**), a sesquiterpene hydroxyquinone with a rearranged drimane skeleton but with a different position for the hydroxyquinone moiety, was isolated from the Philippine sponge *Dysidea* sp. and showed cytotoxicity against HCT-116 (IC_{50} 1.9 μg/ml) [159] and HeLa (IC_{50} 5.45 μM) cells [160]; anti-inflammatory activity inhibiting the human synovial PLA_2 (IC_{50} 0.2 μM), pancreatic PLA_2 (IC_{50} 0.4 μM), and bee venom PLA_2 (IC_{50} 0.1 μM) [161]; and a neuroprotective effect (57% survival) against iodoacetic acid (IAA)-induced cell death at a dose of 10 μM [162].

Dysidine (**149**) was isolated from the Vanuatu Islands sponge *Dysidea* sp., together with bolinaquinone (**148**), and showed high and selective inhibition of the human synovial PLA_2 (IC_{50} 2.0 μM) [161]. Further, dysidine activated the insulin signaling pathway, greatly promoted glucose uptake in 3T3-L1 cells (20 μM) [163], and showed strong insulin-sensitizing activities through inhibition of protein tyrosine phosphatase 1B (hPTP1B) with an IC_{50} value of 6.7 μM [160].

hPTP1B is regarded as a key target for the treatment of Type-II diabetes and obesity because it could hydrolyze phosphotyrosines on the insulin receptor, deactivating it [160].

Dysideamine (**150**), a sesquiterpene amino-hydroxyquinone, was isolated along with bolinaquinone (**148**) from the Indonesian sponge *Dysidea* sp. and showed a neuroprotective effect (43% survival) against IAA-induced cell death at a dose of 10 μM [162].

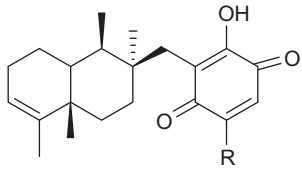

148 R = OCH_3
149 R = $NHCH_2CH_2SO_3H$
150 R = NH_2

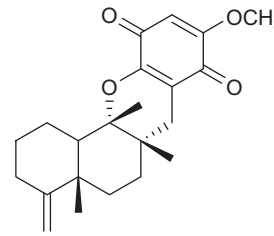

151

From the Okinawan sponge *D. elegans* was isolated neodactyloquinone (**151**) that showed moderate cytotoxic activity against HeLa cells (IC_{50} 86 μM) [164].

Peyssonane Skeleton

Peyssonol B (**152**) was isolated, together with peyssonol A (**88**), from the red alga *Peyssonnelia* sp. [81].

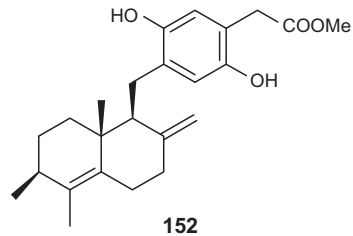

152

The contemporary presence of both **152** and **88** in the same alga suggests that the 3-bromodrimane compound **88** is the natural precursor of peyssonol B (**152**), by the elimination of the C-3 substituent followed by a 1,2-shift of one of the C-4 methyl groups, to C-3, and sequentially abstraction of H-5 to obtain the 4(5) double bond.

Peyssonol B (**152**) strongly inhibited the HIV-1 RT-DDDP (IC_{50} 34.5 μM) and RT-RDDP (IC_{50} 4.3 μM), and HIV-2 RT-DDDP (IC_{50} 28.0 μM) and RT-RDDP (IC_{50} 14.7 μM) [86].

Frondosinane Skeleton

Dysidea frondosa is a rich source of sesquiterpene and nor-sesquiterpene hydroquinone derivatives with a less common bicyclo[5.4.0]undecane ring system, named frondosins. Frondosins A (**153**), B (**154**), D (**155**), and E (**156**) are inhibitors of interleukin-8 (IL-8) receptors and PKC at micromolar levels: the results are reported in Table 5 [165].

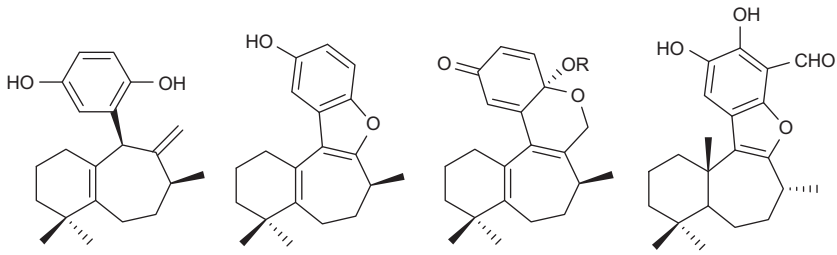

153 **154** **155** R = H, **156** R = CH_3 **157**

IL-8, a chemoattractant for neutrophils, is produced by macrophages, fibroblasts, endothelial, and epithelial cells exposed to TNF and IL-1β. IL-8 promotes the accumulation and activation of neutrophils and has been implicated in a wide range of acute and chronic inflammatory disorders. Hence, inhibitors of IL-8 receptor represent a promising target for novel anti-inflammatory drugs.

Liphagal (**157**), isolated from the sponge *Aka coralliphaga*, selectively inhibited Pl-3 kinase α with an IC_{50} of 100 nM in the primary fluorescent polarization enzyme assay and showed cytotoxicity against LoVo (IC_{50} 0.58 μM), CaCo (IC_{50} 0.67 μM), and MD-468 (IC_{50} 1.58 μM) tumor cell lines [166]. We include this compound in the frondosinane group only because it has a bicyclo[5.4.0]undecane ring system.

TABLE 5 IL-8 Receptors and PKC Activities of Compounds 153–156 [165]

Compound	Mean IC_{50} (μM)		
	IL-8 Rα	*IL-8 Rβ*	*PKC-α*
153	3.4	3.2	1.8
154	9.6	10.8	4.8
155	98	10.8	26
156	64	37.1	30.6

Tricyclic Sesquiterpenoids

Cyclozonarone (**158**), a sesquiterpene-substituted benzoquinone derivative, isolated from the brown alga *Dictyopteris undulate* [167], showed cytotoxicity against gastric adenocarcinoma HM-02 (GI_{50} 5.7 μg/ml), HepG-2 (GI_{50} 9.6 μg/ml), and MCF-7 (GI_{50}>10 μg/ml) cells [65].

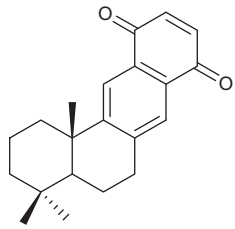

158

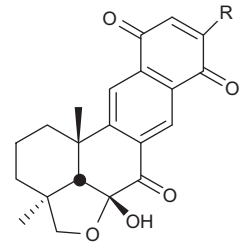

159 R = H
160 R = OCH_3

Alisiaquinones A–C (**159–161**) and alisiaquinol (**162**) were isolated from an unidentified deep water sponge collected in New Caledonia. They showed antimalarial activity against three strains of *P. falciparum* F32 (IC_{50} 9.1, 7.1, 0.15, and 9.9 μM, respectively), FcB1 (IC_{50} 7.4, 8.4, 0.21, and 6.4 μM, respectively), and FcMC29 (IC_{50} 8.5, 2.6, 0.08, and 7.9 μM, respectively), and they inhibited a bovine protein farnesyl transferase (PFTase) with IC_{50} values of 2.8, 2.7, 1.9, and 4.7 μM, respectively.

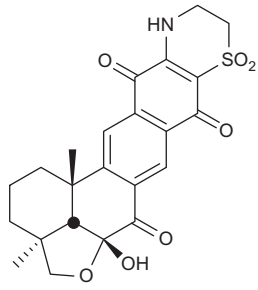

161

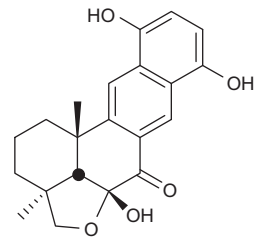

162

Further, alisiaquinone B (**160**) and alisiaquinol (**162**) showed strong cytotoxicity against MCF-7 cells (IC_{50} 0.8 and 1.7 μM, respectively) [168].

DITERPENOIDS GROUP

Brown algae (Phaeophyta) are of current interest owing to their varying and unique metabolites. Phaeophyta and in particular Cystoseiraceae are a rich source of tetraprenyl-toluquinols, also called meroditerpenes. Several of these metabolites have been found to exhibit biological activity.

Linear Diterpenoids

Among brown algae, the genus *Sargassum* is a source of bioactive meroditerpenoids. From the *Sargassum tortile* were isolated sargatriol (**163**) [169], dihydroxysargaquinone (**164**) [170], and hydroxysargaquinone (**165**) [171]. Sargatriol (**163**) and dihydroxysargaquinone (**164**) both exhibited moderate cytotoxic activity (ED_{50} 18.0 μg/ml) [170], while hydroxysargaquinone (**165**) was more cytotoxic (ED_{50} 0.7 μg/ml) [171] against P-388 cells.

Further hydroxylated geranylgeranyl toluoquinones/toluoquinols **166–170** and a related chromene **171** were isolated from *S. micracanthum* [172,173]. These compounds exhibited antioxidant activities as an inhibitory effect on lipid peroxidation (IC_{50} 0.11, 1.0, 0.95, 44.3, 1.15, and 0.28 μg/ml, respectively) [172,173].

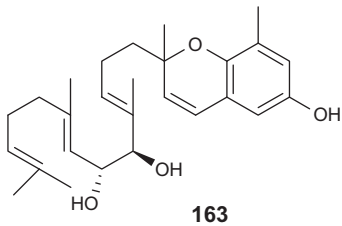

163

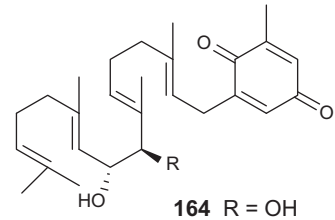

164 R = OH
165 R = H

Compounds **168** and **170** showed relatively strong cytotoxic activity with IC_{50} values of 1.51 and 1.69 μg/ml, respectively, against Colon 26-L5 cells [173], while the chromene **171** showed potent antiviral activity (IC_{50} 0.49 μM) against HCMV human cytomegalovirus [172].

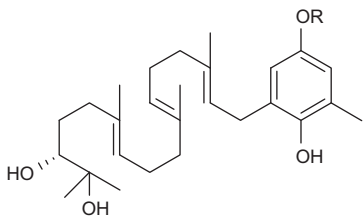

166 R = H

169 R =

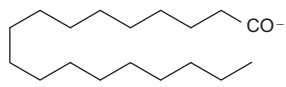

170 R =

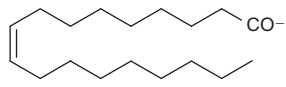

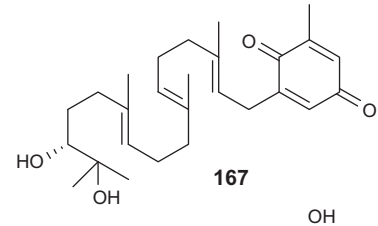

167

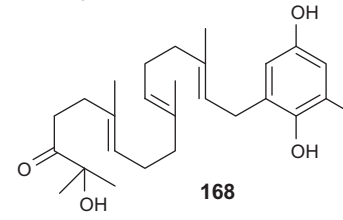

168

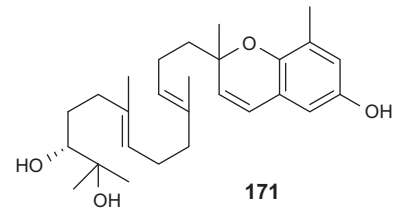

171

From the brown alga *Cystoseira usneoides* were isolated two couples of meroterpenoids, usneoidones *E* (**172**) and *Z* (**173**) [174], and usneidols *E* (**174**) and *Z* (**175**) [175] that exhibited cytotoxic activities in several types of cell lines, including P-388 (IC_{50} 0.8, 1.5, 6.8, and 3.2 μg/ml, respectively), CV-1 (IC_{50} 4.0, 1.0, 4.0, and 3.6 μg/ml, respectively), and BHK baby hamster kidney fibroblast (IC_{50} 6.2, 1.1, 6.2, and 3.7 μg/ml, respectively) [174,175]. In addition, for usneoidones *E* (**172**) and *Z* (**173**), further cytotoxic activities against A-549 (IC_{50} 1.25 and 1.4 μg/ml, respectively), HeLa (IC_{50} 1.0 and 1.3 μg/ml, respectively), and B-16 (IC_{50} 1.0 and 1.5 μg/ml, respectively) were reported [174]. Further, usneoidone *E* (**172**) showed antiviral activity against CV-1 cells infected with herpes simplex virus (HSV-1) with an IC_{50} value of 3.1 μg/ml [174].

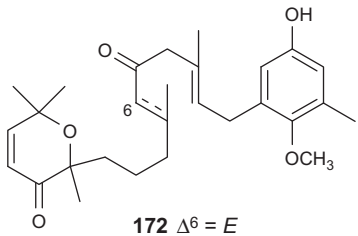

172 $\Delta^6 = E$

173 $\Delta^6 = Z$

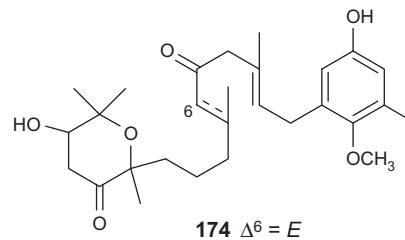

174 $\Delta^6 = E$

175 $\Delta^6 = Z$

Several meroterpenoids were isolated from *C. crinita* [46], but here only those that showed interesting biological activity are reported. Two couples of *E*/*Z* isomers of tetraprenyl-toluquinols (**176** and **177**) and (**178** and **179**), and a dihydroxy derivative (**180**) showed cytotoxic activity against HM-02 (GI_{50} 2.3, 1.8, 0.3, 0.9, and 0.9 μg/ml, respectively), HepG-2 (GI_{50} 7.1, 6.8, 1.8, 1.7, and 1.8 μg/ml, respectively), and MCF-7 (GI_{50} 2.2, 1.8, 1.3, 0.9, and 1.6 μg/ml, respectively) [46].

These data show that the *E*/*Z* geometry of the Δ^6 double bond and the differences in the prenyl chain have little or no influence on the cytotoxic activity of these compounds. Therefore, it can be presumed that the hydroquinone moiety is responsible for the activity.

Sargaquinone (**181**) isolated from the brown algae *Stypopodium zonale* [176], *Cystoseira jabukae* [177], and *Taonia atomaria* [178] exhibited anti-inflammatory activity (IC_{50} 9.4 μM), evaluated by inhibition of LT formation in leukocytes [178].

From the Phaeophyta *Halidrys siliquosa* were isolated several meroterpenoids with antifouling activity.

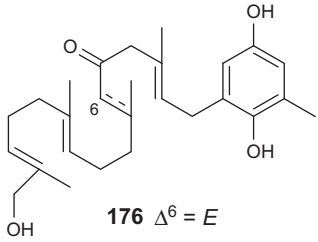

176 $\Delta^6 = E$
177 $\Delta^6 = Z$

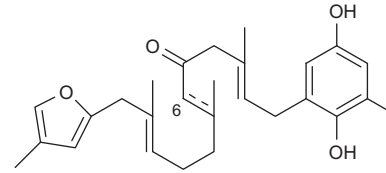

178 $\Delta^6 = E$
179 $\Delta^6 = Z$

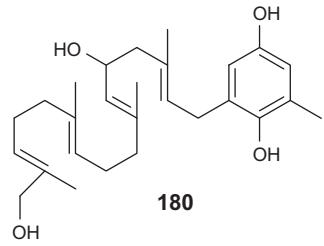

180

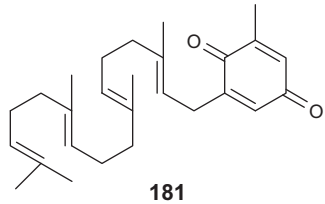

181

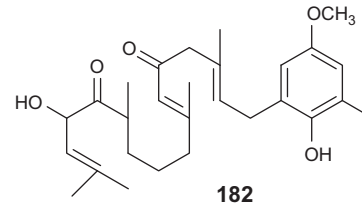

182

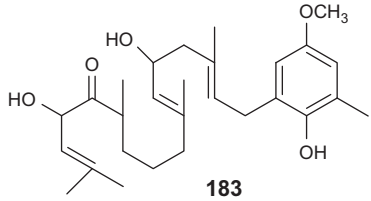

183

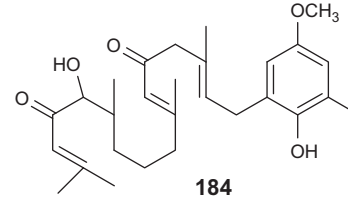

184

The most active compounds were **182–184** that inhibited the growth of four strains of bacteria *Cobetia marina* (MIC 0.5, 1.0, and 2.5 μg/ml, respectively), *Vibrio fischeri* (MIC 0.5, 0.5, and 2.5 μg/ml, respectively), *Marinobacterium stanieri* (MIC 1.0, 1.0, and 1.0 μg/ml, respectively), and *Pseudoalteromonas haloplanktis* (MIC 1.0, 1.0, and 1.0 μg/ml, respectively), and settlement of cyprids of *Balanus amphitrite* (EC_{50} 1.0, 5.0, and 4.0 μg/ml, respectively) [179].

Microbial biofilms and marine fouling organisms, such as barnacles, can cause substantial technical and economic problems on man-made surfaces submerged in seawater. Due to new regulations on toxic antifouling compounds, agents that are effective against biofouling and that are environmentally benign are urgently needed.

Tetraprenyl-toluquinols with the two alkyl groups in the *para* position were isolated from soft corals. From Sodwana Bay (South Africa) *Nephthea* sp. were isolated 2′-tetraprenyl,5′-methyl-hydroquinone (**185**), its 4′-arabinoside, named nephthoside (**186**), and the 4″-acetoxy-nephthoside (**187**), which all showed cytotoxic activity against P-388 cells with an IC_{50} value of 2.0 μg/ml [180].

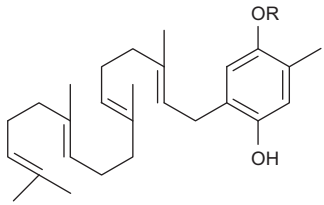

185 R = H
186 R = β-arabinose
187 R = 4-Ac-arabinose

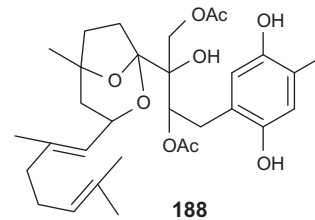

188

Sindurol (**188**), isolated from *Sinularia dura*, showed cytotoxic activity against P-388 cells (IC_{50} 1.2 μg/ml) [180].

Monocyclic Diterpenoids

Bifurcarenone (**189**), with an uncommon monocyclic diterpenoid moiety, was isolated from the brown alga *Bifurcata galapagensis* and inhibited mitotic cell division in the fertilized urchin (*Strongylocentrotus purpuratus*) egg assay (ED_{50} 4.0 μg/ml) [181]. The 4′-metoxy-bifurcarenone (**190**) was isolated from the Mediterranean *Cystoseira amentacea* var. *stricta* and showed less antimitotic activity (ED_{50} 12.0 μg/ml) than that of bifurcarenone, using fertilized eggs of *Paracentrotus lividus* [182].

Jaspaquinol (**191**), isolated from the Papua New Guinea sponges *Jaspis splendens* [183], *Suberea* sp. [184], and *Cacospongia* sp. [185], was a strong inhibitor of the human 15-LO (IC_{50} 0.3 μM) [184], and it showed moderate antimicrobial activity against *Staphylococcus epidermidis* (MIC 5.0 μg/ml) [185].

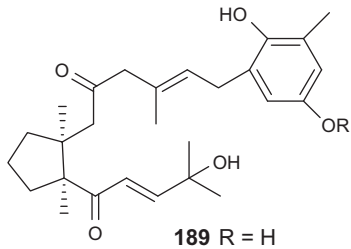

189 R = H
190 R = CH_3

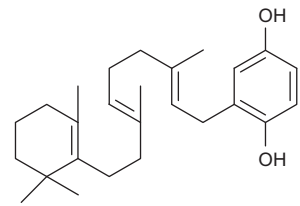

191

Bicyclic Diterpenoids

From the brown alga *S. zonale*, collected off the coast of Lanzarote (Canary Islands, Spain), were isolated stypoquinonic acid (**192**), and atomaric acid (**193**) that inhibited tyrosine kinase ($p56^{lck}$) with IC_{50} values of 79.7 and 92.0 μg/ml, respectively [186].

From the same alga, collected in the Macaronesia Archipelago, was isolated compound **194**, correlated with atomaric acid (**193**), and which showed cytotoxic activity against HT-29 (IC_{50} 2.0 μg/ml), H-116 (IC_{50} 2.5 μg/ml), and A-549 (IC_{50} 2.5 μg/ml) cell lines [187].

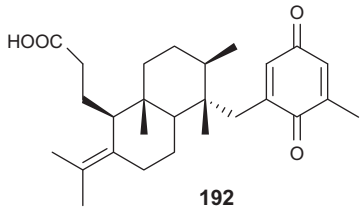

192

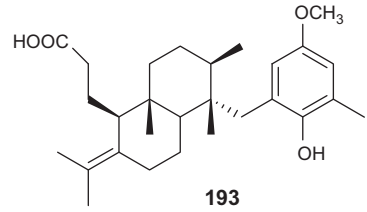

193

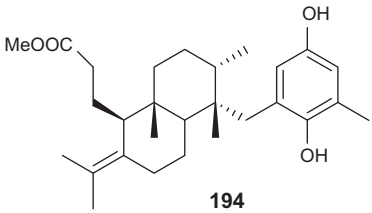

194

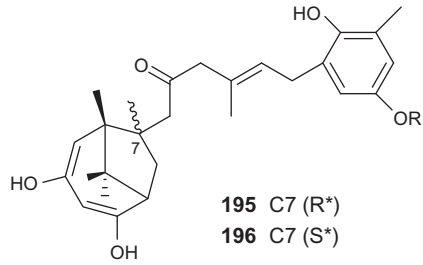

195 C7 (R*)
196 C7 (S*)

The Mediterranean alga *Cystoseira mediterranea* is a rich source of meroditerpenoids with an uncommon bicyclo[4.2.1]nonane ring system. The mixture of mediterraneols A (**195**) and B (**196**) (C-7 epimeres) was the most active, inhibiting mitotic cell division (ED_{50} 2.0 μg/ml) in the *P. lividus* fertilized egg assay [188]. Moreover, the mixture showed antileukemic activity *in vivo*, using the P-388 cell system in NMRI mice (T/C=128% at 32 mg/kg) [189].

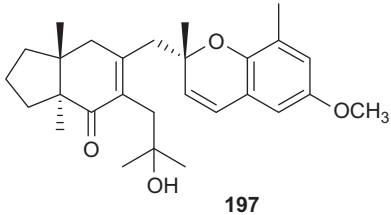

197

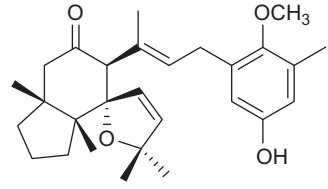

198

From the Atlantic alga *Cystoseira baccata* were isolated several meroditerpenoids that possess a bicyclo[4.3.0]nonane ring system, but only compound **197** showed antifouling activities against growth of the alga *Sargassum muticum* (IC_{50} 2.5 μg/ml) and inhibition of the phenoloxidase (IC_{50} 1.0 μg/ml)

purified from *Mytilus edulis* [190]. Claraenone (**198**), isolated from the brown alga *Cystoseira* sp., showed antitumoral activity against P-388 cells with an IC_{50} value of 5.0 μg/ml [191].

Tricyclic Diterpenoids

Stypoldione (**199**), isolated from the Tropical brown alga *S. zonale*, with a unique spiro-*o*-benzoquinonefuran C_7 unit, showed toxic or strong narcotic effects upon the reef-dwelling herbivorous fish, *Eupomacentrus leucostictus*, at a dose of 1.0 μg/ml, and it probably functions as chemical defence weapon of the alga [176]. Stypoldione (**199**) inhibited the first division of sea urchin (*S. purpuratus*) embryos (IC_{50} 2.5 μM) [192], and it caused modulation of intracellular calcium in rat cerebral granule neurons (CGN), increasing Ca^{2+} influx with an EC_{50} value of 27.8 μM [193]. It was found that stypoldione (**199**) reacts covalently with the sulfhydryl groups of a number of proteins including tubulin and with the sulfhydryl groups of peptides and small molecules. It was suggested that the biological actions of stypoldione (**199**) may be caused by the reaction of this compound with thiol groups of biological molecules [194]. From the alga *Stypopodium flabelliforme* were isolated several meroditerpenoids, but only 2β,3α-epitaondiol (**200**) and stypotriolaldehyde (**201**) showed interesting biological activities [193]. Compound **200** possessed potent sodium channel blocking activity at 0.7 μM, and it was cytotoxic to NCI-H-460 cells with an LC_{50} value of 24.0 μM, while stypotriolaldehyde (**201**) caused a modulation of intracellular calcium in CGN, increasing Ca^{2+} influx with an EC_{50} value of 100 nM [193].

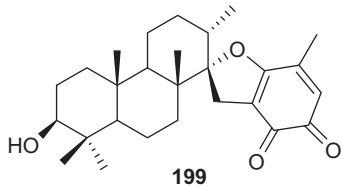

199

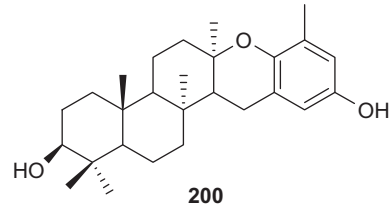

200

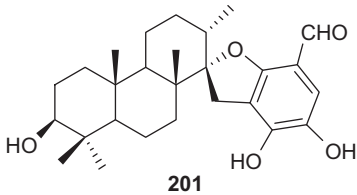

201

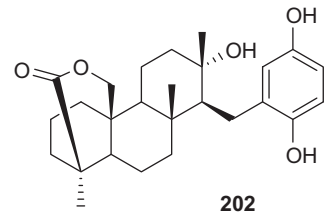

202

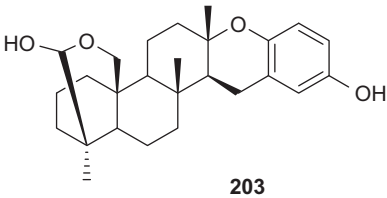

203

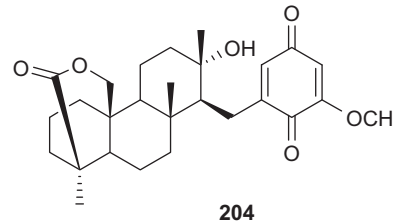

204

Sponges of genus *Strongylophora* are a rich source of meroditerpenoids, named strongylophorines. Only a few interesting bioactivities have been reported for strongylophorines. Strongylophorines 8 (**202**) and 15 (**203**), isolated from *S. strongylata*, showed inhibitory activity on the maturation of starfish (*A. pectinifera*) oocytes with IC_{50} values of 1.1 and 1.2 μM, respectively [195]. From the Papua New Guinea sponge *S. corticata* were isolated the known strongylophorine 8 (**202**) and strongylophorine 26 (**204**), and both compounds inhibited (IC_{50} 7.0 and 1.0 μg/ml, respectively) the invasion of Matrigel by human breast carcinoma MDA-231 cells [196].

The ability of cells to invade adjacent tissues is a biological phenomenon that is crucial for angiogenesis and metastasis. Under the control of angiogenic factors produced by tumor cells, vascular endothelial cells invade solid tumor masses to establish new blood vessels that supply nutrients and oxygen to tumor cells. These newly formed blood vessels can also provide a conduit for metastatic spread, a process that requires the tumor cells themselves to become invasive. Thus, inhibitors of cell invasion may be useful in cancer therapy by preventing both neoangiogenesis and metastasis [197].

From the Philippine sponge *Strongylophora durissima* were isolated strongylophorines 2 (**205**), 3 (**206**), and 8 (**202**) that inhibited (EC_{50} 8.0, 13, and 6.0 μM, respectively) the hypoxia inducible factor-1 (HIF-1) [198].

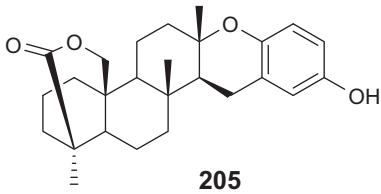

205

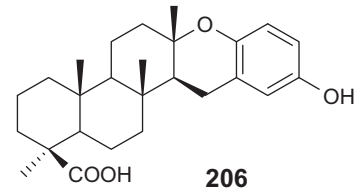

206

A common characteristic of solid tumors is the presence of hypoxic regions (low concentrations of oxygen) that are associated with resistance to both chemotherapy and radiation therapy. Cell survival under hypoxic conditions is mediated in part by the heterodimeric transcriptional factor HIF-1. HIF-1 upregulates expression of genes associated with tumor growth and progression, such as those involved in angiogenesis, glycolysis, and metastasis. The search for inhibitors of the HIF-1 transcriptional pathway has been largely based on accumulating evidence that suggests that selective HIF-1 inhibitors can be developed as molecular-targeted antitumor agents with fewer side effects [199].

Tetracyclic Diterpenoids

Flabellinol (**207**) and flabellinone (**208**) isolated from the brown alga *S. flabelliforme* both possess potent sodium channel blocking activity at 2.0 and 7.0 μM, respectively, and they were cytotoxic to NCI-H-460 cells with LC_{50} values of 9.0 and 14.0 μM, respectively [193].

From the Aegean Sea brown alga *T. atomaria* were isolated two meroditerpenoids, atomarianones A (**209**) and B (**210**), the closest analogues of flabellinone (**208**). Atomarianone A contains an unprecedented *cis* B–C ring fusion, while atomarianone B is the epimer of A at C-7.

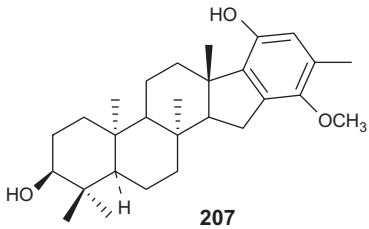

207

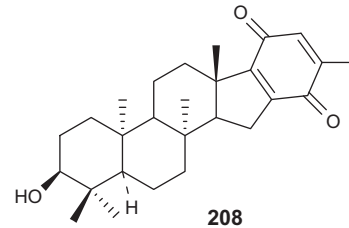

208

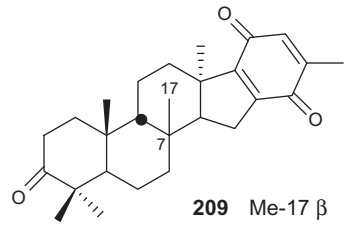

209 Me-17 β
210 Me-17 α

Both compounds exhibited the same significant cytotoxic activity (IC_{50} 7.35 μM) against NSCLC-N6 and A-549 cell lines [200].

SESTERTERPENOIDS GROUP

The sesterterpenes form a rare group of isoprenoids, which occur in widely differing sources and have been isolated from terrestrial fungi, plants, and insects, as well as from marine organisms, mainly from sponges and nudibranches [15]. Marine organisms have provided a large number of sesterterpenoids, possessing novel carbon skeletons, different from those present in terrestrial species, and a wide variety of biological activities. Pentaprenyl quinones/quinols are relatively rare, and those with carbobicyclic and pentacarbocyclic skeletons are dominant.

Bicyclic Sesterterpenoids

Coscinoquinol (**211**) isolated from the Australian sponge *Coscinoderma* sp., with a prenylated labdane skeleton, exhibited cytotoxicity against P-388 (IC_{50} 0.25 μg/ml), A-549 (IC_{50} 0.5 μg/ml), HT-29 (IC_{50} 0.25 μg/ml), and CV-1 (IC_{50} 0.5 μg/ml) cell lines. It showed TOPO II isomerase activity (IC_{50} 0.5 μg/ml) and inhibited dihydrofolate reductase (IC_{50} 2.5 μg/ml) and glutathione reductase (IC_{50} 15.0 μg/ml) [201].

A number of carbobicyclic merosesterterpenoid sulfates were found, including halisulfate 1 (**212**), isolated from *Halichondria* sp. [202]; its antipode coscinosulfate (**213**), isolated from *Coscinoderma mathewsi* [203]; and hipposulfates A (**214**) and B (**215**), isolated from the Okinawan *H. metachromia* [204].

Halisulfate 1 (**212**) was an inhibitor of trypsin (IC_{50} 2.0μg/ml), thrombin (IC_{50} 35.0μg/ml) [205], human 12-LO (IC_{50} 1.0μM), and 15-LO (IC_{50} 0.9μM) [206].

12-LO is involved in the development of psoriasis and controlling cancer cell proliferation, while 15-LO is involved in the development of atherosclerosis and tumorigenesis.

From the sponge *C. mathewsi*, together with halisulfate 1 (**212**), was isolated 1-methylherbipoline salts of halisulfate 1 (**216**), which showed inhibitory activity against trypsin (IC_{50} 25.0μg/ml) [205]. Coscinosulfate (**213**) inhibited Cdc25A phosphatase (IC_{50} 3.0μM) [203].

Cdc25 is a dual specificity family of protein tyrosine phosphatase involved in the regulatory activation of cyclin-dependent kinases (CDKs) by dephosphorylation of a threonine and a tyrosine of the subunit of the CDKs. A family of three analogous genes has been identified in humans Cdc25A, Cdc25B, and Cdc25C. Cdc25A is thought to activate CDK2/cyclin E and thereby trigger the G1/S transition of the cell cycle. Cdc25B appears to play a role in both G1 and G2 phases, while Cdc25C specifically dephosphorylates CDK1/cyclin B, thereby triggering the G2/M transition. Cdc25A and Cdc25B are known to be oncogenic and overexpressed in a number of tumor cell lines. Cdc25 phosphatases constitute attractive screening targets to identify new antimitotic compounds of potential therapeutic interest [207].

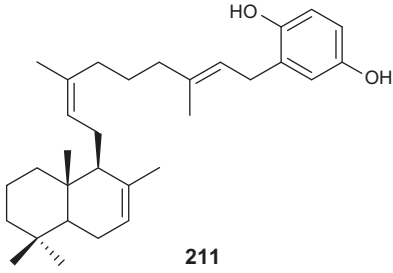

211

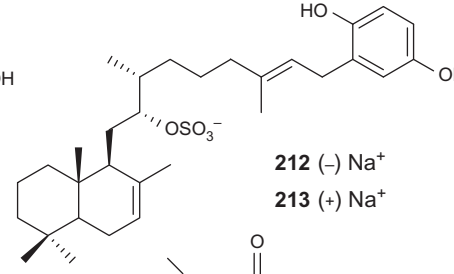

212 (–) Na^+

213 (+) Na^+

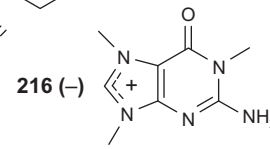

216 (–)

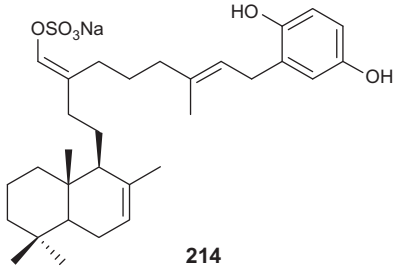

214

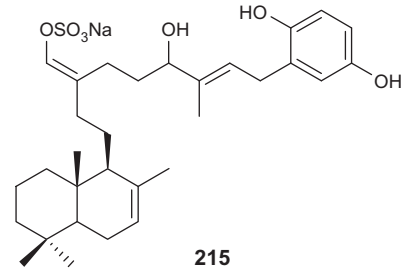

215

Hipposulfate A (**214**) showed cytotoxic activity with an IC_{50} of 2.0 μg/ml against four human tumor cell lines, A-549, P-388, MEL-28, and HT-29 [204].

Pentacyclic Sesterterpenoids

Although numerous marine sesterterpenoids have been found, only a few sesterterpenoids possessing a pentacarbocyclic skeleton have been isolated.

Acanthosulfate (**217**), isolated from the Philippine sponge *Acanthodendrilla* sp., inhibited the proteasome (IC_{50} 4.5 μM), the enzyme responsible for the degradation of endogenous proteins [208].

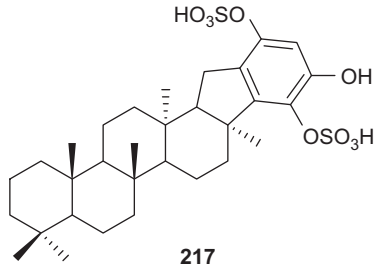

217

TRITERPENOIDS GROUP

Polyprenylated hydroquinones and related secondary metabolites have prevalently been isolated from Demospongiae. Sponges of the order Dictyoceratida are a rich source of linear polyprenylated hydroquinones and related metabolites, while cyclic polyprenylated hydroquinones are isolated from sponges of the order Haplosclerida.

Linear Triterpenoids

2-Hexaprenyl-1,4-hydroquinone (**218**), isolated from *Ircinia spinosula* [209] and *Sarcotragus muscarum* [210], exhibited cytotoxicity against H-4IIE hepatoma cells with an EC_{50} value of 2.5 μM and inhibited the activity of the EGFR (IC_{50} 1.6 μg/ml) [210]. The corresponding chromenol (**219**), isolated from *I. spinosula*, showed anti-inflammatory activity (IC_{50} 1.9 μM), evaluated by inhibition of leukotriene formation in leukocytes [178].

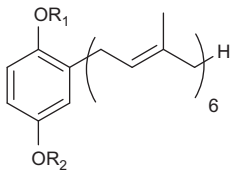

218 $R_1 = R_2 = H$
220 $R_1 = SO_3Na$, $R_2 = H$
221 $R_1 = H$, $R_2 = SO_3Na$

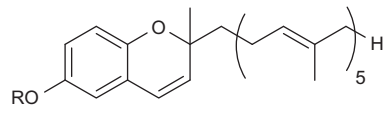

219 R = H
222 $R = SO_3Na$

From the Japanese sponge of genus *Dysidea* was isolated the hexaprenylhydroquinone-1-sodium sulfate (**220**) that inhibited H,K-ATPase (IC_{50} 4.6μM) and PLA_2 (IC_{50} 1.8μM) [211]. Sarcohydroquinone sulfate A (**221**), an isomer of **220**, and sarcochromenol sulfate A (**222**) were isolated from the New Zealand sponge *Sarcotragus spinulosus*. Both compounds inhibited Na^+,K^+-ATPase with an IC_{50} value of 1.6μM [212].

Bicyclic Triterpenoids

The Red Sea sponge *Toxiclona toxius* is a rich source of metabolites with an uncommon hexaprenoid skeleton condensed with a sulfated hydroquinone. Shaagrockol B (**223**) showed antifungal activity against *C. albicans* (IC_{50} 6.0μg/ml) [213] and inhibited HIV-1 RT-RDDP (IC_{50} 8.5μM) and RT-DDDP (IC_{50} 6.7μM) [214].

From the Palauan sponge *Haliclona* sp. were isolated several hexaprenoid hydroquinone sulfates that inhibited the transport of stabilized microtubules by the motor protein kinesin. Adociasulfate 3 (**224**) showed inhibition of ATPase activity in kinesin with an IC_{50} value of 10mM [215].

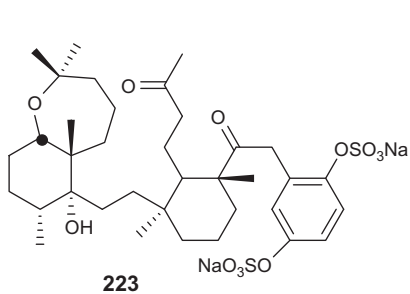

223

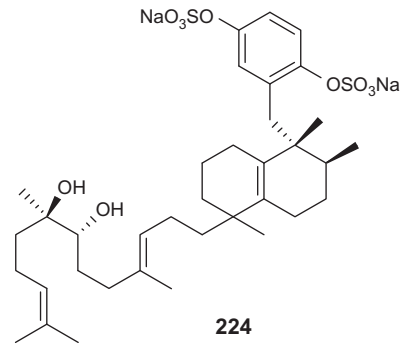

224

Utilizing the energy of ATP hydrolysis, the kinesin superfamily of motor proteins is responsible for movement of cellular cargo along the periphery (anterograde transport). These proteins are important targets for inhibition because they are involved in many dynamic microtubule-mediated events, including cell division and transport of vesicles and organelles [216].

Tricyclic Triterpenoids

Shaagrockol C (**225**), isolated from *T. toxius*, showed antifungal activity against *C. albicans* (IC_{50} 6.0μg/ml) [213] and inhibited HIV-1 RT-RDDP (IC_{50} 3.3μM) and RT-DDDP (IC_{50} 0.8μM) [214].

Adociasulfate 4 (**226**), isolated from the sponge *Haliclona* sp., showed inhibition of ATPase activity in kinesin with an IC_{50} value of 15 mM [215].

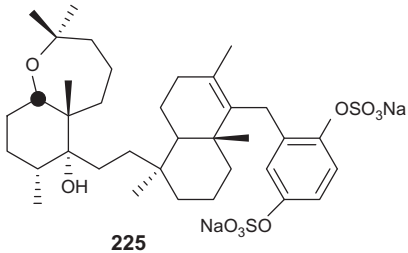

225

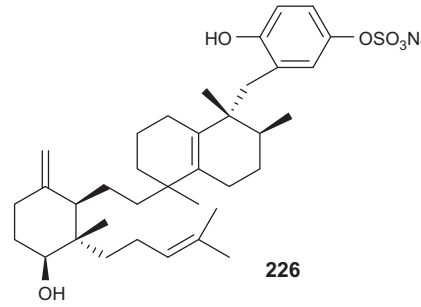

226

Tetracyclic Triterpenoids

Toxiusol (**227**), isolated from *T. toxius*, inhibited various viral reverse transcriptases including HIV-1 RNA-dependent (IC_{50} 1.5 μM) and DNA-dependent (IC_{50} 6.6 μM) [214] murine leukemia virus (MuLV) (IC_{50} 0.76 μM) and equine infectious anemia virus (EIAV) (IC_{50} 1.8 μM) [217]. Toxiusol (**227**) is a noncompetitive inhibitor and binds the enzyme irreversibly. It blocks the first step of DNA polymerization, that is, the formation of the HIV-1 RT-DNA complex [217].

From the Japanese sponge of the genus *Callyspongia* was isolated akaterpin (**228**), an isomer of toxiusol, which inhibited phosphatidylinositol-specific phospholipase C (PI-PLC) with an IC_{50} value of 0.5 μg/ml [218].

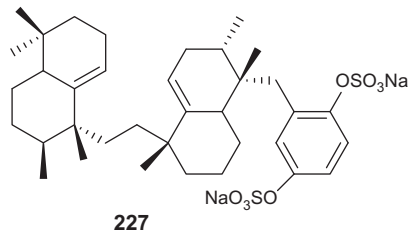

227

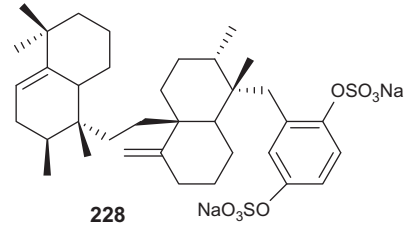

228

PI-PLC hydrolyzes PIP2 into diacylglycerol and inositol-1,4,5-triphosphate. It is considered to be the rate-limiting enzyme of PI turnover; therefore selective inhibitors of PI-PLC are useful as tools for the investigation of signal transduction [219].

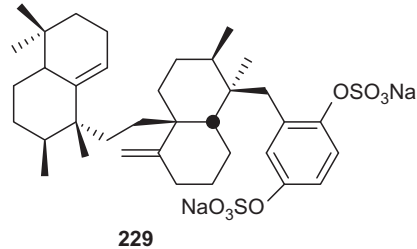

229

Additional sulfated merohexaprenoids were isolated from the Brazilian *Callyspongia* sp., including isoakaterpin (**229**) that inhibited *Leishmania* adenosine phosphoribosyl transferase with an IC_{50} value of 1.05 μM [220].

Pentacyclic Triterpenoids

Toxicols A (**230**) and B (**231**), isolated from *T. toxius*, inhibited HIV-1 RT-RDDP (IC_{50} 3.1 and 3.7 μM, respectively) and RT-DDDP (IC_{50} 2.7 and 8.2 μM, respectively) [214].

Adociasulfates 1 (**232**), 2 (**233**), 5 (**234**), and 6 (**235**), isolated from the Palauan sponge *Haliclona* sp., showed inhibition of ATPase activity in kinesin with IC_{50} values of 12.5, 6.0, 8.0, and 6.0 mM, respectively [215]. Moreover, adociasulfate 1 (**232**) inhibited proton pumping in hen bone-derived membrane (IC_{50} 3.6 μM) and in brain-derived (IC_{50} 4.69 μM) vesicles [221], and adociasulfate 2 (**233**) inhibited the micro-tubule-stimulated kinesin ATPase with an IC_{50} value of 2.7 μM [222].

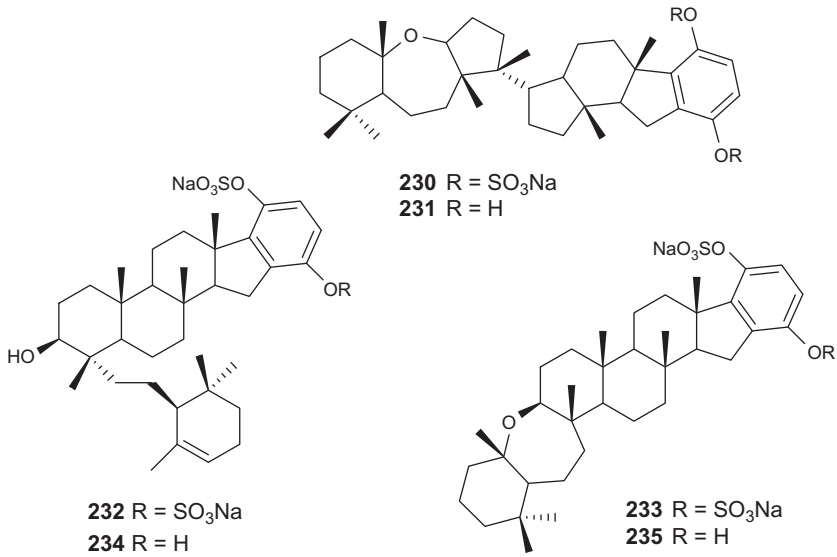

230 R = SO_3Na
231 R = H

232 R = SO_3Na
234 R = H

233 R = SO_3Na
235 R = H

HEPTAPRENYLS GROUP

Polyprenylated hydroquinones and related secondary metabolites with seven or more isoprene units are generally isolated from sponges of class Demospongiae and they have a linear prenyl chain.

2-Heptaprenyl-1,4-hydroquinone (**236**), isolated from the Adriatic Sea sponges *I. spinosula* [223], *S. muscarum*, and *I. fasciculata* [210], inhibited the activity of several protein kinases, including EGFR (IC_{50} 1.4 μg/ml), SRC tyrosine kinase (IC_{50} 3.7 μg/ml), VEGFR-R3 (IC_{50} 8.9 μg/ml), and IGF1-R (IC_{50} 7.4 μg/ml) [210], and it showed toxicity (LC_{50} 0.91 ppm) in

the *Artemia salina* shrimp lethality assay [223]. The corresponding chromenol (**237**), isolated from *I. spinosula*, showed anti-inflammatory activity (IC_{50} 7.5 μM), such as inhibition of leukotriene formation in leukocytes [178].

Sarcohydroquinone sulfate B (**238**), a disulfate heptaprenyl hydroquinone, isolated from the New Zealand sponge *S. spinulosus*, inhibited Na^+,K^+-ATPase with an IC_{50} value of 1.4 μM [212].

2-Heptaprenyl hydroquinone, 4-sodium sulfate (**239**), isolated from *I. spinosula*, showed strong toxicity (LC_{50} 0.02 ppm) in the *A. salina* shrimp lethality assay [223].

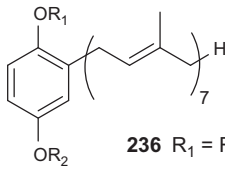

236 $R_1 = R_2 = H$
238 $R_1 = R_2 = SO_3Na$
239 $R_1 = H$, $R_2 = SO_3Na$

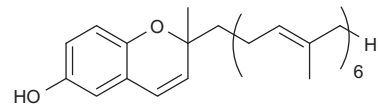

237

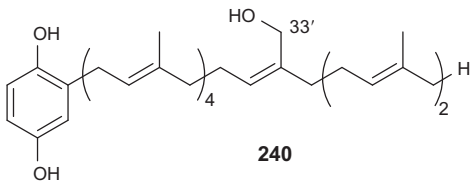

240

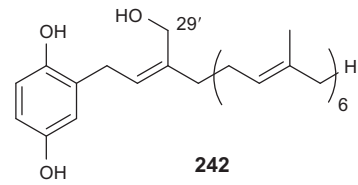

242

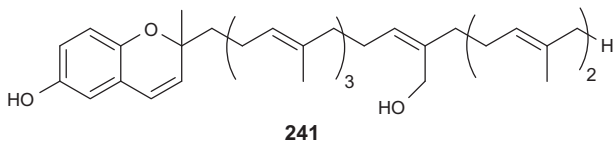

241

Two hydroxylated derivatives of heptaprenyl hydroquinone were isolated from *I. spinosula*, the 2-[33′-hydroxy]heptaprenyl-1,4-hydroquinone (**240**) and the corresponding chromenol (**241**), and showed anti-inflammatory activity (IC_{50} 6.0 and 13.6 μM, respectively), such as inhibition of leukotriene formation in leukocytes [178].

From the deep water sponge *Ircinia* sp. were isolated several polyprenylated hydroquinones and related metabolites, including 2-[29′-hydroxy]heptaprenyl-1,4-hydroquinone (**242**), an isomer of compound **240**, which inhibited tyrosine protein kinase (TPK) (IC_{50} 5.9 μg/ml) [224].

OCTAPRENYLS GROUP

2-Octaprenyl-1,4-hydroquinone (**243**), isolated from the Adriatic Sea sponge *I. spinosula* [223], showed anti-inflammatory activity inhibiting human

synovial PLA_2 in a concentration-dependent manner with an IC_{50} value of 48.7 μM, thromboxane B_2 synthesis and release (IC_{50} 3.9 μM), and A23187-stimulated LT-B_4 production in human neutrophils (IC_{50} 23.1 μM) [225]. Further, it showed toxicity (LC_{50} 0.98 ppm) in the *A. salina* shrimp lethality assay [223].

From the Australian sponge of genus *Sarcotragus* was isolated the octaprenyl-hydroquinone-1-sodium sulfate (**244**) that inhibited α-1,3-fucosyltransferase TVII (Fuc TVII) (IC_{50} 3.9 μg/ml), an enzyme involved in the inflammatory process [226].

Sarcohydroquinone sulfate C (**245**), isolated from the New Zealand sponge *S. spinulosus* [212] and from the Adriatic Sea *I. spinosula* [223], inhibited Na^+,K^+-ATPase with an IC_{50} value of 1.3 μM [212] and showed strong toxicity (LC_{50} 0.04 ppm) in the *A. salina* assay [223]. From the Adriatic Sea *I. spinosula* was also isolated the 37′-hydroxy-2-octaprenyl-hydroquinone (**246**) and its 4-sodium sulfate (**247**) that showed strong toxicity (LC_{50} 0.05, 0.35 ppm, respectively) in the *A. salina* assay [223].

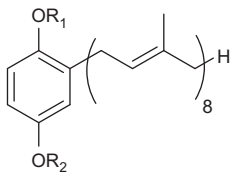

243 $R_1 = R_2 = H$
244 $R_1 = SO_3Na$, $R_2 = H$
245 $R_1 = H$, $R_2 = SO_3Na$

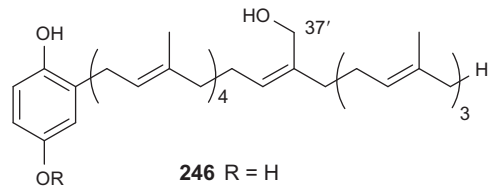

246 R = H
247 R = SO_3Na

Compound **246** showed anti-inflammatory activity inhibiting human synovial PLA_2 in a concentration-dependent manner with an IC_{50} value of 48.0 μM, thromboxane B_2 synthesis and release (IC_{50} 3.4 μM), and A23187-stimulated LT-B_4 production in human neutrophils (IC_{50} 7.4 μM) [225]. The sulfated derivative **247** inhibited the cell cycle regulating phosphatase Cdc25A with an IC_{50} value of 4.0 μM [227].

The Cdc25 phosphatases regulate the cell division cycle by controlling the activity of CDK. Abnormalities in protein phosphorylation are observed essentially in human pathologies, consequently leading to the increasing use of protein kinases and, to a lesser extent, protein phosphatases, as pharmacological targets [228].

NONAPRENYLS GROUP

There are few reports on nonaprenyl quinones/quinols isolated from marine organisms, and to our knowledge, only one paper reports the biological activity for this class of compounds.

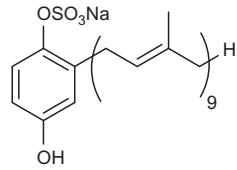

248

From the Australian sponge of genus *Sarcotragus* was isolated the nonaprenyl-hydroquinone-1-sodium sulfate (**248**) that inhibited Fuc TVII with an IC_{50} value of 2.4 μg/ml [226].

ABBREVIATIONS

AChE	Acetylcholinesterase
CDK4	Cyclin-dependent kinase 4
CDKs	Cyclin dependent kinases
CETP	Cholesteryl ester transfer protein
CGN	Cerebral granule neurons
COX	Cyclooxygenase
DPPH	α,α-Diphenyl-β-picrylhydrazyl
EGFR	Epidermal growth factor receptor
fMLP	*N*-formyl-methionyl-leucyl-phenylalanine
HDL	High-density lipoprotein
HIF-1	Hypoxia inducible factor-1
HIV	Human immunodeficiency virus
hPTP1B	Protein tyrosine phosphatase 1B
IGF1R	Insulin-like growth-factor 1 receptor
IL-1β	Interleukin-1β
IL-2	Interleukin-2
IL-8	Interleukin-8
IM	Immunomodulatory
LDL	Low-density lipoprotein
LO	Lipoxygenase
LT-B4	Leukotriene B4
MIC	Minimum inhibitory concentration
MLC	Mixed lymphocyte culture
NF-κB	Nuclear factor-κB
NSAID	Nonsteroidal, anti-inflammatory drugs
PFTase	Protein farnesyl transferase
PI-PLC	Phosphatidylinositol-specific phospholipase C
PLA_2	Phospholipase A_2
PMA	Phorbol myristate acetate
RT	Reverse transcriptase

RTKs	Receptor tyrosine kinases
TBARS	Thiobarbituric acid
TNF-α	Tumour factor-α
TPA	Tetradecanoyl-phorbol acetate
VEGFR1-3	Vascular endothelial growth factor receptors

REFERENCES

[1] A.F. Brodie, B. Revsin, V. Kalra, P. Phillips, E. Bogin, T. Higashi, C.R. Krishna Murti, B. Z. Cavari, E. Marquez, T.W. Goodwin (Ed.), Natural Substance Formed Biologically from Mevalonic Acid, Academic Press, London and NewYork, 1970, pp. 119–143.

[2] R.H. Thomson, Naturally Occurring Quinones, Academic Press, London and, New York, 1971, pp. 1–38.

[3] R.H. Thomson, Naturally Occurring Quinones III: Recent Advances, Chapman and Hall, London and, New York, 1987.

[4] T. Higa, P.J. Scheuer (Ed.), Marine Natural Products, Academic Press, New York and London, 1981, pp. 93–145, vol. 1V.

[5] S. De Rosa, A. De Giulio, C. Iodice, J. Nat. Prod. 57 (1994) 1711–1716.

[6] R.J. Capon, Atta Ur Rahman (Ed.), Studies in Natural Products Chemistry, Elsevier Science B.V., Amsterdam, 1995, pp. 289–326 vol. 15.

[7] I.S. Marcos, A. Conde, R.F. Moro, P. Basabe, D. Diez, J.G. Urones, Mini. Rev. Org. Chem. 7 (2010) 230–254.

[8] R.H. Thomson, Naturally Occurring Quinones VI: Recent Advances, Blackie Academic and Professional, London and, New York, 1997.

[9] T. Higa, P.J. Scheuer (Ed.), Bioorganic Marine Chemistry, Springer-Verlag, Berlin, Heidelberg, 1991, pp. 33–90, vol. 1V.

[10] D.J. Faulkner, Nat. Prod. Rep. 19 (2002) 1–48 and earlier review in the series.

[11] J.W. Blunt, B.R. Copp, M.H.G. Munro, P.T. Northcote, M.R. Prinsep, Nat. Prod. Rep. 27 (2010) 165–237 and earlier review in the series.

[12] L. Minale, P.J. Scheuer (Ed.), Marine Natural Products, Academic Press, New York and London, 1978, pp. 175–240, vol. 1.

[13] D.J. Faulkner, Tetrahedron 33 (1977) 1421–1443.

[14] S. De Rosa, A.P. Rauter, F.B. Palma, J. Justino, M.E. Araújo, S.P. dos Santos (Eds.), Natural Products in the New Millennium: Prospects and Industrial Application, Kluwer Academic Publishers, Dordrecht, 2002, pp. 441–461.

[15] S. De Rosa, M. Mitova, Atta Ur Rahman (Ed.), Studies in Natural Products Chemistry, Elsevier Science B.V., Amsterdam, 2005, pp. 109–168, vol. 32.

[16] L. Minale, Pure Appl. Chem. 48 (1976) 7–23.

[17] J.T. Baker, Pure Appl. Chem. 48 (1976) 35–44.

[18] D. Sladić, M.J. Gašić, Molecules 11 (2006) 1–33.

[19] M. Gordaliza, Mar. Drugs 8 (2010) 2849–2870.

[20] B.M. Howard, K. Clarkson, R.L. Bernstein, Tetrahedron Lett. (1979) 4449–4452.

[21] D.R. Appleton, C.S. Chuen, M.V. Berridge, V.L. Webb, B.R. Copp, J. Org. Chem. 74 (2009) 9195–9198.

[22] C.E. Sansom, L. Larsen, N.B. Perry, M.V. Berridge, E.W. Chia, J.L. Harper, V.L. Webb, J. Nat. Prod. 70 (2007) 2042–2044.

[23] B.C.M. Potts, D.J. Faulkner, R.S. Jacobs, J. Nat. Prod. 55 (1992) 1701–1717.
[24] W. Fenical, H.H. Weber, C.D. Ruggieri (Eds.), Proceedings of the 4th Food-Drugs from the Sea, Marine Technology Society, Washington, DC, USA, 1976, pp. 388–394.
[25] A. Sato, T. Shindo, N. Kasanuki, K. Hasegawa, J. Nat. Prod. 52 (1989) 975–981.
[26] M. Aknin, T.L.-A. Dayan, A. Rudi, Y. Kashman, E.M. Gaydou, J. Agric. Food Chem. 47 (1999) 4175–4177.
[27] A. Rueda, E. Zubia, M.J. Ortega, J. Salva, Nat. Prod. Lett. 11 (1998) 127–130.
[28] L. Garrido, E. Zubía, M.J. Ortega, J. Salvá, J. Nat. Prod. 65 (2002) 1328–1331.
[29] A. Simon-Levert, A. Arrault, N. Bontemps-Subielos, C. Canal, B. Banaigs, J. Nat. Prod. 68 (2005) 1412–1415.
[30] W.R. Markesbery, Free Radic. Biol. Med. 23 (1997) 134–147.
[31] L.K. Shubina, S.N. Fedorov, O.S. Radchenko, N.N. Balaneva, S.A. Kolesnikova, P. S. Dmitrenok, A. Bode, Z. Dong, V.A. Stonik, Tetrahedron Lett. 46 (2005) 559–562.
[32] S.N. Fedorov, O.S. Radchenko, L.K. Shubina, N.N. Balaneva, I.G. Agafonova, A. Bode, J.-O. Jin, J.-Y. Kwak, Z. Dong, V.A. Stonik, Anticancer Res. 28 (2008) 927–932.
[33] H.E. Högberg, R.H. Thomson, T.J. King, J. Chem. Soc. Perkin Trans. 1 (1976) 1696–1701.
[34] N.M. Targett, O.J. McConnell, J. Chem. Ecol. 8 (1982) 115–124.
[35] O.J. McConnell, P.A. Hughes, N.M. Targett, J. Daley, J. Chem. Ecol. 8 (1982) 1437–1453.
[36] M.E. Hay, W. Fenical, K. Gustafson, Ecology 68 (1987) 1581–1591.
[37] A. Aiello, E. Fattorusso, P. Luciano, A. Macho, M. Menna, E. Muñoz, J. Med. Chem. 48 (2005) 3410–3416.
[38] M.E. Wall, M.C. Wani, G. Manikumar, H. Taylor, T.J. Huges, K. Gaetano, W.H. Gerwick, A.T. McPhail, D.R. McPhail, J. Nat. Prod. 52 (1989) 1092–1099.
[39] M. Park, W. Fenical, M.E. Hay, Phytochemistry 31 (1992) 4115–4118.
[40] A.R. Carroll, B.F. Bowden, J.C. Coll, Aust. J. Chem. 46 (1993) 1079–1083.
[41] M. Ochi, H. Kotsuki, S. Inoue, M. Taniguchi, T. Tokoroyama, Chem. Lett. (1979) 831–832.
[42] V. Tiberio, Annali di Igiene Sperimentale 5 (1895) 91–103.
[43] A. Fleming, Br. J. Exp. Pathol. 10 (1929) 226–236.
[44] M.N. Dave, T. Kusumi, M. Ishitsuka, T. Iwashita, H. Kakisawa, Heterocycles 22 (1984) 2301–2307.
[45] B.W. Son, J.C. Kim, H.D. Choi, J.S. Kang, Arch. Pharm. Res. 25 (2002) 77–79.
[46] K.M. Fisch, V. Böhm, A.D. Wright, G.M. König, J. Nat. Prod. 66 (2003) 968–975.
[47] K.H. Jang, B.H. Lee, B.W. Choi, H.-S. Lee, J. Shin, J. Nat. Prod. 68 (2005) 716–723.
[48] N. Fusetani, K. Yasukawa, S. Matsunaga, K. Hashimoto, Tetrahedron Lett. 26 (1985) 6449–6452.
[49] J. Shin, Y. Seo, K.W. Cho, S.S. Moon, Y.I. Cho, J. Org. Chem. 64 (1999) 1853–1858.
[50] G.J. Hooper, M.T. Davies-Coleman, Tetrahedron Lett. 36 (1995) 3265–3268.
[51] G. Cimino, S. De Stefano, L. Minale, Tetrahedron 29 (1973) 2565–2570.
[52] A. Casapullo, L. Minale, F. Zollo, J. Nat. Prod. 56 (1993) 527–533.
[53] E. Zubia, M.J. Ortega, J.L. Carballo, J. Salva, Tetrahedron 50 (1994) 8153–8160.
[54] G. Cimino, S. De Stefano, L. Minale, Experientia 29 (1973) 1063.
[55] J. Ishibashi, Y. Ohizumi, J.-F. Cheng, H. Nakamura, Y. Hirata, T. Sasaki, J. Kobayashi, J. Org. Chem. 53 (1988) 2855–2858.
[56] J. Kobayashi, T. Murayama, Y. Ohizumi, T. Ohta, S. Nozoe, T. Sasaki, J. Nat. Prod. 52 (1989) 1173–1176.
[57] J. Kobayashi, K. Naitoh, T. Sasaki, H. Shigemori, J. Org. Chem. 57 (1992) 5773–5776.
[58] Y.-C. Shen, C.-Y. Chen, Y.-H. Kuo, J. Nat. Prod. 64 (2001) 801–803.
[59] Y. Takahashi, M. Tsuda, J. Fromont, J. Kobayashi, Heterocycles 67 (2006) 791–796.

[60] Y. Takahashi, T. Kubota, J. Fromont, J. Kobayashi, Tetrahedron 63 (2007) 8770–8773.
[61] Y. Takahashi, M. Yamada, T. Kubota, J. Fromont, J. Kobayashi, Chem. Pharm. Bull. 55 (2007) 1731–1733.
[62] O.J. McConnell, R. Longley, M. Gunasekera, Experientia 48 (1992) 891–892.
[63] W. Fenical, J.J. Sims, D. Squatrito, R.M. Wing, P. Radlick, J. Org. Chem. 38 (1973) 2383–2386.
[64] M. Ochi, H. Kotsuki, K. Muraoka, T. Tokoroyama, Bull. Chem. Soc. Jpn. 52 (1979) 629–630.
[65] T. Laube, W. Beil, K. Seifert, Tetrahedron 61 (2005) 1141–1148.
[66] E. Pèrez-Garcìa, E. Zubía, M.J. Ortega, J.L. Carballo, J. Nat. Prod. 68 (2005) 653–658.
[67] C.E. McNamara, L. Larsen, N.B. Perry, J.L. Harper, M.V. Berridge, E.W. Chia, M. Kelly, V.L. Webb, J. Nat. Prod. 68 (2005) 1431–1433.
[68] G. Cimino, S. De Stefano, L. Minale, Experientia 31 (1975) 1117–1118.
[69] A.F. Barrero, E.J. Alvarez-Manzanella, M.M. Herrador, R. Chahboun, P. Galera, Bioorg. Med. Chem. Lett. 9 (1999) 2325–2328.
[70] B. Sullivan, P. Djura, D.E. McIntyre, D.J. Faulkner, Tetrahedron 37 (1981) 979–982.
[71] B. Sullivan, D.J. Faulkner, G.K. Matsumoto, H. Cun-heng, J. Clardy, J. Org. Chem. 51 (1986) 4568–4573.
[72] V.J.R.V. Mukku, R.A. Edrada, F.J. Schmitz, M.K. Shanks, B. Chaudhuri, D. Fabbro, J. Nat. Prod. 66 (2003) 686–689.
[73] K.B. Killday, A.E. Wright, R.H. Jackson, M.A. Sills, J. Nat. Prod. 58 (1995) 958–960.
[74] A. Grube, M. Assmann, E. Lichte, F. Sasse, J.R. Pawlik, M. Köck, J. Nat. Prod. 70 (2007) 504–509.
[75] U. Bickmeyer, A. Grube, K.-W. Klings, J.R. Pawlik, M. Köck, Mar. Biotechnol. 12 (2010) 267–272.
[76] J.A. Chan, A.J. Fryer, B.K. Cartè, M.E. Hemling, G.A. Hofmann, M.R. Mattern, M. A. Mentzer, J.W. Westley, J. Nat. Prod. 57 (1994) 1543–1548.
[77] L. Chen, D.H. Li, S.X. Cai, F.P. Wang, X. Xiao, Q.Q. Gu, Acta Pharmaceutica Sin. 45 (2010) 1275–1278.
[78] S.J. Coval, M.A. Conover, R. Mierzwa, A. King, M.S. Puar, D.W. Phife, J.K. Pai, R. E. Burrier, H.S. Ahn, G.C. Boykow, M. Patel, S.A. Pomponi, Bioorg. Med. Chem. Lett. 5 (1995) 605–610.
[79] T. Laube, A. Bernet, H.-M. Dahse, I.D. Jacobsen, K. Seifert, Bioorg. Med. Chem. 17 (2009) 1422–1427.
[80] J. Wang, H. Qiang, D. Chen, C. Zhang, Y. Zhuang, Clin. Chim. Acta 322 (2002) 85–90.
[81] R. Talpir, A. Rudi, Y. Kashman, Y. Loya, A. Hizi, Tetrahedron 50 (1994) 4179–4184.
[82] K.W.L. Yong, A. Jankam, J.N.A. Hooper, A. Suksamrarn, M.J. Garson, Tetrahedron 64 (2008) 6341–6348.
[83] R.J. Capon, D.R. Groves, S. Urban, R.G. Watson, Aust. J. Chem. 46 (1993) 1245–1253.
[84] R. Kazlauskas, P.T. Murphy, R.G. Warren, R.J. Wells, J.F. Blount, Aust. J. Chem. 31 (1978) 2685–2697.
[85] A. Jankam, M.J. Somerville, J.N.A. Hooper, D.J. Brecknell, A. Suksamrarn, M.J. Garson, Tetrahedron 63 (2007) 1577–1582.
[86] S. Loya, M. Bakhanashvili, Y. Kashman, A. Hizi, Arch. Biochem. Biophys. 316 (1995) 789–796.
[87] E. De Clercq, AIDS Res. Hum. Retroviruses 8 (1992) 119–134.
[88] B.N. Ravi, H.P. Perzanowski, R.A. Ross, T.R. Erdman, P.J. Scheuer, J. Finer, J. Clardy, Pure Appl. Chem. 51 (1979) 1893–1900.

[89] S. Kohmoto, O.J. McConnell, A. Wright, F. Koehn, W. Thompson, M. Lui, K.M. Snader, J. Nat. Prod. 50 (1987) 336.
[90] M.T. Hamann, P.J. Scheuer, M. Kelly-Borges, J. Org. Chem. 58 (1993) 6565–6569.
[91] S.S. Nasu, B.K.S. Yeung, M.T. Hamann, P.J. Scheuer, M. Kelly-Borges, K. Goins, J. Org. Chem. 60 (1995) 7290–7292.
[92] M.L. Bourget-Kondracki, F. Lacombe, M. Guyot, J. Nat. Prod. 62 (1999) 1304–1305.
[93] K.A. El Sayed, P. Bartyzel, X. Shen, T.L. Perry, J.K. Zjawiony, M.T. Hamann, Tetrahedron 56 (2000) 949–953.
[94] A.M. Popov, S.I. Stekhova, N.K. Utkina, N.M. Rebachuk, Pharm. Chem. J. 33 (1999) 71–73.
[95] M.L. Bourget-Kondracki, C. Debitus, M. Guyot, Tetrahedron Lett. 37 (1996) 3861–3864.
[96] P. Djura, D.B. Stierle, B. Sullivan, D.J. Faulkner, E. Arnold, J. Clardy, J. Org. Chem. 45 (1980) 1435–1441.
[97] R.E. Longley, O.J. McConnell, E. Essich, D. Harmody, J. Nat. Prod. 56 (1993) 915–920.
[98] D. Tasdemir, T.S. Bugni, G.C. Mangalindan, G.P. Concepcion, M.K. Harper, C.M. Ireland, Z. Naturforsch. 57c (2002) 914–922.
[99] A.E. Wright, S.S. Cross, N.S. Burres, F. Koehn, PCT WO 9112250 A1, Harbor Branch Oceanographics Institution, Inc., USA, August 22, 1991..
[100] J.-F. Hu, J.A. Schetz, M. Kelly, J.-N. Peng, K.K.H. Ang, H. Flotow, C.Y. Leong, S.B. Ng, A.D. Buss, S.P. Wilkins, M.T. Hamann, J. Nat. Prod. 65 (2002) 476–480.
[101] J.C. Swersey, L.R. Barrow, C.M. Ireland, Tetrahedron Lett. 32 (1991) 6687–6690.
[102] A.E. Wright, S.A. Rueth, S.A. Cross, J. Nat. Prod. 54 (1991) 1108–1111.
[103] L. Minale, R. Riccio, G. Sodano, Tetrahedron Lett. 15 (1974) 3401–3404.
[104] S. De Rosa, L. Minale, R. Riccio, G. Sodano, J. Chem. Soc. Perkin Trans. I (1994) 1408–1414.
[105] A.S. Sarma, P. Chattopadhyay, J. Org. Chem. 47 (1982) 1727–1731.
[106] G. Seibert, W. Raether, N. Dogović, M.J. Gasić, R.K. Zahn, W.E. Müller, Zbl. Bakt. Hyg. 260A (1985) 379–386.
[107] W.E. Müller, A. Maidhof, R.K. Zahn, H.C. Schröder, M.J. Gasić, D. Heidemann, A. Bernd, B. Kurulec, E. Eich, G. Seibert, Cancer Res. 45 (1985) 4822–4826.
[108] A. De Giulio, S. De Rosa, G. Stazzullo, L. Diliberto, P. Obino, M.E. Marongiu, A. Pani, P. La Colla, Antivir. Chem. Chemother. 2 (1991) 223–227.
[109] B. Kurelec, R.K. Zahn, M.J. Gasić, S. Britvić, D. Lucić, W.E.G. Müller, Mutat. Res. 144 (1985) 63–66.
[110] P.S. Sarin, D. Sun, A. Thornton, W.E.G. Müller, J. Natl. Cancer Inst. 78 (1987) 663–666.
[111] W.E. Müller, P.S. Sarin, Y. Kuchino, A. Dorn, G. Hess, K.H. Meyer zum Büschenfelde, M. Rottmann, H.C. Schröder, W. Vettermann, M. Schauzu (Eds.), AIDS, Bundesministerium für Forschung und Technologie, Bonn, 1987, pp. 354–378.
[112] M.L. Ferrándiz, M.J. Sanz, G. Bustos, M. Payá, M.J. Alcaraz, S. De Rosa, Eur. J. Pharmacol. 253 (1994) 75–82.
[113] B. Pejin, C. Iodice, G. Tommonaro, S. De Rosa, J. Nat. Prod. 71 (2008) 1850–1853.
[114] M.A. Belisario, M. Maturo, R. Pecce, S. De Rosa, G.R. Villani, Toxicology 72 (1992) 221–233.
[115] M.A. Belisario, M. Maturo, G. Avagnale, S. De Rosa, F. Scopacasa, M. De Caterina, Pharmacol. Toxicol. 79 (1996) 300–304.
[116] M. Amigó, M. Payá, A. Braza-Boïls, S. De Rosa, M.C. Terencio, Life Sci. 82 (2008) 256–264.
[117] P.F. Lizzul, A. Aphale, R. Malaviya, Y. Sun, S. Masud, V. Dombrovskiy, A.B. Gottlieb, J. Invest. Dermatol. 124 (2005) 1275–1283.

[118] A.I. Bayliffe, R.A. Brigandi, H.J. Wilkins, M.P. Levick, Curr. Opin. Pharmacol. 4 (2004) 306–310.
[119] T. Banno, A. Gazel, M. Blumenberg, J. Biol. Chem. 280 (2005) 18973–18980.
[120] S. De Rosa, A. De Giulio, G. Strazzullo, Trends Org. Chem. 2 (1991) 127–141.
[121] M.J. Gasić, J. Serb. Chem. Soc. 53 (1988) 229–249.
[122] M.A. Belisario, R. Pecce, M. Maturo, S. De Rosa, Toxicology 86 (1994) 89–108.
[123] M. Amigó, M.C. Terencio, M. Mitova, C. Iodice, M. Payá, S. De Rosa, J. Nat. Prod. 67 (2004) 1459–1463.
[124] M. Amigó, M. Payá, S. De Rosa, M.C. Terencio, Br. J. Pharmacol. 152 (2007) 353–365.
[125] L.J. Scott, K.L. Goa, Drugs 60 (2000) 1095–1122.
[126] T. Božić, I. Novaković, M.J. Gašić, Z. Juranić, T. Stanojković, S. Tufegdžić, Z. Kljajić, D. Sladić, Eur. J. Med. Chem. 45 (2010) 923–929.
[127] L. Cariello, M. De Nicola Giudici, L. Zanetti, Comp. Biochem. Physiol. 65C (1980) 37–41.
[128] R. Cozzolino, A. De Giulio, S. De Rosa, G. Strazzullo, M.J. Gašić, D. Sladić, M. Zlatović, J. Nat. Prod. 53 (1990) 699–702.
[129] B.N. Meyer, N.R. Ferrigni, J.E. Putnam, L.B. Jacobsen, D.E. Nichols, J.L. McLaughlin, Planta Med. 45 (1982) 31–34.
[130] A.R. Diaz-Marrero, P. Austin, R. Van Soest, T. Matainaho, C.D. Roskelley, M. Roberge, R. J. Andersen, Org. Lett. 8 (2006) 3749–3752.
[131] A. Crispino, A. De Giulio, S. De Rosa, G. Strazzullo, J. Nat. Prod. 52 (1989) 646–648.
[132] A. De Giulio, S. De Rosa, G. Di Vincenzo, G. Strazzullo, Tetrahedron 46 (1990) 7971–7976.
[133] Y.C. Shen, C.H. Lu, R. Chakraborty, Y.H. Kuo, Nat. Prod. Res. 17 (2003) 83–89.
[134] S. Hirsch, A. Rudi, Y. Kashman, J. Nat. Prod. 54 (1991) 92–97.
[135] S. Loya, A. Hizi, FEBS Lett. 269 (1990) 131–134.
[136] H. Shigemori, T. Madono, T. Sasaki, Y. Mikami, J. Kobayashi, Tetrahedron 50 (1994) 8347–8354.
[137] J. Kobayashi, T. Madono, H. Shigemori, Tetrahedron 51 (1995) 10867–10874.
[138] Y. Takahashi, T. Kubota, J. Ito, Y. Mikami, J. Fromont, J. Kobayashi, Bioorg. Med. Chem. 16 (2008) 7561–7564.
[139] L. Kissau, P. Stahl, R. Mazitschek, A. Giannis, H. Waldmann, J. Med. Chem. 46 (2003) 2917–2931.
[140] L.K. Shubina, S.N. Fedorov, V.A. Stonik, A.S. Dmitrenok, V.V. Isakov, Chem. Nat. Comp. 26 (1990) 296–298 (translated from Kim. Prir. Soedin., 1990, 358–361).
[141] K. Iguchi, A. Sahashi, J. Kohno, Y. Yamada, Chem. Pharm. Bull. 38 (1990) 1121–1123.
[142] R.T. Luibrand, T.R. Erdman, J.J. Vollmer, P.J. Scheuer, J. Finer, J.C. Clardy, Tetrahedron 35 (1979) 609–612.
[143] R.J. Capon, J.K. MacLeod, J. Org. Chem. 52 (1987) 5059–5060.
[144] M.L. Kondracki, M. Guyot, Tetrahedron 45 (1989) 1995–2004.
[145] Y.C. Shen, P.W. Hsieh, J. Nat. Prod. 60 (1997) 93–97.
[146] P.H. Lu, S.C. Chueh, F.L. Kung, S.L. Pan, Y.C. Shen, J.H. Guh, Eur. J. Pharmacol. 556 (2007) 45–54.
[147] S. Loya, R. Tal, Y. Kashman, A. Hizi, Antimicrob. Agents Chemother. 34 (1990) 2009–2012.
[148] P.A. Takizawa, J.K. Yucel, B. Veit, D.J. Faulkner, T. Deerinck, G. Soto, M. Ellisman, V. Malhotra, Cell 73 (1993) 1079–1090.
[149] H.S. Radeke, C.A. Digits, R.L. Casaubon, M.L. Snapper, Chem. Biol. 6 (1999) 639–647.
[150] H.R. Rangel, F. Dagger, R.S. Compagnone, Cell Biol. Int. 21 (1997) 337–339.
[151] M.L. Kondracki, M. Guyot, Tetrahedron Lett. 28 (1987) 5815–5818.

[152] J. Rodriguez, E. Quinoà, R. Riguera, B.M. Peters, L.M. Abrell, P. Crews, Tetrahedron 48 (1992) 6667–6680.
[153] T.P. Evans, L. Cornell, R.W. Peterson, D.J. Faulkner, Nat. Prod. Lett. 4 (1994) 287–291.
[154] F.J. Schmitz, V. Lakshmi, D.R. Powell, D. van der Helm, J. Org. Chem. 49 (1984) 241–244.
[155] N.K. Utkina, V.A. Denisenko, V.B. Krasokhin, J. Nat. Prod. 73 (2010) 788–791.
[156] H.D. Yoo, D. Leung, J. Sanghara, D. Daley, R. van Soest, R.J. Andersen, Pharm. Biol. 41 (2003) 223–225.
[157] B. Cartè, C.B. Rose, D.J. Faulkner, J. Org. Chem. 50 (1985) 2785–2787.
[158] J.R. Carney, P.J. Scheuer, Tetrahedron Lett. 34 (1993) 3727–3730.
[159] F.S. De Guzman, B.R. Copp, C.L. Mayne, G.P. Concepcion, G.C. Mangalindan, L.R. Barrows, C.M. Ireland, J. Org. Chem. 63 (1998) 8042–8044.
[160] Y. Li, Y. Zhang, X. Shen, Y.-W. Guo, Bioorg. Med. Chem. Lett. 19 (2009) 390–392.
[161] C. Giannini, C. Debitus, R. Lucas, A. Ubeda, M. Paya, J.N.A. Hooper, M.V. D'Auria, J. Nat. Prod. 64 (2001) 612–615.
[162] H. Suna, M. Arai, Y. Tsubotani, A. Hayashi, A. Setiawan, M. Kobayashi, Bioorg. Med. Chem. 17 (2009) 3968–3972.
[163] Y. Zhang, Y. Li, Y.W. Guo, H.L. Jiang, X. Shen, Acta Pharmacol. Sin. 30 (2009) 333–345.
[164] H. Mitome, T. Nagasawa, H. Miyaoka, Y. Yamada, R.W.M. van Soest, J. Nat. Prod. 66 (2003) 46–50.
[165] A.D. Patil, A.J. Freyer, L. Killmer, P. Offen, B. Carte, A.J. Jurewicz, R.K. Johnson, Tetrahedron 53 (1997) 5047–5060.
[166] F. Marion, D.E. Williams, B.O. Patrick, I. Hollander, R. Mallon, S.C. Kim, D.M. Roll, L. Feldberg, R. van Soest, R.J. Andersen, Org. Lett. 8 (2006) 321–324.
[167] K. Kurata, K. Taniguchi, M. Suzuki, Phytochemistry 41 (1996) 749–752.
[168] D. Desoubzdanne, L. Marcourt, R. Raux, S. Chevalley, D. Dorin, C. Doerig, A. Valentin, F. Ausseil, C. Debitus, J. Nat. Prod. 71 (2008) 1189–1192.
[169] T. Kikuchi, Y. Mori, T. Yokoi, S. Nakazawa, H. Kuroda, Y. Masada, K. Kitamura, K. Kuriyama, Chem. Pharm. Bull. 31 (1983) 106–113.
[170] A. Numata, S. Kanbara, C. Takahashi, R. Fujiki, M. Yoneda, E. Fujita, Y. Nabeshima, Chem. Pharm. Bull. 39 (1991) 2129–2131.
[171] A. Numata, S. Kanbara, C. Takahashi, R. Fujiki, M. Yoneda, Y. Usami, E. Fujita, Phytochemistry 31 (1992) 1209–1213.
[172] M. Iwashima, J. Mori, X. Ting, T. Matsunaga, K. Hayashi, D. Shinoda, H. Saito, H. Sankawa, T. Hayashi, Biol. Pharm. Bull. 28 (2005) 374–377.
[173] J. Mori, M. Iwashima, H. Wakasugi, H. Saito, T. Matsunaga, M. Ogasawara, S. Takahashi, H. Suzuki, T. Hayashi, Chem. Pharm. Bull. 53 (2005) 1159–1163.
[174] J.G. Urones, P. Basabe, I.S. Marcos, J. Pineda, A.M. Lithgow, R.F. Moro, F.M.S. Brito Palma, M.E.M. Araùjo, M.D.G. Gravalos, Phytochemistry 31 (1992) 179–182.
[175] J.G. Urones, M.E.M. Araùjo, F.M.S. Brito Palma, P. Basabe, I.S. Marcos, R.F. Moro, A.M. Lithgow, J. Pineda, Phytochemistry 31 (1992) 2105–2109.
[176] W.H. Gerwick, W. Fenical, J. Org. Chem. 46 (1981) 22–27.
[177] V. Amico, F. Cunsolo, M. Piattelli, G. Ruberto, Phytochemistry 24 (1985) 1047–1050.
[178] L.A. Tziveleka, D. Abatis, K. Paulus, R. Bauer, C. Vagias, V. Roussis, Chem. Biodivers. 2 (2005) 901–909.
[179] G. Culioli, A. Ortalo-Magne, R. Valls, C. Hellio, A.S. Clare, L. Piovetti, J. Nat. Prod. 71 (2008) 1121–1126.

[180] G. Koren-Goldshlager, P. Klein, A. Rudi, Y. Benayahu, M. Schleyer, Y. Kashman, J. Nat. Prod. 59 (1996) 262–266.
[181] H.H. Sun, N.M. Ferrara, O.J. McConnell, W. Fenical, Tetrahedron Lett. 21 (1980) 3123–3126.
[182] V. Mesguiche, R. Valls, L. Piovetti, B. Banaigs, Phytochemistry 45 (1997) 1489–1494.
[183] L.M. Murray, A. Johnson, M.C. Diaz, P. Crews, J. Org. Chem. 62 (1997) 5638–5641.
[184] J. Carroll, E.N. Jonsson, R. Ebel, M.S. Hartman, T.R. Holman, P. Crews, J. Org. Chem. 66 (2001) 6847–6851.
[185] B.K. Rubio, R.W.M. van Soest, P. Crews, J. Nat. Prod. 70 (2007) 628–631.
[186] M. Wessels, G.M. Konig, A.D. Wright, J. Nat. Prod. 62 (1999) 927–930.
[187] E. Dorta, M. Cueto, I. Brit, J. Darias, J. Nat. Prod. 65 (2002) 1727–1730.
[188] C. Francisco, B. Banaigs, R. Valls, L. Codomier, Tetrahedron Lett. 26 (1985) 2629–2635.
[189] C. Francisco, B. Banaigs, J. Teste, A. Cave, J. Org. Chem. 51 (1986) 1115–1120.
[190] R. Mokrini, M.B. Mesaoud, M. Daoudi, C. Hellio, J.-P. Maréchal, M. El Hattab, A. Ortalo-Magné, L. Piovetti, G. Culioli, J. Nat. Prod. 71 (2008) 1806–1811.
[191] M. Norte, A. Sánchez, A.G. González, Tetrahedron Lett. 34 (1993) 3485–3486.
[192] E.T. O'Brien, R.S. Jacobs, L. Wilson, Mol. Pharmacol. 24 (1983) 493–499.
[193] O.M.M. Sabry, S. Andrews, K.L. McPhail, D.E. Goeger, A. Yokochi, K.T. LePage, T.F. Murray, w.H. Gerwick, J. Nat. Prod. 68 (2005) 1022–1030.
[194] E.T. O'Brien, D.J. Asai, A. Groweiss, B.H. Lipshutz, W. Fenical, R.S. Jacobs, L. Wilson, J. Med. Chem. 29 (1986) 1851–1855.
[195] H. Liu, M. Namikoshi, K. Akano, H. Kobayashi, H. Nagai, X. Yao, J. Asian Nat. Prod. Res. 7 (2005) 661–670.
[196] K. Warabi, L.M. McHardy, L. Matainaho, R. Van Soest, C.D. Roskelley, M. Roberge, R. J. Andersen, J. Nat. Prod. 67 (2004) 1387–1389.
[197] S.A. Eccles, Int. J. Dev. Biol. 48 (2004) 583–598.
[198] K.A. Mohammed, R.C. Jadulco, T.S. Bugni, M.K. Harper, M. Sturdy, C.M. Ireland, J. Med. Chem. 51 (2008) 1402–1405.
[199] G. Powis, D.L. Kirkpatrick, Mol. Cancer Ther. 3 (2004) 647–654.
[200] D. Abatis, C. Vagias, D. Galanakis, J.N. Norris, D. Moreau, C. Roussakis, V. Roussis, Tetrahedron Lett. 46 (2005) 8525–8529.
[201] G.V. Alea, A.R. Carroll, B.F. Bowden, Aust. J. Chem. 47 (1994) 191–194.
[202] M.R. Kernan, D.J. Faulkner, J. Org. Chem. 53 (1988) 4574–4578.
[203] A. Loukaci, I. Le Saout, M. Samadi, S. Leclerc, E. Damiens, L. Meijer, C. Debitus, M. Guyot, Bioorg. Med. Chem. 9 (2001) 3049–3054.
[204] M. Musman, I.I. Ohtani, D. Nagaoka, J. Tanaka, T. Higa, J. Nat. Prod. 64 (2001) 350–352.
[205] J. Kimura, E. Ishizuka, Y. Nakao, W.Y. Yoshida, P.J. Scheuer, M. Kelly-Borges, J. Nat. Prod. 61 (1998) 248–250.
[206] T. Amagata, S. Whitman, T.A. Johnson, C.C. Stessman, C.P. Loo, E. Lobkovsky, J. Clardy, P. Crews, T.R. Holman, J. Nat. Prod. 66 (2003) 230–235.
[207] J.W. Eckstein, Invest. New Drugs 18 (2000) 149–156.
[208] L.M. West, D.J. Faulkner, J. Nat. Prod. 71 (2008) 269–271.
[209] G. Cimino, S. De Stefano, L. Minale, Tetrahedron 28 (1972) 1315–1324.
[210] W. Wätjen, A. Putz, Y. Chovolou, A. Kampkötter, F. Totzke, M.H.G. Kubbutat, P. Proksch, B. Konuklugil, J. Pharm. Pharmacol. 61 (2009) 919–924.
[211] N. Fusetani, M. Sugano, S. Matsunaga, K. Hashimoto, H. Shikama, A. Ohta, H. Nagano, Experientia 43 (1987) 1233–1234.
[212] V.A. Stonik, T.N. Makarieva, A.S. Dmitrenok, J. Nat. Prod. 55 (1992) 1256–1260.
[213] S. Isaacs, Y. Kashman, Tetrahedron Lett. 33 (1992) 2227–2230.

[214] S. Loya, R. Tal, A. Hizi, S. Isaacs, Y. Kashman, J. Nat. Prod. 56 (1993) 2120–2125.
[215] C.L. Blackburn, C. Hopmann, R. Sakowicz, M.S. Berdelis, L.S.B. Goldstein, D.J. Faulkner, J. Org. Chem. 64 (1999) 5565–5570.
[216] N. Hirokawa, Science 279 (1998) 519–526.
[217] S. Loya, M. Bakhanashvili, Y. Kashman, A. Hizi, Biochemistry 34 (1995) 2260–2266.
[218] A. Fukami, Y. Ikeda, S. Kondo, H. Naganawa, T. Takeuchi, S. Furuya, Y. Hirabayashi, K. Shimoike, S. Hosaka, Y. Watanabe, K. Umezawa, Tetrahedron Lett. 38 (1997) 1201–1202.
[219] M.J. Berridge, Annu. Rev. Biochem. 56 (1987) 159–193.
[220] C.A. Gray, S.P. de Lira, M. Silva, E.F. Pimenta, O.H. Thiemann, G. Oliva, E. Hajdu, R. J. Andersen, R.G.S. Berlinck, J. Org. Chem. 71 (2006) 8685–8690.
[221] J.A. Kalaitzis, P. de Almeida Leone, L. Harris, M.S. Butler, A. Ngo, J.N.A. Hooper, R. J. Quinn, J. Org. Chem. 64 (1999) 5571–5574.
[222] R. Sakowicz, M.S. Berdelis, K. Ray, C.L. Blackburn, C. Hopmann, D.J. Faulkner, L.S. B. Goldstein, Science 280 (1998) 292–295.
[223] S. De Rosa, A. Crispino, A. De Giulio, C. Iodice, A. Milone, J. Nat. Prod. 58 (1995) 1450–1454.
[224] G. Bifulco, I. Bruno, L. Minale, R. Riccio, C. Debitus, G. Bourdy, A. Vassas, J. Lavayre, J. Nat. Prod. 58 (1995) 1444–1449.
[225] B. Gil, M.J. Sanz, M.C. Terencio, A. De Giulio, S. De Rosa, M.J. Alcaraz, M. Payá, Eur. J. Pharmacol. 285 (1995) 281–288.
[226] T. Wakimoto, A. Maruyama, S. Matsunaga, N. Fusetani, K. Shinoda, P.T. Murphy, Bioorg. Med. Chem. Lett. 9 (1999) 727–730.
[227] I. Erdogan-Orhan, B. Sener, S. De Rosa, J. Perez-Baz, O. Lozach, M. Leost, S. Rakhilin, L. Meijer, Nat. Prod. Sci. 18 (2004) 1–9.
[228] P. Ohen, Nat. Rev. Drug Discov. 1 (2002) 309–315.

Chapter 7

Chlorosulfolipids

Teppei Kawahara and Tatsufumi Okino
Graduate School of Environmental Science, Hokkaido University, Kita-ku, Sapporo, Japan

INTRODUCTION

The first reported chlorosulfolipids (CSLs) were isolated from the freshwater microalga Chrysophyceae *Ochromonas danica* at the end of the 1960s [1]. They composed about 10% of the total lipid of the organism, including both the chloroplast lipids and the mitochondrial lipids, which together dominate the lipids of the cell. They represented 3% of the dry weight of the cell and more than 50% of the total sulfur content of the cell [2]. In the 1960s, structural studies of the major CSL 2,2,11,13,15,16-hexachlorodocosane-1,14-disulfate (named "danicalipin A" in 2009, **1**) and related precursors revealed planar structures after isolation of the chemical degradation products [3–6]. Some early studies in this class of lipid have been reviewed by Haines [7–9]. Forty years later, they were finally isolated in their natural form by RP-HPLC [10]. The absolute configuration of **1** was elucidated in 2009 by two groups, one using a synthetic chemical approach and the other using an analytical chemical approach [10,11] (Fig. 1). The absolute configurations of the other CSLs in *O. danica* were also determined which were isolated from this alga at the same time.

Chrysomonads in the genera *Ochromonas* and *Poterioochromonas* are known to produce chemicals that are toxic to fish [12,13] and to invertebrates such as daphnia and rotifers [14,15]. The toxins also cause the inhibition of bacterial growth and the lysis of mammalian erythrocytes [16–18]. These toxins were not able to be isolated in the past because they are extremely hygroscopic and viscous. In 2009, CSLs were confirmed as the main toxic chemicals of *O. danica* [10]. However, the biological role of these alga-derived CSLs has not been clearly established. In the previous report, Haines and coworkers concluded that these CSLs were constituents of the cell membranes instead of phospholipids [19,20]. Further, the diol backbone was assumed to be biosynthesized from docosanoic acid or tetracosanoic acid via normal fatty acid biosynthesis [21,22], with the diol then being sulfated

Bioactive Natural Products, Vol. 36. DOI: 10.1016/B978-0-444-53836-9.00024-4

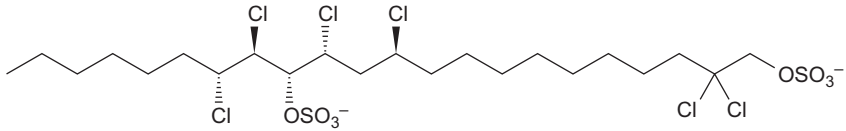

FIGURE 1 Structure of danicalipin A (**1**) from *Ochromonas danica*.

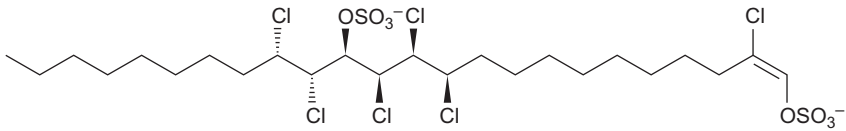

FIGURE 2 Structure of malhamensilipin A (**2**) from *Poterioochromonas malhamensis*.

by phosphoadenosine phosphosulfate (PAPS) [23,24] and chlorinated [23,25] to form the final CSLs.

Malhamensilipin A (**2**) was the first CSL to be isolated in its natural form in 1994 from the freshwater alga *Poterioochromonas malhamensis* [26]. This CSL exhibited moderate protein tyrosine kinase (PTK) inhibition, as well as antiviral and antimicrobial activity. In 2010, the Vanderwal group collaborated with the Gerwick group to revise the structure of **2** [27] (Fig. 2). HR-ESI-MS analysis of **2** revealed its actual molecular weight. The stereochemistry of this disulfate-chlorolipid was also clarified by the same groups.

In the course of investigation into Diarrheic Shellfish Poisoning (DSP) agents, three CSLs (**3**–**5**) were isolated as DSP-toxins from cytotoxic mussels collected in the Adriatic Sea (Fig. 3) [28–30]. In particular, the stereochemistry of a hexachlorosulfolipid (mytilipin A, **3**) was reported for the first time within this class of compounds using advanced NMR techniques. This series of investigations encouraged organic chemists to begin synthesizing these toxic lipids.

As the first syntheses within this class of targets, the Carreira group reported in 2009 that (±)-hexachlorosulfolipid **3** was synthesized via an unexpected five-membered ring through an epoxide-opening reaction [31]. Shortly after Carreira's report, the synthesis of the alga-derived CSL (±)-danicalipin A (**1**) was published by Vanderwal's group [11], as was the synthesis of (+)-malhamensilipin A (**2**) [32]. This synthetic work was done in parallel with structural determination using natural compounds through collaboration with the Gerwick group.

In 2010, the Yoshimitsu/Tanaka group reported the synthesis of (+)-hexachlorosulfolipid **3** [33] by applying their epoxide deoxydichlorination methodology [34]. The total synthesis of (+)-danicalipin A (**1**) and then followed in reports from the Umezawa/Matsuda [35] and the Yoshimitsu/Tanaka groups [36] in 2011. Recently, CSLs were reviewed by Carreira and the Vanderwal group of synthetic chemists [37,38]. Here, we review the current knowledge of CSLs in terms of isolation and structure elucidation.

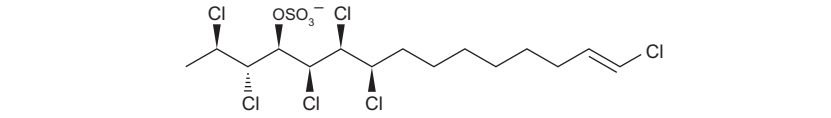

3

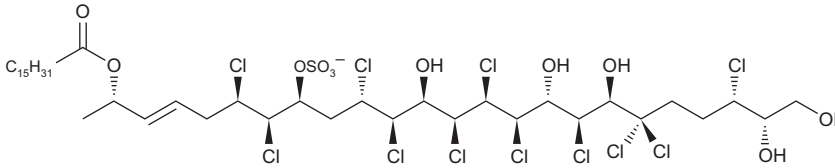

4

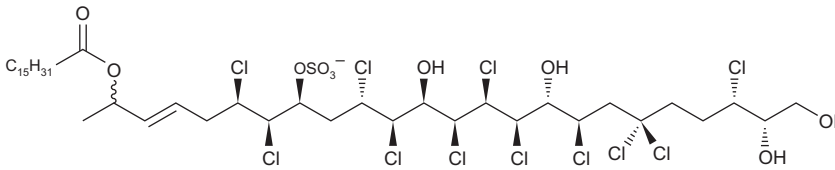

5

FIGURE 3 Structures of chlorosulfolipids (**3**–**5**) from the mussel *Mytilus galloprovincialis*.

CHLOROSULFOLIPIDS FROM *O. DANICA*

Isolation

In 1962, Haines and Block reported on previously unknown lipids from the chrysophyte *O. danica* [1]. The lipids were shown to be mixtures of mono- and disulfated docosane (C-22) and tetracosane (C-24) on a paper chromatogram of ^{35}S-labeled extracts of the cultured cells. Owing to these compounds being extremely hygroscopic and viscous, preparation of these sulfolipids in sufficient purity for structural characterization was difficult. Thus, the crude sulfolipids were obtained by solvent extraction, silica gel chromatography, and ion-exchange gel filtration from *O. danica* extract. Acid hydrolysis of these crude lipids yielded 1,14-docosanediol, 13-chloro-1,14-docosanediol [4,6], and 2,2,11,13,14,15,16-hexachlorodocosane-1,14-diol [3] as hydrolysates of the corresponding disulfates.

In 2009, we successfully isolated the CSLs that are natural components of the cultured freshwater alga *O. danica* (IAM CS-2) [10]. The cultured algal cells (430L) were collected by continuous centrifugation and freeze dried. The freeze-dried cells were extracted with MeOH and EtOAc. The combined extracts were evaporated *in vacuo* and extracted sequentially with hexane, $CHCl_3$, EtOAc, BuOH, and H_2O. The fractionation was performed

by bioassay-guided fractionation (toxicity to *Artemia salina*) and by using an RP-HPLC detected by an evaporative light-scattering detector for final purification because of the very low UV absorbance of these compounds.

The BuOH fraction was separated by silica gel column chromatography (CC) and eluted with combinations of hexane/EtOAc and EtOAc/MeOH. The toxic fractions were subjected to octadecylsilyl (ODS) column chromatography with aqueous MeOH. Danicalipin A (**1**, 825 mg) was obtained from the 80% MeOH aqueous fraction. From the 60% MeOH-eluted fraction, compounds **1** (96.2 mg), **8** (8.0 mg), and **10** (47.9 mg) were isolated by RP-HPLC with CH_3CN/H_2O as the mobile phase on a C30 column. Compounds **9** (5.0 mg), **10** (65.8 mg), and **11** (23.7 mg) were recovered from the other toxic fraction eluted with EtOAc/MeOH and purified in the same manner as described above. The $CHCl_3$ fraction was subjected repeatedly to silica gel column chromatography. The toxic fraction was separated by ODS column chromatography and HPLC, yielding compounds **12** (25.1 mg) and **1** (1 g). The ethyl acetate partition was fractionated by Si gel CC to concentrate the CSLs. Using RP-HPLC for detection, compounds **6** (9.0 mg) and **7** (2.2 mg) were isolated from the fractions eluted with hexane/EtOAc=1:1 and EtOAc, respectively. Further, danicalipin A (**1**, 195.9 mg) was obtained from the other Si gel CC portion (Figs. 4 and 5).

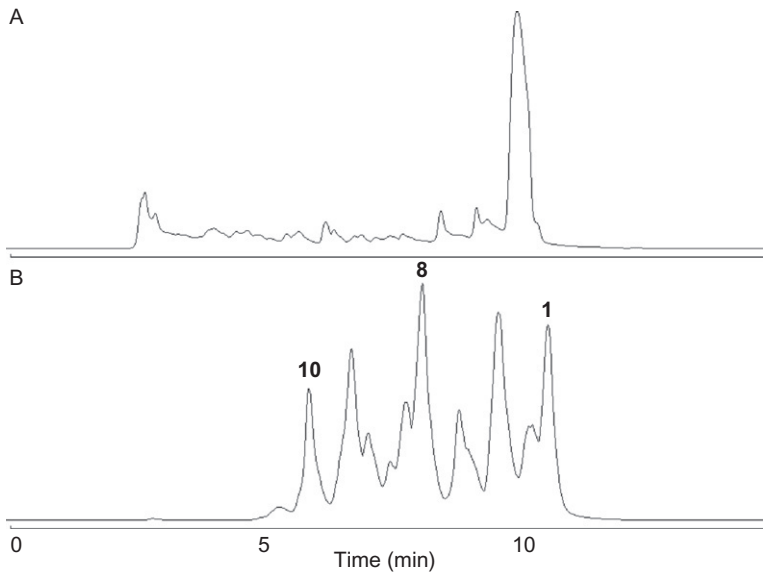

FIGURE 4 HPLC analysis of the chlorosulfolipids. Column: Develosil C30-UG-5 (Nomura chemical, 4.6×150 mm); mobile phase: acetonitrile/H_2O=40:60; flow rate: 1.0 mL/min. (A) UV detection: 210 nm. (B) ELSD: 34.0°C, 1.2 L/min.

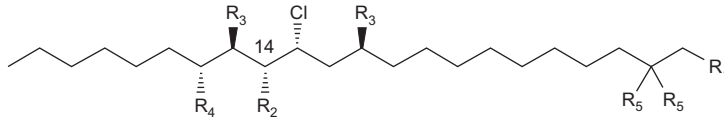

	R_1	R_2	R_3	R_4	R_5
1	OSO_3^-	OSO_3^-	Cl	Cl	Cl
6	OSO_3^-	OH	Cl	Cl	Cl
7	OH	OH	Cl	Cl	Cl
8	OSO_3^-	OSO_3^-	Cl	Cl	H
9	OSO_3^-	OSO_3^-	Cl	H	H
10	OSO_3^-	OSO_3^-	H	H	H

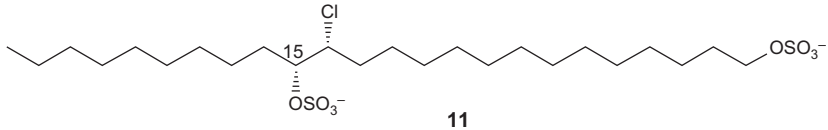

11

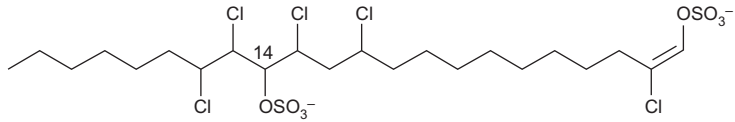

12

FIGURE 5 Structures of the chlorosulfolipids from *O. danica*.

Structural Elucidation

Danicalipin A from the Alga O. danica

Planar Structure

In 1970, Elovson and Vagelos reported the planar structure of danicalipin A (**1**) as the major species of CSL from cultured *O. danica* [3]. Using its pure hydrolysate **13** (hexachlorodiol), structural determination of **1** was carried out by stepwise chemical degradation experiments monitored by mass spectrometry. The analysis of the mass spectrum of a trimethylsilyl (TMS) derivative of **13** allowed assignment of the oxygen-bearing carbon at C-14 from α cleavage fragments (Fig. 6). However, more informative signals which could allow assigning carbons bearing chlorines were not obtained because α cleavages at the carbons attached to electronegative chlorine were not promoted in the MS ionization. Therefore, to locate the chlorine-bearing methines, stepwise degradation was carried out: mild alkali treatment to give epoxides (**14**), further alkali treatment to lose two chlorines for the formation of 2-ketone

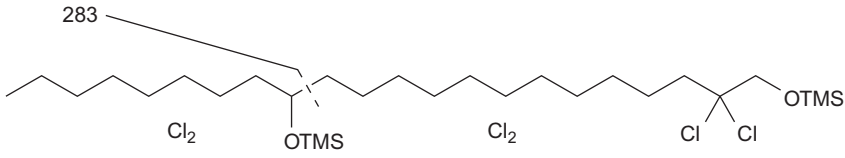

FIGURE 6 MS fragmentation of **13**.

(**15**), periodate cleavage to give the nor-carboxylic acid (**16**, 21 carbons), and PTSA-catalyzed acetolysis to give chloroglycols (**17**) (Fig. 7).

MS analysis of the TMS derivative of **17** and related products modeled by further degradations assigned the chlorine-bearing carbons as C-11, C-13, C-15, and C-16 in **13**. For **14** versus **15**, the difference in the chemical shift values, especially a singlet methylene signal (CH_2-2) at δ_H 3–5 ppm, approved assignment of a dichlorine-bearing carbon at C-2. In this study, Elovson and Vagelos used ^{36}Cl-labeled CSL from *O. danica* cultured in a [^{36}Cl]HCl enriched broth. This condition helped to estimate whether the chlorines were displaced or eliminated by contaminating $^{35}Cl^-$ ions during chemical degradation. Because structure elucidation of this class of compounds is not straightforward, even now, it is amazing that this work was done in the 1960s.

In 2009, we confirmed the planar structure of danicalipin A (**1**) using a pure compound in its natural form through a combination of using analytical instruments and techniques. These included 2D NMR measurements using a high-field FT-NMR (500 or 600 MHz for proton), fast atom bombardment (FAB) mass spectrometry, high-resolution electrospray ionization (ESI) mass spectrometry, and FT-IR. The negative FABMS of **1** showed ions at *m/z* 625, 627, 629, 631, and 633 (Fig. 8). The isotopic ratio of approximately 52:100:80:35:8:1 indicated the presence of six chlorine atoms in **1**. The $[M-2H]^{2-}$ peak exhibited at *m/z* 352 was the principal ion, and the sample admixed with sodium iodide was applied to FABMS to produce sodium adduct ions at *m/z* 727, 729, 731, 733, and 735. With the negative high-resolution ESI-TOF-MS, the molecular related ion peak of **1** at *m/z* 727.0039 for $C_{22}H_{38}{}^{35}Cl_6NaO_8S_2$ was recorded (Fig. 9). The ^{1}H and ^{13}C NMR spectra, with the help of the edited-HSQC measurements, showed the presence of carbons bearing six chlorines and two sulfate esters. A detailed analysis of the DQF-COSY and HMBC spectra of **1** revealed three partial structures (Fig. 10) and three sp^3 methylenes. The ESI-MS/MS data confirmed the length of the methylene chains between the three parts of the molecule (Fig. 11). Thus, the planar structure of **1** was confirmed as danicalipin A. In both approaches, the one used in 1970 and in 2009, mass spectrometry provided very important information.

Stereochemistry

In 1970, there was no method for elucidating the configurations of these acyclic structures. In 2009, the relative configuration of the five chiral centers was assigned using *J*-based configuration analysis (JBCA) [39]. This method

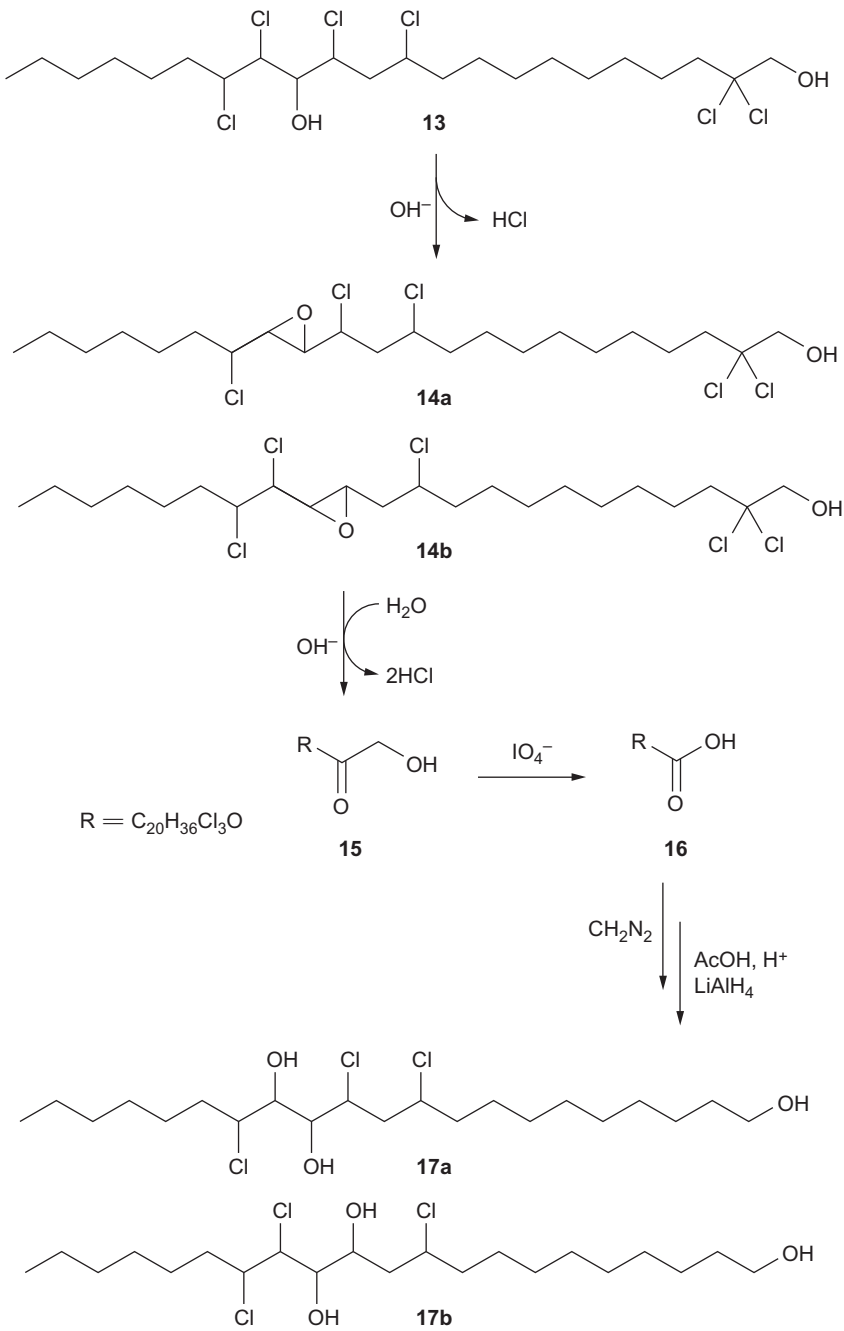

FIGURE 7 Stepwise degradation of 2,2,11,13,15,16-hexachlorodocosane-1,14-diol (**13**).

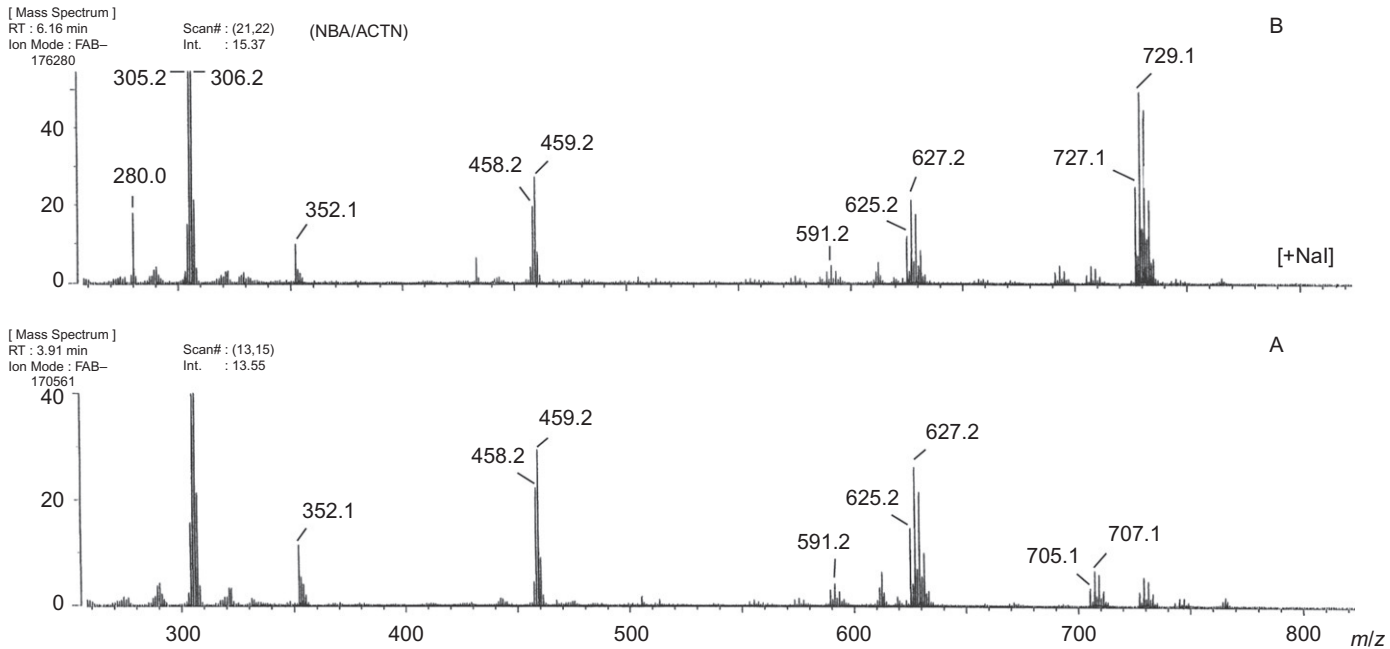

FIGURE 8 Negative ion FAB mass spectra of **1**. (A) Normal and (B) +NaI.

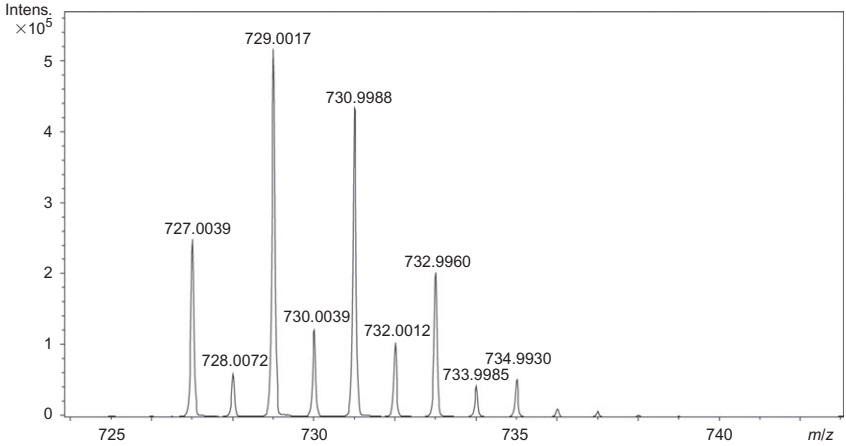

FIGURE 9 Negative ion HR-ESI mass spectrum of **1**.

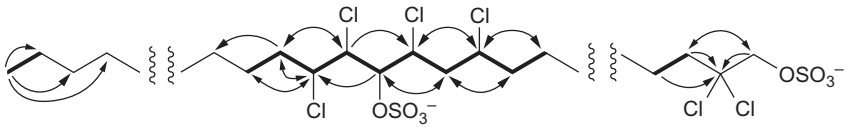

FIGURE 10 The DQF-COSY and HMBC correlations of partial structures of **1**.

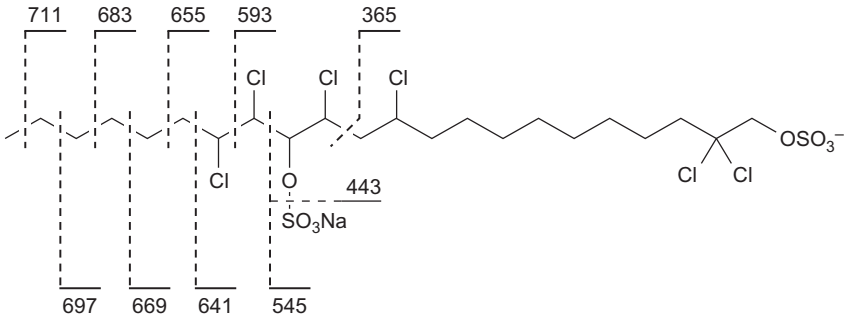

FIGURE 11 MS/MS fragments of **1**.

relies on the extensive use of ^{3}J(H,H) and $^{2,3}J$(C,H) coupling constants in combination with NOE or ROE data. This technique has been widely applied to elucidate the relative configuration of various compounds featuring acyclic chains bearing substituents including hydroxy, alkoxy, and methyl groups; halogens; and even nitrogen. In particular, the substitution of chlorine could be interpreted in the same manner as oxygen, that is, as an electronegative substituent [28–30]. The application of JBCA for chlorinated compounds was proven by synthetic studies on CSLs [11,27,31]. In our study, homonuclear coupling data were obtained from the ^{1}H NMR spectrum. The heteronuclear

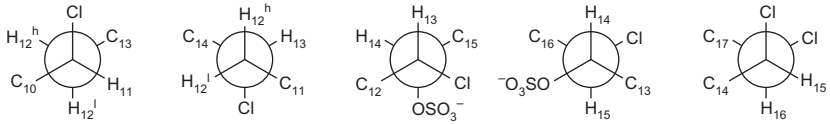

^3J(H11,H12^h) 11.1 Hz	^3J(H12^h,H13) 2.1 Hz	^3J(H13,H14) < 2 Hz	^3J(H14,H15) 10.2 Hz	^3J(H15,H16) 1.1 Hz
^3J(H11,H12^l) 1.2 Hz	^3J(H12^l,H13) 11.1 Hz	^3J(H13,C15) n.s.	^3J(C13,H15) ±3.2 Hz	^3J(C14,H16) ±0.3 Hz
^3J(C10,H12^h) +3.0 Hz	^3J(C11,H13) +2.1 Hz	^3J(C12,H14) ±0.4 Hz	^3J(H14,C16) ±3.5 Hz	^3J(H15,C17) ±5.3 Hz
^3J(C10,H12^l) +1.0 Hz	^2J(H12^h,C13) +1.2 Hz	^2J(C13,H14) ±3.3 Hz	^2J(C14,H15) ±6.3 Hz	^2J(C15,H16) ±0.3 Hz
^3J(H11,C13) +2.1 Hz	^2J(H12^l,C13) –7.8 Hz	^2J(H13,C14) n.s.	^2J(H14,C15) ±6.4 Hz	^2J(H15,C16) ±6.4 Hz
^2J(C11,H12^h) –7.2 Hz				

FIGURE 12 Homo- and heteronuclear coupling constants for the C-11 to C-16 portion of **1**. n.s.: peaks not separated in the *J*-IMPEACH-MBC spectrum.

coupling constants were measured from the HETLOC [40,41] and *J*-IMPEACH-MBC [42] spectra and the gradient-selected *J*-HMBC experiment [43] (Fig. 12).

At the C-11–C-12 axis, the *anti* configuration of H-11–H-12^h was inferred from the large coupling constant between H-11 and H-12^h, whereas H-11–H-12^l was *gauche*, based on the small coupling constant for ^3J(H11/H12^l). In the HETLOC spectrum, small coupling constants for ^3J(C10/H12^l) and ^3J(H11/C13) suggested *gauche* conformations for C-10–H-12^l and H-11–C-13. A large coupling constant value for ^2J(C11/H12^h) was evidence for a *gauche* relationship at Cl-11/H-12^h. For the C-12–C-13 axis, we deduced *gauche* and *anti* conformations for H-12^h/H-13 and H-12^l/H-13, respectively, based on the proton–proton couplings. Analysis of the HETLOC spectrum revealed a small coupling for ^2J(H12^h/C13) and a large coupling for ^2J(H12^l/C13). This was evidence for *anti* and *gauche* relationships at Cl-13/H-12^h and Cl-13/H-12^l, respectively. For the C-13/C-14 axis, the small ^3J(H13/H14) value (<2 Hz) indicated a *gauche* relationship between H-13 and H-14. Unfortunately, the HETLOC spectrum did not contain any peaks related to this axis.

To continue the structure assignment, the *J*-IMPEACH-MBC spectrum was analyzed. Using this method, we were able to observe the corresponding peaks, ^nJ(C,H). However, the values were below the limit of digital resolution (4 Hz), and ^2J(C,H) values below 4 Hz cannot be used to assign either "small" or "medium" values in a disubstituted system [39]. However, the gradient-selected *J*-HMBC yielded small ^3J(C,H) and ^2J(C,H) values. It should be noted that exact values of small heteronuclear couplings are sometimes key to JBCA. The small value for ^3J(C12/H14) suggested that C-12/H-14 was *gauche* and the small value for ^2J(C13/H14) indicated an *anti* conformation at Cl-13/H-14. Further, the lack of NOESY correlation between H-12 and H-15 confirmed the *anti* conformation at C-12/C-15. At the C-14—C-15 bond, a large coupling constant for ^3J(H14/H15) suggested that H-14/H-15 was arranged in the *anti* configuration. The lack of NOESY correlation at H-13/H-16 revealed an *anti* relationship between C-13 and C-16. In addition, the small values for ^3J(C13/H15) and ^3J(H14/C16), obtained using the

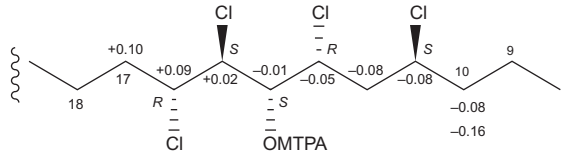

FIGURE 13 $\Delta\delta$ values [$\Delta\delta$ (in ppm)$=\delta_S-\delta_R$] obtained from 1,14-di-(*S*)- and (*R*)-MTPA esters of the hydrolysate of **1**.

gradient-selected *J*-HMBC, supported this conformation. For the C-15—C-16 bond, the *gauche* relationship at H-15/H-16 was inferred due to the small ^3J (H15/H16). From the *J*-IMPEACH-MBC, a large value for ^3J(H15/C17) suggested an *anti* conformation between H-15/C-17. A small value for ^2J(C15/H16) indicated an *anti* relationship between Cl-15 and H-16. Therefore, both the *J* values and the spatial data allowed the unambiguous assignment of the relative configuration of the five chiral carbons in **1**.

The absolute configuration for **1** was determined using a modified Mosher's method after hydrolysis to obtain the corresponding diol. Treatment of the diol with (*R*)-(−)- and (*S*)-(+)-MTPA chloride in anhydrous pyridine gave 1,14-(*S*)- and (*R*)-MTPA diesters, respectively. The chemical shift differences ($\Delta\delta=\delta_S-\delta_R$) are shown in Fig. 13. The $\Delta\delta$ values for H-10–H-13 were negative. In contrast, the values for H-15, 16, and 17 were positive, suggesting that C-14 was arranged in the *S*-configuration. Given this, the absolute configurations of **1** were assigned as 11*S*, 13*R*, 14*S*, 15*S*, and 16*R*.

Other Chlorosulfolipids from the Alga O. danica

In the course of the investigation of alga-derived CSLs, the first identified lipid, in 1967, was docosane-1,14-disulfate (**18**) [4]. This dipolar and detergent-like lipid was confirmed to have a primary and a secondary sulfate by measuring its infrared spectrum before acid hydrolysis. The resultant diol was identified as docosane-1,14-diol by the decisive α cleavage fragmentations in mass spectrometry (Fig. 14). Additionally, the structure of docosane-1,14-diol was confirmed by the ^{1}H NMR spectrum (60 MHz for proton on a Varian A-60, D_2O as solvent): δ_H 0.9 (*t*) assigned for terminal methyl, δ_H 1.3 for aliphatic methylene, and δ_H 3.5 (*t*) for the methylene group of the primary sulfate ester. The chiral center (C-14) was assigned the *S*-configuration by optical rotation.

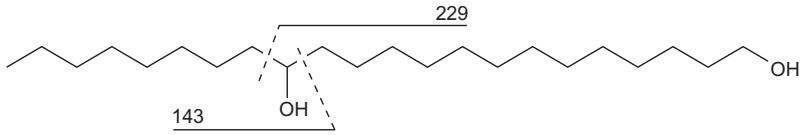

FIGURE 14 MS fragmentation of the hydrolysate of **18**.

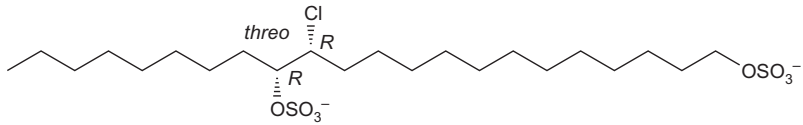

FIGURE 15 Chemical structure of **19**.

In 1969, Elovson and Vagelos reported the MS analysis of *O. danica* lipid extract [2]. In their paper, they found many CSLs, such as 13-chlorodocosane-1,14-disulfate (**19**), 11,15-dichlorodocosane-1,14-disulfate, and other docosane-1,14-disulfates, with three to six chlorine atoms per molecule in the crude lipid extract of *O. danica*. The crude CSL was hydrolyzed to give a mixture of chlorodiols before TMS derivatization. A few months later, Haines and coworkers demonstrated the absolute configuration of **19** as 13*R*, 14*R* by positive optical rotation and through synthetic procedures (Fig. 15) [5]. They also carried out ^{1}H NMR of the hydrolysate of **19** (chlorodiol) in chloroform-*d*: δ_H 0.90 (terminal methyl), δ_H 1.32 (aliphatic methylene), δ_H 3.68 (CH_2, OH terminal), and assorted small peaks (δ_H 3.4–4.1). The detailed characterization of trichloro-, tetrachloro-, and pentachlorosulfolipids from the alga was not published in early studies.

The chemical structures of the other chlorine-containing lipids (**6**–**10**) from *O. danica* culture were obtained along with danicalipin A and reported in 2009 (Fig. 5) [10]. The structures of these isolated lipids were determined in the same manner as for danicalipin A, and most of their stereochemistries were clarified using the same method as that used for danicalipin A.

The molecular formula of **6** was established by negative HR-ESI-MS and the intensity of the isotope peaks ratio (50:100:83:37:8:1). The ^{1}H NMR and ^{13}C NMR spectra were similar to those for danicalipin A (**1**), with the exception of H-14 and C-14 (δ_H 3.76 and δ_C 75.5, respectively, vs. δ_H 4.49 and δ_C 80.8 in **1**). Given this, **6** contained a hydroxy group substituted in place of the 14-sulfate in **1**. The analyses of the DQF-COSY and HMBC spectra established the planar structure of **6** as 2,2,11,13,15,16-hexachloro-14-docosanol-1-sulfate (Fig. 16). To determine the stereochemistry, **6** was hydrolyzed to its

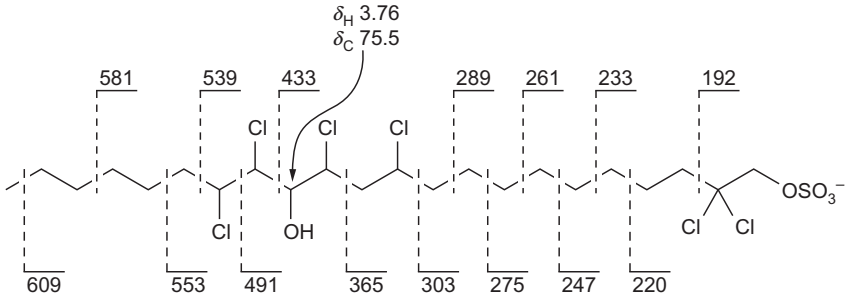

FIGURE 16 MS/MS fragments and ^{13}C and ^{1}H NMR chemical shifts of **6**.

corresponding diol. The ^{1}H NMR chemical shifts and coupling constants of the hydrolysate of **6** were identical to those of the hydrolysate of danicalipin A, suggesting that the relative configuration of **6** was the same. The optical rotation values and signs of these diols were also similar. Based on these results, the absolute configuration of **6** was identified as 11*S*, 13*R*, 14*S*, 15*S*, and 16*R*.

The HR-ESI-MS data of **7** declared its molecular formula as $C_{22}H_{40}Cl_6O_2$, which was confirmed by its isotopic peaks and 1D and 2D NMR data. Further analysis of NMR data concluded that a hydroxy was attached to C-1 in place of the sulfate group of **6** because of the chemical shifts at C-1 (**7**: δ_C 72.6, **6**: δ_C 75.4), C-2 (**7**: δ_C 95.6, **6**: δ_C 91.4), and H-1 (δ_H 3.84 for **7**, δ_H 4.29 for **6**). In addition, the ^{1}H NMR spectrum for **7** matched that of the hydrolysate of **6**. The ESI-MS/MS data confirmed that the planar structure of **7** was 2,2,11,13,15,16-hexachlorodocosane-1,14-diol (Fig. 5). The ^{1}H NMR chemical shifts and coupling constants of **7** were identical to those of the hydrolysate of **6**, suggesting that the relative configuration of **7** was the same as **6**-diol. The optical rotation of **7** was the same sign as that of **1**-diol and **6**-diol, assigning the absolute configuration of **7** as 11*S*, 13*R*, 14*S*, 15*S*, and 16*R*.

Compound **8** was a tetrachlorosulfolipid according to the HR-ESI-MS data. The chemical shifts in the ^{1}H and ^{13}C NMR spectra were very similar to those of **1**, except for the four contiguous methylenes assigned between CH_2-1 (δ_C 69.2; δ_H 3.98, *t*) and CH_2-4 from the HSQC and HMBC spectra. The positions of the oxygen and chlorine substituents were confirmed by ESI-MS/MS measurement (Fig. 5). Further analysis of the NMR spectra satisfied this structure. Thus, the planar structure of **8** was 11,13,15,16-tetrachlorodocosane-1,14-disulfate.

The relative configuration of **8** was determined by JBCA. As the result of analysis of the *J* values and the spatial data, the six relative configurations were the same as those of **1**. The absolute configurations of the chiral centers of **8** (C-11, 13, 14, 15, 16) were then identified as being the same as those of **1** (11*S*, 13*R*, 14*S*, 15*S*, and 16*R*) by a modified Mosher's method.

The ^{1}H and ^{13}C NMR spectra of the trichlorosulfolipid **9** were very similar to those obtained from **8**. However, the characteristic signal for a chlorine-substituted methine was not seen in the spectrum for **9**. This suggested that **9** was a deschloro derivative of **8**. The 2D NMR spectra and the ESI-MS/MS data established the planar structure as 11,13,15-trichlorodocosane-1,14-disulfate.

The relative configuration of **9** was determined by JBCA, as shown in Fig. 17. Given this, the relative configuration of **9** was identical to that of **8**. The absolute configuration of **9** was then established using a modified Mosher's method by the same procedure as for **1** (Fig. 18).

For compound **10**, the HR-ESI-MS data and the intensity ratio of the isotope peaks (100:42) indicated that their molecular formula contained a chlorine and two sulfate esters. The ^{1}H NMR spectrum revealed two methine protons (H-14 and H-13) and a methylene proton (H_2-1), as well as methylene

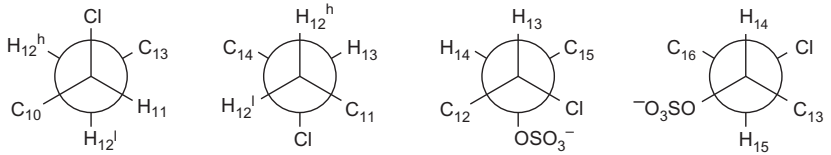

^3J(H11,H12^h) 11.2 Hz
^3J(H11,H12^l) 2.0 Hz
^3J(H11,C13) +1.2 Hz
^2J(C11,H12^h) –6.6 Hz
^2J(C11,H12^l) +1.2 Hz

^3J(H12^h,H13) 2.0 Hz
^3J(H12^l,H13) 11.4 Hz
^3J(C11,H13) +3.1 Hz
^2J(H12^h,C13) +1.2 Hz
^2J(H12^l,C13) –8.4 Hz

^3J(H13,H14) 1.1 Hz

No NOE observed between H-12 and H-15.

^3J(H14,H15) 9.6 Hz
^3J(H14,C16) ±2.0 Hz
^2J(C14,H15) ±6.2 Hz
^2J(H14,C15) ±6.5 Hz

No NOE observed between H-13 and H-16.

FIGURE 17 *J*-based configuration analysis of **9**.

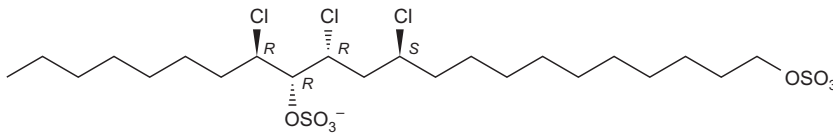

FIGURE 18 Absolute configuration of **9**.

protons and a terminal methyl (H_3-22). The deshielded carbon resonance at δ_C 64.1 (C-13), together with the IR absorption at 588 cm^{-1}, indicated the presence of a chlorine-substituted methine. Further, IR data (ν_{max} 1228 cm^{-1}) and the deshielded methine and methylene carbon signals at δ 81.8 (C-14) and δ 69.2 (C-1) indicated that each carbon was connected to a sulfate ester. Analyses of the COSY and HMBC spectra allowed the assignment of the partial structures. The ESI-MS/MS analysis revealed that the sulfate ester was connected to C-14 and that the chloromethine was located at C-13 (Fig. 5).

The relative configuration of **10** was deduced by *J* values: ^3J(H13,H14), 3.0 Hz; ^3J(C12,H14), −2.4 Hz; ^3J(H13,C15), −1.2 Hz. These values indicated that the axis of C-13/C-14 of **10** was *threo*. Compound **10** was therefore identical to a previously reported CSL (**19**). The absolute configuration of **10** was then identified as 13*R* and 14*R* using a modified Mosher's method after hydrolysis. The absolute configuration of **10** was also identical with **19**, which was determined by comparison of optical rotation after chemical degradation to the alcohol [5].

The molecular formula of **11** was found from HR-ESI-MS data, which suggested that **11** was a monochlorinated linear tetracosane (24 carbons) disulfate. The 1D NMR data and IR spectra of **11** were very similar to those of **10**. However, **11** possessed two additional sp^3 methylenes. The ^1H–^1H COSY, HMBC, edited-HSQC spectra, ESI-MS/MS data, JBCA, and the modified Mosher's method data all suggested that **11** was (14*R*,15*R*)-14-chlorotetracosane-1,15-disulfate (Fig. 19).

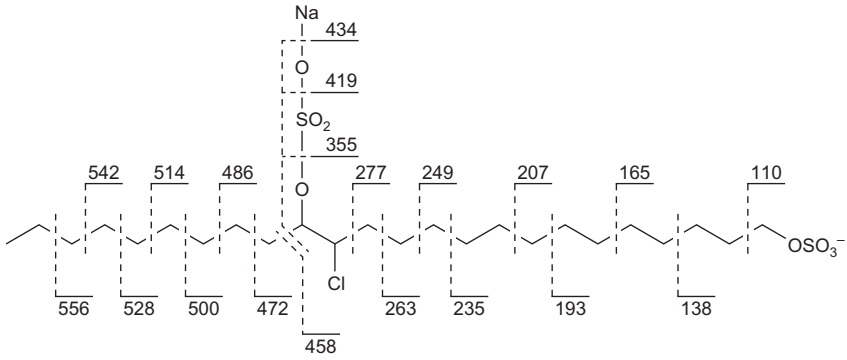

FIGURE 19 MS/MS fragments of **11**.

Compound **12** was expected to be a pentachlorodisulfate, following HR-ESI-MS analysis. However, the ^{1}H NMR spectrum of **12** revealed signals of one oxygenated olefinic proton (δ_H 6.72 for H-1), oxygenated or chlorinated protons (δ_H 4.88, 4.75, 4.53, 4.45, and 4.20 for H-13, 16, 14, 15, and 13, respectively), one primary methyl proton signal (δ_H 0.90, H_3-22), and aliphatic methylene protons (δ_H 1.28–2.52). The ^{13}C NMR chemical shifts obtained from the edited-HSQC spectrum indicated the presence of one olefinic methine (δ_C 136.2, C-1), one quaternary olefinic carbon (δ_C 124.9, C-2), one oxymethine (δ_C 80.7, C-14), four chloromethines (δ_C 68.4, 63.3, 62.4, and 62.3 for C-15, 16, 13, and 11, respectively), one methyl (δ_C 14.5, C-22), and 14 methylenes (δ_C 23.7–45.5). Analysis of the COSY and HMBC spectra and ESI-MS/MS data for **12** determined the planar structure of **12**, as shown in Fig. 5. The geometry of the olefin was proposed to be *E* based on the absence of a NOESY correlation for H-1/H-3. The chemical shifts of this portion matched malhamensilipin A [26,27], but the relative configuration of **12** could not be determined because of its decomposition. Pereira and coworkers have thoroughly discussed the stereochemistry of this type of CSL (see the section on "Total Synthesis of Malhamensilipin A").

In 2007, Darsow and coworkers reported the planar structure of a new tetrachlorosulfolipid (Fig. 20) based on MS^n analyses of an unpurified organic extract via matrix-assisted laser desorption/ionization quadrupole ion trap time-of-flight mass spectrometry (MALDI-QIT-TOF-MS) [44]. The proposed structure, 3,8,12,15-tetrachloroeicosane-1,17,18-triyl tris (hydrogen sulfate),

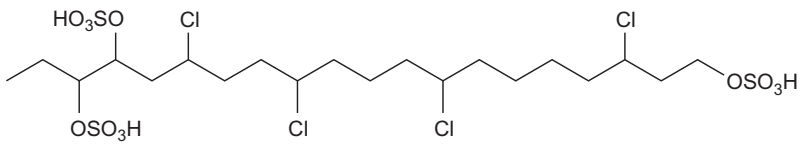

FIGURE 20 Structure of the tetrachlorosulfolipid proposed in 2007.

was not structurally related to danicalipin A or the other precursors described above. In this report, the molecular formula was determined as $C_{20}H_{38}Cl_4O_{12}S_3$, not as $C_{22}H_{40}Cl_6O_8S_2$ (matched to danicalipin A). The difference in the calculated molecular weight between the two potential formulas was 0.0016 Da. Although the authors reported different isotopic ratios for sodium and potassium adducts in the spectrum of the unpurified extract, the compound was not corroborated by any other spectroscopic methods. Further, the strong peak at *m/z* 625, which was ignored by authors, was here assumed to be an important fragment of danicalipin A ($[M-SO_3]^-$). Moreover, the reported isotope patterns of the fragments were in complete agreement with those of danicalipin A. According to the above observations, along with the biogenetical view, we concluded the main component of the analyzed crude lipids was danicalipin A, not a tetrachlorosulfolipid.

MALDI-MS experiments are very useful for finding secondary metabolites from crude extracts. Current MS techniques are very sensitive and are widely used to detect natural products without the requirement for time-consuming purification and collection of sufficient amounts of the sample. However, strong evidence is needed before a new structure can be proposed.

Toxicity of the Chlorosulfolipids

In our study, the isolated chlorosulfolipids from *O. danica* were tested in a brine shrimp toxicity assay [45]. Chlorosulfolipids containing a sulfate were characterized as having higher toxicity to brine shrimp (LC_{50} 0.27 μg/mL), whereas chlorodiol had no toxicity. Other chlorosulfolipids, including danicalipin A, were somewhat toxic (Table 1). These results indicated that the number of chlorine atoms on the chlorosulfolipids did not affect toxicity. Additionally, the Umezawa/Matsuda group described, by evaluation of synthetic chlorosulfolipids (synthetic, enantiomeric, and racemic danicalipin A; Table 1), that the stereochemistry of danicalipin A did not affect its toxicity. According to these results, the toxicity could be caused by the surface-active potency of the amphiphilic molecular character of the chlorosulfolipids.

Biosynthesis of the Chlorosulfolipids in *O. danica*

Although the biosynthetic pathway of chlorosulfolipids is not complete, there is some information available from the early studies, and this is described below. During the 1970s, the groups of Haines [21,23], Elovson [22,46], and Mercer [24,25] independently investigated the biosynthetic pathway of the chlorosulfolipids in *O. danica*. The Haines group declared that the aliphatic chain of chlorosulfolipids was biosynthesized utilizing a normal fatty acid synthesis pathway, as shown by ^{14}C-labeled-acetate-incorporation experiments [21]. They also reported rapid incorporation of carboxy-labeled ^{14}C-oleate and other long-chain fatty acids into the chlorosulfolipids,

TABLE 1 Toxicity of Natural and Synthetic Chlorosulfolipids in Brine Shrimp [10,35]

Compounds		LC_{50} (μg/mL)
Danicalipin A (**1**)		2.2
CSL **6**	(Cl×6, $-OSO_3^-$×1, —OH×1, C_{22})	0.27
CSL **7**	(Cl×6, —OH×2, C_{22})	>30
CSL **8**	(Cl×4, $-OSO_3^-$×2, C_{22})	3.7
CSL **9**	(Cl×3, $-OSO_3^-$×2, C_{22})	6.1
CSL **10**	(Cl×1, $-OSO_3^-$×2, C_{22})	6.9
CSL **11**	(Cl×1, $-OSO_3^-$×2, C_{24})	3.0
CSL **12**	(Cl×3, $-OSO_3^-$×2)	3.8
Synthetic **1**		2.1
Synthetic **1** *ent*-**1**		2.4
Synthetic **1** *rac*-**1**		2.4

suggesting that alkene hydration at C-14 occurred after the aliphatic chain was fully synthesized. In the course of the ^{14}C-labeled incorporation experiments, the Haines group proposed that formation of the diol backbone in the chlorosulfolipids included hydration of an ω-9 unsaturated intermediate [23]. Elovson carried out ^{18}O incorporation experiments *in vivo*. The primary hydroxy group was derived from H_2O of broth, whereas the secondary hydroxy group was derived from molecular oxygen. These results suggested that a docosane 1,14-diol (a precursor of chlorosulfolipids) was synthesized by direct incorporation of a 22(24)-member saturated carbon chain, not via oleic acid [22,46] (Fig. 21). In addition, the Mercer group described the presence of a 3′-phosphoadenosine 5′-phosphosulfate (PAPS)-synthesizing system in *O. danica* and *P. malhamensis*, which suggested the chlorosulfolipids were sulfated through this enzymatic transfer route [24,25].

The system for incorporation of chlorine into the bis-sulfated hydrocarbon backbone, however, was not known completely. The studies performed in the 1970s concluded that the chlorination was caused by enzymes such as haloperoxidases, but at that time, enzymes that catalyzed such oxidations were unknown [23]. Up to the mid-1990s, it was largely accepted that most biological chlorination reactions were catalyzed by chloroperoxidases. However, Dairi *et al*. reported the discovery of a gene that did not code for a chloroperoxidase but was required for halogenation in chlorotetracycline biosynthesis [47]. After that, investigation into new types of enzymatic

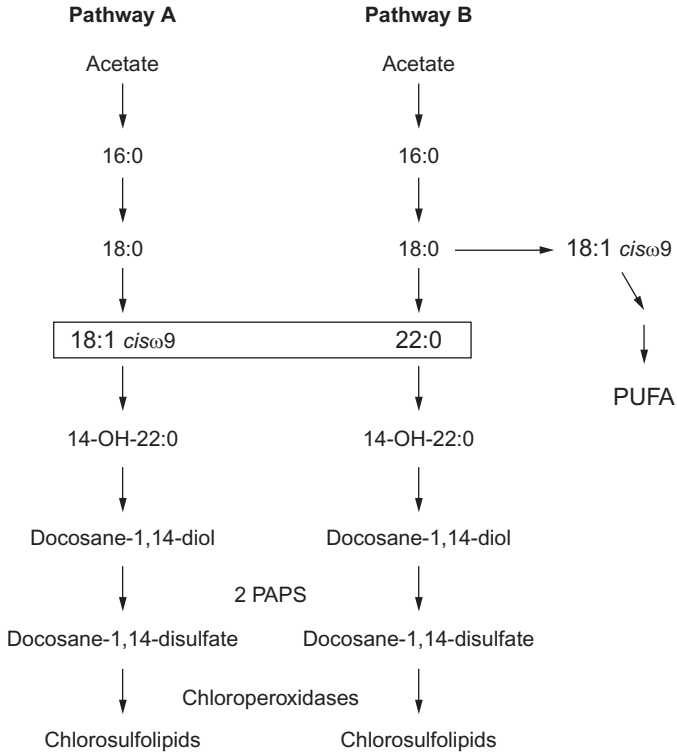

FIGURE 21 Two biosynthetic pathways for chlorosulfolipids in *O. danica*, proposed by the groups of Haines (A) and Elovson (B).

chlorination, such as $FADH_2$-dependent halogenases, non-heme Fe^{II} α-ketoglutarate- and O_2-dependent halogenases, and nucleophilic chlorination, was undertaken [48].

On the basis of our isolation in 2009, danicalipin A and a monochlorosulfolipid **10** comprised ~91% and 5%, respectively, of the total chlorosulfolipids in *O. danica*. We hypothesized that the monochlorinated CSL **10** is an important precursor for chlorosulfolipids. To synthesize danicalipin A, chlorination likely starts in the center of trichloro- and tetrachlorosulfolipid molecules and ends at C-2.

Total Synthesis of Danicalipin A

Between 2009 and 2011, the total synthesis of danicalipin A (**1**) was reported by three independent groups. In 2009, the Vanderwal group reported the first total synthesis of (±)-danicalipin A in parallel with the elucidation of the stereochemistry of danicalipin A hydrolysate, which was first obtained from *O. danica* 40 years ago by Haines [11]. First, the relative stereochemistry of

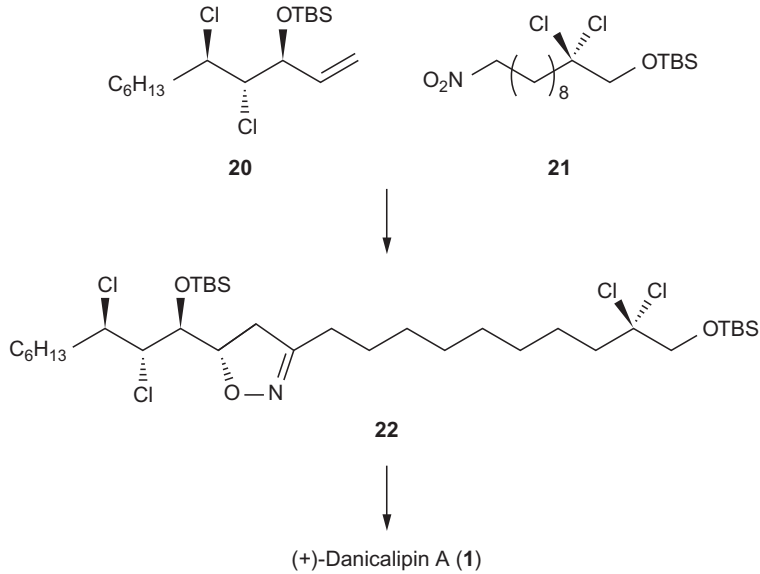

FIGURE 22 Yoshimitsu and Tanaka's synthesis of (+)-danicalipin A (**1**).

the chlorodiol was deduced by JBCA. Total synthesis of (±)-danicalipin A was then carried out using Vanderwal's diastereoselective alkene dichlorination methodology [49,50]. In 2011, the Yoshimitsu/Tanaka [36] and Umezawa/Matsuda groups [35] independently reported the asymmetric total synthesis of (+)-danicalipin A (**1**). Yoshimitsu and Tanaka established the enantiocontroled synthesis of polychlorinated hydrocarbon motifs [34].

Total synthesis of **1** was thus executed via *anti*-isoxazoline **22** by nitrileoxide 1,3-dipolar addition of the stereoselectively chlorinated fragment **20** and nitro compound **21** (Fig. 22) [33]. Umezawa and coworkers achieved the total synthesis of **1** in 17 steps. The *syn*-chlorohydrin **25** was synthesized from the derivative ester of the known chiral epoxide **23**, followed by α-chlorination via aldehyde **26** to yield **27**. A Wittig reaction between **27** and the dichlorinated phosphonium salt **28** furnished *E*-olefin **29** as the major product. The two enantiomeric isomers resulting from dichlorination of *E*-olefin **29** were purified by HPLC. Each hexachloride was sulfated to yield (+)-danicalipin A (**1**) and *ent*-**1** (Fig. 23) [35].

CHLOROSULFOLIPIDS FROM *P. MALHAMENSIS*

Isolation

In 1994, the Gerwick group isolated malhamensilipin A from the alga *P. malhamensis* (Pringsheim) Peterfi. (UTEX L1297), which was cultured in a 50-L Nalgene carboy containing 30L of *Ochromonas* medium with continuous

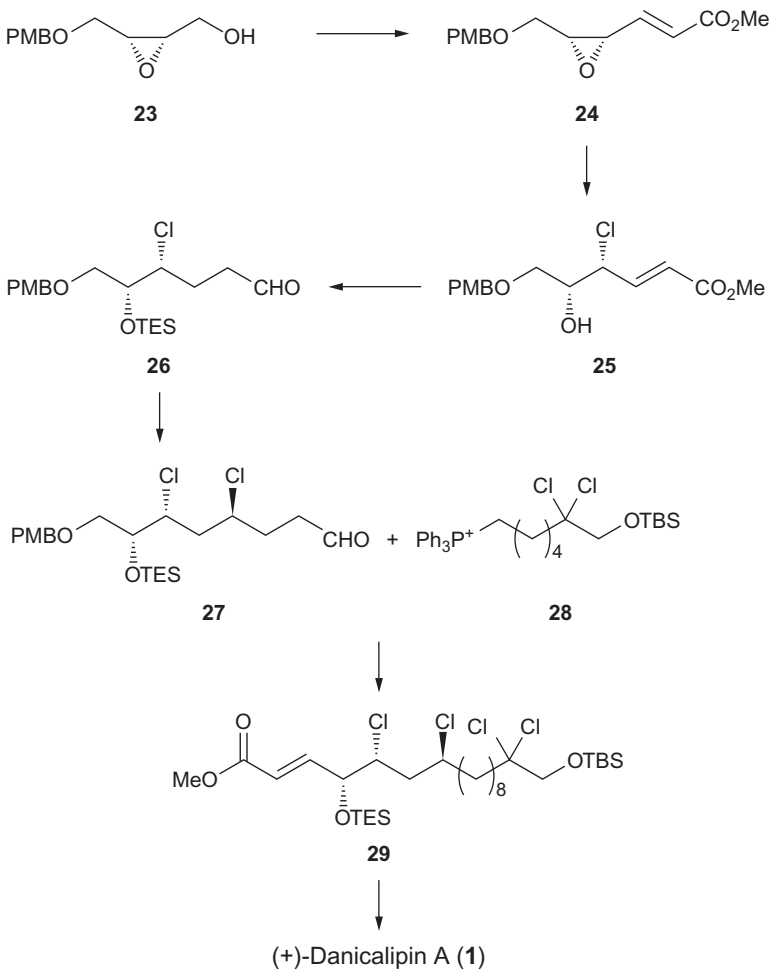

FIGURE 23 Umezawa and Matsuda's synthesis of (+)-danicalipin A (**1**).

stirring at 28 °C for 22 days. The dried cell material (5.56 g) was extracted with $CHCl_3$ and then left overnight in CH_3OH–H_2O (3:1) solution. The extract was then adsorbed with an Amberlite XAD-7 resin. The active MeOH-eluted fraction from XAD-7 was further subjected to Si gel chromatography (MeOH/$CHCl_3$ 12:88) to give **2** as a colorless oil (13.8 mg, ca. 0.25% yield relative to dry weight of cells). Malhamensilipin A (**2**) showed moderate PTK inhibition, as well as antiviral and antimicrobial activity [26].

The same group then reisolated malhamensilipin A in 2010 [27]. *P. malhamensis* (Pringsheim) Peterfi. (SAG 933-1a) was cultured and harvested as described above (30 L of approximately 2×10^5 cells/mL). After filtration through Celite, the cells were lyophilized. The dry material was then extracted

repeatedly with CH_2Cl_2/MeOH (2:1). This portion was fractionated by Si gel CC ($CHCl_3$/CH_3OH 88:12) until an acid-charring material was detected by TLC (33% CH_3OH in $CHCl_3$). This procedure afforded pure **2** (110.5 mg) as a colorless oil.

Structure Elucidation

In 1994, the Gerwick group attempted the structural determination of malhamensilipin A by negative ion HR-FAB-MS and 2D NMR experiments such as ^1H–^1H COSY, ^1H–^1H LRCOSY, HMQC, and HMBC. However, the FAB ionization revealed the $[M-SO_3]^-$ ion as the major fragment, leading to an incorrect molecular formula assignment [26]. They next reported a structure revision and the absolute configuration of malhamensilipin A [27]. The soft ionization by HR-ESI-MS of **2** in MeCN established the actual molecular formula of $C_{24}H_{41}Cl_6O_8S_2$, including two sulfates. To determine the stereochemistry, they created derivatives of **2** with better stability before NMR characterization. The JBCA [39] showed the relative configuration of the middle part of molecule using *J*-resolved NMR pulse sequences like HETLOC and HSQMBC. The geometry of the terminal double bond was deduced as *E* by comparison of NMR data between two model chlorovinyl sulfates, ***Z*-30** and ***E*-30** (Fig. 24). The absolute configuration of **2** was assigned as 14*R* by the modified Mosher's method. Thus, the absolute configuration of **2** was 11*R*, 12*S*, 13*S*, 14*R*, 15*S*, and 16*S*.

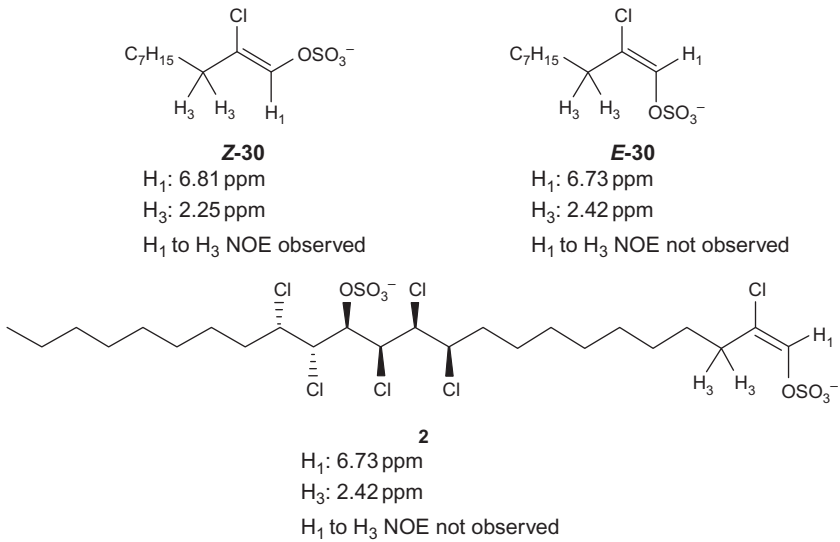

FIGURE 24 Comparison of NMR characteristics between the synthetic model compounds and **2**.

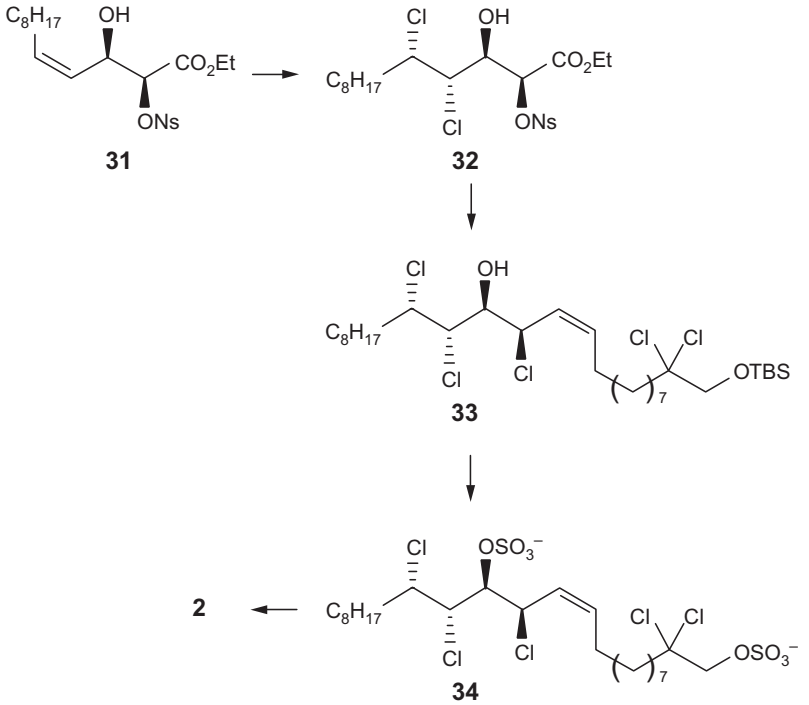

FIGURE 25 The enantioselective synthesis of **2**.

Total Synthesis of Malhamensilipin A

Following the structural revision of malhamensilipin A (**2**), the Vanderwal group started its synthesis. They adopted α-nosylated diol **31** for *anti*-selective dichlorination of *Z*-allylic chloride **33** via stereotetrad **32**. The same procedure used for danicalipin A [11] afforded disulfate **34**. The final step in the total synthesis was carried out using a method that they had developed in model systems to determine the geometry of the chlorovinyl sulfate of **2** (Fig. 25) [32].

CHLOROSULFOLIPIDS FROM ADRIATIC MUSSELS

Hexachlorosulfolipid (Mytilipin A)

Isolation

Mytilipin A (**3**) was isolated from the digestive glands of the mussel *Mytilus galloprovincialis* [28]. The mussels were collected in the autumn of 1998 from one sampling site located along the Emilia Romagna coast of Italy. The digestive glands (4.3 kg) were extracted with acetone. After evaporation, the residual aqueous solution was extracted with EtOAc. The resultant extract

was partitioned between 80% aqueous MeOH and hexane. The 80% MeOH layer was further partitioned between aqueous 60% MeOH and CH_2Cl_2. The dichloromethane soluble portion was then subjected to stepwise ODS column chromatography with MeOH–H_2O (8:2, 9:1, and 10:0), and the last fraction was applied to gel filtration with MeOH. The final HPLC purification was carried out on an ODS column with CH_3CN–H_2O (1:1) as eluent to yield mytilipin A (2.3 mg). Mytilipin A (**3**) was found to inhibit the growth of the cell lines J774, WEHI 164, and P388 with IC_{50} values of 12.1, 16.3, and 10.4 μg/mL, respectively, at 72 h.

Structure Elucidation

The molecular formula of **3** was established by the negative ion HR-FAB-MS spectrum (*m/z* 510.9462; calcd. 510.9419 for $C_{15}H_{23}{}^{35}Cl_5{}^{37}ClO_4S$) and the characteristic isotopic ratio (4:7:6:3:1). The planar structure of **3** was developed from analyses of the IR and NMR spectra including 1D (^1H, ^{13}C, and DEPT) and 2D (^1H–^1H COSY, HOHAHA, HMQC, and HMBC). The *E* geometry of the double bond was determined from the coupling constant between H-14 and H-15 (14.8 Hz), and from the ROESY correlations of H-14/H-12 and H-15/H-13. The planar and absolute configuration of the middle part of **3** was derived from the combination of JBCA [39] and the modified Mosher's method (Fig. 26). This was the first application of JBCA to chlorinated compounds.

Total Synthesis

The first total synthesis of (±)-mytilipin A was achieved by the Carreira group in 2009 [31]. This report was the first laboratory synthesis of a chlorosulfolipid. Regioselective and stereospecific dichlorination, epoxidation, and Wittig olefination afforded olefinic epoxide **36** from ethyl sorbate (**35**). Synthesis of trichloride **38** was accomplished by nucleophilic chlorination of the allylic epoxide of **36** via the unexpected five-member intermediate **37**. Finally, mytilipin A (**3**) was achieved from stereoselective conversion of precursor **38** (Fig. 27).

Asymmetric total synthesis of (+)-mytilipin A (**3**) was accomplished in 2010 by the Yoshimitsu/Tanaka group [33]. They employed their epoxide deoxydichlorination methodology to derive dichloride **40** from protected

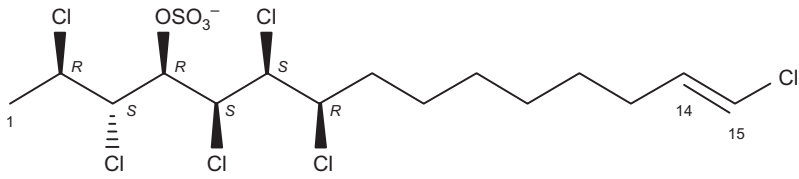

FIGURE 26 Absolute configuration of mytilipin A (**3**).

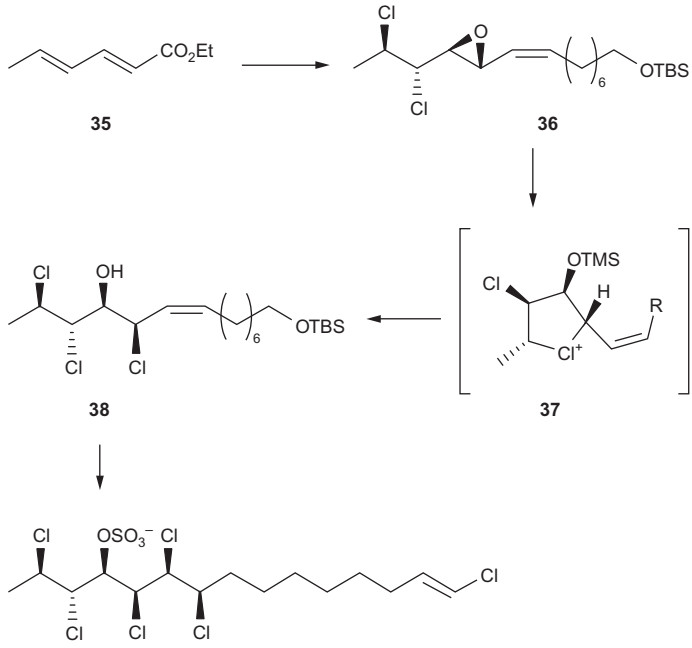

FIGURE 27 The Carreira total synthesis of (±)-mytilipin A (**3**).

epoxide **39**. The stereoselective dichlorination of trichloride **42** from *anti*-alcohol **41** followed Dess–Martin oxidation and allylation of **40**. Allylic oxidation of the *syn*,*syn*-trichloride **42** afforded **43**, followed by alkene cross-metathesis to provide *E*-alkene **44**, which was dichlorinated to afford **45** (Fig. 28).

Polychlorinated Sulfolipids

Isolation

Two chlorosulfolipids were reported by Ciminiello/Fattorusso and coworkers as cytotoxins from digestive glands of the mussel *M. galloprovincialis* [29,30], which were collected from a sampling site located along the Emilia Romagna coast of Italy, in 1999 and 1998 for **4** and **5**, respectively. Mytilipin B (**4**) was isolated from acetone extracts of the digestive glands (1.2kg dry weight). After evaporation, the residue was extracted with EtOAc. The organic solvent was removed and partitioned between hexane and 80% MeOH. The aqueous layer was diluted to 40% MeOH for extraction with CH_2Cl_2. The toxic fraction of the dichloromethane eluate was then evaporated and subjected to ODS column chromatography ($MeOH/H_2O$). The resulting toxic fraction was applied to gel filtration to give the crude toxins. Final purification was carried out by HPLC on an ODS column with 70% MeOH as

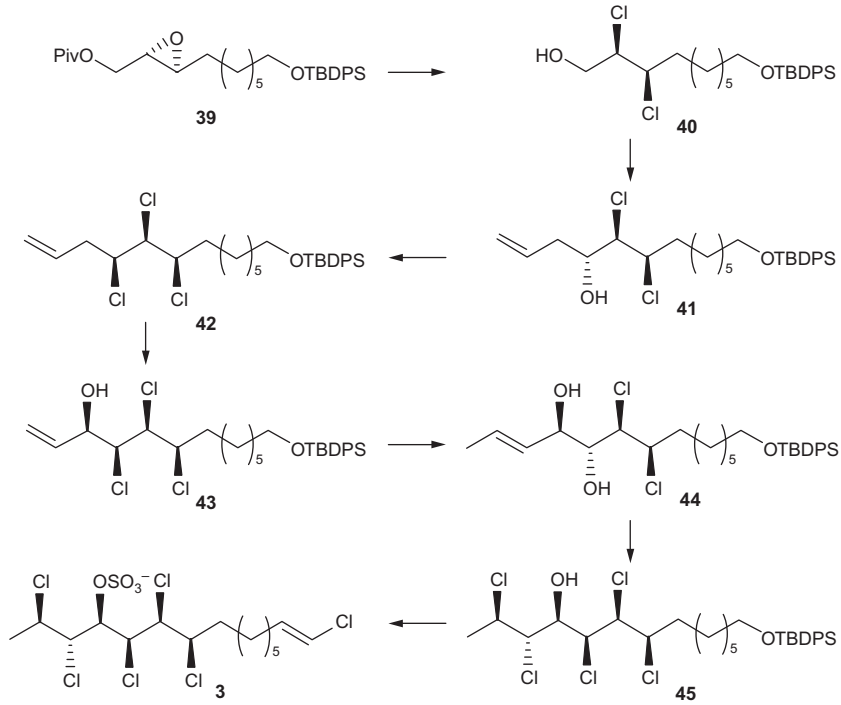

FIGURE 28 The Yoshimitsu/Tanaka asymmetric total synthesis of (+)-mytilipin A (**3**).

eluent to afford pure mytilipin B (**4**) [29]. Mytilipin C (**5**, 2.1mg) was also isolated from the digestive glands (1.8kg dry weight) in a similar way [30].

Structure Elucidation

The negative HR-ESI-MS deduced the molecular formula of mytilipin B (**4**) as $C_{40}H_{66}Cl_{11}O_{11}S$. The combined analyses of 1D and 2D NMR spectra led to the planar structure of the polychlorinated moiety. The residual aliphatic moiety was established by the characteristic NMR signals (δ_H 2.24) coupled to the carbonyl group (δ_C 172.8, C-1), and by the mass fragment ion at *m/z* 255 $[C_{16}H_{31}O_2]^-$ (Fig. 29). The *E* geometry of the olefin was determined by the large proton–proton coupling constant (*J* 15.3Hz) between H-2′ and

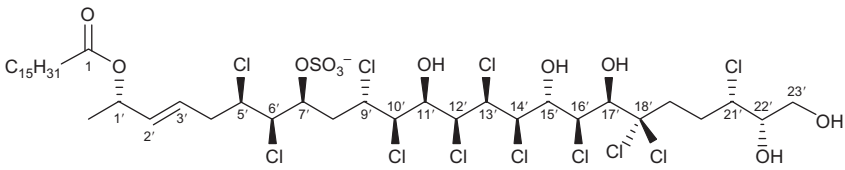

FIGURE 29 Chemical structure of mytilipin B (**4**).

H-3′. The JBCA method [39] was then applied to solve the stereochemistry of the polychlorinated moiety. The absolute configuration of **4** was determined by the modified Mosher's method. In particular, the stereochemistry at C-1 was deduced by analysis of Reguera's simplified approach for the Mosher method [51]. On the basis of this information, the whole absolute configuration of the molecule was consequently assigned as 1′*S*, 5′*R*, 6′*R*, 7′*S*, 9′*S*, 10′*R*, 11′*R*, 12′*S*, 13′*S*, 14′*R*, 15′*R*, 16′*S*, 17′*R*, 21′*S*, and 22′*S* [29].

The structure of mytilipin C (**5**), a 17′-dehydroxy derivative of mytilipin A, was determined by a similar procedure as that used for **4** [30].

CONCLUSIONS

In the early studies, chlorosulfolipids were detected from Xanthophyceae, Chlorophyceae, and Cyanophyceae, but the isolation and the analysis of these lipids were not successful because of the very small quantities in their algae [52]. Subsequently, Mercer and Davis studied the distribution of chlorosulfolipids from a wide range of algal classes (30 species, marine and freshwater). Their results indicated that most of the freshwater species contained a small amount of chlorosulfolipid, but that the golden algae *O. danica* and *P. malhamensis* contained large quantities. They found that no marine species produced chlorosulfolipids [53].

Recently, the Sheu group reported the characterization of mytilipin A, 15-dechlorinated mytilipin A, and the corresponding alcohols from soft coral [54]. As discussed above, chlorosulfolipids had previously been isolated from mussels. It is therefore likely that these chlorosulfolipids in marine animals are derived from marine microalgae.

Ochromonas contains significant quantities of chlorosulfolipids, but does not contain phospholipids. In previous studies, the chlorosulfolipids were thus considered to be a constituent of the cell membranes instead of phospholipids in bilayers. However, Brown and Elovson noted that the polar, diacylated glycerol ether lipid of *N*,*N*,*N*-trimethylhomoserine was the true cell membrane element of the alga [55]. Although this amphiphilic betaine lipid was first isolated from *O. danica*, it is widely distributed in lower plants and algae, as well as in some nonphotosynthetic microorganisms [56]. This issue should be investigated in the future.

The preferred conformations for chlorosulfolipids were found to be mostly *gauche* for the electronegative substituents. These conformational preferences are based on the maximization of relative gauche orientations caused by the "gauche effect." This was attributed primarily to σ-hyperconjugation (in this case, σC—H–σ*C—Cl) [57].

The curved molecular shape of danicalipin A is shown in Fig. 30. In contrast to general bilayer lipids, this lipid has two polar units located at the terminus and center of the molecule. The question of how these lipids behave *in vivo* has not yet been answered.

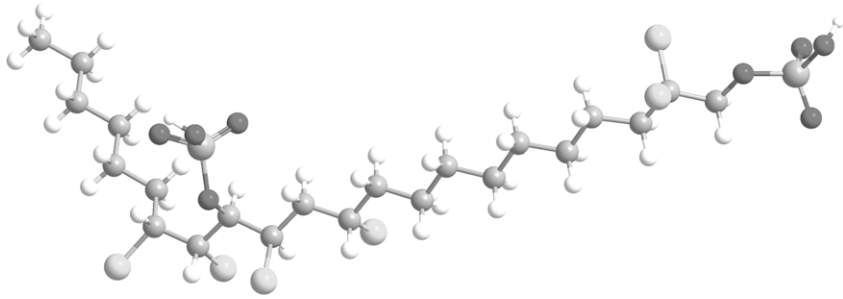

FIGURE 30 Stereochemical model of danicalipin A (**1**).

ABBREVIATIONS

BuOH	butanol
CC	column chromatography
$CHCl_3$	chloroform
CH_3CN	acetonitrile
CSL	chlorosulfolipid
COSY	correlation spectroscopy
DQF	double quantum filter
ELSD	evaporative light-scattering detector
ESI	electrospray ionization
EtOAc	ethyl acetate
FAB	fast atom bombardment
HMBC	heteronuclear multiple-bond connectivity
HPLC	high-performance liquid chromatography
HR	high resolution
HSQC	heteronuclear single quantum coherence
JBCA	*J*-based configuration analysis
MeOH	methanol
MS	mass spectrometry
NMR	nuclear magnetic resonance
NOESY	NOE correlated spectroscopy
ODS	octadecylsilyl
PTSA	*p*-toluenesulfonic acid
PUFA	polyunsaturated fatty acids
TMS	trimethylsilyl
UV	ultraviolet

REFERENCES

[1] T.H. Haines, R.J. Block, J. Protozool. 9 (1962) 33–38.
[2] J. Elovson, P.R. Vagelos, Proc. Natl. Acad. Sci. USA 62 (1969) 957–963.

[3] J. Elovson, P.R. Vagelos, Biochemistry 9 (1970) 3110–3126.
[4] G.L. Mayers, T.H. Haines, Biochemistry 6 (1967) 1665–1671.
[5] T.H. Haines, M. Pousada, B. Stern, G.L. Mayers, Biochem. J. 113 (1969) 565–566.
[6] G.L. Mayers, M. Pousada, T.H. Haines, Biochemistry 8 (1969) 2981–2986.
[7] T.H. Haines, Prog. Chem. Fats Other Lipids 11 (1971) 297–345.
[8] T.H. Haines, Annu. Rev. Microbiol. 27 (1973) 403–412.
[9] T.H. Haines, J.A. Erwin (Ed.), Lipids and Biomembranes of Eukoryotic Microorganisms, Academic Press Inc., New York, 1973, pp. 197–232.
[10] T. Kawahara, Y. Kumaki, T. Kamada, T. Ishii, T. Okino, J. Org. Chem. 74 (2009) 6016–6024.
[11] D.K. Bedke, G.M. Shibuya, A. Pereira, W.H. Gerwick, T.H. Haines, C.D. Vanderwal, J. Am. Chem. Soc. 131 (2009) 7570–7572.
[12] K. Reich, M. Spiegelstein, Isr. J. Zool. 13 (1964) 141.
[13] D.A. Leeper, K.G. Porter, Arch. Hydrobiol. 134 (1995) 207–222.
[14] J.E. Boxhorn, D.A. Holen, M.E. Boraas, Hydrobiologia 387–388 (1998) 283–287.
[15] J. Boenigk, P.J. Stadler, Plankton Res. 26 (2004) 1507–1514.
[16] J.A. Hansen, Physiol. Plant. 29 (1973) 234–238.
[17] S. Halevy, R. Saliternik, L. Avivi, Int. J. Biochem. 2 (1971) 185–192.
[18] A. Magazanik, S. Halevy, Experientia 15 (1973) 310–311.
[19] L.L. Chen, M. Pousada, T.H. Haines, J. Biol. Chem. 251 (1976) 1835–1842.
[20] L.L. Chen, T.H. Haines, J. Biol. Chem. 251 (1976) 1828–1834.
[21] C.L. Mooney, E.M. Mahoney, M. Pousada, T.H. Haines, Biochemistry 11 (1972) 4839–4844.
[22] J. Elovson, Biochemistry 13 (1974) 2105–2109.
[23] C.L. Mooney, T.H. Haines, Biochemistry 12 (1973) 4469–4472.
[24] E.I. Mercer, G. Thomas, J.D. Harrison, Phytochemistry 13 (1974) 1297–1302.
[25] G. Thomas, E.I. Mercer, Phytochemistry 13 (1974) 797–805.
[26] J.L. Chen, P.J. Proteau, M.A. Roberts, W.H. Gerwick, D.L. Slate, R.H. Lee, J. Nat. Prod. 57 (1994) 524–527.
[27] A.R. Pereira, T. Byrum, G.M. Shibuya, C.D. Vanderwal, W.H. Gerwick, J. Nat. Prod. 73 (2010) 279–283.
[28] P. Ciminiello, E. Fattorusso, M. Forino, M. Di Rosa, A. Ianaro, R. Poletti, J. Org. Chem. 66 (2001) 578–582.
[29] P. Ciminiello, C. Dell'Aversano, E. Fattorusso, M. Forino, S. Magno, M. Di Rosa, A. Ianaro, R. Poletti, J. Am. Chem. Soc. 124 (2002) 13114–13120.
[30] P. Ciminiello, C. Dell'Aversano, E. Fattorusso, M. Forino, S. Magno, P. Di Meglio, A. Ianaro, R. Poletti, Tetrahedron 60 (2004) 7093–7098.
[31] C. Nilewski, R.W. Geisser, E.M. Carreira, Nature 457 (2009) 573–577.
[32] D.K. Bedke, G.M. Shibuya, A.R. Pereira, W.H. Gerwick, C.D. Vanderwal, J. Am. Chem. Soc. 132 (2010) 2542–2543.
[33] T. Yoshimitsu, N. Fujumoto, R. Nakatani, N. Kojima, T. Tanaka, J. Org. Chem. 75 (2010) 5425–5437.
[34] T. Yoshimitsu, N. Fukumoto, T. Tanaka, J. Org. Chem. 74 (2009) 696–702.
[35] T. Umezawa, M. Shibata, K. Kaneko, T. Okino, F. Matsuda, Org. Lett. 13 (2011) 904–907.
[36] T. Yoshimitsu, R. Nakatani, A. Kobayashi, T. Tanaka, Org. Lett. 13 (2011) 908–911.
[37] E.M. Carreira, K.C. Nicolaou, J.S. Chen (Eds.), Classics in Total Synthesis III: Further Targets, Strategies, Methods, Wiley-VCH, Weinheim, 2011, pp. 595–614.
[38] D.K. Bedke, C.D. Vanderwal, Nat. Prod. Rep. 28 (2011) 15–25.

[39] N. Matsumori, D. Kaneno, M. Murata, H. Nakamura, K. Tachibana, J. Org. Chem. 64 (1999) 866–876.
[40] M. Kurz, P. Schmieder, H. Kessler, Angew. Chem. Int. Ed. Engl. 30 (1991) 1329–1331.
[41] U. Wollborn, D. Leibfritz, J. Magn. Reson. 98 (1992) 142–146.
[42] R.T. Willamson, B.L. Marquez, W.H. Gerwick, G.E. Martin, V.V. Krishnamurthy, Magn. Reson. Chem. 39 (2001) 127–132.
[43] W. Willker, D. Leibfritz, Magn. Reson. Chem. 33 (1995) 632–638.
[44] K.H. Darsow, H.A. Lange, M. Resch, C. Walter, R. Buchholz, Rapid Commun. Mass Spectrom. 21 (2007) 2188–2194.
[45] B.N. Meyer, N.R. Ferrigni, J.E. Putnam, L.B. Jacobsen, D.E. Nichols, J.L. McLaughlin, Planta Med. 45 (1982) 31–34.
[46] J. Elovson, Biochemistry 13 (1974) 3483–3487.
[47] T. Dairi, T. Nakano, K. Aisaka, R. Katsumata, M. Hasegawa, Biosci. Biotechnol. Biochem. 59 (1995) 1099–1106.
[48] C.D. Murphy, Nat. Prod. Rep. 23 (2006) 147–152.
[49] G.M. Shibuya, J.S. Kanady, C.D. Vanderwal, J. Am. Chem. Soc. 130 (2008) 12514–12518.
[50] J.S. Kanady, J.D. Nguyen, J.W. Ziller, C.D. Vanderwal, J. Org. Chem. 74 (2009) 2175–2178.
[51] S.K. Latypov, J.M. Seco, E. Quinoà, R. Riguera, J. Am. Chem. Soc. 120 (1998) 877–882.
[52] E.I. Mercer, C.L. Davis, Phytochemistry 14 (1975) 1545–1548.
[53] E.I. Mercer, C.L. Davis, Phytochemistry 18 (1979) 457–462.
[54] C.H. Chao, H.C. Huang, G.H. Wang, Z.H. Wen, W.H. Wang, I.M. Chen, J.H. Sheu, Chem. Pharm. Bull. 58 (2010) 944–946.
[55] A.E. Brown, J. Elovson, Biochemistry 13 (1974) 3476–3482.
[56] N. Sato, Bot. Mag. Tokyo 105 (1992) 185–197.
[57] R.W. Hoffmann, Angew. Chem. Int. Ed. 39 (2000) 2054–2070.

Chapter 8

Diversity and Ecological Significance of Fungal Endophyte Natural Products

Soizic Prado, Yanyan Li and Bastien Nay
Muséum National d'Histoire Naturelle, CNRS-UMR 7245, Unité Molécules de Communication et Adaptation des Micro-organismes, Paris, France

INTRODUCTION

The importance of natural products isolated from endophytic fungi has continuously grown in the past 10 years as demonstrated by leading review papers on the subject [1]. According to Arnold's account in 2007 [2], research reports on the diversity of symbiotic endophytes have increased from an average of 1.2 publications per year for the period 1971–1991 to 15 per year from 2001. This resurgence of interest comes along with ecologically relevant studies, including chemical ecology and natural product chemistry of fungal metabolites, since the number of publications in these fields rose from 0.8 publications per year in the 1970s to more than 200 in the past 6 years. However, most of the reported data on natural products from endophytic fungi are dealing with isolation and analysis of bioactive compounds and very few papers focus on the function of these compounds in the environment, particularly with regard to plant–endophyte associations. Even though, it is difficult to link the biological activities measured in the laboratory to any ecological role. Indeed, it is not certain that concentrations used under laboratory conditions are ecologically relevant. Nevertheless, biological screenings shed light, at least in part, on the potential power of endophytic natural products in the plant life and on their environmental consequences.

In this chapter, we chose to focus on the ecological purpose of fungal endophyte natural products. Unfortunately, we had to exclude many structurally interesting compounds due to a lack of knowledge regarding their ecological role. Moreover, on the contrary to the previous review concerning the role of endophytic metabolites in plant protection [3], we chose to organize our

Bioactive Natural Products, Vol. 36. DOI: 10.1016/B978-0-444-53836-9.00025-6

discussion according to the logic of biosynthetic classification, by compound classes rather than by biological activities. Indeed, very often, compound classes are attached to a particular activity and can be shared by many fungal species or genus.

WHAT ARE ENDOPHYTIC FUNGI?

Definition

All plants in natural and anthropogenic ecosystems are colonized by unapparent and symptomless microscopic fungi called endophytes. They invade the living tissues of the host plant for all or part of their life cycles without any symptom of disease. Remarkably, as many as hundreds of species of these microorganisms can be isolated from a specific plant [1,2].

Two major groups of endophytes have been described, sharing different life histories. On the first hand, grass endophytes, restricted to a small number of phylogenetically related species of the *Clavicipitaceae*, are transmitted vertically (from mother to offsprings through seeds) [4] and were reported as the causative agent of toxic syndromes experienced by animals that consume infected grass. These endophytes have been extensively studied and are considered as defensive mutualists of host-grasses [5]. On the other hand, the second group of endophytes, isolated from asymptomatic tissues of all other plants (from ferns to conifers or angiosperms), is mainly represented by highly diverse non-Clavicipitaceous Ascomycetes which are traditionally treated as a single functional group, with different types depending on life history or ecological interactions [6].

Initially, the non-Clavicipitaceous endophytic fungi did not receive much attention before the detection of traces of paclitaxel (Taxol®) in the endophytic fungus *Taxomyces andreanae* isolated from *Taxus brevifolia* [7]. Since then, they have been identified as a rich source of biologically active metabolites [1]. Nevertheless, even if endophytes constitute a large reservoir of unique chemical structures, very little is known about the role of fungal metabolites in the host plant and their ecological significance.

Their Role in the Environmental Context

Clavicipitaceous *Endophytes*

Many *Clavicipitaceous* endophytes can protect their hosts from a variety of biotic and abiotic stresses, particularly from mammalian and insect herbivore damage [5,8]. These benefits arise in part from the production of alkaloidic mycotoxins that are described later in this chapter. Ergot and lolitrem alkaloids primarily affect mammals while peramine and loline alkaloids are generally associated with resistance to insects. This association between the grass and the endophyte is considered mutualistic (Fig. 1) since the association with

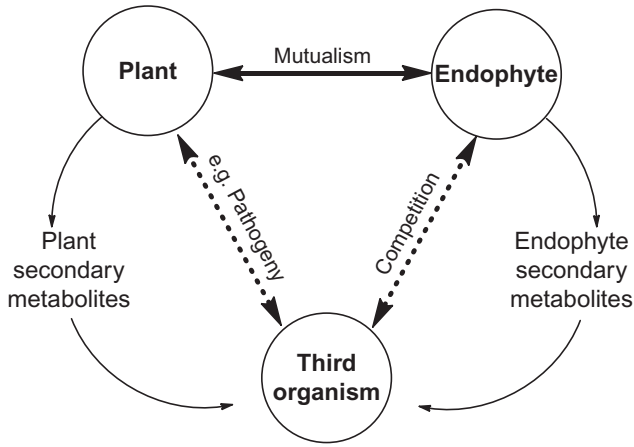

FIGURE 1 Representation of a tripartite relationship between a plant, its endophytic community, and a third organism, for example, a pathogenic fungus.

endophytes helps grasses to gain defensive features. In return, endophytes acquire nutrients and habitat from the host plant.

Other studies have provided evidence for antinematode activity. Infection of tall fescue (*Festuca arundinacea*) with the endophytic fungus *Acremonium coenophialum* has been shown to reduce nematode population in field soils [9]. Activities of grass endophytes against plant pathogens have been reported [10] with indole derivatives, sesquiterpenes, and a diacetamine produced by *Epichloë festucae* accounting for the growth inhibition of other fungi *in vitro*. Similar inhibition of plant pathogens such as *Sclerotina homeocarpa* and *Laetisaria fusiformis* by *E. festucae* has been documented [11]. Moreover, grass endophytes may enhance the ecophysiology of host plants to counter non-biotic stresses (i.e., drought and metal contamination) [12]. *Neothyphodium coenophialum* infection leads to development of the root system, resulting in drought tolerance and/or faster recovery from water stress. Endophytes can also stimulate longer root hair and enhance exudation of "phenolic like compounds" into the rhizosphere, resulting in a more efficient absorption of soil phosphorus and enhanced aluminum tolerance via chelation [12b]. Increased tolerance to other environmental stresses such as heat [13] and low soil fertility [12b] have been reported. The mechanisms responsible for these benefits yet remain unresolved.

Consequently, many endophyte species may have a great economic and ecological importance, such as *Lolium perenne*, *Lolium multiflorum* which colonize pasture and turf (*Festuca pratensis* and *Festuca rubra*). Endophyte infection has clearly the potential of affecting multiple trophic levels, and we have to keep in mind that it may have cascade effects on cocultured plants and their consumers.

Non-Clavicipitaceous *Endophytes*

Non-*Clavicipitaceous* endophytes have also been shown to establish symbiotic associations with their host plants, conferring fitness benefits such as biotic and abiotic stress tolerance, nutrient acquisition, and increased growth and yields [14]. Despite their ubiquitous occurrence in natural and anthropogenic ecosystems, the role of unspecialized fungal endophytes in mediating plant–insect interactions has been largely ignored compared to Clavicipitaceous fungi in grasses. To date, only few studies have stated the effect of these endophytic fungi on insect herbivores [8], with evidence that when endophytes were inoculated into plants, the performance of shoot-feeding by insects was reduced. For example, the endophyte *Acremonium strictum* enhanced the mortality of the polyphagous moth *Helicoverpa armigera*. Similarly, the methanol extract of endophytes isolated from cotton leaves in Australia reduced the larval growth of the same insect pest [15]. It should be noted that some entomopathogenic fungi can behave as endophytes, colonizing plant tissues and providing lasting protection. It is the case of *Beauveria bassiana*, which has been isolated as an endophyte from many plants under natural conditions and of the fungus *Lecanicillium* spp. [16].

Endophytes can also, to some extent, protect hosts against fungal pathogens. For example, the presence of endophytes in the leaves of *Theobroma cacao* can significantly decrease both leaf necrosis and leaf mortality when the plant is challenged with the pathogen *Phytophthora* sp. [14b]. The mechanism of host protection can be mediated either by secondary metabolites or by mycoparasitism or induction of systemic resistance [17]. Endophytic isolates confer resistance to pathogens in barley (*Hordeum vulgare*). This was correlated to increased concentrations of phenolic compounds [18]. Further, the significant antifungal activity of the maize endophyte *Acremonium zeae* against the phytopathogens *Aspergillus flavus* and *Fusarium verticilloides* has been proved to be mediated by the production of complex polyketides (see below) [14e]. A new endophytic species, *Trichoderma stromaticum*, was isolated from the "witches' broom" of *T. cacao* in Brazil, caused by the fungus *Crinipellis perniciosa*. This *Trichoderma*, when applied to dry infected brooms, is able to prevent the formation of new inoculum of *C. perniciosa* through suppression of basidioma formation, thus reflecting a direct parasitism mechanism [19]. Finally, endophytes can contribute to host defense against phytopathogens by controlling plant physiology. Compounds such as indole acetic acid could be responsible for a possible regulation of plant processes by the endophyte [3].

It is clear that endophytes can limit plant stresses through symbiosis. For example, the endophyte *Curvularia protuberate* colonizes all the tissues of the geothermal plant *Dichanthelium lanuginosum*. Nevertheless, when grown separately, neither the plant nor the fungus can endure temperatures above 40°C, while the symbiosis allows both partner to withstand a temperature of 65°C [14a]. Similarly, the growth of the plant *Leymus mollis* is retarded when exposed to levels of salinity in the absence of the endophyte *Fusarium*

culmorum, while both partners in symbiosis can tolerate sea water level of salinity [17]. The cellular mechanisms involved in such stress tolerance and growth enhancement are not known.

The Balance Between Mutualism and Pathogeny

Although it is commonly accepted that endophytes can have profound effects on plant ecology, fitness, and evolution, some examples attest that endophytes can become parasites, cause disease, or reduce fitness of their host plants under certain conditions [20]. Indeed, endophytes and pathogens can both share many of the virulence factors, being able to synthesize phytotoxic mycotoxins and to produce exoenzymes which are necessary to infect and colonize the host [21]. Thus, it is likely that these fungi may be mutualistic or pathogenic depending on circumstances, and the status of the endophyte was regulated at several steps of different physiological processes. The association between fungal endophytes and plant hosts might therefore be regulated by an equilibrium between fungal virulence and plant defence. If such balance is disturbed, a plant disease may develop [1b]. Actually, a recent work has demonstrated that the asymptomatic–endosymbiotic fungus *Diplodia mutila* in the palm *Iriartea deltoidea* can become pathogen under high light exposition, triggering hypersensibility, cell death, and tissue necrosis in the palm [22].

WORKING WITH ENDOPHYTIC FUNGI: PRINCIPLES OF ISOLATION AND CULTIVATION

Isolation of Endophytic Fungi from Plants

The most frequently utilized method to isolate endophytic fungi involves isolation from surface-sterilized host plant tissues [23]. Surface sterilization of plant material can be accomplished by treatment with a strong oxidant followed by sterile rinse. Endophytes are generally isolated by cutting individual plant organs into segments, within 4 h of collection of the plant specimen. Surface sterilization is then realized by sequential immersion (e.g., 5 s in 95% ethanol, then 2 min in 0.5% sodium hypochlorite, and 2 min in 70% ethanol). Fragments will be air-dried under sterile conditions before plating on malt extract agar (MEA) or potato dextrose agar (PDA) which support growth by diverse endophytes. Plates will be sealed and incubated at 25 °C. After several days or weeks of incubation, hyphal tips of the fungal endophyte are removed and transferred to freshly prepared plates.

Identification of Endophytic Fungi

Identification of endophytes requires morphological examination of fungal cultures, mechanisms of sporulation and characteristics of spores. Nevertheless, most of endophytes remain sterile under artificial cultivation, making

morphology-based identification impossible. They are thus identified by analysis of the internal transcribed spacers (ITS) of the 18S ribosomal DNA sequences (ITS1 and ITS2, recognized as a species-level molecular marker in the fungi). Sequences sharing at least 97% pairwise similarity (which is within the range of intraspecific species divergence in fungi) are then grouped in "Operational Taxonomic Units" and identified using the BLAST option in NCBI GenBank database. If no match is found using 18S rDNA, the more conservative 28S rDNA (for which numerous sequences are available in GenBank) can be used to allow, at least, assignment of the taxa to the family or order level. Alternatively, the complementary metagenomic approach, using environmental PCR, can be undertaken to recover endophytes that are not growing on standard culture media or that have obligatory host associations. This approach allows the evaluation of the global (including non-cultivable) diversity of fungal endophytes [24].

Culture Conditions of Endophytic Fungi and Production of Metabolites

A great deal of uncertainty exists between what an endophyte produces in culture and what it may produce in nature. However, quite commonly, endophytes produce secondary metabolites when placed in culture. The temperature, the medium composition, and the degree of aeration will affect the amount and type of compounds that are produced. Paragama and coworkers have investigated the effect of culture conditions on metabolite production by endophytic fungi *Paraphaeosphaeria quadriseptata* and *Chaetomium chiversii* [25]. These studies indicated that the production of the major metabolites by *P. quadriseptata* differs when the water used to make the media was changed from tap water to distilled water. In the same way, the study of the metabolites of the endophytic fungus *Sphaeropsidales* sp. clearly shows that the major breakthrough was solid-phase cultivation in flasks with wet oat grains as a single substrate, probably due to the more natural living conditions compared to standard liquid cultures [26].

This ability of endophytes to produce secondary metabolites, combined with the potential to bring up metabolic variations from a single strain by systematic alteration of its cultivation parameters—known as OSMAC (one strain many compounds) approach [27]—and the use of elicitors to induce or inhibit certain biosynthetic and/or signal transduction pathways, provides new opportunities to maximize chemical diversity. The OSMAC approach results from the observation that very small changes in the cultivation conditions can cause dramatic shift of the metabolic profile of many microorganisms. It would represent a powerful tool to elucidate the secondary metabolome of different endophytes, especially when trying to mimic natural conditions.

STRUCTURES OF ENDOPHYTIC NATURAL PRODUCTS WITH REGARD OF THEIR ECOLOGICAL ROLE

Endophytic Alkaloids: Their Particular Role in Grass Life

Up to now, due to agricultural consequences, the most understood story concerning endophytic alkaloids is related to the mutualistic association between grasses and the fungal family of Clavicipitaceae, Ascomycota (e.g., *Neotyphodium* and its sexual form *Epichloë* associated to *Lolium* and *Festuca* grasses) [4,28]. Not only this association can alter multitrophic interactions by changing food web dynamics [28c], especially when insects are concerned [29], but also plant diversity [30]. We can define four types of alkaloids potentially involved in this relation, on the basis of their biosynthetic origin: isoprenyl-indole alkaloids derived by L-tryptophan (ergot alkaloids), indole-diterpene and -triterpene alkaloids derived by indole-3-glycerol phosphate (tremorgenic alkaloids), loline-related alkaloids derived by L-homoserine and L-proline, and peramine-related cyclodipeptide alkaloids derived by L-proline and L-arginine.

A plethora of indole-terpene alkaloids have been described, with variable complexity on the terpenoid moiety. Their presence leads to a wide range of biological activities to the benefit of the host plant, especially by toxicity against insect, below-ground nematode, or vertebrate herbivores. Indeed, one of the most evident effects of these alkaloids is the neurotoxic syndrome of cattle and livestock which graze endophyte-infected grasses (especially tall fescue and ryegrass) [31]. This may cause serious troubles in agriculture (contaminated forage), although the presence of *Neotyphodium* endophytes which produce alkaloids in crop has also been considered profitable due to improved resistance to insect and increased overwintering survival [32].

The prenyl-indole alkaloids (ergot alkaloids) were first isolated from the crop parasitic genus *Claviceps*. In fact, they are also synthesized by many endophytic fungi of the family Clavicipitaceae, colonizing Poaceae, Polygalaceae, or Convolvulaceae [33]. The typical nucleus is tetracyclic on the model of D-lysergic acid (**1a**) (Fig. 2). Chemical diversity arises from functionalization at C-8, defining alkaloid subclasses (clavines, ergoamides, and ergopeptines). During the past 10 years, mainly already known ergot alkaloids have been isolated from endophytic fungi, and the reader is asked to refer to a more specialized review for details [33]. Endophytic fungi of the *Epichloë*–*Neotyphodium* complex and the genus *Balansia* only produce ergot alkaloids, especially ergovaline (**2**) and lysergic acid amide (**1b**), when they are associated with their host plant, fungal axenic cultures remaining free of alkaloid [34,35]. The presence of ergot alkaloids in a plant would be the signature of symbiosis between an Ascomycota and a plant from the Poaceae or the Convolvulaceae family. Ergovaline (**2**) is nematicidal at 5 µg/mL, providing protection against below-ground herbivores [36] and most of the ergot alkaloids

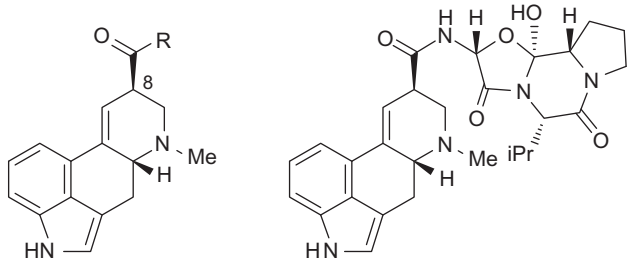

R = OH: D-lysergic acid (**1a**)
R = NH_2: D-lysergic amide (**1b**)

Ergovaline (**2**)

FIGURE 2 Structure of some common ergot alkaloids.

are neurotoxic to mammals due to potent interactions with neurotransmitters in the central nervous system.

The ergot alkaloid biosynthesis (EAS) has been studied in detail at the genetic and functional level in both plant pathogen *Claviceps* species [35] and endophyte *Neotyphodium* species [34,37,38]. Analysis by reverse transcription-PCR revealed that the *eas* genes are specifically expressed *in planta* [35]. Feeding with labeled precursors and gene inactivation experiments have established that the first committed step of the pathway leading to ergopeptines is isoprenylation of tryptophan to form 4-dimethylallyltryptophan (DMAT: **3**), followed by a series of transformations to yield D-lysergic acid (**1a**) (Fig. 3). Subsequent formation of lysergylpeptide is catalyzed by two non-ribosomal peptide synthetases (NRPSs). NRPSs are multifunctional mega-enzymes that are organized into modules. Each module is composed of distinctive active sites (called domains) that are required for activation and incorporation of one amino acid into the peptide chain [40].

As suggested for ergovaline biosynthesis in *Neothyphodium lolii*, D-lysergic acid is activated by LspB (Fig. 3), a single module NRPS, and transferred to the trimodular NRPS LpsA for consecutive elongation with Gly, Val, and Pro. The lysergyl tripeptide is released from the megasynthase as ergopeptam (**4**) followed by a P450 monooxygenase-catalyzed cyclization to form ergovaline (**2**). Major structural differences of ergopeptine alkaloids reside in the composition of the peptide moiety attached to D-lysergic acid. Investigation of the gene cluster for ergopeptines biosynthesis in *Claviceps purpurea* which revealed two additional encoded NRPSs, together with gene inactivation experiments [39], have provided important evidence that amino acid specificity of NRPSs is the biosynthetic origin of ergopeptines chemical diversity.

The indole-diterpenes are known as tremorgenic mycotoxins. They are produced by many Ascomycota fungi, especially the grass-associated endophytes *Neotyphodium* and *Epichloë*. In particular, lolitrem B (**5**) (Fig. 4) has been identified in 1984 after isolation from *N. lolii* and was shown to be the

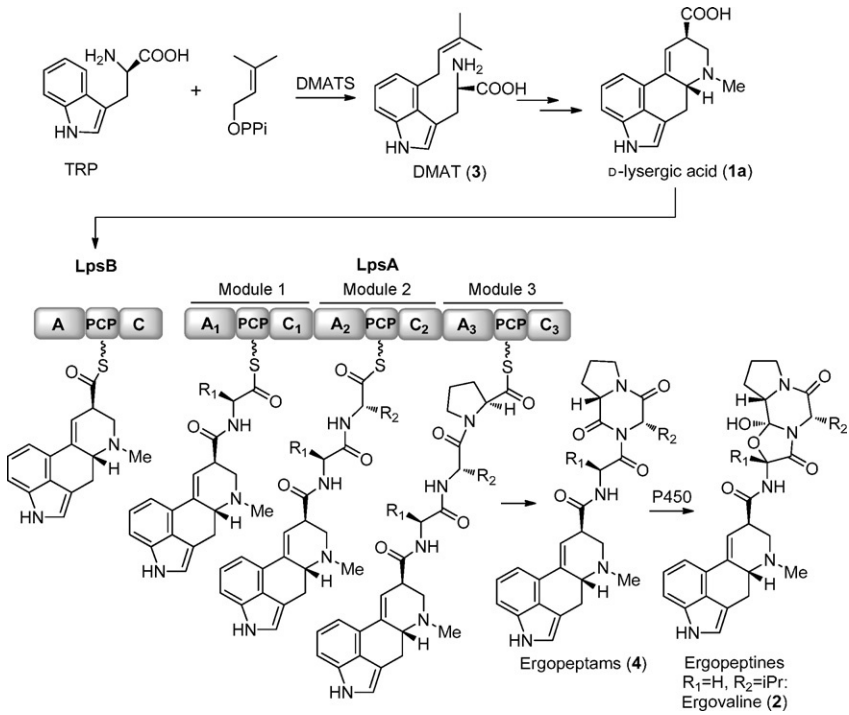

FIGURE 3 Biosynthesis of ergopeptines [39]. *Abbreviations*: A, adenylation domain; PCP, peptidyl carrier protein; C, condensation domain; DMATS, DMAT synthase; EAS enzyme nomenclature according to Fleetwood *et al.* [34].

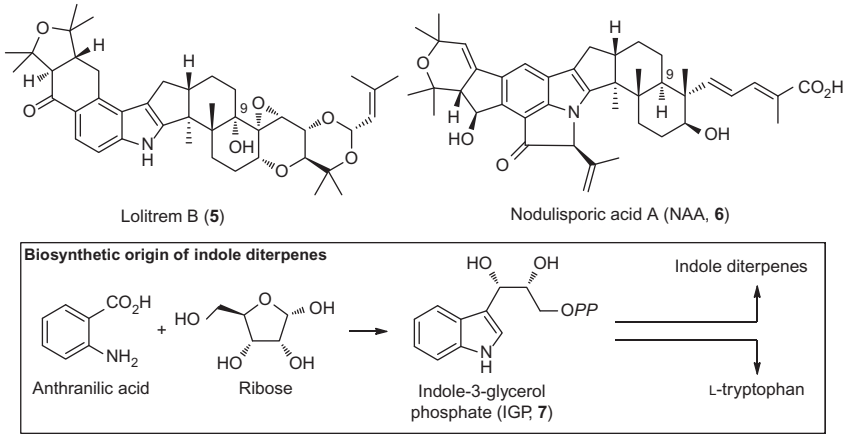

FIGURE 4 Structure and biosynthetic origin of some ecologically relevant indole-diterpene alkaloids.

causative agent of ryegrass staggers disorder in livestock [41]. More recently, related paspalitrem-type alkaloids were isolated from *Cynodon dactylon* (Bermuda grass) infected with *Claviceps cynodontis*, after several decades of cattle stagger intoxications [42].

It has been recently demonstrated that lolitrem gene clusters are highly expressed *in planta* while expression is very low or undetectable in culture condition [34,43]. More recently, some new members of this compound family were reported. Especially, the potent insecticide nodulisporic acid A (NAA: **6**) was discovered from an endophytic strain of *Nodulisporium* sp. isolated from an unidentified woody plant [44] and was soon marked by an important biosynthetic study (see below) [45]. Compared to other members of indole-diterpene alkaloids, it lacks the tertiary hydroxyl group at C-9 which is usually associated with tremorgenic activity, and holds a cyclopentyl ring in the western part of the molecule (Fig. 4). Moreover, the indole nucleus is fused to a highly strained dihydropyrrolone ring derived from isoprenylation, which is unprecedented in indole mycotoxins. NAA showed strong insecticide activity against mosquito larvae, which attracted attention. The biosynthetic study of NAA revealed that the indole nucleus would arise directly from indole-3-glycerol phosphate (IGP: **7**) rather than from L-tryptophan, while the eastern diterpene part would be provided by geranylgeranyl diphosphate [45]. IGP would indeed be a branching point between tryptophan and NAA biosyntheses. Further, isoprenylations would then decorate the western and south moiety of the indole to afford the natural product skeleton. These findings are sharply contrasting with the admitted tryptophan origin of indole-diterpenes which biosynthesis therefore deserves further studies [46]. Indeed, it had previously been shown that isotopically labeled tryptophan was incorporated in the NAA-related compounds paspaline and penitrem A by *Claviceps paspali* and *Penicillium crustosum*, respectively. However, genetic studies have confirmed the IGP origin of indole-diterpenes and highlighted the genetic basis for indole-diterpene diversity in filamentous fungi (Fig. 5) [47].

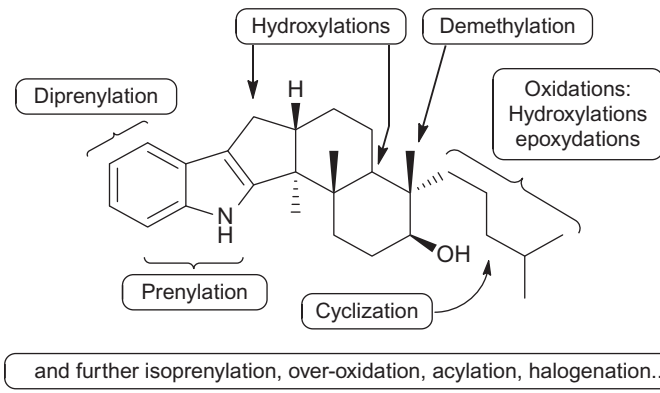

FIGURE 5 Biosynthetic origin of chemical diversity in indole-diterpenes.

Asporyzins A–C (A: **8**, B: **9**, C: **10**) (Fig. 6) have been isolated from an *Aspegillus oryzae* associated with the red alga *Heterosiphonia japonica*, beside known metabolites in the emindole series such as JBIR-03 (**11**) [48]. All isolated compounds were evaluated preliminarily for activities against invertebrate and bacteria in order to probe into their chemical defense functions. It was found that **11** was the more potent against the brine shrimp (*Artemia salina*), yet without anti-acetylcholinesterase activity, and that compound **10** had strong antimicrobial activity against *Escherichia coli*. The effect on shrimps would rather be due to the well known blocking activity of indole-diterpenes on ion channels, like does NAA (**6**) [49]. It was suggested that the endophytic fungus *A. oryzae* may defend the red alga against marine herbivores and bacteria.

The pyrrolizidine class of fungal natural products [50] has been associated to the grass-*Epichloë*/*Neotyphodium* symbiosis, but only recently the proof of their fungal origin was brought by Schardl and coworkers [51]. Indeed, lolines (**12–18**) (Fig. 7) had previously been reported only in plant contaminated by the *Epichloë*/*Neotyphodium* complex (mainly *Lolium* and *Festuca* grasses). They were later found in fungi in minimal culture media that were able to

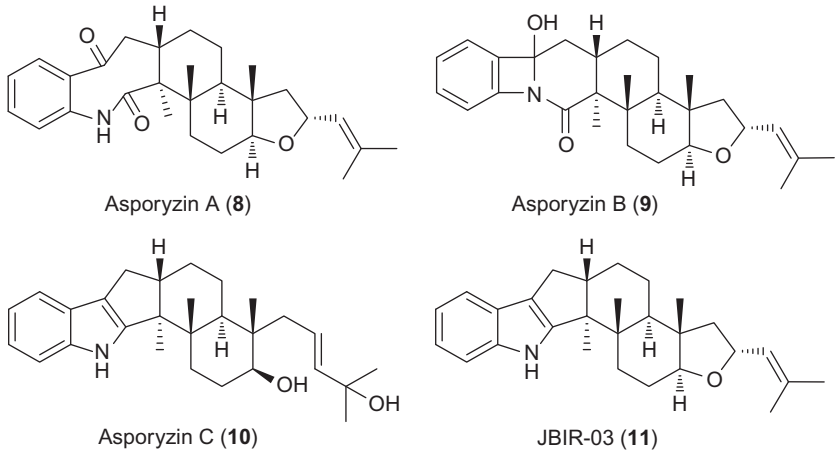

FIGURE 6 Structure of indole-diterpenes from the endophytic fungus *Aspergillus oryzae*.

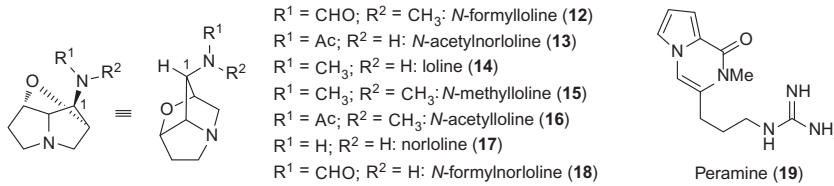

FIGURE 7 Structure of loline pyrrolizidines (**12–18**) and of the unique pyrrolopyrazine peramine (**19**).

mimic the plant tissue (complex media were not effective). Structurally, lolines are oxygen-bridged and differ from plant pyrrolizidines by the lack of CH_2OH at C-1 [52]. The different lolines mainly differ from the substitution pattern at the primary amine group (Fig. 7).

The ecological significance of lolines has been linked to their anti-invertebrate and feeding deterrent activities, while they seem to be weakly or non-toxic to mammalian herbivores [53,54]. Yet the production of lolines by the endophytic fungi in plant is likely to be substantial, approaching up to 2% of the plant dry mass [51b]. Precisely, it might be more concentrated in the vulnerable young parts of the plant, a distribution resulting from regulation by specific plant constituents, especially asparagine [55]. Biosynthetically, lolines are derived from L-proline (precursor of B-ring, including the internal nitrogen) and from L-homoserine (A-ring and the external nitrogen) [56]. The *lol*-gene cluster (containing nine genes) is responsible for their production [57].

The pyrrolopyrazines constitute the fourth class of compounds produced by grass-associated endophytic fungi. The main constituent is peramine (**19**) (Fig. 7) first isolated from *Acremonium lolii* (anterior name of *N. lolii*) [58]. Similar to lolines, **19** can deter herbivorous insects and seems to be present in young plant tissues and seeds only [59]. These alkaloids are exuded in the guttation fluid of endophyte-infected grasses, but it is not clear if an active concentration of the alkaloid would be attained in this case [60]. Peramine is a functionalized cyclodipeptide derived from proline and from arginine in an NRPS-catalyzed biosynthetic pathway [61]. This is probably the most widely distributed *Epichloë* bioprotective metabolites identified to date [61a].

As miscellaneous alkaloids produced by non-Clavicipitaceae fungi (Fig. 8), we can find modified indole alkaloids such as pyrrolyl 4-quinoline derivatives penicinoline (**20**) and penicinotam (**21**) [62]. These compounds were isolated from a mangrove endophytic *Penicillium* sp. and displayed interesting insecticide activities against *Aphis gossypii*, *Plutella xylostella*, and *Heliothis virescens*. The plant auxin indole-3-carboxylic acid (**22**) was isolated from *Botryosphaeria rhodina*, obtained from the Asteraceae *Bidens pilosa* [63]. This kind of phytohormone is responsible for growth stimulation and elongation in plants and it is possible that their production by endophytic fungi is responsible for improving plant growth.

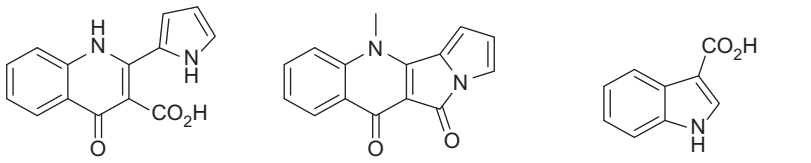

Penicinoline (**20**) Penicinotam (**21**) Indole-3-carboxylic acid (**22**)

FIGURE 8 Miscellaneous indole alkaloids: modified derivatives (**20**, **21**) and an auxin (**22**).

Non-Ribosomal Peptide Derivatives: Diketopiperazines and Cyclopeptides

Diketopiperazines (DKP), the smallest possible cyclic peptides biosynthesized by various fungi, are considered either to be secondary functional metabolites or side products of terminal peptide cleavage [64]. A subgroup of DKP, featuring either thiomethyl groups or disulphide bridges, called epipolythiodioxopiperazines (ETPs: **23**) (Fig. 9), comprises typical toxic metabolites from filamentous fungi, like gliotoxin **24** [65]. Fungal DKPs are typically synthesized by NRPSs [66], which mechanisms have been displayed in Fig. 3, whereas some bacterial DKPs are produced by monofunctional DKP synthases [67].

There is a tremendous structural variety of non-ribosomal peptides biosynthesized by fungi, mainly based on the flexibility of the biosynthetic programming of NRPSs, with adenylation domains responsible for activating a wide variety of nonproteinogenic amino acids, and the formation of main chain heterocycles and linear, macrocyclic, or branched macrocyclic structures with amide, ester, or thioester closure [68]. However, despite their production by many filamentous fungi, few have been described in endophytic fungi and their biological activities are still underexplored.

During bioassay-guided fractionation of the extract of the plant-associated strain *Aspergillus tubingensis*, malformin A_1 (**25**) was reisolated (Fig. 10) [69]. Malformin A1 has been reported to possess plant growth stimulation, mycotoxic activity and phytochrome-mediated response modulation of the bean *Phaseolus vulgaris*.

Another class of fungal peptides is represented by peptaibiotics, defined as linear peptide antibiotics with a molecular weight between 500 and 2200 Da, featuring nonproteinogenic amino acids such as aminoisobutyric acid (Aib) or lipoamino acids, an acetylated N-terminus and an altered C-terminal residue [70]. *Trichoderma* and *Hypocrea* are the most abundant sources of peptaibiotics as approximately half of the known compounds are originating from those two genera. *Trichoderma* are usually considered as soil microorganisms and have been extensively studied for their biocontrol potential. *Trichoderma* represent 60% of sales of biological control agents and are used as biopesticides, biofertilizers, and for soil amendments. Many species of *Trichoderma*

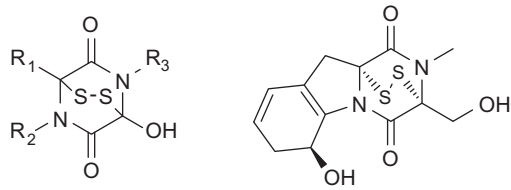

(**23**) Gliotoxin (**24**)

FIGURE 9 Generic structure of ETPs (**23**) and structure of gliotoxin (**24**).

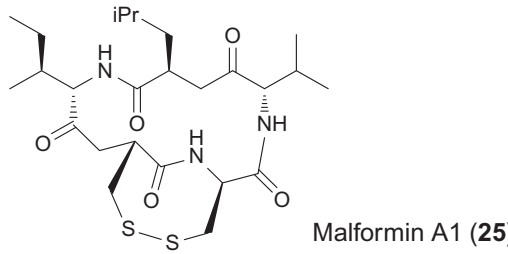

Malformin A1 (**25**)

FIGURE 10 Structure of malformin A1 (**25**).

have been shown to produce a wide heterogeneous range of bioactive metabolites that may contribute to their mycoparasitic and antibiotic activities, including peptaibols [71]. In addition, recent studies have demonstrated that *Trichoderma* colonizes the above ground tissues of *T. cacao* and maintains an endophyte-like symbiotic relationship [14b]. However, the role of peptaibols in host-plant protection has not been demonstrated.

Polyketides

Polyketides constitute the most important group of fungal secondary metabolites, with structural diversity ranging from saturated to aromatic compounds. The biosynthetic origins of these compounds are multifunctional megasynthases, called polyketide synthases (PKSs), which are responsible for acetate oligomerization through Claisen-type condensations. They are organized into modules which are composed of several domains that are required for one round of condensation with acetate-derived units (Fig. 11).

Three types of PKSs have been described and their gene organizations have been well reviewed by others [73]. Fungal PKSs are in general iterative multidomain type I PKSs, that is, domains used iteratively for polypeptide chain elongation. They can be further classified into nonreducing (NR), partially-reducing (PR), and highly reducing (HR) PKSs, accounting for immense chemical diversity of fungal polyketide-derived metabolites (partially saturated linear, macrocyclic, polycyclic, or aromatic compounds). PKSs can also be hybridized with NRPSs which incorporate amino acids into the polyketide backbone [72]. Usually, these megasynthases are associated with accessory enzymes, especially oxidation/reduction enzymes (e.g., P450 monooxygenases) that lead to chain rearrangements and complex cyclizations, as illustrated by the so-called Diels-Alderases [74]. Biologically, polyketides seem to hold a great potential for bioactivity with high ecological significance.

Nonaromatic Polyketides Based on a Decalin System

Solanapyrone A (**26**) (Fig. 12) was first isolated as a phytotoxin from the phytopathogenic fungus *Alternaria solani*, which causes blight disease on potato

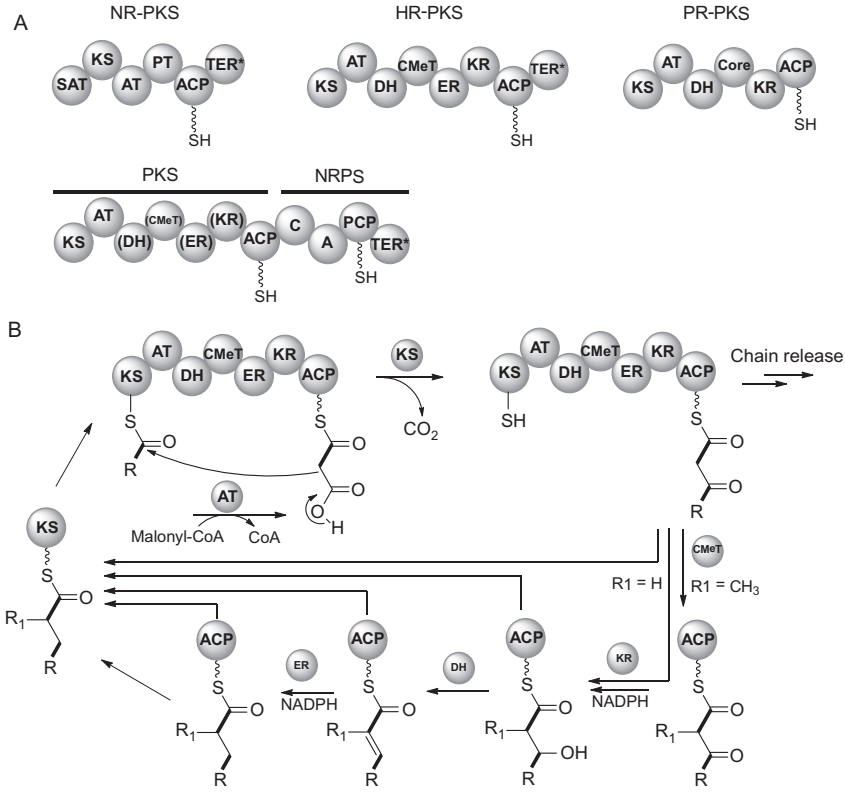

FIGURE 11 (A) Gene organization of fungal iterative multidomain PKSs and PKS/NRPS hybrids. SAT, starter ACP transacylase; ACP/PCP, acyl/peptidyl carrier protein; KS, ketosynthase; AT, acyltransferase; PT, product template; KR, ketoreductase; DH, dehydratase; ER, enoyl reductase; CMeT, C-methyltransferase; Ter*, termination domain that can be a thioesterase, a Claisen cyclase, a reductase, or a Dieckmann cyclase, or can be missing; NR, nonreducing; HR, highly reducing; PR, partially reducing. Domains within parenthesis indicate that they can be non-functional. (B) Example of basic chemical reactions catalyzed by iterative HR-PKS. The growing polyketide chain is passed back and forth between the Cys active site of the KS and the phosphopantethein cofactor of the ACP. The number of cycles and the reductive processing of the nascent β-keto group determine structural complexity. Scheme adapted from Chiang *et al*. [72a] and Cox [72b].

and tomato [75]. Such phytotoxins (**26**, **27**) are also present in endophytic fungi such as a *Nigrospora* sp. from *Azadirachta indica* and have shown little antifungal activities [76]. Solanapyrone A is a selective inhibitor of mammalian DNA polymerases β and λ, but the main interest with regard to this review is the large amount of work undertaken to unravel the biosynthesis of the *cis*-decalin system, at the genetic and enzymatic levels. Solanapyrone biosynthesis begins with the assembling of the linear intermediate prosolanapyrone III (**28**) by an HR-PKS and ends with an intramolecular Diels-Alder

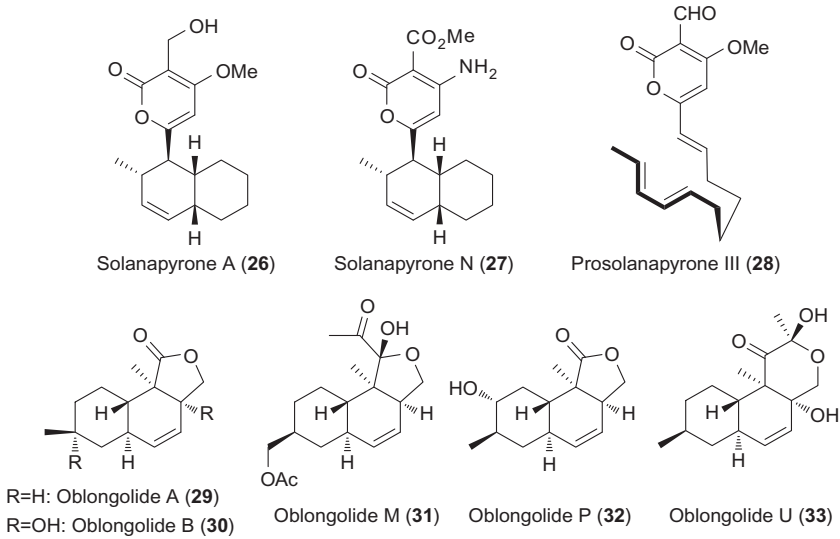

FIGURE 12 Structures of some solanapyrones (**26**, **27**), the biosynthetic precursor prosolanapyrone III (**28**), and oblongolides (**29**–**33**).

reaction of **28** catalyzed by a single flavin-dependent oxidase (solanapyrone synthase) [77]. The presence of phytotoxic solanapyrone analogs in endophytic fungi brings up for discussion the balanced antagonism hypothesized by Schultz and coworkers [18].

Oblongolides hold a *trans*-decalin system related to polyketides as suggested by Shen and coworkers [78], although the first oblongolide was initially classified as a norsesquiterpene [79]. Oblongolide **29** (oblongolide A) (Fig. 12) was first isolated in 1985 from *Phomopsis oblongata*, a latent pathogenic fungus of elm (*Ulmus* sp.) [79]. It was shown to be a boring/feeding deterrent for the *Scolytus* sp. beetles, a vector of the causative agent of the Dutch elm disease (*Ceratocystis ulmi*). It was reisolated from endophytic fungi *Phomopsis* sp. associated to the halotolerant plant *Melilotus dentata* [80], *Phomopsis* sp. of *Camptotheca acuminate* [78], and *Phomopsis* sp. of wild banana leafs (*Musa acuminata*) [81], along with many diversely substituted analogs (**30**–**33**). Some of them exhibited moderate antibacterial, antialgal, and antifungal properties.

Nonaromatic Lactones, Macrolactones, and Macrodiolides

Microcarpalide A (**34**) (Fig. 13) is a nonenolides (10-membered macrolides) isolated from an unidentified strain obtained from the bark of *Ficus microcarpa*, with microfilament-disrupting activity [82]. It is the second member of C_{16} nonenolides ever described, after the isomeric archaetolide reported in 1983 [83]. The antimicrofilament activity of **34** is interesting as it could

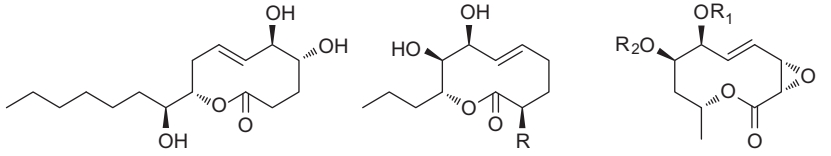

FIGURE 13 Structures of nonenolides isolated from endophytic fungi.

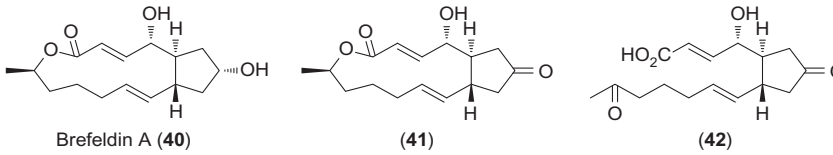

FIGURE 14 Structures of brefeldin A and analogs isolated from *Cylindrocarpon obtusisporum*.

have a wide spectrum of target organisms. However, it is far less active than cytochalasins (see below).

Analogous nonenolides like the C_{12} compounds herbarumins I (**35**) and II (**36**) (Fig. 13) isolated from the pathogenic fungus *Phoma herbarum* have been reported as phytotoxic, causing significant inhibition of radicle growth of plant seedlings [84]. It was shown that in these compounds, both the presence of the diol group and the propyl side chain are necessary to the phytotoxic activity. C_{10} nonenolides have been recently isolated independently from two endophytic *Phomopsis* sp. obtained from *Camptotheca acuminata* [85] and from the Neem tree (*A. indica*) [86]. In particular, 8-*O*-acetylmultiplolide A (**39**) was antifungal at moderate concentrations against the phytopathogenic fungi *Ophiostoma minus* and *Botrytis cinerea* [86]. Interestingly, the 7-*O*-acetyl isomer **38** was not active against these fungi.

The brefeldins are 13-membered macrolactones with the first member brefeldin A (**40**) (Fig. 14) isolated in 1958 from a corn spoiling *Penicillium decumbens* [87]. It has been reisolated with analogous compounds (**41**, **42**) from the endophytic strain *Cylindrocarpon obtusisporum* obtained from the plant *Trewia nudiflora*, which fermentation extract showed strong antifungal activity [88]. In fact, **40** is an inhibitor of protein secretion at an early step of the secretory pathway, and of membrane trafficking, having important impact on organelle structures [89]. Therefore, its production by an endophytic fungus may have important consequences on plant physiology. It has been shown that **40** has a strong inhibition effect on the growth of seedlings of lucerne and rape at the concentration of 20ppm [90].

The genus *Phoma* comprises about 2000 species, some of which have been isolated from healthy plants as endophytes. Macrodiolides like pyrenophorol

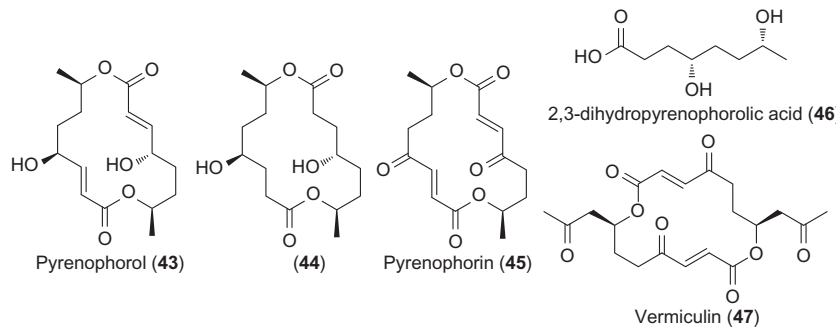

FIGURE 15 Structure of the antimicrobial macrodiolides isolated from *Phoma* sp.

43 (=helmidiol), its tetrahydro derivative **44**, or pyrenophorin **45** (Fig. 15) have been isolated from a strain of *Phoma* sp. associated to the plant *Fagonia cretica*, along with the monomeric acid 4,7-dihydroxyoctanoic acid (**46**) [91]. After cultivation of the fungus, the crude extract showed good herbicidal, algicidal, and moderate fungicidal activities. In fact, the pure compound **43**, previously described as anthelmintic [92], was moderately fungicidal while the algicidal activity was attributed to the monomer **46**. Similar compounds were isolated from another endophytic *Phoma* obtained from the Mediterranean plant *Lycium intricatum* along with ring-opened derivatives, with antifungal, antibacterial, and algicidal activities [93].

Spruce (*Picea glauca*) has provided an endophytic strain responsible for the production of insect toxins [94]. In particular, the macrodiolide vermiculin (**47**) showed toxicity to spruce budworm (*Choristoneura fumiferana*) larvae and cells, which is often invading the tree.

Oxo-Bridged Polycyclic Polyketides

Fusidilactones A–E (**48**–**52**) are ether-bridged polycyclic compounds structurally related to tetronic acids (Fig. 16). They have been isolated from an endophytic *Fusidium* sp. associated to *Mentha arvensis* growing in a German meadow [95]. In particular, fusidilactone C (**52**) is structurally original with a rare oxoadamantane structure, two ether-bridge hemiacetals including a spiroacetal. The metabolites exhibited moderate antifungal, antibacterial, and antialgal properties. Analogous nitrogenated compounds like phaeosphaeride A (**53**) have been isolated from the endophytic fungus *Phaeosphaeria avenaria* which causes the blotch disease of cereals [96].

Dinemasones A–C (**54**–**56**) were isolated from *Dinemasporium strigosum* associated to roots of *Calystegia sepium* [97], with promising antifungal, antibacterial, and antialgal activities. The dimeric compounds pestalotines A and B (A: **57**) were isolated from an endophytic *Pestalotiopsis* sp. of *Chondracis rosee* [98]. They displayed phytotoxic activities by radical growth inhibition of *Cosmos pringlei*.

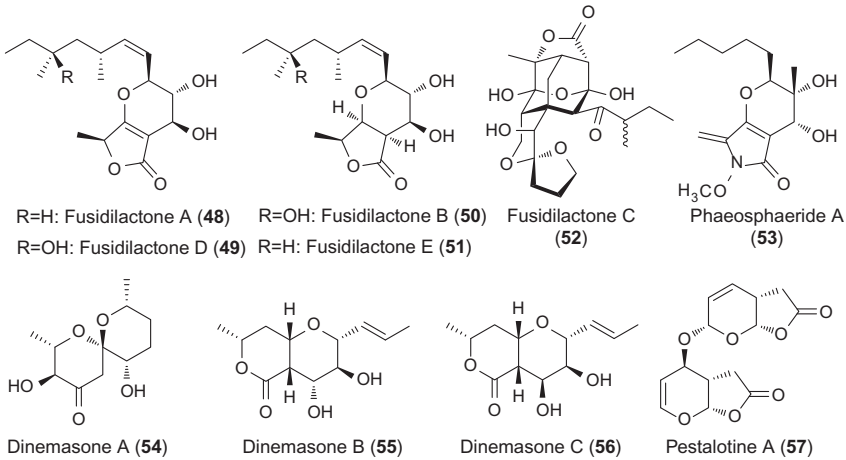

FIGURE 16 Structures of oxo-bridged polycyclic polyketides isolated from endophytic fungi.

Aromatic Polyketides Including a Lactone Moiety

Fourteen-membered resorcylic acid lactones are mycotoxins produced by type I PKS in fungi [99]. They have been associated to potent activities at concentrations in the range of 10–100nM, as inhibitors of important proteins such as the heat shock protein HSP-90, virus proteins or mitogen-activated protein (MAP) kinases. If similar interactions occur in plant or other adverse microorganisms, these molecules could be important as natural mediators or regulators.

Radicicol (**58**) and monocillin I (**59**) (Fig. 17) have been isolated from two plant associated fungi of the Sonoran desert, *C. chiversii* and *P. quadriseptata*, respectively [100]. Radicicol was known as an antibiotic, inhibiting the growth of a number of filamentous fungi and yeasts at moderately low concentrations [101]. Aigialomycins A–E (D: **60**) was first isolated from the endophytic fungus *Aigialus parvus* found in the mangrove wood [102]. Compound **60** was later isolated from an endophytic *Fusarium* sp. originating from the leaves of *Melia azedarach* [103], along with the known compound pochonin N (**61**) and the isocoumarin fusariumin (**62**). Biogenetically, the co-occurrence of these three metabolites in the same fungus suggests that they could share similar biosynthetic pathways. They are likely to be encoded by HR-PKS gene clusters, similar to the biosynthesis of citreoisocoumarin and derivatives in *Aspergillus nidulans* [104]. These compounds displayed significant growth inhibitory activity against the brine shrimp (*A. salina*).

Twelve-membered macrolactones have been isolated from a brown algae (*Sargassum* sp.) endophytic fungus from the South China Sea. They are analogous to lasiodiplodin **63** (Fig. 17), a compound previously isolated from *Lasiodiplodia theobromae* and having potato microtuber inducing activity. These compounds also exhibited moderate antimicrobial activities. Smaller

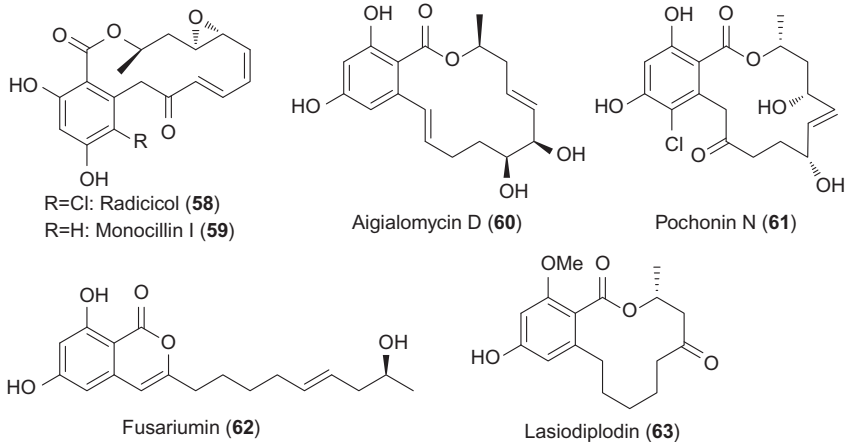

FIGURE 17 Structures of resorcylic macrolactones and an isocoumarin (**62**)

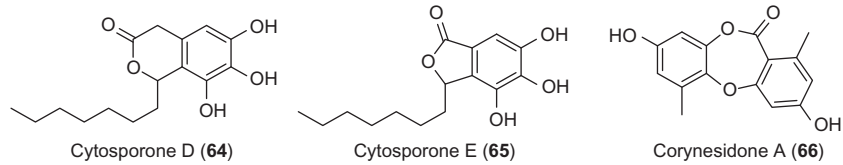

FIGURE 18 Structures of cytosporones and a depsidone.

aromatic, but not resorcylic acid, 10- and 9-membered lactones, phomopsin A–C, and cytosporones, as well as ring-opened derivatives with anti-*Fusarium* properties were isolated from a mangrove endophytic fungus *Phomopsis* sp. [105]. Cytosporones (e.g., **64**, **65**) (Fig. 18) were discovered from the Costa Rica endophytes *Cytospora* sp. and *Diaporthe* sp., which extracts were found to have potent antibiotic activities [106], and have also recently been isolated from a Brazilian endophytic *Cytospora* sp. [107].

Depsidones with antioxidant and radical scavenging activities, like corynesidone A (**66**) (Fig. 18), have been isolated from *Corynespora cassicola*, an endophyte of the Thai medicinal plant *Lindenbergia philippensis* [108]. Depsidones are often isolated from lichens and can prevent UV light-mediated DNA damages, by inhibition of the reactive oxygen species. Similar depsidones with antifungal properties were isolated from *B. rhodina*, an endophyte of the medicinal plant *B. pilosa* [63]. It was suggested that these compounds could participate in modulating fungal populations living within or attacking the host plant.

Phthalides, Isochromans, and Azaphilones Derivatives

Isocoumarins are important PKS-derived fungal metabolites. Mellein (**67**), 5-methylmellein (**68**), and substituted derivatives are typical representatives

of this family of compounds (Fig. 19), with known phytotoxic [109] and antimicrobial properties [110]. The lactone ring can be substituted by a long and more or less substituted polyketide chain. Bioactive isocoumarins monocerin (**69**) and analogs (e.g., **70**) have been isolated from the endophytic fungus *Microdochium bolleyi* associated to the herbaceous plant *F. cretica* [111]. The compounds showed good antifungal, antibacterial, and antialgal activities and were also previously known as insecticidal. Pseudoanguillosporin A (**71**) and B have been isolated from *Pseudoanguillospora* sp. originated from the red algae *Polyides rotundus*, with important activities against phytopathogens [112].

Other isochromans have recently been isolated from an endophytic *Colletotrichum* originated from *Piper ornatum*, and also the phthalide derivative **72** [113]. The compounds displayed strong antioxidant activities. Isopestacin (**73**, naturally racemic) is another antioxidant phthalide isolated from *Pestalotiopsis microspora*, an endophyte of the Combretaceae plant *Terminalia morobensis* [114]. As the parent compound pestacin [115], **73** is able to scavenge superoxide $O_2^{\bullet -}$ and OH• radicals in solution. That may be an important protection to oxidative stress for the fungus. Compound **73** is also moderately antifungal.

Pestaphthalide A (**74**) and the reduced spiro azaphilone **75** (pestafolide A) (Fig. 19) were isolated from *Pestalotiopsis foedan* obtained from a Chinese tree, with moderate antifungal activities [116]. In fact, azaphilones are biogenetically related to isocoumarins as shown in Fig. 20. Evenly, dimerization and amination can occur, like in the cytotoxin chaetoglobin A (**76**) which was isolated from *Chaetomium globosum* originated from the stem of *Imperata cylindrica* [117].

The biosynthesis of isocoumarins has been the subject of interesting work on *Fusarium verticillioides*, suggesting an alternative route through intermolecular ring formation between two linear polyketide intermediates

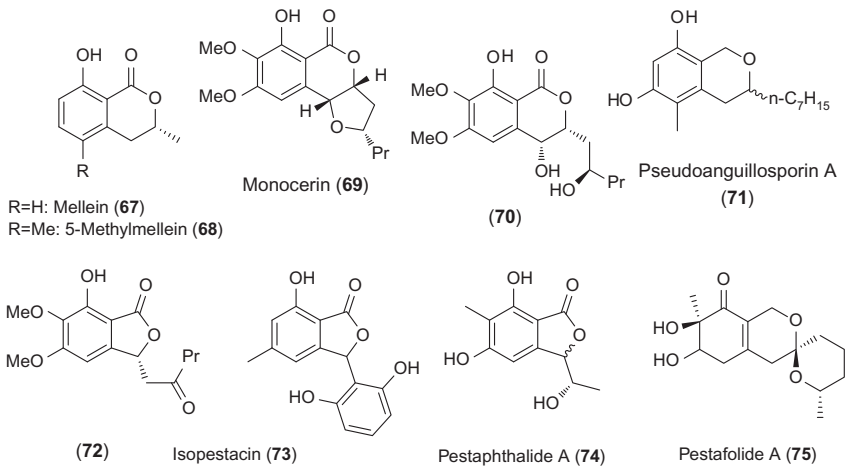

FIGURE 19 Structures of isocoumarins and phthalides.

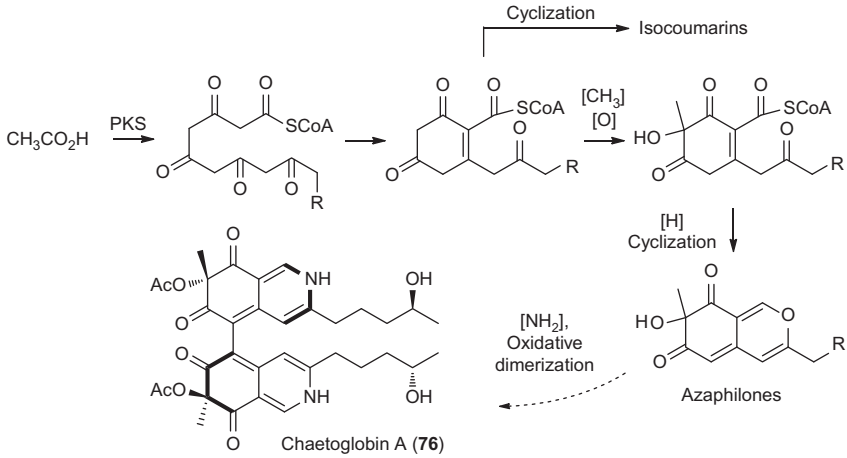

FIGURE 20 Biosynthetic origin of isocoumarins and azaphilones; example of chaetoglobin A.

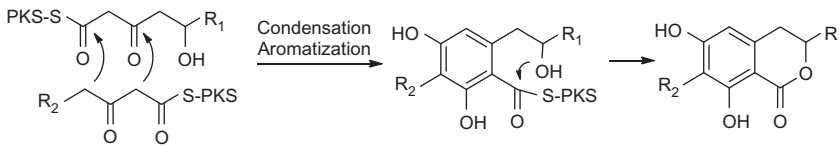

FIGURE 21 Alternative route for the biosynthesis of isocoumarins (adapted from Du *et al.* [118]).

(Fig. 21) [118]. In fact, this route may also be applicable to cyclohexenones and epoxyquinols which are discussed in the following section.

Cyclohexenones and Epoxyquinols

Cyclohexenone derivatives have been isolated from endophytic *Pestalotiopsis* spp. and *Monochaetia* sp. discovered in rainforest plants. Especially, ambuic acid (**77**) (Fig. 22) was isolated by bioassay-guided fractionation with *Pythium ultimum* as the test organism [119]. It is a highly functionalized isoprenylated cyclohexenone[1] structurally related to the previously discovered torreyanic acid (**78**) isolated from an endophytic fungus [120]. Ambuic acid (**77**) was later reisolated concomitantly with a torreyanic acid analog from an endolichenic fungus *Pestalotiopsis* sp. [121]. Compound **77** was active against several plant pathogenic fungi (*Fusarium* sp., *Diplodia natelensis*, *Cephalosporium gramineum*), suggesting a possible role of this compound in the fungus–plant relationship, being protective to the plant by virtue of its antimycotic activity.

[1] It is worth noting that for these compounds, isoprenylation has been invoked for their biosynthesis, but following the hypothesis of Fig. 21, the isoprenyl chain may also derive by the polyketide route.

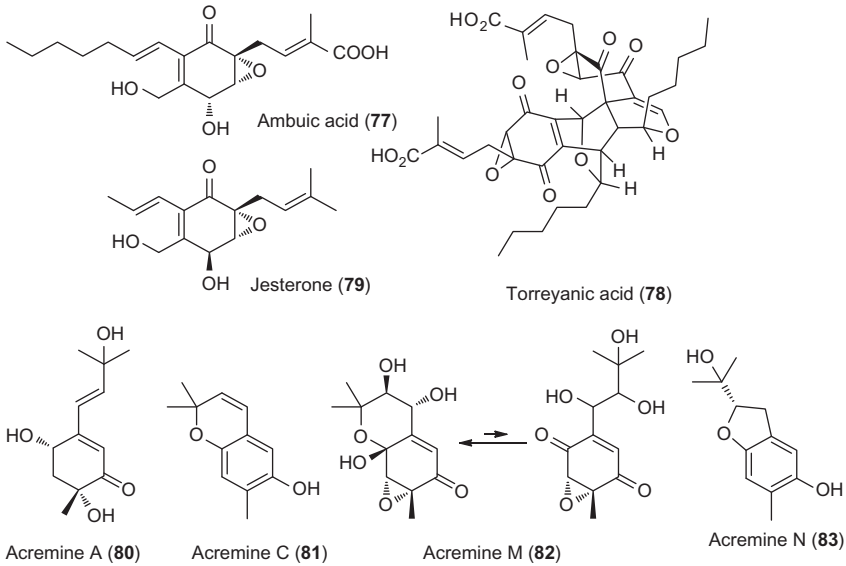

FIGURE 22 Structures of cyclohexenone derivatives.

The dimeric nature of torreyanic acid is supposed to come from an intermolecular Diels-Alder reaction. The oxygenated cycles would be derived from an oxidation/electrocyclization process. This hypothesis was demonstrated by biomimetic synthetic studies [122].

Jesterone (**79**) (Fig. 22) and hydroxy-jesterone are two other branched cyclohexenone derivatives isolated from *Pestalotiopsis jesteri*, an endophytic fungus obtained from the Gentianaceae *Fragraea bodenii* harvested in Papua New Guinea [123]. The most noticeable activity of these compounds was observed on the oomyceteous fungi *P. ultimum*, *Aphanomyces* sp., *Phytophthora citrophthora*, and *Phytophthora cinnamomi* which are important plant pathogenic fungi. Other dimeric epoxyquinols isolated from *Pestalotiopsis* sp. have been described with cytotoxic properties and additional decorations like tetrahydropyran ring, halogenated positions, or an endoperoxide bridge [124]. Diverse 2,3-epoxycyclohexenes and biosynthetically related isocoumarins have been isolated from the endophytic fungus *Phomopsis* sp. from *Laurus azorica* [125]. They displayed good antimicrobial activities.

Acremines A–F (A: **80**, C: **81**) (Fig. 22) have been isolated from the sporangiophores of the grapevine pathogen oomycetes *Plasmopara viticola* [126]. Compound **81** showed the strongest inhibition against sporangia germination of *P. viticola*, in the range of 1 mM. Similar activities were observed with analogous acremines G–N (M: **82**, N: **83**) isolated from *Acremonium byssoides*, a residential endophyte parasiting *P. viticola* in a wild Sicilian vineyard [127].

The rearranged polycyclic sequoiatones (e.g., **84**, **85**) and sequoiamonascins (e.g., **86**, **87**) (Fig. 23) have been isolated through brine shrimp lethality-guided fractionation from *Aspergillus parasiticus* associated to the inner bark of *Sequoia sempervirens*, a coast redwood tree [128]. They are biosynthetically related although sequoiatones are organized around a cyclopentene ring, while sequoiamonascins all share a cyclohexene ring. The shrimp tests revealed possible toxicity against arthropods.

Chromone, Xanthone, and Benzophenone Derivatives

The chlorinated benzophenone derivatives pestalachlorides A–C (A: **88**, B: **89**) (Fig. 24) were discovered from the endophytic fungus *Pestalotiopsis adusta* obtained from an unidentified tree [129]. They displayed significant antifungal activities against three plant pathogens, *Fusarium culmorum*, *Gibberella zeae*, and *Verticillium albo-atrum*. Compound **88** more specifically strongly inhibited *F. culmorum*.

Phomoxanthone A (**90**) is a dimeric xanthone isolated from *Phomopsis* sp. originated from the stems of a Costaceae plant, which crude extract displayed good antibacterial and antifungal activities [130]. Indeed, **90** showed high activity against the Gram-positive bacterium *Bacillus megaterium* and moderate inhibition of the alga *Chlorella fusca*, showing a potential phytotoxic activity. It also showed strong activity in a crop protection screening against a number of harmful fungi, in particular against the dangerous riceblast pathogen *Pyricularia oryzae*.

Chromone dimers phomopsis-H76 A–C (A: **91**, C: **92**) were isolated from a mangrove endophytic fungus *Phomopsis* sp. [131]. Compounds **91** and **92** altered the development of the Zebrafish embryo. The antifungal compound diversonol (**93**) was isolated at the same time as monomeric chromone related to **91**, from an endophytic *Microdiplodia* sp. derived from the schrub

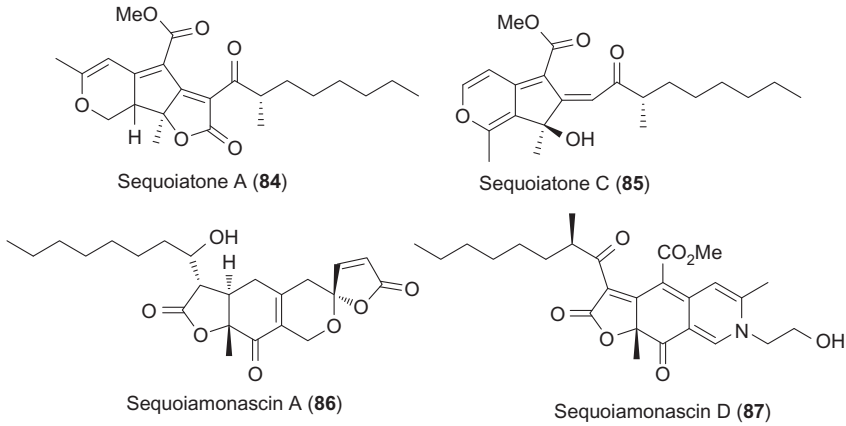

FIGURE 23 Structures of sequoiatones and sequoiamonascins from *Aspergillus parasiticus*.

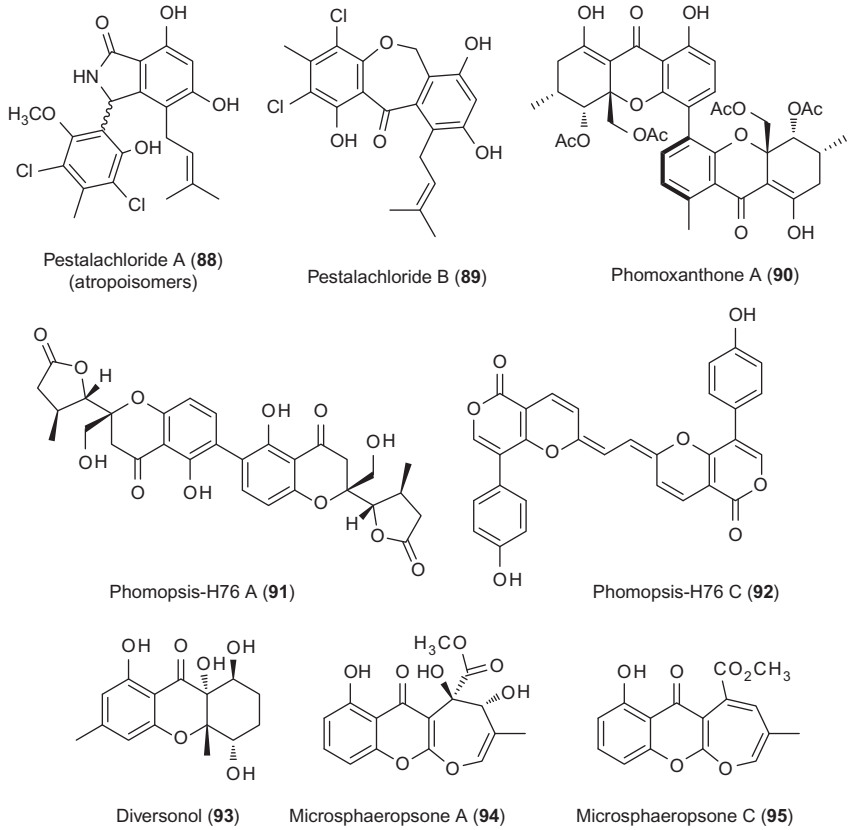

FIGURE 24 Structures of benzophenones, xanthones, and chromones metabolites.

Lycium intricatum [132]. Other antimicrobial and herbicide compounds in the same series (blennolides A–G) were isolated from *Blennoria* sp., an endophytic fungus from *Carpobrotus edulis* [133]. The unique oxepino[2,3-*b*]chromen-6-one of microsphaeropsones A–C (e.g., **94**, **95**) can be recognized as ring-enlarged lactones [134]. They were isolated from *Microsphaeropsis* sp., an endophytic fungus originated from the shoots of *L. intricatum*. They displayed antibacterial and antialgal activities. Interestingly, **94** and **95** were not antifungal but the oxidation of the allylic alcohol of **94** led to significant antifungal activity.

Anthraquinones, Bisanthraquinones, Tetralones, and Other Polycarbocyclic Aromatic Compounds

In 1978, Carroll and Carroll first suggested that endophytes recovered from coniferous trees (needles) might be mutualist symbionts [135]. Especially, conifer needle endophytes may produce anti-insect compounds. Indeed, Miller and coworkers demonstrated that the needles colonized by a rugulosin

(**96**)-producing endophyte contain rugulosin in concentrations that are effective *in vitro* at retarding the growth of spruce budworm larvae (*Choristineura fumiferana*), at least under nursery conditions [136]. The implicated endophytes would be a species of *Phialocephala* [137] or a *Nemania serpens* or a *Lophodermium* [138]. Rugulosin (**96**) (Fig. 25) has been known for more than half a century as a bisanthraquinone [139] and it holds a wide range of biological activities, including DNA damage properties. *In vitro*, it was shown to reduce body weight and affect instar development in *fumiferana fumerana* [136b]. *In vivo* measurements of rugulosin concentrations in endophyte-infected needles revealed that the mycotoxin is present in the range of 1 μg/g, which in the range of the toxic concentration *in vitro* (*ca.* 20 μM) [137]. In this context, it is possible that **96** and related compounds play a role in the mutualistic relation between conifers and their associated endophytes against insect herbivores. Many bisanthraquinones have been isolated from fungi and it has been suggested that they would derive from the dimerization reaction of anthraquinone monomers [140], a point confirmed by biomimetic synthetic works [141].

Cytoskyrins A (**97**) and B were isolated from the endophytes *Cytospora* sp. originated from a branch of *Conocarpus erecta* (buttonwood tree) [142]. As **96**, **97** was active in the biochemical induction assay (BIA) which measures the induction of the SOS response in bacteria and is used to identify compounds that inhibit DNA replication or DNA modifications.

Monomeric naphthoquinones and tetralones have been isolated at the same time as anthraquinones, showing very close biogenetic relationship [143]. Many of them were described as phytotoxic compounds. Interesting structures were described, showing the high propensity of the naphthalene derivatives to rearrangements [144] and heterodimerization. Preussomerins G–L (G: **98**) (Fig. 26), with moderate antimicrobial activities and farnesyl transferase inhibition, were isolated from an endophytic *Mycelia sterile* obtained from *Atropa belladona* [145]. Allelochemical preussomerins (**99**, **100**) and a palmarumycin (**101**) were isolated from the endophytic fungus *Edenia gomezpompae* originated from the leaves of a Verbenaceae collected in Mexico [146]. The

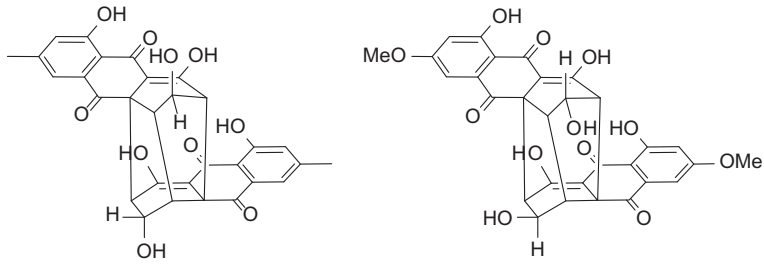

FIGURE 25 Structures of bisanthraquinones.

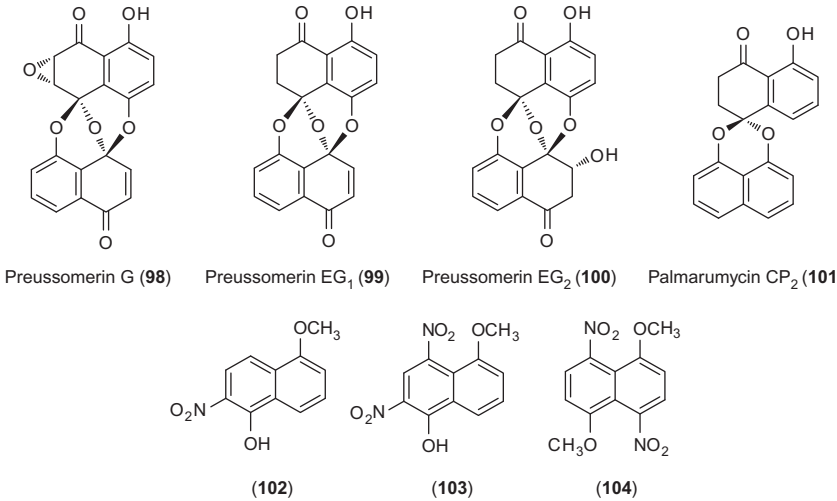

FIGURE 26 Structures of preussomerins and monomeric naphthalenoids.

bioactivity of the mycelial organic extracts and the pure compounds was tested against endophytic fungi (*Colletotrichum* sp., *Phomopsis* sp., and *Guignardia manguifera*) isolated from the same plant species and against economically important phytopathogenic microorganisms (two oomycetes: *Phytophthora capsici* and *Phytophthora parasitica*, and the fungi *Fusarium oxysporum* and *Alternaria solani*). Significant growth inhibitions of most of these fungal competitors were described. Further, it is important to note that three palmarumycins closely related to **101** were isolated from the stem of the plant *Jatropha curcas* in appreciable quantities (172mg from 3kg of the stems) [147]. The question was raised about the exact origin of these metabolites. Similar results were obtained when working on the dried fruits of *Diospyros ehretioides*, showing the presence of palmarumycins and dimeric naphthoquinones [148]. The compounds were not present in fresh fruits, and it was shown that they appeared during the drying process with the development of palmarumycin-producing fungi.

Unusual nitronaphthalene derivatives (**102**–**104**) (Fig. 26) have been isolated from the endophytic fungus *Coniothyrium* sp. originated from the shrub of *Sideritis chamaedryfolia* [149]. Some of them (**102** and **103**) displayed significant antifungal activities against the phytopathogen *Microbotryum violaceum*, while compound **104** was inactive.

Nonadrides and Maleic Anhydride Derivatives

The nonadrides are rare secondary metabolites whose structures are based on formal C_9-units represented by 2-(1-butenyl)-3-methylmaleic anhydrides encountered as linear or cyclic di- or trimeric derivatives. Anti-insect extracts from an endophytic strain of *Dwayaangam colodena* has provided the maleic anhydrides **105**–**107** (Fig. 27), which may be responsible for the anti-insect

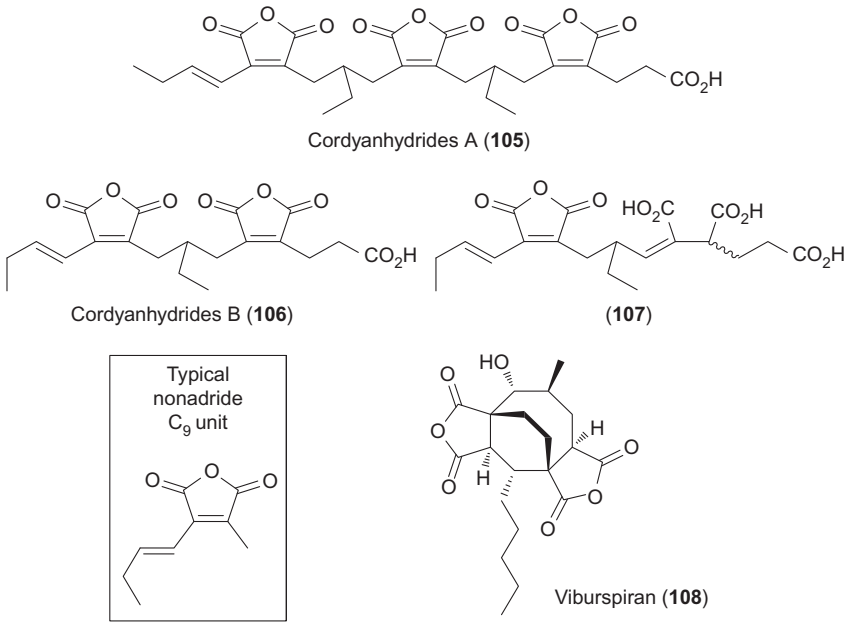

FIGURE 27 Structures of nonadrides and maleic anhydride derivatives.

properties of the fungal extract on *Choristineura fumiferana* (eastern spruce budworm) [150]. Compounds **105** and **106** had previously been described as cordyanhydrides A and B, respectively, from the insect pathogenic fungus *Cordyceps pseudomilitaris* [151]. Moreover, it was shown that numerous members of the nonadride group are inhibitors of protein phosphatases and have herbicidal, antifungal, and antibacterial activities [152].

Recently, Viburspiran (**108**) was reported as a new antifungal derivative classified as an "octadride," by comparison with the known nine-membered nonadrides. It was isolated from the endophyte *Cryptosporiopsis* sp. originated from *Viburnum tinus* [153].

Polyketides Derived by the Mixed PKS–NRPS Pathway and Featuring the Presence of a Tetramic Acid Part

In the PKS–NRPS hybrid natural products, the amino acid is most often hidden in a tetramic acid moiety resulting from the condensation of its activated acyl group with a PKS β-ketothioester adduct. The chemical diversity of these compounds is extremely important, not only resulting from the diversity of the ketide and amino acid constituents but also from the high reactivity of the biosynthetic intermediates following the PKS–NRPS assembly line and post-assembly line modifications. The tetramic acid moiety can be overoxidized or reduced [154] as exemplified by the compound L-755,807 (**109**) (Fig. 28) isolated from an endophytic *Microsphaeropsis* sp. (overoxidized

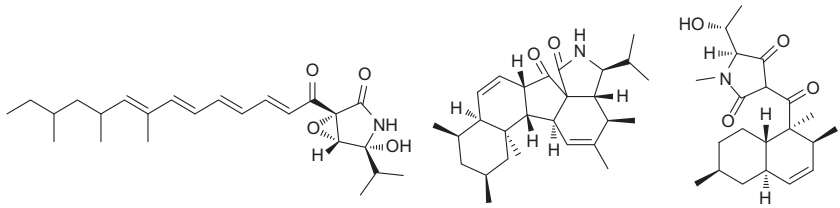

FIGURE 28 Example of chemical diversity in the PKS–NRPS hybrid metabolites.

tetramic acid derived by leucin and bearing a linear acyl chain) [155] or by chaetochalasin A (**110**) isolated from the mycoparasitic fungus *Chaetomium brasiliense* (reduced tetramic acid fused with a tetracyclic system) [156].

Cryptocin (**111**) is a decalin tetramic acid originated from the endophytic fungus *Cryptosporiopsis cf. quercina* which was isolated from the inner bark of the stems of *Triptergyium wilfordii* [157]. It showed potent antimycotic activity against the pathogenic fungus *P. oryzae* at 0.39 μg/mL, the causal agent of rice blast disease, and other plant pathogenic fungi, but not against human pathogens. In fact, the presence of this compound could explain the impressive antibiosis observed on agar plates against a plethora of other plant-associated fungi including pathogenic ones. Further, the inoculation of *C. quercina* in both the oak *Quercus alba* or *T. wilfordii* under experimental conditions gave healthy plants even after 2 years of observation, therefore suggesting a symbiotic state.

Cytochalasins are also derived from the PKS–NRPS hybrid pathway. They have to be considered in this account owing to their marked biological activities and their important place in fungal natural product chemistry [158]. Some of them are indeed particularly active in the depolymerization of actin filaments from animals or plants, thus inhibiting cytokinesis. Consequently, the presence of any chalasin-producing endophytic fungus in a host plant is susceptible to interfere with plant life and physiology, as regard to root hair growth inhibition [159], pollen germination and tube growth [160], gravitropic response of flowering shoots [161], molecular interaction between glycoproteins at plant cell surface and in-cell microtubules [162]. All these processes are indeed disrupted by the presence of cytochalasin D, a compound used as a tool in cell biology. Cytochalasins could also act as virulence factors and phytotoxins [163], or as anti-insectan [164].

Despite their plant adverse effects, cytochalasins have been isolated from endophytic fungi. *Chaetomium globosum* has provided several examples of bioactive compounds in this series. In particular, an endophytic strain isolated from *Ginkgo biloba* has provided chaetoglobosins A (**112**) and C (**113**) (Fig. 29) [165]. Both compounds were toxic against the brine shrimp *A. salina* (mortality rate of 83% and 75% at 10 μg/mL), which may account for an anti-arthropod activity for the benefit of the plant, and were also significantly

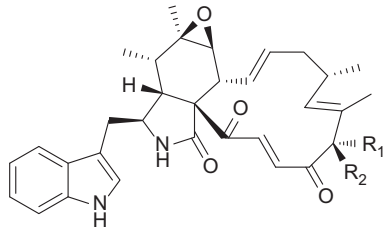

R_1=H, R_2=OH: Chaetoglobosin A (**112**)
R_1=R_2=O: Chaetoglobosin C (**113**)

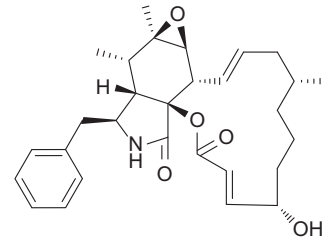

Cytochalasin F (**114**)

FIGURE 29 Structures of some chalasin natural compounds isolated from endophytic fungi.

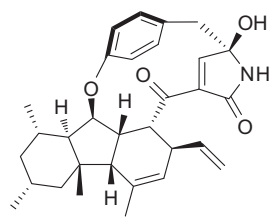

Pyrrocidine A (**115**)

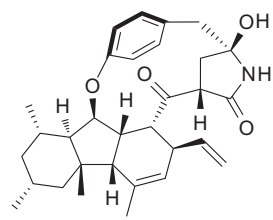

Pyrrocidine B (**116**)

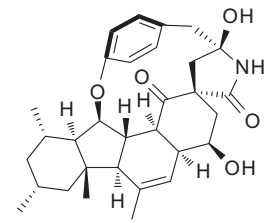

Pyrrospirone A (**117**)

FIGURE 30 Structure of the antibiotic pyrrocidines A and B, and the related pyrrospirone A.

antifungal against *Mucor miehei*. Recently, the gene cluster for chaetoglobosin biosynthesis was identified in *Penicillium expansum*, encoding one HR-PKS–NRPS, two regulators, and four enzymes involved in oxidation/reduction [166]. This provides insights into the cytochalasan assembly, notably a Diels-Alder reaction involved in the isoindolone formation.

Cytochalasin F (**114**) was reisolated from *Geniculosporium* sp., an endophytic fungus residing in *Teucrium scorodonia* [167]. It was algicidal and showed an inhibitory effect on photosynthesis, suggesting an ecological function in the plant–symbiont relationship. Other recent examples of bioactive endophytic cytochalasins have been reported in fungi like *Aspergillus terreus*, *Aspergillus flavipes*, *Eutypella scoparia*, *Endothia gyrosa*, or other strains of *C. globosum*, yet with only medicinal but no environmental purpose [168].

By the past 10 years, there has been a growing family of chalasin-related polycyclic PKS–NRPS natural products isolated from filamentous fungi, especially endophytic ones. All share a common 6-5-6 fused polycyclic system decorated with an *ansa*-bridged macrocyclic ring including a *p*-cyclophane and a pyrrolidinone originated from tyrosine. Among them, pyrrocidines A (**115**) and B (**116**) (Fig. 30) are two antibiotics with antibacterial activities produced by a strain of *Cylindrocarpon* LL-Cyan426 isolated in 2003 from a mixed douglas fir hardwood forest on Crane Island Preserve [169].

The same compounds were isolated from the endophytic fungus *Acremonium zeae*, a protective microorganism grown from maize [14e,170]. *A. zeae* is one of the most prevalent colonists of preharvest maize, typically producing symptomless kernel infections. Its presence within the germ and endosperm tissues would prevent pathogen attacks, especially *A. flavus* infections, at the seed and seedling stage where natural enemies of the plant would have the greatest impact on fitness [170a,171]. The antagonistic effect of *A. zeae* against *A. flavus* and aflatoxin contamination in maize was known from the 1980s [172]. Pyrrocidines **115** and **116** were isolated during a screening program aiming at identifying antifungal metabolites which inhibit the growth of *A. flavus* and/or *F. verticillioides* (causing stalk- or ear-rotting in maize). Both compounds were isolated from the culture broth of *A. zeae* on corn or maize kernel substrate. They were shown to be strongly inhibitory to the growth of several pathogens and fungal competitors such as *F. verticillioides*, *A. flavus*, *F. graminearum*, *Nigrospora oryzae*, *Rhizoctonia zeae*, *Alternaria alternata*, or *Curvularia lunata*. Compound **115** also exhibited potent antibacterial activity against the maize pathogen *Clavibacter michiganense* subsp. *nebraskense* [170]. It was suggested that the ability of *A. zeae* to produce these antibiotics could be important to fungal endophyte interactions with competing microbes and contributes to fungal survival in maize cultivation. Moreover, there may be a strong selection for pyrrocidine production among *A. zeae* endophyte populations in regions where crops are exposed to drought and temperature stress, which usually makes them more vulnerable to pathogen attack [170c].

Pyrrocidines are very close to pyrrospirones A and B (A: **117**) isolated from the endophytic fungus *Neonectria ramulariae* (Fig. 30) and to the antibiotic hirsutellones, a series of compounds with a lower methylation pattern isolated from the entomopathogenic fungus *Hirsutella nivea* (hirsutellones A–E) [173] and from the seed fungus *Trichoderma gelatinosum* found in a Leguminosae [174]. There has been no data on the ecological significance of these compounds. Further, the antitumor GKK1032A_2 fungal metabolite holds the same skeleton and was isolated from a non-endophytic *Penicillium* strain [175]. Oikawa's account on the biosynthesis of GKK1032A_2 gives a significant description of the biochemical origin of the series [175b].

Terpenoids

Terpenoids in plant-associated microorganisms are derived from isoprene units that are produced by the mevalonate or methyl-D-erythritol-4-phosphate pathway [176]. Sesquiterpenoids, diterpenoids, triterpenoids, and steroids can be found, as well as hybrid metabolites with the terpenoid skeletons linked to polyketides (most meroterpenoids) or to indoles (indole-diterpenoids). However, despite a wide chemical diversity and a wide range of biological activities (cytotoxic, antiviral, antimicrobial), few reports have described their ecological role, especially in the plant–fungus symbiosis.

Punctaporonins (e.g., **118**) (Fig. 31) are caryophyllene sesquiterpenoids originally isolated from the coprophilous fungus *Poronia punctata* [177]. Three new related compounds have been isolated from the fungicolous isolate of *Pestalotiopsis disseminata* and **118** exhibited a moderate antibacterial activity against the soil bacterium *Bacillus subtilis* [178].

Two sesquiterpenes in the epiisopetalol series (**119** and **120**) were isolated from the unidentified endophytic strain CSB 121944 present on the needles of *Picea rubens* (red spruce) [150]. Initially, this strain was selected for its toxicity against the forest pest *Choristineura fumiferana* (eastern spruce budworm) out of 150 foliar fungal endophytes isolated. Indeed, the extract of CBS 121944 significantly reduced the weight of insects in dietary bioassays. This effect may be attributed to the presence of both compounds **119** and **120**. The metabolites are biosynthetically related to the known insect PR toxin (**121**) and analogs isolated from *Penicillium* species.

In the course of a screening of fungal extracts for metabolites with activity against the infective agent of rice *Magnaporthe grisea*, extracts of the basidiomycete *Coprinus heptemerus* were selected and led to the isolation of heptemerones A–G (G: **122**) (Fig. 32). These compounds are new diterpenoids [179] and are closely related to the guanacastepenes A–O (A: **123**) which were previously reported as metabolites of the unidentified endophytic fungus growing on the *Daphnopsis americana* tree in Costa Rica [180]. Moreover, all compounds exhibited potent inhibition of fungal germination of the plant pathogen *M. grisea*. Heptemerone G (**122**) is the most active compound with a MIC around 1 µg/mL.

An original approach consisting in the dual culture of the callus of *Trewia nudiflora* and its endophytic fungus *Fusarium* sp. WXE was undertaken by Wu and coworkers [181]. In these conditions, they isolated three new *ent*-trachylobane diterpenoids (**124**–**126**) which had never been observed in a pure endophytic culture. This suggests that such compounds are specifically involved in the communication between the host plant and the fungus.

A new macrophorin analog, the meroterpenoid **127** (Fig. 33), was isolated from the fungicolous fungus *Hymenopsis* sp. obtained from the surface of a black stroma of an unidentified pyrenomycete collected on a dead hardwood branch from an Eucalyptus forest in Hawai [182]. This compound displayed a potent activity against the phytopathogen *F. verticillioides* and against

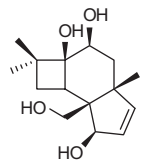

6-hydroxypunctaporonin (**118**)

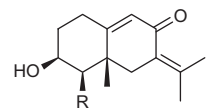

R=CH_3 : 3-epiisopetasol (**119**)
R=CH_2OH 15-hydroxy-epiisopetasol (**120**)

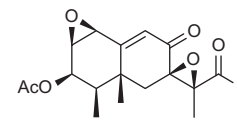

PR toxin (**121**)

FIGURE 31 Structures of sesquiterpenoids.

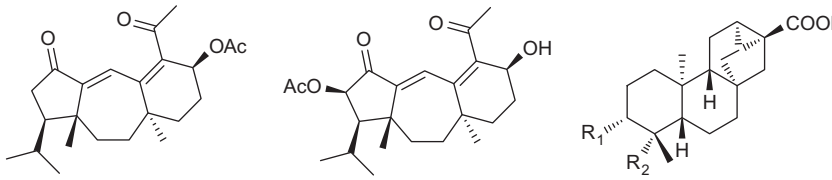

Heptemerone G (**122**) Guanacastepene A (**123**) Trachylobane derivatives:
R_1=OH, R_2=COOMe (**124**)
R_1=H, R_2=COOMe (**125**)
R_1=H, R_2=COOH (**126**)

FIGURE 32 Structure of diterpenoids in the guanacastepene and trachylobane series.

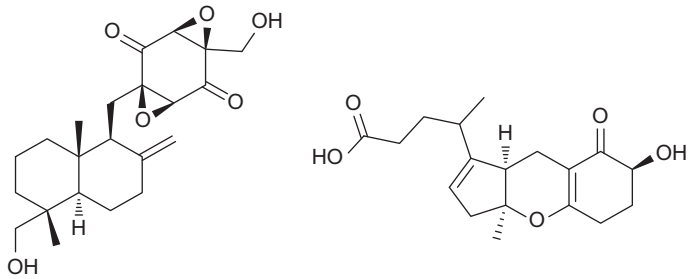

(**127**) Tricycloalternarene A (**128**)

FIGURE 33 Structure of meroterpenoids: A macrophorin analog and tricycloalternarene A

A. flavus known for its ability to contaminate peanut (*Arachis hypogae* L.) and to produce aflatoxin.

A. alternata is a known phytopathogen causing brown spot disease of mandarins tobacco, and other plants. It was isolated from an endophytic fungus of *Maytenus hookeri*. Cultivating the fungus in the presence of a plant supplemented medium led to the isolation of the meroterpenoid tricycloalternarenes (**128**) characterized by the combination of three isoprene units and a non-terpenoid six-membered α,β-unsaturated ketone. These compounds are known to inhibit leaf growth by causing spreading brown lesions and necrotic effects. They also strongly inhibit germination of *Spirodela polyrhiza* turions [183].

Miscellaneous Compounds

The chemical exploration of endophytic crude extracts with antimycobacterial activities (mainly from *Phomopsis* sp.) has led to the identification of 3-nitropropionic acid (3-NPA), a small molecule with known potent neurotoxicity [184]. The yield after purification was important, up to 178 mg/L. Since 3-NPA has also been identified in Leguminosae plant [185], it was questioned if this compound may be produced by associated endophytic fungi. This question has not been answered yet.

3-Hydroxypropionic acid was isolated by bioactivity-guided fractionation of extracts of endophytic fungi originated from above-ground plant organs [186]. It was identified as a nematicidal principle in endophytic fungi, having activity against the plant-parasitic nematode *Meloidogyne incognita* with LD_{50} values of *ca.* 15 μg/mL.

The *Muscodor* fungal genus has provided many examples of endophytic fungi producing volatile organic compounds (VOCs) with allelochemical effects. *Muscodor albus* strains were isolated from the Lauraceae *Cinnamomum zeylanicum* [187] and from the Sterculiaceae *Guazuma ulmifolia* [188]. *Muscodor crispans* was isolated from *Ananas ananassoides* [189]. GC–MS analyses of these fungi revealed the presence of methyl-substituted butanoic acids, butenols, butanols, and other alcohols, butenal, 1-octene-3-ethyl-guaiol, *N*-(1-methylpropyl)formamide, some azulene and naphthalene derivatives, caryophyllene, phenylethyl alcohol, 2-phenylethyl acetate, bulnesene, and various 2-methylpropanoic acid derivatives. The production of VOCs by *M. albus* in bioassay Petri plate test had an important antagonistic effect with lethality to other fungi. The antimicrobial profile of activity was dependent on the *Muscodor* species. Similar allelochemical effects were observed with volatile compounds and organic extracts from *Muscodor yucatanensis*, a tropical endophytic fungus from *Bursera simaruba* [190]. Further, naphthalene was identified as the insect repellent almost exclusively produced by *Muscodor vitigenus*, an endophytic fungus of *Paullinia paullinioides*. Agar plugs supporting growth of the fungus and producing known amounts of naphthalene effectively repelled the adult stage of the wheat stem sawfly, *Cephus cinctus*, in Y-tube bioassay tests.

THE PRODUCTION OF PLANT-DERIVED COMPOUNDS BY ENDOPHYTIC FUNGI

Some endophytes can produce secondary metabolites similar to those of their host plant. This is the case of the endophyte *Taxomyces andreanae* isolated from the phloem of the pacific yew *Taxus brevifolia* that produces paclitaxel (**129**) (Fig. 34) [191]. This spectacular discovery was first only based on the identical electrospray mass spectra of culture fluids of the fungus and authentic samples of the paclitaxel from yews. Further studies using ^{14}C-labeled precursors demonstrated the presence of fungal-derived taxol in the culture medium [7].

These results raised questions with regard to horizontal gene transfer from the host plant to endophytes acquiring the enzymatic machinery for the production of host-plant metabolites.

Thereafter, the endophyte *Pestalotiopsis microscopra*, isolated from a bald cypress (non-*Taxus* spp.), also turned out to biosynthesize paclitaxel (**129**) [192]. From this first example of paclitaxel-producing endophyte residing in another plant than *Taxus* spp., many other observations have been accumulated. For instance, **129** was found in endophytes isolated from the pine

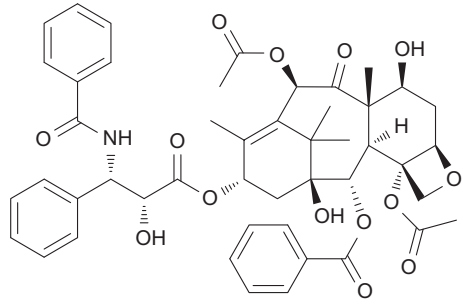

FIGURE 34 Structure of paclitaxel (**129**).

Wollemia nobilis and from the rubiaceous *Maguirethamnus speciosus* [193]. Generally, it appears that paclitaxel-producing endophytes are widespread and not confined to yew trees. Strobel and coworkers provided an ecological explanation for such a wide distribution of fungi producing **129** [1c]. According to them, **129** would be antifungal against plant pathogens such as *Phytophthora* spp. and *Phytium* spp. which are known to be sensitive to taxane derivatives and also to be the most important phytopathogens worldwide. Thus, phytopathogens would be strong competitors against endophytic fungi in the plant niches and endophytes would synthetize paclitaxel to protect the host plant from degradation and disease caused by these pathogens.

Nevertheless, a more recent report of Stanieck and coworkers suggested another hypothesis. The authors showed that commercial *T. andreanae* strain possesses the taxadiene synthase (TXS) and the phenylpropanoyl transferase (BAPT), two of the crucial enzymes implicated in the biosynthesis of paclitaxel (**129**) *in planta* [194]. However, they did not find the presence of **129** in the fungus extracts despite the existence of these enzymes. Accordingly, they suggested that a specific plant environment may be required for the induction of paclitaxel biosynthesis genes in the fungal symbiont.

Similarly, Kusari and coworkers investigated the biosynthetic pathways of hypericin (**132**) and emodin (**130**) (Fig. 35) in the endophyte *Thielavai subthermophila*, isolated from *Hypericum perforatum*, which produces both plant compounds [195]. A hypothetical biosynthetic pathway was proposed after the isolation and characterization of hypericin (**132**). Further, Bais and coworkers reported the biochemical and molecular characterization of the enzyme Hyp-1 from *H. perforatum* cell cultures that catalyzes the conversion of **130** into **132** (Fig. 35) [196].

Thus, in axenic submerged culture of the endophyte *T. subthermophila*, neither emodin anthrone (**131**) nor protohypericin (**133**), the hypothetical precursors of hypericin were detected. Moreover, no homologous sequence of the gene *hyp-1* in the endophyte was found. This is suggesting a different biosynthetic pathway and/or a different molecular regulation mechanism in the

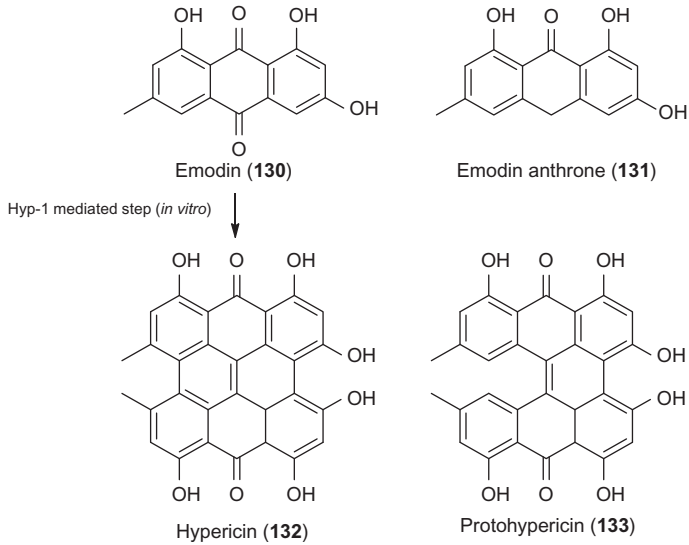

FIGURE 35 Emodin anthrone, protohypericin, and Hyp-1 mediated pathway from emodin to hypericin.

endophytic fungus than in the host plant. Thus, horizontal gene transfer might not be the only mechanism explaining the production of plant-derived metabolites by endophytes. The authors assumed that the endophyte and the host plant started coexisting, followed by some random gene transfer. However, it is possible that the fungus underwent independent evolution and developed its own machinery subjected to specific selection pressure. The production of plant-derived compounds by fungi could thus be the result of a convergent evolution of fungi and host plants. Therefore, the horizontal gene transfer hypothesis should be revisited and further investigated. The identification of the regulatory mechanisms could be of considerable interest for a deeper understanding of such plant–microbe interactions.

It was demonstrated that the production of known vegetal compounds in endophytes is by no mean restricted to paclitaxel and hypericin but also extends to other pharmacologically natural compounds like camptothecin (**134**) and podophyllotoxin (**135**) (Fig. 36). The discovery of fungal endophytes that produce plant-derived medicinal compounds would have significant biological and commercial implications. Up to now, many attempts have been made to increase the yield of fungal paclitaxel [197]. Nevertheless, yields are still very low when compared to yew cell cultures. It is likely due to the low tolerance of fungi to high level of taxol. In any case, advances in the molecular biology of fungal secondary metabolisms could allow a better understanding of the regulation of biosynthetic gene clusters and optimization of fungal metabolite production in laboratory conditions.

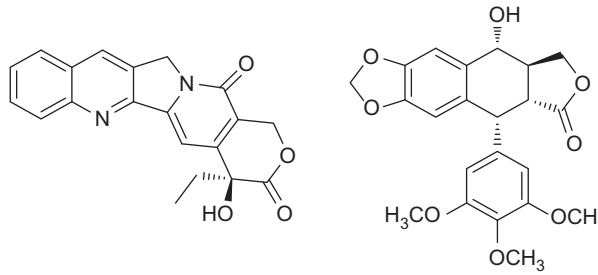

Camptothecin(**134**) Podophyllotoxin (**135**)

FIGURE 36 Further examples of plant-derived compounds produced by endophytic fungi.

THE REGULATION OF SECONDARY METABOLITE BIOSYNTHESIS IN ENDOPHYTIC FUNGI

The production of fungal secondary metabolites is subject to complex and multilevel regulation. Extensive studies on model fungi *Aspergillus* have provided insights into the molecular mechanisms of secondary metabolite regulation in fungi. Readers are referred to several in-depth reviews for details [198]. Here, we briefly cover current knowledge of this subject in fungi, and particularly focus on the regulation of endophytic fungal secondary metabolite production *in planta*. Like in bacteria, fungal genes involved in the biosynthesis of one particular metabolite are located adjacent to one another, forming a contiguous cluster [199]. Although the evolutionary origin of such gene clustering in fungi remains unknown, it is generally acknowledged that it underlines an advantage for a coordinated regulation. At the transcriptional level, two types of transcription factors have been reported. In some cases, a pathway-specific transcription factor is embedded in the gene cluster that directly activates/represses expression of the pathway, as exemplified by the positive regulator AlfR in the biosynthetic cluster for aflatoxin in *A. flavus* [200]. However, a more frequent mechanism in fungi involves global wide-domain regulators. They are not confined to a particular pathway and control production of various secondary metabolites in response to a wide range of environmental stimuli such as carbon/nitrogen source, pH, temperature, osmotic conditions, or light. Further, recent discovery of a novel global regulator in *Aspergillus* species has linked chromatin remodeling and epigenetic controls to secondary metabolites biosynthesis, representing a higher-hierarchical level of regulation [198c,201].

Although less studied, it is conceivable that endophytic fungi utilize the same regulation mechanisms for secondary metabolite production as elucidated for other non-endophytic fungi. For example, four conserved motifs matching wide-domain regulators were identified in promoters of the lolines biosynthetic cluster [202]. Preliminary data also accumulated to demonstrate the effect of biochemical regulators on EAS, by inhibition of histone deacetylases in

Claviceps species [35]. Given the highly regulated and coordinated nature of endophyte growth *in planta* [20,203], the plant host must control metabolic pathways of the symbiont or *vice versa* in order to maintain a balanced interaction. This view is substantiated by common observations that some fungal compounds, particularly those contribute to plant defence such as lolines [54] and ergot alkaloids [34], are synthesized only *in planta* and not in axenic cultures. Production of anti-insect lolines *in symbio* has been studied extensively. It was influenced by types and development stages of the plant tissues as well as environmental stresses [204]. Of particular relevance, artificial plant damages or that caused by herbivores were demonstrated to play a role in regulating loline synthesis [205]. In meadow fescue (MF)-*Neotyphodium* symbiota, it was shown that substrate availability accounted for a high level of lolines in young leaves [55]. On the contrary, in MF with the sexual species *E. festucae*, low yields of lolines were mainly due to downregulation of a positive regulator gene *lolA* [206]. Taken together, plant controlled production of endophyte metabolites is a sophisticated and specialized process. Future efforts will be required to elucidate the underlining molecular mechanisms, which will be indispensable to fully exploit the metabolic potential of endophytic fungi.

CONCLUSION

In this chapter, we have seen many examples of endophytic natural products which may play a role in fungi and plant life and physiology. Most of the bioactivities were evaluated *in vitro* and an extrapolation only can be done about their role, if expressed, *in planta*. Yet several studies have been undertaken *in vivo*, including the effect of plant–fungi association on the local ecosystem, and measurement of endophytic alkaloids within colonized plants, showing real consequences of the presence of endophytic metabolites (e.g., alkaloids) in the plant, in particular against herbivores and phytopathogens.

The fungal community is responsible for an impressive diversity of bioactive secondary metabolites, whose biosynthesis responds to environmental pressures. In the laboratory, culturing endophytic fungi in variable conditions can lead to deep modifications of their metabolism. The challenge will be to mimic the natural conditions *in planta* if we are to understand the functions and regulation mechanisms of fungal secondary metabolism. This should be a multidisciplinary task, from natural product chemistry, biochemistry, and chemical ecology to environmental ecology. At last, all observations concerning bioactive metabolites could be highly valuable to the humankind.

ABBREVIATIONS

3-NPA	3-Nitropropionic acid
A	Adenylation domain
AT	Acyl transferase

ACP	Acyl carrier Protein
BLAST	Basic local alignment search tool
C	Condensation domain
CMeT	C-Methyltransferase
DH	Dehydratase
DKP	Diketopiperazine
DMAT	4-Dimethylallyltryptophan
EAS/*eas*	Ergot alkaloid synthesis
ER	Enoyl reductase
ETP	Epipolythiodioxopiperazines
GC–MS	Gas chromatography–mass spectrometry
HR	Highly reducing (applied to PKS)
IGP	Indole-3-glycerol phosphate
ITS	Internal transcribed spacer
KR	Ketoreductase
KS	Ketosynthase
MAP	Mitogen-activated protein
MEA	Malt extract agar
MF	Meadow fescue
NAA	Nodulisporic acid
NCBI	National Center for Biotechnology Information
NR	Nonreducing (applied to PKS)
NRPS	Non-ribosomal peptide synthase
OSMAC	One strain many compounds
PCP	Peptidyl carrier protein
PCR	Polymerase chain reaction
PDA	Potato dextrose agar
PKS	Polyketide synthetase
PT	Product template
PR	Partially reducing (applied to PKS)
SAT	Starter ACP transacylase
VOC	Volatile organic compound

REFERENCES

[1] (a) For leading reviews on the chemistry of endophytic fungi, the reader can refer to: R.X. Tan, W.X. Zou, Nat. Prod. Rep. 18 (2001) 448–459; (b) B. Schulz, C. Boyle, S. Draeger, A.-K. Römmert, K. Krohn, Mycol. Res. 106 (2002) 996–1004; (c) G. Strobel, B. Daisy, Microbiol. Mol. Biol. Rev. 67 (2003) 491–502; (d) H.W. Zhang, Y.C. Song, R.X. Tan, Nat. Prod. Rep. 23 (2006) 753–771; (e) A.A.L. Gunatilaka, J. Nat. Prod. 69 (2006) 509–526; (f) A. H. Aly, A. Debbab, J. Kjer, P. Proksch, Fungal Divers. 41 (2010) 1–16.

[2] A.E. Arnold, Fung. Biol. Rev. 21 (2007) 51–66.

[3] C. Giménez, R. Cabrera, M. Reina, A. González-Coloma, Curr. Org. Chem. 11 (2007) 707–720.

[4] K. Clay, C. Schardl, Am. Nat. 160 (2002) S99–S127.
[5] K. Clay, Ecology 69 (1988) 10–16.
[6] R.J. Rodriguez, J.F. White Jr., A.E. Arnold, R.S. Redman, New Phytol. 182 (2009) 314–330.
[7] A. Stierle, G. Strobel, D. Stierle, Science 260 (1993) 214–216.
[8] S.E. Hartley, A.C. Gange, Ann. Rev. Entomol. 54 (2009) 323–342.
[9] C.A. Kimmons, Plant Dis. 74 (1990) 757–761.
[10] C. Yue, C.J. Miller, J.F.J. White, M. Richardson, J. Agric. Food Chem. 48 (2000) 4687–4692.
[11] (a) B.B. Clarke, J.F.J. White, R.H. Hurley, M.S. Torres, S. Sun, D.R. Huff, Plant Dis. 90 (2006) 994–998; (b) S.A. Bonos, M.M. Wilson, W.A. Meyer, C.R. Funk, Appl. Turfgrass Sci. 10 (2005) 1094.
[12] (a) M. Arechavaleta, C.W. Bacon, C.S. Hoveland, D.E. Radcliffe, Agron. J. 81 (1989) 83–90; (b) D.P. Malinowski, D.P. Belesky, Crop Sci. 40 (2000) 923–940.
[13] S. Marks, K. Clay, New Phytol. 133 (1996) 727–733.
[14] (a) R.S. Redman, K.B. Sheehan, R.G. Stout, R.J. Rodriguez, J.M. Henson, Science 298 (2002) 1581; (b) A.E. Arnold, L.C. Mejia, D. Kyllo, E.I. Rojas, Z. Maynard, N. Robbins, A.E. Herre, Proc. Natl. Acad. Sci. USA 23 (2003) 15649–15654; (c) M. Mucciarelli, S. Scannerini, C. Bertea, M. Maffei, New Phytol. 158 (2003) 579–591; (d) F. Waller, B. Achatz, H. Baltruschat, J. Fodor, K. Becker, M. Fischer, T. Heier, R. Huckelhoven, C. Neumann, D. von Wettstein, Proc. Natl. Acad. Sci. USA 201 (2005) 13386–13391; (e) D.T. Wicklow, S. Roth, S.T. Deyrup, J.B. Gloer, Mycol. Res. 109 (2005) 610–618.
[15] P.A. McGee, Aust. J. Exp. Agric. 42 (2002) 995–999.
[16] B.H. Ownley, K.D. Gwinn, F.E. Vega, Biocontrol 55 (2010) 113–128.
[17] R.J. Rodriguez, J. Henson, E. van Volkenburgh, M. Hoy, L. Wright, F. Beckwith, Y. Kim, R.S. Redman, Int. Soc. Microb. Ecol. J. 2 (2008) 404–416.
[18] B. Schulz, A.-K. Römmert, U. Dammann, H.-J. Aust, D. Strack, Mycol. Res. 103 (1999) 1275–1283.
[19] G.J. Samuel, R. Pardo-Schultheiss, K.P. Hebbar, R.D. Lumsden, C.N. Bastos, J.C. Costa, J.L. Bezerra, Mycol. Res. 104 (2000) 760–764.
[20] K.H. Kogel, P. Franken, R. Huckelhoven, Curr. Opin. Plant Biol. 9 (2006) 358–363.
[21] B. Schulz, C. Boyle, Mycol. Res. 109 (2005) 661–686.
[22] P. Alvarez-Loayza, J.F. White Jr., M.S. Torres, H. Balslev, T. Kristiansen, J.-C. Svenning, N. Gil, PLos One 6 (2011) 1–8.
[23] B. Schulz, J. Sucker, H.J. Aust, K. Krohn, K. Ludewig, P.G. Jone, D. Doring, Mycol. Res. 99 (1995) 1007–1015.
[24] (a) A.E. Arnold, D.A. Henk, R.L. Eells, F. Lutzoni, R. Vilgalys, Mycologia 99 (2007) 185–206; (b) A. Nieguitsila, M. Deville, T. Jamal, L. Halos, M. Berthelemy, R. Chermette, S. Latouche, P. Arne, J. Guillot, J. Microbiol. Methods 70 (2007) 86–95; (c) H.E. O'Brien, J.L. Parrent, J.A. Jackson, J.M. Moncalvo, R. Vilgalys, Appl. Environ. Microbiol. 71 (2005) 5544–5550.
[25] P.A. Paranagama, E.M.K. Wijeratne, A.A. Gunatilaka, J. Nat. Prod. 70 (2007) 1939–1945.
[26] H.B. Bode, R. Hofs, B. Bethe, A. Zeeck, ChemBioChem 3 (2002) 619–627.
[27] (a) T.O. Larsen, J. Smedsgaard, K.F. Nielsen, M.E. Hansen, J.C. Frisvad, Nat. Prod. Rep. 22 (2005) 672–695; (b) K. Scherlach, C. Hertweck, Org. Biomol. Chem. 7 (2009) 1753–1760.
[28] (a) C. Schardl, Fungal Genet. Biol., 33 (2001) 69–82; (b) J.A. Rudgers, K. Clay, J. Dighton, J.F. White, P. Oudemans (Eds.), The Fungal Community, Its Organization and Role in the Ecosystem, third ed., CRC Press, New York, 2005, pp. 423–442; (c) C. Schardl, A. Leuchtmann, J. Dighton, J.F. White, P. Oudemans (Eds.), The Fungal Community, Its Organization and Role in the Ecosystem, third ed., CRC Press, New York, 2005,

pp. 475–503; (d) J.F. Bischoff, J.F. White Jr., J. Dighton, J.F. White, P. Oudemans (Eds.), The Fungal Community, Its Organization and Role in the Ecosystem, third ed., CRC Press, New York, 2005, pp. 505–518; (e) C.W. Bacon, P. Lyons, J. Dighton, J.F. White, P. Oudemans (Eds.), The Fungal Community, Its Organization and Role in the Ecosystem, third ed., CRC Press, New York, 2005, pp. 519–531.
[29] M. Omacini, E.J. Chaneton, C.M. Ghersa, C.B. Müller, Nature 409 (2001) 78–81.
[30] K. Clay, J. Holah, Science 285 (1999) 1742–1744.
[31] (a) C.W. Bacon, J.K. Porter, J.D. Robbins, E.S. Luttrell, Appl. Environ. Microbiol. 34 (1977) 576–581; (b) F.N. Thompson, J.A. Stuedemann, Agric. Ecosyst. Environ. 44 (1993) 263–281.
[32] S.H. Faeth, C.J. Hayes, D.R. Gardner, Microb. Ecol. 60 (2010) 496–504.
[33] C. Wallwey, S.-M. Li, Nat. Prod. Rep. 28 (2011) 496–510.
[34] D.J. Fleetwood, B. Scott, G.A. Lane, A. Tanaka, R.D. Johnson, Appl. Environ. Microbiol. 73 (2007) 2571–2579.
[35] N. Lorenz, T. Haarmann, S. Pažoutová, M. Jung, P. Tudzynski, Phytochemistry 70 (2009) 1822–1832.
[36] (a) D.G. Panaccione, J.B. Kotcon, C.L. Schardl, R.D. Johnson, J.B. Morton, Nematology 8 (2006) 583–590; (b) A.A. Bacetty, M.E. Snook, A.E. Glenn, J.P. Noe, N. Hill, A. Culbreath, P. Timper, P. Nagabhyru, C.W. Bacon, Phytopathology 99 (2009) 1336–1345.
[37] D.G. Panaccione, R.D. Johnson, J. Wang, C.A. Young, P. Damrongkool, B. Scott, C.L. Schardl, Proc. Natl. Acad. Sci. USA 98 (2001) 12820–12825.
[38] J. Wang, C. Machado, D.G. Panaccione, H.F. Tsai, C.L. Schardl, Fungal Genet. Biol. 41 (2004) 189–198.
[39] T. Haartmann, C. Machado, Y. Lübbe, T. Correia, C.L. Schardl, D.G. Panaccione, P. Tudzynski, Phytochemistry 66 (2005) 1312–1320.
[40] M.A. Fischbach, C.T. Walsh, Chem. Rev. 106 (2006) 3468–3496.
[41] R.T. Gallagher, A.D. Hawkes, P.S. Steyn, R. Vleggaar, J. Chem. Soc. Chem. Commun. (1984) 614–616.
[42] S. Uhlig, C.J. Botha, T. Vrålstad, E. Rolén, C.O. Miles, J. Agric. Food Chem. 57 (2009) 11112–11119.
[43] C.A. Young, S. Felitti, K. Shields, G. Spangenberg, R.D. Johnson, G.T. Bryan, S. Saikia, B. Scott, Fungal Genet. Biol. (2006) 679–693.
[44] J.G. Ondeyka, G.L. Helms, O.D. Hensens, M.A. Goetz, D.L. Zink, A. Tsipouras, W. L. Shoop, L. Slayton, A.W. Dombrowski, J.D. Polishook, D.A. Ostlind, N.N. Tsou, R. G. Ball, S.B. Singh, J. Am. Chem. Soc. 119 (1997) 8809–8816.
[45] K.M. Byrne, S.K. Smith, J.G. Ondeyka, J. Am. Chem. Soc. 124 (2002) 7055–7060.
[46] P.G. Mantle, Phytochemistry 70 (2009) 7–10.
[47] S. Saikia, M.J. Nicholson, C. Young, E.J. Parker, B. Scott, Mycol. Res. 112 (2008) 184–199.
[48] M.-F. Qiao, N.-Y. Ji, X.-H. Liu, K. Li, Q.-M. Zhu, Q.-Z. Xue, Bioorg. Med. Chem. Lett. 20 (2010) 5677–5680.
[49] V. Raymond-Delpech, K. Matsuda, B.M. Sattelle, J.J. Rauh, D.B. Sattelle, Invert. Neurosci. 5 (2005) 119–133.
[50] For a recent review article on this topic, see: C.L. Schardl, R.B. Grossman, P. Nagabhyru, J.R. Faulkner, U.P. Mallik, Phytochemistry 68 (2007) 980–996.
[51] (a) J.D. Blankenship, M.J. Spiering, H.H. Wilkinson, F.F. Fannin, L.P. Bush, C.L. Schardl, Phytochemistry 58 (2001) 395–401; (b) K.D. Craven, J.D. Blankenship, A. Leuchtmann, K. Hignight, C.L. Schardl, Sydowia 53 (2001) 44–73.
[52] R.G. Powell, R.J. Petroski, S.W. Pelletier (Ed.), The Alkaloids: Chemical and Biological Perspectives, Springer, Berlin, 1992, pp. 320–338 vol. 8.

[53] J.A. Jackson, D.R. Varney, R.J. Petroski, R.G. Powell, L.P. Bush, M.R. Siegel, R.W. Hemken, P.M. Zavos, Drug Chem. Toxicol. 19 (1996) 85–96.
[54] H.H. Wilkinson, M.R. Siegel, J.D. Blankenship, A.C. Mallory, L.P. Bush, C.L. Schardl, Mol. Plant Microbe Interact. 13 (2000) 1027–1033.
[55] D.X. Zhang, P. Nagabhyru, C.L. Schardl, Plant Physiol. 150 (2009) 1072–1082.
[56] J.D. Blankenship, J.B. Houseknecht, S. Pal, L.P. Bush, R.B. Grossman, C.L. Schardl, ChemBioChem 6 (2005) 1016–1022 [Erratum in *Chembiochem* 7 (2006) 404].
[57] (a) D.X. Zhang, A.J. Stromberg, M.J. Spiering, C.L. Schardl, Fungal Genet. Biol. 46 (2009) 517–530; (b) M.J. Spiering, C.D. Moon, H.H. Wilkinson, C.L. Schardl, Genetics 169 (2005) 1403–1414.
[58] D.D. Rowan, M.B. Hunt, D.L. Gaynor, J. Chem. Soc. Chem. Commun. (1986) 935–936.
[59] (a) O.J.-P. Ball, G.M. Barker, R.A. Prestidge, D.R. Lauren, J. Chem. Ecol. 23 (1997) 1419–1434; (b) M.J. Spiering, G.A. Lane, M.J. Christensen, J. Schmid, Phytochemistry 66 (2005) 195–202.
[60] A. Koulman, G.A. Lane, M.J. Christensen, K. Fraser, B.A. Tapper, Phytochemistry 68 (2007) 355–360.
[61] (a) A. Tanaka, B.A. Tapper, A. Popay, E.J. Parker, B. Scott, Mol. Microbiol. 57 (2005) 1036–1050; (b) R. Johnson, C. Voisey, L. Johnson, J. Pratt, D. Fleetwood, A. Khan, G. Bryan, Fungal Genet. Biol. 44 (2007) 1180–1190.
[62] C.-L. Shao, C.-Y. Wang, Y.-C. Gu, M.-Y. Wei, J.-H. Pan, D.-S. Deng, Z.-G. She, Y.-C. Lin, Bioorg. Med. Chem. Lett. 20 (2010) 3284–3286.
[63] R. Abdou, K. Scherlach, H.-M. Dahse, I. Sattler, C. Hertweck, Phytochemistry 71 (2010) 110–116.
[64] M.B. Martins, I. Carvalho, Tetrahedron Lett. 63 (2007) 9923–9932.
[65] D.O. Guimarães, W.S. Borges, N.J. Vieira, L.F. de Oliveira, C.H.T.P. da Silva, N.P. Lopes, L.G. Dias, R. Durán-Patrón, I.G. Collado, M.T. Pupo, Phytochemistry 71 (2010) 1423–1429.
[66] C.J. Balibar, C.T. Walsh, Biochemistry 45 (2006) 15029–15038.
[67] S. Lautru, M. Gondry, R. Genet, J.L. Pernodet, Chem. Biol. 9 (2002) 1355–1364.
[68] R. Süssmuth, J. Müller, H. von Döhren, I. Molnàr, Nat. Prod. Rep. 28 (2011) 99–124.
[69] J. Zhang, K.B. Gunaherath, E.M.K. Wijeratne, L.A.A. Gunatilaka, Phytochemistry 68 (2007) 368–372.
[70] T. Degenkolb, H. von Döhren, K.F. Nielsen, G.J. Samuels, H. Brückner, Chem. Biodivers. 5 (2008) 671–680.
[71] L. Maddau, A. Cabras, A. Franceschini, B.T. Linaldeddu, S. Crobu, T. Roggio, D. Pagnozzi, Microbiology 155 (2009) 3371–3381.
[72] (a) Y.M. Chiang, B.R. Oakley, N.P. Keller, C.C.C. Wang, Appl. Microbiol. Biotechnol. 86 (2010) 1719–1736; (b) R.J. Cox, Org. Biomol. Chem. 5 (2007) 2010–2026.
[73] (a) M.A. Fischbach, C.T. Walsh, Chem. Rev. 106 (2006) 3468–3496; (b) C. Hertweck, Angew. Chem. Int. Ed. 48 (2009) 4688–4716.
[74] (a) H. Oikawa, T. Tokiwano, Nat. Prod. Rep. 21 (2004) 321–352; (b) W.L. Kelly, Org. Biomol. Chem. 6 (2008) 4483–4493.
[75] A. Ichihara, H. Tazaki, S. Sakamura, Tetrahedron Lett. 24 (1983) 5373–5376.
[76] S.-H. Wu, Y.-W. Chen, S.-C. Shao, L.-D. Wang, Y. Yu, Z.-Y. Li, L.-Y. Yang, S.-L. Li, R. Huang, Chem. Biodivers. 6 (2009) 79–85.
[77] K. Kasahara, T. Miyamoto, T. Fujimoto, H. Oguri, T. Tokiwano, H. Oikawa, Y. Ebizuka, I. Fujii, ChemBioChem 11 (2010) 1245–1252.
[78] T. Lin, X. Lin, C. Lu, Z. Hu, W. Huang, Y. Huang, Y. Shen, Eur. J. Org. Chem. (2009) 2975–2982.

[79] M.J. Begley, J.F. Grove, J. Chem. Soc. Perkin Trans. 1 (1985) 861–863.
[80] J. Dai, K. Krohn, D. Gehle, I. Kock, U. Flörke, H.-J. Aust, S. Draeger, B. Schulz, J. Rheinheimer, Eur. J. Org. Chem. (2005) 4009–4016.
[81] T. Bunyapaiboonsri, S. Yoiprommarat, P. Srikitikulchai, K. Srichomthong, S. Lumyong, J. Nat. Prod. 73 (2010) 55–59.
[82] A.S. Ratnayake, W.Y. Yoshida, S.L. Mooberry, T. Hemscheidt, Org. Lett. 3 (2001) 3479–3481.
[83] B. Bodo, L. Molho, D. Davoust, D. Molho, Phytochemistry 22 (1983) 447–451.
[84] J.F. Rivero-Cruz, G. García-Aguirre, C.M. Cerda-García-Rojas, R. Mata, Tetrahedron 56 (2000) 5337–5344.
[85] Q. Tan, X. Yan, X. Lin, Y. Huang, Z. Zheng, S. Song, C. Lu, Y. Shen, Helv. Chim. Acta 90 (2007) 1811–1817.
[86] S.-H. Wu, Y.-W. Chen, S.-C. Shao, L.-D. Wang, Z.-Y. Li, L.-Y. Yang, S.-L. Li, R. Huang, J. Nat. Prod. 71 (2008) 731–734.
[87] V.L. Singleton, N. Bohonos, A.J. Ullstrup, Nature 181 (1958) 1072–1073.
[88] B.-Z. Yu, N. Zhu, Z.-Z. Du, Helv. Chim. Acta 93 (2010) 324–328.
[89] R.D. Klausner, J.G. Donaldson, J. Lippincott-Schwartz, J. Cell Biol. 116 (1992) 1071–1080.
[90] Y. Suzuki, H. Tanaka, H. Aoki, T. Tamura, Agric. Biol. Chem. 34 (1970) 395–413.
[91] K. Krohn, U. Farooq, U. Flörke, B. Schulz, S. Draeger, G. Pescitelli, P. Salvadori, S. Antus, T. Kurtán, Eur. J. Org. Chem. (2007) 3206–3211.
[92] R. Kind, A. Zeeck, S. Grabley, R. Thiericke, M. Zerlin, J. Nat. Prod. 59 (1996) 539–540.
[93] W. Zhang, K. Krohn, H. Egold, S. Draeger, B. Schulz, Eur. J. Org. Chem. (2008) 4320–4328.
[94] J.A. Findlay, G. Li, J.D. Miller, T.O. Womiloju, Can. J. Chem. 81 (2003) 284–292.
[95] (a) K. Krohn, C. Biele, K.-H. Drogies, K. Steingröver, H.-J. Aust, S. Draeger, B. Schulz, Eur. J. Org. Chem. (2002) 2331–2336; (b) S. Gin, K. Krohn, U. Flörke, B. Schulz, S. Draeger, G. Pescitelli, P. Salvadori, S. Antus, T. Kurtán, Eur. J. Org. Chem. (2009) 3279–3284.
[96] K.N. Maloney, W. Hao, J. Xu, J. Gibbons, J. Hucul, D. Roll, S.F. Brady, F.C. Schroeder, J. Clardy, Org. Lett. 8 (2006) 4067–4070.
[97] K. Krohn, M.H. Sohrab, T. van Ree, S. Draeger, B. Schulz, S. Antus, T. Kurtán, Eur. J. Org. Chem. (2008) 5638–5646.
[98] Y.L. Zhang, H.M. Ge, F. Li, Y.C. Song, R.X. Tan, Chem. Biodivers. 5 (2008) 2402–2407.
[99] For a feature article on resorcylic acid lactones, see:N. Wissinger, S. Barluenga, Chem. Commun. (2007) 22–36.
[100] T.J. Turbyville, E.M.K. Wijeratne, M.X. Liu, A.M. Burns, C.J. Seliga, L.A. Luevano, C.L. David, S.H. Faeth, L. Whitesell, A.A.L. Gunatilaka, J. Nat. Prod. 69 (2006) 178–184.
[101] G. Avans, N.H. White, Trans. Brit. Mycol. Soc. 49 (1966) 563–576.
[102] M. Isaka, C. Suyarnsestakorn, M. Tanticharoen, P. Kongsaeree, Y. Thebtaranonth, J. Org. Chem. 67 (2002) 1561–1566.
[103] S.-X. Yang, J.-M. Gao, Q. Zhang, H. Laatsch, Bioorg. Med. Chem. Lett. 21 (2011) 1887–1889.
[104] A. Watanabe, I. Fujii, U. Sankawa, M.E. Mayorga, W.E. Timberlake, Y. Ebizuka, Tetrahedron Lett. 40 (1999) 91–94.
[105] Z. Huang, X. Cai, C. Shao, Z. She, X. Xia, Y. Chen, J. Yang, S. Zhou, Y. Lin, Phytochemistry 69 (2008) 1604–1608.

[106] (a) S.F. Brady, M.M. Wagenaar, M.P. Singh, J.E. Janso, J. Clardy, Org. Lett. 2 (2000) 4043–4046; (b) M.P. Singh, J.E. Janso, S.F. Brady, Mar. Drugs 5 (2007) 71–84.
[107] L.M. Abreu, R.K. Phipps, L.H. Pfenning, C.H. Gotfredsen, J.A. Takahashi, T.O. Larsen, Tetrahedron Lett. 51 (2010) 1803–1805.
[108] P. Chomcheon, S. Wiyakrutta, N. Sriubolmas, N. Ngamrojanavanish, S. Kengtong, C. Mahidol, S. Ruchirawat, P. Kittakoop, Phytochemistry 70 (2009) 407–413.
[109] (a) A. Ballio, S. Barcellona, B. Santurbano, Tetrahedron Lett. 31 (1966) 3723–3726; (b) T. Okuno, S. Oikawa, T. Goto, K. Sawai, H. Shirahama, T. Matsumoto, Agric. Biol. Chem. 50 (1986) 997–1001.
[110] For the antimicrobial activities of isocoumarins, see for example the following publication, and references therein:K. Krohn, I. Kock, B. Elsässer, U. Flörke, B. Schulz, S. Draeger, G. Pescitelli, S. Antus, T. Kurtán, Eur. J. Org. Chem. (2007) 1123–1129.
[111] W. Zhang, K. Krohn, S. Draeger, B. Schulz, J. Nat. Prod. 71 (2008) 1078–1081.
[112] I. Kock, S. Draeger, B. Schulz, B. Elsässer, T. Kurtán, A. Kenéz, S. Antus, G. Pescitelli, P. Salvadori, J.-B. Speakman, J. Rheinheimer, K. Krohn, Eur. J. Org. Chem. (2009) 1427–1434.
[113] K. Tianpanich, S. Prachya, S. Wiyakutta, C. Mahido, S. Ruchirawat, P. Kittakoop, J. Nat. Prod. 74 (2011) 79–81.
[114] G. Strobel, E. Ford, J. Worapong, J.K. Harper, A.M. Arif, D.M. Grant, P.C.W. Fung, R.M. W. Chau, Phytochemistry 60 (2002) 179–183.
[115] J.K. Harper, A.M. Arif, E. Ford, G. Strobel, J.A. Porco Jr., D.P. Tomer, K.L. Oneill, E.M. Heider, D.M. Grant, Tetrahedron 59 (2003) 2471–2476.
[116] G. Ding, S. Liu, L. Guo, Y. Zhou, Y. Che, J. Nat. Prod. 71 (2008) 615–618.
[117] H.M. Ge, W.Y. Zhang, G. Ding, P. Saparpakorn, Y.C. Song, S. Hannongbua, R.X. Tan, Chem. Commun. (2008) 5978–5980.
[118] X. Zhu, F. Yu, X.-C. Li, L. Du, J. Am. Chem. Soc. 129 (2007) 36–37.
[119] J.Y. Li, J.K. Harper, D.M. Grant, B.O. Tombe, B. Bashyal, W.M. Hess, G.A. Strobel, Phytochemistry 56 (2001) 463–468.
[120] J.C. Lee, G.A. Strobel, E. Lobkovsky, J.C. Clardy, J. Org. Chem. 61 (1996) 3232–3233.
[121] G. Ding, Y. Li, S. Fu, S. Liu, J. Wei, Y. Che, J. Nat. Prod. 72 (2009) 182–186.
[122] L. Chaomin, R.P. Johnson, J.A. Porco, J. Am. Chem. Soc. 125 (2003) 5095–5106.
[123] J.Y. Li, G.A. Strobel, Phytochemistry 57 (2001) 261–265.
[124] (a) L. Liu, S. Niu, X. Lu, X. Chen, H. Zhang, L. Guo, Y. Che, Chem. Commun. 46 (2010) 460–462; (b) D. Ding, F. Zhang, H. Chen, L. Guo, Z. Zou, Y. Che, J. Nat. Prod. 74 (2011) 286–291.
[125] H. Hussain, N. Akhtar, S. Draeger, B. Schulz, G. Pescitelli, P. Salvadori, S. Antus, T. Kurtán, K. Krohn, Eur. J. Org. Chem. (2009) 749–756.
[126] G. Assante, S. Dallavante, L. Malpezzi, G. Nasini, S. Burruano, L. Torta, Tetrahedron 61 (2005) 7686–7692.
[127] (a) A. Arnone, G. Nasini, W. Panzeri, O.V. de Pava, L. Malpezzi, J. Nat. Prod. 71 (2008) 146–149; (b) A. Arnone, G. Assante, A. Bava, S. Dallavalle, G. Nasini, Tetrahedron 65 (2009) 786–791.
[128] (a) For the isolation of sequoiatones A and B:A.A. Stierle, D.B. Stierle, T. Bugni, J. Org. Chem. 64 (1999) 5479–5484; (b) For the isolation of sequoiatones C–F:A.A. Stierle, D.B. Stierle, T. Bugni, J. Nat. Prod. 64 (2001) 1350–1353; (c) For the isolation of sequoiamonascins A–D:A.A. Stierle, D.B. Stierle, T. Bugni, J. Org. Chem. 68 (2003) 4966–4969.
[129] E. Li, L. Jiang, L. Guo, H. Zhang, Y. Che, Bioorg. Med. Chem. 16 (2008) 7894–7899.

[130] B. Elsässer, K. Krohn, U. Flörke, N. Root, H.J. Aust, S. Draeger, B. Schulz, S. Antus, T. Kurtán, Eur. J. Org. Chem. (2005) 4563–4570.
[131] J. Yang, F. Xu, C. Huang, J. Li, Z. She, Z. Pei, Y. Lin, Eur. J. Org. Chem. (2010) 3692–3695.
[132] I.N. Siddiqui, A. Zahoor, H. Hussain, I. Ahmed, V.U. Ahmad, D. Padula, S. Draeger, B. Schulz, K. Meier, M. Steiner, T. Kurtán, U. Flörke, G. Pescitelli, K. Krohn, J. Nat. Prod. 74 (2011) 365–373.
[133] W. Zhang, K. Krohn, Zia-Ullah, U. Flörke, G. Pescitelli, L. Di Bari, S. Antus, T. Kurtán, J. Rheinheimer, S. Draeger, B. Schulz, Chem. Eur. J. 14 (2008) 4913–4923.
[134] K. Krohn, S.F. Kouam, G.M. Kuigoua, H. Hussain, S. Cludius-Brandt, U. Flörke, T. Kurtán, G. Pescitelli, L. Di Bari, S. Draeger, B. Schulz, Chem. Eur. J. 15 (2009) 12121–12132.
[135] G.C. Carroll, F.E. Carroll, Can. J. Bot. 56 (1978) 3034–3043.
[136] (a) J.D. Miller, S. Mackenzie, M. Foto, G.W. Adams, J.A. Findlay, Mycol. Res. 106 (2002) 471–479; (b) M.W. Sumarah, J.D. Miller, G.W. Adams, Mycologia 97 (2005) 770–776.
[137] (a) M.W. Sumarah, G.W. Adams, J. Berghout, G.J. Slack, A.M. Wilson, J.D. Miller, Mycol. Res. 112 (2008) 731–736; (b) J.D. Miller, M.W. Sumarah, G.W. Adams, J. Chem. Ecol. 34 (2008) 362–368.
[138] Stains of these fungi have been studied by the authors but only yielded non insecticide wanthones and melleins:M.W. Sumarah, E. Puniani, B.A. Blackwell, J.D. Miller, J. Nat. Prod. 71 (2008) 1393–1398.
[139] J. Breen, J.C. Dacre, H. Raistrick, G. Smith, Nature 60 (1955) 618–626.
[140] (a) N. Takeda, S. Seo, Y. Ogihara, U. Sankawa, I. Iitaka, I. Kitagawa, S. Shibata, Tetrahedron 29 (1973) 3703–3719; (b) S. Seo, U. Sankawa, Y. Ogihara, I. Iitaka, S. Shibata, Tetrahedron 29 (1973) 3721–3726.
[141] K.C. Nicolaou, Y.H. Lim, C.D. Papageorgiou, J.L. Piper, Angew. Chem. 117 (2005) 8131–8135.
[142] S.F. Brady, M.P. Singh, J.E. Janso, J. Clardy, Org. Lett. 2 (2000) 4047–4049.
[143] K. Trisuwan, N. Khamthong, V. Rukachaisirikul, S. Phongpaichit, S. Preedanon, J. Sakayaroj, J. Nat. Prod. 73 (2010) 1507–1511.
[144] (a) Rearranged products with a spiro-nonadiene skeleton have been described:S.A. van der Sar, J.W. Blunt, M.H.G. Munro, Org. Lett. 8 (2006) 2059–2061; (b) X. Chen, Q. Shi, G. Lin, S. Guo, J. Yang, J. Nat. Prod. 72 (2009) 1712–1715.
[145] K. Krohn, U. Flörke, M. John, N. Root, K. Steingröver, H.-J. Aust, S. Draeger, B. Schulz, S. Antus, M. Simonyi, F. Zsila, Tetrahedron 57 (2001) 4343–4348.
[146] M.L. Marcias-Rubalcava, B.E. Hernandez-Bautista, M. Jimenez-Estrada, M.C. Gonzales, A.E. Glenn, R.T. Hanlin, S. Hernandez-Ortega, A. Saucedo-Garcia, J.M. Muria-Gonzalez, A.L. Anaya, Phytochemistry 69 (2008) 1185–1196.
[147] N. Ravindranath, M.R. Reddy, G. Mahender, R. Ramu, K.R. Kumar, B. Das, Phytochemistry 65 (2004) 2387–2390.
[148] A. Prajoubklang, B. Sirithunyalug, P. Charoenchai, R. Suvannakad, N. Sriubolmas, S. Piyamongkol, P. Kongsaeree, P. Kittakoop, Chem. Biodivers. 2 (2005) 1358–1367.
[149] K. Krohn, S.F. Kouam, S. Cludius-Brandt, S. Draeger, B. Schulz, Eur. J. Org. Chem. (2008) 3615–3618.
[150] M.W. Sumarah, E. Puniani, D. Sørensen, B.A. Blackwell, J.D. Miller, Phytochemistry 71 (2010) 760–765.
[151] M. Isaka, M. Tanticharoen, Y. Thebtaranonth, Tetrahedron Lett. 41 (2000) 1657–1660.
[152] X. Chen, Y. Zheng, Y. Shen, Chem. Rev. 107 (2007) 1777–1830.
[153] M. Saleem, H. Hussain, I. Ahmed, S. Draeger, B. Schulz, K. Meier, M. Steinert, G. Pescitelli, T. Kurtán, U. Flörke, K. Krohn, Eur. J. Org. Chem. (2011) 808–812.

[154] (a) For a review on tetramic and tetronic acids, see:R. Schobert, A. Schlenk, Bioorg. Med. Chem. 16 (2008) 4203–4221; (b) For a review on modified tetramic acids, see:B. Nay, N. Riache, L. Evanno, Nat. Prod. Rep. 26 (2009) 1044–1062.
[155] Y.K. Lam, O.D. Hensens, R. Ransom, R.A. Giacobbe, J. Polishook, D. Zink, Tetrahedron 52 (1996) 1481–1486.
[156] H. Oh, D.C. Swenson, J.B. Gloer, D.T. Wicklow, P.F. Dowd, Tetrahedron Lett. 39 (1998) 7633–7636.
[157] J.Y. Li, G. Strobel, J. Harper, E. Lobkovsky, J. Clardy, Org. Lett. 2 (2000) 767–770.
[158] K. Scherlach, D. Boettger, N. Remme, C. Hertweck, Nat. Prod. Rep. 27 (2010) 869–886.
[159] T. Ketelaar, C. Faivre-Moskalenko, J.J. Esseling, N.C.A. de Ruijter, C.S. Grierson, M. Dogterom, A.M.C. Emons, Plant Cell 14 (2002) 2941–2955.
[160] Y.-F. Wang, L.-M. Fan, W.-Z. Zhang, W. Zhang, W.H. Wu, Plant Physiol. 136 (2004) 3892–3904.
[161] H. Friedman, J.W. Vos, P.K. Hepler, S. Meir, A.H. Halevy, S. Philosoph-Hadas, Planta 216 (2003) 1034–1042.
[162] H.S. Sardar, J. Yang, A.M. Showalter, Plant Physiol. 142 (2006) 1469–1479.
[163] N. Moebius, C. Hertweck, Curr. Opin. Plant Biol. 12 (2009) 390–398.
[164] A. Vilcinskas, V. Matha, P. Götz, J. Insect Physiol. 43 (1997) 1149–1159.
[165] J.-C. Qin, Y.-M. Zhang, J.-M. Gao, M.-S. Bai, S.-X. Yang, H. Laatsch, A.-L. Zhang, Bioorg. Med. Chem. Lett. 19 (2009) 1572–1574.
[166] J. Schümann, C. Hertweck, J. Am. Chem. Soc. 129 (2007) 9564–9565.
[167] G.M. König, A.D. Wright, H.-J. Aust, S. Draeger, B. Schulz, J. Nat. Prod. 62 (1999) 155–157.
[168] (a) H.-W. Zhang, J. Zhang, S. Hu, Z.-J. Zhang, C.-J. Zhu, S.W. Ng, R.-X. Tan, Planta Med. 76 (2010) 1616–1621; (b) Z.-J. Lin, G.-J. Zhang, T.-J. Zhu, R. Liu, H.-J. Wei, Q.-Q. Gu, Helv. Chim. Acta 92 (2009) 1538–1544; (c) W. Pongcharoen, V. Rukachaisirikul, S. Phongpaichit, N. Rungjindamai, J. Sakayaroj, J. Nat. Prod. 69 (2006) 856–858; (d) S. Xu, H.M. GE, Y.C. Song, Y. Shen, H. Ding, R.X. Tan, Chem. Biodivers. 6 (2009) 739–745; (e) G. Ding, Y.C. Song, J.R. Chen, C. Xu, H.M. Ge, X.T. Wang, R.X. Tan, J. Nat. Prod. 69 (2006) 302–304; (f) C.-M. Cui, X.-M. Li, C.-S. Li, P. Proksch, B.-G. Wang, J. Nat. Prod. 73 (2010) 729–733.
[169] (a) H. He, H.Y. Yang, R. Bigelis, E.H. Solum, M. Greenstein, G.T. Carter, Tetrahedron Lett. 43 (2002) 1633–1636(b)H. He, H.Y. Yang, R. Bigelis, Patent Application US 20040127540A1 (2004).
[170] (a) D.T. Wicklow, S.M. Poling, Phytopathology 96 (2006) S122; (b) D.T. Wicklow, S.M. Poling, R.C. Summerbell, Can. J. Plant Pathol. 30 (2008) 425–433; (c) D. T. Wicklow, S.M. Poling, Phytopathology 99 (2009) 109–115.
[171] S.H. Faeth, Oikos 98 (2002) 25–36.
[172] (a) D.T. Wicklow, C.W. Hesseltine, O.L. Shotwell, G.L. Adams, Phytopathology 70 (1980) 761–764; (b) D.T. Wicklow, B.W. Horn, O.L. Shotwell, C.W. Hesseltine, R.W. Caldwell, Phytopathology 78 (1988) 68–74.
[173] (a) M. Isaka, N. Rugseree, P. Maithip, P. Kongsaeree, S. Prabpai, Y. Thebtaranonth, Tetrahedron 61 (2005) 5577–5583; (b) S. Madla, M. Isaka, P. Wongsa, Lett. Appl. Microbiol. 47 (2008) 74–78.
[174] (a) M. Isaka, W. Prathumpai, P. Wongsa, M. Tanticharoen, Org. Lett. 8 (2006) 2815–2817; (b) S. Supothina, M. Isaka, P. Wongsa, Lett. Appl. Microbiol. 44 (2007) 531–537.
[175] (a) F. Koizumi, K. Hasegawa, K. Ando, T. Ogawa, A. Hara, Patent Application JP 2001147574A2 (2001).(b) H. Oikawa, J. Org. Chem. 68 (2003) 3552–3557.

[176] S.C. Roberts, Nat. Chem. Biol. 3 (2007) 387–395.
[177] (a) J.R. Anderson, C.E. Briant, R.L. Edwards, M.P. Mabellis, J.P. Poyser, H. Spencer, A.J. Whalley, J. Chem. Soc. Chem. Commun. (1984) 405–406; (b) J.R. Anderson, R.L. Edwards, A.A. Freer, M.P. Mabellis, J.P. Poyser, H. Spencer, A.J. Whalley, J. Chem. Soc. Chem. Commun. (1984) 917–919; (c) J.R. Anderson, R.L. Edwards, J.P. Poyser, A.J. Whalley, J. Chem. Soc. Perkin Trans. 1 (1988) 823–831.
[178] S.T. Deyrup, D.C. Swenson, J.B. Gloer, D.T. Wicklow, J. Nat. Prod. 69 (2006) 608–611.
[179] C. Valdivia, M. Kettering, H. Anke, E. Thines, O. Sterner, Tetrahedron 61 (2005) 9527–9532.
[180] (a) S.F. Brady, M.P. Singh, J.E. Janso, J. Clardy, J. Am. Chem. Soc. 122 (2000) 2116–2117; (b) S.F. Brady, S.M. Bondi, J. Clardy, J. Am. Chem. Soc. 123 (2001) 9900–9901.
[181] X. Wu, C.-H. Lu, Y.-M. Shen, Helv. Chim. Acta 92 (2009) 2783–2789.
[182] L.E. Schmidt, S.T. Deyrup, J. Baltrusaitis, D.C. Swenson, D.T. Wicklow, J.B. Gloer, J. Nat. Prod. 73 (2010) 404–408.
[183] L. Yuan, P.-J. Zhao, J. Ma, G.-H. Li, Y.-M. Shen, Helv. Chim. Acta 91 (2008) 1588–1594.
[184] P. Chomcheon, S. Wiyakrutta, N. Sriubolmas, N. Ngamrojanavanich, D. Isarangkul, P. Kittakoop, J. Nat. Prod. 68 (2005) 1103–1105.
[185] C.R. Hipkin, D. Simpson, S.J. Wainwright, M.A. Salem, Nature 430 (2004) 98–101.
[186] M. Schwarz, B. Köpcke, R.W.S. Weber, O. Sterner, H. Anke, Phytochemistry 65 (2004) 2239–2245.
[187] (a) G.A. Strobel, E. Dirkse, J. Sears, C. Markworth, Microbiology 147 (2001) 2943–2950; (b) D. Ezra, W.M. Hess, G.A. Strobel, Microbiology 150 (2004) 4023–4031.
[188] G.A. Strobel, K. Fluck, W.M. Hess, J. Sears, D. Ezra, P.N. Vargas, Microbiology 153 (2007) 2613–2620.
[189] A.M. Mitchel, G.A. Strobel, E. Moore, R. Robison, J. Sears, Microbiology 156 (2010) 270–277.
[190] M.L. Marcías-Rubalcava, B.E. Hernández-Bautista, F. Oropeza, G. Duarte, M.C. González, A.E. Glenn, R.T. Hanlin, A.L. Anaya, J. Chem. Ecol. 36 (2010) 1122–1131.
[191] A. Stierle, G. Strobel, D. Stierle, Science 260 (1993) 154–155.
[192] J.Y. Li, G.A. Strobel, R. Shidu, W.M. Hess, Microbiology 142 (1996) 2223–2226.
[193] (a) G.A. Strobel, W.M. Hess, J.Y. Li, E. Ford, J. Sears, R.S. Sidhu, B. Summerell, Aust. J. Bot. 45 (1997) 1073–1082; (b) G.A. Strobel, E. Ford, J.Y. Li, J. Sears, R.S. Sidhu, W.M. Hess, Syst. Appl. Microbiol. 22 (1999) 426–433.
[194] A. Stanieck, H.J. Woerdenbag, O. Kayser, Planta Med. 75 (2009) 1561–1566.
[195] S. Kusari, M. Lamshoft, S. Zühlke, M. Spiteller, J. Nat. Prod. 71 (2009) 159–162.
[196] H.P. Bais, R. Vepachdu, C.B. Lawrence, F.R. Stremirtz, J.M. Vivance, J. Biol. Chem. 278 (2003) 32413–32422.
[197] X. Zhou, H. Zhu, L. Liu, J. Lin, K. Tang, Appl. Microbiol. Biotechnol. 86 (2010) 1707–1717.
[198] (a) N.P. Keller, G. Turner, J.W. Bennett, Nat. Rev. Microbiol. 3 (2005) 937–947; (b) D. Hoffmeister, N.P. Keller, Nat. Prod. Rep. 24 (2007) 393–416; (c) J. Strauss, Y. Reyes-Dominguez, Fungal Genet. Biol. 48 (2011) 62–69; (d) A.A. Brakhage, M. Thön, P. Spröte, D.H. Scharf, Q. Al-Abdallah, S.M. Wolke, P. Hortschansky, Phytochemistry 70 (2009) 1801–1811.
[199] N.P. Keller, T.M. Hohn, Fungal Genet. Biol. 21 (1997) 17–29.
[200] K.C. Ehrlich, B.G. Montalbano, P.J. Cotty, Fungal Genet. Biol. 38 (2003) 63–74.
[201] J. Bok, N. Keller, Euk. Cell 3 (2004) 527–535.

[202] B.L. Kutil, C. Greenwald, G. Liu, M.J. Spiering, C.L. Schardl, H.H. Wilkinson, Fungal Genet. Biol. 44 (2007) 1002–1010.
[203] C.J. Eaton, M.P. Cox, B. Scott, Plant Sci. 180 (2011) 190–195.
[204] (a) M. Justus, L. Witte, T. Hartmann, Phytochemistry 44 (1997) 51–57; (b) C.W. Kennedy, L.P. Bush, Crop. Sci. 23 (1983) 547–552; (c) D.W. Tong, J.Y. Wang, P. Brain, R. Gooneratne, Agric. Sci. China 5 (2006) 793–797.
[205] (a) T.L. Bultman, G. Bell, W.D. Martin, Ecology 85 (2004) 679–685; (b) T.J. Sullivan, J. Rodstrom, J. Vandop, J. Librizzi, C. Graham, C.L. Schardl, T.L. Bultman, New Phytol. 176 (2007) 673–679.
[206] D.X. Zhang, P. Nagabhyru, J.D. Blankenship, C.L. Schardl, Plant Signal. Behav. 5 (2010) 1419–1422.

Chapter 9

Flavonoids as Anti-Inflammatory and Analgesic Drugs: Mechanisms of Action and Perspectives in the Development of Pharmaceutical Forms

Waldiceu A. Verri Jr.[*], Fabiana T.M.C. Vicentini[†], Marcela M. Baracat[‡], Sandra R. Georgetti[‡], Renato D.R. Cardoso[*], Thiago M. Cunha[§], Sergio H. Ferreira[§], Fernando Q. Cunha[§], Maria J.V. Fonseca[†] and Rubia Casagrande[‡]

[*]*Departamento de Ciencias Patologicas, Centro de Ciencias Biologicas, Universidade Estadual de Londrina, Rod. Celso Garcia Cid, Campus Universitario, Londrina, Parana, Brazil*

[†]*Department of Pharmaceutical Sciences of Ribeirao Preto, University of Sao Paulo, Ribeirao Preto, Sao Paulo, Brazil*

[‡]*Departamento de Ciencias Farmaceuticas, Centro de Ciencias da Saude, Universidade Estadual de Londrina, Londrina, Parana, Brazil*

[§]*Department of Pharmacology, School of Medicine of Ribeirao Preto, University of Sao Paulo, Ribeirao Preto, Sao Paulo, Brazil*

INTRODUCTION

Flavonoids constitute a large group of aromatic amino acids widely distributed in the plant kingdom [1–3]. In fact, flavonoids are important components of the human diet. The intake of flavonoids can range between 50 and 800 mg/day, depending on the consumption of vegetables and fruits [4–6]. Flavonoids are free radical scavengers (chain-breaking antioxidants) because they are highly reactive as hydrogen or electron donors, which has led to their potential use as therapeutic drugs [2,3,5,7–9].

In this chapter, we will discuss the current knowledge on the anti-inflammatory and analgesic effects and mechanisms of flavonoids. The basic chemistry of

Bioactive Natural Products, Vol. 36. DOI: 10.1016/B978-0-444-53836-9.00026-8

flavonoids, structure–activity relationship, preclinical evidence and models, and the development of pharmaceutical forms for their administration are also addressed.

CHEMISTRY AND CLASSIFICATION

Flavonoids are formed in plants from the aromatic amino acids phenylalanine and malonate. As shown in Fig. 1, the basic flavonoid structure is the flavan nucleus, which consists of 15 carbon atoms arranged in three rings (C-6–C-3–C-6) that are labeled A, B, and C. The various classes of flavonoids differ in the level of oxidation and the pattern of substitution of the C ring, whereas individual compounds within a class differ in the pattern of substitution of the A and B rings as presented in Fig. 2. The flavonoid classes are flavones, flavanones, isoflavones, flavonols, flavanonols, flavan-3-ols, anthocyanidins, chalcones, and aurones. The dimerization of flavonoids has also been shown [10].

Flavonoids are primarily found in plants as glycosides, whereas aglycones (the forms lacking sugar moieties) are found less frequently. At least eight different monosaccharides or combinations of these (di- or trisaccharides) can bind to different hydroxyl groups of the flavonoid aglycone [11]. The most common sugar moieties include D-glucose and L-rhamnose. The glycosides are typically *o*-glycosides with the sugar moiety bound to the hydroxyl group at the C-3 or C-7 position [12].

ANTI-INFLAMMATORY AND ANALGESIC FLAVONOIDS AND THEIR MECHANISMS

Inflammation involves the development of four phenomena: edema, pain, erythema, and an increase in temperature/fever. Depending on the intensity of these cardinal signs, there can be loss of function. Although it is not a cardinal inflammatory sign, the recruitment and activity of cells during inflammation is important for the host response against infections and tissue repair. The development of inflammation is initiated by the release of mediators of different structures/classes through many cellular sources. Regarding the cellular sources, resident cells, including macrophages and mast cells, are the first to

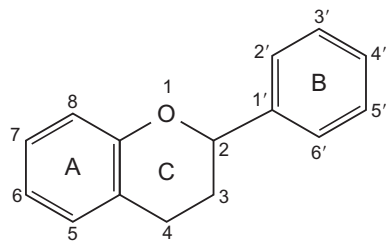

FIGURE 1 Core structure of flavonoids.

respond to inflammatory stimuli, and they communicate to the other cells of the host by producing inflammatory mediators, which have been shown to organize the host response and indicate what cells should be recruited to the inflammatory foci and what activity should be performed by these cells. A didactic description of inflammatory mediators examines those that are produced by cells and those that are produced from components present in the plasma. The mediators produced by cells are serotonin, histamine, cytokines and chemokines, nitric oxide (NO), reactive oxygen species (ROS), and lipid mediators, such as prostanoids, leukotrienes, and lipoxins. Those derived from components present in the plasma include bradykinin and members of the complement and coagulation system [13]. Flavonoids interfere with these molecules at various degrees, depending on the concentration/doses of flavonoids used *in vitro* and *in vivo*. In the following sections, we will discuss the anti-inflammatory and analgesic mechanisms of flavonoids as antioxidants,

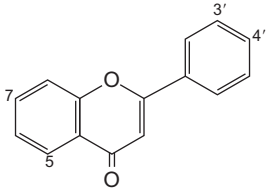

Flavones

	5	6	7	3′	4′
Luteolin	OH		OH	OH	OH
Apigenin	OH		OH	OH	
Chrysin	OH		OH		
Baicalein	OH	OH	OH		
Baicalin	OH	OH			

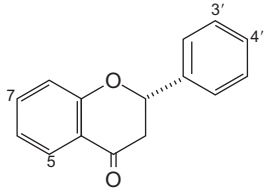

Flavonones

	5	7	3′	4′
Hesperetin	OH	OH	OH	OCH_3
Narigenin	OH	OH		OH

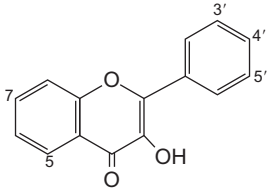

Flavonols

	5	7	3′	4′	5′
Quercetin	OH	OH	OH	OH	
Kaempferol	OH	OH		OH	
Galangin	OH	OH			
Fisetin		OH	OH	OH	
Myricetin	OH	OH	OH	OH	OH
Isoquercetin	OH	OH	OH	OH	
Myricetrin	OH	OH	OH	OH	OH
Rutin	OH	OH	$O_9C_{12}H_{21}$	OH	OH

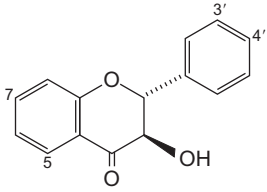

Flavanolol

	5	7	3′	4′
Taxifolin	OH	OH	OH	OH

FIGURE 2 (A) Structural characteristics of flavonoids.

continued

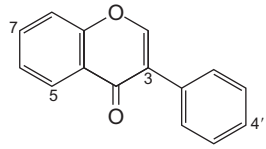

Isoflavones

	5	7	4′
Genistein	OH	OH	OH
Genistin	OH	Oglc	OH
Daidzein		OH	OH
Daidzin		Oglc	OH
Biochanin A	OH	OH	OCH_3
Formononetin		OH	OCH_3
Dehydroequol		OH	OH
Equol		OH	OH
Isoequol		OH	OH

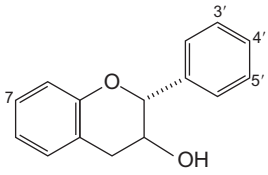

Flavan-3-ols

	3	5	7	3′	4′	5′
(+)-catechin	βOH	OH	OH	OH	OH	
(-)-epicatechin	αOH	OH	OH	OH	OH	
(-)-epigallocatechin	αOH	OH	OH	OH	OH	OH
gallate						
Procyanidins		OH	OH	OH	OH	

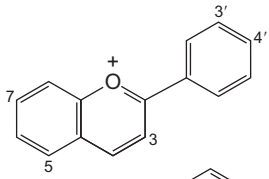

Anthocyanidins

	3	5	7	3′	4′
Cyanidin	OH	OH	OH	OH	OH
Cyanin	O-glc	OH	OH	OH	OH
Pelargonidin	OH	OH	OH		OH

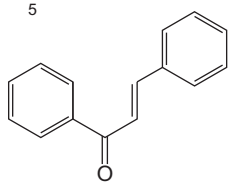

Chalcones

	3	5	3′	4′
Butein	OH	OH	OH	OH
2-hidroxychalcone			OH	

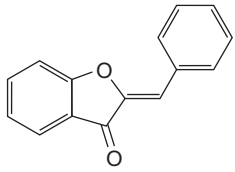

Aurones

	4	6	7	3′	4′
Auresidin	OH	OH		OH	OH
Leptosidin		OH	OCH_3	OH	OH

FIGURE 2—cont'd (B) Structural characteristics of flavonoids.

inhibitors of cytokine production and cyclooxygenase (COX) expression, and inhibitors of a variety of intracellular pathways.

Antioxidant Effect of Flavonoids and Structure–Activity Relationship

Many of the biological functions of flavonoids are attributed to their antioxidant effects. The mechanisms are related to the neutralization of ROS, such as peroxide anions, superoxide anion, hydroxyl radicals, lipid peroxides, and hydroperoxides. Flavonoids also prevent oxidation of low-density lipoproteins, which have been implicated in atherosclerosis [14].

The prominent antioxidant activity of flavonoids is related to their low redox potential (0.23<E7<0.75) [15]; therefore, they are thermodynamically able to reduce free radicals with redox potentials between 2.13 and 1.0 V. Structure–activity studies of flavonoids have shown that three main components are important for their activity: (1) *o*-dihydroxy on the B ring confers the high stability to the flavonoid after the H atom donation, forming a phenoxyl radical by participating in the electron delocalization; (2) the presence of 2,3-double bound bond in conjugation with a 4-oxo group on the C ring allows for the dislocation of an electron from the phenoxyl radicals on the B ring to the C ring; and (3) the 3-hydroxy group in combination with the 2,3-double bound increases the resonance stabilization for electron dislocation across the molecule [16]. Flavonoids have been shown to chelate metals, which is a characteristic associated with the presence of *o*-dihydroxy group in the B ring, 3-hydroxy and 4-oxo groups in the C ring, and 5-hydroxy and 4-oxo groups in the C and A rings as shown in Fig. 1. Variations in these structures resulted in variations in activity. It is noteworthy to mention that quercetin is considered a standard flavonoid because it contains these three structures related to flavonoids activity (Fig. 1). Figure 2 shows the basic structure of the other members of the flavonoid family with substituent groups forming some prominent flavonoids.

Flavonoids have also been shown to inhibit xanthine oxidase, which is involved in the production of superoxide anion and hydrogen peroxide. Therefore, this is a likely antioxidant mechanism of flavonoids [17].

Interestingly, flavonoids can also exert pro-oxidant activities, which are related to the presence of hydroxyl groups, especially in the B ring. Further, the unsaturated 2,3-bond and 4-oxo arrangement of flavones may promote the formation of ROS induced by divalent copper in the presence of oxygen. These data suggest that the same structural attributes that increased the antioxidant capacity could also exacerbate oxidative stress and the damage to functional and structural cellular molecules [18].

Inhibition of Production and Activity of Cytokines and Other Related Molecules by Flavonoids

There is evidence that free radicals could activate oxidative stress sensitive transcription factors, such as nuclear factor κB (NF-κB). NF-κB is known as a pro-inflammatory transcription factor that induces the production of COX-2, cytokines, and other pro-inflammatory molecules. In this vein, free radicals are also pro-inflammatory molecules. Further, this is reciprocal because cytokines, such as tumor necrosis factor α (TNFα), have been shown to activate nicotinamide adenine dinucleotide phosphate-oxidase (NADPH oxidase) to produce superoxide anion, which, in turn, could activate NF-κB, although this relationship was not found in every cell and experimental condition [19]. This could be one mechanism for the inhibition of cytokine production or cytokine-dependent inflammation by flavonoids. Cytokines induce the

production of other cytokines and chemokines, and the inhibition of cytokine effects limits this amplification system [20]. Cytokines have been shown to induce the production of prostanoids, such as prostaglandin E_2 (PGE_2), from COX-2 and have been shown to induce NF-κB activation, resulting in increased COX-2 expression (enzyme that produced prostaglandin). Thus, this modulation of cytokines and NF-κB activity might explain other effects of flavonoids, such as the inhibition of prostaglandin synthesis [19,21,22].

An interesting study investigated the mechanisms of baicalin (7-glucuronic acid 5,6-dihydroxy-flavone), which is a flavonoid derived from *Scutellaria baicalensis* Georgi. Baicalin acts through an NF-κB-independent mechanism and selectively binds to chemokines (subtype of cytokines), such as stromal cell-derived factor (SDF), IL-8, MIP-1β, MCP-2, and C lymphotactin without interacting with fractalkine (CX3C chemokine), neurotactin, or other cytokines, such as TNFα and IFNγ. Baicalin does not compete with chemokines for receptor binding; thus, it is not a receptor antagonist. Therefore, the anti-inflammatory mechanism of baicalin could be attributed to selectively binding/scavenging chemokines and limiting their biological activity [23].

In addition, studies have shown that flavonoids also induced the expression of anti-inflammatory molecules, such as IL-1 receptor antagonist (IL-1ra), as shown for luteolin in alveolar macrophages. Luteolin has been shown to increase IL-1ra mRNA expression in alveolar macrophages without affecting the mRNA expression of the anti-inflammatory cytokine IL-10 [24].

Therefore, flavonoids can inhibit NF-κB-dependent cytokine production, act as a scavenger of some chemokines or induce the expression of anti-inflammatory cytokines, such as IL-1ra. This role is important in inflammation because cytokines and chemokines initiate the inflammatory response. Cytokines and chemokines activate and induce the increased expression of adhesion molecules allowing the rolling of leukocytes over the endothelium, which is necessary for their recruitment. Chemokines are important for the selective recruitment of leukocytes during a variety of inflammatory conditions. Cytokines are also involved in the development of fever by inducing the production of prostaglandins, which act on EP3 (subtype of PGE_2 receptor) [25] receptors to alter the activity of warm and cold sensitive neurons in the hypothalamus to induce thermodysregulation. Another component of inflammation is pain, which results from the activation and sensitization of nociceptors (neurons transmitting the painful stimulus). Cytokines can directly modulate nociceptor activity via their receptors. Thus, during inflammation, flavonoids function to inhibit pro-inflammatory cytokine production and inducing anti-inflammatory cytokines or scavenging chemokines. As described for baicalin, the scavenging effects were selective for some chemokines and were similar to those observed with soluble receptors or anti-cytokine antibodies. In this sense, because not all flavonoids may present the same effects described for the general form, every flavonoid must be analyzed separately in different *in vivo* and/or *in vitro* assays.

Cytokines have also been shown to increase the expression of inducible nitric oxide synthase (iNOS), which is responsible for NO synthesis in inflammatory states [26]. The inhibition of iNOS-derived NO production is an important anti-inflammatory mechanism of flavonoids because excessive NO production is one of the components responsible for tissue destruction in inflammation. In contrast, flavonoids, such as baicalin, increased the expression of heme oxygenase-1 (HO-1) during ischemia/reperfusion injury model, which mediated the reduction of NF-κB localization in the nucleus (active NF-κB) and inhibition of IκB degradation. Therefore, the reduction of TNFα, IL-6, and COX-2 mRNA expression was observed [27]. Flavonoids modulate the activity of other enzymes, such as myeloperoxidase, which is an enzyme found in neutrophils and macrophages that produce the microbicidal molecule hypochlorite. Flavonoids, such as myricitrin and quercetin, are substrates for myeloperoxidase and inactivate it *in vitro* and *in vivo* [22,28,29].

During inflammation, cytokines activate and increase the expression of adhesion molecules, which are responsible for the interactions between leukocytes and endothelial cells resulting in the sequence of rolling, firm adhesion and transmigration of leukocytes culminating in leukocyte recruitment toward the inflammatory foci. The three main groups of adhesion molecules include selectins, integrins, and adhesion molecules of the immunoglobulin super family. Their expression was reduced by the treatment with flavonoids [30–33].

Thus, flavonoids affect the biology of cytokines/chemokines and other systems, such as iNOS/NO and HO-1, to different extents and mechanisms. Figure 3 summarizes these data.

Effect of Flavonoids on the Production of Lipid Mediators

It has been shown that flavonoids inhibit the peroxidase active site of COX-1, COX-2, and 5-lipoxygenase (5-LO) [62], resulting in inhibition of prostanoids (prostaglandins and tromboxanes) and leukotrienes production, respectively. In fact, flavonoids inhibited the production of PGE_2, which was consistent with the inhibition of COX activity. In addition to the inhibition of the COX-2 peroxidase active site [62], there is evidence that flavonoids inhibited the NF-κB-dependent expression of COX-2 [63].

The inhibition of COX has the potential to be used as clinical activity because of the use of selective and nonselective COX inhibitors, which have been classified as nonsteroidal anti-inflammatory drugs (NSAIDs). Prostaglandins contributed to edema as a consequence of increased vascular permeability and modulated the activity of neurons responsible for painful stimuli perception and thermal regulation [13]. It is noteworthy that COX-1 inhibitors have side effects, such as an increase in gastric and intestinal ulcers, because prostaglandins have been shown to increase protective mucus production, and

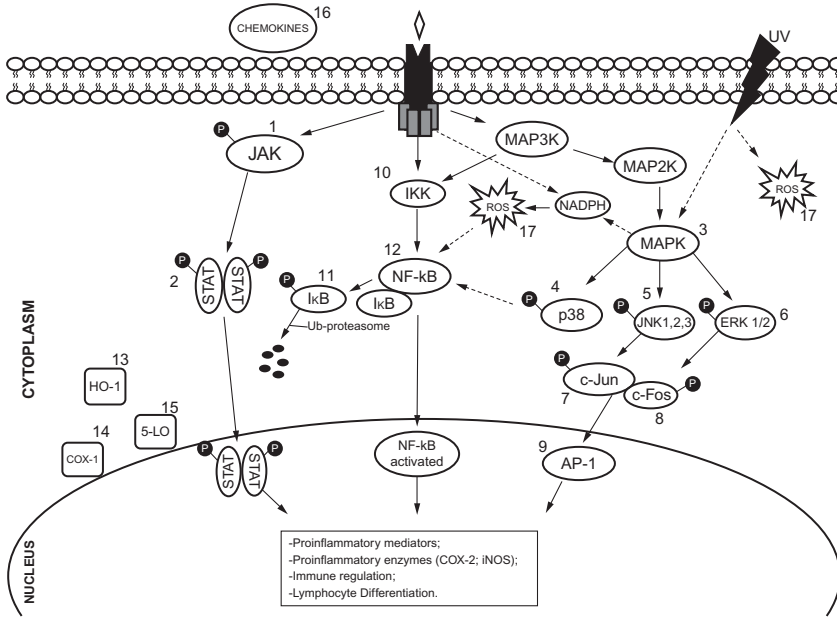

FIGURE 3 Intracellular targets of flavonoids in inflammation. A variety of inflammatory stimuli activate cells via receptors to produce inflammatory mediators that regulate the inflammatory process. This cellular activation depends on intracellular signaling pathways. Receptor-independent mechanisms also exist, such as those activated by UV radiation. Some examples of flavonoid classes regulating inflammation by modulating/blocking JAK (janus kinase)/STAT (signal transducers and activators of transcription), MAPKs (mitogen-activated protein kinases), AP-1 (activating protein 1) and NF-κB (nuclear factor κB) pathways are shown. These data support that the flavonoid apigenin (flavone) inhibited the expression of 1–2 [34] and 7–10 [35,36], decreased 13 [37] production and inhibited the phosphorylation of 4–6 [38]. Delphinidin (anthocyanidins) inhibited 4–6, 9, 11–12 [39,40]. The epigallocatechin gallate (aflavan-3-ols) suppressed 12 and 9 activation [41], phosphorylation of 5 and 6 [42], upregulated 13 [43] and inhibited 16 [44]. The isoflavone genistein also inhibited the activation of 2–4 and 12 [45] and upregulates 13 [43]. Naringenin (flavonones) suppressed the activation of 1–4, 6, and 8 pathways and the downstream signal transducer of 2 and 12 [34,46,47] and induced production of 13 [48]. Quercetin (flavonols) modulated 1–2 [49] and 12–13 pathways [32,50], reduced the expression of 14 and 16 [32,51], inhibited 11 [52] degradation and attenuated the activation of points 3–10 [32,53]. Butein (chalcone) inhibited 11 degradation [54] and 1–2, 4–6, and 12 activation [54,55]. Taxifolin (flavonolol) inhibited the activation of 1–3 and 6 [56,57]. Baicalein reduced 1–2, 4–6, 11, and 15 [29,58,59] activation and scavenged 16 [60]. Fisetin (flavonol) targeted 4 [61] and increased 13 expression [61]. In addition to the inhibition of COX-2 expression, flavonoids also inhibited the peroxidase site of COX-2 [62]. Finally, all flavonoids have antioxidant activities and, therefore, inhibited 17. This is a general scheme of flavonoid targets [13,14,18]. However, it is important to note that not all cellular mechanisms are shown, and the flavonoids present in this study may have other targets that are not presented in this figure.

treatment with COX-2 inhibitors increased the cardiovascular risk because the COX-2-derived PGE_2 produced by endothelial cells present anti-aggregating and vascular relaxing activities [64,65]. However, because the activity of flavonoids do not rely exclusively on the inhibition of COX enzymes but affect other pathways concomitantly to COX inhibition, they do not present these common side effects of NSAIDs that target COX enzymes. In fact, flavonoids have opposite effects compared to the COX inhibitors. The treatment with extracts containing flavonoids and/or flavonoid-rich fractions of extracts reduced the gastric lesions induced by NSAIDs, such as aspirin and indomethacin, or even promoted tissue healing [66,67]. Studies have also shown that isolated flavonoids, such as rutin, reduced ulcers [68]. Moreover, in a randomized clinical trial, a cream containing quercetin caused pain relief and aphthous ulcer healing [69]. The analgesic mechanisms are discussed in a separated section.

Regarding leukotrienes, there are 5-LO inhibitors and leukotriene receptor antagonists available for clinical use. Because inhibition of leukotriene synthesis [62] is a possible mechanism of action for some flavonoids, it is possible that flavonoids inhibit inflammatory conditions that depend on leukotrienes. In fact, isoquercitrin inhibited leukotriene-induced airway contraction in guinea pigs [70], and genistein inhibited leukotriene synthesis in eosinophils in asthma [71]. Further, flavonoids have additional mechanisms. Narigenin reduced mucus secretion by modulating ROS production and inhibited NF-κB activity via epidermal growth factor receptor (EGFR)/phosphatidylinositol 3-kinase (PI3K)-Akt/extracellular-regulated kinase (ERK) mitogen activated protein kinase (MAP kinases) signaling in human airway epithelial cells [72], quercetin induced a bronchodilator effect in an acute asthma model [73], and apigenin reduced allergen-induced airway inflammation [74]. Therefore, it is likely that flavonoids could represent a possible therapeutic approach in asthma and in leukotriene-related diseases because leukotriene synthesis inhibitors and receptor antagonists are in clinical use. Further, flavonoids have a low toxicity, whereas leukotriene inhibitors have neurological side effects and induce liver toxicity (more information on leukotriene inhibitors can be found at www.fda.gov); therefore, flavonoids are safer than leukotriene synthesis inhibitors and receptor antagonists.

Flavonoids can also modulate other lipid mediators. Isoflavones, such as genistein and daidzein, inhibited the hydrolysis of anandamide by fatty acid amide hydrolase (FAAH) at low micromolar concentrations. Among the flavonoids tested by Thors *et al*. [75], kaempferol was the most potent and was shown to inhibit FAAH in a competitive manner. The implications of this mechanism of action included the reduced degradation of endocannabinoids and, therefore, the enhancement of the activation of cannabinoid receptors. The consequences would be the increase in the analgesic effect of endogenous and exogenous cannabinoids in cancer and inflammatory pain [76–78].

Inhibition of Intracellular Signaling Pathways by Flavonoids During Inflammation and Possible Implications Regarding Their Antioxidant Effects

During inflammation, a variety of signaling pathways can be activated depending on the inflammatory mediators, type of antigen and type of cell. For example, PI3K and the three main MAP kinases, ERK, p38, and c-Jun N-terminal kinase (JNK), are triggered during inflammation and may be responsible for NADPH oxidase activation/oxidative burst, leukocyte recruitment and activation of transcription factors, such as NF-κB and activating protein-1 (AP-1) [79]. In inflammation, inhibition of one MAP kinase reduced the production of free radicals and inflammatory mediators. For instance, TNFα-induced superoxide anion production via NADPH oxidase activation depends on three pathways: (i) PI3K-induced PKC (protein kinase C) δ, (ii) PI3K/ERK-induced PKCδ, and (iii) p38 activation of NADPH oxidase in a PKCδ-independent manner. As a consequence, inhibition of MAP kinases reduced superoxide anion production [80]. Therefore, because a variety of flavonoids have been shown to inhibit MAP kinases, including p38, JNK, and ERK [72,81,82], it is possible that flavonoids do not act as antioxidants only by scavenging free radicals but also by inhibiting NADPH oxidase-dependent production of superoxide anion and other ROS. Further, excessive NADPH oxidase activation may lead to tissue lesions; thus, flavonoids could limit tissue lesions. Because these MAP kinases and PI3K pathways lead to NF-κB and/or AP-1 activation and, consequently, pro-inflammatory mediators (e.g., cytokines) and enzymes (e.g., COX-2), their inhibition by flavonoids also reduced the production of these inflammatory mediators [24,29,72,83].

Leukocyte recruitment is an important feature of inflammation because leukocytes, such as neutrophils, must reach the inflammatory foci to phagocytose and eliminate the foreign antigen. However, excessive leukocyte recruitment and activation, in general, resulted in tissue lesions. Therefore, it is important to limit the leukocyte recruitment to reduce tissue lesions. In autoimmune diseases, leukocytes have a major role in tissue destruction, and inhibiting their recruitment was shown to be beneficial [84,85]. MAP kinases and PI3K are also activated during leukocyte recruitment with different kinases activated based on the inflammatory stimulus and leukocyte. Because flavonoids inhibit the activation of those kinases, this is a possible mechanism that is involved in flavonoid inhibition of leukocyte recruitment. Nevertheless, the efficacy of each flavonoid in each inflammatory condition needs to be demonstrated [72,81,82].

Intracellular signaling pathways are involved in flavonoid-induced activation of antioxidant mechanisms. In human umbilical vein endothelial cells (HUVECs), it was demonstrated that treatment with small interfering RNA (siRNA) and pharmacological inhibitors targeting PKCδ and p38 MAPK attenuated HO-1 induction by fisetin (flavonol). The fisetin-induced

HO-1 expression was dependent on increased nuclear factor (erythroid-derived 2)-like 2 (Nrf2) translocation and antioxidant response element (ARE), as detected by luciferase activity. Consistent with this, the treatment with an HO-1 inhibitor reduced the inhibitory effect of fisetin for H_2O_2 production [86].

Therefore, several models were able to demonstrate that the signaling pathways were inhibited by flavonoids. It was difficult to present all signaling pathways affected by flavonoids. In this vein, some additional intracellular mechanisms targeted by flavonoids are summarized in Fig. 3.

Structure–Activity Relationship of Flavonoids in Inflammation

There are some slight differences in the intracellular pathways inhibited by the different classes of flavonoids, but they share many similar targets as shown in Fig. 3. Unfortunately, the majority of studies that examined the activity of flavonoids did not investigate the structure–activity relationship. However, there were several studies that did examine this relationship.

Tran *et al*. [87] synthesized derivatives from 2′-hydroxychalcone and investigated their effect on lipopolysaccharide (LPS)-induced PGE_2 synthesis in macrophages. They concluded that the structure required the combination of at least two alkoxy groups on the B ring of chalcones (see Fig. 2 for the basic structure) where one group was substituted at position 4 and the other group was substituted at positions 3 or 5 of B ring, which may enhance the inhibitory activity of PGE_2 production. The benzyloxy moiety plays an important role in establishing strong interactions between chalcone and COX-2. Importantly, the inhibition of PGE_2 production from RAW 264.7 cells by 2-hydroxychalcone derivatives was not associated with their cytotoxicity, which further corroborates the safety of flavonoids.

Interestingly, previous studies have found the effects of flavonols (kaempferol, quercetin, and myricetin) and flavones (flavone, chrysin, apigenin, luteolin, baicalein, and baicalin) on the TNFα-stimulated ICAM-1 (adhesion molecule) expression. Among the flavonoids tested, quercetin, kaempferol, chrysin, apigenin, and luteolin inhibited TNFα-induced ICAM-1 expression. These results suggest that the activity was independent of the flavonoid class (flavonols and flavones) (Fig. 2). The TNFα-induced expression of ICAM-1 was dependent on the activation of MAP kinases (ERK, JNK, and p38), NF-κB, and AP-1. Apigenin and luteolin (flavones) inhibited TNFα-induced activation of all MAP kinases, AP-1, and IKK/NF-κB pathways. In comparison, kaempferol (flavonols) and chrysin (flavones) only inhibited JNK and AP-1 activity. Further, kaempferol (flavonols) and chrysin (flavones) showed similar mechanisms of action, whereas flavones (apigenin and luteolin compared to chrysin) signaled through a unique mechanism. Thus, the flavonoid class does not define the mechanism of action, but the –OH group at positions 5 and 7 of the A ring and at position 4 of the B ring is an important structural component for determining the flavonoid mechanisms of action (see Fig. 2 for

the basic structure). Further, the presence of an –OH group at position 3 of the B ring reduced the activity, whereas the –OH group at position 5 of the B ring abolished the activity [29].

Previous studies have also shown that kaempferol had increased activity than quercetin regarding the inhibition of the expression of adhesion molecules (VCAM-1, ICAM-1, and L-selectin) [32], which was consistent with the data mentioned above [29]. However, quercetin showed increased inhibition of iNOS and COX-2 protein expression and NF-κB and AP-1 than kaempferol [32]. These compounds differ by the presence of the –OH at position 3 in the B ring in quercetin. This structural difference was considered to be predictive of the reduced activity in the study of Chen *et al*. [29], as described above. In contrast, the –OH group at positions 3 and 4 in the B ring found in quercetin conferred high stability to the flavonoid after H atom donation, forming a phenoxyl radical by participating in the electron delocalization, and represents one out of three possible antioxidant mechanisms of flavonoids, as described above [16]. Because iNOS and COX-2 could be induced by transcription factors, including NF-κB and AP-1, and that free radicals activate NF-κB, the presence of the –OH group at positions 3 and 4 in the B ring and the resulting antioxidant effect might account for the inhibition of gene expression and NF-κB and AP-1 activation by LPS [32]. Therefore, it is likely that depending on the experimental model, the –OH groups may result in contrasting data regarding the structure–activity relationship.

Analgesic Flavonoids

The sensitization of primary sensory neurons is essential to inflammatory pain. Nonetheless, previously, the sensitization of nociceptors was believed to be the result of the excitatory action of a "soup" of various inflammatory mediators released at the site of inflamed or damaged tissue. However, this hypothesis was challenged by the discovery of the mechanism of action of NSAIDs by Vane's group [88] and by the demonstration, in humans and in animals, that eicosanoids were primarily responsible for nociceptor sensitization and not overt pain [89]. In addition to PGE_2, other inflammatory mediators, including sympathetic amines, endothelin, substance P, bradykinin, and NGF, also possessed the same nociceptor-sensitizing property. These mediators acted directly on neuronal receptors, triggering molecular mechanisms that facilitated the electrical activity of the neuronal membrane. Although our understanding of the molecular mechanisms of nociceptor sensitization is not complete, there is a general agreement that the stimulation of G-protein-coupled receptors by inflammatory mediators activate the enzyme adenylate cyclase to produce cyclic adenosine monophosphate (cAMP). This substance, in turn, triggers the activation of a group of protein kinases [protein kinase A (PKA) and C (PKC)], which leads to the phosphorylation of ion channels in the membrane. These data were a result of a facilitation of the

inward sodium current via tetrodotoxin (TTX)-resistant Na^+ channels, a facilitation of inward Ca^{2+} currents, and an inhibition of outward K^+ currents. This sequence of events is the basic peripheral mechanism of hyperalgesia, a state in which a slight or normally non-noxious thermal, mechanical, or chemical stimulus becomes painful [21].

We refer to the mediators that act directly on the primary nociceptor as "final mediators," which was in contrast with "intermediate" mediators released during inflammation by resident and migrating cells or by plasma, which stimulated the release of the final mediators. Whereas the inflammatory signs and symptoms were similar, the resident and migrating cells and the intermediate and final mediators varied depending on the time frame, the type of tissue, and the type of inflammatory stimuli. In general, measurements of mediators in exudates or inflamed tissues at a single time point gave a distorted picture of the evolution of the pathological process and suggested a disorganized "soup" of cells and mediators. In fact, sequential release of inflammatory mediators or cellular events observed after a challenge by inflammatory stimuli could be observed only by performing a series of measurements. Commonly, it is this temporal and pathophysiological hierarchy that allowed the researcher to discover the site of action of existing drugs or to propose targets for new drug development [21].

Studies have shown that flavonoids have analgesic effects. They have been shown to inhibit both inflammatory and neuropathic pain through mechanisms involving the inhibition of cytokine production (e.g., IL-1β) and prostaglandin and inducing NO production and endogenous opioid-dependent mechanisms. These data were demonstrated for quercetin and other flavonoids (e.g., myricitrin, hesperidin, and dihydroxy flavones) in models of overt pain-like behavior, such as acetic acid and phenyl-*p*-benzoquinone-induced abdominal contortions and in the formalin test, in models of mechanical hyperalgesia induced by carrageenan and in thermal hyperalgesia in streptozotocin-induced diabetes [90–95]. Depending on the experimental model, flavonoids inhibited the production of intermediate and directly acting nociceptive mediators in inflammatory pain [93] as well as directly antagonized nociceptor sensitization by activating neuronal mechanisms, including the release of endogenous opioids in streptozotocin-induced diabetic neuropathy [90]. Previous studies have demonstrated that myrecetin reduced, in a concentration- and p38-dependent manner, the K^+ currents in dorsal root ganglia (DRG) neurons using whole cell patch-clamp recordings. This effect does not induce analgesia. Therefore, it is unlikely that the analgesic mechanism of a flavonoid would depend on the direct modulation of K^+ currents in neurons [96]. In contrast, studies have shown that the inhibition of TNFα-induced activation of MAP kinase, p38, in DRG neurons reduced the activation of TTX-resistant Na^+ channels, such as Nav 1.8, that have been implicated in inflammatory and neuropathic pain [21]. Thus, the inhibition of these Na^+ currents is an analgesic mechanism [97]. Together with the data demonstrating that

flavonoids inhibited MAP kinase activation [81], it would be appropriate to determine whether flavonoids reduce TTX-resistant sodium channels currents in DRG neurons.

In support of the involvement of the inhibition of oxidative stress in flavonoids analgesic mechanisms of action, quercetin has been shown to inhibit carrageenan-induced mechanical hyperalgesia and the accompanying reduction in the decreased glutathione levels [92]. Interestingly, baicalin reduced streptozotocin-induced neuropathic pain by inhibiting p38 activation, oxidative–nitrosative stress, and 12/15-lipoxygenase overexpression and activation without affecting glucose levels [98]. Therefore, as discussed for other inflammatory signs, it is likely that flavonoids function through more than one mechanism. Further, glucocorticosteroids (steroidal anti-inflammatory drugs) increased the blood glucose levels, which is a relevant side effect for diabetic patients. In this sense, the ability of baicalin to reduce pain without affecting glucose levels indicates that it would be a potential treatment option for diabetic patients' pain management [98].

Structure modifications are also an interesting approach to increase the activity of flavonoids. El-Sabbagh *et al.* [99] synthesized 2,3-dihydroquinazolin-4 (1*H*)-one derivatives bearing chalcone moieties. One compound showed a significant analgesic effect in the acetic acid-induced writhing test and in the reduction of carrageenan-induced paw edema compared to celecoxib (a commonly used NSAID that selectively inhibits COX-2), and it also exhibited a similar loss of gastric effects, as compared to celecoxib, which were reduced compared to COX-1 inhibitors, such as indomethacin. Therefore, structural modifications of flavonoids could be a promising approach to increase their analgesic and anti-inflammatory activities. However, it remains to be determined whether the side effects are also maintained in very low levels.

Evidence of Flavonoids Effects in Human Inflammatory Diseases and Human Cell Models of Disease

To further corroborate the data discussed above on the anti-inflammatory effects, mechanisms and structure–activity relationship of flavonoids, studies support their use in *in vitro* models to evaluate inflammatory signaling using human cells and in human diseases.

Dietary supplementation of quercetin at 900 mg/day for 4 weeks did not change the blood biomarkers of inflammation and disease severity of rheumatoid arthritis patients [100]. However, there are some concerns to be mentioned. Quercetin has poor oral absorption, and therefore, optimized pharmaceutical formulation might help increase its absorption. The patients were recommended to refrain from ingesting nutritional antioxidants because their ingestion normally ranged between 50 and 800 mg/day [4–6]. Thus, the treatment with quercetin at the dose tested would only replenish the deficit of intake. Moreover, only one dose was tested and the period was short. Further, these patients were

under conventional medical treatments that made it difficult to observe the additional anti-inflammatory effects with quercetin treatment [100].

In contrast, quercetin has been shown to inhibit phorbol 12-myristate 13-acetate (PMA)- and calcium ionophore A23187 (PMACI)-induced gene expression and the production of TNFα, IL-1β, IL-6, and IL-8 in a human mast cell line. Quercetin also attenuated PMACI-induced activation of NF-κB and p38 MAP kinase in mast cells [101]. Because mast cells play an important role in the pathogenesis of rheumatoid arthritis, modulation of the production of inflammatory mediators by these cells could be a target of quercetin [85]. Further data regarding rheumatoid arthritis demonstrated that hesperitin and myricetin also reduced IL-1β-induced production of metalloprotease and IL-6 in human synovial cell line in a JNK and JNK- and p38-dependent manner, respectively [102,103]. Luteolin also reduced IL-1β-induced cytokine and metalloprotease activation by inhibiting MAP kinases, NF-κB, and AP-1 in a human synovial sarcoma cell line [104].

In another autoimmune disease, lupus, patients need alternatives to steroids and cytotoxic drugs. Apigenin inhibited autoantigen-presenting and stimulatory functions of antigen presenting cells (APCs) necessary for the activation and expansion of autoreactive Th1 and Th17 cells and B cells in lupus. Apigenin also has been shown to cause apoptosis of hyperactive lupus APCs and T and B cells by inhibiting expression of NF-κB-regulated anti-apoptotic molecules, especially COX-2 and cellular caspase-8 (FLICE)-like inhibitory protein (c-FLIP), which are hyper-expressed by lupus immune cells. Increasing the bioavailability of dietary plant-derived COX-2 and NF-κB inhibitors, such as apigenin, could be valuable for suppressing inflammation in lupus and other Th17-mediated diseases, such as rheumatoid arthritis, Crohn's disease, and psoriasis, and in the prevention of inflammation-based tumors overexpressing COX-2 (colon and breast) [105].

Interestingly, one study addressed the effect of flavonoid intake in chronic diseases. People with an increased quercetin intake had a lower mortality from ischemic heart disease. The incidence of cerebrovascular disease was lower with a higher intake of kaempferol, naringenin, and hesperetin. Men with increased quercetin intake had a lower lung cancer incidence, and men with higher myricetin intake had a lower prostate cancer risk. The incidence of asthma was lower with increased quercetin, naringenin, and hesperetin intakes. A trend toward a reduction in the risk of type 2 diabetes was associated with higher quercetin and myricetin intakes [106]. Therefore, there are data suggesting a protective role of flavonoids in human disease and/or human cell systems. Of note, the effects of flavonoids, as shown in humans [106], might depend on long-term treatment.

Evidence also suggests that flavonoids might be useful to reduce the excessive inflammatory responses induced in the presence of bacterial (e.g., LPS and fMLP) products by inhibiting the activation of MAP kinases, PI3K, and NF-κB and inhibiting the production of pro-inflammatory cytokines and NO

[107–109]. Further, long-term ultraviolet-induced skin inflammation has been shown to contribute to cancer development, and flavonoids have been shown to reduce the inflammatory state by mechanisms that are discussed in the section regarding topical formulation development [110–113].

DEVELOPMENT OF ORAL FORMULATIONS CONTAINING FLAVONOIDS

Encapsulation of Flavonoids

The research and application of flavonoids have been areas of great interest in the functional foods, nutraceutical and pharmaceutical industries due to their high spectrum of biological activities, including antioxidant, anti-inflammatory, antibacterial, and antiviral functions [86–118]. However, the effectiveness of nutraceutical products, including flavonoids, in preventing diseases is dependent on preserving the bioavailability of the active ingredients. This can be difficult because only a small proportion of the molecules remain available following oral administration due to insufficient gastric residence time, low permeability and/or solubility within the gut, and their instability under conditions encountered in food processing and storage (temperature, oxygen, and light) or in the gastrointestinal tract (pH, enzymes, and in the presence of other nutrients) [119].

In fact, flavonoids have weak water solubility and could undergo degradation in the acidic stomach environment. These properties cause low flavonoid dissolution rates from solid, oral dosage forms, such as capsules and tablets, from meals or from the partial degradation in the harsh pH conditions of the gastric environment, resulting in a low absorption and bioavailability. Thus, to encapsulate flavonoids in gastro-resistant polymers to transport them directly to the intestine may improve their bioavailability after oral administration [120]. To increase the effectiveness of flavonoids, formulations must provide protective mechanisms that can maintain the active molecular form until the time of consumption and deliver this form to the physiological target within the organism [121].

Most of the bioactive food components were administered in encapsulated forms to overcome the drawbacks of their instability, alleviate unpleasant tastes or flavors, and improve the bioavailability and half-life of the compound *in vivo* and *in vitro* [122–129].

Microencapsulation is defined as a process in which tiny particles or droplets of the active ingredient(s) are surrounded by a coating or embedded in a homogeneous or heterogeneous matrix, generally of polymeric materials, to give small capsules that may range from sub-microns to several millimeters in size with many useful properties [130]. Nanoencapsulation involves the formation of active, loaded particles with diameters ranging from 1 to 1000 nm [129]. The term nanoparticle is a collective name for both nanospheres and nanocapsules. Nanospheres have a matrix type structure. Active particles

may be absorbed at the sphere surface or encapsulated within the particle. Nanocapsules are vesicular systems in which the active particle is confined to a cavity consisting of an inner liquid core surrounded by a polymeric membrane [131]. Compared to micron-sized particles, nanoparticles provide a greater surface area and have the potential to increase the solubility due to a combination of large interfacial adsorption of the core compound, enhanced bioavailability, and improved controlled release, which enabled better precision targeting of the encapsulated materials [130,132].

The encapsulation, depending on the polymers and technology used, may stabilize these labile compounds and extend their shelf-life. From an industrial perspective, encapsulated powders would be easy to handle and to use in food and pharmaceutical processing, keeping their initial flavonoid content, bioactivity, and safety for prolonged storage. In nano- and microsystems, stabilization occurred because the wall/coating material acts as a physical barrier; therefore, for this reason, the shelf-life of the encapsulated drugs was prolonged. Moreover, polymers may modulate the release rate and solubility in intestinal fluid [120,133–135].

Various techniques have been used for encapsulation, including spray-drying, spray freezing, extrusion, coacervation, liposome entrapment, inclusion complexation, lyophilization, and emulsion [136,137,133].

Spray-Drying

Spray-drying encapsulation is commonly used in pharmaceutical and biochemical fields and in the food industry due to the large availability of equipment and for the ease of industrialization. It is also a mild, "one-step" processing operation to move from a liquid feed into a powder product [138,139]. The spray-drying process is an economical, flexible, continuous operation that produces particles of good quality. The typical shape of spray-dried particles is spherical, with a mean size range of 10–100mm [137]. Because the fast solvent evaporation keeps the droplet temperature far below the drying air temperature, spray-drying is strongly recommended for heat sensitive materials, such as flavonoids [114]. Ersus and Yurdagel [140] microencapsulated the flavonoid anthocyanin pigments of the black carrot by spray-drying using maltodextrins as a carrier and coating agents to protect the flavonoids from oxidation. The ethanolic extracts of black carrots that were dried with high air inlet temperatures (>160–180°C) caused greater anthocyanin losses, whereas the maltodextrin of 20–21 DE (Glucodry® 210) gave the highest anthocyanin content powder at the end of drying process [140]. The maltodextrin could also be mixed with arabic gum as wall material. A mixture of maltodextrin (60%) and arabic gum (40%) has been used for encapsulation of procyanidins from grape seeds [141]. The encapsulation efficiency was up to 89%, and the procyanidin was not changed during drying. The stability of the products was improved by spray-drying.

Other flavonoids, such as naringin and rutin, that present different structures and physicochemical characteristics were microencapsulated by spray-drying using cellulose-derived polymers [142]. The protective ability of cellulose derivatives was based either on the ability to form amorphous matrices loading drugs during the spray-drying process or on their pH dependent solubility. Cellulose acetate phthalate (CAP) was as insoluble and stable in acidic gastric fluid as in its nonionized form. It becomes soluble, swellable, and disintegrable as the phthalic acid groups ionized above pH 6 in intestinal fluid [143]. However, these results showed that satisfactory, gastro-resistant microsystems were produced only for the more soluble glycosides, such as rutin and naringin [142,144]. Nevertheless, in the development of gastro-resistant microparticles containing low-solubility, the ingredients required a compromise between the enhancement of the dissolution rate and protection in the gastric environment. An incomplete flavonoid release in the simulated intestinal fluid was observed for the slightly water-soluble, such as quercetin [142,144]. Sansone *et al*. [120] produced naringenin and quercetin gastro-resistant microparticles by spray-drying and investigated the effects of the combined use of CAP as coating polymer and three different materials (sodium dodecylbenzensulfonate, tween-85, and sodium carboxymethylcellulose crosslinked) that were able to enhance the dissolution test. The presence of a combination of CAP and surfactants or swelling agents in the formulations produced microparticles with a good resistance at a low gastric fluid pH and complete flavonoid release in the intestinal environment. The spray-drying technique and the process conditions selected have produced good encapsulation efficiencies and product yields. Chitosan has also been used as a wall material in spray-drying of olive leaf extract (OLE) [145]. Another wall material successfully used for encapsulation of polyphenol was the protein–lipid (sodium caseinate–soy lecithin) emulsion, which has been used in spray-drying of grape seed extract, apple polyphenol extract, and olive leaf extract [146]. Therefore, there is an increase in groups attempting to develop gastro-resistant formulations containing flavonoids to increase their availability.

Coacervation

Complex coacervation is commonly associated with no definite forms and is an expensive method for encapsulating food ingredients [147]; however, this process should be related to the potential benefits it might offer, especially to high value, labile functional ingredients, such as the encapsulation of flavonoids [148]. The size of the capsule and its characteristics can be varied by changing the pH, the ion concentration, the ratio of matrix molecule and the bioactive component, and the type of matrix. The technique is primarily driven by electrostatic interactions, but hydrophobic interactions are also involved [136,148,149]. This is immobilization rather than encapsulation technology and is, therefore, mostly proposed and applied for bioactive food

molecules rather than for bioactive, living cells. The technique is applied for flavors, oils, and for some water-soluble bioactive molecules [119].

The studies on encapsulation of flavonoids by coacervation used wall materials, such as calcium alginate and calcium alginate-chitosan, to encapsulate yerba mate extract [125], gelatin to encapsulate (−) epigallocatechin gallate [150], glucan to encapsulate black currant extract [151], and propolis extract was encapsulated using pectin and soy protein [126]. Other coacervation coating systems such as gliadin, heparin/gelatin, carrageenan, soy protein, polyvinyl alcohol, gelatin/carboxymethylcellulose, b-lactoglobulin/gum acacia, and guar gum/dextran have also been studied [147]. However, most of the core materials in these studies were essential oils rather than flavonoids.

Liposomes

Liposomes are spherical bilayers that enclose bioactive molecules. The liposomes are formed by dispersion of polar lipids (mostly phospholipids) in an aqueous solution. Liposomes can be utilized in the entrapment, release of water-soluble, lipid-soluble, and amphiphilic materials [152]. Bioactive agents encapsulated into liposomes can be protected from digestion in the stomach and showed significant levels of absorption in the gastrointestinal tract, leading to the enhancement of bioactivity and bioavailability [153]. A variety of liposome techniques have been employed for the encapsulation of flavonoids, such as film evaporation, sonication, reverse phase evaporation, melting, and freezing–thawing [154]. The encapsulating efficiency of liposomes was highest when they were prepared by freezing–thawing, followed by thin film evaporation, then reverse phase evaporation, whereas melting and sonication have the lowest efficiency. Liposomal systems prepared by sonication, melting, and reverse phase evaporation displayed better dispersion.

The nature of the core materials is another factor that affects the efficiency of liposome encapsulation. The isomers of (+)-catechin and (−)-epicatechin entrapped in liposomes showed similar encapsulation levels and release rates [155]. However, another type of catechin, (−)-epigallocatechin-3-gallate (EGCG), has been observed to have an increased level of encapsulation for the same liposome system. EGCG contains a galloyl group, indicating a greater lipophilicity. Hence, it is possible that EGCG was more effective when localized within the liposome bilayers, thereby increasing the entrapment.

There is evidence of quercetin liposomes prepared from egg phosphatidylcholine/cholesterol (2:1). A lower dose (20 μg/kg body weight) and a faster rate of absorption were observed with intranasal quercetin liposomes when compared with oral quercetin (300 mg/kg body weight). These results suggest that intranasal delivery of quercetin in the form of liposomes to the brain could allow for a reduction in the dose to reduce the potential of toxicity of the quercetin [156].

Inclusion Encapsulation—Cyclodextrins

Cyclodextrins can envelop molecular structures by forming molecular inclusion complexes. Cyclodextrins have a hydrophobic interior and a hydrophilic exterior. The hydrophobic interior of the capsule can be varied in size by varying the number of glucose units of the cyclodextrin molecules [157,158]. It has been applied to increase the solubility of hydrophobic molecules and to protect molecules from inactivation or degradation.

The inclusion of hesperetin and hesperidin in (2-hydroxypropyl)-β-cyclodextrin (HP-β-CD) [159]; quercetin and myricetin in HP-β-CD, maltosyl-β-CDs, and β-CDs [160]; kaempferol, quercetin, and myricetin in HP-β-CD [161]; 3-hydroxyflavone (3-OHeF), morin, and quercetin in α- and β-CDs [162]; and rutin in β-CD [163] have been studied, and their water solubility improved by encapsulation. In addition, their antioxidant activities were shown to be increased in these CD-encapsulated systems. The improved antioxidant efficacy of the inclusion complex may be a result of the protection of the flavonoid against rapid oxidation by free radicals [161], which may, in part, be explained by an increase in their solubility in the biological moiety [163]. The encapsulation efficacy of CD inclusion was affected by the core materials. In general, the higher the hydrophobicity and the smaller the molecule, the greater the affinity for the CD was.

Freeze-Drying

Freeze-drying is an industrial process used to ensure the long-term stability and to preserve the original properties of pharmaceutical and biological products [164]. Freeze-drying, also known as lyophilization or cryodesiccation, is a process used for the dehydration most heat-sensitive materials and aromas. Freeze-drying works by freezing the material, reducing the surrounding pressure, and adding enough heat to allow the frozen water in the material to sublimate directly from the solid phase to the gas phase. Encapsulation by freeze-drying is achieved as the core materials homogenize in matrix solutions and then co-lyophilize, resulting in uncertain forms.

Due to the long dehydration period required (generally 20h), this technology is rarely applied but may serve as a solution of specific encapsulation issues for encapsulating water-soluble essences and natural aromas and drugs [137]. Freeze-dried samples of pomace containing anthocyanin and maltodextrin have shown good shelf life stability during storage at 50°C/0.5 water activity for up to 2 months [165]. Laine *et al*. [166] encapsulated phenolic-rich cloudberry extract by freeze-drying, using maltodextrins as wall materials. The microencapsulated cloudberry extract offered better protection for phenolics during storage, whereas the antioxidant activity remained the same or even improved slightly. However, studies have shown that freeze-drying induced encapsulation was unable to improve stability or bioactivity. When

Hibiscus anthocyanin extract was encapsulated in pullulan by freeze-drying, the free anthocyanins were shown to have 1.5–1.8 times faster degradation than the pullulan–anthocyanin co-lyophilized materials [167]. These results showed that they can be both free and co-lyophilized with pullulan, Hibiscus anthocyanins exhibited good antiradical activity throughout storage, and no significant differences were observed between the materials, suggesting that the encapsulation might not be necessary if the Hibiscus anthocyanin extract is to be freeze dried.

DEVELOPMENT OF TOPICAL FORMULATIONS CONTAINING FLAVONOIDS

The UV components of sunlight are now recognized as major environmental factors that are deleterious to human health. Acute exposure to ultraviolet radiation (UVR) from the sun is harmful to the skin, causing sunburn, immune suppression, DNA damage, and connective tissue degradation. Accumulated damage resulting from chronic sun exposure has been shown to cause skin cancer and premature skin aging (photoaging) [168]. The genesis of skin diseases due to UVR exposure is a result of the generation of free radicals and mobilization of transition metal ions, and, thus, inflammation [22].

In principle, the conscientious use of sunscreens/blocks or protective clothing should prevent UV exposure to the skin. Nevertheless, as epidemiological studies have indicated that the use of sunscreen and sun block are not completely effective in preventing UV-induced skin injuries, further approaches are needed to more effectively protect human skin against UV-caused damage [169]. Instead of only blocking the UVR from being absorbed by the skin, as is usually found with UV absorbers and sunscreens, the skin could also be protected by preventing the formation of the photooxidants that result in radical damage and cutaneous diseases [170].

There is increased interest in the identification of natural product sources for novel anti-inflammatory and antioxidant compounds that might prove to be of superior efficacy in preventing and/or treating the skin from the photodamage [171,172]. Naturally occurring agents are considered to be less toxic and more effective approaches in controlling various human malignancies [173,174]; thus, a new concept in cosmetics research and development is the use of the so-called “biological filters,” such as the potent antioxidants, vitamins, and flavonoids, which can have protective effects against UVR and may also have biologically relevant filtering activity [175].

In addition to their innate antioxidant activity, flavonoids, which are widely distributed in medicinal plants, are known as natural anti-inflammatory agents [176], which strongly suggest the potential of these compounds to antagonize critical UV-induced damaging events. Therefore, their topical use may provide the necessary photoprotection in addition to human sunscreens.

The topical delivery of bioactive substances is a powerful strategy to avoid possible systemic toxicity and, at the same time, to restrict the therapeutic effects to specific tissues [177] because it is the considered route of administration of agents against the UV-induced skin damages. Nevertheless, the most difficult aspect of a topical delivery system is to overcome the barrier of the stratum corneum (SC) against foreign substances [178,179]. Further, most flavonoids are highly lipophilic substances, and their penetration across the SC (epidermis' outermost layer) and into viable skin layers may be difficult due to their affinity for SC components (principally lipophilic in nature) and the tendency to be retained in this layer [180].

Therefore, adequate cutaneous absorption is known to be an essential requirement for topically applied photoprotective agents [181], and the vehicle in which the drug is applied could effectively influence its release from a topical pharmaceutical preparation [177]. When a delivery system is applied topically to the skin, the active agent must be released from its carrier (vehicle) before it contacts the epidermal surface and be available for penetration into the SC and lower layers of the skin [182,183]. Thus, the percutaneous absorption of a drug could be influenced by the partition of the active agent between the vehicle and SC, which was influenced by active agent–vehicle–skin interactions [184].

In addition, to propose the topical application of flavonoids or delivery systems containing these agents, extensive *in vivo* studies are required to test the long-term treatment effects of the proposed agents, their half-life and the optimum dose for beneficial effects. Recently, many studies were designed to evaluate the *in vivo* efficacy against the UV-induced damage of different flavonoids when topically applied.

Quercetin, the best studied and one of the most common flavonoids found in nature, which was shown to have a poor ability to permeate through excised human skin [177], has been incorporated into different delivery systems to inhibit the oxidative skin damage and the inflammatory processes induced by the solar UVR.

Among the first studies that incorporated quercetin into two different oil-in-water emulsions, with a distinct lipid content, was developed by Casagrande *et al*. [22,177], and they evaluated their potential application as a topical carrier system for the delivery of this flavonoid. The *in vivo* results suggested that these functionally stable formulations containing quercetin may be used as a topical active product to control UVB-induced skin damage.

Based on these promising results, further studies investigated the design of novel administration forms to increase the quercetin effectiveness when topically applied. In this context, quercetin was incorporated into a liquid, crystalline formulation, and the influence of this carrier in the *in vitro* antioxidant activity of this flavonoid was evaluated. Vehicles having a liquid, crystalline structure allowed for an easier diffusion of biologically active substances through the skin have a considerable solubilizing capacity for both oil- and water-soluble compounds; in addition, liquid crystals were thermodynamically

stable and could be stored for long periods of time without phase separation [185]. In fact, Scalia and Mezzena [186] demonstrated that the incorporation of quercetin in lipid microparticles improved the photo- and chemical stability of the flavonoid, and the biocompatibility of the lipoparticle carrier system represents an additional advantage for the development of quercetin-based products for skin care.

In addition, quercetin was also incorporated into water-in-oil (w/o) microemulsion and evaluated regarding its protective effect against UVB-induced damage in the hairless mouse skin. These results confirmed the possible usefulness of topical formulations containing quercetin to prevent UVB radiation skin as suggested by Casagrande *et al*. [22]. However, the incorporation into the w/o microemulsion optimized the effects of the flavonoid because a dose approximately sixfold smaller produced the same *in vivo* results obtained with nonionic emulsion containing quercetin. The optimization was due to the significant increase in quercetin skin penetration caused by its incorporation into w/o microemulsion [21]. Further, by evaluating the effects of this w/o microemulsion incorporating quercetin in UV-induced erythema formation and histopathological changes, we suggest that the protective effects of this formulation on UV-induced responses was not secondary to the interference of UV transmission (i.e., blocking the UVB radiation from being absorbed by the skin), as is usually performed with UVB absorbers and sunscreens, but was due to different biological effects of this flavonoid [168].

Microemulsion systems, which represent pharmaceutically versatile formulations for various applications, have received increasing attention during recent years because they have several advantages, such as ease of manufacturing, thermodynamic stability, and high solubilizing power, that allow for the incorporation of large amounts of poorly soluble compounds and increased drug permeation rates [179,187].

This type of formulation was also employed as a carrier of another flavonoid with lipophilic characteristics. Hesperetin, a flavanone compound, which has been demonstrated to have protective effects for skin damage [188], was incorporated into microemulsions for topical whitening products after UVR. This *in vivo* study demonstrated that hesperetin-loaded microemulsions showed significant topical whitening effects and diminished skin irritations when compared with the nontreated group. The authors suggested that the observed inhibition on the irritation effect might be due to the anti-inflammatory effect of flavonoids [178]. It was also observed that there was an *in vivo* protective effect of hesperetin that was incorporated into a cream formulation when combined with a combination of the penetration enhancers, such as menthol, linoleic acid, and lecitin [179].

The evaluation of the *in vivo* effect of different extracts where flavonoids were among the main chemical constituents has also been shown. Typically, as a first step, the extracts that have previously been shown to have anti-inflammatory and antioxidant activities, in addition to other pharmacological properties, were incorporated into a topical administration forms, and its

release and its skin penetration were evaluated to select the most promising system to deliver the studied active agent.

Gebre-Mariam *et al*. [182] incorporated the extract of *Melilotus elegans* into three different types of formulations (hydrophilic, amphiphilic, and lipophilic cream) and evaluated the release profiles of the kaempferol glycosides from these formulations. As expected, the faster and higher release was obtained by employing the lipophilic cream in which the glycoside forms of flavonoids, due to their polarity, have less affinity for the cream base.

The postirradiation, topical application of lotions containing increasing levels of the plant extract, pycnogenol B, significantly inhibited the acute inflammation-edema response to solar-simulated UVR [190].

The potential of a topical preparation (SK Ato Formula) containing flavonoid mixtures from *S. baicalensis* Georgi roots and *Ginkgo biloba* L. leaves with an extract of *Gentiana scabra* Bunge roots was evaluated in an animal model of chronic skin inflammation. In this study, the animals were treated with 12-*O*-tetradecanoylphorbol-13-acetate for 7 consecutive days to induce a chronic skin inflammation, and when topically applied in this model, the studied formulation reduced these responses. Further, it inhibited PGE_2 generation and suppressed the expression of pro-inflammatory genes, COX-2, and IL-1β in the skin lesion [176].

Reseada luteola L., which is a natural source of luteolin (flavone), was used to obtain a luteolin-rich extract to be investigated in the prevention or treatment of inflammatory skin diseases (e.g., sunburn). Due to poor solubility of the *Reseada* extract, a nanoparticular soluble state of the extract (s-RE) was used and clinically assessed on its anti-inflammatory properties in a standardized test model in human volunteers *in vivo*. These results showed that topical application of a solubilized luteolin-rich extract from *R. luteola* effectively reduced UVB-induced skin inflammation [189].

Fonseca *et al*. [172] investigated the potential use of extracts from *Calendula officinalis* L. (also known as marigold), which is used primarily for cutaneous and internal inflammatory diseases of several origins that was added in various topical formulations to prevent or to treat the UVB irradiation-induced skin damage. The topical application of the gel formulation containing *C. officinalis* reduced the histological skin changes induced by UVB irradiation, providing a photoprotective effect in the hairless mice.

Studies have shown that topically applied isoflavones and their metabolites may offer protection from UV-induced inflammation and immunosuppression [191]. The topical administration may also be a suitable route for soy isoflavones to obtain systemic bioavailability because of their rapid clearance from the plasma [192].

Widyarini *et al*. [193] assessed the effect of several red clover (*Trifolium pratense*) isoflavones on UVR-induced skin inflammation that was measured as the edema component of this reaction by the increase in the irradiated skinfold thickness and on the systemic suppression of immune function measured as the contact hypersensitivity response. This study had shown that topical

application of lotions containing genistein, equol, isoequol, or dehydroequol provided protection not only against UVR-induced cutaneous inflammation observed as the sunburn reaction but also against photoimmune suppression, which was evident as a defective contact hypersensitivity reaction that was initiated by the UV-irradiated skin.

Several isoflavonoid derivatives have been identified as metabolites produced from dietary isoflavones by the gastrointestinal microflora in humans and found to have various potent biological activities [189]. Studies that have focused on equol ([*S*]-4′,7-dihydroxyisoflavane) because it was shown that its contribution to the protection against solar-simulated UVR-induced erythemal-associated edema and immunosuppression [190] showed a potential role in the prevention of human skin cancer [190] by acting as a sunscreen and, thus, inhibiting DNA photodamage [191] when topically applied as a lotion.

Soybeans are a rich source of flavonoids called isoflavones, with the most potent isoflavones being genistein and daidzein and the soybean cake, a byproduct obtained during the processing of soybean oil that has been shown to be a rich source of isoflavones and other functional components. Chiu *et al*. [194] found that isoflavone extract from soybean cake could decrease the early activation of the signaling pathway in response to UVB and could prevent skin cell apoptosis, erythema, and inflammation reactions. Thus, this extract might be a good candidate for an anti-photoaging agent in skin care that has many advantages, such as convenience, economy, and environmental protection.

Propolis is a resinous material that honeybees (*Apis mellifera* L.) collect from various plant species and mix with wax and other substances. In general, it is a complex mixture of different constituents, including flavonoids, aromatic acids and esters, aldehydes and ketones, fatty acids and esters, terpenes, steroids, amino acids, polysaccharides, hydrocarbons, alcohols, hydroxybenzene, and several other compounds in trace amounts [195]. Although its composition varies with the source, most samples share significant similarity in their overall chemical nature, and approximately 50% of the raw propolis is represented by resin, composed of flavonoids and related phenolic acids [196]. Many of these constituents were biologically active and were involved in a broad spectrum of pharmacological properties of propolis, with the main properties being antimicrobial, immunomodulatory, and anti-inflammatory [197,198]. It has been suggested that these properties may arise from complex mechanisms or synergistic interactions between compounds [199]. The topical application of a crude de-waxed ethanolic extract of "Sydney" propolis in the Skh:hr-1 albino hairless mouse was effective in reducing inflammation, immunosuppression, and oxidative damage caused by UV exposure [171].

In contrast, although Fonseca *et al*. [199] had demonstrated that oral treatment of the hairless mice with two Brazilian propolis extracts (green and brown) prevented irradiation-induced oxidative stress by preventing GSH depletion, the topical pretreatment of animals with solutions containing both propolis extracts was not effective. The low topical effectiveness of both extracts could be explained by poor diffusion of the active compounds

through the SC and viable epidermis of mouse skin. To this end, topical formulations that diffuse more effectively through the skin could be developed and additional studies should be performed.

Finally, the topical application of dermocosmetic formulations containing an association of vitamins and bioflavonoids showed relevant biological activity in terms of photoprotection, demonstrating the potentiality of using the association of active substances with different mechanisms of action against the UV-induced skin damages [147].

In conclusion, the above-mentioned findings suggest that the *in vivo* topical application of flavonoids has the potential to antagonize critical damaging events, such as the inflammatory reaction, induced by UVR and could be developed as dermatological and cosmetic products in addition to sunscreens that would provide photoprotection for humans.

CONCLUSIONS

In this chapter, we described evidence that demonstrated the anti-inflammatory and analgesic effects of flavonoids by mechanisms involving the inhibition of oxidative stress, cytokines and lipid mediators production, scavenging chemokines, NF-κB, AP-1, JAK/STAT, MAP kinases and PI3K activation, IκB degradation, myeloperoxidase, and stimulation of endogenous opioids release, NO production, IL-1ra, and HO-1 expression. There have been studies that examined the structure–activity relationship of flavonoids, but there have not been conclusive data. Further, there has been an increased focus on developing novel formulations and pharmaceutical forms that could improve the stability and absorption of flavonoids for oral administration and that could be incorporated into topical formulations for the protection against UV radiation-induced skin damage. Finally, the use of flavonoids may represent a better pharmacological approach compared to current therapies because flavonoids do not act by a single mechanism, but they have been shown to inhibit the activity and expression of pro-inflammatory enzymes (e.g., COX-1, COX-2, and 5-LO), inhibit cytokine production and scavenge them, inhibit intracellular signaling pathways essential for inflammation/pain induction (e.g., MAP kinases and PI3K), transcription factors (e.g., NF-κB and AP-1), and oxidative stress while presenting a better profile regarding side effects, such as gastrointestinal and renal lesions, as compared to nonselective and selective COX-2 inhibitors, respectively. Moreover, steroidal anti-inflammatory drugs increased blood glucose levels, and there is evidence that it does not occur, at least for some flavonoids, suggesting a better profile for diabetic patients. Thus, flavonoids represent a promising class of drugs for anti-inflammatory and analgesic use, and there is increasing attention on the development of pharmaceutical forms of flavonoids. Further studies using human cells and long-term clinical trials are necessary to confirm their usefulness.

ACKNOWLEDGMENTS

We thank the financial support of Fundação de Amparo a Pesquisa do Estado de São Paulo (FAPESP), Conselho Nacional de Desenvolvimento Científico e Tecnológico (CNPq), Coordenação de Aperfeiçoamento de Pessoal de Nível Superior (CAPES), Fundação Araucária and Governo do Estado do Paraná/SETI, Brazil.

ABBREVIATIONS

5-LO	5-lipoxygenase
AP-1	activating protein-1
APCs	antigen presenting cells
CAP	cellulose acetate phthalate
cFLIP	cellular caspase-8 (FLICE)-like inhibitory protein
COX	cyclooxygenase
DRG	dorsal root ganglia
EGCG	(−)-epigallocatechin-3-gallate
EP3	PGE_2 receptor 3
ERK	extracellular signal-regulated kinase
FAAH	fatty acid amide hydrolase
GSH	reduced glutathione
IKK	Iκ B kinase
IL	interleukin
iNOS	inducible nitric oxide synthase
JNK	Jun N-terminal Kinase
MAP kinases	mitogen-activated protein kinases
MCP-2	monocyte chemotatic protein-2
MIP-1β	macrophage inflammatory protein-1
NADPH oxidase	nicotinamide adenine dinucleotide phosphate-oxidase
NF-κB	nuclear factor κB
NO	nitric oxide
NSAIDS	nonsteroidal anti-inflammatory drugs
PGE_2	prostaglandin E_2
PI3K	phosphoinositide 3-kinase
PMA	phorbol 12-myristate 13-acetate
PMACI	PMA calcium ionophore A23187
ROS	reactive oxidative species
SC	stratum corneum
SDF	stromal cell-derived factor
Th	T helper
UVR	ultraviolet radiation
w/o	water-in-oil

REFERENCES

[1] J. Peterson, J. Dwyer, Nutr. Res. 18 (1998) 1995–2018.
[2] N. Cotelle, Curr. Top. Med. Chem. 1 (2001) 569–590.
[3] D. Amic, D. Davidovic-Amic, D. Beslo, N. Trinajstic, Croat Chem. Acta 76 (2003) 55–61.
[4] P.C. Hollman, M.B. Katan, Food Chem. Toxicol. 37 (1999) 937–942.
[5] B. Yang, A. Kotani, K. Arai, F. Kusu, Anal. Sci. 17 (2001) 599–604.
[6] A. Lugasi, J. Hóvári, K.V. Sági, L. Bıró, Acta Biol. Szeged. 47 (2003) 119–125.
[7] C. Kaur, H. Kapoor, Int. J. Food Sci. Technol. 36 (2001) 703–725.
[8] A.S. Pannala, T.S. Chan, P.J. O'Brien, C.A. Rice-Evans, Biochem. Biophys. Res. Commun. 282 (2001) 1161–1168.
[9] M.A. Soobrattee, V.S. Neergheen, A. Luximon-Ramma, O.I. Aruoma, T. Bahorun, Mutat. Res. 579 (2005) 200–213.
[10] P.-G. Pietta, J. Nat. Prod. 63 (2000) 1035–1042.
[11] J.B. Harbone, C.A. Williams, Phytochemistry 55 (1992) 481–504.
[12] I. Erlund, Nutr. Res. 24 (2004) 851–874.
[13] S.L. Robbins, V. Kumar, A.K. Abbas, R.S. Cotran, N. Fausto, Hardback, Saunders/Elsevier, Philadelphia, 2010, pp. 43–78.
[14] R.J. Williams, J.P.E. Spencer, C. Rice-Evans, Free Radic. Biol. Med. 36 (2004) 838–849.
[15] S.V. Jovanovic, S. Steenken, M. Tosic, B. Marjanovic, M.G. Simic, J. Am. Chem. Soc. 116 (1994) 4846–4851.
[16] W. Bors, W. Heller, C. Michel, M. Saran, Methods Enzymol. 186 (1990) 343–355.
[17] A.K. Verma, R. Pratap, Nat. Prod. Rep. 27 (2010) 1571–1593.
[18] K.E. Heim, A.R. Tagliaferro, D.J. Bobilya, J. Nutr. Biochem. 13 (2002) 572–584.
[19] A. Bowie, L.A. O'Neill, Biochem. Pharmacol. 59 (2000) 13–23.
[20] D. Porath, C. Riegger, J. Drewe, J. Schwager, J. Pharmacol. Exp. Ther. 315 (2005) 1172–1180.
[21] W.A. Verri Jr., T.M. Cunha, C.A. Parada, S. Poole, F.Q. Cunha, S.H. Ferreira, Pharmacol. Ther. 112 (2006) 116–138.
[22] R. Casagrande, S.R. Georgetti, W.A. Verri Jr., D.J. Dorta, A.C. dos Santos, M.J. Fonseca, J. Photochem. Photobiol. B 84 (2006) 21–27.
[23] B.Q. Li, T. Fu, W.H. Gong, N. Dunlop, H. Kung, Y. Yan, J. Kang, J.M. Wang, Immunopharmacology 49 (2000) 295–306.
[24] C.Y. Chen, W.H. Peng, K.D. Tsai, S.L. Hsu, Life Sci. 81 (2007) 1602–1614.
[25] M. Lazarus, K. Yoshida, R. Coppari, C.E. Bass, T. Mochizuki, B.B. Lowell, C.B. Saper, Nat. Neurosci. 10 (2007) 1131–1133.
[26] S. Prasad, K. Phromnoi, V.R. Yadav, M.M. Chaturvedi, B.B. Aggarwal, Planta Med. 76 (2010) 1044–1063.
[27] S.J. Kim, Y.J. Moon, S.M. Lee, J. Nat. Prod. 73 (2010) 2003–2008.
[28] F.C. Meotti, R. Senthilmohan, D.T. Harwood, F.C. Missau, M.G. Pizzolatti, A.J. Kettle, Free Radic. Biol. Med. 44 (2008) 109–120.
[29] C.C. Chen, M.P. Chow, W.C. Huang, Y.C. Lin, Y.J. Chang, Mol. Pharmacol. 66 (2004) 683–693.
[30] M.E. Gerritsen, W.W. Carley, G.E. Ranges, C.P. Shen, S.A. Phan, G.F. Ligon, C.A. Perry, Am. J. Pathol. 147 (1995) 278–292.
[31] H. Kobuchi, S. Roy, C.K. Sen, H.G. Nguyen, L. Packer, Am. J. Physiol. 277 (1999) 403–411.

[32] I. Crespo, M.V. García-Mediavilla, B. Gutiérrez, S. Sánchez-Campos, M.J. Tuñón, J. González-Gallego, Br. J. Nutr. 100 (2008) 968–976.
[33] S. Tribolo, F. Lodi, C. Connor, S. Suri, V.G. Wilson, M.A. Taylor, P.W. Needs, P.A. Kroon, D.A. Hughes, Atherosclerosis 197 (2008) 50–56.
[34] H. Lim, H. Park, H.P. Kim, J. Pharmacol. Sci. (2011) 1–11.
[35] Y.P. Hwang, K.N. Oh, H.J. Yun, H.G. Jeong, J. Dermatol. Sci. 61 (2011) 23–31.
[36] K. Yamagata, A. Myiashita, H. Matsufuji, M. Chino, J. Nutr. Biochem. 21 (2010) 116–124.
[37] A. Abate, G. Yang, R.J. Wong, H. Schroder, D.K. Stevenson, P.A. Dennery, Free Radic. Biol. Med. 39 (2005) 711–718.
[38] J. Kowalski, A. Samojedny, M. Paul, G. Pietsz, T. Wilczok, Pharmacol. Rep. 57 (2005) 390–394.
[39] C.T. Yeh, G.C. Yen, J. Agric. Food Chem. 53 (2005) 1740–1749.
[40] S.S. Hecht, C. Huang, G.D. Stoner, J. Li, M.J. Patrick, S.J. Sturla, S.G. Carmella, Carcinogenesis 27 (2006) 1617–1627.
[41] P.A. Abboud, P.W. Hake, T.J. Burroughs, K. Odoms, M. O'Connor, P. Mangeshkar, H.R. Wong, B. Zingarelli, Eur. J. Pharmacol. 579 (2008) 411–417.
[42] S.J. Kima, H.J. Jeonga, K.M. Leeb, N.Y. Myungc, N.H. Anc, W.M. Yangd, S.K. Parkd, H.J. Leee, S.H. Hongc, H.M. Kima, J.H. Uma, J. Nutr. Biochem. 18 (2007) 587–596.
[43] C.C. Wu, M.C. Hsu, C.W. Hsieh, J.B. Lin, P.H. Lai, B.S. Wung, Life Sci. 78 (2006) 2889–2897.
[44] M.H. Hong, M.H. Kim, H.J. Chang, N.K. Kim, B.A. Shin, B.W. Ahn, Y.D. Jung, Life Sci. 80 (2007) 1957–1965.
[45] E.K. Kima, K.B. Kwon, M.Y. Songa, S.W. Seo, S.J. Park, S.O. Kaa, K.A. Kima, D.G. Ryub, H.S. Sod, J.W. Park, B.H. Park, Mol. Cell. Endocrinol. 278 (2007) 18–28.
[46] K. Vafeiadou, D. Vauzour, H.Y. Lee, A. Rodriguez-Mateos, R.J. Williams, J.P.E. Spencer, Arch. Biochem. Biophys. 484 (2009) 100–109.
[47] R. Mukai, Y. Shirai, N. Saito, Y. Fukuda, S. Nishiumi, K. Yoshida, H. Ashida, Arch. Biochem. Biophys. 501 (2010) 134–141.
[48] H.Y. Lin, S.C. Shen, Y.C. Chen, J. Cell. Physiol. 202 (2005) 579–590.
[49] G. Muthian, J.J. Bright, J. Clin. Immunol. 24 (2004) 542–552.
[50] M. Matsushima, K. Takagi, M. Ogawa, E. Hirose, Y. Ota, F. Abe, K. Baba, T. Hasegawa, Y. Hasegawa, T. Kawabe, Inflamm. Res. 58 (2009) 705–715.
[51] S.R. Panickera, P. Sreenivasb, M.S. Babuc, D. Karunagarand, C.C. Karthac, Pharmacol. Res. 62 (2010) 328–336.
[52] Z.J. Sun, G. Chen, X. Hu, W. Zhang, Y. Liu, L.X. Zhu, Q. Zhou, Y.F. Zhao, Apoptosis 15 (2010) 850–863.
[53] B. Ying, T. Yang, X. Song, X. Hu, H. Fan, X. Lu, L. Chen, D. Cheng, T. Wang, D. Liu, X. Xu, Y. Wei, F. Wen, Mol. Biol. Rep. 36 (2009) 1825–1832.
[54] M.K. Pandey, S.K. Sandur, B. Sung, G. Sethi, A.B. Kunnumakkara, B.B. Aggarwal, J. Biol. Chem. 282 (2007) 17340–17350.
[55] M.K. Pandey, B. Sung, K.S. Ahn, B.B. Aggarwal, Mol. Pharmacol. 75 (2009) 525–533.
[56] T. Bitoa, S. Royb, K. Senb, T. Shirakawac, A. Gotohc, M. Uedad, M. Ichihashid, L. Packera, FEBS Lett. 520 (2002) 145–152.
[57] Y.H. Wanga, W.Y. Wangb, J.F. Liaoa, C.F. Chena, Y.C. Houc, K.T. Liouf, Y.C. Chou, J.H. Tieng, Y.C. Shend, Biochem. Pharmacol. 67 (2004) 2251–2262.
[58] S. Liu, Z. Ma, H. Cai, Q. Li, W. Rong, M. Kawano, Eur. J. Haematol. 84 (2010) 137–144.
[59] S. Yoo, S. Han, Y.S. Park, J.H. Lee, U. Oh, S.W. Hwang, Mol. Cells 27 (2009) 417–422.

[60] Z.F. Li, X.M. Xia, C. Huang, S. Zhang, J. Zhang, A.J. Zhang, Hepatobiliary Pancreat. Dis. Int. 8 (2) (2009) 201–208.
[61] R.R. de Sousa, K.C. Queiroz, A.C. Souza, S.A. Gurgueira, A.C. Augusto, M.A. Miranda, M.P. Peppelenbosch, C.V. Ferreira, H. Aoyama, J. Enzyme Inhib. Med. Chem. 22 (2007) 439–444.
[62] B.P. Burnett, Q. Jia, Y. Zhao, R.M. Levy, J. Med. Food 10 (2007) 442–451.
[63] K. Morikawa, M. Nonaka, M. Narahara, I. Torii, K. Kawaguchi, T. Yoshikawa, Y. Kumazawa, S. Morikawa, Life Sci. 74 (2003) 709–721.
[64] T.D. Warner, F. Giuliano, I. Vojnovic, A. Bukasa, J.A. Mitchell, J.R. Vane, Proc. Natl. Acad. Sci. USA 96 (1999) 7563–7568.
[65] M.A. Buerkle, S. Lehrer, H.Y. Sohn, P. Conzen, U. Pohl, F. Krötz, Circulation 110 (2004) 2053–2059.
[66] M.S. Alam, M.A. Alam, S. Ahmad, A.K. Najmi, M. Asif, T. Jahangir, Toxicol. Mech. Methods 20 (2010) 572–578.
[67] P.C. Vasconcelos, M.A. Andreo, W. Vilegas, C.A. Hiruma-Lima, C.H. Pellizzon, J. Ethnopharmacol. 131 (2010) 146–153.
[68] I.T. Abdel-Raheem, Basic Clin. Pharmacol. Toxicol. 107 (2010) 742–750.
[69] A.A. Hamdy, M.A. Ibrahem, J. Contemp. Dent. Pract. 11 (2010) 9–16.
[70] J. Fernandez, R. Reyes, H. Ponce, M. Oropeza, M.R. Vancalsteren, C. Jankowski, M.G. Campos, Eur. J. Pharmacol. 522 (2005) 108–115.
[71] R. Kalhan, L.J. Smith, M.C. Nlend, A. Nair, J.L. Hixon, P.H. Sporn, Clin. Exp. Allergy 38 (2008) 103–112.
[72] J. Yang, Q. Li, X.D. Zhou, V.P. Kolosov, J.M. Perelman, Mol. Cell. Biochem. 351 (2011) 29–40.
[73] M. Joskova, S. Franova, V. Sadlonova, Bratisl. Lek. Listy 112 (2011) 9–12.
[74] R.R. Li, L.L. Pang, Q. Du, Y. Shi, W.J. Dai, K.S. Yin, Immunopharmacol. Immunotoxicol. 32 (2010) 364–370.
[75] L. Thors, M. Belghiti, C.J. Fowler, Br. J. Pharmacol. 155 (2008) 244–252.
[76] N. Clayton, F.H. Marshall, C. Bountra, C.T. O'Shaughnessy, Pain 96 (2002) 253–260.
[77] L.J. Kehl, D.T. Hamamoto, P.W. Wacnik, D.L. Croft, B.D. Norsted, G.L. Wilcox, D.A. Simone, Pain 103 (2003) 175–186.
[78] T. Gutierrez, J.N. Farthing, A.M. Zvonok, A. Makriyannis, A.G. Hohmann, Br. J. Pharmacol. 150 (2007) 153–163.
[79] E. Herlaar, Z. Brown, Mol. Med. Today 5 (1999) 439–447.
[80] L.E. Kilpatrick, S. Sun, H. Li, T.C. Vary, H.M. Korchak, J. Leukoc. Biol. 87 (2010) 153–164.
[81] T.W. Nam, C.I. Yoo, H.T. Kim, C.H. Kwon, J.Y. Park, Y.K. Kim, J. Bone Miner. Metab. 26 (2008) 551–560.
[82] L. Navarro-Núñez, M.L. Lozano, C. Martínez, V. Vicente, J. Rivera, Fitoterapia 81 (2010) 75–80.
[83] A. Xagorari, C. Roussos, A. Papapetropoulos, Br. J. Pharmacol. 136 (2002) 1058–1064.
[84] H. Jonsson, P. Allen, S.L. Peng, Nat. Med. 11 (2005) 666–671.
[85] W.A. Verri Jr., F.O. Souto, S.M. Vieira, S.C. Almeida, S.Y. Fukada, D. Xu, J.C. Alves-Filho, T.M. Cunha, A.T. Guerrero, R.B. Mattos-Guimaraes, F.R. Oliveira, M.M. Teixeira, J.S. Silva, I.B. McInnes, S.H. Ferreira, P. Louzada-Junior, F.Y. Liew, F.Q. Cunha, Ann. Rheum. Dis. 69 (2010) 1697–1703.
[86] S.E. Lee, S.I. Jeong, H. Yang, C.S. Park, Y.H. Jin, Y.S. Park, J. Cell. Biochem. 112 (2011) 2352–2360, doi:10.1002/jcb.23158.

[87] T.D. Tran, H. Park, H.P. Kim, G.F. Ecker, K.M. Thai, Bioorg. Med. Chem. Lett. 19 (2009) 1650–1653.
[88] J.R. Vane, Nat. New Biol. 231 (1971) 232–235.
[89] S.H. Ferreira, Nat. New Biol. 240 (1972) 200–203.
[90] M. Anjaneyulu, K. Chopra, Prog. Neuropsychopharmacol. Biol. Psychiat. 27 (2003) 1001–1005.
[91] M. Anjaneyulu, K. Chopra, Indian J. Exp. Biol. 42 (2004) 766–769.
[92] A.W. Filho, V.C. Filho, L. Olinger, M.M. de Souza, Arch. Pharm. Res. 31 (2008) 713–721.
[93] D.A. Valério, S.R. Georgetti, D.A. Magro, R. Casagrande, T.M. Cunha, F.T. Vicentini, S.M. Vieira, M.J. Fonseca, S.H. Ferreira, F.Q. Cunha, W.A. Verri Jr., J. Nat. Prod. 72 (2009) 1975–1979.
[94] K. Vidyalakshmi, P. Kamalakannan, S. Viswanathan, S. Ramaswamy, Pharmacol. Biochem. Behav. 96 (2010) 1–6.
[95] M.M. Córdova, M.F. Werner, M.D. Silva, A.P. Ruani, M.G. Pizzolatti, A.R. Santos, Neurosci. Lett. 495 (2011) 173–177.
[96] T. Hagenacker, I. Hillebrand, D. Büsselberg, M. Schäfers, Brain Res. Bull. 83 (2010) 292–296.
[97] X. Jin, R.W. Gereau, J. Neurosci. 26 (2006) 246–255.
[98] R. Stavniichuk, V.R. Drel, H. Shevalye, Y. Maksimchyk, T.M. Kuchmerovska, J.L. Nadler, I.G. Obrosova, Exp. Neurol. 230 (2011) 106–113.
[99] O.I. El-Sabbagh, S.M. Ibrahim, M.M. Baraka, H. Kothayer, Arch. Pharm. 343 (2010) 274–281.
[100] S.C. Bae, W.J. Jung, E.J. Lee, R. Yu, M.K. Sung, J. Am. Coll. Nutr. 28 (2009) 56–62.
[101] Y.D. Min, C.H. Choi, H. Bark, H.Y. Son, H.H. Park, S. Lee, J.W. Park, E.K. Park, H.I. Shin, S.H. Kim, Inflamm. Res. 56 (2007) 210–215.
[102] E.M. Choi, Y.S. Lee, Cell. Immunol. 264 (2010) 1–3.
[103] Y.S. Lee, E.M. Choi, Int. Immunopharmacol. 10 (2010) 812–814.
[104] E.M. Choi, Y.S. Lee, Food Chem. Toxicol. 48 (2010) 2607–2611.
[105] H.K. Kang, D. Ecklund, M. Liu, S.K. Datta, Arthritis Res. Ther. 11 (2009) R59.
[106] P. Knekt, J. Kumpulainen, R. Järvinen, H. Rissanen, M. Heliövaara, A. Reunanen, T. Hakulinen, A. Aromaa, Am. J. Clin. Nutr. 76 (2002) 560–568.
[107] C. Nicholas, S. Batra, M.A. Vargo, O.H. Voss, M.A. Gavrilin, M.D. Wewers, D.C. Guttridge, E. Grotewold, A.I. Doseff, J. Immunol. 179 (2007) 7121–7127.
[108] K. Shanmugam, L. Holmquist, M. Steele, G. Stuchbury, K. Berbaum, O. Schulz, O. Benavente-García, J. Castillo, J. Burnell, V. Garcia-Rivas, G. Dobson, G. Münch, Mol. Nutr. Food Res. 52 (2008) 427–438.
[109] F.O. Souto, A.C. Zarpelon, L. Staurengo-Ferrari, V. Fattori, R. Casagrande, M.J. Fonseca, T.M. Cunha, S.H. Ferreira, F.Q. Cunha, W.A. Verri Jr., J. Nat. Prod. 74 (2011) 113–118.
[110] F.T. Vicentini, T. He, Y. Shao, M.J. Fonseca, W.A. Verri Jr., G.J. Fisher, Y. Xu, J. Dermatol. Sci. 61 (2011) 162–168.
[111] U. Wölfle, P.R. Esser, B. Simon-Haarhaus, S.F. Martin, J. Lademann, C.M. Schempp, Free Radic. Biol. Med. 50 (2011) 1081–1093.
[112] Y.N. Wang, W. Wu, H.C. Chen, H. Fang, J. Dermatol. Sci. 58 (2010) 19–27.
[113] J.H. Huang, C.C. Huang, J.Y. Fang, C. Yang, C.M. Chan, N.L. Wu, S.W. Kang, C.F. Hung, Toxicol. In Vitro 24 (2010) 21–28.
[114] A. Bennick, Crit. Rev. Oral Biol. Med. 13 (2002) 184–196.
[115] E. Haslam, J. Nat. Prod. 59 (1996) 205–215.
[116] S. Quideau, K.S. Feldman, Chem. Rev. 96 (1996) 475–503.

[117] C. Manach, A. Scalbert, C. Morand, C. Rémésy, L. Jiménez, Am. J. Clin. Nutr. 79 (2004) 727–747.
[118] A. Scalbert, C. Manach, C. Morand, C. Rémésy, L. Jiménez, Crit. Rev. Food Sci. Nutr. 45 (2005) 287–306.
[119] P. De Vos, M.M. Faas, M. Spasojevic, J. Sikkema, Int. Dairy J. 20 (2010) 292–302.
[120] F. Sansone, P. Picerno, T. Mencherini, F. Villecco, A.M. D'Ursi, R.P. Aquino, M.R. Lauro, J. Food Eng. 103 (2011) 188–196.
[121] L. Chen, G.E. Remondetto, M. Subirade, Trends Food Sci. Technol. 17 (2006) 272–283.
[122] M.C. Andry, H. Vezin, I. Dumistracel, J.L. Bernier, M.C. Le´vy, Int. J. Pharm. 171 (1998) 217–226.
[123] A.M. Bakowska-Barczak, P.P. Kolodziejczyk, Ind. Crops Prod. 34 (2011) 1301–1309.
[124] M. Chávarri, I. Marañón, R. Ares, F.C. Ibáñez, F. Marzo, M.C. Villarán, Int. J. Food Microbiol. 142 (2010) 185–189.
[125] L. Deladino, P.S. Anbinder, A.S. Navarro, M.N. Martino, Carbohydr. Polym. 71 (2008) 126–134.
[126] M.P. Nori, C.S. Favaro-Trindade, S.M. Alencar, M. Thomazini, J.C.C. Balieiro, C.J.C. Castillo, LWT - Food Sci. Technol. 44 (2011) 429–435.
[127] C. Saénz, S. Tapia, J. Chávez, P. Robert, Food Chem. 114 (2009) 616–622.
[128] A.S. Saraf, Fitoterapia 81 (2010) 680–689.
[129] H. Vila-Real, A.J. Alfaia, M.E. Rosa, A.R. Calado, M.H.L. Ribeiro, Process Biochem. 45 (2010) 841–850.
[130] Z. Fang, B. Bhandari, Trends Food Sci. Technol. 21 (2010) 510–523.
[131] P. Couvreur, C. Dubernet, F. Puisieux, Eur. J. Pharm. Biopharm. 41 (1995) 2–13.
[132] C.P. Reis, R.J. Neufeld, A.J. Ribeiro, F. Veiga, Nanomedicine: NBM 2 (2006) 8–21.
[133] B.F. Gibbs, S. Kermasha, I. Alli, C.N. Mulligan, Int. J. Food Sci. Nutr. 50 (1999) 213–224.
[134] C. Manach, G. Williamson, C. Morand, A. Scalbert, C. Rémésy, Am. J. Clin. Nutr. 81 (2005) 230–242.
[135] L. Sagalowicz, M.E. Leser, Curr. Opin. Colloid Interface 15 (2010) 61–72.
[136] M.A. Augustin, Y. Hemar, Chem. Soc. Rev. 38 (2009) 902–912.
[137] K.G.H. Desai, H.J. Park, Dry Technol. 23 (2005) 1361–1394.
[138] K. Cal, K. Sollohub, J. Pharm. Sci. 99 (2010) 575–586.
[139] K. Sollohub, K. Cal, J. Pharm. Sci. 99 (2010) 587–597.
[140] S. Ersus, U. Yurdagel, J. Food Eng. 80 (2007) 805–812.
[141] L. Zhang, D. Mou, Y. Du, J. Agric. Food Chem. 87 (2007) 2192–2197.
[142] M.R. Lauro, L. Maggi, U. Conte, F. De Simone, R.P. Aquino, J. Drug Deliv. Sci. Technol. 15 (2005) 363–369.
[143] S.R. Béchard, L. Levy, S.D. Clas, Int. J. Pharm. 114 (1995) 205–213.
[144] M.R. Lauro, F. De Simone, F. Sansone, P. Iannelli, R.P. Aquino, J. Drug Deliv. Sci. Technol. 17 (2007) 119–124.
[145] S.L. Kosaraju, L. D'ath, A. Lawrence, Carbohyd. Polym. 64 (2006) 163–167.
[146] S.L. Kosaraju, D. Labbett, M. Emin, I. Konczak, L. Lundin, Nutr. Dietetics 65 (2008) 48–52.
[147] S. Gouin, Trends Food Sci. Technol. 15 (2004) 330–347.
[148] M. Girard, C. Sanchez, S.I. Laneuville, S.L. Turgeon, S.F. Gauthier, Colloid Surf. B 35 (2004) 15–22.
[149] S.I. Laneuville, S.L. Turgeon, C. Sanchez, P. Paquin, Langmuir 22 (2006) 7351–7357.
[150] T.G. Shutava, S.S. Balkundi, Y.M. Lvov, J. Colloid Interf. Sci. 330 (2009) 276–283.
[151] S. Xiong, L.D. Melton, A. Easteal, D. Siew, J. Agric. Food Chem. 54 (2006) 6201–6208.

[152] V. Schafer, H. Von Briesen, R. Andreesen, A.M. Steffan, C. Royer, S. Troster, J. Kreuter, H. Rubsamen-Waigmann, Pharm. Res. 9 (1992) 541–546.
[153] M. Takahashi, K. Inafuku, T. Miyagi, H. Oku, K. Wada, T. Imura, D. Kitamoto, J. Oleo Sci. 56 (2007) 35–42.
[154] M.H. Fan, S.Y. Xu, S.Q. Xia, X.M. Zhang, J. Agric. Food Chem. 55 (2007) 3089–3095.
[155] J.Y. Fang, T.L. Hwang, Y.L. Huang, C.L. Fang, Int. J. Pharm. 310 (2006) 131–138.
[156] A. Priprem, J. Watanatorn, S. Sutthiparinyanont, W. Phachonpai, S. Muchimapura, Nanomedicine: NBM 4 (2008) 70–78.
[157] E. Bilensoy, A.A. Hincal, Expert Opin. Drug Deliv. 6 (2009) 1161–1173.
[158] A. Harada, Y. Takashima, H. Yamaguchi, Chem. Soc. Rev. 38 (2009) 875–882.
[159] S. Tommasini, M.L. Calabrò, R. Stancanelli, P. Donato, C. Costa, S. Catania, V. Villari, P. Ficarra, R. Ficarra, J. Pharm. Biomed. 39 (2005) 572–580.
[160] C. Lucas-Abellán, M.I. Fortea, J.M. López-Nicolás, E. Núnez-Delicado, Food Chem. 104 (2007) 39–44.
[161] M. Mercader-Ros, C. Lucas-Abellán, M.I. Fortea, J.A. Gabaldón, E. Núnez-Delicado, Food Chem. 118 (2010) 769–773.
[162] M.L. Calabrò, S. Tommasini, P. Donato, D. Raneri, R. Stancanelli, P. Ficarra, R. Ficarra, C. Costa, S. Catania, C. Rustichelli, G. Gamberini, J. Pharm. Biomed. 35 (2004) 365–377.
[163] H. Ding, J. Chao, G. Zhang, S. Shuang, J. Pan, Spectrochim. Acta A 59 (2003) 3421–3429.
[164] W. Abdelwahed, G. Degobert, H. Fessi, J Int. Pharm. 324 (2006) 74–82.
[165] F. Delgado-Vargas, A.R. Jimenez, O. Paredes-Lopez, Crit. Rev. Food Sci. 40 (2000) 173–289.
[166] P. Laine, P. Kylli, M. Heinonen, K. Jouppila, J. Agric. Food Chem. 56 (2008) 11251–11261.
[167] G. Gradinaru, C.G. Biliaderis, S. Kallithraka, P. Kefalas, C. Garcia-Viguera, Food Chem. 83 (2003) 423–436.
[168] F.T. Vicentini, Y.M. Fonseca, D.L. Pitol, M.M. Iyomasa, M.V. Bentley, M.J. Fonseca, J. Pharm. Pharm. Sci. 13 (2008) 274–285.
[169] S. Cooper, J. Ranger-Moore, T.G. Bowden, Mol. Carcinog. 43 (2005) 108–116.
[170] S. Maalouf, M. El-Sabban, N. Darwiche, H. Gali-Muhtasib, Mol. Carcinog. 34 (2002) 121–130.
[171] N. Cole, P.W. Sou, A. Ngo, K.H. Tsang, J.A. Severino, S.J. Arun, C.C. Duke, V.E. Reeve, Int. Arch. Allergy Immunol. 152 (2010) 87–97.
[172] Y.M. Fonseca, C.D. Catini, F.T. Vicentini, A. Nomizo, R.F. Gerlach, M.J. Fonseca, J. Ethnopharmacol. 127 (2010) 596–601.
[173] S. Dhanalakshmi, G.U. Mallikarjuna, R.P. Singh, R. Agarwal, Carcinogenesis 25 (2004) 1459–1465.
[174] B.R. Zhou, B.J. Lin, S.L. Jin, D. Luo, Photodermatol. Photoimmunol. Photomed. 25 (2009) 250–258.
[175] P.M. Maia Campos, M.D. Gianeti, A. Kanashiro, Y.M. Lucisano-Valim, L.R. Gaspar, Photochem. Photobiol. 82 (2006) 683–688.
[176] H. Lim, K.H. Son, H.W. Chang, S.S. Kang, H.P. Kim, Arch. Pharm. Res. 29 (2006) 503–507.
[177] R. Casagrande, S.R. Georgetti, W.A. Verri Jr., M.F. Borin, R.F. Lopez, M.J. Fonseca, Int. J. Pharm. 328 (2007) 183–190.
[178] Y.H. Tsai, K.F. Lee, Y.B. Huang, C.T. Huang, P.C. Wu, Int. J. Pharm. 388 (2010) 257–262.
[179] Y.B. Huang, K.F. Lee, C.T. Huang, Y.H. Tsai, P.C. Wu, Chem. Pharm. Bull. 58 (2010) 611–614.

[180] L.B. Lopes, H. VanDeWall, H.T. Li, V. Venugopal, H.K. Li, S. Naydin, J. Hosmer, M. Levndusky, H. Zheng, M.V. Bentley, R. Levin, M.A. Hass, J. Pharm. Sci. 99 (2010) 1346–1357.
[181] Y.M. Fonseca, C.D. Catini, F.T. Vicentini, J.C. Cardoso, R.L. Cavalcanti De Albuquerque Junior, M.J. Vieira Fonseca, J. Pharm. Sci. 100 (2011) 2182–2193.
[182] T. Gebre-Mariam, K. Asres, M. Getie, A. Endale, R. Neubert, P.C. Schmidt, Eur. J. Pharm. Biopharm. 60 (2005) 31–38.
[183] F. Marquele-Oliveira, Y.M. Fonseca, O. de Freitas, M.J. Fonseca, Int. J. Pharm. 342 (2007) 40–48.
[184] C.D. Ropke, T.M. Kaneko, R.M. Rodrigues, V.V. da Silva, S. Barros, T.C. Sawada, M.J. Kato, S.B. Barros, Int. J. Pharm. 249 (2002) 109–116.
[185] F.T. Vicentini, R. Casagrande, W.A. Verri Jr., S.R. Georgetti, M.V. Bentley, M.J. Fonseca, AAPS Pharm. Sci. Technol. 9 (2008) 591–596.
[186] S. Scalia, M. Mezzena, J. Pharm. Biomed. Anal. 49 (2009) 90–94.
[187] F.T. Vicentini, T.R. Simi, J.O. Del Ciampo, N.O. Wolga, D.L. Pitol, M.M. Iyomasa, M.V. Bentley, M.J. Fonseca, Eur. J. Pharm. Biopharm. 69 (2008) 948–957.
[188] P. Dekker, W.E. Parish, M.R. Green, Photochem. Photobiol. 81 (2005) 837–842.
[189] F. Casetti, W. Jung, U. Wolfle, J. Reuter, K. Neumann, B. Gilb, A. Wahling, S. Wagner, I. Merfort, C.M. Schempp, J. Photochem. Photobiol. B 96 (2009) 260–265.
[190] S. Sime, V.E. Reeve, Photochem. Photobiol. 79 (2004) 193–198.
[191] S. Widyarini, N. Spinks, A.J. Husband, V.E. Reeve, Photochem. Photobiol. 74 (2001) 465–470.
[192] M.G. Busby, A.R. Jeffcoat, L.T. Bloedon, M.A. Koch, T. Black, K.J. Dix, W.D. Heizer, B.F. Thomas, J.M. Hill, J.A. Crowell, S.H. Zeisel, Am. J. Clin. Nutr. 75 (2002) 126–136.
[193] S. Widyarini, A.J. Husband, V.E. Reeve, Photochem. Photobiol. 81 (2005) 32–37.
[194] T.M. Chiu, C.C. Huang, T.J. Lin, J.Y. Fang, N.L. Wu, C.F. Hung, J. Ethnopharmacol. 126 (2009) 108–113.
[195] F. Hu, H.R. Hepburn, Y. Li, M. Chen, S.E. Radloff, S. Daya, J. Ethnopharmacol. 100 (2005) 276–283.
[196] P.G. Pietta, C. Gardana, A.M. Pietta, Fitoterapia 73 (2002) 7–20.
[197] G.A. Burdock, Food Chem. Toxicol. 36 (1998) 347–363.
[198] A.H. Banskota, Y. Tezuka, S. Kadota, Phytother. Res. 15 (2001) 561–571.
[199] Y.M. Fonseca, F. Marquele-Oliveira, F.T. Vicentini, N.A. Furtado, J.P. Sousa, Y.M. Lucisano-Valim, M.J. Fonseca, Evid. Based Complement Alternat. Med. 2011 (2011) pii:863917.

Chapter 10

Antileishmanial Natural Products from Plants

Ifedayo V. Ogungbe, Meenakshi Singh and William N. Setzer
Natural Products Drug Discovery Group, Department of Chemistry, University of Alabama in Huntsville, Huntsville, Alabama, USA

INTRODUCTION

Leishmaniases are diseases caused by various species of the protozoan genus, *Leishmania*, six of which cause leishmaniasis in humans [1]. The parasites are transmitted to the mammalian host by sandflies (*Phlebotomus* spp. and *Lutzomya* spp.). It was reported at the beginning of last decade that a steady increase in the cases of leishmaniases is being recorded all over the world [2], largely because resources devoted to combat this re-emerging disease have been grossly insufficient. Clinical manifestations of these diseases in humans are classified as visceral, diffuse cutaneous, subcutaneous, cutaneous, and recidivans leishmaniasis. Visceral leishmaniasis (VL) and cutaneous leishmaniasis are, however, the main clinical forms of the disease in humans. In the mammalian host, *Leishmania* survive and multiply as intracellular non-motile amastigotes in the phagolysosomes of macrophages or other reticulo-endothelial cells. After ingestion by a sandfly vector, the parasites multiply in the gut as flagellated promastigotes, migrate to the proboscis, and enter a new vertebrate host when the fly bites. The UNICEF/UNDP/World Bank/WHO special program on Tropical Diseases Research (TDR) estimates that about 12 million people are currently infected with the disease and that nearly 350 million people are at risk of infection in over 88 countries. The incidence of VL is estimated to be as high as half a million cases per year in the Indian subcontinent alone, while an estimated 1.5 million cases of cutaneous leishmaniasis are recorded annually [3]. Leishmaniasis has also been widely reported as an opportunistic infection in HIV/AIDS patients, thus making it a serious public health concern in endemic populations [4].

Proven chemotherapeutics for leishmaniasis include the antimonials sodium stibogluconate (pentostam) and meglumine antimoniate (glucantime). There are adverse side effects associated with these compounds, and drug

Bioactive Natural Products, Vol. 36. DOI: 10.1016/B978-0-444-53836-9.00027-X

resistance is emerging [5]. Alternative antileishmanial chemotherapies include amphotericin B and pentamidine, but these are generally more toxic than the pentavalent antimonials. The alkylphosphocholine miltefosine is currently in clinical use in India and may find more widespread use in the future. The aminoglycoside antibiotic paromomycin is also currently used in the treatment of VL. Combination therapies with better treatment regimens are also being explored for the treatment of leishmaniasis. A recent study revealed that a combination of miltefosine and liposomal amphotericin B was successful in treating VL [3,6]. Combination therapy involving paromomycin plus sodium stibogluconate as well as allopurinol plus sodium stibogluconate has also been tried in the past [7,8]. Proponents of combination therapy have argued that it could help in halting the development of drug resistance by the parasite and in reducing drug adverse effects, and, as a result of shorter treatment regimen, it could ensure patient treatment compliance. The development of vaccines against the parasites has also been pursued extensively; however, those efforts have yet to result in any clinically acceptable vaccine [9].

Drug Targets in *Leishmania* spp.

Successful sequencing of the *Leishmania major*, *Leishmania infantum*, and *Leishmania braziliensis* [10,11] genomes, like those of many other disease-causing pathogens, has provided a myriad of information about potential cellular targets in *Leishmania* spp. Comparative genomic and proteomic analyses on these targets in various *Leishmania* spp. and their homologues in humans are expected to provide a guide for several drug discovery efforts in the future. While a great deal still needs to be done on target validation, several reports have indicated that some targets are druggable, are essential for parasite survival, and could deliver on the promise of new chemotherapy against leishmaniasis. Some of the drug targets that have been reported to offer such promise include farnesyl pyrophosphate synthase, histone deacetylase, CRK3 cyclin-dependent kinase, dihydrofolate reductase–thymidylate synthase, cysteine protease B, GDP-mannose pyrophosphorylase, glycogen synthase kinase-3, *N*-myristoyltransferase, ornithine decarboxylase, and fumarate reductase [12–26]. In addition to these targets, a plethora of other potential drug targets are also made available by TDR through its chemogenomics resource database (www.TDRtargets.org). The use of bioinformatics to identify potential drug targets in *L. major* using the resources made available by TDRtargets.org was recently demonstrated by Crowther and co-workers [27].

Natural Products as Antileishmanial Agents

Natural products are a very attractive source of chemical diversity and without any question, the most important source of therapeutic agents against parasitic diseases. Newman and Cragg [28–30] have continually pointed out that

natural products contribute overwhelmingly to the number of newly approved small molecule-based drugs and that the exploration of Mother Nature for novel therapeutic agents requires an expansion. The success of natural products is evident in the case of malaria. The most effective chemotherapy against malaria, so far, has been based on natural product pharmacophores, and several reports have indicated that many natural products have antileishmanial activity. Excellent reviews on natural products with antileishmanial activity have been written by Rocha and co-workers [31] and by Salem and Werbovetz [32], in which they surveyed compounds that have been reported to have antileishmanial activity. These reviews were followed by a survey of the most promising leishmanicidal natural products by Polonio and Efferth [33]. Since those reviews, several antileishmanial compounds have been reported, and, as our contribution to this volume, we provide a survey of pure compounds and extracts from plants that have been reported to have biological activity against several species of *Leishmania*. We hope that this will encourage subsequent isolation and synthetic or biosynthetic efforts to provide natural products libraries that can support high-throughput pharmacological screening of compounds as possible drug leads against leishmaniasis.

Antileishmanial Phenolics

The flavonoids kaempferol, quercetin, trifolin, 6″-*O*-acetylhyperoside and their *O*-acetyl derivatives, tetra-*O*-acetylkaempferol, penta-*O*-acetylquercetin, hepta-*O*-acetyltrifolin, and octa-*O*-acetylhyperoside isolated from the aerial parts of *Consolida oliveriana* were tested for their leishmanicidal activity against the promastigote forms of *L.* (*V.*) *peruviana* and *L.* (*V.*) *braziliensis*. The acetylated flavonoids penta-*O*-acetylquercetin, hepta-*O*-acetyltrifolin, and octa-*O*-acetylhyperoside had leishmanicidal activity against *L.* (*V.*) *peruviana* promastigotes, with IC_{50} values of 11.18, 10.53, and 7.35 μM, respectively, while hepta-*O*-acetyltrifolin and octa-*O*-acetylhyperoside had IC_{50} values of 8.72 and 6.21 μM against *L.* (*V.*) *braziliensis*, respectively. These acetylated flavonoids were shown to be more active against the two *Leishmania* spp. than pentostam and glucatim in addition to being less toxic toward the macrophage cell line, J774.2. Their antiproliferative effects were also confirmed by the observed morphological alterations and by the detected metabolic imbalances in the parasites, which included disruption of the cytoplasm, intense vacuolization of the parasites, reduction in the excretion of catabolites like acetate and succinate, and increased production of L-alanine and D-lactate [34]. The prenylated xanthone 1,4,5-trihydroxy-3-(3-methylbut-2-enyl)-9*H*-xanthen-9-one isolated from the root bark of *Garcinia livingstonei* (Clusiaceae) had moderate activity against the amastigotes of *L. infantum*, with an IC_{50} value of 27 μM (Figs. 1 and 2) [35].

Machilin-G and veraguensin, lignans isolated from the bark of *Nectandra megapotamica* (Lauraceae), showed activity against the promastigote form of

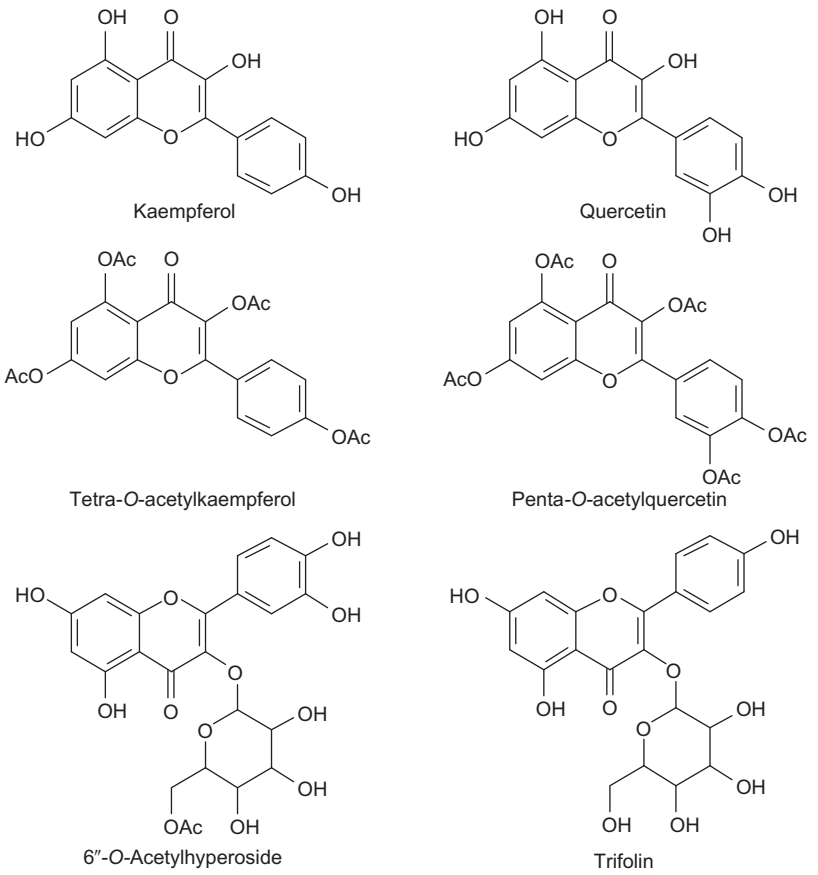

FIGURE 1 Structures of antileishmanial phenolics.

Leishmania donovani. The IC_{50} of Machilin-G was determined to be 50.5 μM, while the IC_{90} of veraguensin was 96.7 μM. These compounds did not display any toxicity against the African green monkey kidney fibroblast at the concentrations tested [36]. Also, the cannaboid 5-acetyl-4-hydroxycannabigerol isolated from *Cannabis sativa* (Cannabaceae) was shown to have antileishmanial activity against *L. donovani*, with IC_{50} and IC_{90} values of 10.7 and 18.7 μM, respectively [37]. Piceatannol, a protein kinase inhibitor isolated from the seeds of *Euphorbia lagascae* (Euphorbiaceae), displayed antileishmanial activity against promastigotes of *L. donovani*, *L. major*, and *L. infantum*, with LD_{50} values of 17.2, 16, and 23.3 μM, respectively. Its LD_{50} value against intracellular amastigotes of *L. donovani* was 30.3 μM. The kinase inhibitor also showed toxicity toward noninfected RAW macrophages [38]. Also, isoxanthochymol isolated from the stem bark of the Indonesian plant *Garcinia griffithii* (Clusiaceae) exhibited activity against *L. infantum*, with an IC_{50} value of 2.03 μM.

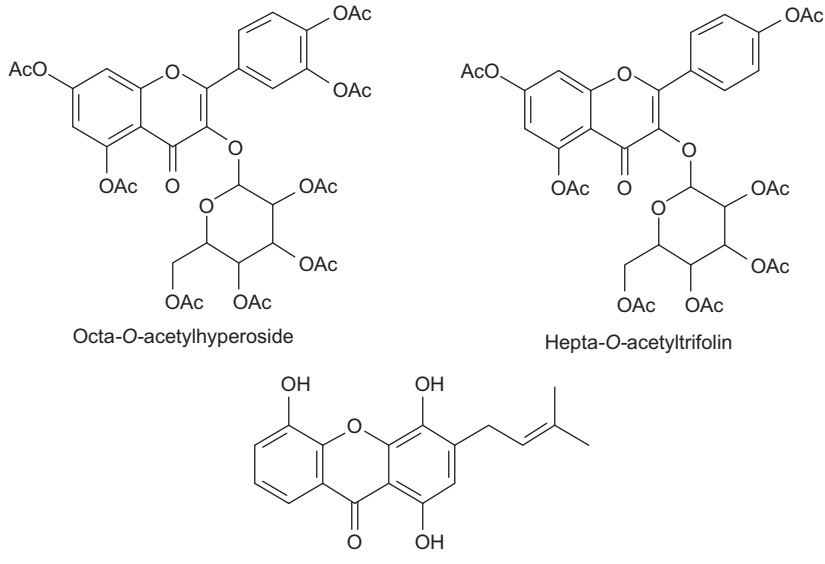

Octa-*O*-acetylhyperoside

Hepta-*O*-acetyltrifolin

1,4,5-Trihydroxy-3-(3-methylbut-2-enyl)-9*H*-xanthen-9-one

FIGURE 2 Structures of antileishmanial phenolics.

It also had a high toxicity against MRC-5 cells with an IC_{50} value of 7.26μM. It also displayed activity against *Trypanosoma cruzi*, *Trypanosoma brucei*, and *Plasmodium falciparum* (Fig. 3) [39].

1,2-Dihydroxy-6-8-dimethoxy xanthone (TDR13011), the compound with previously reported antimalarial activity [40], was reported to have leishmanicidal activity against *L. infantum* amastigotes. Its IC_{50} value against the parasites was determined to be 27.8μM. It was isolated from the roots of the Indian medicinal plant, *Andrographis paniculata* (Acanthaceae) [41]. The prenylated benzoic acid derivative 3-(3,7-dimethyl-2,6-octadienyl)-4-methoxy-benzoic acid isolated from the leaves of *Piper aduncum* (Piperaceae) exhibited activity against the promastigotes of *L. braziliensis*, with an IC_{50} value of 22.3μM. Its reported activity was higher toward the parasite than that of pentamidine (IC_{50} value of 29.4μM) [42]. Also, benzoic acid derivative methyl 3,4-dihydroxy-5-(3-methyl-2-butenyl)benzoate isolated from the leaves of *Piper glabratum* showed antileishmanial activity against promastigote forms of *L. braziliensis*, *Leishmania amazonensis*, and *L. donovani*, with IC_{50} values of 58.4, 77.1, and 78.4μM, respectively [43]. Gallic acid (EC_{50} value of 25.9μM) and its methyl ester, methyl 3,4,5-trihydroxybenzoate (EC_{50} value of 67.9μM), isolated from the roots of *Pelargonium sidoides* (Geraniaceae) were shown to significantly reduce the intracellular survival of *L. donovani* amastigotes within murine macrophages. These reductions were suspected to have been caused by a possible activation of leishmanicidal apparatus in the macrophages due to the

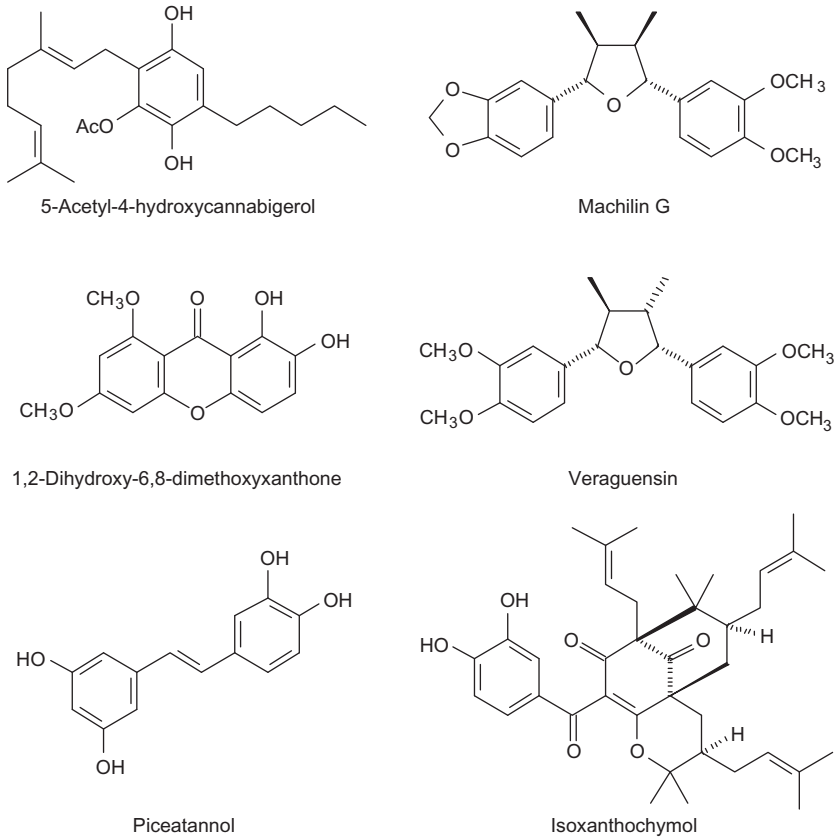

FIGURE 3 Structures of antileishmanial phenolics.

presence of the cytokine, tumor necrosis factor, and inorganic nitric oxides in the supernatants of sample-treated macrophage cultures (Fig. 4) [44,45].

5-(11′(*S*)-Hydroxy-8′-heptadecenyl)resorcinol and 5-(12′(*S*)-hydroxy-8′,14′-heptadecadienyl)resorcinol, new hydroxyalkenylresorcinols isolated from leaves of *Stylogyne turbacensis* (Myrsinaceae), were reported to have good antileishmanial activity. Their IC_{50} values against *L. donovani* were determined to be 7 and 3 μM, respectively [46]. The isoflavone 5,7,3′,4′- tetrahydroxy-2′-(3,3-dimethylallyl)isoflavone and the chalcone isoliquiritigenin isolated from the roots of *Psorothamnus arborescens* (Fabaceae) displayed leishmanicidal activity against axenic amastigotes of *L. donovani*. The IC_{50} values of the flavonoids against the parasite were 13.0 and 20.7 μM, respectively, although their low selectivity (around threefold) for the parasites was also revealed, due to their toxicity toward the mammalian Vero cells (Fig. 5) [47].

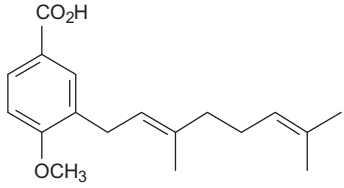

3-(3,7-Dimethyl-2,6-octadienyl)-
4-methoxybenzoic acid

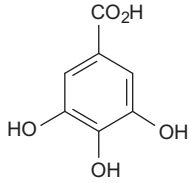

Gallic acid

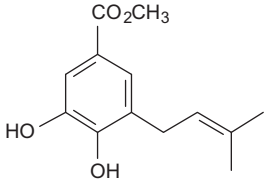

Methyl 3,4-dihydroxy-5-
(3-methyl-2-butenyl)benzoate

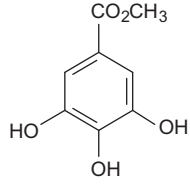

Methyl-3,4,5-trihydroxybenzoate

FIGURE 4 Structures of antileishmanial phenolics.

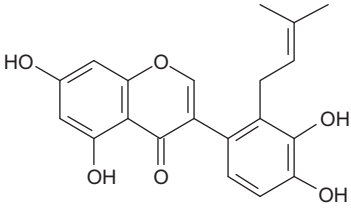

5,7,3′,4′-Tetrahydroxy-2′-
(3,3-dimethylallyl)isoflavone

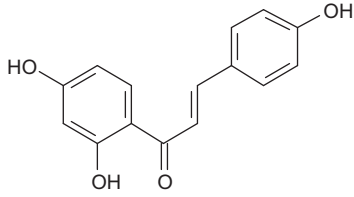

Isoliquiritigenin

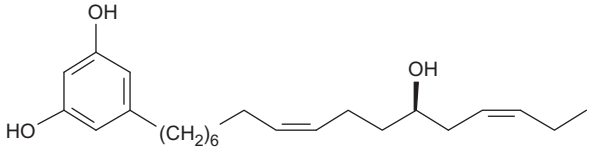

5-(12′(*S*)-Hydroxy-8′,14′-heptadecadienyl)resorcinol

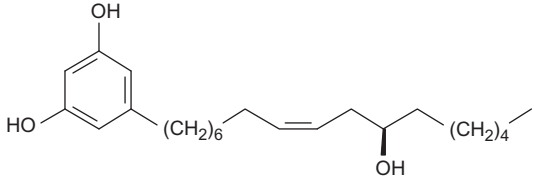

5-(11′(*S*)-hydroxy-8′-heptadecenyl)resorcinol

FIGURE 5 Structures of antileishmanial phenolics isolated from *Stylogyne turbacensis* and *Psorothamnus arborescens*.

Malabaricones A and B were reported to have antileishmanial activity against *L. donovani* promastigotes. The IC_{50} values of these diarylnonanoids against the parasites were determined to be 49 and 64.2 μM, respectively. They were isolated from the fruit peels of *Myristica malabarica* (Myristiceae), along with the less active malabaricones C and D [48]. The chalcone, isocordoin, and its derivatives isolated from the roots of *Lonchocarpus xuul* (Fabaceae) were reported to have antileishmanial activity. Isocordoin had an IC_{50} value of 7.70 μM against *Leishmania mexicana* promastigotes, while its derivative 2′,4′-diacetoxy-3′-(3-methylbut-2-enyl)-chalcone had an IC_{50} value of 3.10 μM against similar parasites. Both of these compounds had a low selectivity index toward the parasites because of their cytotoxicity. However, methylation of isocordoin significantly increased its selectivity index from 1.14 to 358.00 with a concomitant decrease in its antileishmanial activity (IC_{50} value of 23.00 μM) [49]. Also, flavokavain B, a chalcone isolated from the leaves of *Piper rusbyi* (Piperaceae), was found to have leishmanicidal activity against promastigotes of *L. amazonensis*, *L. braziliensis*, and *L. donovani* with a remarkably identical IC_{50} value of 11.2 μM for all three parasites, a value lower than the IC_{50} value of the control drug, pentamidine (IC_{50} value of 16.8 μM). Subsequent evaluation of flavokavain B in *L. amazonensis*-infected mice which were treated with 5 mg/kg/day of the compound suggests significant *in vivo* activity that is promising for drug development [50].

Also, the evaluation of quercetin 3-*O*-α-L-arabinopyranosyl (1→2)-α-L-rhamnopyranoside, quercetin 3-*O*-α-L-rhamnopyranoside (quercitrin), and quercetin in *L. amazonensis*-infected mice by Muzitano and co-workers revealed that the flavonoids were able to reduce parasite load and control the growth of lesions in murine models at a dose of 16 mg/kg body weight. It was suggested that the activity of the glycosylated quercetins might be due to the aglycone, quercetin, and its conjugates derived upon catabolism. Quercetin itself and quercitirin have also been previously reported to have *in vitro* antileishmanial activity against *L. amazonesis* amastigotes (Figs. 6 and 7) [51,52].

The isoflavonoid 6,7-dimethoxy-3′,4′-methylenedioxyisoflavone isolated from the roots of *Millettia puguensis* (Fabaceae) was found to have moderate activity against *L. infantum* amastigotes with IC_{50} values of 32 μM. It also displayed toxicity toward MRC-5 cells with an IC_{50} value of 43 μM [53]. Calceolarioside A isolated from the leaves of *Nyctanthes arbor-tristis* (night jasmine, Oleaceae) was found to have *in vitro* and *in vivo* activity against *L. donovani*. Its IC_{50} value against promastigotes of *L. donovani* was determined to be 41.8 μM. It was also reported to cause significant hepatic and splenic parasite burden reduction in infected hamsters at a dose of 20 mg/kg body weight. A synergistic effect was observed when the hamsters were cotreated with sodium antimony gluconate [54]. Apigenin, a potent inhibitor of cytochrome P450 2C9, and the ubiquitous flavones luteolin and luteolin 7-*O*-β-glucopyranoside were reported to have antileishmanial activity against amastigotes

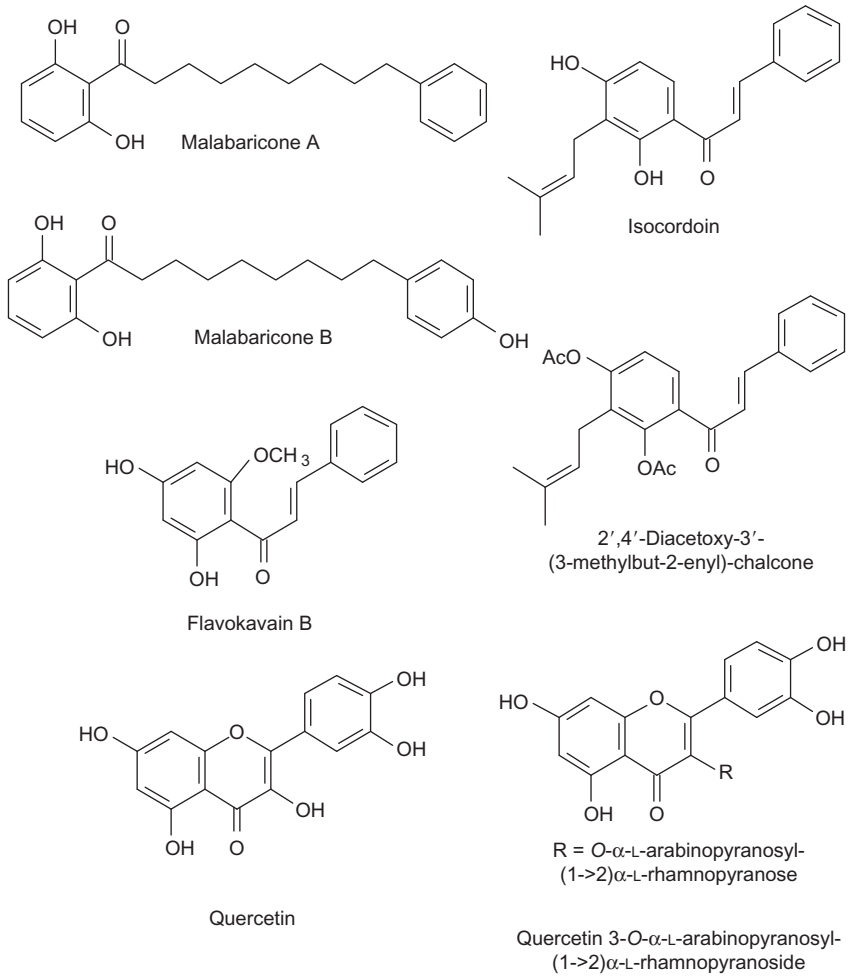

FIGURE 6 Structures of some antileishmanial phenolics.

of *L. donovani*, with IC_{50} values of 27.8, 10.5, and 15.6 μM, respectively. They were isolated from the aerial parts of *Melampyrum arvense* [55].

Antileishmanial Alkaloids

The naphthylisoquinoline alkaloid 5-*epi*-6-*O*-methylancistrobertsonine A was reported to exhibit activity against amastigotes of *L. donovani* with an IC_{50} value of 3.7 μM. It was isolated from the roots of the Congolese *Ancistrocladus* plant (Ancistrocladaceae) [56]. The *N*,*C*-coupled naphthyldihydroisoquinoline alkaloids ancistrocladinium A and the *atropo*-diastereomers ancistrocladinium B and *N*-6′-*epi*-ancistrocladinium B, isolated from the leaves of the same

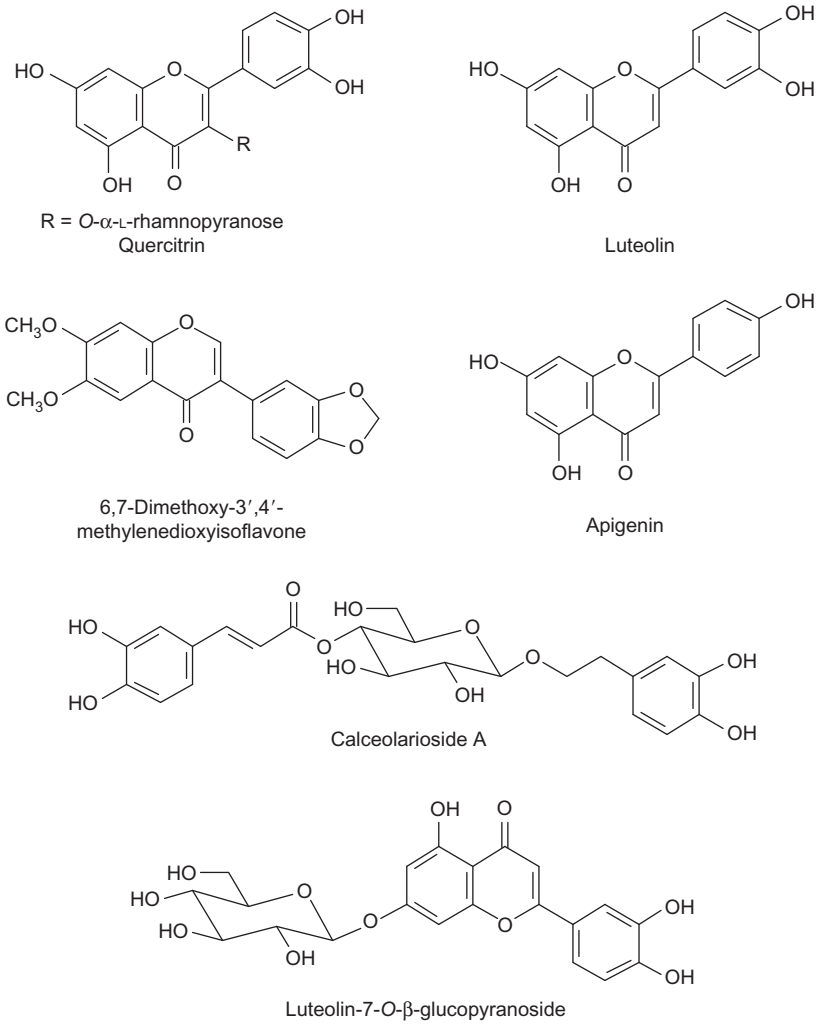

FIGURE 7 Structures of some antileishmanial phenolics.

Congolese plant species, were also shown to have antileishmanial activities. The IC_{50} values of ancistrocladinium A against *L. donovani* and *L. major* were reported as 1.7 and 7.3 μM, respectively, while a mixture of the diastereoisomers ancistrocladinium B and *N-6′-epi*-ancistrocladinium B had IC_{50} values of 2.7 and 6.6 μM against *L. donovani* and *L. major*, respectively. In addition to their antileishmanial activity, they also displayed considerable toxicity toward rat skeletal myoblast L-6 cells and the macrophage cell line, J774.1 [57]. Costa and co-workers reported that annomontine has antileishmanial activity. Its IC_{50} value against *L. braziliensis* promastigotes was determined

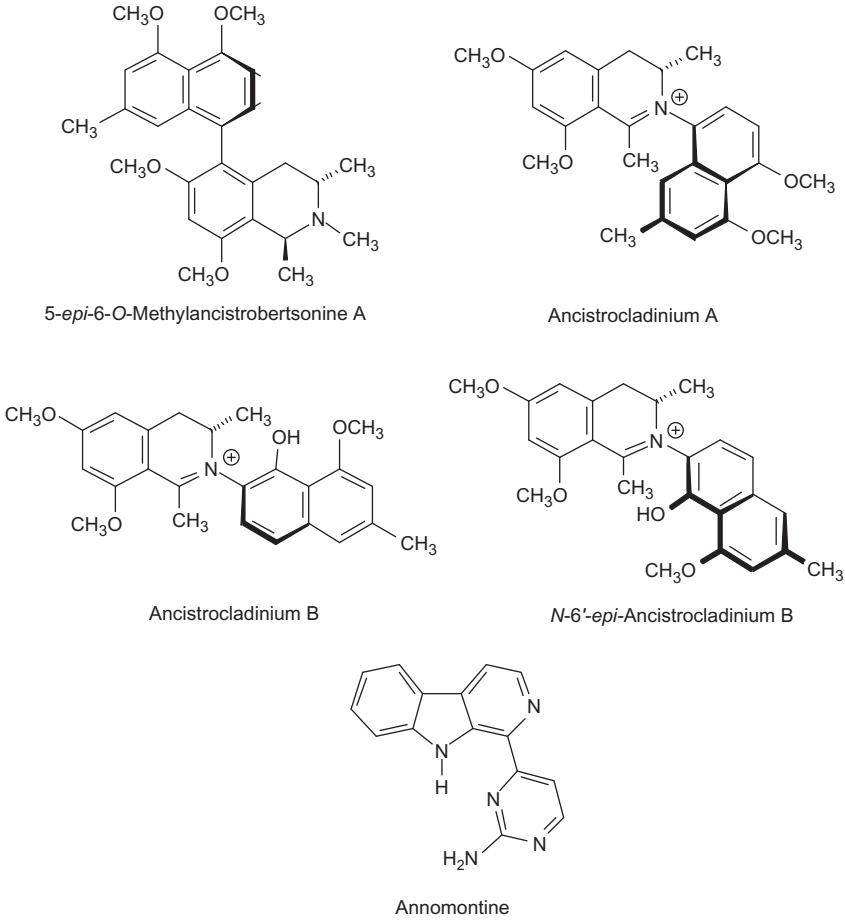

FIGURE 8 Structures of some antileishmanial alkaloids.

to be 34.8 μM. It was isolated, along with the previously characterized antileishmanial compound liriodenine, from the bark of *Annona foetida* (Annonaceae) (Fig. 8) [58,59].

The steroidal alkaloids hookerianamide H, hookerianamide I, hookerianamide J, hookerianamide K, vagenine A, sarcovagine C, and dehydrosarsalignone were reported to be active against promastigotes of *L. major*. They had IC_{50} values of 22.4, 8.8, 11.3, 6.8, 3.3, 1.5, and 21.3 μM, respectively. They were isolated from the evergreen plant *Sarcococca hookeriana* (Buxaceae) (Fig. 9) [60].

Cryptolepine, an indoloquinoline alkaloid, and its dimeric form, biscryptolepine, displayed leishmanicidal activity against the axenic amastigotes of *L. donovani*, with IC_{50} values of 2.68 and 1.15 μM, respectively. They were isolated from the African medicinal plant *Cryptolepis sanguinolenta*

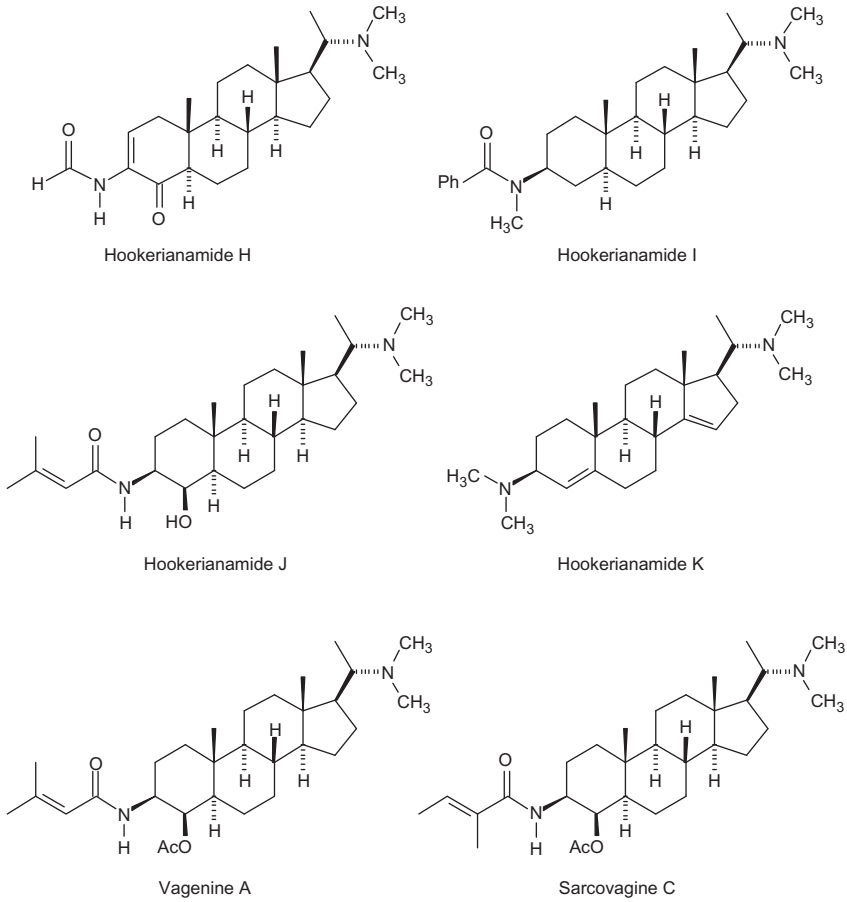

FIGURE 9 Structures of antileishmanial alkaloids isolated from *Sarcococca hookeriana*.

(Asclepiadaceae) [61]. Dihydrochelerythrine, 6-acetonyldihydrochelerythrine, lucidamine A, and lucidamine B were reported to have leishmanicidal activity against the axenic amastigote of *L. donovani*. Their IC_{50} values were 2.0, 6.6, 10.8, and 6.8 μM, respectively. The extent of dihydrochelerythrine's activity against the parasites was comparable to that of pentamidine, and it was less toxic than the drug to Vero cells. These alkaloids were isolated from the stem bark of *Garcinia lucida* (Clusiaceae) (Fig. 10) [62].

(+)-Neolitsine was isolated from the leaves of *Guatteria dumetorumi* (Annonaceae), and it was found to be active against promastigotes of *L. mexicana*, with a 25-fold selectivity index over its toxicity toward murine macrophages. Its reported IC_{50} value was 15.4 μM [63]. 17-Oxo-3-benzoylbuxadine and other related triterpenoidal alkaloids isolated from the aerial parts of *Buxus hyrcana* (Buxaceae) were shown to have weak antileishmanial activity.

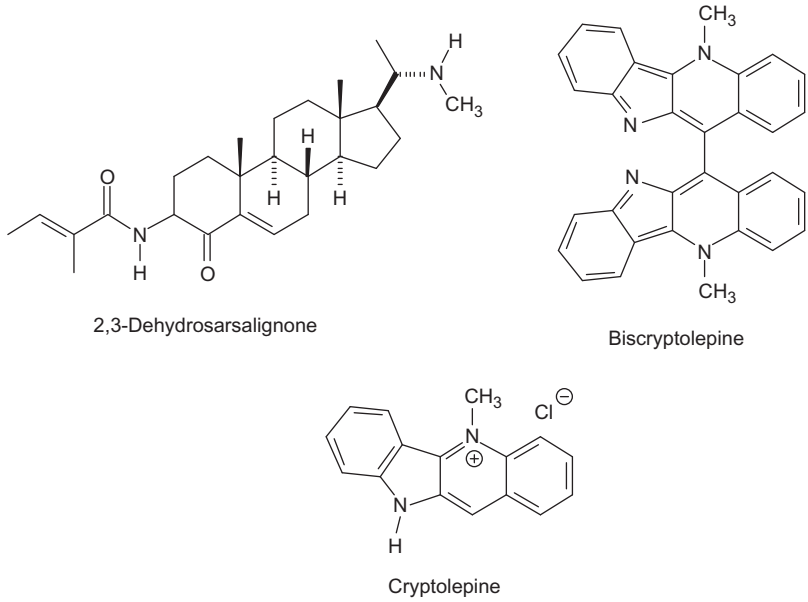

FIGURE 10 Structures of antileishmanial alkaloids.

17-Oxo-3-benzoylbuxadine being the most active of them had an IC_{50} value of 58 μM. Their activities were tested against the intracellular amastigotes of *L. donovani* (Fig. 11) [64].

Antileishmanial Terpenes and Terpenoids

(−)-α-Bisabolol, the principal component of *Chamomilla recutita* essential oil, was reported to have leishmanicidal activity against promastigotes of *L. infantum*. It had an IC_{50} value of 49.4 μM, and its activity was reported to compete favorably with pentamidine as an antileishmanial agent [65]. Also, the citral-rich essential oil from *Cymbopogon citratus* (Poaceae) was reported to have promising antileishmanial properties. Citral, the main component of the oil, was reported to induce significant morphological alterations in the parasites, and its IC_{50} value against *L. amazonensis* promastigotes was determined to be 52.5 μM [66]. (+)-δ-Cadinene, a minor component of basil oil (from *Ocimum basilicum*), had an appreciable activity against promastigotes of *L. donovani*. Its IC_{50} and IC_{90} values against the parasites were reported as 19.6 and 34.3 μM, respectively. Other minor components of the oil including δ-3-carene, α-humulene, citral, and (−)-(*E*)-caryophyllene also showed antileishmanial activity, with IC_{50} values of 198, 93, 124.8, and 93 μM, respectively (Figs. 12 and 13) [67].

The cycloartane triterpenoids bicusposide C and 3-*O*-β-D-xylocyclosiversigenin isolated from the Fabaceae plant *Astragalus bicuspis* were reported to

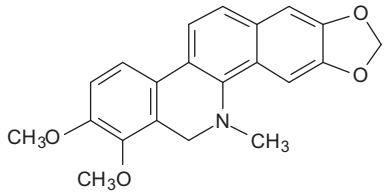

Dihydrochelerythrine

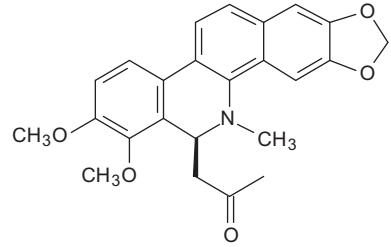

6-Acetonyldihydrochelerythrine

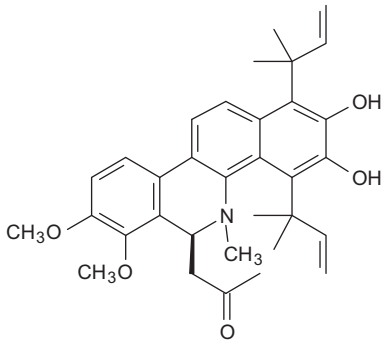

Lucidamine B

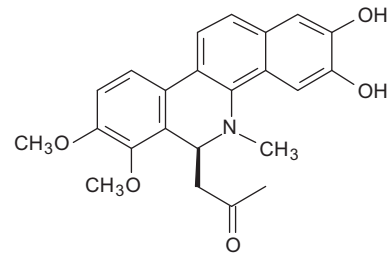

Lucidamine A

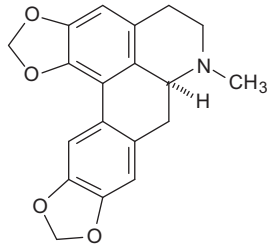

(+)-Neolitsine

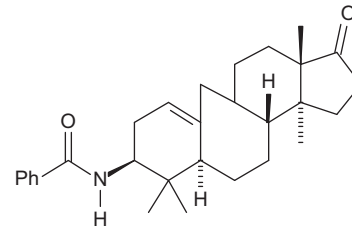

17-Oxo-3-benzoylbuxadine

FIGURE 11 Structures of antileishmanial alkaloids.

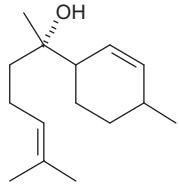

(–)-α-Bisabolol

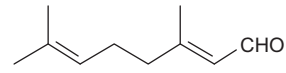

Citral

FIGURE 12 Structures of antileishmanial terpenoids present in the essential oils of *Chamomilla recutita* and *Cymbopogon citratus*.

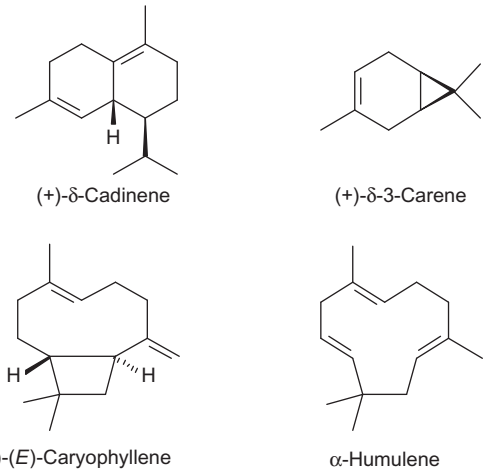

FIGURE 13 Structures of antileishmanial terpenes.

have weak leishmanicidal activity against promastigotes of *L. major*. Their IC_{50} values were reported as 64.35 and 56.51 μM, respectively [68]. 6α,7α,15β,16β,24-Pentacetoxy-22α-carbomethoxy-21β,22β-epoxy-18β-hydroxy-27,30-bisnor-3,4-secofriedela-1,20(29)-dien-3,4 R-olide (LLD-3) isolated from the wood powder of *Lophanthera lactescens* (Malpighiaceae) exhibited good leishmanicidal activity against intramacrophage amastigote forms of *L. amazonensis*. The reported IC_{50} value was 500 nM. In addition to its good antiproliferative activity, it was reported that LLD-3 lacked any toxicity toward mouse peritoneal macrophages. Also, blood levels of creatinine, urea, glutamyl oxalacetic transaminase, and glutamyl pyruvic transaminase, clinical markers for kidney and liver function, were not altered in LLD-3-treated animals as well as there were no noticeable histopathological alterations in the tissues examined [69]. Costunolide, a sesquiterpene lactone, exhibited *in vitro* leishmanicidal activity (IC_{50} value of 9.4 μM) against the amastigote form of *L. mexicana*. It was isolated, along with some novel germacranes, from the young leaves of *Magnolia sororum* (Figs. 14 and 15) [70].

7-Deacetylgedunin and 7-deacetyl-7-oxogedunin were shown to have good *in vitro* activity against axenic amastigotes of *L. donovani*. The reported IC_{50} values were 3.2 and 2.3 μM, respectively. These gedunin derivatives were isolated from the roots of *Pseudocedrela kotschyi* (Meliacae) [71]. The triterpenoid saponin arborenin isolated by the bioassay-guided fractionation of the methanolic extract from *Careya arborea* leaves was reported to have antileishmanial activity against the promastigote and amastigote forms of *L. donovani*. The IC_{50} values were 18.8 and 15.7 μM against the promastigote and amastigote forms, respectively. The compound did not display any detectable toxicity toward human peripheral blood mononuclear cells [72]. Totarol,

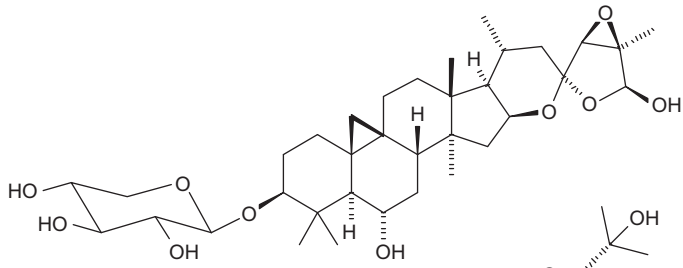

Bicusposide C

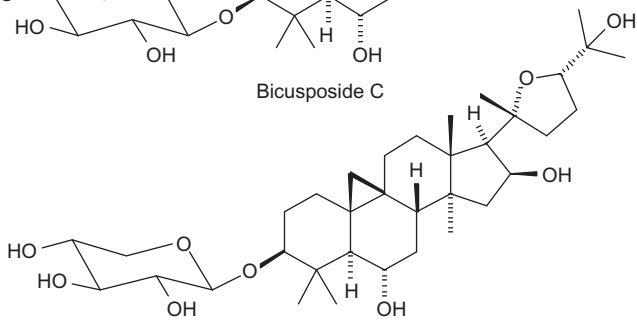

3-*O*-β-Xylocyclosiversigenin

FIGURE 14 Structures of some antileishmanial terpenoids.

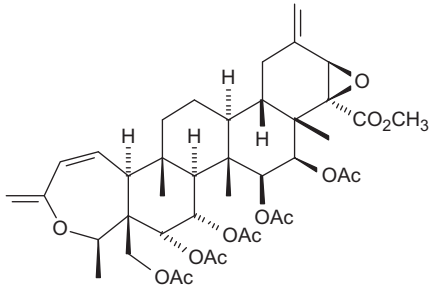

6α,7α,15β,16β,24-Pentacetoxy-22α-carbomethoxy-21β,22β-epoxy-18β-hydroxy-27,30-bisnor-3,4-secofriedela-1,20(29)-dien-3,4 R-olide (LLD-3)

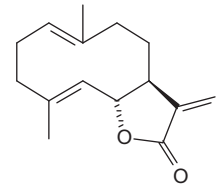

Costunolide

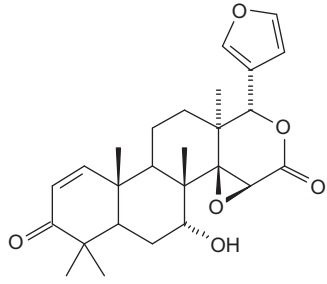

7-Deacetylgedunin

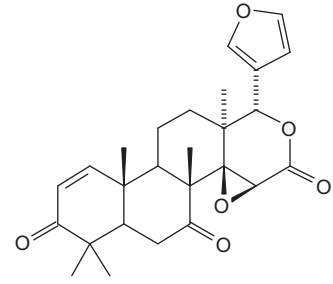

7-Deacetyl-7-oxogedunin

FIGURE 15 Structures of some antileishmanial terpenoids.

ferruginol, and 7β-hydroxyabieta-8,13-diene-11,12-dione, the abietane diterpenes isolated from the berries of *Juniperus procera* (Cupressaceae) by Samoylenko and co-workers, were reported to inhibit the growth of *L. donovani* promastigotes. The IC_{50} and IC_{90} values of totarol were 12.2 and 24.1 μM, while those of ferruginol were 12.2 and 24.4 μM, and those of 7β-hydroxyabieta-8,13-diene-11,12-dione were 14.5 and 69.5 μM, respectively [73]. The sterol clerosterol exhibited antileishmanial activity against *Leishmania chagasi* promastigotes and intracellular amastigotes. Its activity was characterized by IC_{50} values of 24.3 μM for the promastigote form and 43.9 μM for the intracellular amastigotes. While clerosterol was about 3.6-fold less toxic than pentamidine toward peritoneal macrophages, pentamidine was about 100-fold more active against the promastigote form of the parasite. The sterol was isolated from the fruits of *Cassia fistula* (Fabaceae) (Fig. 16) [74].

Several diterpenes from *Cistus creticus* (Cistaceae), and their semisynthetic derivatives, were tested against *L. donovani* promastigotes. The most

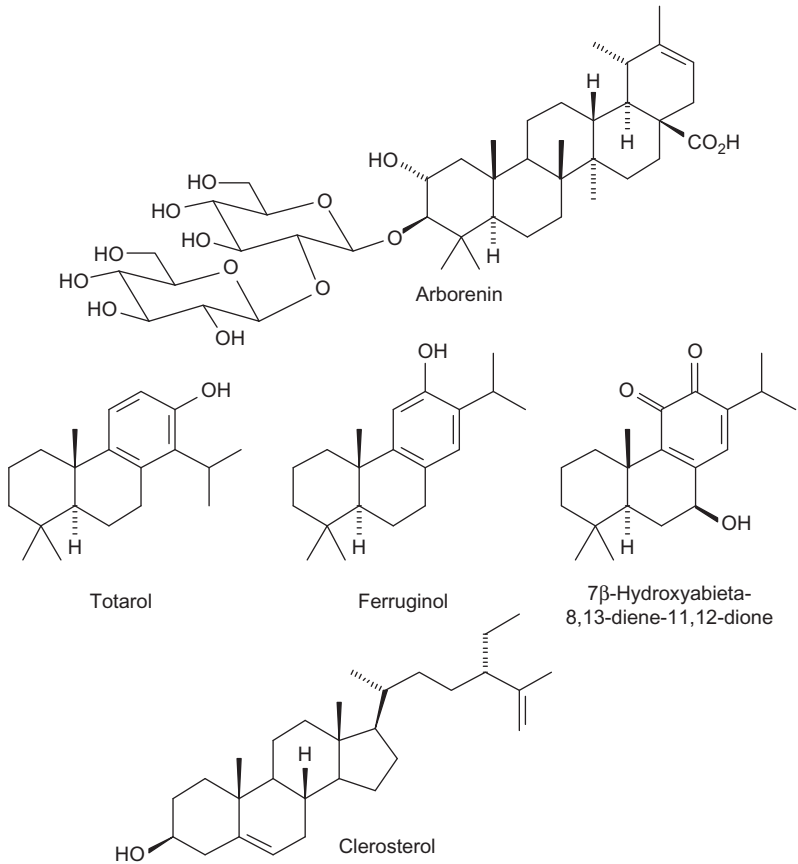

FIGURE 16 Structures of some antileishmanial terpenoids.

active of these compounds were the *cis*-clerodane diterpenes: 18-acetoxy-*cis*-clerod-3-en-15-ol (the IC_{50} and IC_{90} values were 9.4 and 19.3 μM, respectively), 15,18-diacetoxy-*cis*-clerod-3-ene (the IC_{50} and IC_{90} values were 8.6 and 18.4 μM), and 13-(*E*)-8α-hydroxylabd-13-en-15-ol-2-chloroethylcarbamate (the IC_{50} and IC_{90} values were 8.5 and 18.1 μM, respectively), a chlorinated carbamate derivate of 13-(*E*)-8α-hydroxylabd-13-en-15-ol malonate. These activities compare favorably with those reported for pentamidine (the IC_{50} and IC_{90} values were 4.7 and 23.5 μM, respectively), and they display selectivity in their activity by having weaker activity toward the African green monkey epithelial cells [75]. Onoseriolide isolated from the bark of *Hedyosmum angustifolium* (Chloranthaceae) was reported to exhibit growth-inhibiting activity against the axenic amastigotes of *L. amazonensis* and *L. infantum*, and the intramacrophagic form of *L. infantum*. The IC_{50} values were determined to be 19.8, 20.97, and 24.3 μM, respectively [76]. The hydroperoxycycloartanes 24-hydroperoxycycloart-25-en-3β-ol and 25-hydroperoxycycloart-23-en-3β-ol isolated from *Blepharodon nitidum* (Asclepiadaceae) exhibited antileishmanial activity against axenic amastigotes of *L. amazonensis*, with IC_{50} values of 5.2 and 5.0 μM, respectively (Figs. 17 and 18) [77].

The sesquiterpene lactone 8-epixanthatin 1β,5β-epoxide, isolated from the dichloromethane extract of the aerial parts of *Xanthium brasilicum* (Asteraceae), was found to have potent antileishmanial activity. It had an IC_{50} value of 0.6 μM against the axenic amastigotes of *L. donovani* [78]. Also, the sesquiterpene lactones anthecotulide, 4-hydroxyanthecotulide, and 4-acetoxyanthecotulide isolated from the aerial parts of *Anthemis auriculata* (Asteraceae) were found to have leishmanicidal activity against axenic amastigotes of *L. donovani* with IC_{50} values of 32.9, 12.4, and 40.8 μM, respectively. However, these compounds were also found to display significant toxicity against L6 cells [79]. The bioassay-guided fractionation of the root bark extract of *Elaeodendron schlechteranum* (Celastraceae) led to the isolation of tingenin B (22-hydroxytingenone). Its activity against *L. infantum* was characterized by an IC_{50} value of 1.2 μM. It was also reported to have antibacterial, antitrypanosomal, and antiplasmodial activities. It was also very toxic toward MRC-5 cells (Fig. 19) [80].

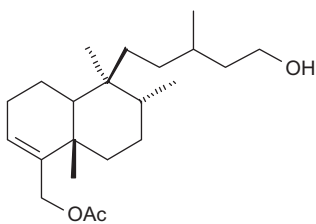

18-Acetoxy-*cis*-clerod-3-en-15-ol

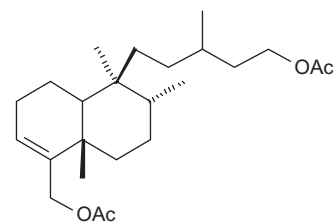

15,18-Diacetoxy-*cis*-clerod-3-ene

FIGURE 17 Structures of antileishmanial terpenoids from *Cistus creticus*.

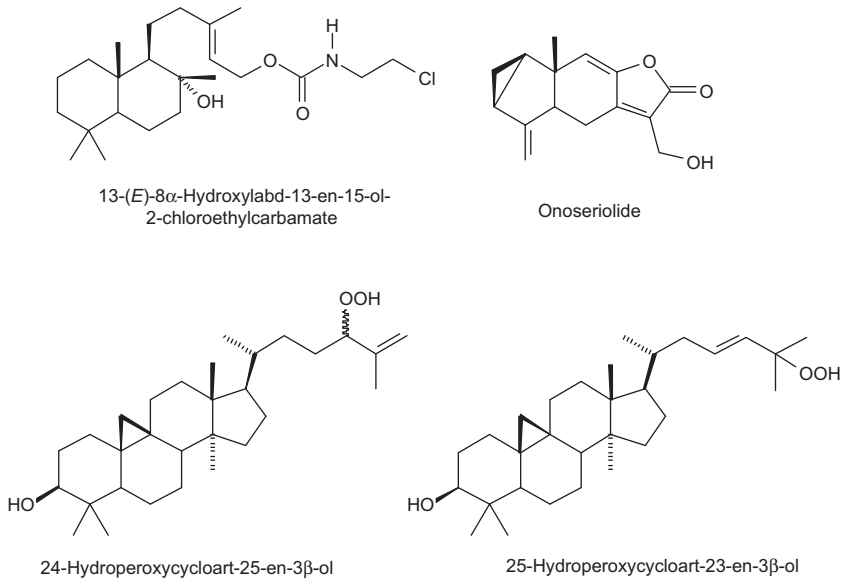

13-(*E*)-8α-Hydroxylabd-13-en-15-ol-2-chloroethylcarbamate

Onoseriolide

24-Hydroperoxycycloart-25-en-3β-ol

25-Hydroperoxycycloart-23-en-3β-ol

FIGURE 18 Structures of antileishmanial terpenoids.

The hydroperoxy-cycloartane triterpenoids musambins A and B isolated from the leaves of the east African plant *Markhamia lutea* (Bignoniaceae) were reported to have antileishmanial activity against the promastigote form of *L. donovani*. The reported EC_{50} values were 57.5 and 49.5 μM, respectively [81].

Antileishmanial Quinones

The quinones cordiachrome A and cordiachrome B isolated from the methanol extract of *Cordia fragrantissima* wood were reported to have good antileishmanial activity against promastigote forms of *L. major* with IC_{50} values of 16.9 and 10.3 μM, respectively. Also isolated from the same plant were the related compounds: cordiaquinol J, cordiaquinol C, alliodorin, and acetylcordiaquinol C (a semisynthetic derivative of cordiaquinol C). Their IC_{50} values against promastigote forms of *L. major* were reported as 10.3, 10.2, 26.9, and 4.3 μM, respectively. In addition, cordiaquinol I, cordiaquinol J, cordiachrome C, and alliodorin were reported to have good activity against promastigotes of *Leishmania guyanensis* with IC_{50} values of 25.7, 11.4, 24.8, and 6.9 μM, respectively, as well as against promastigotes of *L. panamensis*, with IC_{50} values of 47.7, 6.9, 22.7, and 6.9 μM, respectively. The toxicity of these compounds toward the epithelial-like African green monkey kidney cells (COS-7) and the human liver cancer cells (HuH-7) was considerably low when compared to their leishmanicidal activities (Figs. 20 and 21) [82].

7-{[(2*R**)-3,3-Dimethyloxiran-2-yl]methoxy}-8-[(2*R**,3*R**)-3-isopropenyloxiran-2-yl]-2H-chromen-2-one, 7-methoxy-8-(4-methyl-3-furyl)2H-chromen-

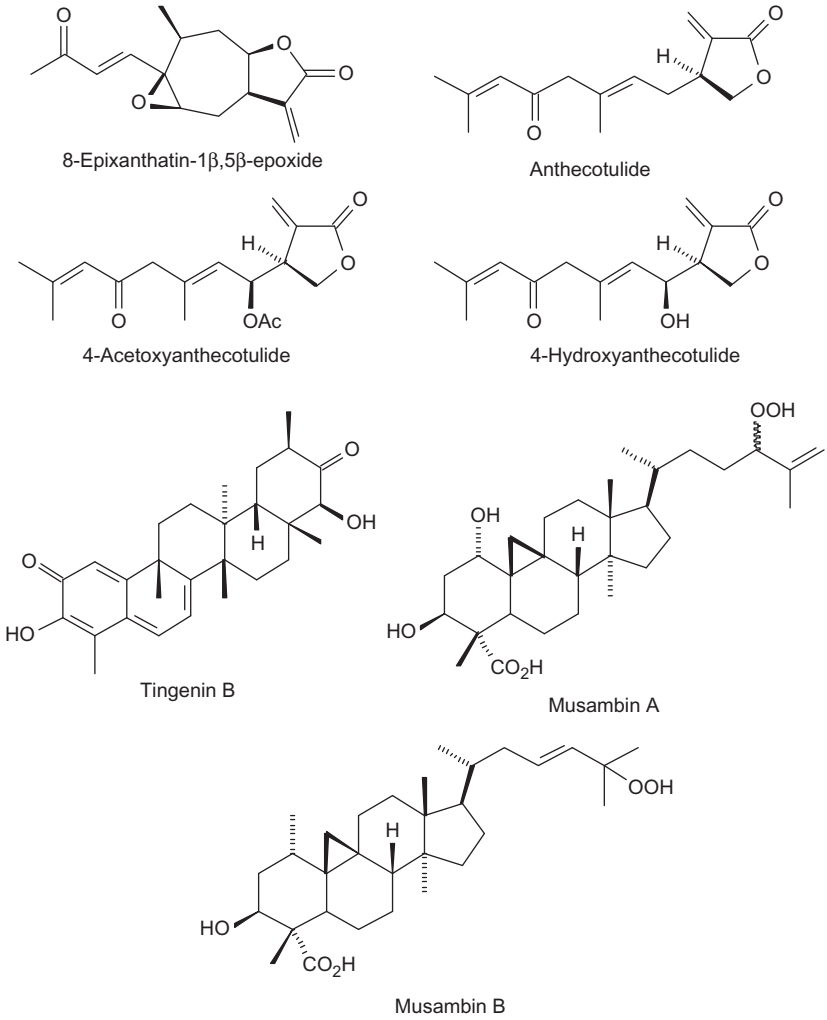

FIGURE 19 Structures of antileishmanial terpenoids.

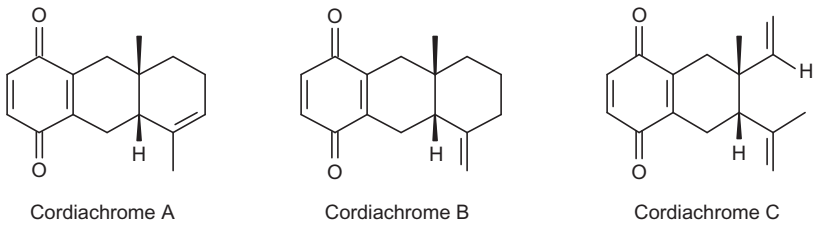

FIGURE 20 Structures of antileishmanial cordiachromes isolated from *Cordia fragrantissima* wood.

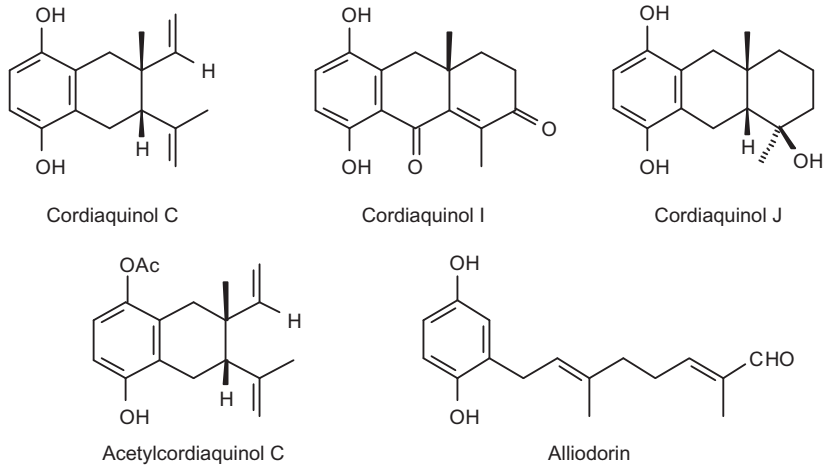

FIGURE 21 Structures of antileishmanial cordiaquinols and alliodorin isolated from *Cordia fragrantissima* wood.

2-one, and phebalosin exhibited activity against the axenic amastigotes of *L. panamensis* and the human promonocytic U-937 cells. Their reported EC_{50} values were 30.1, 41, and 54.6 μM, respectively. These coumarins were isolated from the leaves of *Galipea panamensis* (Rutaceae) [83]. Dioncoquinones A and B isolated from the cell material of *Triphyophyllum peltatum* (Dioncophyllaceae) were reported to have specific activity against *L. major*. Dioncoquinone A was reported to inhibit the growth of the parasites by 49.6% at 2.1 μM, while dioncoquinone B inhibited their growth by 79.2% at a concentration of 3.6 μM [84]. 4-Hydroxy-3,5-dimethoxy-2-naphthaldehyde, diospyrin, and 8′-hydroxyisodiospyrin isolated from the roots of *Diospyros assimilis* (Ebenaceae) were found to be active against the axenic amastigotes of *L. donovani*, with IC_{50} values of 38.78, 8.82, and 16.66 μM, respectively. Cytotoxicity studies revealed that the dimeric quinones, diospyrin and 8′-hydroxyisodiospyrin were toxic to L-6 cells while 4-hydroxy-3,5-dimethoxy-2-naphthaldehyde was about 10-fold less toxic than the quinones. Diospyrin has been previously reported to have leishmanicidal activity (Figs. 22 and 23) [85,86].

The coumestan derivative tephcalostan D isolated from the roots of *Tephrosia calophylla* (Fabaceae) was found to be active against the axenic amastigotes of *L. donovani*. The reported IC_{50} value was 15.63 μM, which is considerably higher than that reported for miltefosine (IC_{50} value was reported as 0.47 μM). Tephcalostan D was, however, reported to be over 1000-fold less toxic to L-6 cells than miltefosine [87]. Auraptene and umbelliprenin isolated from the roots of *Ferula szowitsiana* (Apiaceae) significantly inhibited the growth of *L. major* promastigotes. The IC_{50} values reported for

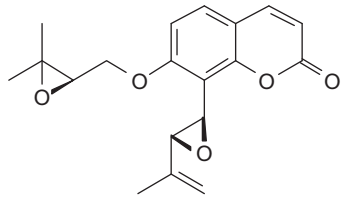

7-{[(2*R**)-3,3-Dimethyloxiran-2-yl]methoxy}-8-[(2*R**,3*R**)-3-isopropenyloxiran-2-yl]-2*H*-chromen-2-one

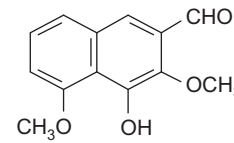

4-Hydroxy-3,5-dimethoxy-2-naphthaldehyde

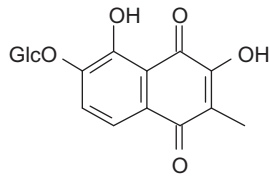

Dioncoquinone A

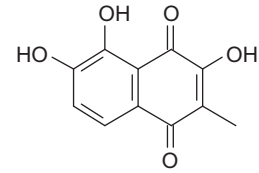

Dioncoquinone B

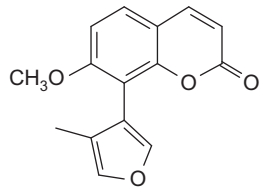

7-Methoxy-8-(4-methyl-3-furyl)-2*H*-chromen-2-one

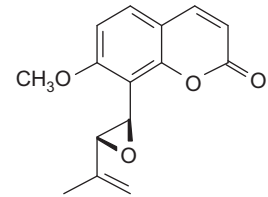

Phebalosin

FIGURE 22 Structures of some antileishmanial compounds from plants.

these compounds were 17.1 and 13.3 μM, respectively. It has been previously reported by Napolitano and co-workers that auraptene has antileishmanial activity [88,89]. The antileishmanial activity of 12,16-dideoxyaegyptinone B isolated from the roots of *Zhumeria majdae* (Lamiaceae) was reported by Moein and co-workers. Its activity was characterized by an IC_{50} value of 2.5 μM against promastigotes of *L. donovani*. The antileishmanial activity and its selectivity index were comparable to those reported for pentamidine [90].

Miscellaneous Antileishmanial Compounds

The polyacetylenes 8-hydroxyheptadeca-4,6-diyn-3-yl ethanoate, 8-hydroxyheptadeca-1-ene-4,6-diyn-3-yl ethanoate, and 16-acetoxy-11-hydroxyoctadeca-17-ene-12,14-diynyl ethanoate, isolated from the petroleum ether extract of the root bark of the Tanzanian medicinal plant, *Cussonia zimmermannii*

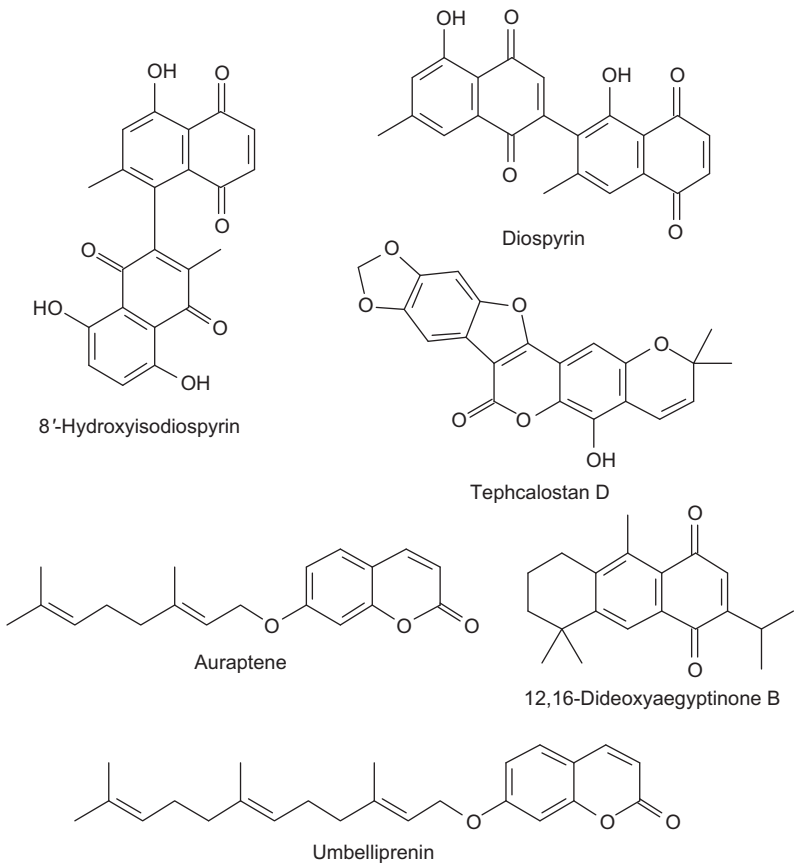

FIGURE 23 Structures of some antileishmanial quinones.

(Araliaceae), were found to have significant activity against the axenic and intramacrophagic amastigote forms of *L. donovani*. Their IC_{50} values against the axenic form were 7.8, 0.13, and 0.14 μM, respectively. They had, however, IC_{50} values of >10, 0.32, and 2.3 μM, respectively, against the intramacrophagic forms of the parasite [91]. Another related compound, (3*S*)-16,17-didehydrofalcarinol, isolated from the methanol extract of *Tridax procumbens* (Asteraceae), exhibited antileishmanial activity against the promastigote and amastigote forms of *L. mexicana*, with IC_{50} values of 0.55 and 0.485 μM, respectively [92,93]. Grandiuvarone isolated from the bark of *Uvaria grandiflora* (Annonaceae) was reported to have antileishmanial activity. Its IC_{50} and IC_{90} values against promastigotes of *L. donovani* were determined to be 2.3 and 5 μM, respectively. Although the extent of grandiuvarone's cytotoxicity was not described in that report, it showed better antileishmanial activity than

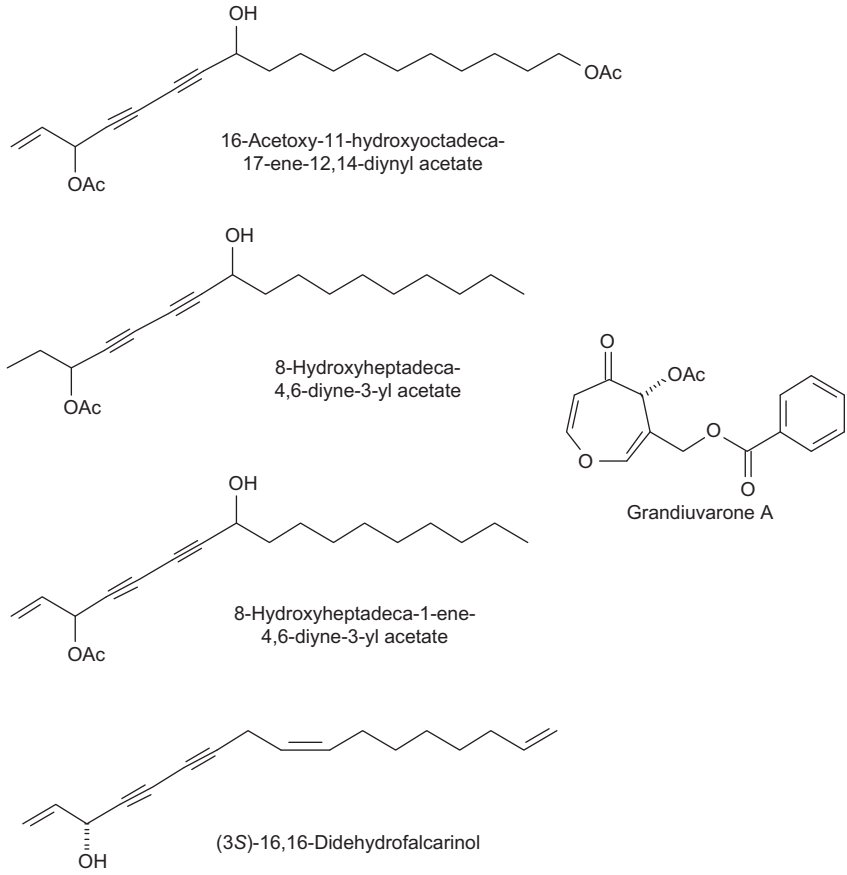

FIGURE 24 Structures of some antileishmanial compounds.

pentamidine (IC_{50} and IC_{90} values were reported to be 4.7 and 19.4 μM, respectively) (Fig. 24) [94].

Plants Extracts

A small percentage of all characterized plant species has been explored over the years for pharmaceutical applications [95]. The list of antileishmanial compounds that we surveyed and those that have been reported prior to this shows the enormous potential of plants as sources of drug leads. In Table 1, we provide a list of plants whose extract(s) have been reported to have antileishmanial activity. Their activities were reported using various terms, as indicated in Table 1. We hope research programs can be developed around these plant families for the isolation and characterization of their antileishmanial principles.

TABLE 1 Plant Species Reported to Have Antileishmanial Activity

Family	Plant	Origin	Parts of Plant (Solvent)[a]	Organism Tested	Percentage Survival (Concentration)	References
Clusiaceae	*Psorospermum guineense* Hochr.	Marché de Médine, Bamako, Mali	Root bark (DCM)	*Leishmania major* (Amastigotes)	14.0±0.6 (35μg/mL)	[96]
Clusiaceae	*Psorospermum guineense* Hochr.	Marché de Médine, Bamako, Mali	Root bark (DCM)	*Leishmania major* (Promastigotes)	3.5±0.3 (35μg/mL), 12.8±0.9 (17.5μg/mL)	[96]
Fabaceae	*Bobgunnia madagascarensis* J. H. Kirkbr. and Wiersema	Siby, Mali	Root bark (DCM)	*Leishmania major* (Amastigotes)	0.4±0.1 (35μg/mL), 3.6±0.3 (17.5μg/mL)	[96]
Fabaceae	*Bobgunnia madagascarensis* J. H. Kirkbr. and Wiersema	Siby, Mali	Root bark (DCM)	*Leishmania major* (Promastigotes)	0.2±0.0 (35μg/mL), 0.6±0.1 (17.5μg/mL)	[96]
Fabaceae	*Entada africana* Gill. and Perr.	Marché de Médine, Bamako, Mali	Roots (H_2O)	*Leishmania major* (Amastigotes)	5.0±0.9 (35μg/mL), 7.3±1.1 (17.5μg/mL)	[96]
Fabaceae	*Entada africana* Gill. and Perr.	Marché de Médine, Bamako, Mali	Roots (H_2O)	*Leishmania major* (Promastigotes)	15.3±1.4 (35μg/mL)	[96]
Meliaceae	*Pseudocedrela kotschyi* (Schweinf.) Harms	Marché de Médine, Bamako, Mali	Roots (DCM)	*Leishmania major* (Amastigotes)	5.6±1.2 (35μg/mL), 9.2±0.8 (17.5μg/mL)	[96]

Continued

TABLE 1 Plant Species Reported to Have Antileishmanial Activity—Cont'd

Family	Plant	Origin	Parts of Plant (Solvent)[a]	Organism Tested	Percentage Survival (Concentration)	References
Rubiaceae	*Sarcocephalus latifolius* (Smith) Bruce	Marché de Médine, Bamako, Mali	Stem bark (DCM)	*Leishmania major* (Amastigotes)	18.5±2.1 (35 μg/mL)	[96]
Rubiaceae	*Sarcocephalus latifolius* (Smith) Bruce	Marché de Médine, Bamako, Mali	Stem bark (DCM)	*Leishmania major* (Promastigotes)	15.0±0.6 (35 μg/mL)	[96]
Rubiaceae	*Sarcocephalus latifolius* (Smith) Bruce	Marché de Médine, Bamako, Mali	Stem bark (MeOH)	*Leishmania major* (Promastigotes)	16.7±1.4 (35 μg/mL)	[96]
Rutaceae	*Zanthoxylum zanthoxyloides* (Lam.) Zepernick and Timler	Marché de Médine, Bamako, Mali	Root bark (DCM)	*Leishmania major* (Amastigotes)	0.9±0.3 (35 μg/mL), 6.0±1.4 (17.5 μg/mL)	[96]
Rutaceae	*Zanthoxylum zanthoxyloides* (Lam.) Zepernick and Timler	Marché de Médine, Bamako, Mali	Root bark (H_2O)	*Leishmania major* (Amastigotes)	14.5±0.4 (35 μg/mL), 17.7±0.5 (17.5 μg/mL)	[96]

Family	Plant	Origin	Parts of Plant (Solvent)	Organism Tested	% Viability (CV)[b] (100 μg/mL)	References
Asteraceae	*Chromolaena hirsuta* (Hook. and Arn.)	Minas Gerais, Brazil	Leaves (DCM)	*Leishmania amazonensis* (Promastigotes)	67.91 (6.55)	[97]

Asteraceae	*Chromolaena hirsuta* (Hook. and Arn.)	Minas Gerais, Brazil	Leaves (EtOH)	*Leishmania amazonensis* (Promastigotes)	86.42 (6.36)	[97]
Asteraceae	*Chromolaena hirsuta* (Hook. and Arn.)	Minas Gerais, Brazil	Flowers (DCM)	*Leishmania amazonensis* (Promastigotes)	30.22 (2.57)	[97]
Asteraceae	*Chromolaena hirsuta* (Hook. and Arn.)	Minas Gerais, Brazil	Flowers (EtOH)	*Leishmania amazonensis* (Promastigotes)	76.06 (4.25)	[97]

Family	**Plant**	**Origin**	**Parts of Plant (Solvent)**	**Organism Tested**	**Mortality (%) Extract Concentration (1mg/mL)**	**References**
Aloeaceae	*Aloe nyeriensis*	Kiambu, Kenya	Leaves (MeOH)	*Lieshmania major* (Promastigotes)	68.4±6.3	[98]
Aloeaceae	*Aloe nyeriensis*	Kiambu, Kenya	Leaves (H_2O)	*Lieshmania major* (Promastigotes)	53.3±5.10	[98]
Fabaceae	*Albizia coriara*	Kajulu, Kenya	Stem bark (H_2O)	*Lieshmania major* (Promastigotes)	66.7±5.00	[98]
Fabaceae	*Acacia tortilis*	Kitui, Kenya	Stem bark (H_2O)	*Lieshmania major* (Promastigotes)	52.9±6.55	[98]

Continued

TABLE 1 Plant Species Reported to Have Antileishmanial Activity—Cont'd

Family	Plant	Origin	Parts of Plant (Solvent)	Organism Tested	Mortality (%) Extract Concentration (1mg/mL)	References
Liliaceae	*Asparagus racemosus*	Meka, Kenya	Roots (MeOH)	*Lieshmania major* (Promastigotes)	58.3±8.22	[98]
Liliaceae	*Asparagus racemosus*	Meka, Kenya	Roots (H_2O)	*Lieshmania major* (Promastigotes)	56.8±6.58	[98]

Family	Plant	Origin	Parts of Plant (Solvent)	Organism Tested	Infection Rate (%) Extract Concentration (1000μg/mL)	References
Aloeaceae	*Aloe nyeriensis* var. *kedongensis*	Kiambu, Kenya	Leaves (MeOH)	*Lieshmania major* (Amastigotes)	30±1.22	[98]
Euphorbiaceae	*Suregada zanzibariensis*	Gedi Ruins, Kenya	Leaves (MeOH)	*Lieshmania major* (Amastigotes)	28±2.11	[98]
Fabaceae	*Albizia coriaria*	Kajulu, Kenya	Stem bark (MeOH)	*Lieshmania major* (Amastigotes)	44±3.69	[98]
Fabaceae	*Acacia tortilis*	Kitui, Kenya	Stem bark (H_2O)	*Lieshmania major* (Amastigotes)	44±5.59	[98]
Liliaceae	*Asparagus racemosus*	Meka, Kenya	Roots (H_2O)	*Lieshmania major* (Amastigotes)	42±3.84	[98]

Family	Plant	Origin	Parts of Plant (Solvent)	Organism Tested	Multipication Indices (%) Extract Concentration (1000 μg/mL)	References
Aloeaceae	*Aloe nyeriensis* var. *kedongensis*	Kiambu, Kenya	Leaves (MeOH)	*Lieshmania major* (Amastigotes)	31.1 ± 2.22	[98]
Aloeaceae	*Aloe nyeriensis*	Kiambu, Kenya	Leaves (H_2O)	*Lieshmania major* (Amastigotes)	46.7 ± 3.28	[98]
Euphorbiaceae	*Suregada zanzibariensis*	Gedi Ruins, Kenya	Leaves (MeOH)	*Lieshmania major* (Amastigotes)	29.4 ± 2.15	[98]
Fabaceae	*Albizia coriaria*	Kajulu, Kenya	Stem bark (MeOH)	*Lieshmania major* (Amastigotes)	28.5 ± 1.43	[98]
Fabaceae	*Acacia tortilis*	Kitui, Kenya	Stem bark (H_2O)	*Lieshmania major* (Amastigotes)	35.9 ± 3.49	[98]
Fabaceae	*Albizia coriaria*	Kajulu, Kenya	Stem bark (H_2O)	*Lieshmania major* (Amastigotes)	47.5 ± 3.21	[98]

Family	Plant	Origin	Parts of Plant (Solvent)	Organism Tested	EC_{50} (μg/mL)	References
Annonaceae	*Uvaria afzelii* Sc. Elliot	Cote d'ivoire	Leaves (MeOH)	*Leishmania donovani* (Promastigotes)	12.5	[99]
Annonaceae	*Uvaria afzelii* Sc. Elliot	Cote d'ivoire	Roots (DCM)	*Leishmania donovani* (Promastigotes)	12.5	[99]

Continued

TABLE 1 Plant Species Reported to Have Antileishmanial Activity—Cont'd

Family	Plant	Origin	Parts of Plant (Solvent)	Organism Tested	EC_{50} (μg/mL)	References
Apocynaceae	*Pagiantha cerifera* (Pancher and Sébert) Markgraf	New Caledonia and Vanuatu	Leaves (DCM)	*Leishmania donovani* (Promastigotes)	5.0	[100]
Chenopodiaceae	*Chenopodium ambrosioides* L.	Cuba	Aerial parts (essential oil)	*Leishmania donovani* (Promastigotes)	4.45	[101]
Chenopodiaceae	*Chenopodium ambrosioides* L.	Cuba	Aerial parts (essential oil)	*Leishmania donovani* (Amastigotes)	5.1	[101]
Chenopodiaceae	*Chenopodium ambrosioides* L.	Cuba	Aerial parts (essential oil)	*Leishmania amazonensis* (Promastigotes)	3.7	[102]
Chenopodiaceae	*Chenopodium ambrosioides* L.	Cuba	Aerial parts (essential oil)	*Leishmania amazonensis* (Amastigotes)	4.6	[102]
Euphorbiaceae	*Codiaeum peltatum* (Labillardière) P.S. Green	New Caledonia and Vanuatu	Bark (DCM)	*Leishmania donovani* (Promastigotes)	5.0	[100]
Rubiaceae	*Gardenia urvillei* Montrouzier	New Caledonia and Vanuatu	Flowers (hexane)	*Leishmania donovani* (Promastigotes)	4.5	[100]
Rutaceae	*Zieridium melicopaefolium* Guillaumin	New Caledonia and Vanuatu	Bark (EtOH)	*Leishmania donovani* (Promastigotes)	3.5	[100]

Sapindaceae	*Cupaniopsis glomeriflora* Radlkofer	New Caledonia and Vanuatu	Leaves (EtOH)	*Leishmania donovani* (Promastigotes)	3.3	[100]
Verbenaceae	*Lippia multiflora* Moldenke	Cote d'ivoire	Leaves (DCM)	*Leishmania donovani* (Promastigotes)	12.5	[99]
Zingiberaceae	*Aframomum sceptrum* (Oliv. and T. Hanb.) K. Schum.	Cote d'ivoire	Leaves (DCM)	*Leishmania donovani* (Promastigotes)	12.5	[99]

Family	**Plant**	**Origin**	**Parts of Plant (Solvent)**	**Organism Tested**	**IC_{50} (μg/mL)**	**References**
Acanthaceae	*Aphelandra scabra* (Vahl) Sm.	Yucatan peninsula	Leaves (MeOH)	*Leishmania mexicana* (Promastigotes)	15	[103]
Aceraceae	*Acer laurinum* var. *petelotii*	Thai Nguyen province, Vietnam	Leaves (EtOH)	*Leishmania infantum* (Amastigotes)	2	[104]
Annonaceae	*Annona foetida* Martius	Manaus, Amazonas, Brazil	Leaves (essential oil)	*Leishmania amazonensis* (Promastigotes)	16.2±1.9	[105]
Annonaceae	*Annona foetida* Martius	Manaus, Amazonas, Brazil	Leaves (essential oil)	*Leishmania braziliensis* (Promastigotes)	9.9±1.2	[105]
Annonaceae	*Annona foetida* Martius	Manaus, Amazonas, Brazil	Leaves (essential oil)	*Leishmania chagasi* (Promastigotes)	27.2±6.2	[105]

Continued

TABLE 1 Plant Species Reported to Have Antileishmanial Activity—Cont'd

Family	Plant	Origin	Parts of Plant (Solvent)	Organism Tested	IC_{50} (μg/mL)	References
Annonaceae	*Annona foetida* Martius	Manaus, Amazonas, Brazil	Leaves (essential oil)	*Leishmania guyanensis* (Promastigotes)	4.1±0.2	[105]
Annonaceae	*Polyalthia suaveolens* Engl. and Diels syn. *Greenwenyadendron suaveolens* (Engl. and Diels) Verdc.	Estuaire region, Gabon	Stem barks (MeOH)	*Leishmania infantum* (Promastigotes)	1.8	[106]
Annonaceae	*Annona muricata* L.	Colombia	Leaves (EtOAc)	*Leishmania amazonensis* (Promastigotes)	25	[107]
Annonaceae	*Annona muricata* L.	Colombia	Leaves (EtOAc)	*Leishmania braziliensis* (Promastigotes)	25	[107]
Annonaceae	*Annona muricata* L.	Colombia	Leaves (EtOAc)	*Leishmania donovani* (Promastigotes)	25	[107]
Annonaceae	*Rollinia exsucca* (DC. ex Dunal) A. DC.	Colombia	Stems (hexane)	*Leishmania amazonensis* (Promastigotes)	20.8	[107]
Annonaceae	*Rollinia exsucca* (DC. ex Dunal) A. DC.	Colombia	Stems (hexane)	*Leishmania braziliensis* (Promastigotes)	20.8	[107]

Annonaceae	*Rollinia exsucca* (DC. ex Dunal) A. DC.	Colombia	Stems (hexane)	*Leishmania donovani* (Promastigotes)	20.8	[107]
Annonaceae	*Xylopia aromatica* (Lam.) Mart.	Colombia	Leaves (MeOH)	*Leishmania amazonensis* (Promastigotes)	20.8	[107]
Annonaceae	*Xylopia aromatica* (Lam.) Mart.	Colombia	Leaves (MeOH)	*Leishmania braziliensis* (Promastigotes)	20.8	[107]
Annonaceae	*Xylopia aromatica* (Lam.) Mart.	Colombia	Leaves (MeOH)	*Leishmania donovani* (Promastigotes)	20.8	[107]
Annonaceae	*Rollinia pittieri* Saff.	Colombia	Leaves (hexane)	*Leishmania amazonensis* (Promastigotes)	12.6	[107]
Annonaceae	*Rollinia pittieri* Saff.	Colombia	Leaves (EtOAc)	*Leishmania amazonensis* (Promastigotes)	20.8	[107]
Annonaceae	*Rollinia pittieri* Saff.	Colombia	Leaves (MeOH)	*Leishmania amazonensis* (Promastigotes)	19.7	[107]
Annonaceae	*Rollinia pittieri* Saff.	Colombia	Stems (hexane)	*Leishmania amazonensis* (Promastigotes)	13.3	[107]

Continued

TABLE 1 Plant Species Reported to Have Antileishmanial Activity—Cont'd

Family	Plant	Origin	Parts of Plant (Solvent)	Organism Tested	IC_{50} (μg/mL)	References
Annonaceae	*Rollinia pittieri* Saff.	Colombia	Stems (EtOAc)	*Leishmania amazonensis* (Promastigotes)	20.8	[107]
Annonaceae	*Rollinia pittieri* Saff.	Colombia	Leaves (hexane)	*Leishmania braziliensis* (Promastigotes)	10.7	[107]
Annonaceae	*Rollinia pittieri* Saff.	Colombia	Leaves (EtOAc)	*Leishmania braziliensis* (Promastigotes)	20.8	[107]
Annonaceae	*Rollinia pittieri* Saff.	Colombia	Leaves (MeOH)	*Leishmania braziliensis* (Promastigotes)	31.4	[107]
Annonaceae	*Rollinia pittieri* Saff.	Colombia	Stems (hexane)	*Leishmania braziliensis* (Promastigotes)	15.1	[107]
Annonaceae	*Rollinia pittieri* Saff.	Colombia	Stems (EtOAc)	*Leishmania braziliensis* (Promastigotes)	25.0	[107]
Annonaceae	*Rollinia pittieri* Saff.	Colombia	Leaves (hexane)	*Leishmania donovani* (Promastigotes)	10.7	[107]

Annonaceae	*Rollinia pittieri* Saff.	Colombia	Leaves (EtOAc)	*Leishmania donovani* (Promastigotes)	20.8	[107]
Annonaceae	*Rollinia pittieri* Saff.	Colombia	Leaves (MeOH)	*Leishmania donovani* (Promastigotes)	43.8	[107]
Annonaceae	*Rollinia pittieri* Saff.	Colombia	Stems (hexane)	*Leishmania donovani* (Promastigotes)	15.1	[107]
Annonaceae	*Rollinia pittieri* Saff.	Colombia	Stems (EtOAc)	*Leishmania donovani* (Promastigotes)	19.7	[107]
Apocynaceae	*Pagiantha cerifera* (Pancher and Sébert) Markgraf	New Caledonia and Vanuatu	Leaves (DCM)	*Leishmania amazonensis* (Amastigotes)	12.5	[100]
Apocynaceae	*Himatanthus sucuuba* (Spruce ex Muell. Arg.) Woodson	Peru	Stem bark (EtOH)	*Leishmania amazonensis* (Axenic amastigotes)	5	[108]
Apocynaceae	*Himatanthus sucuuba* (Spruce ex Muell. Arg.) Woodson	Peru	Stem bark (EtOH)	*Leishmania amazonensis* (Promastigotes)	20	[108]
Apocynaceae	*Tabernaemontana sananho* Ruiz and Pav.	Peru	Roots (EtOH)	*Leishmania amazonensis* (Promastigotes)	9	[109]

Continued

TABLE 1 Plant Species Reported to Have Antileishmanial Activity—Cont'd

Family	Plant	Origin	Parts of Plant (Solvent)	Organism Tested	IC_{50} (μg/mL)	References
Asteraceae	*Baccharis dracunculifolia* DC.	Brazil	Leaves (essential oil)	*Leishmania donovani* (Promastigotes)	42	[110]
Asteraceae	*Milleria quinqueflora* L.	Yucatán Peninsula, Mexico	Roots (MeOH)	*Leishmania mexicana* (Promastigotes)	49	[103]
Asteraceae	*Tridax procumbens* L.	Yucatán Peninsula, Mexico	Whole plant (MeOH)	*Leishmania mexicana* (Promastigotes)	3	[103]
Asteraceae	*Vernonia polyanthes* Less.	Juiz de Fora, Minas Gerais, Brazil	Leaves (MeOH)	*Leishmania amazonensis* (Promastigotes)	4	[111]
Asteraceae	*Calea montana* Klatt	Yanesha, Peru	Leaves (EtOH)	*Leishmania amazonensis* (Axenic amastigotes)	10±5.6	[112]
Asteraceae	*Elephantopus mollis* Kunth	Ecuador	Leaves (DCM)	*Leishmania donovani* (Axenic amastigotes)	0.6	[113]
Asteraceae	*Clibadium sylvestre* (Aubl.) Baill.	Chayahuita, Peru	Aerial parts (EtOH)	*Leishmania amazonensis* (Axenic amastigotes)	15.7±2	[114]

Calophyllaceae	*Calophyllum brasiliense* Cambess.	Cerrado biome, Brazil	Root wood (DCM)	*Leishmania* (*L.*) *chagasi* (Promastigotes)	27.6± 0.82	[115]
Caricaceae	*Carica papaya* L.	Yanesha, Peru	Leaves (EtOH)	*Leishmania amazonensis* (Axenic amastigotes)	11±1.2	[112]
Clusiaceae	*Garcinia pedicillata* Seeman	New Caledonia and Vanuatu	Leaves (DCM)	*Leishmania amazonensis* (Amastigotes)	12.5	[100]
Clusiaceae	*Harungana madagascariensis* Lam. ex Poir.	Bazou, Cameroon	Seeds (MeOH)	*Leishmania donovani* (Amastigotes)	1.6±0.6	[116]
Cupressaceae	*Juniperus oxycedrus* L.	Coimbra, Portugal	Berries (essential oils)	*Leishmania infantum* (Promastigotes)	51	[117]
Ebenaceae	*Diospyros hispida* A. DC.	Cerrado biome, Brazil	Roots (EtOAc)	*Leishmania* (*L.*) *chagasi* (Promastigotes)	18.9± 0.53	[115]
Fabaceae	*Diphysa carthagenensis* Jacq.	Yucatán Peninsula, Mexico	Leaves (MeOH)	*Leishmania mexicana* (Promastigotes)	35	[103]
Fabaceae	*Desmodium axillare* Sw. DC.	Chayahuita, Peru	Aerial parts (EtOH)	*Leishmania amazonensis* (Axenic amastigotes)	17±2.5	[114]

Continued

TABLE 1 Plant Species Reported to Have Antileishmanial Activity—Cont'd

Family	Plant	Origin	Parts of Plant (Solvent)	Organism Tested	IC_{50} (μg/mL)	References
Fabaceae-Caesalpiniodeae	*Copaifera reticulata* Ducke	Belém, Pará State, Brazil	Copaiba oils (oleoresins from the trunks)	*Leishmania amazonensis* (Promastigotes)	5.0	[118]
Fabaceae-Caesalpiniodeae	*Copaifera reticulata* Ducke	Belém, Pará State, Brazil	Copaiba oils (oleoresins from the trunks)	*Leishmania amazonensis* (Axenic amastigotes)	15.0	[118]
Fabaceae-Caesalpiniodeae	*Copaifera reticulata* Ducke	Belém, Pará State, Brazil	Copaiba oils (oleoresins from the trunks)	*Leishmania amazonensis* (Intracellular amastigotes)	20.0	[118]
Goodneniaceae	*Scaevola balansae* Guillaumin	New Caledonia	Bark (DCM)	*Leishmania donovani* (Promastigotes)	8.7 ± 1.4	[119]
Guttiferae	*Clusia flava* Jacq.	Yucatán Peninsula, Mexico	Leaves (MeOH)	*Leishmania mexicana* (Promastigotes)	32	[103]
Icacinaceae	*Apodytes dimidiata*	Thai Nguyen province, Vietnam	Roots (EtOH)	*Leishmania infantum* (Amastigotes)	2	[104]

Lamiaceae	*Thymus capitelatus* Hoffmanns and Link	Coimbra, Portugal	Aerial parts (essential oils)	*Leishmania infantum* (Promastigotes)	37	[117]
Lamiaceae	*Ocimum gratissimum* L.	Juiz de Fora, Minas Gerais, Brazil	Leaves (MeOH)	*Leishmania chagasi* (Promastigotes)	71	[111]
Lamiaceae	*Hyptis lacustris* A. St.-Hil. ex Benth.	Yanesha, Peru	Leaves (EtOH)	*Leishmania amazonensis* (Axenic amastigotes)	10±7.2	[112]
Lamiaceae	*Premna serratifolia* L.	New Caledonia	Bark (DCM)	*Leishmania donovani* (Promastigotes)	4.4±0.4	[119]
Lauraceae	*Aniba canelilla* (H.B.K.) Mez	Amazonas state, Brazil	Leaves (essential oil)	*Leishmania amazonensis* (Promastigotes)	40.0±1.2	[120]
Lauraceae	*Licaria canella* (Meissner) Kostermans	Amazonas state, Brazil	Leaves (essential oil)	*Leishmania amazonensis* (Promastigotes)	19.0±0.9	[120]
Malpighiaceae	*Byrsonima bucidaefolia* Standl.	Yucatán Peninsula, Mexico	Bark (MeOH)	*Leishmania mexicana* (Promastigotes)	36	[103]
Malpighiaceae	*Byrsonima crassifolia* (L.) Kunth in H.B.K.	Yucatán Peninsula, Mexico	Bark (MeOH)	*Leishmania mexicana* (Promastigotes)	14	[103]

Continued

TABLE 1 Plant Species Reported to Have Antileishmanial Activity—Cont'd

Family	Plant	Origin	Parts of Plant (Solvent)	Organism Tested	IC_{50} (μg/mL)	References
Menispermaceae	*Triclisia patens* Oliv	Ghana	Aerial parts (MeOH)	*Leishmania donovani* (Promastigotes)	1.50± 0.16	[121]
Moraceae	*Dorstenia contrajerva* L.	Yucatán Peninsula, Mexico	Whole plant (MeOH)	*Leishmania mexicana* (Promastigotes)	23	[103]
Myrsinaceae	*Cybianthus anthuriophyllus* Pipoly	Chayahuita, Peru	Roots (EtOH)	*Leishmania amazonensis* (Axenic amastigotes)	12±1	[114]
Myrsinaceae	*Ardisia myrsinoides*	Thai Nguyen province, Vietnam	Roots (EtOH)	*Leishmania infantum* (Amastigotes)	2	[104]
Myrsinaceae	*Ardisia viburnifolia*	Thai Nguyen province, Vietnam	Roots (EtOH)	*Leishmania infantum* (Amastigotes)	2	[104]
Myrsinaceae	*Ardisia quinquegona* var. *oblonga*	Thai Nguyen province, Vietnam	Stems (EtOH)	*Leishmania infantum* (Amastigotes)	3	[104]
Myrsinaceae	*Ardisia angusta*	Thai Nguyen province, Vietnam	Roots (EtOH)	*Leishmania infantum* (Amastigotes)	2	[104]

Myrsinaceae	*Ardisia caudata*	Thai Nguyen province, Vietnam	Twigs (EtOH)	*Leishmania infantum* (Amastigotes)	9	[104]
Myrsinaceae	*Ardisia roseiflora*	Thai Nguyen province, Vietnam	Roots (EtOH)	*Leishmania infantum* (Amastigotes)	8	[104]
Myrsinaceae	*Ardisia amherstiana*	Thai Nguyen province, Vietnam	Twigs (EtOH)	*Leishmania infantum* (Amastigotes)	8	[104]
Myrsinaceae	*Maesa ambigua*	Thai Nguyen province, Vietnam	Twigs (EtOH)	*Leishmania infantum* (Amastigotes)	8	[104]
Myrsinaceae	*Maesa argentea*	Belgian National Botanical Garden, Meise, Belgium	Leaves (MeOH)	*Leishmania infantum* (Amastigotes)	<0.125	[104]
Myrsinaceae	*Maesa brevipaniculata*	Thai Nguyen province, Vietnam	Leaves (EtOH)	*Leishmania infantum* (Amastigotes)	<0.125	[104]
Myrsinaceae	*Maesa japonica*	Belgian National Botanical Garden, Meise, Belgium	Leaves (MeOH)	*Leishmania infantum* (Amastigotes)	<0.125	[104]

Continued

TABLE 1 Plant Species Reported to Have Antileishmanial Activity—Cont'd

Family	Plant	Origin	Parts of Plant (Solvent)	Organism Tested	IC_{50} (μg/mL)	References
Myrsinaceae	*Maesa perlarius*	Thai Nguyen province, Vietnam	Twigs (EtOH)	*Leishmania infantum* (Amastigotes)	2	[104]
Myrsinaceae	*Myrsine affinis*	Thai Nguyen province, Vietnam	Twigs (EtOH)	*Leishmania infantum* (Amastigotes)	6	[104]
Olacaceae	*Minquartia guianensis* Aubl.	Ecuador	Bark (DCM)	*Leishmania donovani* (Axenic amastigotes)	2.8	[113]
Olacaceae	*Minquartia guianensis* Aubl.	Ecuador	Leaves (DCM)	*Leishmania donovani* (Axenic amastigotes)	0.3	[113]
Papaveraceae	*Bocconia integrifolia*	Ecuador	Bark (DCM)	*Leishmania donovani* (Axenic amastigotes)	0.5	[113]
Papaveraceae	*Bocconia integrifolia*	Ecuador	Bark (hexane)	*Leishmania donovani* (Axenic amastigotes)	1.8	[113]
Papaveraceae	*Bocconia integrifolia*	Ecuador	Bark (MeOH)	*Leishmania donovani* (Axenic amastigotes)	0.7	[113]

Piperaceae	*Piper auritum* Kunt	Cuba	Aerial parts (essential oil)	*Leishmania major* (Promastigotes)	29.1±1.4	[122]
Piperaceae	*Piper auritum* Kunt	Cuba	Aerial parts (essential oil)	*Leishmania mexicana* (Promastigotes)	63.3±2.6	[122]
Piperaceae	*Piper auritum* Kunt	Cuba	Aerial parts (essential oil)	*Leishmania braziliensis* (Promastigotes)	52.1±3.1	[122]
Piperaceae	*Piper auritum* Kunt	Cuba	Aerial parts (essential oil)	*Leishmania donovani* (Promastigotes)	12.8±2.8	[122]
Piperaceae	*Piper auritum* Kunt	Cuba	Aerial parts (essential oil)	*Leishmania donovani* (Intracellular amastigotes)	22.3±1.8	[122]
Piperaceae	*Piper dennisii* Trel.	Yanesha, Peru	Leaves (EtOH)	*Leishmania amazonensis* (Axenic amastigotes)	10±1.5	[112]
Piperaceae	*Piper hispidum* var. *hispidum* Sw.	Peru	Leaves (EtOH)	*Leishmania amazonensis* (Axenic amastigotes)	5	[109]

Continued

TABLE 1 Plant Species Reported to Have Antileishmanial Activity—Cont'd

Family	Plant	Origin	Parts of Plant (Solvent)	Organism Tested	IC_{50} (μg/mL)	References
Piperaceae	*Piper strigosum* Trel	Peru	Leaves (EtOH)	*Leishmania amazonensis* (Axenic amastigotes)	7.8	[109]
Piperaceae	*Piper* sp. 2	Ecuador	Leaves (DCM)	*Leishmania donovani* (Axenic amastigotes)	2.2	[113]
Piperaceae	*Piper loretoanum* Trel.	Chayahuita, Peru	Aerial parts (EtOH)	*Leishmania amazonensis* (Axenic amastigotes)	13.6±0.6	[114]
Piperaceae	*Piper sanguineispicum* Trel.	Chayahuita, Peru	Stem (EtOH)	*Leishmania amazonensis* (Axenic amastigotes)	15±1	[114]
Poaceae	*Cymbopogon citratus* (DC) stapf.	Coimbra, Portugal	Aerial parts (essential oils)	*Leishmania infantum* (Promastigotes)	25	[117]
Primulaceae	*Anagallis arvensis*	Belgian National Botanical Garden, Meise, Belgium	Whole plant (MeOH)	*Leishmania infantum* (Amastigotes)	<0.125	[104]

Primulaceae	*Primula elatior*	Belgian National Botanical Garden, Meise, Belgium	Leaves (butanol extraction of methanol extract)	*Leishmania infantum* (Amastigotes)	1	[104]
Rhamnaceae	*Gouania lupuloides* (L.) Urb.	Ecuador	Bark/branches (DCM)	*Leishmania donovani* (Axenic amastigotes)	1.9	[113]
Rhamnaceae	*Gouania lupuloides* (L.) Urb.	Ecuador	Bark/branches (MeOH)	*Leishmania donovani* (Axenic amastigotes)	2.9	[113]
Rubiaceae	*Pavetta crassipes* K. Schum	Kankan, Guinea	Leaves (alkaloid extract)	*Leishmania infantum* (Amastigotes)	10.77	[123]
Rutaceae	*Spiranthera odoratissima* A. St.-Hil	Cerrado biome, Brazil	Roots (hexane)	*Leishmania* (*L.*) *chagasi* (Promastigotes)	22.3 ± 0.45	[115]
Sapindaceae	*Cupania dentata* D.C.	Yucatán Peninsula, Mexico	Bark (MeOH)	*Leishmania mexicana* (Promastigotes)	13	[103]
Scrophulariaceae	*Scoparia dulcis* L.	Ecuador	Whole plant (DCM)	*Leishmania donovani* (Axenic amastigotes)	1.8	[113]

Continued

TABLE 1 Plant Species Reported to Have Antileishmanial Activity—Cont'd

Family	Plant	Origin	Parts of Plant (Solvent)	Organism Tested	IC_{50} (μg/mL)	References
Solanaceae	*Cestrum racemosum* Ruiz and Pav.	Yanesha, Peru	Leaves (EtOH)	*Leishmania amazonensis* (Axenic amastigotes)	9.8±2.6	[112]
Solanaceae	*Brugmansia Pers.* sp. 1	Ecuador	Leaves (DCM)	*Leishmania donovani* (Axenic amastigotes)	3.0	[113]
Verbenaceae	*Vitex gaumeri* Greenm.	Yucatán Peninsula, Mexico	Bark (MeOH)	*Leishmania mexicana* (Promastigotes)	31	[103]
Verbenaceae	*Lantana* sp.	Yanesha, Peru	Leaves (EtOH)	*Leishmania amazonensis* (Axenic amastigotes)	10±2.1	[112]
Zingiberaceae	*Hedychium coronarium* J. König	Yanesha, Peru	Rhizomes (EtOH)	*Leishmania amazonensis* (Axenic amastigotes)	10±2.6	[112]
Zingiberaceae	*Renealmia alpinia* (Rottb.) Maas	Yanesha, Peru	Rhizomes (EtOH)	*Leishmania amazonensis* (Axenic amastigotes)	9±0.6	[112]

[a]*EtOH, ethanol; MeOH, methanol; DCM, dichloromethane; H_2O, water; EtOAc, ethyl acetate.*
[b]*CV, coefficient of variation.*

Concluding Remarks

It is evident that the list of antileishmanial agents from natural sources is extensive. It is important to point out that pharmacological evaluation of reported antileishmanials after the initial isolation and characterization is rarely carried out. To that end, efforts should be made by organizations such as TDR to establish viable natural product banks as a complement to existing chemoinformatic databases or libraries that can coordinate standardized screening and pharmacological evaluation of samples submitted by researchers around the world. As the world population becomes more integrated than ever before, it is our hope that with continued funding and efforts, novel chemotherapies against leishmaniasis and other tropical diseases will soon be developed.

REFERENCES

[1] E. Handman, Clin. Microbiol. Rev. 14 (2001) 229–243.
[2] R.W. Ashford, Int. J. Parasitol. 30 (2000) 1269–1281.
[3] WHO/TDR Annual report. Accessed on 02/10/2010. http://apps.who.int/tdr/publications/about-tdr/annualreports/bl10-annual-report/pdf/bl10-annual-report-2009.pdf. 2009.
[4] J. Alvar, P. Aparicio, A. Aseffa, M. Den Boer, C. Cañavate, J. Dedet, L. Gradoni, R. Ter Horst, Clin. Microbiol. Rev. 21 (2008) 334–359.
[5] S.L. Croft, S. Sundar, A.H. Fairlamb, Drug resistance in leishmaniasis, Clin. Microbiol. Rev. 19 (2006) 111–126.
[6] S. Sundar, T.K. Jha, C.P. Thakur, J. Engel, H. Sindermann, C. Fischer, K. Junge, A. Bryceson, J. Berman, N. Engl. J. Med. 347 (2002) 1739–1746.
[7] C.N. Chunge, G. Gachihi, R. Muigai, K. Wasunna, J.R. Rashid, J.D. Chulay, G. Anabwani, C.N. Oster, A.D. Bryceson, Trans. R. Soc. Trop. Med. Hyg. 79 (1985) 715–718.
[8] C.N. Chunge, J. Owate, H.O. Pamba, L. Donno, Trans. R. Soc. Trop. Med. Hyg. 84 (1990) 221–225.
[9] L. Kedzierski, J. Glob. Infect. Dis. 2 (2010) 177–185.
[10] A.C. Ivens, C.S. Peacock, E.A. Worthey, L. Murphy, G. Aggarwal, M. Berriman, E. Sisk, M. Rajandream, E. Adlem, R. Aert, A. Anupama, Z. Apostolou, P. Attipoe, N. Bason, C. Bauser, A. Beck, S.M. Beverley, G. Bianchettin, K. Borzym, G. Bothe, C.V. Bruschi, M. Collins, E. Cadag, L. Ciarloni, C. Clayton, R.M.R. Coulson, A. Cronin, A.K. Cruz, R.M. Davies, J. de Gaudenzi, D.E. Dobson, A. Duesterhoeft, G. Fazelina, N. Fosker, A.C. Frasch, A. Fraser, M. Fuchs, C. Gabel, A. Goble, A. Goffeau, D. Harris, C. Hertz-Fowler, H. Hilbert, D. Horn, Y. Huang, S. Klages, A. Knights, M. Kube, N. Larke, L. Litvin, A. Lord, T. Louie, M. Marra, D. Masuy, K. Matthews, S. Michaeli, J.C. Mottram, S. Müller-Auer, H. Munden, S. Nelson, H. Norbertczak, K. Oliver, S. O'Neil, M. Pentony, T.M. Pohl, C. Price, B. Purnelle, M.A. Quail, E. Rabbinowitsch, R. Reinhardt, M. Rieger, J. Rinta, J. Robben, L. Robertson, J.C. Ruiz, S. Rutter, D. Saunders, M. Schäfer, J. Schein, D.C. Schwartz, K. Seeger, A. Seyler, S. Sharp, H. Shin, D. Sivam, R. Squares, S. Squares, V. Tosato, C. Vogt, G. Volckaert, R. Wambutt, T. Warren, H. Wedler, J. Woodward, S. Zhou, W. Zimmermann, D.F. Smith, J.M. Blackwell, K.D. Stuart, B. Barrell, P.J. Myler, Science 309 (2005) 436–442.
[11] C.S. Peacock, K. Seeger, D. Harris, L. Murphy, J.C. Ruiz, M.A. Quail, N. Peters, E. Adlem, A. Tivey, M. Aslett, A. Kerhornou, A. Ivens, A. Fraser, M.-A. Rajandream, T. Carver,

H. Norbertczak, T. Chillingworth, Z. Hance, K. Jagels, S. Moule, D. Ormond, S. Rutter, R. Squares, S. Whitehead, E. Rabbinowitsch, C. Arrowsmith, B. White, S. Thurston, F. Bringaud, S.L. Baldauf, A. Faulconbridge, D. Jeffares, D.P. Depledge, S.O. Oyola, J.D. Hilley, L.O. Brito, L.R.O. Tosi, B. Barrell, A.K. Cruz, J.C. Mottram, D.F. Smith, M. Berriman, Nat. Genet. 39 (2007) 839–847.

[12] M.H. Gelb, L. Brunsveld, C.A. Hrycyna, S. Michaelis, F. Tamanoi, W.C. Van Voorhis, H. Waldmann, Nat. Chem. Biol. 2 (2006) 518–528.

[13] A. Mai, I. Cerbara, S. Valente, S. Massa, L.A. Walker, B.L. Tekwani, Antimicrob. Agents Chemother. 48 (2004) 1435–1436.

[14] J.C. Mottram, B.P. McCready, K.G. Brown, K.M. Grant, Mol. Microbiol. 22 (1996) 573–583.

[15] K.M. Grant, M.H. Dunion, V. Yardley, A. Skaltsounis, D. Marko, G. Eisenbrand, S.L. Croft, Antimicrob. Agents Chemother. 48 (2004) 3033–3042.

[16] A. Cruz, S.M. Beverley, Nature 348 (1990) 171–173.

[17] A. Cruz, C.M. Coburn, S.M. Beverley, Proc. Natl. Acad. Sci. USA 88 (1991) 7170–7174.

[18] S. Khabnadideh, D. Pez, A. Musso, R. Brun, L.M.R. Pérez, D. González-Pacanowska, I. H. Gilbert, Bioorg. Med. Chem. 13 (2005) 2637–2649.

[19] P.M. St. Hilaire, L.C. Alves, F. Herrera, M. Renil, S.J. Sanderson, J.C. Mottram, G. H. Coombs, M.A. Juliano, L. Juliano, J. Arevalo, M. Meldal, J. Med. Chem. 45 (2002) 1971–1982.

[20] A. Ponte-Sucre, R. Vicik, M. Schultheis, T. Schirmeister, H. Moll, Antimicrob. Agents Chemother. 50 (2006) 2439–2447.

[21] A.J. Davis, M.A. Perugini, B.J. Smith, J.D. Stewart, T. Ilg, A.N. Hodder, E. Handman, J. Biol. Chem. 279 (2004) 12462–12468.

[22] K. Lackovic, J.P. Parisot, N. Sleebs, J.B. Baell, L. Debien, K.G. Watson, J.M. Curtis, E. Handman, I.P. Street, L. Kedzierski, Antimicrob. Agents Chemother. 54 (2010) 1712–1719.

[23] E. Xingi, D. Smirlis, V. Myrianthopoulos, P. Magiatis, K.M. Grant, L. Meijer, E. Mikros, A. Skaltsounis, K. Soteriadou, Int. J. Parasitol. 39 (2009) 1289–1303.

[24] J.A. Brannigan, B.A. Smith, Z. Yu, A.M. Brzozowski, M.R. Hodgkinson, A. Maroof, H. P. Price, F. Meier, R.J. Leatherbarrow, E.W. Tate, D.F. Smith, A.J. Wilkinson, J. Mol. Biol. 396 (2010) 985–999.

[25] J.M. Boitz, P.A. Yates, C. Kline, U. Gaur, M.E. Wilson, B. Ullman, S.C. Roberts, Infect. Immun. 77 (2009) 756–763.

[26] M. Chen, L. Zhai, S.B. Christensen, T.G. Theander, A. Kharazmi, Antimicrob. Agents Chemother. 45 (2001) 2023–2029.

[27] G.J. Crowther, D. Shanmugam, S.J. Carmona, M.A. Doyle, C. Hertz-Fowler, M. Berriman, S. Nwaka, S.A. Ralhp, D.S. Roos, W.C. Van Voorhis, F. Agüero, PLoS Negl. Trop. Dis. 4 (2010) e804.

[28] D.J. Newman, G.M. Cragg, J. Nat. Prod. 70 (2007) 461–477.

[29] D.J. Newman, G.M. Cragg, K.M. Snader, J. Nat. Prod. 66 (2003) 1022–1037.

[30] G.M. Cragg, D.J. Newman, K.M. Snader, J. Nat. Prod. 60 (1997) 52–60.

[31] L.G. Rocha, J.R.G.S. Almeida, R.O. Macêdo, J.M. Barbosa-Filho, Phytomedicine 12 (2005) 514–535.

[32] M.M. Salem, K.A. Werbovetz, Curr. Med. Chem. 13 (2006) 2571–2598.

[33] T. Polonio, T. Efferth, Int. J. Mol. Med. 22 (2008) 277–286.

[34] C. Marín, S. Boutaleb-Charki, J.G. Díaz, O. Huertas, M.J. Rosales, G. Pérez-Cordon, R. Guitierrez-Sánchez, M. Sánchez-Moreno, J. Nat. Prod. 72 (2009) 1069–1074.

[35] Z.H. Mbwambo, M.C. Kapingu, M.J. Moshi, F. Machumi, S. Apers, P. Cos, D. Ferreira, J.P. J. Marais, D.V. Berghe, L. Maes, A. Vlietinck, L. Pieters, J. Nat. Prod. 69 (2006) 369–372.
[36] A.A. da Silva Filho, E.S. Costa, W.R. Cunha, M.L.A. Silva, N.P.D. Nanayakkara, J.K. Bastos, Phytother. Res. 22 (2008) 1307–1310.
[37] M.M. Radwan, M.A. Elsohly, D. Slade, S.A. Ahmed, I.A. Khan, S.A. Ross, J. Nat. Prod. 72 (2009) 906–911.
[38] N. Duarte, O. Kayser, P. Abreu, M.U. Ferreira, Phytother. Res. 22 (2008) 455–457.
[39] E. Elfita, M. Muharni, M. Latief, D. Darwati, A. Widiyantoro, S. Supriyatna, H.H. Bahti, D. Dachriyanus, P. Cos, L. Maes, K. Foubert, S. Apers, L. Pieters, Phytochemistry 70 (2009) 907–912.
[40] V.K. Dua, V.P. Ojha, R. Roy, B.C. Joshi, N. Valecha, C. Usha Devi, M.C. Bhatnagar, V.P. Sharma, S.K. Subbarao, J. Ethnopharmacol. 95 (2004) 247–251.
[41] V.K. Dua, G. Verma, A.P. Dash, Phytother. Res. 23 (2009) 126–128.
[42] N. Flores, I.A. Jiménez, A. Giménez, G. Ruiz, D. Gutiérrez, G. Bourdy, I.L. Bazzocchi, Phytochemistry 70 (2009) 621–627.
[43] N. Flores, I.A. Jiménez, A. Giménez, G. Ruiz, D. Gutiérrez, G. Bourdy, I.L. Bazzocchi, J. Nat. Prod. 71 (2008) 1538–1543.
[44] O. Kayser, H. Kolodziej, A.F. Kiderlen, Phytother. Res. 15 (2001) 122–126.
[45] H. Kolodziej, O.A. Radtke, A.F. Kiderlen, Phytochemistry 69 (2008) 3103–3110.
[46] C. Jiménez-Romero, D. Torres-Mendoza, L.D. Ureña González, E. Ortega-Barría, K.L. McPhail, W.H. Gerwick, L. Cubilla-Rios, J. Nat. Prod. 70 (2007) 1249–1252.
[47] M.M. Salem, K.A. Werbovetz, J. Nat. Prod. 69 (2006) 43–49.
[48] R. Sen, A.K. Bauri, S. Chattopadhyay, M. Chatterjee, Phytother. Res. 21 (2007) 592–595.
[49] R. Borges-Argáez, T. Vela-Catzín, A. Yam-Puc, M.J. Chan-Bacab, R.E. Moo-Puc, M. Cáceres-Farfán, Planta Med. 75 (2009) 1336–1338.
[50] N. Flores, G. Cabrera, I.A. Jiménez, J. Piñero, A. Giménez, G. Bourdy, F. Cortés-Selva, I.L. Bazzocchi, Planta Med. 73 (2007) 206–211.
[51] M.F. Muzitano, L.W. Tinoco, C. Guette, C.R. Kaiser, B. Rossi-Bergmann, S.S. Costa, Phytochemistry 67 (2006) 2071–2077.
[52] M.F. Muzitano, C.A.B. Falcão, E.A. Cruz, M.C. Bergonzi, A.R. Bilia, F.F. Vincieri, B. Rossi-Bergmann, S.S. Costa, Planta Med. 75 (2009) 307–311.
[53] M.C. Kapingu, Z.H. Mbawanbo, M.J. Moshi, J.J. Magudula, P. Cos, D.V. Berghe, L. Maes, M. Thenius, S. Apers, L. Pieters, Planta Med. 72 (2006) 1341–1343.
[54] A. Poddar, A. Banerjee, S. Ghanta, S. Chattopadhyay, Planta Med. 74 (2008) 503–508.
[55] H. Kirmizibekmez, I. Atay, M. Kaiser, R. Brun, M.M. Cartagena, N.M. Carballeira, E. Yesilada, D. Tasdemir, Phytother. Res. 25 (2011) 142–146.
[56] G. Bringmann, J. Spuziak, J.H. Faber, T. Gulder, I. Kajahn, M. Dreyer, G. Heubl, R. Brun, V. Mudogo, Phytochemistry 69 (2008) 1065–1075.
[57] G. Bringmann, I. Kajahn, M. Reichert, S.E.H. Pedersen, J.H. Faber, T. Gulder, R. Brun, S.B. Christensen, A. Ponte-Sucre, H. Moll, G. Heubl, V. Mudogo, J. Org. Chem. 71 (2006) 9348–9356.
[58] E.M.K. Wijeratne, Y. Hatanaka, T. Kikuchi, Y. Tezuka, A.A.L. Gunatilaka, Phytochemistry 6 (1996) 1703–1706.
[59] E.V. Costa, M. Lúcia, B. Pinheiro, C.M. Xavier, J.R.A. Silva, A.C.F. Amaral, A.D.L. Souza, A. Barison, F.R. Campos, A.G. Ferreira, G.M.C. Machado, L.L.P. Leon, J. Nat. Prod. 69 (2006) 292–294.
[60] K.P. Devkota, B.N. Lenta, J.D. Wansi, M.I. Choudhary, D.P. Kisangau, N.Q. Samreen, N. Sewald, J. Nat. Prod. 71 (2008) 1481–1484.

[61] S. Van Miert, S. Hostyn, B.U.W. Maes, K. Cimanga, R. Brun, M. Kaiser, P. Mátyus, R. Dommisse, G. Lemière, A. Vlietinck, L. Pieters, J. Nat. Prod. 68 (2005) 674–677.
[62] J. Fotie, D.S. Bohle, M. Olivier, M.A. Gomez, S. Nzimiro, J. Nat. Prod. 70 (2007) 1650–1653.
[63] J.H. Correa, H.C. Ríos, A.R. Castillo, L.I. Romero, E. Ortega-Barría, P.D. Coley, T.A. Kursar, M.V. Heller, W.H. Gerwick, L.C. Rios, Planta Med. 72 (2006) 270–272.
[64] A. Ata, C.D. Iverson, K.S. Kalhari, S. Akhter, J. Betteridge, M.H. Meshkatalsadat, I. Orhan, B. Sener, Phytochemistry 71 (2010) 1780–1786.
[65] M. Morales-Yuste, F. Morillas-Marquez, J. Martín-Sanchez, A. Valero-López, M.C. Navarro-Moll, Phytomedicine 17 (2010) 279–281.
[66] M.R. Santin, A.O. dos Santos, C.V. Nakamura, B.P.D. Filho, I.C.P. Ferreira, T. Ueda-Nakamura, Parasitol. Res. 105 (2009) 1489–1496.
[67] V.D. Zheljazkov, C.L. Cantrell, B. Tekwani, S.I. Khan, J. Agric. Food Chem. 56 (2008) 380–385.
[68] M.I. Choudhary, S. Jan, A. Abbaskhan, S.G. Musharraf, Samreen, S.A. Sattar, Atta-ur-Rahman, J. Nat. Prod. 71 (2008) 1557–1560.
[69] M.G.M. Danelli, D.C. Soares, H.S. Abreu, L.M.T. Peçanha, E.M. Saraiva, Phytochemistry 70 (2009) 608–614.
[70] L.A. Sánchez, Z. Capitan, L.I. Romero, E. Ortega-Barría, W.H. Gerwick, L. Cubilla-Rios, Nat. Prod. Commun. 2 (2007) 1065–1069.
[71] A. Hay, J. Ioset, K.M. Ahua, D. Diallo, R. Brun, K. Hostettmann, J. Nat. Prod. 70 (2007) 9–13.
[72] D. Mandal, N. Panda, S. Kumar, S. Banerjee, N.B. Mandal, N.P. Sahu, Phytochemistry 67 (2006) 183–190.
[73] V. Samoylenko, D.C. Dunbar, M.A. Gafur, S.I. Khan, S.A. Ross, J.S. Mossa, F.S. El-Feraly, B.L. Tekwani, J. Bosselaers, I. Muhammad, Phytother. Res. 22 (2008) 1570–1576.
[74] P. Sartorelli, S.P. Andrade, M.S.C. Melhem, F.O. Prado, A.G. Tempone, Phytother. Res. 21 (2007) 644–647.
[75] N. Fokialakis, E. Kalpoutzakis, B.L. Tekwani, A.L. Skaltsounis, S.O. Duke, Biol. Pharm. Bull. 29 (2006) 1775–1778.
[76] L. Acebey, V. Jullian, D. Sereno, S. Chavalley, Y. Estevez, C. Moulis, S. Beck, A. Valentin, A. Gimenez, M. Sauvain, Planta Med. 76 (2010) 365–368.
[77] J.C. Aponte, Y. Estevez, R.H. Gilman, H.W. Lewis, R. Rojas, M. Sauvain, A.J. Valsberg, G.B. Hammond, Planta Med. 74 (2008) 1–4.
[78] A.M.M. Nour, S.A. Khalid, M. Kaiser, R. Brun, W.E. Abdallah, T.J. Schmidt, Planta Med. 75 (2009) 1363–1368.
[79] A. Karioti, H. Skaltsa, M. Kaiser, D. Tasdemir, Phytomedicine 16 (2009) 783–787.
[80] S.M. Maregesi, N. Hermans, L. Dhooghe, K. Cimanga, D. Ferreira, C. Pannecouque, D.A. Vanden Berghe, P. Cos, L. Maes, A.J. Vlietinck, S. Apers, L. Pieters, J. Ethnopharmacol. 129 (2010) 319–326.
[81] D. Lacroix, S. Prado, A. Deville, S. Krief, V. Dumontet, J. Kasenene, E. Mouray, C. Bories, B. Bodo, Phytochemistry 70 (2009) 1239–1245.
[82] K. Mori, M. Kawano, H. Fuchino, T. Ooi, M. Satake, Y. Agatsuma, T. Kusumi, S. Sekita, J. Nat. Prod. 71 (2008) 18–21.
[83] V. Arango, S. Robledo, B. Séon-Méniel, B. Figadère, W. Cardona, J. Sáez, F. Otálvaro, J. Nat. Prod. 73 (2010) 1012–1014.
[84] G. Bringmann, S. Rüdenauer, A. Irmer, T. Bruhn, R. Brun, T. Heimberger, T. Stühmer, R. Bargou, M. Chatterjee, Phytochemistry 69 (2008) 2501–2509.

[85] O. Hiraoka, H. Satake, S. Iguchi, A. Matsuda, T. Ueda, Y. Wataya, Biochem. Biophys. Res. Commun. 134 (1986) 1114–1121.
[86] S. Ganapaty, P.S. Thomas, G. Karagianis, P.G. Waterman, R. Brun, Phytochemistry 67 (2006) 1950–1956.
[87] S. Ganapaty, G.V.K. Srilakshmi, S.T. Pannakal, H. Rahman, H. Laatsch, R. Brun, Phytochemistry 70 (2009) 95–99.
[88] H.B. Napolitano, M. Silva, J. Ellena, B.D.G. Rodrigues, A.L.C. Almeida, P.C. Vieira, G. Oliva, O.H. Thiemann, Braz. J. Med. Biol. Res. 37 (2004) 1847–1852.
[89] M. Iranshahi, P. Arfa, M. Ramezani, M.R. Jaafari, H. Sadeghian, C. Bassarello, S. Piacente, C. Pizza, Phytochemistry 68 (2007) 554–561.
[90] M.R. Moein, R.S. Pawar, S.I. Khan, B.L. Tekwani, I.A. Khan, Phytother. Res. 22 (2008) 283–285.
[91] M. Senn, S. Gunzenhauser, R. Brun, U. Séquin, J. Nat. Prod. 70 (2007) 1565–1569.
[92] Z. Martín-Quintal, R. Moo-Puc, F. González-Salazar, M.J. Chan-Bacab, L.W. Torres-Tapia, S.R. Peraza-Sánchez, J. Ethnopharmacol. 122 (2009) 463–467.
[93] Z. Martín-Quintal, M. del Rosario García-Miss, M. Mut-Martín, A. Matus-Moo, L. W. Torres-Tapia, S.R. Peraza-Sánchez, Phytother. Res. 24 (2010) 1004–1008.
[94] S. Ankisetty, H.N. ElSohly, X. Li, S.I. Khan, B.L. Tekwani, T. Smillie, L. Walker, J. Nat. Prod. 69 (2006) 692–694.
[95] S.M.K. Rates, Toxicon 39 (2001) 603–613.
[96] K.M. Ahua, J. Ioset, K.N. Ioset, D. Diallo, J. Mauël, K. Hostettmann, J. Ethnopharmacol. 110 (2007) 99–104.
[97] S.H. Taleb-Contini, M.J. Salvador, J.M.F. Balanco, S. Albuquerque, D.C.R. de Oliveira, Phytother. Res. 18 (2004) 250–254.
[98] E.V.M. Kigondu, G.M. Rukunga, J.M. Keriko, W.K. Tonui, J.W. Gathirwa, P.G. Kirira, B. Irungu, J.M. Ingonga, I.O. Ndiege, J. Ethnopharmacol. 123 (2009) 504–509.
[99] T. Okpekon, S. Yolou, C. Gleye, F. Roblot, P. Loiseau, C. Bories, P. Grellier, F. Frappier, A. Laurens, R. Hocquemiller, J. Ethnopharmacol. 90 (2004) 91–97.
[100] M. Billo, A. Fournet, P. Cabalion, J. Waikedre, C. Bories, P. Loiseau, E. Prina, A.R. de Arias, G. Yaluff, C. Fourneau, R. Hocquemiller, J. Ethnopharmacol. 96 (2005) 569–575.
[101] L. Monzote, M. García, A.M. Montalvo, R. Scull, M. Miranda, J. Abreu, Phytother. Res. 21 (2007) 1055–1058.
[102] L. Monzote, A.M. Montalvo, A.S. Almanonni, R. Scull, M. Miranda, J. Abreu, Chemotherapy 52 (2006) 130–136.
[103] S.R. Peraza-Sánchez, F. Cen-Pacheco, A. Noh-Chimal, F. May-Pat, P. Simá-Polanco, E. Dumonteil, M.R. García-Miss, M. Mut-Martín, Fitoterapia 78 (2007) 315–318.
[104] M. Vermeersch, K. Foubert, R.I. da Luz, L.V. Puyvelde, P. Cos, L. Pieters, L. Maes, Phytother. Res. 23 (2009) 1404–1410.
[105] E.V. Costa, M.L.B. Pinheiro, J.R.A. Silva, B.H.L.N.S. Maia, M.C.T. Duarte, A.C. F. Amaral, G.M.C. Machado, L.L. Leon, Quim. Nova 32 (2009) 78–81.
[106] M. Lamidi, C. DiGiorgio, F. Delmas, A. Favel, C.E. Mve-Mba, M.L. Rondi, E. Ollivier, L. Nze-Ekekang, G. Balansard, J. Ethnopharmacol. 102 (2005) 185–190.
[107] E. Osorio, G.J. Arango, N. Jiménez, F. Alzate, G. Ruiz, D. Gutiérrez, M.A. Paco, A. Giménez, S. Robledo, J. Ethnopharmacol. 111 (2007) 630–635.
[108] D. Castillo, J. Arevalo, F. Herrera, C. Ruiz, R. Rojas, E. Rengifo, A. Vaisberg, O. Lock, J.-L. Lemesre, H. Gornitzka, M. Sauvain, J. Ethnopharmacol. 112 (2007) 410–414.
[109] Y. Estevez, D. Castillo, M.T. Pisango, J. Arevalo, R. Rojas, J. Alban, E. Deharo, G. Bourdy, M. Sauvain, J. Ethnopharmacol. 114 (2007) 254–259.

[110] N.A. Parreira, L.G. Magalhães, D.R. Morais, S.C. Caixeta, J.P.B. de Sousa, J.K. Bastos, W.R. Cunha, M.L.A. Silva, N.P.D. Nanayakkara, V. Rodrigues, A.A.S. Filho, Chem. Biodivers. 7 (2010) 993–1001.
[111] F.G. Braga, M.L.M. Bouzada, R.L. Fabri, M.O. Matos, F.O. Moreira, E. Scio, E.S. Coimbra, J. Ethnopharmacol. 111 (2007) 396–402.
[112] V. Céline, P. Adriana, D. Eric, A. Joaquina, E. Yannick, L.F. Augusto, R. Rosario, G. Dionicia, S. Michel, C. Denis, B. Geneviève, J. Ethnopharmacol. 123 (2009) 413–422.
[113] M.S. Gachet, J.S. Lecaro, M. Kaiser, R. Brun, H. Navarrete, R.A. Muñoz, R. Bauer, W. Schühly, J. Ethnopharmacol. 128 (2010) 184–197.
[114] G. Odonne, G. Bourdy, D. Castillo, Y. Estevez, A. Lancha-Tangoa, J. Alban-Castillo, E. Deharo, R. Rojas, D. Stien, M. Sauvain, J. Ethnopharmacol. 126 (2009) 149–158.
[115] L.C. Albernaz, J.E. de Paula, G.A.S. Romero, M.R.R. Silva, P. Grellier, L. Mambu, L.S. Espindola, J. Ethnopharmacol. 131 (2010) 116–121.
[116] B.N. Lenta, C. Vonthron-Sénécheau, R.F. Soh, F. Tantangmo, S. Ngouela, M. Kaiser, E. Tsamo, R. Anton, B. Weniger, J. Ethnopharmacol. 111 (2007) 8–12.
[117] M. Machado, G. Santoro, M.C. Sousa, L. Salgueiro, C. Cavaleiro, Flavour Fragr. J. 25 (2010) 156–160.
[118] A.O. Santos, T. Ueda-Nakamura, B.P. Dias Filho, V.F. Veiga Junior, A.C. Pinto, C.V. Nakamura, J. Ethnopharmacol. 120 (2008) 204–208.
[119] J. Desrivot, J. Waikedre, P. Cabalion, C. Herrenknecht, C. Bories, R. Hocquemiller, A. Fournet, J. Ethnopharmacol. 112 (2007) 7–12.
[120] J.R.A. Silva, D.F.M. do carmo, É.M. Reis, G.M.C. Machado, L.L. Leon, B.O. da silva, J.L. P. Ferreira, A.C.F. Amaral, J. Braz. Chem. Soc. 20 (2009) 1071–1076.
[121] M.D.R. Camacho, J.D. Phillipson, S.L. Croft, P.N. Solis, S.J. Marshall, S.A. Ghazanfar, J. Ethnopharmacol. 89 (2003) 185–191.
[122] L. Monzote, M. García, A.M. Montalvo, R. Scull, M. Miranda, Mem. Inst. Oswaldo Cruz 105 (2010) 168–173.
[123] E.S. Baldé, V. Megalizzi, M.S. Traoré, P. Cos, L. Maes, C. Decaestecker, L. Pieters, A.M. Baldé, J. Ethnopharmacol. 130 (2010) 529–535.

Index

B

C

D

E

F

G

H

I

J

K

L

M

N

O

P

Q

R

S

T

U

V

W

X

Y

Z